UNIVERSITE DE BOURGOGNE
ECOLE DOCTORALE ENVIRONNEMENT - SANTE – STIC

UMR Agroécologie INRA 1347/Agrosup/Université de Bourgogne, Pôle Interactions Plantes Microorganismes ERL 6300 CNRS, BP 86510, 21065 Dijon Cedex, France

Département Environnement et Agro-Biotechnologies, Centre de Recherche Public-Gabriel Lippmann, 41, rue du Brill, L-4422, Belvaux, Luxembourg

THÈSE

Pour obtenir le grade de

Docteur de l'Université de Bourgogne
Spécialité Biochimie, Biologie Cellulaire et Moléculaire

Par

Cosette ABDALLAH

Technical improvements for analysis of recalcitrant proteins by LC-MS: the mycorrhiza responsive membrane proteome as a case study

Le 26 octobre 2012 devant le jury

Graziella Berta, Professeur, Università del Piemonte Orientale	Rapporteur
André Almeida, Chargé de recherches, Universidade Nova de Lisboa	Rapporteur
Christophe Roux, Professeur, Université Paul Sabatier de Toulouse	Examinateur
Benoit Valot, Chargé de recherches, INRA de Paris	Examinateur
Eliane Dumas-Gaudot, Directrice de recherches INRA de Dijon	Co-directeur de thèse
Ghislaine Recorbet, Chargé de recherches, INRA de Dijon	Co-directeur de thèse
Jenny Renaut, Responsable de la plateforme de protéomique, CRP Gabriel Lippmann, Luxembourg	Co-directeur de thèse

To my family and Antoine

Acknowledgements

"The teacher who is indeed wise does not bid you to enter the house of his wisdom but rather leads you to the threshold of your mind" Gibran Khalil Gibran.

First and foremost my sincere and deep thanks go to my honourable thesis supervisors Jenny Renaut, Eliane Dumas-Gaudot and Ghislaine Recorbet. Jenny, the joy and enthusiasm you had for research was contagious and motivational for me. I am happy that I witnessed the birth of your adorable daughter, Emily. Eliane, I am deeply thankful for your encouragement and thoughtful guidance all over these years. I want also to express my deep thank to Ghislaine, your willingness, continuous contribution and invaluable advices were mandatory to complete this PhD dissertation.

My debt of gratitude is due to the supportive adviser Kjell Sergeant for sharing my workload and for his unflagging encouragement. This work would not have been possible without your suggestions and comments to improve the legibility of the manuscript.

I would like to acknowledge honorary Lucien Hoffmann, head of EVA department in CRP Gabriel Lippmann, and Daniel Wipf, head of Pôle Interactions Plantes Microorganismes group at INRA, for their confidence and for giving me the opportunity to perform my PhD within the research units of both institutes. My thoughts go as well to the INRA staff, many thanks to Silvio, Vivienne, Franck, Francine and Jonathan.

I am grateful to the jury members for the care with which they accepted to review this work. I am particularly thankful to André Almeida and Graziella Berta, your helpful suggestions will increase the quality and reduce ambiguity of the thesis manuscript.

I would like also to thank Michel Zivy and Benoit Valot for the great collaboration and the constructive data that they have supplied. Special thanks to my thesis committee members Christelle Guillier, Estelle Goulas and Françoise Simon-Plas for their support, guidance and helpful suggestions.

I gratefully acknowledge the funding source Fonds National de la Recherche du Luxembourg, TR-PHD BFR 08-078, that made my PhD work possible.

I would like also to thank the technical staff in the CRP proteomics Platform. Sébastien Planchon who rescued me in many bioinformatics related issues. Céline Leclercq, thank you for your technical support and help. Foremost thanks for your friendship, good mood and your presence has helped to better integrate and carry on throughout all these years.

"In the sweetness of friendship let there be laughter, and sharing of pleasures" Gibran Khalil Gibran.

I would like to use this opportunity to thank all my friends and colleagues who have helped me through all these years. I owe them my heartfelt appreciation.

To start, I would like to thank André Jobard and Germaine Chabanaud for being like a second family for me in Dijon.

The thank goes to Anastasia Georgantzopoulou, spelling and pronouncing properly your family name is another achievement in my life :) thank you for your friendship, for supporting me in my ups and downs and being the guide of "what is must to do in Luxembourg". I am looking forward to make more journeys together :)

Lisa, my cinema partner every Wednesday and with whom I shared the first unforgettable camping experience :) thank you and I wish you all the best.

A big thanks is for my office colleagues, I enjoyed their company in a friendly atmosphere. Raquel, thank you for your good mood, Sebastian, thanks for your informatics skills and keep me updated on your targeted "juicy market". Frédéric, the office secretary thank you for everything. Bruno, I will miss our enthusiastic political debates. Good luck for all of you in finishing your PhD.

My thoughts go as well to my friend Roy, I will miss exchanging mails with you, thank you for all the laughter and good luck in achieving your PhD. Rachid thank you for your support. Laura, Tommaso, Mauricio, Xavier, Hélène, Imad, Ali, Tiphaine and Périne many thanks for your presence and assistance.

"A friend who is far away is sometimes much nearer than one who is at hand" Gebran Khalil Gebran.

I could not complete my work without invaluable friendly assistance that meant more to me than I could ever express. The thank goes to my Lebanese friends: the beautiful bride Diane, Dédé thanks for being so close regardless the distance, Johnny my childhood friend, Charbel thanks for the great time that we shared together, and Zeina thank you for your help in Dijon and I wish you all the best in your personal and professional life.

"Your children are not your children. They are the sons and daughters of Life's longing for itself" Gebran Khalil Gebran.

My sincerest thanks indebted to my parents who raised me with love and supported me in all my pursuits. You accepted to be far away from your children, wishing them to make better future and reach higher issues. Thank you for your prayers, love and financial aids.
The thank goes as well to my sister Marie who was always present and supportive regardless the distance and who encouraged me to seek further knowledge, you deserve all the best in your professional and private life. Thanks for the support of my brother in law Elie. I am not forgetting my brother Gilbert who was always source of enthusiasm and joy, thanks for your encouragements.

"Love is the only flower that grows and blossoms without the aid of the seasons" Gebran Khalil Gebran.
Antoine, I deeply thank you for your love, continuous support to cope with ups and downs, successes and failures, doubts and certainties. "*yesterday is today's memory and tomorrow is today's dream*" I am looking forward to be together.

Résumé

La symbiose mycorhizienne à arbuscules (SMA) est le résultat de l'interaction entre les racines de plus de 80% des familles de plantes terrestres et les champignons MA. Divers types de membranes jouent un rôle crucial dans la mise en place et le fonctionnement de la SMA chez l'hôte végétal. Si l'électrophorèse bidimensionnelle (2-DE) reste la méthode la plus couramment utilisée pour des analyses protéomiques quantitatives dans la SMA, elle résout difficilement les protéines membranaires en raison de leur hydrophobicité, leur précipitation au point isoélectrique (pI) et leur faible abondance comparativement aux protéines cytosoliques. Donc peu nombreuses sont les protéines membranaires identifiées comme étant régulées en réponse à la symbiose. Afin d'avoir accès à cette catégorie de protéines et contourner les défauts de la 2-DE, l'application de nouvelles méthodes permet de réaliser des analyses quantitatives avec marquage chimique (comme l'iTRAQ) ou non (label-free). Dans ce contexte, deux méthodes de protéomique quantitative, iTRAQ-OFFGEL-CL-SM/SM et « label-free » 1-DE-CL-SM/SM, sont adoptées dans ce travail visant à identifier et quantifier les variations d'accumulation des protéines microsomales de racines de *Medicago truncatula* inoculées par *Rhizophagus irregularis*, préalable indispensable à l'analyse de leur rôle fonctionnel dans la SMA. Un protocole d'extraction donnant accès à des fractions radiculaires enrichies en protéines microsomales nécessaires pour les analyses ultérieures est décrit dans cette étude. En plus de l'analyse quantitative du protéome membranaire en réponse à la SMA, une approche méthodologique a été mise en place afin d'étudier l'impact du marquage iTRAQ sur le pI des peptides.

Mots-clés : symbiose mycorhizienne à arbuscules, *Medicago truncatula*, protéines membranaires, protéomique hors gel, protéomique sans marquage.

Abstract

Arbuscular mycorrhizas (AM) are widespread symbiotic associations between plant roots and AM fungi. Deep membrane alterations are the foremost morphological changes occurring in the host plant in response to AM symbiosis. Two-dimensional gel electrophoresis (2-DE) is the workhorse method in AM proteomics. Membrane proteins are under-represented in 2-DE because of their hydrophobicity, low abundance, and precipitation at their isoelectric point, thereby few are the identified membrane proteins involved in sustaining the AM symbiosis. Membrane proteomics is still challenging due to 2-DE related shortcomings, however latest trends and advancements in mass spectrometry (MS)-based quantitative proteomics offer enormous potential to monitor membrane protein change in abundance in large scale experiments. In the current work microsomal proteins of *Medicago truncatula* roots inoculated with *Rhizophagus irregularis* were, for the first time, scrutinised by state-of-the-art MS-based proteomic approaches iTRAQ-OFFGEL-LC-MS/MS and label-free 1-DE-LC-MS/MS. The applied workflows combine two novel proteomic procedures, label-based and -free, targeting an insight view on the membrane proteome changes in AM symbiosis. A subcellular fractionation method is herein described to access the total membrane-associated proteins with sufficient recovery and purity for their subsequent in-depth analysis. In addition to the biological gain by shedding the light on candidate AM-related membrane proteins, a methodological approach was carried out in the present work in order to elucidate the iTRAQ labelling impact on peptide isoelectric points.

Keywords: arbuscular mycorrhizal symbiosis, *Medicago truncatula*, membrane-associated proteins, gel-free proteomics and label-free proteomics.

List of abbreviations

ACN: Acetonitrile
AFC: Affinity chromatography
AM: Arbuscular mycorrhiza
AMF: Arbuscular mycorrhizal fungi
ANOVA: Analysis of variance
APEX: Absolute protein expression
AX: Anion-exchange chromatography

BN-PAGE : Blue native-PAGE

CHCA: α-cyano-4-hydroxycinnamic acid
CID: Collision induced dissociation
CX: Cation-exchange chromatography

DDA: Data-dependent analysis
DIA: Data-independent analysis
DTT: Dithiothreitol

EDTA: Ethylenediaminetetraacetic acid
emPAI: Exponentially modified Protein abundance index
EMRT: Exact mass retention time
ERM: Extra-radical mycelium
EST: Expressed sequence tag

FA: Formic acid
FDR: False discovery rates

HCD: High energy collisional dissociation
HILEP: Hydroponic isotope labelling of entire plants

IAA: 2-iodoacetamide
ICAT: Isotope-coded affinity tags
ICPL: Isotope-coded protein labelling
IEC: Ion-exchange chromatography
IEF: Isoelectric focusing
IPG: Immobilized pH gradient
IRM: Intra-radial mycelium
iTRAQ: Isobaric tags for relative and absolute quantitation

JA: Jasmonic acid

LC: Liquid chromatography

MALDI-TOF: Matrix assisted laser desorption ionisation time of flight
Mbp: Million base pair
MeOH: Methanol
MES: 2-(N-morpholino)ethanesulfonic acid
ms: Millisecond

MS: Mass spectrometry
MS^E: High-energy scan mode
MudPIT: Multidimensional protein identification technology
MW: Molecular weight
m/z: Ratio mass/charge

NSAF: Normalized spectral abundance factor
NMWL: Nominal molecular weight limit

OGE: OFFGEL electrophoresis

PAI: Protein abundance index
PCA: Principle component analysis
pI: Isoelectric point
PMSF: Phenylmethylsulfonyl fluoride
PPA: Pre-penetration apparatus

RNF: Rhizobial nitrogen-fixing
ROS: Reactive oxygen species
RP: Reversed-phase chromatography
Rt: Retention time

s: second
SCX: Strong-cation exchange
SDS: Sodium dodecyl sulphate
SEC: Size exclusion chromatography
SILAC: Stable isotopic labelling with amino acids in cell culture
SILIP: Stable isotope labelling in planta
SL: Strigolactone

TEAB: Triethylammonium bicarbonate
TFA: Trifluoroacetic acid
TMT: Tandem Mass Tag
Tris: Tris(hydroxymethyl)aminomethane

1-DE: One-dimensional gel electrophoresis
2-DE: Two-dimensional gel electrophoresis
2D-DIGE: Difference gel electrophoresis
2D-LC: Two-dimensional liquid chromatography

Table of contents

List of tables

Table of figures

List of additional files

Synopsis de la thèse

Dans la nature, les relations plantes-microorganismes sont principalement du type parasitisme, commensalisme, ou mutualisme. C'est parmi cette dernière catégorie de relations que s'inscrit la symbiose mycorhizienne à arbuscules (SMA) (Smith & Read, 2008). Les premières traces de la SMA remontent à 400 millions d'années avec la découverte de fossiles de plantes présentant dans leurs tissus les mêmes structures fongiques que les plantes contemporaines (Remy *et al.*, 1994). Ces observations confirment une étude moléculaire datant l'apparition des champignons MA de 353 à 462 millions d'années (Simon *et al.*, 1993). Cette apparition et les premières traces de la symbiose endomycorhizienne coïncideraient avec le début de la colonisation du milieu terrestre par les plantes. Le terme mycorhize provient des mots grecs "mûkes" et "rhiza" signifiant respectivement "champignon" et "racine". Il désigne l'interaction réciproque entre certains champignons du sol et les racines d'une plante. La SMA est le résultat de l'interaction entre les racines de plus de 80% des familles de plantes terrestres et les champignons MA. Ces derniers sont des biotrophes obligatoires c'est-à-dire qu'ils ne peuvent se développer qu'en présence des racines de la plante hôte. Leurs besoins en composés carbonés sont satisfaits *via* la symbiose grâce aux photosynthétats de la plante permettant ainsi d'accomplir leur cycle de vie (Smith & Gianinazzi-Pearson, 1988). En parallèle, la plante hôte bénéficie d'une meilleure nutrition minérale vis-à-vis de divers éléments y compris des éléments traces engendrant ainsi le plus souvent un gain en biomasse (Smith & Gianinazzi-Pearson, 1988) et une meilleure résistance aux stress biotiques et abiotiques (Pozo & Azcon-Aguilar, 2007). Avant tout contact physique, chaque partenaire décèle la présence de l'autre par l'intermédiaire de signaux moléculaires diffusibles qui contribuent aux mécanismes de reconnaissance entre les deux partenaires (Giovannetti *et al.*, 1993). L'hôte végétal exsude par ses racines de multiples molécules capables de stimuler la germination des spores et/ou la prolifération cellulaire des champignons MA (Buee *et al.*, 2000; Sbrana & Giovannetti, 2005). Découvertes plus récemment (Akiyama *et al.*, 2005; Besserer *et al.*, 2006), les strigolactones sont des apocaroténoïdes à très forte activité biologique capables d'activer en quelques minutes, et à des concentrations inférieures au nano-molaire, le métabolisme mitochondrial du partenaire fongique (Besserer *et al.*, 2006;

Besserer *et al.*, 2008; Besserer *et al.*, 2009). En échange, les champignons MA produisent des signaux diffusibles capables de modifier l'expression des gènes de la plante et de provoquer des réponses racinaires comme des variations calciques cytosoliques ou la production de racines latérales (Weidmann *et al.*, 2004; Kosuta *et al.*, 2008; Kuhn *et al.*, 2010). La mise en place de la SMA requiert une coordination fine des programmes cellulaires du champignon et de la plante. Ainsi, la colonisation de la racine par l'hyphe du champignon s'effectue selon un enchaînement de séquences définies que l'on peut brièvement résumer comme suit: après la germination des spores et la formation d'hyphes, ces derniers interagissent avec la paroi de la racine et forment une structure particulière nommée « hyphopodium », le champignon va coloniser le cortex de la racine en développant des hyphes entre les cellules. Ces hyphes vont croître dans le cortex et se différencier dans les cellules du parenchyme cortical en une structure d'échange privilégiée connue sous le nom d'arbuscule, lieu privilégié d'échange de nutriments entre les deux partenaires. Finalement, le champignon développe un réseau d'hyphes extra-radiculaires en même temps qu'il forme des vésicules ou des cellules auxiliaires et de nouvelles spores représentant des éléments de réserve (Bonfante & Genre, 2008). Durant les 4 à 5 premières heures qui suivent la formation de l'hyphopodium, une structure subcellulaire appelée « PrePenetration Apparatus » (PPA) se forme (Genre *et al.*, 2005). La membrane cytoplasmique de la cellule épidermique s'invagine créant ainsi un tube dont l'orientation est prédéfinie par le noyau (Genre *et al.*, 2005). Le cytosquelette, le réticulum endoplasmique et l'appareil de Golgi interviennent activement dans la formation de ce tunnel. Puis le champignon va progresser par des hyphes intercellulaires en direction de la zone corticale de la racine où il va pénétrer et se ramifier par croissance dichotomique afin de former la structure typique de cette symbiose *i.e.* l'arbuscule. Les arbuscules se développent dans un compartiment résultant de l'invagination de la membrane hôte appelée membrane périarbusculaire (Parniske, 2000). La surface de la membrane plasmique végétale va plus ou moins quadrupler pour former la membrane périarbusculaire. Lors de la formation de l'arbuscule, un certain nombre de modifications des membranes et paroi intervient pour faciliter les échanges entre le champignon et la plante hôte (Harrison 1999). En outre, la mise en place de ces structures en forme de petit arbre (Parniske, 2008) s'accompagne de profonds réarrangements dans les cellules corticales de la plante hôte incluant des mouvements du noyau, la multiplication et réorganisation de

nombreux organites dans les cellules colonisées et l'augmentation de la surface des membranes plasmique et tonoplastique. L'ensemble de ces remaniements suppose donc que divers types de membranes jouent un rôle crucial dans la mise en place et le fonctionnement de la SMA à la fois chez le micro-symbiote et l'hôte végétal. Des études ont permis l'identification de quelques transporteurs localisés dans les zones de colonisation comme les transporteurs de phosphate MtPT4 et de sucrose MtSuc1 chez *M. truncatula* (Javot et al., 2007; Baier et al., 2010), deux transporteurs ABC (Zhang *et al.*, 2010) et la « blue copper binding protein » (Valot *et al.*, 2006; Pumplin & Harrison, 2009). D'autres travaux effectués sur les protéines membranaires ont révélé aussi la régulation d'une vingtaine de protéines en réponse à la symbiose (Valot *et al.*, 2005; Valot *et al.*, 2006). En dépit des connaissances récemment acquises sur les rôles des protéines dans l'établissement et le fonctionnement de cette symbiose, de nombreuses questions sont encore à résoudre concernant les protéines membranaires et ce d'autant plus que l'étude à grande échelle de cette catégorie de protéines se heurte à des difficultés méthodologiques. Si l'électrophorèse bidimensionnelle (2-DE) reste la méthode la plus couramment utilisée pour des analyses protéomiques quantitatives, elle résout difficilement les protéines membranaires en raison de leur hydrophobicité, leur faible dissolution dans le tampon d'isofocalisation utilisé, leur précipitation au point isoélectrique (pI) et leur faible abondance comparativement aux protéines cytosoliques (Ephritikhine *et al.*, 2004; Haynes & Roberts, 2007). Afin d'avoir accès à cette catégorie de protéines, un recours aux méthodes de protéomique de type « shotgun » s'avère indispensable. En effet, l'utilisation de cette stratégie de protéomique est reconnue pour augmenter le nombre d'identifications des protéines hydrophobes et peu abondantes (Haynes & Roberts, 2007) pouvant ainsi donner accès aux protéines membranaires intrinsèques. Le développement de nouvelles méthodes permet désormais de réaliser des analyses quantitatives sans (label-free) ou avec marquage chimique (ICAT, iTRAQ, SILAC, etc..).

Les objectifs de cette thèse sont de mettre en œuvre des méthodes d'analyse protéomique améliorant la couverture et la quantification des protéines membranaires de plantes. Une introduction sous forme de deux articles de revue permet d'un part de dresser un état des lieux des connaissances actuelles des protéines reliées à la SMA **(publication n° 1, soumise)** et d'autre part des méthodologies envisageables pour la quantification des protéines par spectrométrie de masse (SM) **(publication n°2,**

soumise). La SMA a été choisie comme modèle d'étude en raison des importants remaniements membranaires qui caractérisent cette interaction, particulièrement dans le couple *Medicago truncatula* - *Rhizophagus irregularis*. *M. truncatula* est reconnue comme l'une des plantes modèles pour les recherches sur les légumineuses grâce à son petit génome et la disponibilité de nombreux mutants, sa forte synthénie avec la plupart des légumineuses cultivées et la facilité de sa culture et transformation. En outre, *Arabidopsis thaliana* ne pouvant pas établir de symbiose mycorhizienne, *M. truncatula* a été choisie comme plante hôte mycotrophe de choix pour le décryptage des événements moléculaires gouvernant les interactions symbiotiques avec les bactéries fixatrices d'azote et/ou la SMA (Henckel *et al.*, 2009).

L'accès aux protéines membranaires reste très limité par la seule utilisation d'une approche globale. Dans ce contexte, deux méthodes de protéomique subcellulaires sont adoptées dans ce travail visant à caractériser les protéines microsomales des racines de *M. truncatula* et ceci, afin d'élucider leur rôle fonctionnel dans la SMA. Ces travaux de recherche s'articulent en trois parties : la première approche méthodologique a consisté à mettre en œuvre un protocole de digestion des protéines microsomales en solution et étudier l'impact du marquage iTRAQ (isobaric tags for relative and absolute quantification) sur le pI des peptides **(publication n° 3, sous presse).** La seconde partie est consacrée à l'utilisation d'une technologie innovante de fractionnement des peptides en solution (OFFGEL) compatible avec le marquage isotopique iTRAQ pour comparer l'abondance des protéines microsomales entre racines témoins et mycorhizées **(publication n° 4, soumise)**. Enfin, dans une dernière partie, nous avons eu recours à la méthode dénommée « label-free » 1-DE-CL-SM/SM, qui n'est pas basée sur un marquage chimique et permet d'accéder à la quantification relative des protéines **(publication n° 5, soumise).**

Quelle que soit la technique protéomique appliquée, la qualité de l'échantillon de départ est une étape cruciale pour la suite de l'analyse. Dans cet objectif, nous avons utilisé une méthode d'enrichissement en microsomes adaptée de celle décrite par Stanislas *et al.* (2009). L'atout majeur de ce protocole est l'utilisation d'un broyeur électrique qui permet l'obtention d'un broyat homogène et l'accès à des

fractions radiculaires enrichies en microsomes à partir des racines mycorhizées ou non par le champignon *R. irregularis* nécessaires pour les analyses ultérieures.

Dans un premier temps, les protéines microsomales ont été analysées par la méthode iTRAQ-OFFGEL-CL-SM/SM. Le marquage iTRAQ a été décrit pour la première fois par Ross *et al.* (2004) et permet la comparaison simultanée de 4 à 8 conditions. Il repose sur le marquage des amines primaires en position N-terminale des peptides et en chaîne latérale de la lysine. Les différents échantillons protéiques sont digérés en solution, marqués avec un tag iTRAQ particulier, mélangés, fractionnés et puis analysés en spectrométrie de masse (SM). Les tags étant isobariques, les différents peptides marqués apparaissent lors du scan SM sous la forme d'un seul et même pic. En SM/SM, les différents échantillons sont distingués par la libération des groupements rapporteurs de *m/z* 114 à 121. L'intensité de ces ions est proportionnelle à la quantité relative du peptide dans chacune des conditions auxquelles ils se rapportent. Le reste du spectre SM/SM est classique et permet de visualiser les différents fragments du peptide et donc de l'identifier. Les étapes d'identification et de quantification sont réalisées simultanément durant l'analyse SM/SM. La fenêtre de *m/z* 114 à 121 a été choisie car aucun fragment ou ion immonium pouvant fausser la quantification ne se situe dans cette zone. Récemment, la technologie OFFGEL a émergé comme étant d'un grand intérêt en protéomique (Fraterman *et al.*, 2007). Cette technique permet la séparation des peptides en fonction de leur pI en milieu liquide. La séparation se déroule sur une bandelette de gel (bandelette ou « strip » de 12 ou 24 cm), contenant un gradient de pH immobilisé, sur lequel se trouve 12 ou 24 cupules formant des fractions tout au long de la bandelette. L'échantillon peptidique, dilué dans un tampon contenant des ampholytes et du glycérol, est réparti dans chacune des fractions. L'application d'un courant induit la migration des peptides, la bandelette servant de « pont » reliant les différentes fractions les unes aux autres. A la fin de l'IEF, chaque fraction liquide contient l'ensemble des peptides ayant un pI correspondant à la gamme de pH de la fraction. L'avantage majeur de cette approche, outre le préfractionnement de l'échantillon, est de pouvoir déterminer le pI des peptides et de l'utiliser comme un filtre supplémentaire pour valider les identifications en SM.

Nos premiers objectifs méthodologiques sont la vérification de l'efficacité de l'isofocalisation des peptides en OFFGEL, la compatibilité de ce système avec l'iTRAQ et l'effet de ce dernier sur le pI des peptides. Dans cette stratégie, la digestion protéique doit être réalisée en solution avant le marquage des digestats aux iTRAQ. La digestion des protéines en gel génère des extraits peptidiques dépourvus de sels et de détergents, lesquels sont préjudiciables à l'analyse subséquente en SM. En revanche, celle réalisée en solution nécessite des étapes de dessalage et de nettoyage d'échantillons avant de les analyser en SM, en regard des différents réactifs ajoutés au cours de la réduction et alkylation des protéines avant leur digestion à la trypsine. Ces détergents, même en faible concentration, peuvent inhiber la digestion enzymatique et dominer les spectres à cause de leur ionisation facile (Arnaud *et al.*, 2005). Un protocole modifié de la méthode FASP (« filter aided sample preparation ») de Wiśniewski *et al.*, (2009) est décrit, dans cette partie du travail, pour la digestion des protéines en solution. Il s'agit de réaliser les différentes étapes de réduction et alkylation des protéines ainsi que la digestion trypsique dans des tubes à filtre. Le filtre joue un rôle clé de « réacteur protéomique » qui retient les molécules de haut poids moléculaire (protéines) et permet le passage de ceux de faible poids moléculaire (impuretés et peptides) (Wisniewski *et al.*, 2009). Les résultats en SM ont prouvé l'efficacité de cette méthode à éliminer les interférents et assurer le marquage des peptides. Ensuite, la qualité du fractionnement des peptides par OFFGEL a été analysée. Celle-ci est évaluée en étudiant la répartition d'un peptide unique dans des fractions OFFGEL successives. Les résultats ont révélé que 70% des peptides, marqués ou non à l'iTRAQ, sont enrichis dans une fraction unique d'OFFGEL et qu'environ 90% d'entre eux sont présents dans au maximum 2 fractions successives. L'OFFGEL présente donc une bonne qualité de séparation des peptides et ces résultats confirment que le marquage iTRAQ ne perturbe pas la qualité de la focalisation. En outre, un nombre plus élevé de peptides marqués a été identifié dans les fractions au pH basique comparé à leurs homologues non marqués et un effet de marquage sur le pI des peptides est remarqué. En effet, l'ion rapporteur de l'iTRAQ est une pipérazine qui possède deux fonctions amines tertiaires. Lorsque ce groupe vient se lier au N-terminal du peptide et à la chaîne latérale d'une lysine, un remplacement d'une amine primaire par deux autres tertiaires est réalisé ce qui pourrait augmenter la basicité des peptides. Ainsi, il semble que ce marquage induit une modification des pIs des peptides ce qui s'est traduit par un déplacement (« shift ») surtout vers les zones les

plus basiques. Les outils actuellement disponibles pour le calcul des pIs ne prennent pas en considération l'addition d'un réactif iTRAQ sur les N-terminaux des peptides, ainsi leur pI après le marquage ne peut pas être calculé. Afin de mieux comprendre et expliquer cet effet, un autre outil a été employé dans cette étude, disponible en accès libre (http://www.chemaxon.com/marvin/sketch), qui permet de dessiner les structures des peptides (acides aminés et molécules ajoutés aux peptides) et d'ensuite calculer le pI avant et après le marquage. Effectivement, cet outil a conduit à une meilleure interprétation de nos résultats tout en confirmant un changement de pI des peptides à la suite de leur marquage.

Le marquage iTRAQ se présente comme un puissant outil en protéomique quantitative permettant d'étudier l'expression différentielle des protéines entre plusieurs échantillons et de faire des comparaisons intra-échantillons en améliorant la reproductibilité qui fait souvent défaut aux techniques classiques d'électrophorèse. L'intérêt de ce marquage est sa capacité, grâce à la somme des signaux en SM, d'augmenter la sensibilité de détection en favorisant l'identification et la quantification des protéines peu abondantes et récalcitrantes, faisant de cette technique une méthode de choix pour l'étude des protéines membranaires. Malgré son utilisation accrue en protéomique quantitative, uniquement quelques spectromètres de masse sont capables d'analyser des peptides marqués aux iTRAQ. Ceci est dû à la limitation de la méthode de fragmentation en CID (collision induced dissociation) qui génère des spectres non informatifs aux bas poids moléculaires induisant une perte de la zone qui contient les ions rapporteurs de l'iTRAQ. Afin de contourner ce défaut, une complémentarité de méthodes de fragmentation tel que le couple CID-HCD (high collision dissociation) a été proposée et s'est révélée être une méthode de choix pour les analyses des échantillons marqués aux iTRAQ.

Dans une deuxième partie du travail, une démarche choisie pour l'étude différentielle des protéines microsomales en réponse à la SMA a été réalisée en utilisant l'approche iTRAQ-OFFGEL-CL-SM/SM. Tout d'abord, un protocole d'enrichissement en protéines microsomales, indispensable pour une étude plus approfondie du protéome membranaire, a été utilisé. La vérification de l'enrichissement par analyse protéomique a permis de révéler que moins de 12% des protéines identifiées ont été classées comme protéines potentiellement non membranaires ce qui représente une pureté d'enrichissement suffisamment élevée

pour la suite de l'analyse. Ce résultat rend robuste le choix du protocole d'extraction des microsomes employé et met en évidence son rendement qualitatif. Dans cette analyse, le spectromètre de masse Orbitrap Elite Velos est utilisé, c'est un appareil hybride de haute résolution capable de combiner différents types de fragmentation. Ainsi, les ions parents (ou précurseurs) sont sélectionnés pour être analysés dans deux cellules de collision différentes et les ions issus de ces fragmentations sont ensuite utilisés ensemble pour la recherche dans les bases de données. Le spectre CID permet l'identification de la séquence peptidique, l'abondance étant quant à elle obtenue grâce au spectre HCD. Ce dernier permet notamment une fragmentation à plus haute énergie que le mode CID sans perte de fragments et contient la signature des ions iTRAQ à *m/z* 114-121 rendant possible le calcul du rapport des ions rapporteurs. Malgré un nombre élevé de spectres, 151 protéines ont été identifiées avec succès dans l'ensemble des échantillons provenant des fractions enrichies en microsomes des extraits de racines témoins et mycorhizés. Ce nombre limité d'identification protéique a été associée à l'inconvénient majeur du fractionnement en tandem (OFFGEL-CL) qui augmente les risques de pertes durant la préparation de l'échantillon. En outre, le marquage iTRAQ se fait relativement tard dans le procédé de préparation de l'échantillon, après la digestion à la trypsine, ce qui pourrait aussi augmenter les différents biais expérimentaux. Quant aux résultats de quantification, ils se sont avérés peu reproductibles. En effet, l'intensité de l'ion rapporteur à *m/z* 117 était majoritairement plus forte que celle de l'ion à *m/z* 114 induisant des biais dans les résultats de quantification et diminuant la confiance dans leur validité. Le même effet était obtenu en analysant ces échantillons au MALDI-TOF/TOF. Malgré sa popularité accrue, plusieurs désavantages ont été liés au marquage iTRAQ, parmi lesquels la distorsion des calculs de ratios des ions rapporteurs causant un vrai problème de crédibilité envers les résultats de quantification. Afin de pallier à ces inconvénients, l'utilisation de la méthode de fragmentation hybride CID-HCD et la décomplexification des échantillons par fractionnement ont été conseillées. Dans notre étude, les deux recommandations ont été prises en compte, puisque les peptides ont été, dans une première dimension, fractionnés selon leur pI en OFFGEL suivi de leur séparation en CL. Les analyses en SM ont été ensuite réalisées en appliquant la méthode de fragmentation hybride et ceci n'a pas permis de réduire les biais liés à la quantification des protéines. Une co-sélection de contaminants dans la même fenêtre de l'ion parent en SM pourrait être à l'origine de ce manque de fiabilité dans la

mesure de l'intensité des ions rapporteurs en SM/SM. Christoforou et Lilley (2012) ont montré que 90% des spectres des peptides non marqués, censés être incapables de produire des ions rapporteurs, contiennent au moins 2 de ces 8 ions d'iTRAQ (Christoforou & Lilley, 2012). Donc cette distorsion imprédictible, due à l'omniprésence des contaminants, pourrait être limitée en réduisant la largeur de la fenêtre de sélection de l'ion parent. En outre, l'addition d'un standard interne dans l'échantillon à analyser permettrait d'évaluer le degré de l'erreur observée. Ainsi l'ajout d'une quantité connue d'un peptide protéotypique particulier à un digestat complexe peut servir d'un standard interne et d'outil de validation de la précision de la quantification. Il est aussi indispensable de souligner l'importance de réaliser des expériences pilotes afin de choisir la technique protéomique la plus appropriée à l'analyse d'un type d'échantillon.

L'approche iTRAQ s'est avérée peu adéquate à l'analyse du protéome membranaire en réponse à la SMA d'où la nécessité de trouver une méthode alternative. Au vu du coût élevé et de la relative difficulté expérimentale du marquage isotopique, différentes alternatives de quantification sans marquage ont été proposées. Dans ces méthodologies les échantillons à comparer sont analysés les uns après les autres dans les mêmes conditions expérimentales pour favoriser la reproductibilité. En effet, il existe un très large panel de techniques pour identification, caractérisation et quantification des protéines en SM. L'avantage clé de ces techniques dites « label-free » réside dans leur capacité à réaliser la quantification des protéines sans marquage ou modification préalable des échantillons. Deux types de méthodes sans marquage sont distingués : l'une basée sur le dénombrement des spectres et l'autre reposant sur le calcul de l'aire sous le pic d'un peptide. La première méthode est simple et semi-quantitative et consiste à décompter les spectres SM/SM acquis pour chaque protéine. Le nombre de peptides identifiant une protéine augmente avec l'abondance de la protéine : plus une protéine est abondante, plus les signaux de ses peptides seront élevés. Un index d'abondance (PAI) est ensuite calculé, il dépend du nombre de peptides, de la qualité et de l'exactitude des identifications. Le PAI est calculé en normalisant le nombre de peptides observés par le nombre de peptides théoriquement observables pour la protéine d'intérêt. La deuxième méthode de quantification, plus fiable et précise, repose sur le calcul de l'intensité du signal du pic chromatographique. La haute précision des spectromètres de masse et la

reproductibilité de la CL sont des facteurs critiques pour le succès de cette approche et la limitation des variabilités.

Dans une 3ème partie du travail, nous avons adopté la méthode « label-free » 1-DE-CL-SM/SM pour pouvoir discriminer les protéines différentiellement exprimées entre les échantillons témoins et mycorhizés **(publication N° 5).** La puissance de cette méthodologie est l'assurance de la solubilité des protéines en SDS-PAGE. Le SDS est un agent anionique qui se fixe sur les protéines, en formant un complexe anionique ayant une charge nette négative, et permet une meilleure solubilisation des protéines. Les protéines sont ensuite séparées selon leur poids moléculaire sur gel pour préfractionner les échantillons complexes avant leur analyse en SM. La digestion protéique en gel donne accès à des fractions peptidiques dépourvues de substances interférentes avec les analyses ultérieures. Néanmoins, le pouvoir de cette séparation reste relativement faible vu la présence de nombreuses protéines par bande de gel. Afin de s'affranchir de cette limitation, cette technique est couplée avec un système de CL. Dans cette stratégie, deux étapes de séparations sont donc réalisées, une au niveau protéique et une autre au niveau peptidique. Le principal avantage de cette approche est son aptitude à analyser les protéines basiques et hydrophobes, son principal champ d'application est donc bien l'analyse des protéomes membranaires. L'enrichissement des fractions radiculaires en protéines microsomales a été en premier lieu évalué par des analyses en Western Blot en utilisant l'anticorps, marqueur du cytosol, anti-UDP-glucose pyrophosphorylase (UGPase). L'intensité du signal correspondant à la bande spécifique de cet anticorps à 51 kDa a été fortement diminuée dans les fractions microsomales des racines témoins et mycorhizées, reflétant un appauvrissement de ces 2 fractions en protéines cytosoliques. La quantification des protéines est réalisée en utilisant un logiciel MassChroQ développé dans la plateforme de PAPPSO (http://pappso.inra.fr/). Cette approche a permis l'identification de 1047 protéines de racines de *M. truncatula* témoins et mycorhizées. Parmi celles-ci uniquement 164 protéines sont potentiellement des protéines solubles, contaminantes de la fraction microsomale. Ceci permet d'estimer l'enrichissement en protéines membranaires à 84.3%, un résultat qui devance les essais préalablement effectués sur le protéome membranaire du maïs et de *M. truncatula*. La majorité de ces protéines est localisée dans le chloroplaste, le noyau et la membrane plasmique et est impliquée dans le transport membranaire, la synthèse protéique et le métabolisme

primaire. L'abondance de 19 protéines diminue significativement dans les racines mycorhizées alors que celle de 22 protéines augmente dans les racines mycorhizées. La protéine associée à la membrane plasmique « Mtha1 » s'est révélée spécifiquement exprimée en réponse à la SMA. Uniquement une protéine est induite et une autre réprimée en réponse à la SMA. Ces résultats ont mis en avant la présence d'un répertoire de protéines membranaires conservé entre les racines de *M. truncatula* témoins et mycorhizées. Parmi les protéines surexprimées dans les racines mycorhizées, l'expression de la « blue copper protein, MtBcp1 » a 10 fois augmenté en réponse à la symbiose. Cette protéine a été préalablement prouvée pour être induite en réponse à la symbiose et localisée dans les zones de colonisation du champignon MA. En outre, la SMA est connue pour induire de profondes réorganisations du cytosquelette d'où l'accumulation dans les racines mycorhizées de « actin-like proteins », et des protéines impliquées dans la synthèse et le devenir protéique comme des histones, des protéines ribosomales et des « cyclophilins ». Ceci est corrélé à l'activation de la machine nucléaire, reflétant une plus forte activité transcriptionnelle de la plante dans le génome des cellules colonisées par rapport aux cellules non-colonisées. Dans cette analyse comparative, les quantités de 3 isoformes de transporteurs de phosphate « plasma membrane-located phosphate transporters, MtPT1, MtPT2 and MtPT3 » diminuent dans les racines mycorhizées. Les plantes mycorhizées possèdent deux voies d'assimilation du phosphate, une voie d'assimilation directe « interface sol/plante » et une voie indirecte à travers le réseau mycélien du champignon MA «sol/MA/plante ». Chez certaines espèces de plantes, la voie directe d'assimilation de phosphate est inactivée par la plante alors que 100% du phosphate est transféré à la plante *via* les hyphes fongiques des champignons. Dans le même contexte de besoins en phosphate satisfaits par la SMA, la sous expression de « vacuolar H^+PPiase », « UDP-glucose pyrophosphorylase », « protein proteases », « PDR (pleiotropic drug resistant)-like ABC transporter », et « protein phosphatase 2C » a été observée dans les racines mycorhizées de *M. truncatula*. Les résultats obtenus ont permis l'identification des protéines membanaires qui sont directement ou indirectement impliquées dans les voies de signalisation et transduction de signaux nécessaires entre les deux partenaires.

En se développant, la symbiose mycorhizienne à arbuscules induit un ensemble de modifications morphologiques et physiologiques au niveau des racines de la plante hôte. Ce processus de colonisation se caractérise par un réarrangement

des parois et des membranes plasmiques végétales facilitant les échanges entre les deux symbiotes. Notre étude a consisté à développer des approches de protéomique « shotgun » pour l'analyse des protéines microsomales préalablement enrichies en fractions membranaires par centrifugation différentielle. Parallèlement, deux stratégies d'analyse protéomique susceptibles de contourner les biais induits par l'électrophorèse bi-dimensionnelle à l'encontre des protéines membranaires ont été testées et validées afin d'analyser la composition protéique des fractions microsomales obtenues. Tout d'abord, d'un point de vue méthodologique nos travaux ont permis de mettre en œuvre un protocole de digestion des protéines membranaires en solution donnant accès à des fractions peptidiques dépourvues de substances interférentes. Ensuite, un effet du marquage iTRAQ sur le pI des peptides marqués a été pour la première fois démontré. Quant à l'analyse quantitative utilisant l'iTRAQ, elle s'est avérée moins adéquate pour nos échantillons que l'analyse protéomique en « label-free » 1-DE-CL-SM/SM, qui a permis de révéler l'identité de nouvelles protéines membranaires impliquées dans le processus de colonisation.

Les résultats de ce travail de thèse sont discutés dans le chapitre 5 de la conclusion et les perspectives qui découlent de nos recherches sont également présentées. Les différentes méthodes sont regroupées en annexe et la thèse est close par les références bibliographiques.

Introduction

The introduction encompasses two chapters. While the first one presents the state of art of the arbuscular mycorrhizal symbiosis (article n°1), the second one reviews gel- and mass spectrometry- based quantitative proteomic approaches that are available to date (article n°2).

Chapter 1.1

Proteins sustaining arbuscular mycorrhizal symbiosis: falling silent for function reveals a new generation of underground-working desperate housewives

Ghislaine Recorbet[1], Cosette Abdallah[1,2], Jenny Renaut[2], Daniel Wipf[1] and Eliane Dumas-Gaudot[1]

[1]*UMR Agroécologie INRA 1347/Agrosup/Université de Bourgogne, Pôle Interactions Plantes Microorganismes ERL 6300 CNRS, BP 86510, 21065 Dijon Cedex, France.*

[2]*Département Environnement et Agro-Biotechnologies, Centre de Recherche Public- Gabriel Lippmann, 41, rue du Brill, L-4422, Belvaux, Luxembourg.*

Recorbet *et al.*, 2012 Proteins sustaining arbuscular mycorrhizal symbiosis: falling silent for function reveals a new generation of underground-working desperate housewives. *New Phytologist* (submitted)

Summary

The roots of most land plants can enter a symbiotic relationship with soil-borne fungi belonging to the phylum *Glomeromycota*, whereby helping the host to cope with nutrient-limited and adverse environments. This symbiosis with arbuscular mycorrhizal (AM) fungi belongs to the so-called biotrophic plant–microbe interactions involving the intracellular accommodation of a microorganism by a living plant cell without causing the death of the host. The mechanisms by which this is achieved remain largely unknown but proteins happen to take the lion's share in the paradigms that currently govern biotrophy by playing key roles in mediating signalling, nutrient transport and plant cell differentiation. Although profiling technologies performed during the last decade have generated an increasing depository of plant and fungal proteins eligible as actors of the AM symbiotic program, a bottleneck actually exists for their functional analysis as these experiments turn-out to be time-consuming and difficult to carry out with AM fungi by reason of their obligatory biotrophy together with the absence of sequenced genomes for Glomeromycetes. Nonetheless, in recent years, the expansion of legume genome data banks coupled to gene-to phenotype reverse genetic tools such as RNAi, have been proved very efficient in elucidating some of the plant-related protein candidates sustaining AM symbiosis. Likewise, despite the recurrent absence of transformation tools for AM fungi, host-induced gene silencing succeeded for the first time in knocking-down fungal gene expression *in planta*, thus unlocking a technological limitation in deciphering the functional pertinence of glomeromycotan gene products in mycorrhizal establishment. This review is thus intended to draw a picture of our current knowledge in the plant and fungal protein actors that have been demonstrated as functionally implicated in sustaining AM symbiosis.

I. Casting

The intracellular accommodation of a microorganism by a living plant cell, which is referred to as a biotrophic association, can either lead to plant beneficial or detrimental effects, so that these interactions play major roles in agriculture (Parniske, 2000; O'Connell & Panstruga, 2006; Paszkowski, 2006; Gianinazzi *et al.*, 2010). The distinction between parasitic and beneficial biotrophs has its origin in the availability of nutrients to the microorganism. Typically, most parasitic biotrophs responsible for devastating plant pathologies like mildews, rusts, and smuts derive nutrients from shoot tissue without having any alternative energy source (Schulze-Lefert & Panstruga, 2003). By contrast, most beneficial biotrophic microorganisms like mycorrhizal fungi and nitrogen-fixing rhizobia colonize root tissues and have access to nutrients outside the plant, raising the possibility for bi-directional nutrient movement and the development of a mutualist rather than a parasitic interaction (Smith & Smith, 1990). In arbuscular mycorrhiza (AM), the symbiosis that most terrestrial plant roots engage with soil-borne fungi of the phylum *Glomeromycota*, AM fungal extra-radical hyphae absorb from the soil water and mineral nutrients, mainly phosphorus and nitrogen, which are supplied to the host plant in exchange for sugars generated by photosynthesis (Parniske, 2008). Actually, in contrast to plants that can survive in the absence of symbiotic fungi, AM symbionts are categorized within obligate biotrophs in that they strictly depend on carbohydrates from their hosts for growth and reproduction (Bonfante & Genre, 2010). Although leading to different outcomes, mutualistic and parasitic biotrophs share the ability to penetrate the plant cell through the differentiation of specialized intracellular accommodation structures corresponding to haustoria in most pathogenic interactions, haustoria termed arbuscules in the AM symbiosis, or bacteroids in the rhizobial nitrogen-fixing (RNF) symbiosis (Parniske, 2000). Because these structures are always surrounded by a host-derived plant plasma membrane, microbial biotrophs remain separated from the host cytoplasm. A resulting common feature of plant-biotroph associations corresponds to the existence of an interface, thought to be the main site of nutrient and signal flow between cells, which comprises the plant and the microbial membranes separated by a plant-derived apoplast (Smith & Smith, 1990; Harrison, 1999; Parniske, 2000; Perfect & Green, 2001). For a successful interaction, biotrophs have to either avoid or suppress plant defence reactions together with redirecting the host

metabolic flow to their benefit without killing the host. The mechanisms by which this is achieved remain largely unknown but proteins happen to take the lion's share in the paradigms that currently govern this kind of plant-microbe interactions by playing key roles in mediating recognition, signalling, nutrient transport, plant cell differentiation and compatibility (Panstruga, 2003; Schulze-Lefert & Panstruga, 2003; Schmidt & Panstruga, 2011). Although a vast majority of the crop plants used to feed human population form the AM symbiosis, which contributes to an overall improvement of plant fitness as reflected by an increased plant biomass and a better protection of host plants against biotic and abiotic stresses (Smith & Read, 2008; Gianinazzi *et al.*, 2010), the elucidation of key protein actors governing this mutualistic plant-fungus interaction is far from being as developed as that involved in other biotrophic systems (Schmidt & Panstruga, 2011), mainly by reason of typical developmental and genetic traits.

Noteworthy, unlike several pathogens with a complete (*Cladosporium fulvum*, *Ustilago maydis*) or hemi-biotrophic (*Magnaporthe*, *Colletotrichum spp*.) lifestyle, AM fungi so far have escaped cultivability in the absence of a host plant. A more drastic feature limiting functional analyses in AM symbiosis relates to the fact that *Glomeromycota*, for which no sexual cycle is known, are unique in that their spores and coenocytic hyphae contain multiple nuclei in a common cytoplasm, making classical Mendelian genetic approaches unsuitable and transformation attempts so far unsuccessful in generating permanent transgenic expression (Bonfante & Genre, 2010). Additionally, knowledge of fungal genetics is essentially based on Ascomycota and Basidiomycota, two phyla highly divergent from glomeromycotan fungi, preventing comparative studies to be confidently achieved reviewed in Sanders & Croll (2010). Finally, the genomes of AMF are not assembled yet, and consequently comprehensive predictions for putative actors sustaining symbiosis yet cannot be performed (Martin *et al.*, 2008). As a result, AM fungi have not yet entered the post-genomics area that many biotrophic pathogens are facing now (Schmidt & Panstruga, 2011). Nevertheless, besides approaches aiming at targeting fungal proteins eligible as being involved in nutrient uptake and assimilation, including phosphate and nitrogen compounds (Harrison & van Buuren, 1995; Lopez-Pedrosa *et al.*, 2006; Cappellazzo *et al.*, 2008), the recent application to AM symbionts of high throughput technologies including proteomics and transcriptomics have pointed out candidate symbiosis-

related traits in the model AM fungus *Rhizophagus irregularis (formerly Glomus intraradices*) (Recorbet *et al.*, 2009; Tisserant *et al.*, 2012). Noticeably, in the first genome-wide inventory of gene expression in *R. irregularis* using sequencing of cDNA libraries from germinated spores, extra and intra-mycelium, off the 18751 coding sequences detected by oligoarrays, more than 5% were found regulated in intra-radial mycelium (IRM) relative to germinated spores, among which genes involved in nitrogen, phosphate and lipid metabolism, displayed a higher expression (Tisserant *et al.*, 2012). With regard to the conserved accommodation program displayed by mycotrophic host plants toward AM fungi, whereas depicted as a chronological series of events including the pre-symbiotic phase, contact and fungal entrance, intra-radical fungal proliferation, and cell invagination and nutrient transfer (Figure 1.1), establishment of the AM symbiosis in the whole root is highly asynchronous with all developmental stages being present simultaneously, thus making difficult a specific targeting of symbiosis-related structures and processes after plant penetration (Paszkowski, 2006). Consequently, although plant mutants are key tools for the genetic dissection of mycorrhizal development, the most frequently described phenotypes so far consist of hosts compromised for root penetration events and fungal growth arrest at the plant-fungus contact stage (Marsh & Schultze, 2001; Parniske, 2008). The use of model legumes has paved the way for isolating corresponding genes from loss-of-function mutant backgrounds and defining the common SYM pathway that mediates signalling processes essential for both RNF and AM symbioses, and comprises a plasma membrane-located leucine-rich repeat receptor-like kinase (DMI2 in *Medicago truncatula* and SYMRK in *Lotus japonicus*), several components in the nuclear envelope among which two cation-ion channels required for Ca^{2+} spiking (*M. truncatula* DMI1a, DMI1b and *L. japonicus* CASTOR and POLLUX), subunits of nuclear pores (*L. japonicus* NUP85, NUP133 and NENA), and a nuclear localized calcium calmodulin-dependent kinase (CCaMK) (*M. truncatula* DMI3 and *L. japonicus* CCaMK) that acts in cooperation with the nuclear porin MtIPD3/LjCYCLOPS as decoder of Ca^{2+} spiking reviewed in (Groth *et al.*, 2010; Kouchi *et al.*, 2010).

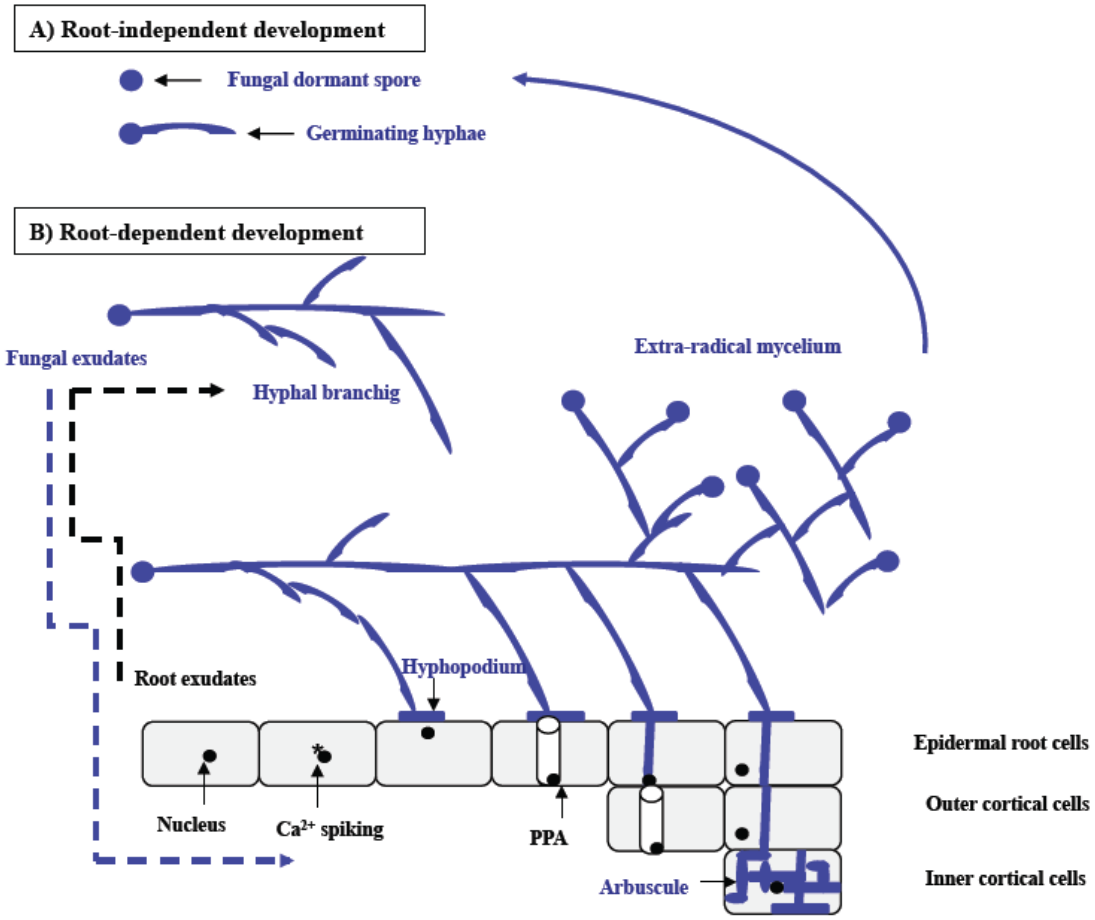

Figure 1.1: Schematic overview of the life cycle of an AM fungus
It is adapted from (Bonfante & Genre, 2010)). **A)** Hyphae germination at the expense of spore storage lipids.
B) In the vicinity of a host plant, root exudates trigger hyphal branching and concomitantly, the fungal exudates perceived by the host lead to calcium spiking through the activation of the common SYM pathway, which generates a reprogramming of the elicited and adjacent root cells in order to accommodate the fungus. Following contact between the two partners, the AM symbiont differentiates a root-adhering hyphal structure, the hyphopodium that triggers the formation of the prepenetration apparatus (PPA) in the contacted and underlying outer cortical cells. The PPA guides the fungal development from epidermal to inner cortical cells where a highly branched fungal structure, the arbuscule, can differentiate to form an extensive surface area for nutrient exchange. Concomitantly, the AM fungus develops an extra-radical mycelium to explore the soil for resources and new hosts. Blue and dark colours refer to fungal and plant structures or metabolites, respectively.

The early signalling cascade shared by both AM and RNF symbioses is not only essential for successful infection events but it also required to activate a feedback phenomenon referred to as autoregulation (AUT) of mutualism. As very comprehensively reviewed in Hause & Schaarschmidt (2009), host plants indeed are able to control the degree of their associations with rhizobia and AM fungi in order to

minimize the carbon resources they invest in symbiosis. Once first steps of interactions are initiated, further establishment of symbionts above a critical threshold level is restricted, leading to AUT. On the basis of loss-of-AUT mutants that display a supernodulating and supermycorrhizal phenotype (increased abundance of nodules and arbuscules, respectively), the key actor mediating AUT was identified as a CLAVATA1-like leucine-rich repeat receptor-like kinase acting in the shoot. Upon perception of a long distance-transported signal generated in the roots, activation of the AUT receptor kinase leads to the production of a shoot-derived inhibitor that upon its transports down to the roots, negatively affects the early signalling cascade by interfering with DMI3/CCaMK, thus inhibiting subsequent AM and RNF infection events reviewed in Staehelin *et al.* (2011).

By reason of the evolutionary divergent nature of AM and RNF interactions it has nonetheless been anticipated that additional and AM-specific genes might govern endomycorrhizal formation and functioning, pointing to the necessity of performing more holistic approaches to unravel unusual suspects (Harrison, 2005; Parniske, 2008). In this respect, transcriptomics, proteomics, and metabolomics had allowed shedding light on plant proteins and metabolic pathways candidates for the AM symbiotic program by virtue of their differential expression between mycorrhized and nonmycorrhized hosts, including transcriptomic changes (Liu *et al.*, 2003; Manthey *et al.*, 2004; Guimil *et al.*, 2005; Hohnjec *et al.*, 2005; Kistner *et al.*, 2005; Krajinski & Frenzel, 2007), protein abundance modifications (Bestel-Corre *et al.*, 2002; Valot *et al.*, 2005; Amiour *et al.*, 2006; Valot *et al.*, 2006; Aloui *et al.*, 2009; Campos-Soriano *et al.*, 2011), and metabolic reorientations (Lohse *et al.*, 2005; Schliemann *et al.*, 2006; Walter *et al.*, 2007; Walter *et al.*, 2010). Such initiatives have mainly targeted legumes including *M. truncatula*, *Glycine max*, *L. japonicus* but also *Oriza sativa* and *Solanum lycopersicum* as non-legume plant hosts, and the technical requirements for such large-scale methods have been reviewed by Ané *et al.* (Ane *et al.*, 2008) for *M. truncatula*. Altogether, profiling technologies performed during the last decade led to the identification of hundreds of AM-activated genes and proteins in different plant species among which the phosphate transporter MtPt4 (Harrison *et al.*, 2002), the serine-carboxypeptidase MtScp1 (Liu *et al.*, 2003), the protease-inhibitor MtTil (Grunwald *et al.*, 2004), the lectins MtLec5 and MtLec (Frenzel *et al.*, 2005; Frenzel *et al.*, 2006) the chitinase Mtchit3-3 (Elfstrand *et al.*, 2005), the glutathione–S-

transferase MtGst1 (Wulf *et al.*, 2003), the endo-1,4-ß-D-glucanase MtCel1 (Liu *et al.*, 2003) and the blue copper binding protein MtBcp1 (Hohnjec *et al.*, 2005; Paradi *et al.*, 2010) display an expression pattern driven by mycorrhiza-specific promoters in *M. truncatula* reviewed in Hohnjec *et al.* (2005); Krajinski & Frenzel (2007); Kuster *et al.* (2007). As a result, both targeted and untargeted approaches have generated an increasing depository of plant and fungal candidates eligible as actors of the AM symbiotic program but there is a bottleneck for their functional analysis as these experiments are time-consuming and difficult to carry out with AM fungi (AP & Howlett, 2011). Nonetheless, recent years have seen fascinating contributions in demonstrating the role of proteins in AM symbiosis, which have been driven by the realisation that mutualistic and parastic plant biotrophs shared many parallels together with the progress made in reverse genetics and cell biology tools ((Guimil *et al.*, 2005; Paszkowski, 2006; Ane *et al.*, 2008; Parniske, 2008; Bhadauria *et al.*, 2009; Bonfante & Genre, 2010; Nunes & Dean, 2012) and references therein). This review is thus intended to draw a picture of our current knowledge in the plant and fungal protein actors that have been demonstrated as functionally implicated in sustaining AM symbiosis.

II. Fashion victims: copy and paste for guest entry between AM symbiosis and more recently evolved plant interactions

1. The dress code to make friends: branching out before symbiont contact

The AM symbiosis is the result of a complex exchange of molecular information that starts before the partners engage physical contact. Because root colonization is crucial for AM fungi, the release in the plant rhizosphere of soluble signals is thought to enlarge the ability for symbionts to encounter each other before depletion of the fungal spore resources that sustain a short-term living pre-symbiotic hyphal elongation (Bonfante & Requena, 2011). In this respect, a first major breakthrough in deciphering this pre-symbiotic crosstalk relates to the identification of plant root-exuded metabolites, the so-called strigolactones (SLs), which stimulate branching of germinated hyphae of AM fungi to encourage host-root colonization (Akiyama *et al.*, 2005; Akiyama, 2007). SLs were originally identified as stimulators of the germination of root-parasitic weeds of the genera *Striga*, *Orobanche*, and *Phelipanche*, which are obligate plant biotrophs that threaten resource-limited agriculture (Cook *et al.*, 1966). The finding that parasitic plant infection is partially

controlled though the SYM pathway has reinforced the view that more recently evolved parasitic plants have co-opted part of the AM symbiosis communication program (Fernandez-Aparicio *et al.*, 2009; Kubo *et al.*, 2009). Besides their role as rhizophere signalling molecules, SLs were also identified as a novel class of plant hormones synthesized in roots and stem that inhibit shoot branching after transport through the xylem (Gomez-Roldan *et al.*, 2008; Umehara *et al.*, 2008; Kohlen *et al.*, 2011). Noticeably, it has been demonstrated that up-regulation of SLs biosynthesis during phosphate starvation played a role in the reduced shoot-branching phenotype even in the nonmycorrhizal host *Arabidopsis*, suggesting that this response enables plants to invest energy in lateral root formation in phosphate limiting environmental conditions (Kohlen *et al.*, 2011). During the last decade, genes encoding enzymes essential for SL biosynthesis or perception/signalling have been identified through their cloning from a series of mutants displaying increased shoot branching phenotypes, referred to as *decreased apical dominance* (*dad*) in petunia, *ramosus* (*rms*) in pea, *more axillary growth* (*max*) in *Arabidopsis*, and *dwarf* and *high tillering dwarf* (*d/htd*) in rice reviewed in Xie & Yoneyama (2010). Results showed that SLs are synthesized from a carotenoid substrate by sequential cleavages involving two carotenoid cleavage dioxygenases (CCD)7 (RMS5/MAX3/D17) and 8 (RMS1/MAX4/D10/DAD1) and a subsequent oxidation by a cytochrome P450 (MAX1). Three other genes *D27*, *D14* and *D3* were identified in rice, which encode a plastid-located iron-containing protein involved in SL biosynthesis, an α/ß-fold hydrolase and a F-box protein involved in signal perception, respectively (Figure 1.2, (Xie & Yoneyama, 2010)).

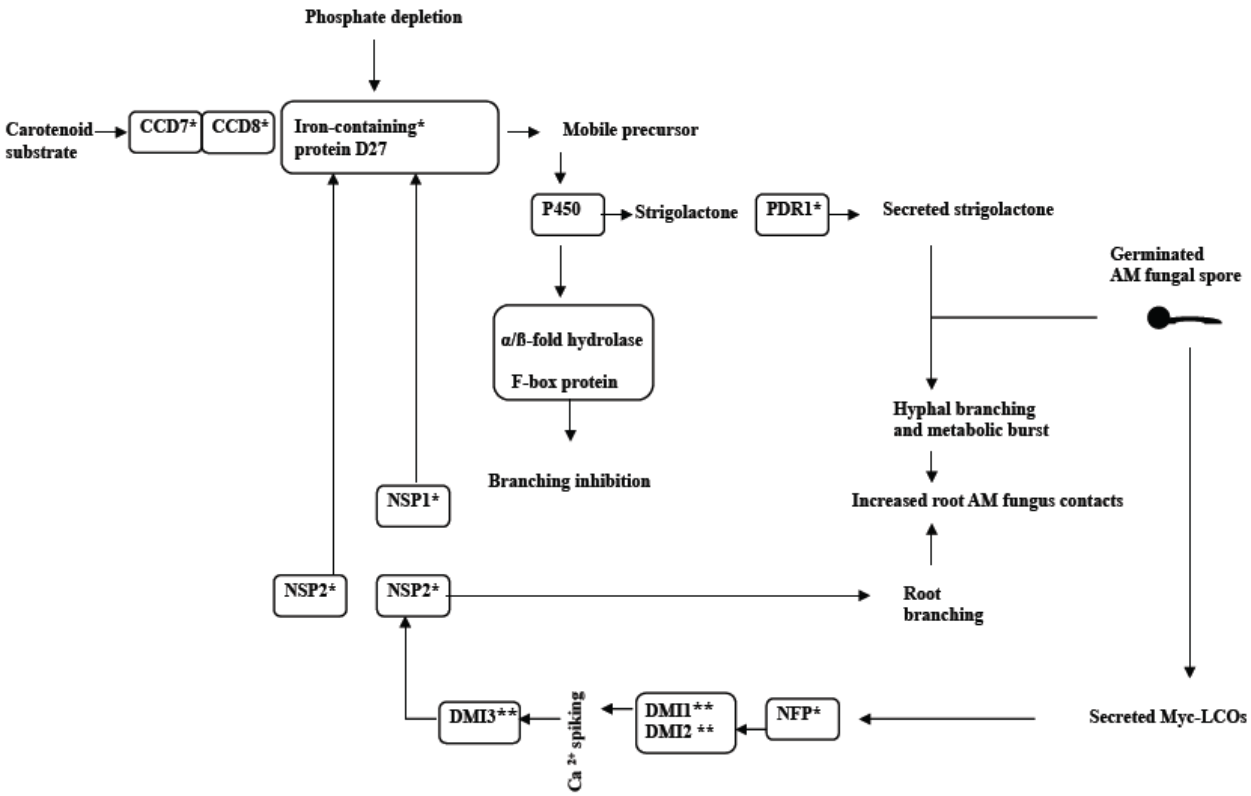

Figure 1.2: Schematic overview of the SL and Myc-LCO-related pathways that mediate AM hyphal and root branching responses.
It is adapted according to Xie & Yoneyama (2010); Liu *et al.* (2011); Maillet *et al.* (2011); Kretzschmar *et al.* (2012). Single asterisks indicate plant proteins believed to maximize plant-fungus contact events in that reduced expression of the corresponding genes results into quantitative differences in root colonisation without affecting arbuscule development. Double asterisks correspond to plant proteins belonging to the SYM pathway required for fungal infection.

Initial functional demonstrations for a role of SLs in sustaining the AM symbiotic program come from SL biosynthesis knockout mutants *(ccd8*) in tomato and pea, which display a reduction in mycorrhizal colonization of roots (Gomez-Roldan *et al.*, 2008; Koltai *et al.*, 2010). Likewise, a targeted analysis of strigolactones and AM-induced apocarotenoids revealed major decreases in the levels of these compounds in *cdd7* antisense lines generated in tomato, coupled to a decreased in arbuscule abundance (*S. lycopersicum*) (Vogel *et al.*, 2010). Very recently, new insights in the functional characterization of the SL-dependent symbiotic signalling were obtained from silencing-based experiments performed in barrel medic, rice and petunia. In the search for efflux carriers for strigolactones, Kretzschmar and co-workers isolated ABC transporters of *Petunia hybrida* on the basis of their abundance in phosphate-

starved or in mycorrhizal roots (Kretzschmar *et al.*, 2012). Using promoter-GUS reporter fusion constructs the candidate PDR1 was found to localize to the plasma membrane and gene expression was demonstrated substantial in individual subepidermal cells of the lateral roots that resemble hypodermal passage cells, which are devoid of suberin and serve as entry points for AM hyphae (Sharda & Koide, 2008). Noteworthy, GUS staining was reported more prominent in root grown under phosphate–deficient conditions and in mycorrhizal roots, particularly in regions containing or flanking arbuscules, suggesting a role for PDR1 in AM during pre-symbiotic development and during intra-radical growth. *PDR1* silencing and/or transposon-mediated loss of function allowed demonstrating that PDR1 acts as a strigolactone export carrier in that only extra-radical SL levels (orobanchol) were affected in *pdr1* mutants, in which root exudates showed a reduced activity for stimulating hyphal branching of AM fungi relative to wild-type. Likewise, petunia *pdr1* knockout or down lines display a significant reduced ability to accommodate mycosymbionts without exhibiting defects in arbuscule morphology, suggesting that quantitative differences in colonisation were due to decreased hyphal penetration events and retarded intra-radical expansion, rather than to defects in intracellular development. Overall, a role was proposed to PDR1 in mediating strigolactone secretion from HPCs, which under low phosphate conditions creates local rhizosphere gradients that guide AM hyphae to entry points (Figure 1.2, (Kretzschmar *et al.*, 2012)).

More recently, a second milestone decisive in understanding the pre-symbiotic crosstalk between mycosymbionts and plants roots was the chemical elucidation of some diffusible AM fungal signalling molecules belonging to the so-called Myc factors, which stimulate root growth and branching through a calcium signal that determines the activation of essential symbiotic genes (Bonfante & Requena, 2011). It has been shown that *R. irregularis* secretes symbiotic signals corresponding to a mixture of sulphated and non-sulphated simple lipochitooligosaccharides (Myc-LCOs), thus confirming the working hypothesis that Myc signals, produced by fungi able to synthesize chitin, are ancestors of the more recent LCO-like Nod factors produced by most rhizobia and required for early steps of legume infection and nodule organogenesis (Maillet *et al.*, 2011). Strikingly, recent studies also revealed that the intricacy between Nod and Myc signalling was more complex than previously

anticipated. Initially, the symbiotic signalling pathway identified in *M. truncatula* included genes coding for Nod factor perception (*NFP* and *LYK3*), calcium signalling (*DMI1*, *DMI2* and *DMI3*), and transcription factors (*NSP1 NSP2* and *ERN*). NFP and LYK3 correspond to Nod factor membrane receptors so far described dispensable for AM fungi signal-induced calcium oscillations in epidermal cells and subsequent mycorrhiza formation. Likewise, the three transcription factors were thought specifically activated upon Nod factor perception. On the contrary DMI1, 2 and 3 are required both for nodulation and mycorrhization. However, Op den Camp and co-workers provided evidence that in *Parasponia*, the only nonlegume partner of rhizobia, a single cell surface receptor can recognize both the fungal and bacterial signals and induce the common SYM pathway to promote the intracellular accommodation of AM fungi and rhizobia, in that silencing the unique *NFP* ortholog in *Parasponia* impairs the formation of both symbioses (Op den Camp *et al.*, 2011). Likewise, the data obtained by Maillet *et al.* (Maillet *et al.*, 2011) suggested that NFP is partly involved in the Myc-signal-elicited root branching response, as inferred from the reduced root branching response observed in *nfp* mutants relative to the wild-type. Additionally, by reason of a 40% lower colonisation level than wild-type plants exhibited in the *nsp2* mutant, a NSP2-dependent signalling pathway was found to facilitate mycorrhizal root colonization, thus indicating that the transcriptional activator NSP2 does not function exclusively in rhizobium Nod factor signalling (Maillet *et al.*, 2011). In accord with this view, recent comparative gene expression studies in symbiotic mutants demonstrated that transcriptional reprogramming by AM fungal LCOs strictly depends on MtNSP and largely requires MtDMI3. Noteworthy, none of the genes related to functional AM stages was activated by Myc-LCOs, suggesting that the function of Myc-LCOs is restricted to presymbiotic AM stages (Czaja *et al.*, 2012). On the basis of transcript profiling experiments in *nsp1* and *nsp2* knockout mutants, which were attempted to identify genes activated by NSP1 and NSP2 under non symbiotic conditions, it was also shown that NSP1 and NSP2 are indispensable for strigolactone biosynthesis in *M. truncatula* and in rice (Liu *et al.*, 2011). The disturbed SL biosynthesis in *nsp1 nsp2* mutant backgrounds was found to correlate with reduced expression of *D27* that encodes the plastid-located iron-containing protein essential for SL biosynthesis. In contrast to nodulation, none of the components of the Nod factor signalling pathway, not even the kinase CCaMK

directly active upstream of NSP1 and NSP2, are required for *D27* expression. It was thus proposed that NSP1 and NSP2 proteins fulfil dual regulatory functions to control downstream targets after rhizobium-induced signalling as well as SL synthesis in nonsymbiotic conditions. With regard to AM fungal infection, the *M. truncatula nsp1 nsp2* double mutant shows a reduction in mycorrhizal root infection but without defects in arbuscule development, suggesting that SLs stimulate root colonization exclusively *ex-planta* (Liu *et al.*, 2011).

Overall, it appears from the above-cited data that at least seven plant proteins (NFP, NSP1, NSP2, CCD7, CCD8, D27, PDR1) were recently demonstrated as either directly or indirectly involved in the fungal-root branching-induced crosstalk that takes place during pre-symbiosis as schematized in Figure 1.2. Because reduced expression in the corresponding genes mostly results into quantitative differences in root colonisation without affecting arbuscule morphology, it rather seems likely that these proteins play roles in AM symbiosis through maximizing hyphal penetration events than through mediating intra-radical development.

2. Holding a reception

Following exudates-mediated hyphae and root branching events, the pre-symbiotic phase of AM symbiosis ends up once a hyphal tip has contacted the root epidermis. Unlike aerial pathogens that have to penetrate the hydrophobic leaf cuticle through the differentiation of an appressorium that generates a glycerol-mediated turgor pressure, glomeromycotan root-infecting fungi develop hyphododia, which correspond to glycerol-free, nonmelanized and nonseptate small swellings structures at the hyphal tip that mediate adhesion to epidermal root cells through the formation of protrusions in the fungal cell wall (Genre *et al.*, 2009; Bonfante & Genre, 2010). In this regard, a third outstanding breakthrough in understanding the plant AM symbiotic program relates to the root responses elicited upon hyphopodium formation, among which the formation of a pre-penetration apparatus (PPA) that outlines the route for hyphal growth across the plant cell lumen belongs to (Genre *et al.*, 2005). Following a cytoplasmic aggregation, which consists of a cytoskeleton–driven accumulation of organelles including the plant nucleus, at the contacted epidermal site, the host cell develops a transcellular cytoplasmic column, the PPA, whose elongation follows the migration of the plant nucleus toward the inner cell wall facing the root cortex (Figure 1.1). The PPA has overlap with cell division processes in that it is particularly rich in

secretory membranes, ER, cytoskeletal elements, and requires the production of a cell wall within the lumen. This apparatus also appears reminiscent of infection thread formation, which facilitates rhizobium entry into legume root hairs that guide them into the root cortex. In addition, cytoplasmic aggregation in epidermal cells similarly occurs in several pathogenic plant-microbe interactions, where it is believed to form part of a plant defence response that leads to the formation of cell wall appositions (papillae) and the localized release of defence-related compounds (Bonfante & Genre, 2008; Genre *et al.*, 2009; Anderson *et al.*, 2010). In this line, when using roots of *M. truncatula* expressing a green fluorescent tag for the ER, which were challenged with an AM fungus, a necrotrophic pathogen, a hemibiotrophic pathogen, a noncompatible endomycorrhizal fungus, or abiotic stimuli, a correlation was underlined between physical stimulation at the cell surface and nuclear repositioning. By contrast, cytoplasmic aggregation was only induced by compatible fungi and the PPA only triggered by AM fungi. The DMI3 protein (CCaMK) also turned out to be required both for cytoplasmic aggregation and PPA formation, thus extending the role of DMI3 from symbiotic to pathogenic interactions (Genre *et al.*, 2009). CCaMK, a key conserved component of the common SYM pathway is currently believed to decode the Ca^{2+} spiking that is activated in the host epidermis during initial recognition of endosymbiotic and to trigger appropriate downstream signalling pathways leading to gene transcription in association with LjCYCLOPS/MtIPD3. Recently, it has been reported that distinct Ca^{2+} spiking profiles correlate with specific stages of transcellular apoplastic infection (Sieberer *et al.*, 2012). Outer cortical cells were found to exhibit low-frequency Ca^{2+} spiking during the intracellular remodelling that precedes infection; which appears to be a prerequisite for the formation of either pre-infection threads in RNF symbiosis or the PPA in AM symbiosis, both of which are fully reversible processes. Low-frequency spiking cells are characterized by nuclear migration to the site of future cell infection and associated cytoplasmic reorganization in the vicinity of the nucleus. By contrast, there is an increase in the frequency of Ca^{2+} spiking just before and during initial cortical cell entry by both bacterial and fungal symbionts, which involves an irreversible cell wall disassembly and *de novo* interface synthesis linked to membrane invagination. In this respect, it has been proposed that the protein Vapyrin could mediate Ca^{2+}-mediated membrane and cytoskeleton rearrangements during initial stages of root cell infection by rhizobia and AM fungi

((Ercolin & Reinhardt, 2011; Sieberer *et al.*, 2012), Figure 1.3). Actually, besides the SYM signalling pathway that is crucial for epidermal infection, Vapyrin has been discovered as a new component required for epidermal and cortical cell colonization by rhizobia and AM fungi (Reddy *et al.*, 2007; Feddermann *et al.*, 2010; Pumplin *et al.*, 2010; Murray *et al.*, 2011). In *M. truncatula*, Vapyrin RNAi roots show a high frequency of hyphopodia that attempt but fail to penetrate the epidermal cells (Pumplin *et al.*, 2010), as observed in the common *sym* mutants (Parniske, 2008). Interestingly, *MtVapyrin* was reported to be induced upon Myc-LCOs application, suggesting that the encoded protein already acts in presymbiotic stages (Czaja *et al.*, 2012) (Czajaet al. 2012). When the AM fungus succeeds entering the cortex of Vapyrin RNAi roots, intercellular hyhae spread laterally but no arbuscules are formed; a phenotype reminiscent of that displayed in the *cyclops/ipd3* and *pam1* mutants of *L. japonicus* and petunia (Reddy *et al.*, 2007). As a result, it has been suggested that a common cellular mechanism may be required to sustain hyphal growth through epidermal cells and arbuscule development in the cortex (Pumplin *et al.*, 2010). Notably, in contrast to common *sym* mutants impaired in initial endosymbiotic signalisation, in Vapyrin RNAi roots, the fungus attempts to penetrate the cells as exemplified by the hyphal projections existing below hyphopodia. Consequently, Pumplin and co-workers hypothesized that the signalling process necessary to induce fungal penetration was not affected in *vapyrin* knockdown lines, but that the cellular machinery supporting fungal entry and membrane invagination was impaired (Pumplin *et al.*, 2010). In support for this idea, was the activation of genes related to membrane dynamics and secretion events upon symbiont contact (Siciliano *et al.*, 2007b). the vesicle-like cytoplasmic localization of Vapyrin complexes that may be involved in the deposition of membrane material, which contrasts with the nuclear localization of the signalling proteins CCaMK/DMI3 and CYCLOPS/IPD3, together with the two domains composing the protein that can mediate structural changes within the cell (Pumplin *et al.*, 2010). A critical role for membrane reorganization was also approached for fungal accommodation at the early stage of AM symbiosis by Kuhn and co-workers who reported that down regulation of the membrane steroid-binding protein 1 *MtMSBP1* through RNAi led to an aberrant mycorrhizal phenotype characterized by thick and septated hyphopodia with aborted penetration attempts, septated intracellular hyphae, decrease number of arbuscules

and distorted arbuscule morphology, pointing once again to a common mechanism sustaining epidermal and cortical fungus development (Kuhn *et al.*, 2010). *MtMSBP1* expression happened to be DMI2-dependent, induced before fungal contact by a diffusible signal from branched hyphae and observed in epidermal and subepidermal cells in the vicinity of approaching hyphae and in hyphopodium-enriched root areas. Because *MtMSBP1* encodes a membrane steroid-binding protein having role in sterol homeostasis, it has been proposed that alteration of lipid metabolism is required to sustain PM invagination and intracellular accommodation of symbionts in the cortex (Kuhn *et al.*, 2010). Strikingly, both Vapyrin- and MtMSBP1-encoding genes are activated by a diffusible fungal signal, although probably different in nature. Actually, *MtVapyrin* was reported to be induced upon Myc-LCOs application in contrast to *MtMSBP1* (Czaja *et al.*, 2012).

Besides cellular remodelling events in response to AM fungus sensing, evidences were also obtained for the modulation of plant cell defence mechanisms for the initial accommodation of the symbiont. The early stages of AM symbiosis are generally accompanied by a transient induction of markers of defence (Garcia-Garrido & Ocampo, 2002; Liu *et al.*, 2003; Liu *et al.*, 2007), which are thought to represent a first reaction of the plant to unspecific microbial signals (elicitors) from the AM fungus before the recognition of some Myc factors that trigger the switch to the symbiotic program and the concomitant suppression of the plant defence response (Reinhardt, 2007). Consistent with this view, it was recently shown that silencing of the Rac1 GTPase *MtROP9* triggers the stimulation of early root colonization by the AM fungus *R. irregularis* and the pathogenic oomycete *Aphanomyces eutiches*, coupled to an inhibition of reactive oxygen species (ROS) production and anti-oxidative compounds production in *M. truncatula* roots (Kiirika *et al.*, 2012). Because RAC proteins are plant-specific small GTPases that function as molecular switches within elementary signal transduction pathways, including the regulation of ROS generation via activation of plasma membrane-associated NADPH oxidases, it was concluded that ROS signalling did play a role in mounting a general defence barrier against fungal and fungal-like invaders, including mycorrhizal mycosymbionts. Most interestingly, the PPA triggered by AM fungi was found to elicit a specific transcriptome response in epidermal cells including the DMI3-dependent up-regulation of genes encoding expansin-like and Nod-like proteins, the former likely

having role in cell wall plasticity, and down-regulation of the defence-related gene *ACRE264* encoding the Avr9/Cf-9 Rapidity-Elicited protein 264, identified as a protein kinase (ACK1) required for full resistance to *Cladosporium fulvum* strains expressing the *Avr9* gene (Siciliano *et al.*, 2007a; Siciliano *et al.*, 2007b). Consequently, the DMI3-mediated suppression of defence-related genes like *ACRE264* after physical contact with the hyphopodium led Siciliano and co-workers hypothesized that plant-AM fungus compatibility requires basal defence responses to be kept under control similarly to what observed in compatible plant-pathogen interactions. In this line of reasoning, a fourth significant recent advance in understanding the early steps mediating symbiont accommodation by plant cells was the discovery that AM fungi do use effector proteins to short-circuit the plant defence program (Kloppholz *et al.*, 2011). Actually, plants are known to have a basal defence system trained to recognize conserved traits of microbial pathogens termed MAMPS for microbial-associated molecular patterns. Recognition of these epitopes by pattern recognition receptors induces MAMP-triggered immunity, a first line of plant defences to prevent further colonization of the host. In return, microbial invaders have evolved the capacity to deliver effector proteins inside host cells to cope with MAMP-triggered immunity often through suppression of host defences or to protect themselves against plant arms (De Wit *et al.*, 2009; Hogenhout *et al.*, 2009; De Jonge *et al.*, 2011; Zamioudis & Pieterse, 2012). When investigating whether AM fungi use effector proteins to short-circuit the plant defence program, Kloppholz and co-workers showed that *R. irregularis* secreted a protein, SP7, which can crosses plant membranes to interact with the defense-related ethylene (ET)-responsive factor ERF19 in the plant nucleus to block the ERF19-mediated transcriptional program (Kloppholz *et al.*, 2011). ERF transcription factors are known to activate expression of target defence proteins, including pathogenesis-related proteins (PR) PR1, PR2 and PR4, and Osmotin. Interestingly, *MtERF19* expression can not only be induced by application of crude extracts of *R. irregularis*, but also from that of several different fungi, including plant pathogens and non-plant pathogens, pointing to the existence of a common fungal MAMP. The constitutive expression of *SP7* in roots was reported to lead to higher mycorrhization while reducing the levels of the fungal pathogen *Colletotrichum trifolii*-mediated defence responses, as assessed by the PR10 marker. Noteworthy, *SP7* expression in the rice blast fungus *Magnaporthe oryzae*, a

hemibiotrophic pathogen that can infect both leaves and roots of host plants, results in the reduced expression of defence genes encoding PR10 proteins in rice roots and extends the length of the biotrophic phase, delaying the root decay that characterized the necrotrophic phase. Overall, the results obtained by Kloppholz and co-workers (2011) support the view that SP7 acts as a universal effector to promote the biotrophic phase of a fungus inside a plant. Aside from this report, the use of transformable hemibiotroph fungal pathogens like *Colletotrichum* spp. and *M. oryzae* whose development share common features with the AM fungal lifecycle (spore, appressoria and/or hyphopodia, haustoria), coupled to comparative analyses of genome sequences from plant-infecting fungi also proved successful in revealing AM fungal proteins mediating plant cell entry. In this regard, Tollot and co-workers investigated whether the transcription factor STE12 that is essential for hyphal penetration of leaf surfaces from appressoria and in some cases for subsequent invasive growth by hemibiotrophic plant pathogens could play role in early steps of AM symbiosis (Tollot *et al.*, 2009). Introduction of *GinSTE*, a *STE12* homolog, isolated from *R. irregularis*, into a noninvasive mutant of *C. lindemuthianum* was found to restore penetration and infectivity of the fungal pathogen in *Phaseolus vulgaris* leaves. Additionally, *GinSTE* expression specifically localized in extra-radical AM fungal structures and was up-regulated when *R. irregularis* penetrated roots of wild-type *M. truncatula* roots as compared to the incompatible *dmi3* mutant, suggesting a possible common role of GinSTE in mediating early steps of plant tissue penetration between pathogenic and symbiotic fungi. Likewise, Erl1, a Ras-like GTPase from the rice blast *M. oryzae* was found to be homologous to the mature amino terminal part of the Gin1 protein of *R. irregularis*. Deletion of ERL1 in *M. oryzae* resulted in delayed appressorium formation, slow growth *in planta* and reduced intracellular colonization without defect in the necrotic ability of the fungus, indicating that ERL1 is required for invasive growth of root tissues. Because root browning defect of Δ*erl1* strains could be complemented by the AM fungus gene, it was suggested that Erl1 and Gin-N are orthologs and might be involved in the control of polar hyphal growth *in planta*, thus extending the hypothesis of common genetic features underlying plant colonization strategies among different fungi (Heupel *et al.*, 2010).

Taken together, the results described above sustain the view, on the basis of localization, silencing, and/or complementation experiments, that fungal entry within

epidermal plant cells requires the modulation of plant defence reactions coupled to cellular remodelling events in both symbionts. Besides the common SYM pathway, the identification of nine additional proteins involved in the early intracellular accommodation of AM fungi allows proposing a hypothetical model illustrating the protein pattern associated with AM fungal entry into plant cells at the early stages of symbiosis, as schematised in Figure 1.3.

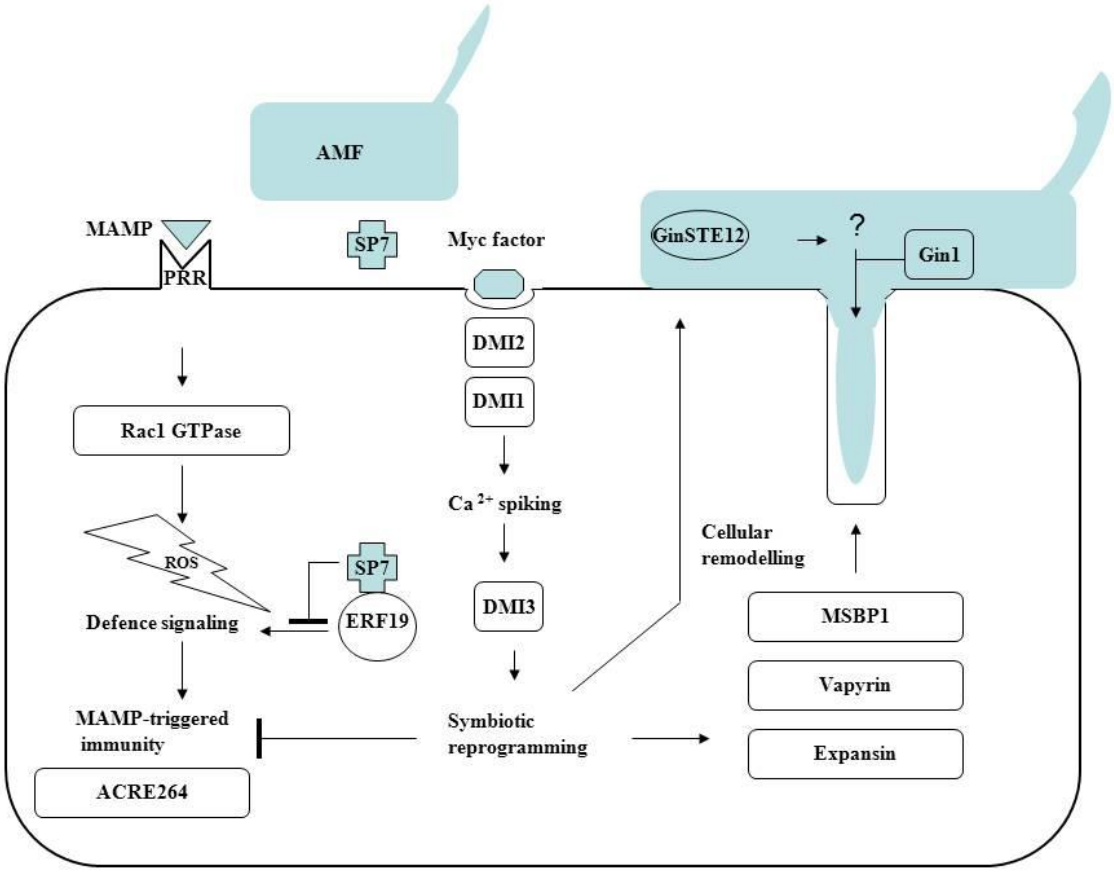

Figure 1.3: Schematic representation of a model protein pattern associated with AM fungal entry into plant cells at the early stages of symbiosis.
It is modified from (Siciliano *et al.*, 2007a; Siciliano *et al.*, 2007b; Ercolin & Reinhardt, 2011; Zamioudis & Pieterse, 2012). Host plants initially recognize arbuscular mycorrhizal fungi (AMF) as potential invaders through pattern-recognition receptors (PRR) that perceive microbe-associated molecular patterns (MAMPs). As a result, a signalling cascade likely involving Rac1-mediated reactive oxygen species (ROS) production (Kirika et al. 2012) is induced, which results in MAMP-triggered immunity (MTI) through the production of defence-related compounds. The perception of Myc factors induces the symbiotic program through the SYM pathway (DMI1, DMI2, DMI3) that triggers suppression of MTI, as exemplified by the DMI3-dependent down-regulation of the defence-related protein ACRE264 (Siciliano et al. 2007 a, b), and activation of cellular remodelling events in plant (MSP1, Vapyrin, Expansin) and fungal (GinSTE12) cells. The AMF *R. irregularis* secretes the SP7 protein effector into the plant cytosol, which upon targeting to the nucleus, interacts

with the defence-related transcription factor ERF19 to block the ERF19-mediated transcriptional program. Blue and dark colours refer to fungal and plant structures or proteins, respectively.

III. Home sweet corner. A 400-Myr old but any rest housekeeping investment to accommodate arbuscules

After traversing the epidermis and outer cortical layers, AM fungal hyphae enter cortical cells via invagination of the plasma membrane that is suspected to proceed from fusion of PPA vesicles (Bonfante & Genre, 2008). Inside a cortical cell, the intracellular hypha branches repeatedly to develop the specialized tree-like structure, known as arbuscule, which is enveloped by an extension of the host plasma membrane, the periarbuscular membrane that separates the fungus from the plant cell cytoplasm. This delineates as depicted in Figure 1.4, the interface compartment, an apoplastic space that surrounds the fungus and mediates nutrient exchange (Bonfante & Genre, 2008). Although the composition of the apoplastic space is somehow reminiscent of that of the primary plant cell wall with cellulose, pectins and hemicellulose, a structured cell wall is not present, indicative of the specialized nature of this compartment (Balestrini *et al.*, 2005). Likewise, despite consisting of an extension of the plant plasma membrane, the periarbuscular membrane displays specific protein features compared to the host PM, including the presence of the AM symbiosis-specific phosphate transporters MtPT4 and OsPT11 (Harrison *et al.*, 2002; Kobae & Hata, 2010), the AM-inducible ammonium transporter GmAMT4.1 (Kobae *et al.*, 2010), STR half-ABC transpoters (Zhang *et al.*, 2010; Gutjahr *et al.*, 2012), and VAMP721d/e proteins (Ivanov *et al.*, 2012). Imaging also revealed that the periarbuscular membrane is at least composed of two distinct specific protein-containing compartments, corresponding to an arbuscule-branch domain that specifically harbours MtPT4, OsPT11, GmAMT4, STR transporters and VAMP721s, as opposed to an arbuscule-trunck domain that contains the blue copper-binding protein MtBcp1 (of unknown function), which also localizes to the host PM (Figure 1.4).

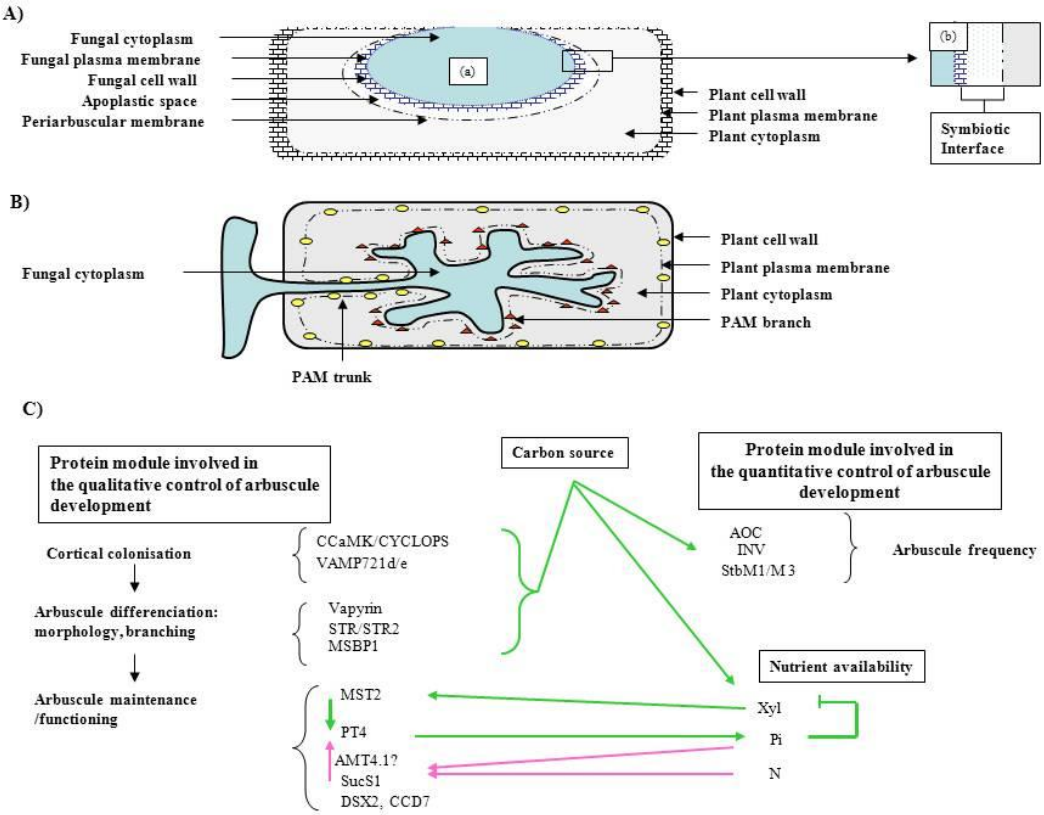

Figure 1.4: Schematic representation of the structure and regulation of an arbuscule.
A) Diagrammatic view of an arbusculated cortical plant cell into which fungal hyphae (**a**) are enveloped by the periarbuscular membrane, an extension of the host plasma membrane. This delineates (**b**) the symbiotic arbuscule/cortical cell interface that comprises the plant and the microbial membranes separated by the plant-derived apoplast
B) Illustration according to (Pumplin & Harrison, 2009) of the polarisation of the periarbuscular membrane (PAM) that is at least composed of two distinct specific protein-containing compartments, corresponding to an arbuscule-branch domain that specifically harbours MtPT4, OsPT11, GmAMT4, STR transporters and VAMP721s (red triangles), as opposed to the arbuscule trunk domain that contains the blue copper-binding protein MtBcp1 (yellow circles), which also localizes to the host PM. This suggests the occurrence of a *de novo* membrane biogenesis process associated with the dichotomous branching of hyphae. **C**) Hypothetical model representing the protein and nutrient-mediated mechanisms involved in the regulation of arbuscular morphogenesis and functioning. Protein roles are inferred from the phenotype(s) displayed in their corresponding loss-of-function backgrounds (Table 1.1). The role of Pi, N and Xyl originate from the data reported in ((Baier *et al.*, 2010), pink arrows) and ((Helber *et al.*, 2011), green arrows).

This suggests the occurrence of a *de novo* membrane biogenesis process associated with the dichotomous branching of the hyphae (Pumplin & Harrison, 2009; Kobae & Hata, 2010; Kobae *et al.*, 2010; Zhang *et al.*, 2010; Ivanov *et al.*, 2012). Interestingly, the polar targeting of MtPT4 to the periarbuscular membrane happens mediated by a

transient reorientation of secretion favouring vesicle fusion with the developing periarbuscular membrane rather than with the PM, and a coincident change in the newly synthesized protein cargo entering the secretory system (Pumplin *et al.*, 2012). In parallel to the development of the periarbuscular membrane, arbusculated cells display a drastic architectural reorganization to support deposition of membrane and newly synthesized proteins, as illustrated by the presence of organelles involved in synthetizing and secreting proteins (nucleus, ER, Golgi, plastids) in the close vicinity of the periarbuscular membrane, together with cytoskeletal components (actins, microtubules) to direct secretion ((Pumplin & Harrison, 2009; Gutjahr *et al.*, 2011) and references therein). In addition to these changes schematized in Figure 1.4, an accumulation of peroxisomes around collapsing arbuscules also has been documented, suggesting either an active lipid breakdown through β-oxidation and/or the sequestration of the ROS generated during membrane breakdown (Pumplin & Harrison, 2009).

Despite this fifth recent major breakthrough in the understanding of arbuscule morphogenesis, the protein-encoding genes sustaining the cortical phase of AM symbiosis have been a long time coming relative to those involved in hyphal penetration. This probably reflects the fact that, historically, mycorrhizal mutant phenotypes were first uncovered through genetic screens for plant defective in nodulation leading to the resolution of the early common symbiosis signalling pathway, together with the difficulty in visually detecting plants compromised for arbuscules in that they reside inside root cells (Morandi *et al.*, 2005; Morandi *et al.*, 2009). Nowadays, the blind dissection of the molecular components sustaining arbuscule development/functioning largely beneficiates from the combination of whole-genome transcriptome profiling of mycorrhizal roots (Liu *et al.*, 2003; Guimil *et al.*, 2005; Hohnjec *et al.*, 2005; Kistner *et al.*, 2005) together with mutant resources and/or reverse genetic screenings for altered mycorrhizal phenotypes (Hirochika *et al.*, 2004; Porceddu *et al.*, 2008; Kuromori *et al.*, 2009; Revalska *et al.*, 2011). Likewise, the ever increasing number of completed plant and fungal genome sequencing projects also has improved the analogy-based targeted search of proteins involved in AM symbiosis (Schmidt & Panstruga, 2011). Overall, the proteins that have so far been demonstrated to play role in sustaining arbuscule formation/functioning can be divided into either two distinct phenotypic classes

corresponding to those already involved in epidermal penetration and those only required for cortical infection/reprogramming, and/or into functional groups, which encompass processes related to signalling, membrane biogenesis/protein trafficking, nutrient transport and plastidial metabolism.

1. Gossip girls for signalization

Regarding the common SYM pathway whose distinctive roles in the early and late accommodation of both rhizobia and AM fungi have been very comprehensively reviewed in Ercolin & Reinhardt (2011), mutations in *SYM* genes generally lead to an arrest of AM hyphal infection. However, under high inoculum pressure, a few *sym* mutants can be forced into AM colonization and the development of arbuscules can proceed normally indicating that cortical infection is not strictly dependent on *SYM* gene signalling (Morandi *et al.*, 2005; Bonfante & Genre, 2010). Nonetheless, two exceptions actually exist in that the common *SYM* genes *CYCLOPS/IPD3* and *CCaMK/DMI3* that operate downstream calcium spiking are indispensable both for epidermal infection as well as for cortical infection and arbuscule formation (Levy *et al.*, 2004; Chen *et al.*, 2007; Gutjahr *et al.*, 2008; Yano *et al.*, 2008). CCAMK/DMI3 is thought to transduce calcium signals and physically interacts with and phosphorylates CYCLOPS (INTERACTING PROTEIN OF DMI3 (IPD3)) (Messinese *et al.*, 2007), and act together as a signal transduction complex required for infection (Yano *et al.*, 2008). Interestingly, recent experiments have shown that a dominant active form of CCaMK expressed in *sym* mutant backgrounds allows successful AM infection despite the fact that the normal signal transduction pathway leading to calcium spiking has been circumvented (Hayashi *et al.*, 2010). These results gave evidence that the common symbiosis genes upstream calcium spiking is only required for the activation of CCaMK and that this activation allows symbiotic accommodation of both rhizobia and AM fungi in *L. japonicus*. In other words, activation of CCaMK alone is sufficient to mediate symbiont accommodation within cortical cells. Additionally, it has been shown that calcium spiking has different signatures depending on RNF or AM symbiotic interactions, leading to the transmission of RNF- or AM-specific information to the downstream pathways (Kosuta *et al.*, 2008). In contrast, gain-of-function of CCaMK does not discriminate the roots either infected by rhizobia or AM fungi, implying that a specific signal, other than those mediated by common *SYM* genes, plays role in the determination of

downstream pathways responsible for each of the symbioses (Hayashi *et al.*, 2010). Likewise, a transition from low- to high-frequency calcium spiking occurs concomitantly with endosymbiotic microbe entry into cortical root cells and the spiking profiles associated with cell entry are similar in term of periodicity in response to rhizobia and AM fungi (Sieberer *et al.*, 2012). Consequently, it has been proposed that calcium signatures discriminate bacterial and fungal symbionts prior to infection, but that a conserved calcium spiking profile is required for activating pathways required for cortical infection. Finally, as very comprehensively reviewed in Singh & Parniske (2012), recent data also indicate that a negative regulation of CCaMK via autophosphorylation of the CaM binding site is essential for symbiotic infection. Actually, Liao and co-workers showed that the *ccamk-14* mutant that carries a single amino acid substitution in a newly discovered autophosphorylation site in the calmodulin binding domain is impaired specifically in the infection of cortical cells by rhizobia or AM fungi (Liao *et al.*, 2012). Biochemical analysis indicates that phosphorylation at this site inhibits calmodulin binding, thus negatively interfering with CCaMK activation.

2. Interior designers for membrane biogenesis and protein trafficking

As aforementioned (fungal entry), the pattern of impaired epidermal penetration together with lack of arbuscule in the *cyclops* and *ccamk* mutants, was also observed in *Vapyrin* knock-down plants (Feddermann *et al.*, 2010; Pumplin *et al.*, 2010). In petunia and barrel medic, Vapyrin was reported indispensable for arbuscule differentiation in cortical cells, whereas its function is conditional for epidermal colonisation at high infection pressure. Using confocal microscopy, it was shown that the cortical cells of the mutant were indeed colonized, but that arbuscule development was arrest at an early point of branching (Feddermann *et al.*, 2010). By contrast, in wild-type colonized cells, Vapyrin become increasingly localized in areas of intense hyphal branching to membrane-bound structures associated with the tonoplast, referred to as tonospheres, which may function as a mobile reservoir of membrane material. This hypothesis could explain why Vapyrin is more critical in cortical cells than in epidermal cells, by reason of a more extensive need in membrane production (Pumplin & Harrison, 2009). In the same line, aside from resulting in septated hyphopodia with aborted penetration attempts, inactivation of the membrane steroid-binding proteins MtMSBP1 leads to a decreased number of arbuscules, some of them

having a distorted morphology, suggesting that alteration of sterol metabolism with regard to membrane biogenesis is required for fungal accommodation (Kuhn *et al.*, 2010). In relation to protein trafficking, Takeda and co-workers investigated in *L. japonicus* the relevance for mycorrhizal development of two AM-specific subtilases, SbtM1 and SbtM3, by negatively interfering with their expression through RNAi (Takeda *et al.*, 2009). Suppression of *SbtM1* or *SbtM3* caused a decrease in intra-radical hyphae and arbuscule frequency without affecting the number of fungal penetration attempts, indicating that the two subtilases play an indispensable role during the fungal infection process in particular arbuscule development. The predicted proteolytic activity of SbtM1 and SbtM3, together with their localization in the apoplastic perifungal and periarbuscular spaces, suggested that cleavage of structural proteins within and between plant cell walls by subtilases might be required for elongation of fungal hyphae in the intracellular space and for penetration into the host cell during arbuscule formation. Interestingly, AM-induced proteases were found to be secreted at the symbiotic interface. Actually, when testing the functionality of the subtilase signal peptide by fusion to the N-terminus of Venus protein, strong fluorescence was detected around fungal hyphae traversing plant cells and in the periarbuscular space, suggesting first that protein trafficking towards the periarbuscular space follows the canonical secretory pathway, and second, that the increase in membrane surface during arbuscule development may cause a significant portion of trans-Golgi vesicles to fuse with the periarbuscular membrane, and then to redirect proteins entering the secretory pathway to the periarbuscular space (Takeda *et al.*, 2009). Very recently, Ivanov and co-workers investigated whether an exocytotic pathway might similarly control the formation of the symbiotic interface in both RNF and AM symbioses (Ivanov *et al.*, 2012). Exocytosis that involves focalized fusion of transport vesicles (with a specific cargo) with their target (plasma) membrane, is mediated in plants by a group of proteins belonging to the VAMP72 (vesicle-associated membrane proteins), which have been shown to be recruited in the *Arabidopsis* interaction with biotrophic fungi (Kwon *et al.*, 2008). Upon mining of *M.* EST and genome sequence data, a putative "symbiotic" *VAMP721* subgroup, including *MtVAMP721d* and *–e* without *Arabidopsis* homologs, was retrieved as the best candidate to be involved in symbiosis-related membrane compartments. Localisation studies show that the corresponding proteins localize to over the

periarbucular membrane, especially at the fine branches, and subsequent RNAi-based silencing of *VAMP721d/e* genes blocks symbiosome as well as arbuscule formation in RNF and AM symbiosis, respectively. It was thus concluded that arbuscule formation is specifically controlled by the MtVAMP721d/e-regulated exocytotic pathway whose switch-on allows the targeting of vesicles with a different cargo to facilitate the development of a symbiotic interface with specific protein composition. Overall, the current data confirm that the periarbuscular endomembrane compartment is apoplastic despite its intracellular nature (Ivanov *et al.*, 2012).

Also related to the processes that may drive arbuscule extension/differenciation, transcriptional analyses revealed the occurrence of transporter genes that are induced in mycorrhizal roots but happened rather more likely involved in the export of unknown signalling molecules into the periarbuscular space than in the direct uptake of nutrients from the plant-fungus interface (Benedito *et al.*, 2010; Gaude *et al.*, 2012). Actually, in *M .truncatula*, Zhang and co-workers identified from a mycorrhiza-defective mutant background two half-ABC transporters designated STR and STR2 (for stunted arbuscule), which happen essential for arbuscule development but dispensable for RNF symbiosis, as inferred from the wild-type nodulation phenotype displayed in *str* mutants (Zhang *et al.*, 2010). Expression of both *STR* genes was induced in cortical cells containing arbuscules and silencing of STR2 by RNA interference resulted in a stunted arbuscule phenotype identical to that of *str*. Noteworthy, interaction data show that STR and STR2 function as a heterodimer that resides in the periarbuscular membrane, more specifically around arbuscule branches. Based on the transport activity of most ABC transporters coupled to localization data, the authors supposed that unlike the phosphate transporters MtPT4 and OsPT11, STR/STR2 functions as a pump to export from the cortical cells to the periarbuscular apoplastic space in direction to the AM fungus a substrate molecule, which might be a lipid or a secondary metabolite. Previously, it was shown that the lysolipid lyso-phosphatidylcholine (LPC) may serve as a signal to induce symbiotic Pi transporter gene expression (Drissner *et al.*, 2007), but LPC was excluded as a putative substrate for STR/STR2 because the *M. truncatula* symbiotic Pi transporter *PT4* is expressed appropriately in *str* backgrounds. By reason of the slow growth and reduced branching phenotype of arbuscules typical of *str* phenotypes, it was thus proposed that strigolactones might play a role in stimulating the dichotomous branching of intra-

radical hyphae to create the arbuscule (Zhang *et al.*, 2010). However, in a parallel study that analyses the function of STR/STR2 heterologous proteins in rice, this hypothesis was discarded in that *d17* and *d10* rice lines that carry mutations in carotenoid cleavage dioxygenases 7 and 8, respectively, which are required for SL biosynthesis, displayed wild-type like branched arbuscules (Gutjahr *et al.*, 2012). Likewise, not only the expression profile of AM-specific markers including that of the mycorrhiza-specific Pi transporter gene *OsPT11* actually persists in *str* rice lines, which is consistent with what observed in *M. truncatula*, but also the *str* phenotype was not complemented by wild-type nurse plants, suggesting that carbon flux to the AM symbiont is unlikely involved in restricting arbuscule branching. Overall, the hypothesis of either a plant Pi- or fungal carbon malnutrition in mediating stunted arbuscule formation fails to be sustained in rice (Gutjahr *et al.*, 2012), pointing to the possible involvement of membrane-required phospholipid-related compounds as alternative substrates of the STR transporter complex.

3. On a permanent slimming diet: the phosphate price for success

As a central feature of biotrophic mutualism in the AM symbiosis, a bi-directional nutrient flux corresponding to carbon delivery to the fungus versus mineral nutrient import to the plant, has been for a long time anticipated to proceed through protein transporters located to the arbuscule/cortical cell interface that comprises the plant and the microbial membranes separated by the plant-derived apoplast (Smith & Smith, 1990). Regarding phosphorus (P), which remains considered as the main symbiosis-mediated benefit for the host probably by reason of the low mobility of its ionic forms in the soil, two pathways can mediate its acquisition by plants as orthophosphate (Pi): the direct uptake pathway at the root-soil interface that involves high-affinity Pi transporters located to the epidermis and root hairs, as opposed to the mycorrhizal pathway that extends from extra-radical hyphae to cortical arbuscules. Pi is actually believed to translocate to fungal hyphae as polyphosphate, which upon hydrolysis by polyphosphatases in the arbuscule, generates Pi that is exported to the periarbuscular space. Subsequently, plant Pi transporters (PT), which use an H^+ gradient to drive the transport process (Gianinazzi-Pearson *et al.*, 2000), mediate Pi import to the root cell across the periarbuscular membrane (Parniske, 2008). Currently, AM-inducible Pi transporters, which all belong to the clade Pht1, have

been identified in many plant species and cluster in subfamilies I and III (Javot *et al.*, 2007).

Transporters in subfamily III are expressed in roots, and some members such as such as StPT3 of potato and LjPT3 of *L. japonicus* are induced in cortical cells during AM symbiosis. Noteworthy, in *L. japonicus* roots colonized with *G. mosseae*, *LjPT3* transcripts were detected in arbuscule-containing cells of the inner cortex and partial suppression of *LjPT3* through RNAi led to a two-fold reduction in Pi transfer coupled to a decreased arbuscule number, suggesting that LjPT3 actually contributes to the symbiotic transport of Pi and that insufficient Pi uptake and/or low expression of *LjPT3* prevents further development of fungal structures (Maeda *et al.*, 2006). Relative to subfamily III, Pi transporters belonging to subfamily I such as OsPT11 of rice, MtPT4 of *M. truncatula* and LePT4 of tomato, only accumulate during symbiosis within arbuscule-containing cells, and at least for MtPT4 and OsPT11, their location in the perirbuscular membrane, notably in the arbuscule-branch domain, has been demonstrated (Pumplin & Harrison, 2009; Kobae & Hata, 2010), and thereby they are also referred to as mycorrhiza-specific transporters (Javot *et al.*, 2007).

The functional demonstration for a role of subfamily I transporters in sustaining symbiotic Pi transport comes from *mtpt4* knockout mutants in *M. truncatula*, which fail to display mycorrhiza-associated increases in Pi (Javot *et al.*, 2007). Likely as a sixth decisive breakthrough in deciphering mycorrhiza functioning, Pi transport by MtPT4 appears clearly essential for AM symbiosis as inferred from the premature death of arbuscules and fungal growth arrest in mutants lacking MtPT4 function, suggesting that the import of Pi by MtPT4 serves as a signal to the plant cell not only to permit continued arbuscule development but also to sustain fungal existence within plant roots (Javot *et al.*, 2007). Consistent with the idea of a causal relationship between Pi transport and arbuscule maintenance, proteins MtPT4 and OsPT11:GFP were no longer detectable on degenerating arbuscules in wild-type roots of *M. truncatula* and rice, respectively (Harrison *et al.*, 2002; Kobae & Hata, 2010). Likewise, in petunia plants it was noticed that repression of phosphate transporter–encoding genes upon Pi addition precedes the reduction in colonization, indicating that PT loss-of-function actually represents a cause, but not a consequence, of decreased symbiosis (Breuillin *et al.*, 2010). Unexpectedly, the N status of the plant was found to impact the *mpt4* mycorrhizal phenotype in that premature arbuscule

degeneration is relieved when plants are deprived of N, whereas fungal death is not rescued when the fungus has access to carbon from a nurse plant, indicating that arbuscule lifespan is regulated in part by N, but unlikely by C availability (Javot *et al.*, 2011). In this respect, AM symbionts are known to transfer N to the plant (Hodge *et al.*, 2001), and the existence of AM-inducible ammonium transporter genes has been documented especially in *L. japonicus* and *G. max* (Guether *et al.*, 2009; Kobae *et al.*, 2010). Interestingly, in soybean the AM-inducible ammonium transporter GmAMT4.1 localizes to the arbuscule-branch domain similarly to MtPT4 in *M. truncatula* (Kobae *et al.*, 2010). It is therefore conceivable that ammonium symbiotic delivery by the AM fungus at the cortical plant-symbiont interface can also act as a signal to sustain arbuscule functioning in order to provide the plant with N when the environmental conditions are limiting. Unfortunately, it is currently unknown whether the AMT4.1 protein disappears upon arbuscule death in natural mycorrhiza nor whether AMT4 loss-of-function triggers symbiosis arrest as observed for MtPT4. Regarding the putative signalling processes involved in the phosphate control of AM symbiosis, Drissner and co-workers identified LPC as a signalling molecule which activates the expression of *LePT3*, *StPT3* and *StPT4*, which are mycorrhiza-inducible PT genes in tomato (*S. lycopersicum*) and potato (*Solanum tuberosum*) (Drissner *et al.*, 2007). By contrast, in *P. hybrida*, the mycorrhiza-specific phosphate transporter gene *PhPT4*, was found suppressed by LPC, suggesting that lysolipid may not act as an universal signal in AM symbiosis (Tan *et al.*, 2012). Whatever the case, a series of promoter truncation and mutation analyses led recently to the identification of two conserved *cis*-acting elements, MYCS and P1BS, involved in the regulation of mycorrhiza-activated Pi transporters in eudicot species, which may provide new insights in the Pi signalling pathways during AM symbiosis (Chen *et al.*, 2011).

4. Shopping centre addiction: the fuel dispenser

Regarding plant carbon delivery to the AM fungus, sucrose (Suc), which channels a substantial portion of the photosynthetic fixed CO_2, is used for long-distance carbon and energy transport into diverse heterotrophic sinks and represents the preferred carbohydrate translocated to the mycorrhizal interface (Bucking & Shachar-Hill, 2005). Higher transcript levels of sucrose transporters (SUT), as well as accumulation of sucrose and monosaccharides in sink organs were observed in mycorrhized roots of tomato (*Solanum lycopersicum*) and white clover (*Trifolium repens*) plants, indicating

an increased movement of sucrose from photosynthesizing leaves (Wright *et al.*, 1998; Boldt *et al.*, 2011). Very recently, the characterization of the complete sucrose transporter family from *M. truncatula* and the identification of two key members upregulated in mycorrhized plants (*MtSUT1.1* and *MtSUT4.1*) reinforce this idea of an increased movement from source leaves towards mycorrhizzed roots (Doidy *et al.*, 2012). Interestingly, the overexpression of the phloem loading SoSUT1 of potato (*Solanum tuberosum*) shaped the plant-fungus interaction by increasing *R. irregularis* colonization, compared to WT plants, when high-phosphate conditions were applied (Gabriel-Neumann *et al.*, 2011). The fact that no effects on mycorrhization rates were observed in low-phosphate conditions, nor when antisense inhibition lines of this transporter were assessed; coupled with previous evidences showing an altered leaf C-partitioning and tuber metabolism when this gene was overexpressed (Leggewie *et al.*, 2003), might suggest a non-direct effect of SoSUT1 on the AM interaction. Additional evidences of transcriptional regulation of genes involved in sucrose transport were reported in the AM interaction between tomato plants and *Glomus fasciculatum* (Tejeda-Sartorius *et al.*, 2008). Nevertheless, contrasting evidences on SUTs regulation have been reported for the LeSUT1 of tomato, which showed to be down-regulated in AM mycorrhized roots (Ge *et al.*, 2008).

Because intra-radical fungal structures are unable to take-up Suc together with the lack of evidence in favour of Suc-cleaving activities in AM fungi, Suc is believed to be hydrolysed prior to fungal utilization by cytosolic Suc synthases (SucS), producing UDP-Glc and Fru, or invertases (Inv), producing Glc and Fru. Particularly, extracellular invertases have a key function in supporting increasing sink strength, a feature of mycorrhizal roots; and may thus directly deliver utilizable carbohydrates to the apoplast-located fungal structures. Unexpectedly, artificially augmented hexose availability to the AM fungus, obtained by yeast-derived apoplastic Inv active in the arbuscule interface of transgenic mycorrhizal *M. truncatula* roots, failed to improve AM colonization significantly (Schaarschmidt *et al.*, 2007). These data suggested that carbohydrate supply in AM cannot be improved by root-specifically increased hexose levels, implying that under normal conditions sufficient carbon is available in mycorrhizal roots. By contrast, transgenic tobacco plants expressing an inhibitor of Inv functioning showed reduced apoplastic invertase activities in roots that also had lower contents of Glc and Fru coupled to a diminished mycorhization, thus showing

that the carbon supply in the AM interaction actually depends on the activity of hexose-delivering apoplastic invertases in roots (Schaarschmidt *et al.*, 2007). Concomitantly, to study the relevance of the SucS-mediated symplastic sink near the plant fungus interface, Baier and co-workers (Baier *et al.*, 2010) used *M. truncatula* lines displaying partial suppression of *MtSucS1*, the only *MtSucS* gene currently known as activated under endosymbiotic conditions and for which a role for biological N fixation in root nodules was demonstrated (Baier *et al.*, 2007). Antisensing MtSuc1 led to an internal mycorrhization-defective phenotype as inferred from reduced frequencies in internal hyphae, vesicle and arbuscule development. Strikingly, arbuscules were not only degenerating, similarly to the early symbiosome senescence observed in *Rhizobium*-inoculated *MtSuc1*-knockdown lines, but often showed a lower branching network, resulting in a reduced functional symbiotic interface also evident from the recorded down-regulation of periarbuscular membrane transcript markers. This phenotype, somehow reminiscent of that displayed in *MtMTP4*-repressed constructs (Javot *et al.*, 2007), correlated with reduced phosphorus and nitrogen levels and was proportional to the extent of MtSuc1 knockdown, as represented in Figure 1.4. Overall, it was concluded that plant sucrose synthase MtSuc1 functioning is directly or indirectly a prerequisite, not to induce, but to sustain normal arbuscule maturation and lifetime (Baier *et al.*, 2010).

In parallel, the long time-dating hypothesis of a subsequent carbon uptake by AM fungi, occurring in form of hexoses at the plant-fungal interface, has been supported by the isolation of a monosaccharide transporter from *Geosiphon pyriformis*, a member of the *Glomeromycota* that undergoes AM-like endosymbiosis with cyanobacteria, but not with higher plants (Schussler *et al.*, 2006; Schussler *et al.*, 2007). Nonetheless, a recent seventh likely-decisive step forward the understanding of mycorrhizal mutualism comes from the first isolation of a *R. irregularis* monosaccharide transporter operating at several symbiotic root locations (Helber *et al.*, 2011). Using a preliminary draft of the sequencing project of *R. irregularis*, Helber and co-workers actually identified the monosaccharide transporter gene *MST2*, which is expressed not only in arbuscules but also in intercellular hyphae, indicating that sugar uptake can proceed in both fungal structures (Helber *et al.*, 2011). MST2 was found able to transport Glc, and Fru, but also Xyl, Man, Gal, glucuronic and galacturonic acids that are components of the no linked primary cell wall-like

apoplastic plant-fungus interface, thus corroborating the idea that AM fungi can indeed feed on cell wall components (Smith & Smith, 1990). Furthermore, *MST2* expression *in planta* was clearly found to depend on the symbiotic phosphate delivery pathway. Actually, upon Pi fertilization, the expression of *MST2* was down-regulated concomitantly to that of the mycorrhiza-specific Pi transporter *PT4*. Most interestingly, knockdown *MST2* lines through host-induced gene silencing indicates that MST2 is indispensable for a functional symbiosis as inferred from lower mycorhization levels coupled to the appearance of not fully developed and early senescing arbuscules, a phenotype that parallels the abolished expression of *MtPT4*. Unexpectedly, it also turned out that Xyl can specifically induce the expression of *MST2* in the extra-radical mycelium (ERM), a tissue believed so far unable of sugar uptake, suggesting that Xyl may act as a signal to trigger *MST2* expression *in planta*. On the basis of these outstanding data, Helber and co-workers proposed a model according to which AM fungal growth within the cortex induces a signal-mediated increase in carbon sink coupled to Xyl availability that triggers MTS2 expression; and subsequent arbuscule formation induces PT4 activation (Helber *et al.*, 2011). As a feedback control, a high phosphate symbiotic delivery might act by reducing Xyl levels and consequently repress *MST2* induction.

5. The face pack of house-keepers: a plastid-derived colored and hormonal control.

Upon AM symbiosis, colonized cortical cells are known to accumulate within the plastids surrounding arbuscules two types of apocarotenoids (carotenoid cleavage products) of unknown function, which lead to the typical macroscopically visible yellow coloration of mycorrhizal roots, and are assumed to originate from a common carotenoid precursor (Fester *et al.*, 2002; Floss *et al.*, 2008). Namely, the chromophor of this yellow complex is an acyclic C_{14} apocarotenoid polyene called mycorradicin that occurs in a complex mixture of derivatives, coupled to the concomitant accumulation of C_{13} cyclohexanone apocarotenoid derivatives (Schliemann *et al.*, 2006). To investigate the elusive role of cyclohexanone and mycorradicin accumulation in AM symbiosis, Floß and co-workers suppressed the expression of *MtDSX2* (1-deoxy-D-ribulose 5-phosphate synthase) that catalyzes the first step of the plastidial methylerythritol phosphate (MEP) pathway, which supplies isoprenoid precursors in parallel to an alternative cytosolic pathway (Floss *et al.*, 2008). RNAi-

mediated repression of *MtDSX2* led to a strong and reproducible reduction in the accumulation of the two AM-inducible apocarotenoids coupled to a shift towards a greater number of older, degrading and dead arbuscules at the expense of mature ones. Overall, these data reveal a requirement for DXS2-dependent MEP pathway-based isoprenoid products to sustain mycorrhizal functionality at late stages of symbiosis. In accord with this view, Vogel and co-workers reported that a knock-down approach performed in tomato on the *carotenoid cleavage dioxygenase 7* (*cdd7*) gene located downstream in the pathway of apocarotenoid biosynthesis resulted in major decreases in the levels of AM-induced apocarotenoids in *cdd7* antisense lines, coupled to a decreased in arbuscule abundance (Vogel *et al.*, 2010). Although the role of cyclohexanone and mycorradicin during AM symbiosis still remains to be solved, it turns out that a specific consequence of the absence of apocarotenoids might be the accumulation of older arbuscules (Floss *et al.*, 2008). In this respect, a high exogenous supply of Pi in mycorrhizal petunia roots was found to repress genes involved not only in phosphate transport and intracellular accommodation, but also in carotenoid biosynthesis (Breuillin *et al.*, 2010). Taken together, these data support a hypothesis according to which apocarotenoids sustain directly or indirectly arbuscule maintenance/functioning.

Finally, and as very comprehensively reviewed in (Hause & Schaarschmidt, 2009), the involvement of the plastid-located lipid-derived phytohormone jasmonic acid (JA) as a regulator of AM symbiosis has been observed in diverse plant species. Initially noticed from application experiments that resulted in a promotion of mycorrhizal root colonization, a positive effect of JA on AM symbiotic development was also drawn from the increased endogenous JA levels observed after the initial step of the symbiotic interaction, indicating that partner recognition may not be linked to the expression of JA-biosynthetic genes and to elevated JA levels. A functional demonstration for a role of JA in mycorrhiza establishment comes from a *M. truncatula* antisense line that displays a partial suppressed expression of *MtAOC1*, which encodes the JA-biosynthetic enzyme allene oxide synthase (AOC) (Isayenkov *et al.*, 2005). The reduction in the amount of MtAOC protein through antisense-mediated suppression resulted in a decrease in endogenous JA level in mycorrhizal roots accompanied by an overall reduction in arbuscule frequency rather than to an abnormal infection process. Immunocytology indicated that in mycorrhizal roots

MtAOC clearly localizes to plastids that develop around arbuscules, whereas the cortex cells of nonmycorrhizal roots were label-free. Notably, the AOC protein also seems to be present in arbuscule-containing cells independent of their developmental stage, suggesting the absence of a relationship between JA synthesis and arbuscule maintenance. In this line, when considering genes the repression of which upon Pi fertilization may potentially affect AM colonization in petunia, a homologue of the JA-inducible *JA2* transcript was slightly increased, in contrast to the phosphate-mediated suppression of those essential for symbiosis (Breuillin *et al.*, 2010). Consequently, the petunia transcriptional Pi-related proxy rather sustains a helper/signalling effect of JA biosynthesis in mycorrhizal colonization rather than a prominent role of the phytohormone in sustaining AM functioning. Nonetheless, because jasmonates can affect mycorhization in multiple ways, including alteration in flavonoid biosynthesis, microtubular pattern, defence reaction, cytokinin action together with an increase in the stimulation of carbohydrate synthesis, additional experiments based on metabolite, protein and/or transcript profiling are required to elucidate the processes mediated by jasmonates during AM symbiosis (Isayenkov *et al.*, 2005).

Overall, contrasting with the last decade that has been essentially dominated by the dissection of the role played by the common SYM pathway in the cortical infection by AM fungi (reviewed in Singh & Parniske, 2012), recent years have seen not only an extraordinary increase in the protein repertoire sustaining arbuscule development and functioning, but also an unexpected specialization of the protein machinery mediating arbuscule morphogenesis coupled to a network of interacting regulators that turns out to be quite more complex than anticipated, a protein scenario we have attempted to schematise and list in Figure 1.4 and Table 1.1, respectively.

Table 1.1: List of proteins essential for arbuscules.
Repertoire of the proteins listed in the current study for which partial or total loss-of-function supports a role in sustaining arbuscule (Arb) development and/or functioning.

Protein	Origin	Function	Location	Origin of loss-of function	Loss-of-function phenotype in AM symbiosis	Main literature cited
CCaMK	Plant	Signalling	Plant nucleus	Nodulation defective mutant	Arb defective	Reviewed in Singh and Parniske (2012)
CYCLOPS	Plant	Signalling	Plant nucleus	Nodulation defective mutant	Arb defective	Reviewed in Singh and Parniske (2012)
Vapyrin	Plant	Membrane biogenesis	Membrane-bound structures	RNAi	Arb branching defective	(Feddermann *et al.*, 2010; Pumplin *et al.*, 2010)
MSBP1	Plant	Membrane biogenesis	ER	RNAi	Decreased arb number, arb morphology defects	(Kuhn *et al.*, 2010)
SbtM1/M3	Plant	Protein trafficking	Apoplastic symbiotic interface	RNAi	Decreased IRM and arb number	(Takeda *et al.*, 2009)
VAMP72s	Plant	Membrane biogenesis	PAM branches	RNAi	Arb defective	(Ivanov *et al.*, 2012)
STR/STR2	Plant	Transport	PAM branches	RNAi	Slow growth, reduced branching	(Zhang *et al.*, 2010) (Gutjahr *et al.*, 2012)
PT4	Plant	Transport	PAM branches	RNAi	Arb premature death, growth arrest	(Javot *et al.*, 2007)
Inv	Plant	Suc cleavage	Apoplaste	Activity inhibitor	Reduced mycorrhization	(Schaarschmidt *et al.*, 2007)
SucS1	Plant	Suc cleavage	Cytoplasme	RNAi	Decreades IRM and vesicles. Arb branching defects and senescence	(Baier *et al.*, 2010)
MST2	Fungus	Transport	Arbuscule/ IRM/ERM	HIGS	Reduced mycorrhization, not fully developed arb, arb senescence	(Helber *et al.*, 2011)
DXS2	Plant	Carotenoid biosynthesis	Plastid	RNAi	Arb senescence	(Floss *et al.*, 2008)
CDD7	Plant	Carotenoid biosynthesis	Plastid	RNAi	Reduced mycorrhization, arb senescence	(Vogel *et al.*, 2010)
AOC	Plant	JA biosynthesis	Plastid	RNAi	Reduced mycorrhization	(Isayenkov *et al.*, 2005)

IV. The gardener, the chemist, and the trader as desperados' serial lovers. - "Because mycorrhiza worth it":

In recent years, the expansion of legume genome data banks coupled to imaging and gene-to phenotype reverse genetic tools such as RNAi, have been proved very efficient methods to elucidate some of the plant-related protein-related mechanisms sustaining AM symbiosis development and functioning. Although expected, but likely to a lesser extent, most of the resulting data support a drastic role of membrane organogenesis and differentiation in accommodating AM fungal symbionts, through which C, Pi and N turned out to play unsuspected decisive roles. Likewise, despite the multinucleate nature of AM fungi and the recurrent absence of transformation tools, host induced gene silencing succeeded for the first time in silencing fungal gene expression *in planta*, thus unlocking a methodological bottleneck in deciphering the functional pertinence of Glomeromycotan fungi-gene products during AM symbiosis. In this respect, methodological refinements and future insights regarding AM fungal dependence upon plant metabolites, as above exemplified with Xyl, might help inoculum producers in optimizing an improved propagule delivery for sustainable agricultural processes. Likewise, symbiosis with AM beneficial fungi is known to promote plant fitness and help hosts to cope with biotic and abiotic stresses, a phenomenon somehow anticipated, on the basis of previous results obtained with cadmium tolerance of mycorrhizal plants (Aloui *et al.*, 2009; Aloui *et al.*, 2011), to depend upon the constitutive symbiotic protein program. Consequently, one can expect that "falling for function" might not only help in retrieving functions essential to the AM symbiotic partnership, but also in understanding the processes by which mycorrhiza turn out to be so human-friendly in relieving anthropogenic miss activities.

Acknowledgments: CA, EDG, DW and GR acknowledge financial support by the Burgundy Regional Council (PARI Agrale 8) and "Fonds National de la Recherche du Luxembourg" AFR TR-PHD BFR 08-078 The authors are grateful to H-N Truong-Cellier and D. van Tuinen for their quite kind critical reading and to Morgane who provided the integral season of her every-day favourites. GR would like to sincerely thank Silvio Gianinazzi for his initial trust and his constant human support within a ten year travel through his mycorrhizal world.

Chapter 1.2

Gel-based and gel-free quantitative proteomics approaches at a glance

Cosette Abdallah[1,2], Eliane Dumas-Gaudot[2], Jenny Renaut[1] and Kjell Sergeant[1]

[1]*Département Environnement et Agro-Biotechnologies, Centre de Recherche Public- Gabriel Lippmann, 41, rue du Brill, L-4422, Belvaux, Luxembourg.*

[2]*UMR Agroécologie INRA 1347/Agrosup/Université de Bourgogne, Pôle Interactions Plantes Microorganismes ERL 6300 CNRS, BP 86510, 21065 Dijon Cedex, France.*

Abdallah *et al.*, 2012 Gel-based and gel-free quantitative proteomics approaches at a glance. *International Journal of Plant Genomics* (accepted)

Abstract

Two-dimensional gel electrophoresis (2-DE) is widely applied and remains the method of choice in proteomics; however, pervasive 2-DE-related concerns undermine its prospects as a dominant separation technique in proteome research. Consequently, the state-of-the-art shotgun techniques are slowly taking over and utilising the rapid expansion and advancement of mass spectrometry (MS) to provide a new toolbox of gel-free quantitative techniques. When coupled to MS, the shotgun proteomic pipeline can fuel new routes in sensitive and high-throughput profiling of proteins, leading to a high accuracy in quantification. Although label-based approaches, either chemical or metabolic, gained popularity in quantitative proteomics because of the multiplexing capacity, these approaches are not without drawbacks. The burgeoning label-free methods are tag-independent and suitable for all kind of samples. The challenges in quantitative proteomics are more prominent in plants due to difficulties in protein extraction, some protein abundance in green tissue and the absence of well-annotated and completed genome sequences. The goal of this perspective assay is to present the balance between the strengths and weaknesses of the available gel-based and -free methods and their application to plants. The latest trends in peptide fractionation amenable to MS analysis are as well discussed.

Abdallah *et al.*, 2012 Gel-based and gel-free quantitative proteomics approaches at a glance. *International Journal of Plant Genomics* (accepted)

1- Introduction

"*In the wonderland of complete sequences, there is much that genomics cannot do, and so the future belongs to proteomics, the analysis of complete complements of proteins*" (Fields, 2001).

Originally coined by Marc Wilkins in 1995, proteomics by name is now over 15 years old. The term "proteome" refers to the entire PROTEin complement expressed by a genOME (Wilkins *et al.*, 1996). Proteomics is thus the large-scale analysis of proteins in a cell, tissue or whole organism at a given time under defined conditions. The cutting-edge proteomics techniques offer several advantages over genome-based technologies as they directly deal with the functional molecules rather than genetic code or mRNA abundance. Even though there is only one definitive genome of an organism, it codes for multiple proteomes since the accumulation of a protein changes in relation to the environment and is the result of a combination of transcription, translation, protein turnover, and posttranslational modifications.

The field of proteomics has grown at an astonishing rate, mainly due to tremendous improvements in the accuracy, sensitivity, speed and throughput of the mass spectrometry (MS) and the development of powerful analytical software. It appears to be gaining momentum as proteomic techniques become increasingly widespread and applied to an expanding smorgasbord of biological assays. Recently, proteomics has expanded from mere protein profiling to accurate and high-throughput protein quantification between two or multiple biological samples.

Most of the early developments in quantitative proteomics were driven by research on yeast and mammalian cell lines (Schulze & Usadel, 2010). The incidence of proteomic studies on plants has increased over the past years but still lags behind human and animal proteomics, moreover model organisms and cash crops (e.g., *Arabidopsis* and rice) continue to be dominant in the plant proteomic literature. Most quantitative proteomic techniques used for human, animal or other eukaryotic organisms can essentially also be employed for plant systems but plants, possessing distinct properties with regard to their genome, physiology, and culture, can impose high demands on proteomic sample handling. However, these advanced strategies have helped and facilitated the study of plant proteins and many new reports on differential

Abdallah *et al.*, 2012 Gel-based and gel-free quantitative proteomics approaches at a glance. *International Journal of Plant Genomics* (accepted)

expression, as well as global and organellar proteomic elucidation, have been put forth.

Quantitative proteomic approaches can be classified as either gel-based or gel-free methods as well as "label-free" or "label-based", of which the latter can be further sub-divided into the various types of labelling approaches such as chemical and metabolic labelling. In the present work, the thorough description and current status of commonly used gel-based and -free proteomic methodologies is provided. An overview of their suitability, potential and bottleneck applications in plant proteomics is discussed.

2- Gel-based proteomics

"Electrophoresis today and tomorrow: helping biologist's dreams come true" (Kleparnik & Bocek, 2010)

2.1- Two-dimensional gel electrophoresis (2-DE): the workhorse of proteomics

Since it was first introduced in 1975 (O'Farrell, 1975), 2-DE has evolved at different levels and became the workhorse of protein separation and the method of choice for differential protein expression analysis. Proteins first undergo isoelectric focusing (IEF) based on their net charge at different pH values and in the orthogonal second dimension further separation is performed based on the molecular weight (MW). This technique has an excellent resolving power and today, it is possible to visualize over 10,000 spots corresponding to over 1,000 proteins, multiple spots containing different molecular forms of the same protein, on a single 2-DE gel (Schulze & Usadel, 2010). Due to the pivotal problem of protein solubility, the overwhelming majority of electrophoretic protein separations is made under denaturing conditions. Two types of reagents are used in 2-DE buffers to ensure protein solubility and denaturation. The first type, chaotropes (e.g., urea, thiourea) used at multimolar concentrations, is able to unfold proteins by weakening non-covalent bonds (hydrophobic interactions, hydrogen bonds) between proteins (Gordon & Jencks, 1963). The second one is ionic detergents, in which SDS (Sodium Dodecyl Sulfate) is the archetype. It is made of a long and flexible hydrocarbon chain linked to an ionic polar head. The detergent molecules will bind through their hydrophobic hydrocarbon tail to hydrophobic amino acids. This binding favours amino acid-detergent interactions over amino acid-amino acid interactions, thereby promoting denaturation. Moreover, nonionic or zwitterionic

detergents such as Triton X-100 are also used for protein solubilisation, since IEF requires low ion concentration in the sample (Vertommen *et al.*, 2011). The detection method post-gel migration is achieved either by the use of visible stains such as silver and Coomassie or fluorescent stains such as Sypro Ruby, Lava- and Deep Purple.

Nevertheless, 2-DE has lately come under assault due to its known limitations and in part to the development of alternative MS-based approaches. Some of the reasons behind this trend include issues related to reproducibility (Lilley *et al.*, 2002), poor representation of low abundant proteins (Gygi *et al.*, 2000), highly acidic/basic proteins, or proteins with extreme size or hydrophobicity (Ong & Pandey, 2001), and difficulties in automation of the gel-based techniques (Tonge *et al.*, 2001). Moreover, the co-migration of multiple proteins in a single spot renders comparative quantification rather inaccurate.

Although no technique has a better resolving power than classical 2-DE, many endeavours were made to step forward and make it suitable to study membrane proteins (Vertommen *et al.*, 2011), and to overcome the protein ratio errors due to low gel-to-gel reproducibility by the inclusion of Difference Gel Electrophoresis (2D-DIGE) (Unlu *et al.*, 1997). This technique enables protein detection at subpicomolar levels and relies on pre-electrophoretic labelling of samples with one of three spectrally resolvable fluorescent CyDyes (Cy2, Cy3 and Cy5). These dyes have an NHS-ester reactive group that covalently attaches to the ε-amino group of protein lysines *via* an amide linkage. The ratio of dye to protein is specifically designed to ensure that the dyes are limiting in the reaction and approximately cover 1-2% of the available proteins where only a single lysine per protein is labelled. Inter-gel comparability is achieved by the use of an internal standard (mixture of all samples in the experiment) labelled with Cy2 and co-resolved on the gels that each contains individual samples labelled with Cy3 or Cy5. Since every sample is multiplexed with an equal aliquot of the same Cy2 standard mixture, each resolved feature can be directly related to the Cy2-labelled internal standard, and ratios can be normalized to all other ratios from other samples and across different gels. This can be done with extremely low technical variability and high statistical power (Alban *et al.*, 2003; Friedman *et al.*, 2004; Karp & Lilley, 2009).

For quantitative analysis, imaging software is required to align gel spots and measure their intensities. To this end, gels need to be digitalised either by using a scanner recording light transmitted through or reflected from the stained gel or fluorescent scanner. The images are subsequently imported into dedicated commercially available 2-DE image analysis softwares such as DeCyder (GE Healthcare), Proteomweaver (Bio-Rad), PDQuest (Bio-Rad), and Progenesis Same Spots (Nonlinear Dynamics). Most of these analysis software tools are user-friendly and allow (i) image alignment and spot matching across the gels, (ii) normalization, background adjustment and noise removal, (iii) spot detection, (iv) quantification by calculation of the spot volumes and statistical analysis to highlighting differentially-present proteins. Background cleaning allows the enhancement of the protein signal and distinguishes the noise from a spot. The global background correction consists of subtraction of all pixels below a set threshold of the maximum intensity. For matching, typically a reference gel is chosen and all gels are then automatically matched to the master one. Matching represents the most laborious step since frequent mistakes are made due to gel-to-gel and spot migration variability. Therefore, user intervention is needed to manually correct the software and improve the accuracy in spot matching. The quantification is performed through a summation of the pixel intensities localized within the defined spot area. The softwares use multivariate statistical packages such as ANOVA (Analysis of Variance) based on spot size and intensity, spots are then assigned to *p*-values, fold changes between groups. Most packages furthermore apply FDR (False Discovery Rates) or *q*-values to avoid the wrongful assignment of significant changes. PCA (Principle Component Analysis) is also often carried out. These available statistical tests make the 2-DE analyses and quantification more straightforward. However, the challenges associated with computational 2-DE analysis are technical problems such as experimental variation between gels and a high probability of piling several proteins under one spot.

Gel-based proteomics has so far been the main approach used in plant proteomics. 2D-DIGE has been successfully applied to investigate symbiosis- and pathogenesis-related protein in *Medicago truncatula* (van Noorden *et al.*, 2007; Schenkluhn *et al.*, 2010) and to study the impact of abiotic stresses such as drought in oak (Sergeant *et al.*, 2011), frost in *Arabidopsis* (Li *et al.*, 2011), ozone and heavy metals in poplar

(Kieffer *et al.*, 2008; Durand *et al.*, 2010; Bohler *et al.*, 2011).

2.2- Electrophoretic separations of native proteins

In their endeavour to study the protein complexes of the respiratory chain of mitochondria, Schägger and von Jagow developed a gel-based system able to separate protein complexes involved in oxidative phosphorylation in their native state (Schagger & von Jagow, 1991). This technique enables the separation of protein complexes under native conditions followed by the separation of individual proteins under denaturing conditions, thereby providing insight into the stoichiometry of the complexes. A charge-shifting agent, the dye Coomassie Brilliant Blue G-250, is added to the cathode buffer in order to stick to proteins conferring a uniform electric charge without unfolding the protein structure. Thus, intact protein complexes can be separated on a non-denaturing gradient gel roughly according to their MW, but the size and shape of each complex also influences how far that complex migrates into the gel. The gel lane is then cut out and separated on a second gel, orientated perpendicularly to the first axis of separation. This second dimension, a classic SDS-PAGE, is performed to separate the component proteins of each complex according to their MW. Blue Native-PAGE (BN-PAGE) studies were mainly focused on the analysis of electron transfer chain complexes in plastids and mitochondria; the potential application of this technique in plant proteomics was previously discussed and reviewed (Eubel *et al.*, 2005). More recently, this strategy was used efficiently to analyze the proteome of wheat chloroplast protein complexes (Meng *et al.*, 2011). BN-PAGE was highly linked to membrane proteomics showing a deep interest to improve the hydrophobic proteome coverage of gel-based approaches (Kota & Goshe, 2011).

BN-PAGE appears to be unsuitable to resolve small protein complexes (<100 kDa) due to the small separation distance of the first gel step, nevertheless a protocol for bacteria and eukaryotic cells allowing the identification of complexes in the range of 20-1,300 kDa was recently reported (Lasserre & Menard, 2012). However, distinct complexes of similar molecular masses may co-migrate and the constitutive proteins appear then to be present in the same complex. Despite the trick of the use of a charge-shifting agent, BN-PAGE is difficult to optimize and it is quite common to observe some trailing of the bands, which indicates insufficient protein solubilisation.

To improve the resolution, three-dimensional electrophoresis can be performed, combining 2 variants of native electrophoresis in the first and second dimension and SDS-PAGE in the third dimension (Vertommen *et al.*, 2011).

2.3- One-dimensional gel electrophoresis (1-DE): the birth of proteomics

Soon after its inception, one-dimensional gel electrophoresis (1-DE) became the most popular method for at least two purposes: fast determination of protein MW and assessing the protein purity. Today, this widespread technique is used for many applications: comparison of protein composition of different samples, analysis of the number and size of polypeptide subunits, Western blotting coupled to immuno-detection, and, of course, as a second dimension in 2-DE maps.

Taking advantage of both gel-based protein and gel-free peptide separation properties 1-DE is, nowadays, coupled to subsequent analysis in liquid chromatography (LC) prior to MS. After protein separation on SDS gel, the entire gel lane is excised and divided into slices prior to the proteolytic digestion. Afterwards, peptide fractions are subjected to a second separation in LC prior to MS/MS analysis. The main advantages of this technique are the harsh ionic detergent use of the SDS that ensures protein solubility during the size-separation step and the reduced sample complexity prior to LC which renders the chance of identifying low abundant proteins higher. Recently comparisons of 1-DE-LC approach to other fractionation methods (e.g., cation exchange, isoelectric focusing, etc.) at both protein and peptide level, demonstrated its superior performance and higher proteome coverage (Hahne *et al.*, 2008; Fang *et al.*, 2010; Piersma *et al.*, 2010). Thus, by increasing the solubility (the major bottleneck in protein separations) and dwindling the complexity of the system by cutting the protein gel lane, 1-DE coupled to LC/MS analysis represents an attractive technique in proteomics studies. In plants 1-DE-LC-MS/MS approach has been broadly applied, as an example the study on *M. truncatula* plasma membrane changes in response to arbuscular mycorrhizal symbiosis (Valot *et al.*, 2006) and on *Arabidopsis thaliana* chloroplast envelope (Froehlich *et al.*, 2003). Lately, this approach has also been used for the compilation of a protein expression map of the *Arabidopsis* root providing the identity and cell type-specific localization of nearly 2,000 proteins (Petricka *et al.*, 2012).

3- Proteomics: from gel-based to gel-free techniques

"A la carte proteomics with an emphasis on gel-free techniques"(Gevaert *et al.*, 2007).

Two-dimensional gel electrophoresis is a now a mature and well-established technique, however it suffers from some ongoing concerns regarding quantitative reproducibility and limitations on the ability to study certain classes of proteins. Therefore in recent years, most developmental endeavours have been focused on alternative approaches, such as promising gel-free proteomics. With the appearance of MS-based proteomics, an entirely new toolbox has become available for quantitative analysis. In shotgun proteomics (bottom-up strategy) complex peptide fractions, generated after protein proteolytic digestion, can be resolved using different fractionation strategies, which offer high-throughput analyses of the proteome of an organelle or a cell type and provide a snapshot of the major protein constituents.

Although these novel approaches were initially pitched as replacements for gel-based methods, they should probably be regarded as complements to rather than replacements of 2-DE. There are many points of comparison and contrast between the standard 2-DE and shotgun analyses, such as sample consumption, depth of proteome coverage, analyses of isoforms and quantitative statistical power. Both platforms have the ability to resolve hundreds to thousands of features, so the choice between the different platforms is often determined by the biological question addressed. Currently there is no single method, which can provide qualitative and quantitative information of all protein components of a complex mixture. Ultimately, these approaches are both of great value to a proteomic study and often provide complementary information for an overall richer analysis.

4- Peptide fractionation procedures

"*The introduction of multidimensional peptide resolving techniques is of unquestionable value for the characterization of complex proteomes*" (Manadas *et al.*, 2010).

Since there is no method or instrument that is capable of identifying and quantifying the components of a complex sample in a single-step operation, there is ample evidence that high dimensional fractionation is required for deep exploration of complex proteomes and low abundant proteins. The basic principle of

multidimensional fractionation is to separate peptides according to various orthogonal physicochemical properties and/or affinity interactions, resulting in much less complex fractions. There are numerous methodologies of separation available that can be used in tandem to perform a reduction in sample complexity. Each method has its own merits and drawbacks, therefore, the downstream needs of the workflow determine the optimal method for sample analysis.

4.1- Ion-exchange chromatography (IEC)

This type of chromatography involves peptide separation according to their electric charge. In cation-exchange chromatography (CX), negative functional groups attract positively charged peptides at acidic pH, while in anion-exchange chromatography (AX), positive functional groups have affinity for negatively charged peptides at basic pH. Strong cation-exchange chromatography (SCX) encompasses a strong exchanger group that can be ionised over a broad pH range. For peptide separation using SCX columns, the peptide mixture is loaded under acidic conditions so that the positively charged peptides bind to the column. By increasing the salt concentration, peptides are displaced according to their charge, while by applying a pH gradient, peptides are resolved according to their isoelectric point (pI). Thus, positively charged peptides bind to the SCX column when the actual buffer pH is lower than their pI.

4.2- Reversed-phase chromatography (RP)

This most widespread LC-method applied in proteomics allows neutral peptide separation according to their hydrophobicity. The separation is based on the analyte partition coefficient between the polar mobile phase and the hydrophobic (non-polar) stationary phase. The trapped peptides are then eluted using an organic phase gradient, usually acetonitrile. The ion-pair chromatography relies upon the addition of ionic compounds to the mobile phase to promote the formation of ion pairs with charged analytes. These reagents are comprised of an alkyl chain with an ionisable terminus. The introduction of ion pair-reagents increased the retention of charged analytes and improved peak shapes. Trifluoroacetic acid (TFA) and formic acid (FA) have been extensively used as ion-pairing reagents (Manadas *et al.*, 2010).

4.3- Two-dimensional liquid chromatography (2D-LC)

Multidimensional analytical methods, having orthogonal separation power, are required to reduce sample complexity and increase the proteome coverage. The

separation of peptide mixtures by 2D-LC has been performed using several orthogonal combinations such as AX coupled to RP (AX/RP), size exclusion chromatography coupled to RP (SEC/RP), and affinity chromatography coupled to RP (AFC/RP). In most shotgun proteomic analyses, the second dimension is performed by RP because the mobile phase is compatible with MS (Fournier *et al.*, 2007).

It has been shown that SCX is an excellent match to RP for multidimensional proteomic separations. In offline mode, the eluted fractions of the first dimension (SCX) are collected and then subjected to the second dimension (RP). Online approaches are faster with less sample loss due to the direct coupling of the two dimensions. In Multidimensional Protein Identification Technology (MudPIT) the SCX and RP stationary phase are packed together in the same microcapillary column. It was developed in the Yates laboratory and the results showed a high number of protein identifications, including low abundant ones (Washburn *et al.*, 2001). This technology shows a good separation power and presents a prime example of the enhanced proteome coverage in bottom-up proteomic approaches (Mathy & Sluse, 2008). Several studies employed MudPIT in plant proteomics and its usage in this field was been previously reviewed (Park, 2004; Jorrin *et al.*, 2007).

4.4- OFFGEL electrophoresis (OGE)

The recently developed OFFGEL fractionator allows liquid phase peptide IEF. The separation is carried out in a two-phase system with an upper liquid phase, containing carrier ampholites and buffer-free solution, divided into 12 or 24 compartments and a lower phase, which is the IPG strip (Horth *et al.*, 2006). After sample loading into the wells and application of a voltage gradient, peptides migrate through the IPG strip until they reach their pI at a given compartment. After IEF, peptides can be easily recovered in solution for further analysis. OGE has high loading capacity and resolution power (Horth *et al.*, 2006). Unlike LC fractionation, OGE provides additional physiochemical information such as peptide pI, which is a highly valuable tool to corroborate MS results, sort false positive rates, and increase the reliability of the identification procedure. While a study comparing MudPIT to OGE fractionation for the high-resolution separation of peptides revealed comparable results using both platforms (Elschenbroich *et al.*, 2009), others showed that the IPG as a first dimension separation strategy is superior to SCX with a salt gradient (Essader *et al.*, 2005) or pH

gradient (Manadas *et al.*, 2009) for the analysis of complex mixtures. In contrast, Yang and co-workers reported that RP-LC offered better resolution and yielded more unique peptide and protein identifications in comparison to OGE in proteomic analysis of differentially expressed proteins in long term cold storage of potato tubers (Yang *et al.*, 2011). During the last few years the use of OGE in plant proteomics has increased. Its unprecedented application allowed the recovering of wheat soluble proteins extracted from leaves (Vincent, 2011). OGE was furthermore compared to classical IEF on microsomal fractions of 5 plant species. OGE performed slightly better in the identification of proteins with transmembrane domains and significantly increased the number of proteins in the alkaline range (Meisrimler & Luthje, 2012). Finally, this technique has also been used on microsomal proteins extracted from *M. truncatula* roots to investigate the iTRAQ labelling effect on peptide isoelectric point and thus their focusing behaviour in OGE (Abdallah *et al.*, 2012).

The long running time of OGE (which varies from few hours to 2-3 days) in comparison with other offline technique was the main disadvantage associated to this novel technique.

5- MS-based quantitation

"Mass spectrometry-based proteomics turns quantitative" (Ong & Mann, 2005).

In the last decade, MS has known a tremendous progress in proteomics and has increasingly established itself as a key tool for the analysis of complex protein samples notably after the availability of protein sequence databases and the development of more sensitive and user-friendly MS equipment (Aebersold & Mann, 2003). A new toolbox of label-based and label-free quantitative proteomic methods is currently available. "To label or not to label", to answer this question and select the appropriate quantitative approach some considerations should be taken into account. Different proteomic approaches vary in their sensitivity, and the variability of each method should be defined *a priori* together with the workflow and sample-specific characteristics (Cairns, 2011). The number of biological and technical replicates is also critical, the greater the number of replicates, the more representative the results will be for the general population. Several studies have focused on the comparison of label-based and label-free methods for quantitative proteomics and the results showed that

there is no superiority and that the accuracy of the acquired results depends on the experimental set-up (Filiou *et al.*, 2012).

6- Overview of label-based proteomic approaches

"Stable isotope methods for high-precision proteomics" (Schneider & Hall, 2005).

The labelling methods for relative quantification studies can be classified into two main groups: chemical isotope tags and metabolic labelling. These approaches are based on the fact that both labelled and unlabelled peptides exhibit the same chromatographic and ionisation properties but can be distinguished from each other by a mass-shift signature. In metabolic labelling, the label is introduced to the whole cell organism through the growth medium, while in chemical labelling, proteins or peptides are tagged through a chemical reaction (Schulze & Usadel, 2010).

6.1- Chemical labelling

6.1.1- Proteolytic labelling

^{18}O stable-isotope labelling is a simple, fast, and reliable method that takes place during proteolytic digestion in presence of heavy water ($H_2{}^{18}O$) (Yao *et al.*, 2001). Samples undergo enzymatic digestion either in presence of $H_2{}^{16}O$ (unlabelled sample) or $H_2{}^{18}O$ (labelled sample). The natural catalytic activity of serine proteases (e.g., trypsin, Lys-C, Arg-C) can exchange both C-terminal oxygen atoms with a "heavy" ^{18}O from water in the surrounding solution. The first ^{18}O atom is introduced upon the cleavage of the peptidic amide bond, while the second ^{18}O atom is introduced when the cleaved peptide is bound to the enzyme as an reaction-mechanism intermediate (Table 1.2). The resulting peptides, 2 or 4 Da heavier than their unlabelled counterparts, are pooled with the unlabelled peptide mixture and peak intensities of the isotopic envelopes are compared, which can be resolved in medium-high resolution mass spectrometers (Stewart *et al.*, 2001). Trypsin-catalyzed ^{18}O isotopic labelling has not often been used in plant proteomics and only one application was found (Table 1.3). Nelson and co-authors has used ^{18}O isotopic labelling for relative quantification of the degree of enrichment of *Arabidopsis* plasma membrane proteins (Nelson *et al.*, 2006). The main drawback of this technique, despite optimization by Staes *et al.* (Staes *et al.*, 2004)**,** is that the exchange reaction is rarely complete for all peptides, resulting in a complex isotopic pattern due to the overlap of the unlabelled, singly and doubly labelled peptides.

Table 1.2: The various available isotopic labels, their sites of labelling and structures.

Label	Modified site	Structure
^{18}O One atome of ^{18}O is introduced by the reaction cleaving the peptide bond. A second ^{18}O is introduced by repeated binding/hydrolysis cycles with the proteolytic peptide fragment as a pseudosubstrate (Yao *et al*., 2001)	^{18}O incorporation at lysine and arginine *via* trypsin during the proteolytic digestion	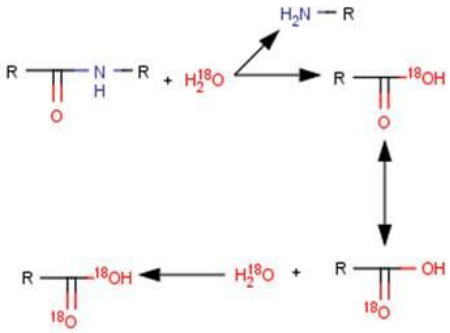
ICAT Isotope-Coded Affinity Tags (Gygi *et al*., 1999)	Thiol group	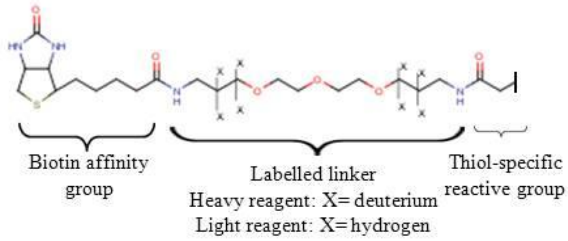
ICPL Isotope-Coded Protein Labelling (Schmidt *et al*., 2005)	Free amino group	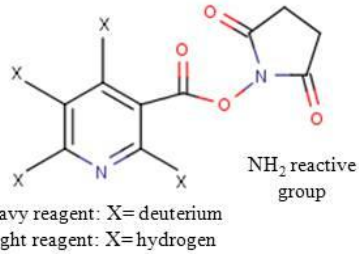

Abdallah *et al*., 2012 Gel-based and gel-free quantitative proteomics approaches at a glance. *International Journal of Plant Genomics* (accepted)

Label	Modified site	Structure
iTRAQ isobaric Tags for Relative and Absolute Quantification (Ross *et al.*, 2004)	Peptide N-termini and ε-amino group of lysine	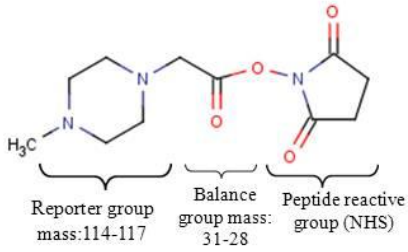
TMT Tandem Mass Tag (Thompson *et al.*, 2003)	Free amino group	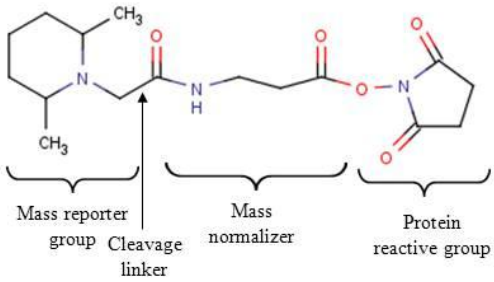
SILAC Stable Isotopic Labelling with Amino Acids in Cell Culture (Mann, 2006)	Metabolic incorporation of lysine or arginine	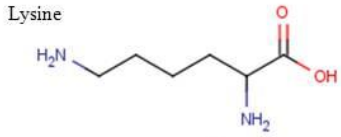 Heavy lysine: 6x ^{13}C

6.1.2- Isotope-Coded Affinity tags (ICAT)

One of the first labels used for differential isotope labelling consists of three functional elements: a specific chemical reactive group that binds to sulfhydryl groups of cysteinyl residues, an isotopically coded linker with light or heavy isotopes, and a biotin tag for affinity purification (Table 1.2) (Gygi *et al.*, 1999). The proteins containing cysteine residues are labelled either with light or heavy isotopes, where the latter form has eight ^{13}C atoms. Afterwards, light and heavy labelled samples are pooled and proteolytically cleaved. Subsequently, the complexity of the sample is reduced prior to MS-analysis through the purification of tagged cysteine-containing peptides by affinity chromatography using biotin-avidin affinity columns. Peptide pairs with 8 Da mass-shifts are detected in MS scans and their ion intensities are compared for relative quantitation. ICAT labelling takes place at the protein level allowing samples to be pooled prior to protease treatment, thus eliminating vial-to-vial

variations. However, cysteine is not very abundant and approximately one in seven proteins do not contain this amino acid, greatly reducing the completeness of the study (Thelen & Peck, 2007).

In plants, Dunkley and co-workers have studied the localization of organelle proteins by isotope tagging (LOPIT) to discriminate endoplasmic reticulum, Golgi, plasma membrane, and mitochondria or plastids proteins in *Arabidopsis*. This technique involves partial separation of the organelles by density gradient centrifugation followed by the analysis of protein distributions in the gradient by ICAT and MS (Dunkley *et al.*, 2004). Taking advantage of the ICAT labelling specificity to cysteinyl groups, this approach was used to study the redox-status of proteins allowing a quantitative analysis of the redox proteome and ozone stress in plants (Stroher & Dietz, 2006; Hagglund *et al.*, 2008; Miles *et al.*, 2009; Hagglund *et al.*, 2010). To increase the functional information about S-nitrosylation sites in plants, Fares and colleagues combined both "biotin-switch" method (BSM) and ICAT labelling, and succeeded in identifying 53 endogenous nitrosocysteines in *Arabidopsis* cells (Fares *et al.*, 2011). ICAT was also used to identify wheat seed proteins and to understand their interactions and expression in relation to chromosome deletion, which were reported to be difficult by 2-DE due to co-synthesis of proteins by genes from three genomes, A, B and D (Islam *et al.*, 2003). A cross-comparison of gel-based and -free quantitative methods (2-DE, ICAT, and label-free) was performed by analysing the differential accumulation of maize chloroplast proteins in bundle sheath versus mesophyll cells. Among the 125 chloroplast proteins quantified in the 3 methods, only 20 proteins were quantified in common, demonstrating the complementary nature of these quantitative approaches (Majeran *et al.*, 2005). More applications of ICAT quantitative approach in plant proteomics are listed in Table 1.3.

6.1.3- Isotope-Coded Protein Labelling (ICPL)

This approach termed ICPL is based on isotopic labelling of all free amino groups in proteins. Two protein mixtures are reduced and alkylated to ensure easier access to free amino groups that are subsequently derivatised with the deuterium-free (light) or 4 deuterium containing (heavy) form, respectively (Table 1.2). Light and heavy labelled samples are then mixed, fractionated, and digested prior to high throughput MS analysis. Since peptides of identical sequence derived from the two differentially

labelled protein samples differ in mass (4 Da), they appear as doublets in the acquired MS-spectra. From the ratios of the ion intensities of these sister peptide pairs, the relative abundance of their parent proteins in the original samples can be determined (Schmidt *et al.*, 2005). Recently, a detailed experimental protocol called post-digest ICPL was published highlighting a better protein identification and quantification (Fleron *et al.*, 2010; Leroy *et al.*, 2010) and when compared to iTRAQ, both techniques have shown comparable number of identified and quantified proteins in the endosperm of castor bean seeds at three developmental stages (Nogueira *et al.*, 2012). So far, the latter study is the unique reported quantitative proteomic investigation on plants using ICPL (Table 1.3). The main drawback of this method is the isotopic effect of deuterated tags that interferes with retention time of the labelled peptides during LC (Brunner *et al.*, 2010).

6.1.4- Isobaric Tags for Relative and Absolute Quantification (iTRAQ)

Unlike ICAT and ICPL, iTRAQ tags are isobarics and primarily designed for the labelling of peptides rather than proteins. The overall molecule mass is kept constant at 145 Da and 304 Da for iTRAQ-4plex and -8plex, respectively. The structure of the iTRAQ-8plex balancer group has not been published while the iTRAQ-4plex molecule consists of a reporter group (based on *N*-methylpiperazine), a mass balance group (carbonyl), and a peptide reactive group (NHS ester) (Table 1.2) (Ross *et al.*, 2004). The iTRAQ reagents label peptide N-termini and ε-amino groups of lysine side chains and allow comparison of up to eight samples in the same experiment. Another difference from the pre-cited methods is that the quantification occurs in MS/MS scans after peptide fragmentation. In fact, iTRAQ labelled peptides appear as a single unresolved precursor at the same *m/z* in the MS spectrum. Upon peptide fragmentation, the iTRAQ labels fragment to produce reporter ions in a "silent region", usually unpopulated, at low *m/z* range (e.g., 114-121). Measurements of the reporter ion intensities enable relative quantification of the peptide in each sample.

This method has quickly gained popularity in proteomics and benefits from increased MS sensitivity compared to for instance ICAT due to the contribution of all samples to the precursor ion signal. The iTRAQ reagent was furthermore reported to increase the number of lysine-terminated tryptic peptides identified by database searches to equivalence with arginine-terminated peptides (Ross *et al.*, 2004). Ow and co-authors

evaluated iTRAQ relevance, accuracy, and precision for biological interpretation and entitled their verdict "the good, the bad and the ugly" of iTRAQ quantitation (Ow *et al.*, 2009). "The good" is the potential of iTRAQ to provide accurate quantification spanning two orders of magnitude. However, that potential is limited by two factors: isotopic impurities "the bad", and peptide co-fragmentation (inadvertently selecting two or more closely spaced peptides for MS/MS instead of one) "the ugly" (Perkel, 2009). In the same study, a putative contamination of the reporter ion region with the second isotope of the phenylalanine immonium ion on the 121 *m/z* peak, which can interfere with peptide quantification was mentioned (Ow *et al.*, 2009).

The iTRAQ has shown a high utility in large-scale quantitative proteomics (Table 1.3) to study plant responses to pathogens: *Pseudomonas syringae* in *Arabidopsis* (Kaffarnik *et al.*, 2009), *Lobesia botrana* and *Erysiphe necator* in grape (Marsh *et al.*, 2010; Melo-Braga *et al.*, 2012), *Huanglongbing* in sweet orange (Fan *et al.*, 2011), *Fusarium graminearum* in maize (Mohammadi *et al.*, 2011). Quantitative shotgun proteomic approaches using iTRAQ were furthermore used for characterizing the differential phosphorylation of *Arabidopsis* in response to microbial elicitation (Jones *et al.*, 2006) and the study of protein degradation in chloroplasts (Rudella *et al.*, 2006). The potency of iTRAQ was used for better understanding mechanisms of plant tolerance to boron in barley (Patterson *et al.*, 2007), cadmium in barley (Schneider *et al.*, 2009) and *Brassica juncea* (Alvarez *et al.*, 2009), and cold in potato and rice (Neilson *et al.*, 2011b; Yang *et al.*, 2011). An example of iTRAQ application in plant membrane proteomics is the study of differentiated state of bundle sheath and mesophyll chloroplast thylakoid and envelope membrane proteomes in maize (Majeran *et al.*, 2008).

6.1.5- Tandem Mass Tag (TMT)

A novel MS/MS-based quantitative method using isotopomer labels, similar to iTRAQ, and referred as "tandem mass tags" (TMT) was recently developed (Table 1.2) (Thompson *et al.*, 2003). Both techniques share several common features: (i) these reagents employ *N*-hydroxy-succinimide (NHS) chemistry that permits specific tagging of primary amino groups. (ii) They were designed to allow multiplexing of several samples by chemical derivatization with different forms of the same isobaric tag that appear as a single peak in full MS scans. (iii) The release of "daughter ions" in

MS/MS analysis (between 126 and 131 Da for TMT) that can be used for relative quantification. The cysteine-reactive TMT (cysTMT) reagents enable selective labelling and relative quantitation of cysteine-containing peptides from up to six biological samples. This technique has been used for the redox proteomic analysis of the tomato leaves in response to the pathogen *P. syringae* pv. tomato strain DC3000 (Table 1.3) (Parker *et al.*, 2012). Aside from this study, TMT labelling approach has so far not been fully exploited for the analysis of plant proteomes.

A study comparing TMT and iTRAQ showed that the performance of both techniques was similar in terms of quantitative precision and accuracy, however the number of identified peptides and proteins was higher with iTRAQ 4-plex compared to TMT 6-plex (Pichler *et al.*, 2010).

6.2- Metabolic labelling

Although chemical labelling presents a wide range of approaches for quantitative proteomics, this group of techniques suffers from sample variability and induces a technical bias since the labelling occurs after the protein extraction or even after proteolytic digestion. In addition, the high cost of these reagents can be a limiting factor for large-scale experiments. Therefore metabolic labelling, which allows protein labelling at the time of protein synthesis, presents a valuable alternative strategy for quantitative proteomics.

6.2.1- Stable Isotopic Labelling with Amino Acids in Cell Culture (SILAC)

In vivo metabolic labelling, in which two populations of cells are cultured either in a medium containing a “light” (unlabelled) amino acid or encompassing a “heavy” (labelled), one typically arginine or lysine labelled with ^{13}C and/or ^{15}N are used (Mann, 2006). The mass shift induced by the incorporation of the heavy amino acid into a peptide, is known and allows comparison between a peptide in both samples (e.g., 6 Da in the case of $^{13}C_6$-Lys, Table 1.2). Samples are then combined prior to protein extraction, which minimizes technical variation arising during sample processing. In MS spectra, each peptide appears as a pair and the ratio of peak intensities yields the protein abundance in the sample since the light and heavy amino acids are chemically identical and only isotopically distinguished.

Although probably the most general and global labelling strategy, SILAC appears less suited for quantitative proteomic studies in plants. Being autotrophic organisms, plants

are metabolic specialists capable of synthesising all amino acids from inorganic nitrogen, and therefore, have lower incorporation efficiency of the exogenously supplied labelled amino acids. The labelling efficiency achieved using exogenous amino acid feeding of *Arabidopsis* cell cultures has been found to average only 70–80% (Gruhler *et al.*, 2005). Considering these limitations and the high cost of isotopically labelled amino acids, SILAC appears likely to be inadequate for quantitative proteomics studies in plants; albeit it seems less restricted to study algae such as *Chlamydomonas reinhardtii* and *Ostreococcus tauri* (Table 1.3) (Naumann *et al.*, 2007; Martin *et al.*, 2012; Mastrobuoni *et al.*, 2012).

6.2.2- $^{14}N/^{15}N$ labelling

In this method, the label is introduced to the whole cell or organism through the growth medium. Samples can easily be labelled metabolically *via* growth media containing ^{15}N-labelled inorganic salts, typically $K^{15}NO_3$ (Ippel *et al.*, 2004). The quantification process is based on the intensity of extracted ion chromatograms of survey scans containing the pair of labelled (^{15}N, heavy) and unlabelled (^{14}N, light) peptide isoforms.

Unlike SILAC, this approach achieved more than 98% incorporation in both plants (Ippel *et al.*, 2004) and cell cultures (Engelsberger *et al.*, 2006), and is more efficient at allowing large-scale quantitative analysis. The trade-off is that all amino acids will incorporate the label, thus the mass shift will be peptide-sequence dependent. Metabolic ^{15}N-labelling is becoming the method of choice for quantitative proteomics in plant studies (Table 1.3). It was used to study plant membrane proteome changes in response to cadmium and cryptogenin elicitor in *Arabidopsis* and tobacco cells, respectively (Lanquar *et al.*, 2007; Stanislas *et al.*, 2009). Such a quantitative proteomic strategy was applied in quantitative phosphoproteomics to study differentiated proteins in response to fungal or microbial elicitors in *Arabidopsis* cells (Benschop *et al.*, 2007). Moreover, other metabolic labelling strategies have been developed such as Hydroponic Isotope Labelling of Entire Plants (HILEP) which has proven to be very efficient and robust method to completely label the whole mature plants. Nearly 100% of ^{15}N-labelling efficiency was achieved in *Arabidopsis* plants by growing them in hydroponic media containing 2.5 mM ^{15}N potassium nitrate and 0.5 mM ^{15}N ammonium nitrate (Palmblad *et al.*, 2007a; Bindschedler *et al.*, 2008). A

similar quantitative proteomic method, SILIP (Stable Isotope Labelling In Planta), was developed for labelling tomato plants growing in sand in a greenhouse environment (Schaff *et al.*, 2008). An alternative strategy for quantitative proteomics that relies upon the subtle changes in isotopic envelope shape resulting from partial metabolic labelling to compare relative abundances of labelled and unlabelled peptides has been developed in *Arabidopsis*. Both partial and full labelling have been proven to be comparable with respect to dynamic range, accuracy and reproducibility, and both are suitable for quantitative proteomics characterization (Huttlin *et al.*, 2007).

7- Label-free quantitative proteomics

"Comparative LC-MS: a landscape of peaks and valleys" (America & Cordewener, 2008).

"Less label, more free" (Neilson *et al.*, 2011a).

Quantitative proteomics based on stable isotope-coding strategies often require expensive labelling reagents, high amount of starting samples, multiple sample preparation steps resulting in considerable sample loss and reduced detection sensitivity. Label-free LC/MS methods represent attractive alternatives (Lundgren *et al.*, 2010) since they are amenable to all type of biological samples, are simple, reproducible, cost effective, and less prone to errors and side reactions related to the labelling process.

Given the fact that, theoretically, the peak intensity of any ion should be proportional to its abundance the ion signals in MS have been used, for decades, as a quantification technique for small molecules in analytical chemistry. However, technical variation, at both LC and ionization levels, might render comparisons of peak intensities between experiments unreliable. The recent advances in LC/MS approaches allowed circumvention of the looming replicate biases and recently the observation of a correlation between protein abundance and peak areas (Bondarenko *et al.*, 2002; Chelius & Bondarenko, 2002) or number of MS/MS spectra (Liu *et al.*, 2004) has widened the choice of analytical procedure in the field of quantitative proteomics. The general framework of label-free quantification can be summarised as follows: for the two samples that need to be compared quantitatively, the LC-MS/MS experiment is first performed for both samples separately, and precursor ion *m/z* and retention time

(Rt) file is generated for all MS/MS spectra of each identified protein, creating a 2D map (*m/z*, Rt) allowing peptide match in several samples.

Depending on the MS acquisition mode, two analytical methods can be distinguished: the data-dependent analysis (DDA) and the data-independent analysis (DIA). DDA involves acquisition of a MS survey scan followed, for an allotted period of time, by precursor ion selection based on its intensity for subsequent fragmentation (Geromanos *et al.*, 2009). In this approach, quantification can be achieved using DDA-based spectral counting or spectral peak intensities. Venable and co-authors described DIA in which no parent ion is pre-selected; the instrument constantly operates in MS/MS mode and data acquisition of all charge states of eluted peptides is performed by rapid switching of the collision energy between low and high-energy states (Venable *et al.*, 2004).

7.1 Spectral counting

Spectral counting or peptide identification frequency is becoming popular in label-free quantification due to its simple procedure that does not require chromatographic peak integration or retention time alignment. It is based on the rationale that peptides from more abundant proteins will be more selected for fragmentation and will thus produce a higher number of MS/MS spectra. Thus, the number of MS/MS scans is tabulated and the protein abundance is inferred from the total number of MS/MS spectra that match peptides from the protein (Liu *et al.*, 2004). The ability to accurately quantify proteins by spectral counting largely depends on the number of spectra obtained and the coverage of sampling. The relative difference in protein abundance is estimated by calculating the protein abundance index (PAI), which corresponds to the number of observed peptides in the experiment divided by the number of theoretical tryptic peptides for each protein within a given mass range of the employed mass spectrometer (Rappsilber *et al.*, 2002). The exponential form of PAI minus one (10^{PAI}-1), exponentially modified Protein Abundance Index (emPAI) (Ishihama *et al.*, 2005), takes into account the fact that generally more peptides are detected for larger proteins and is directly proportional to the protein content in the sample. The absolute protein expression (APEX) index, a very similar approach to emPAI, is a derived measurement of protein abundance in a given sample based on the analytical features in mass spectrometric analysis (Lu *et al.*, 2007). It has been used to generate a protein

abundance map of the *Arabidopsis* proteome (Baerenfaller *et al.*, 2008) and to determine the abundance of stromal proteins in *A. thaliana* chloroplast (Zybailov *et al.*, 2008). Spectral counting based quantitative proteomics has been widely used in the field of plant proteomics (Table 1.3). The accuracy and reliability of label-free spectral counting in the relative quantitative analysis of soybean leaf proteome was evaluated by comparing nine technical replicates (Cooper *et al.*, 2010). Gammulla and co-authors quantified and identified temperature stress responsive proteins in rice leaves by calculating the NSAF (Normalized Spectral Abundance Factor), which is given by the total number of MS/MS spectra (SpC) identifying a protein, divided by the protein's length (L), divided by the sum of SpC/L for all proteins in the experiment (Gammulla *et al.*, 2010; Gammulla *et al.*, 2011). Spectrum counting has been used to study drought stress response in root nodules of *M. truncatula* (Larrainzar *et al.*, 2007) and in large-scale plant proteomics in response to pathogen infection in bean (*Phaseolus vulgaris*) (Lee *et al.*, 2009).

7.2- Spectral peak intensities

Other label-free methods use the signal intensities of individual peptides rather than the spectral counts to compare the relative abundance of proteins between samples (Silva *et al.*, 2005). It is based on the principle that the relative abundance of the same peptide in different samples can be estimated by the precursor ion signal intensity across consecutive LC/MS runs, given that the measurements are performed under identical conditions. In contrast to differential labelling, every biological specimen needs to be measured separately in a label-free experiment. Typically, peptide signals are detected at the MS level, their patterns are then tracked across the retention time dimension and used to reconstruct a chromatographic elution profile of the monoisotopic peptide mass. The total ion current of the peptide signal is then integrated and the measurement of the chromatographic peak areas is used as a quantitative measurement for the original peptide concentration. Profiling methods based on ion intensity were applied to define the sucrose-induced phosphorylation changes in *Arabidopsis* plasma membrane proteins (Niittyla *et al.*, 2007). It has been furthermore used to detect twelve phosphopeptides from 50 identified phosphoproteins in different amounts during the hypersensitive response in tomato plants (Stulemeijer *et al.*, 2009). Moreover, the ion intensity method was used as strategic track to study

soybean plasma membrane proteins following 24 h flooding and 48 h osmotic stress (Table 1.3) (Komatsu *et al.*, 2009; Nouri & Komatsu, 2010).

Spectral counting and spectral peak intensities were compared and results obtained from both methods are generally in good accordance (Old *et al.*, 2005; Wienkoop *et al.*, 2006) with spectral counting covering a slightly higher dynamic range and measurements of ion abundance being more accurate for the identification of protein ratios (Old *et al.*, 2005). Both techniques have also been used to investigate the major allergens in transgenic peanut lines (Stevenson *et al.*, 2009).

Unlike labelling methods, in which quantitative analyses are limited to the tagged peptides, label-free approaches offer the quantitative comparison of all peptide constituents of the sample. However, they are more susceptible to errors due to parallel sample processing and thus suffer from increased analytical variability. Therefore, label-free methods are very replicate dependent. To be statistically significant, chromatographic separation reproducibility must be very high. The high-resolution power of MS, high scanning rates, high accurate mass measurements and exact chromatogram alignment are prerequisite for the success of this quantitative technique (Silva *et al.*, 2005; Palmblad *et al.*, 2007b). The extensive workflow ranging from peptide detection, alignment, normalization, identification, quantitative comparisons and statistical analysis has triggered the development of several sophisticated software algorithms.

7.3- Data-independent analysis (DIA)

LC/MS^E, a quantitative comparison of ions emanating from identically prepared control and experimental samples, was developed by using a reproducible chromatographic separation system along with the high mass resolution and mass accuracy of an orthogonal time-of-flight mass spectrometer (Silva *et al.*, 2005). In this method, the instrument alternates between low and high collision energies in MS analysis. While the low collision energy scan mode leads to the determination of accurate precursor ion masses, the high-energy scan mode (MS^E) generates accurate peptide fragmentation data (Kota & Goshe, 2011). The use of multiplex parallel fragmentation of LC/MS^E yields uniformly product ion information of all peptides across their entire chromatographic peaks (Silva *et al.*, 2005), which provides continuous MS data throughout the entire acquisition. Product ions are time aligned

and correlated to precursor ions to generate a list of Exact Mass Retention Time (EMRT) signatures (Silva *et al.*, 2005). The integrated peak areas of EMRT are compared across different biological replicates to determine the differences in protein abundances.

The LC/MS^E approach is well suited for relative and absolute quantification (Blackburn *et al.*, 2010b) and it was shown to increase the signal-to-noise ratio by a factor 3-5 and could identify peptides undetected in a parent ion scan (Carvalho *et al.*, 2010). This recent achievement in MS-based proteomics has provided a basis to qualitatively and quantitatively assess the transition from dark to light of maize seedlings (Shen *et al.*, 2009) and to study the salicylic acid-induced changes in the *Arabidopsis* and *Apium graveolens* secretome (Cheng *et al.*, 2009; Blackburn *et al.*, 2010a). MS^E has also been implemented to study the changes in barley protein expression in response to UV-B treatment (Table 1.3) (Kaspar *et al.*, 2010).

Table 1.3: An overview of the latest MS-based quantitative proteomic studies on plant systems.
The table shows the implemented quantitative approaches, plant species, biological questions, and reference of the corresponding paper.

Quantitative approach	plant	Biological study	Authors
^{18}O labelling	*Arabidopsis thaliana*	Quantification of the degree of plasma membrane protein enrichment	(Nelson *et al.*, 2006)
ICAT	*Arabidopsis thaliana*	Localization of integral membrane proteins by using the localization of organelle proteins by isotope tagging (LOPIT)	(Dunkley *et al.*, 2004)
ICAT	*Hordeum vulgare*	Identification of specific disulfide targets of barley thioredoxin in proteins released from barley aleurone layers	(Hagglund *et al.*, 2010)
ICAT	*Arabidopsis thaliana*	Understanding of AtMPK6 role in transducing ozone-derived signals	(Miles *et al.*, 2009)
ICAT	*Arabidopsis thaliana*	Functional information about S-nitrosylation sites in plants	(Fares *et al.*, 2011)
ICAT	*Triticum aestivum*	Identification of wheat seed proteins and their related expression to chromosome deletion	(Islam *et al.*, 2003)
ICAT, 2-DE, label-free	*Zea mays*	Quantitative comparative proteome analysis of purified mesophyll and bundle sheath chloroplast stroma in maize	(Majeran *et al.*, 2005)
ICAT	*Oryza sativa*	Protein profiling of uninucleate stage rice anther and identification of the CMS-HL related proteins	(Sun *et al.*, 2009)
ICAT	*Arabidopsis thaliana*	ProCoDeS (Proteomic Complex Detection using Sedimentation) for profiling the sedimentation of a large number of proteins	(Hartman *et al.*, 2007)
ICPL, iTRAQ	*Ricinus communis*	Quantitative proteomic comparison of ICPL *vs* iTRAQ on *ricinus communis* seeds	(Nogueira *et al.*, 2012)
iTRAQ	*Solanum tuberosum*	Comparative proteomic approach of potato tubers after 0 and 5 months of storage at 5°C	(Yang *et al.*, 2011)
iTRAQ	*Arabidopsis thaliana*	Quantitative study of the secreted proteins from *Arabidopsis* cells in response to *Pseudomonas syringae*	(Kaffarnik *et al.*, 2009)
iTRAQ	*Vitis vinifera*	Comparative proteomic study of dynamic changes in control and infected *Vitis vinifera*	(Melo-Braga *et al.*, 2012)
iTRAQ	*Vitis vinifera*	Comparative analysis of differentially expressed proteins in *Erysiphe necator* infected grape	(Marsh *et al.*, 2010)
iTRAQ	*Citrus sinensis*	Comparative proteomic approach of the pathogenic process of HLB in affected sweet orange leaves	(Fan *et al.*, 2011)
iTRAQ	*Zea mays*	Proteomic approach of two maize inbreds in the early infection by *Fusarium graminearum*	(Mohammadi *et al.*, 2011)
iTRAQ	*Arabidopsis thaliana*	Changes tack of the *Arabidopsis* phosphoproteome during the defence response to *Pseudomonas*	(Jones *et al.*,

		syringae	2006)
iTRAQ	*Arabidopsis thaliana*	Investigation of the proteomic changes in the chloroplasts of clpr2-1	(Rudella *et al.*, 2006)
iTRAQ	*Hordeum vulgare*	Comparative proteomic study of boron-tolerant and -intolerant barley	(Patterson *et al.*, 2007)
iTRAQ	*Hordeum vulgare*	Quantitative proteomic approach to unravel the contribution of vacuolar transporters to Cd^{2+} detoxification	(Schneider *et al.*, 2009)
iTRAQ, 2D-DIGE	*Brassica juncea*	Quantitative proteomic approaches to understand the effect of cadmium on *Brassica juncea* roots	(Alvarez *et al.*, 2009)
iTRAQ, label-free	*Oryza sativa*	Quantitative proteomic response of rice seedling to 48, 72 and 96 h of cold stress	(Neilson *et al.*, 2011b)
iTRAQ, BN-PAGE, label-free	*Zea mays*	Comparative analysis of protein abundance in chloroplast thylakoid and envelope membrane proteomes in maize	(Majeran *et al.*, 2008)
Cys-TMT	*Solanum lycopersicum*	Study of the redoxproteomic analysis of the *Pseudomonas syringae* tomato DC3000 treated tomato leaves	(Parker *et al.*, 2012)
SILAC	*Chlamydomonas reinhardtii*	Dynamic changes of proteome turnover under salt stress	(Mastrobuoni *et al.*, 2012)
SILAC	*Ostreococcus tauri*	Quantitative proteomics on synthesis and degradation rate constants of individual proteins in autotrophic organisms	(Martin *et al.*, 2012)
SILAC	*Chlamydomonas reinhardtii*	Comparative proteomics on the iron deficiency impact in *Chlamydomonas reinhardtii*	(Naumann *et al.*, 2007)
$^{14}N/^{15}N$ labelling	*Solanum tuberosum*	Effectiveness of fully label a plant with ^{15}N isotopes	(Ippel *et al.*, 2004)
$^{14}N/^{15}N$ labelling	*Arabidopsis thaliana*	Demonstration of plant ^{15}N labelling as a powerful comparative quantitative proteomic approach	(Engelsberger *et al.*, 2006)
$^{14}N/^{15}N$ labelling	*Arabidopsis thaliana*	Comparative analysis of *Arabidopsis* cells following a cadmium exposure	(Lanquar *et al.*, 2007)
$^{14}N/^{15}N$ labelling	*Nicotiana tabacum*	Quantitative proteomic approach of the detergent-resistant membranes of tobacco cells in response to cryptogenin	(Stanislas *et al.*, 2009)
$^{14}N/^{15}N$ labelling	*Arabidopsis thaliana*	Quantitative approach of phosphorylated sites in signaling and protein response in flg22 or xylanase *Arabidopsis* treated cells	(Benschop *et al.*, 2007)
HILEP	*Arabidopsis thaliana*	Demonstration of HILEP suitability for relative plant quantitative proteomic subjected to oxidative stress	(Bindschedler *et al.*, 2008)
SILIP	*Solanum lycopersicum*	SILIP development for homogeneously ^{15}N incorporation within the whole plant proteome.	(Schaff *et al.*, 2008)

$^{14}N/^{15}N$ labelling	*Arabidopsis thaliana*	Investigation of both partial and full ^{15}N labelling effect on quantitative analysis in a complex mixture	(Huttlin *et al.*, 2007)
Spectral counting	*Arabidopsis thaliana*	Proteome map of *Arabidopsis thaliana*	(Baerenfaller *et al.*, 2008)
Spectral counting	*Arabidopsis thaliana*	Comprehensive *Arabidopsis* chloroplast proteome analysis	(Zybailov *et al.*, 2008)
Spectral counting	*Glycine max*	Evaluation of the suitability of spectral counting to quantitative soybean proteome study	(Cooper *et al.*, 2010)
Spectral counting	*Oryza sativa*	Differential proteomic response of rice leaves exposed to high- and low-temperature stress	(Gammulla *et al.*, 2010)
Peak ion intensity	*Arabidopsis thaliana*	Sucrose-induced phosphorylation changes of plasma membrane proteins in *Arabidopsis*	(Niittyla *et al.*, 2007)
Peak ion intensity	*Solanum lycopersicum*	Quantitative proteomics of phosphoproteins in tomato hypersensitive response	(Stulemeijer *et al.*, 2009)
Peak ion intensity, 2-DE	*Glycine max*	Investigation of the soybean plasma membrane function in response to flooding stress	(Komatsu *et al.*, 2009)
Spectral counting + peak ion intensity	*Medicago truncatula*	Comparison of two label-free quantitative approaches on nodule protein extracts from *Medicago truncatula*	(Wienkoop *et al.*, 2006)
Spectral counting + peak ion intensity	*Arachis hypogaea*	Investigation of major allergens in transgenic peanut lines	(Stevenson *et al.*, 2009)
MS^E	*Apium graveolens*	Analysis of the *Apium graveolens* protein response to salicylic acid	(Blackburn *et al.*, 2010b)
MS^E	*Zea mays*	Proteomic approach assessment of the transition from dark to light in maize seedlings	(Shen *et al.*, 2009)
MS^E	*Arabidopsis thaliana*	Proteomic changes in the cell wall proteome in response to salicylic acid	(Cheng *et al.*, 2009)
MS^E	*Hordeum vulgare*	Study of the UV-B irradiation effect on the barley proteome	(Kaspar *et al.*, 2010)

8- Conclusion

Proteomics, the promising new "omics", has become an important complementary tool to genomics providing novel information and greater insight into plant biology. The application of gel-based and -free proteomics methods to study plant physiology has strongly increased in recent years. Here, a broad perspective is offered on the available techniques.

So far, most quantitative plant proteomics was performed on *Arabidopsis thaliana*, the model plant due to various traits including its small (and annotated) genome size (125 MBp), short generation time, high transformation efficiency, and the large panel of available mutants. The completion of more plant genome sequencing projects such as rice, barley, tomato and *M. truncatula* is scheduled for the near future and will permit the proteome probing of these plant systems. In the meantime, extensive EST databases for numerous important crop plants represent alternative sources of sequence information to the full genome sequences. Moreover, with the technical maturity attained in MS and protein/peptide fractionation tools, comparative plant proteomics will move out of the beginner realm and emerge as high valuable discipline to enhance the comprehension of plant systems, their subcellular membranes and organelles. It is worth noting that combining multiple quantitative proteomic techniques is highly beneficial, as these approaches yield complementary datasets which improve the understanding of biological issues and provide in-depth characterization of proteins with respect to their abundance. These technical advancements coupled to well-designed experiments will significantly reveal the protein function in plant growth, development, and provide a wealth of information on plant proteome changes occurring in response to external stimuli, biotic, and abiotic stresses.

Acknowledgements

This work was supported by grants from the "Fonds National de la Recherche du Luxembourg" AFR TR-PHD BFR 08-078 and Conseil Régional de Bourgogne (PARI 20100112095254682-1). Ghislaine Recorbet and Daniel Wipf are thanked for their assistance and support.

Objectives and outline

In plants, MS-based proteomics has been largely used for protein identification while quantitative proteomics is still bourgeoning. The shotgun proteomic approaches may allow the identification of recalcitrant, membrane proteins, which could easily escape to 2-DE, and shed the light on their role in AM symbiosis. The overall work presented here aims at further revealing the membrane proteome changes in *Medicago truncatula* roots colonized by *Rhizophagus irregularis*. To this goal, a not yet implemented label-based and -free approaches on plant roots-AM fungi symbiosis, was herein applied to circumvent the 2-DE related shortcomings in order to study membrane proteins. Whatever the gel-free or gel-based proteomic approach was used, *Medicago truncatula* were cultivated in presence/absence of *R. irregularis* for four weeks. Microsomal proteins were extracted from *M. truncatula* roots by using the differential centrifugation-based strategy originally developed for *Nicotiana tabacum* cultured cells (Stanislas *et al.*, 2009). The following research framework is divided into 3 chapters as depicted in figure 1.5.

Chapter 2 deals with the first application of iTRAQ-OGE-LC-MS/MS proteomic approach on *M. truncatula* microsomal proteins. The main objective of this study is methodological. To this purpose, straightforward and iTRAQ compatible in-filter protein digestion is developed. Then, the effective resolution power of OGE fractionator in pI-based peptide separation in solution is assessed on free and iTRAQ labelled samples. Furthermore, the investigation of the iTRAQ labelling effect on peptide electrofocusing in OGE fractionator is carried out on the *M. truncatula* membrane protein digests.

This first exploratory view on iTRAQ-OGE-LC-MS/MS approach is a starting point of its further application on microsomal proteins extracted from *M. truncatula* roots to track their changes in response to AM symbiosis. Therefore, chapter 3 focuses on the ability of this method to perform comparative differential proteomic study on control and mycorrhized roots. Moreover, the enrichment of membrane protein fractions is assessed after the protein identifications to corroborate the ability of the employed fractionation protocol to recover membrane proteins.

Guided by previous results of the aforementioned method, chapter 4 encompasses the application of a label-free 1-DE-LC-MS/MS approach to have an insight view into the membrane proteome changes in response to AM symbiosis. This

chapter forms a first step towards more characterization of membrane proteins orchestrating this interaction.

Finally, chapter 5 presents the general conclusions and prospects for future proteomic research studies on AM symbiosis.

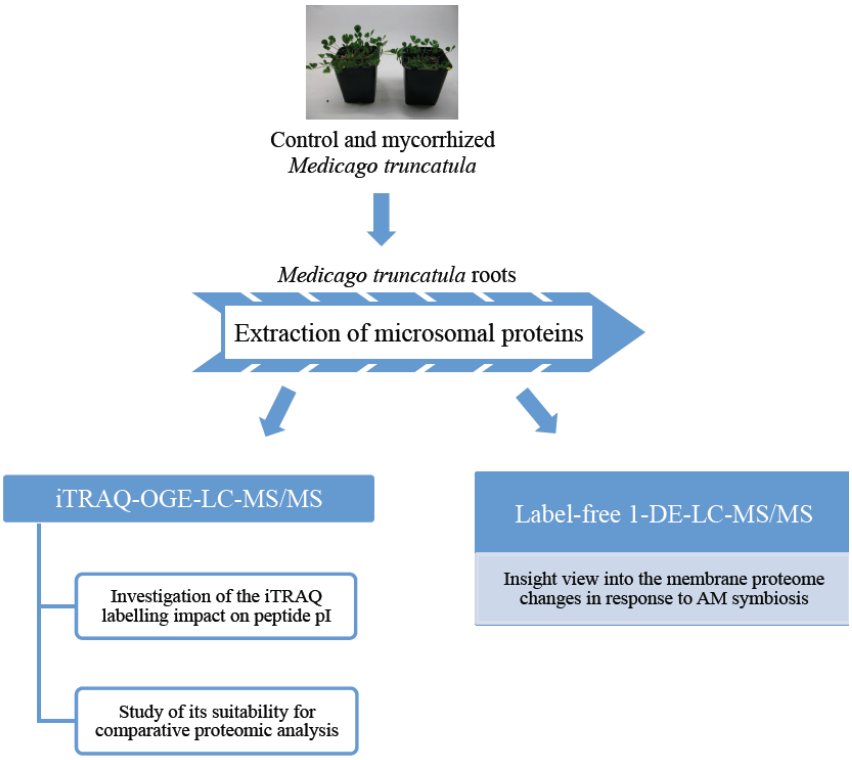

Figure 1.5: Research outline of the presented study

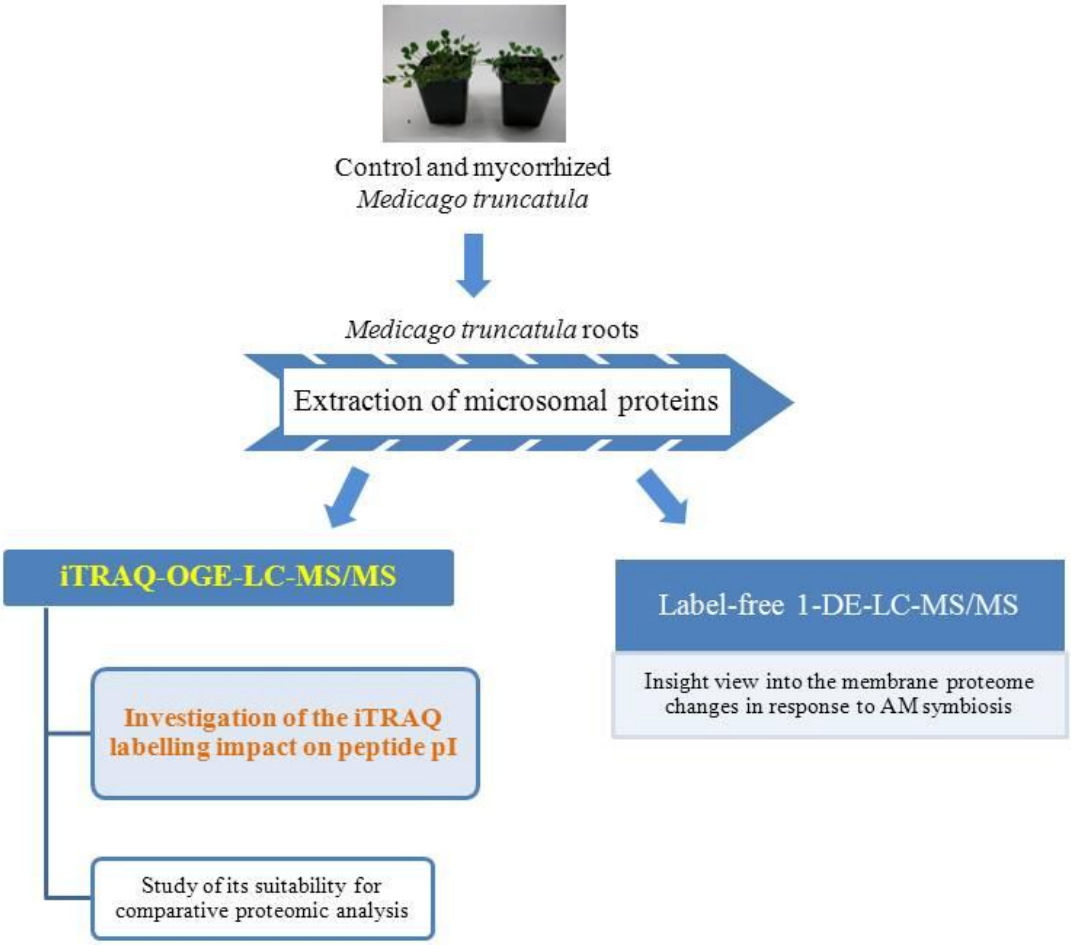

Abdallah *et al.*, Optimization of iTRAQ labelling coupled to OFFGEL fractionation as a proteomic workflow to the analysis of microsomal proteins of *Medicago truncatula* roots. *Proteome Science* 2012, 10:37

Results & discussion

Chapter 2

Optimization of iTRAQ labelling coupled to OFFGEL fractionation as a proteomic workflow to the analysis of microsomal proteins of *Medicago truncatula* roots

Cosette Abdallah[1,3], Kjell Sergeant[1], Christelle Guillier[2], Eliane Dumas-Gaudot[3], Céline C. Leclercq[1] and Jenny Renaut[1]

[1]*Département Environnement et Agro-Biotechnologies, Centre de Recherche Public- Gabriel Lippmann, 41, rue du Brill, L-4422, Belvaux, Luxembourg.*

[2]*UMR 1347 Agroécologie, CNRS, ERL CNRS 6300, BP 86510, Dijon 21000, France.*

[3]*UMR 1347 Agroécologie, INRA, BP 86510, Dijon 21000, France.*

Recently high numbers of robust, sensitive and advanced gel-free proteomic approaches have emerged with a new toolbox of plethora and powerful quantitative proteomic methodologies. Isobaric tagging such as iTRAQ has proven its popularity in quantitative proteomics and shown its compatibility with OFFGEL electrophoresis (OGE), which permits isoelectric point peptide separation in solution. In the current study iTRAQ-OGE-LC-MS/MS has been applied for the first time on microsomal proteins extracted from *Medicago truncatula* roots with foremost analytical objectives starting from sample preparation and up to protein identifications. Given that good sample preparation is the foundation of an analysis success, a protein extraction protocol based on differential centrifugation and allowing membrane-enriched fractions is described. Then a new, straightforward and home-made in-solution protein digestion leading to peptide fractions, free of iTRAQ interfering compounds, is developed for the downstream analysis. Multidimensional peptide separations prior to MS analysis are crucial for low abundant and recalcitrant protein identifications, therefore iTRAQ labelled peptides were pre-fractionated in OGE prior to their separation on a C18 column. Literature lacks critical discussion on the iTRAQ labelling effect on peptide isoelectric point, thus its impact on peptide electrofocusing behaviour in OGE fractionation in a wide pH range (3-10) is herein investigated on *Medicago truncatula* membrane protein digests, to offer an insight view on the compatibility of iTRAQ labelling with OGE.

Abstract

Background

Shotgun proteomics represents an attractive technical framework for the study of membrane proteins that are generally difficult to resolve using two-dimensional gel electrophoresis. The use of iTRAQ, a set of amine-specific isobaric tags, is currently the labelling method of choice allowing multiplexing of up to eight samples and the relative quantification of multiple peptides for each protein. Recently the hyphenation of different separation techniques with mass spectrometry was used in the analysis of iTRAQ labelled samples. OFFGEL electrophoresis has proved its effectiveness in isoelectric point-based peptide and protein separation in solution. Here we describe the first application of iTRAQ-OFFGEL-LC-MS/MS on microsomal proteins from plant material. The investigation of the iTRAQ labelling effect on peptide electrofocusing in OFFGEL fractionator was carried out on *Medicago truncatula* membrane protein digests.

Results

In-filter protein digestion, with easy recovery of a peptide fraction compatible with iTRAQ labelling, was successfully used in this study. The focusing quality in OFFGEL electrophoresis was maintained for iTRAQ labelled peptides with a higher than expected number of identified peptides in basic OFFGEL-fractions. We furthermore observed, by comparing the isoelectric point (pI) fractionation of unlabelled versus labelled samples, a non-negligible pI shifts mainly to higher values.

Conclusions

The present work describes a feasible and novel protocol for in-solution protein digestion in which the filter unit permits protein retention and buffer removal. The data demonstrates an impact of iTRAQ labelling on peptide electrofocusing behaviour in OFFGEL fractionation compared to their native counterpart by the induction of a substantial, generally basic pI shift. Explanations for the occasionally observed acidic shifts are likewise presented.

Keywords

Sample preparation, Membrane proteomics, Gel-free proteomics, OFFGEL peptide fractionation, iTRAQ labelling, *Medicago truncatula*

Background

Two-dimensional gel electrophoresis (2-DE) coupled to mass spectrometry (MS) has been the trademark method for relative protein quantification in plant proteomics. Nevertheless, lack of quantitative reproducibility (Lilley *et al.*, 2002), poor representation of low abundant proteins, highly acidic/basic proteins (Gygi *et al.*, 2000), or proteins with extreme size or hydrophobicity (Ong & Pandey, 2001) are the principal shortcomings of 2-DE, this related to the low tolerance of the technique for detergents and ionic compounds. However, handling membrane proteins requires detergent and buffer use for membrane solubilisation and homogenization followed by their removal prior to further analysis in MS. Proteomic analysis of membrane proteins remains a major challenge and represents an ongoing topic of myriad investigations. Therefore, MS-based 2D-gel-free proteomic approaches have recently bypassed the status of descriptive tool to become the new mainstream method for quantitative proteome studies.

Isobaric tags for relative and absolute quantitation (iTRAQ) are recently developed chemical labelling reagents (Ross *et al.*, 2004) that quickly gained popularity in proteomics (Aggarwal *et al.*, 2006; Zieske, 2006). The iTRAQ label modifies peptide N-termini and ε-amino groups of lysine side chains. It was shown to increase the number of peptides identified by MS, a finding attributed to a greater number of lysine-terminated peptides detected (Ernoult *et al.*, 2008). Protein quantification relies on reporter ions generated in a "silent region" at low molecular mass of peptide MS/MS spectra. iTRAQ labelling proved compatibility with different kind of samples, providing in-depth knowledge in several biological pathways and has been applied in plant shotgun proteomics (Schulze & Usadel, 2010). Majeran and co-workers used iTRAQ for a comparative analysis of the chloroplast envelope proteome in maize (Majeran *et al.*, 2008), and the approach was likewise used to study the changes in the *Arabidopsis* plasma membrane in response to flagellin treatment (Nuhse *et al.*, 2007).

Immobilized pH gradient isoelectric focusing (IPG-IEF) has emerged as a highly promising alternative to strong-cation exchange fractionation as the first separation dimension in shotgun proteomics (Cargile *et al.*, 2005), especially for membrane proteome analysis (Chick *et al.*, 2008; Eriksson *et al.*, 2008). OFFGEL

electrophoresis (OGE) combines the traditional IEF using IPG strips with the convenience of a liquid-based system. Proteins or peptides migrate through the IPG strip until they reach their isoelectric point (pI) at a given compartment, and after completion of the run samples can be easily recovered in solution for further analysis. OGE separation as first step was recently compared to MudPIT for the analysis of membrane proteins and resulted in comparable results for protein/peptide identification and reproducibility (Elschenbroich *et al.*, 2009). The inclusion of OGE into the proteomic workflow furthermore offers the opportunity to determine the pI of peptides which is an independent validating and filtering tool for false positive identifications (Horth *et al.*, 2006). The additional use of a pI filter enhances the stringency of the peptide validation criteria and increases the identification confidence. However, most frequently used pI calculation algorithms use only native peptide sequences, and the addition of modifications such as the iTRAQ label is cumbersome. The question whether an iTRAQ labelled peptide will exhibit the same pI-value as the native counterpart is therefore not trivial. In the present study, an online tool for chemical drawing, MarvinSketch calculator (http://www.chemaxon.com/marvin/sketch) has been used to calculate pI of unlabelled and iTRAQ labelled peptides to explain some experimentally observed pI shifts (Csizmadia, 2000).

A quantitative proteomic approach using iTRAQ-IEF combination was successfully applied on *Staphylococcus aureus* membrane extracts (Scherl *et al.*, 2006). Moreover, Chenau and co-authors evaluated the efficiency of OGE fractionation for iTRAQ labelled peptides from the human secretome and plasma (Chenau *et al.*, 2008). When evaluating OGE fractionation of iTRAQ labelled peptides, one must consider that the iTRAQ-label incorporates a highly basic group "*N*-methylpiperazine" at peptide N-termini and ε-amino groups of lysine side chains. This can alter the pI of peptides and consequently the isoelectrofocusing behaviour in IPG-IEF or OGE. This impact was previously studied using proteins from a colon cancer cell line using a small, acidic pH range between pI 3.4 and 4.9; and there any observed shift in pI could only be small or absent (Lengqvist *et al.*, 2007).

To date, the iTRAQ/OGE couple has been applied on complex eukaryotic samples and different types of matrices, but none dealing with plant membrane proteins

(Ernoult *et al.*, 2008; Besson *et al.*, 2011). Here we present, for the first time, the application of an iTRAQ-OGE-LC-MS/MS proteomic approach on microsomal proteins from *Medicago truncatula* roots. A feasible protocol is described for in-solution protein digestion allowing the recovery of a "clean" protein digest from *Medicago truncatula* cv Jemalong 5 roots inoculated or not with *Rhizophagus irregularis*. Furthermore by comparing the OGE fractionation of native and labelled peptides, the predictable basic shift induced by iTRAQ labelling was studied using a wide pH-range (3-10).

Results and discussion

Experimental design

During the last decade, proteomics has gained popularity in plant science, but still mostly relies on 2-DE. Not all types of proteins are amenable to gels and this method often falls short to study low-abundant and recalcitrant proteins. Therefore a gel-free proteomic approach was implemented here on *Medicago truncatula* membrane proteome. For microsome preparation a previously optimised method based on differential centrifugation has been employed (Stanislas *et al.*, 2009). Microsomal proteins were cleaved using a homemade protocol for in-solution protein digestion allowing the recovery of a "clean" peptide fraction. Subsequently, these protein digests from *M. truncatula* roots inoculated or not with *Rhizophagus irregularis*, were labelled with iTRAQ and fractionated using OGE prior to RP-HPLC-MS/MS, a first time this type of approach is used on membrane proteins of plant material. OGE prefractionation was performed in 12 wells using a 12 cm strip covering the pH range of 3 to10. iTRAQ labelled and pre-fractionated samples were then separated using liquid chromatography (LC) followed by MALDI-TOF/TOF analysis. Searches in the databases were carried out using ProteinPilot software. A schematic summary of the workflow performed in the current study is illustrated in Figure 2.1.

The OGE-LC separation of 100 µg of unlabelled microsomal protein digest allowed the identification of 241 peptides and 107 proteins, whilst 266 peptides and 130 proteins were identified in iTRAQ labelled samples. The enrichment of membrane protein fraction was assessed by the subcellular localisation of the identified proteins. Seventy percent of proteins in both experiments had at least one membrane

localisation experimentally demonstrated (results not shown). Furthermore only 7 and 5% of the identified proteins were predicted to be localised in the cytosol in unlabelled and iTRAQ labelled experiments, respectively (results not shown).

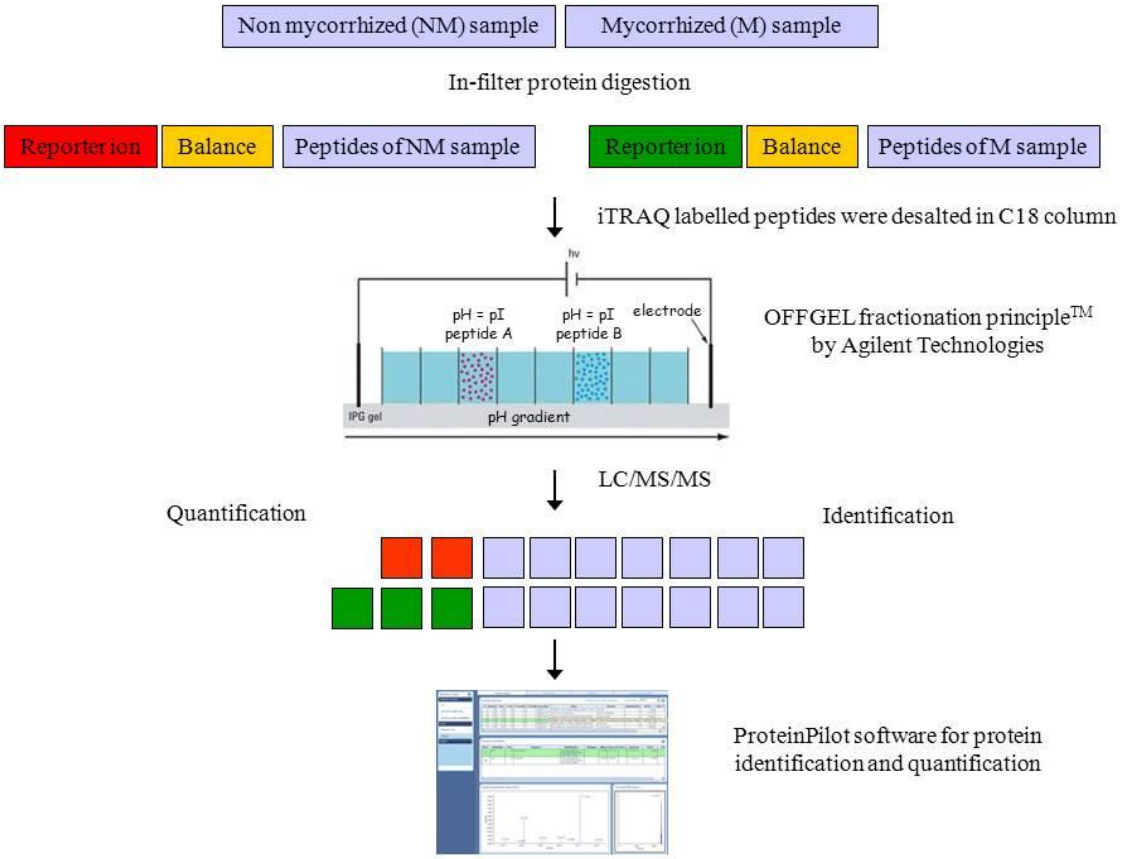

Figure 2.1: Schematic representation of the experimental workflow of iTRAQ-OGE-LC-MS/MS.
The flowchart shows the peptide OGE fractionation process designed by Agilent Technologies.

In-filter protein digestion

One of the most critical steps in all proteome analyses is sample preparation. Detergents are indispensable tools for the solubilisation and fractionation of membrane proteins. However, they can dominate mass spectra and preclude peptide analysis in MS, even in minute concentrations. As a consequence, the majority of studies on membrane proteins use in-gel digestion to remove detergents prior to mass spectrometric analysis (Nagaraj *et al.*, 2008). Therefore, gel-free proteomic approaches require adequate protocols for in-solution protein digestion while avoiding the use of high-ionic strength buffers and detergents. To overcome these difficulties,

various alternative approaches have been described and the use of filtration columns appears to be the most promising (Manza *et al.*, 2005). Based on the filter-aided sample preparation (FASP) workflow (Wisniewski *et al.*, 2009) a method has been developed in the current study in which the protein digestion took place in a commercially available ultra-filtration device used for protein retention, buffer exchange and removal (Figure 2.2). The key feature of this method is the ability to remove interfering compounds associated with the sample during protein digestion through the filter device and to recover resulting peptides by centrifugation. Wiśniewski and co-workers compared the distribution of molecular weights of the identified proteins using either a 3k or 10k filter. They found that the 10k filter efficiently retained small proteins (5-10kDa) and efficiently released peptides up to 5,000 Da (Wisniewski *et al.*, 2009). Therefore, Amicon Ultra filter devices (Millipore), with relative molecular mass cut-off of 10,000 NMWL (Nominal Molecular Weight Limit) have been used in the subsequent experiment. The in-solution protein digestion protocol was made up of 3 main steps: (1) DTT was first added to reduce protein disulphide bonds. Then, (2) carbamidomethylation of thiols was achieved by the addition of iodoacetamide. All the reagents added during these steps were easily removed by centrifugation. Afterwards, (3) protein digestion was carried out by adding trypsin and leaving it overnight at room temperature. Finally, the peptide fraction, free of unwanted, interfering compounds, was obtained by centrifugation. One of the aims of the current study was to develop an alternative in-solution protein digestion to the one proposed by iTRAQ reagent kit in order to be able to produce peptide fraction free of interfering compounds such as urea, Tris and DTT. Consequently, in-filter protein digestion represented the method of choice allowing the removal of residual interfering buffers associated with the sample. At one step to iTRAQ labelling, any buffer added through sample preparation should be "primary amine free" to avoid the quenching of the iTRAQ labelling. Hence, ammonium bicarbonate's substitution was a mandatory step. Triethylammonium bicarbonate (TEAB) was chosen as a good tertiary amine buffer, which is also very volatile, and can therefore be easily removed *in vacuum*. Thus in our protocol, the in-filter protein digestion described above was convenient for protein digestion and sample clean-up prior to iTRAQ labelling.

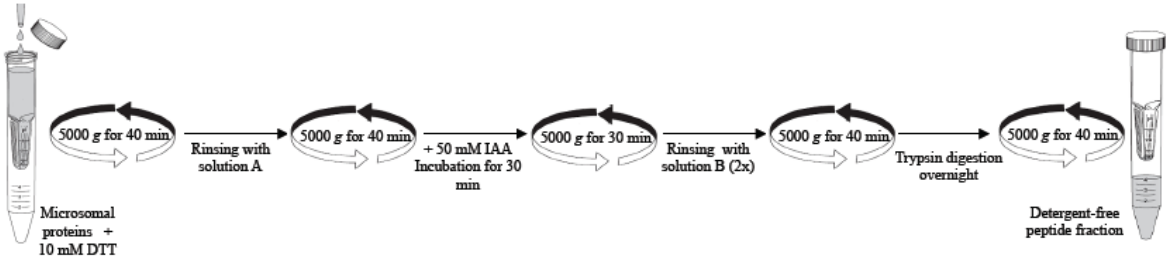

Figure 2.2 Depiction of in-filter protein digestion protocol using Amicon Ultra filter devices™ (Millipore).

Peptide isobaric tagging

After the labelling process, samples must be ready for OGE separation. Nevertheless, excess iTRAQ reagents in the sample mixture should be removed since their presence can suppress the signal obtained from target peptides and thus reduces the level of achievable sensitivity and reproducibility. The supplier recommended the use of cation exchange (CX) cartridge, delivered with the iTRAQ kit, as a desalting step prior to LC-MS/MS analysis. However since peptides will be eluted of the CX-column in 10 mM potassium phosphate in 25% (v/v) of acetonitrile (ACN) and 350 mM of potassium chloride, when using the OGE fractionator, an alternative desalting method was an absolute requirement. Several tests with alternative desalting steps have been conducted, and it was found that the use of a C18 column was well suited to clean-up iTRAQ labelled samples (results not shown). Ernoult and co-authors have also used C18 cartridge to desalt the iTRAQ labelled samples prior to OGE (Ernoult *et al.*, 2008).

Since we have used an alternative in-solution digestion protocol, which contains DTT, IAA and Tris categorized as potential interfering substances with the labelling process, the utility of this method for the removal of these compounds and thus the creation of an iTRAQ-compatible environment needed to be established. One example of a labelled peptide is shown in Figure 2.3. Figure 2.3A presents the MS/MS spectrum of CALVYGQMNEPPGAR at *m/z* 1806.94, while 2.3B shows the low mass region covering daughter ions (114 and 117) released in MS/MS. Further empirical evidence that the applied procedure was successful in removing interfering compounds was obtained by researching all datasets but omitting the fixed

modification with the iTRAQ label (not added or added as variable modification). None of these searches resulted in the significant identification of a peptide, so if not all interfering compounds are completely eliminated at least their effect on labelling was not observable in our data.

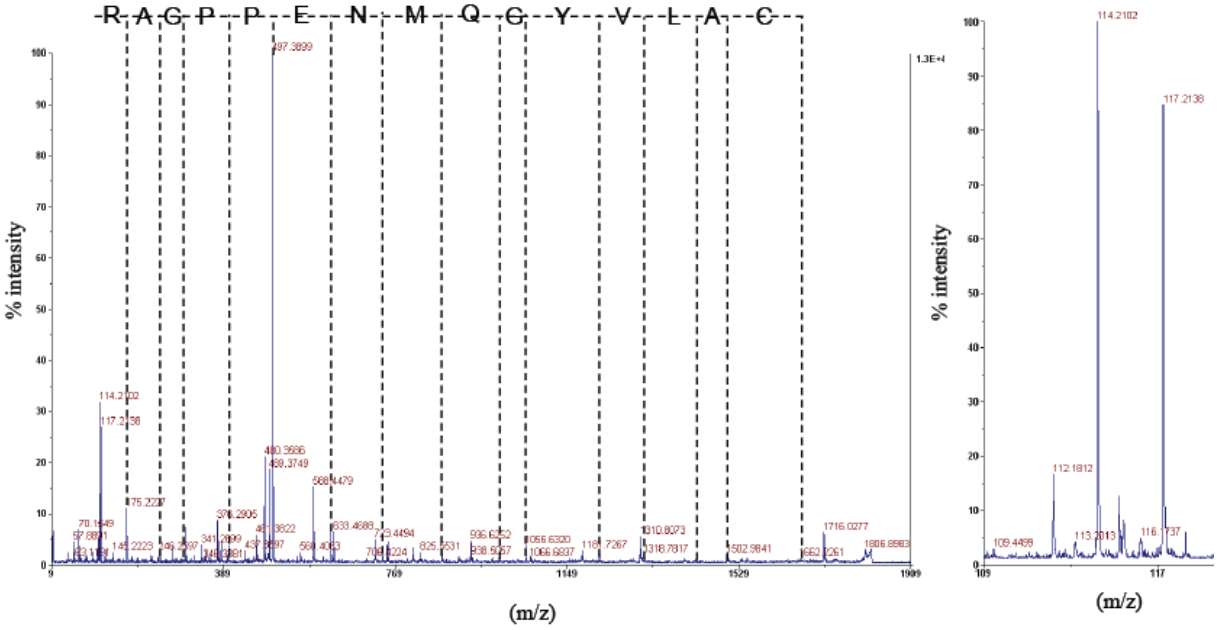

Figure 2.3 Spectrum of an iTRAQ labelled peptide of control (114) and mycorrhized (117) protein digest.
(A) MS/MS spectrum of iTRAQ labelled CALVYGQMNEPPGAR at *m/z* 1806.94. (B) iTRAQ reporter ions at *m/z* 114 and 117, their peak areas are used to calculate the relative abundance of a given peptide

Peptide OGE fractionation

IPG as first dimension separation strategy has proved to be superior to SCX with a salt or pH gradient (Essader *et al.*, 2005; Manadas *et al.*, 2009). Therefore, OGE has been chosen to separate peptides according to their isoelectric point in a liquid phase. The novelty and strengths of this method can be resumed by the ability to directly introduce pI-fractionated peptides to LC-MS/MS analysis. Nonetheless, glycerol in peptide focusing buffer interfered with SpeedVac concentration (increased viscosity), direct injection into reverse phase LC and with crystallization on a MALDI target. This problem was previously mentioned by Fraterman and co-workers (Fraterman *et*

al., 2007), in which study the glycerol content of the focusing buffer was reduced by 50% (v/v) in deviation from the supplier's protocol, while others indicated the use of even lower concentrations (Hubner *et al.*, 2008; Warren *et al.*, 2010). Several other studies did not mention the concentration of glycerol proposed by the OGE manufacturers (6%) as a problem (Chenau *et al.*, 2008; Ernoult *et al.*, 2008). In the present work, reducing the concentration of glycerol by 50% (v/v), final concentration equals 3%, was not enough to avoid the clogging of the pre-column after few runs or to solve the crystallization problem on a MALDI target. According to Agilent Technologies, reducing and even omitting glycerol content in peptide focusing buffer does not affect the efficiency of the IEF, therefore the glycerol concentration was reduced to 5% (v/v) (final concentration equals 0.3%) in deviation of the original protocol. Hubner and co-workers demonstrated that the loading capacity for optimal peptide focusing on 12 cm strip is below 100 µg (Hubner *et al.*, 2008; Warren *et al.*, 2010), therefore in this study, 100 µg of protein digest were separated in OGE. The isoelectrofocusing of peptides offers the possibility to exploit the deviation between expected and observed peptide pI distribution across the IPG strip. It has been reported that the average pI values of peptides fits fairly well with the pH range of the corresponding OGE fractions (Horth *et al.*, 2006; Chenau *et al.*, 2008; Ernoult *et al.*, 2008).

Hence, the effective resolution obtained in the 12 OGE fractions of free and iTRAQ labelled samples was assessed by determining the number of peptides identified in single versus multiple fractions (Figure 2.4). Peptides were unevenly distributed along the IPG strip in both labelled and unlabelled samples. In native samples, over 70% of identified peptides were localized in only one fraction and more than 90% were found in one or two successive fractions. These findings were in agreement with previous studies (Horth *et al.*, 2006). In iTRAQ labelled samples, more peptides were identified in basic region compared to the acidic one. Only 3, 10 and 8 peptides in total were respectively found in fraction 1, 2 and 4 while 63 peptides were identified in fraction 10. Moreover, the fractionation quality in basic fractions was greater than in acidic ones. More than 80% of peptides were recovered in single fraction (fractions 6 to 12) while this percentage fell to 20% in fraction 2 and no unique peptide was found in fraction 1. As Ernoult *et al.* (2008) have shown, more peptides were recorded

in iTRAQ labelled samples giving the fact that iTRAQ improves MALDI ionisation (Horth *et al.*, 2006; Chenau *et al.*, 2008; Ernoult *et al.*, 2008). Our results confirmed that the slightly modified version of the initial OGE protocol applied did not affect the quality of peptide IEF. Interestingly, iTRAQ labelled peptides showed a better OGE fractionation quality in basic fractions where a greater number of peptides have been identified compared to acidic ones. This observation will be discussed in more detail below.

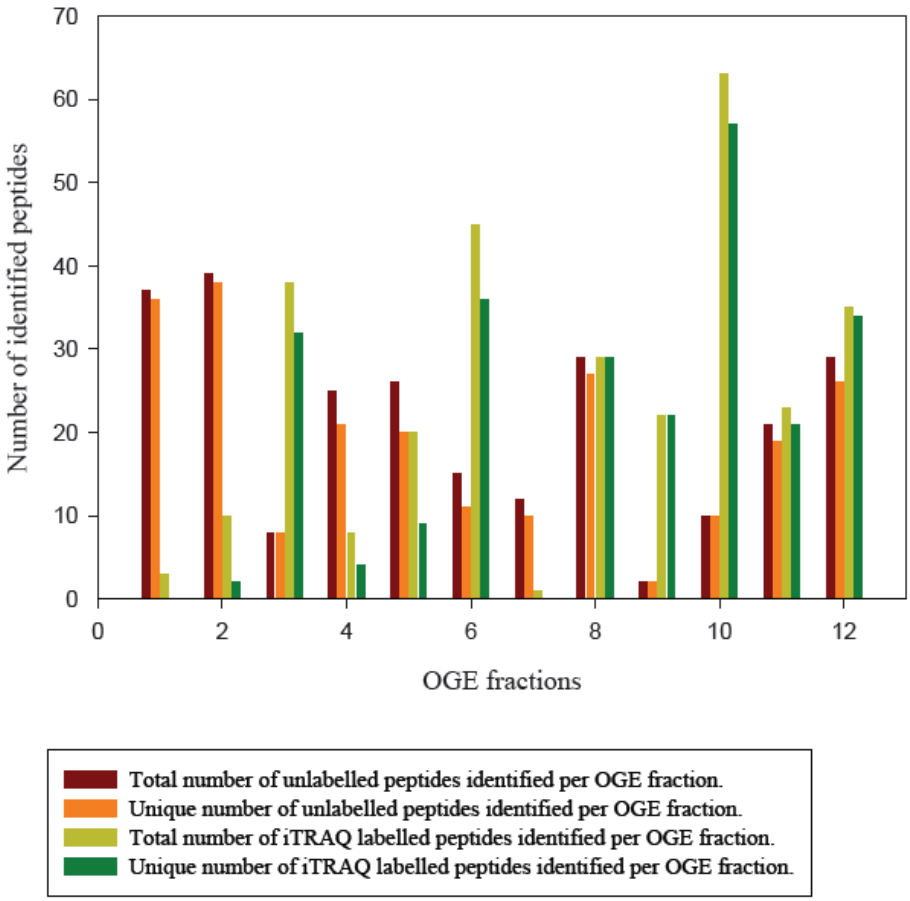

Figure 2.4: Number of peptides identified per OGE fraction.
Brown and light green bars represent the total number of unlabelled and iTRAQ labelled peptides identified in each fraction, respectively. Orange and dark green bars indicate the unique number of unlabelled and iTRAQ labelled peptides identified per fraction, respectively.

iTRAQ impact on peptide OGE fractionation

The assumption that iTRAQ labelling induces a negligible increase in peptide isoelectric point (Lengqvist *et al.*, 2007) prompted us to investigate the validity of this claim on peptide OGE fractionation on a wide pH range (3-10). Hence, peptide distribution on the 12 cm strip pH 3-10 was examined when peptides were either labelled or not with iTRAQ reagents. The current survey delineated 4 different groups of labelled peptides found in at least 3 replicates of labelled samples with a high reproducibility in these independent experiments (Chapter 2, additional file S2.1).

Table 2.1 shows a set of 70 peptides (group A) found in more basic fractions after iTRAQ labelling, this finding being highly related to the incorporation of the basic group "*N*-methylpiperazine" at peptide N-termini and ε-amino groups of lysine side chains. As an example, 2 ions were assigned to EQMGYTFDALK by Paragon search with 99% of confidence. The unlabelled peptide with a *m/z* of 1301.58 was found in fraction 1 while the labelled (*m/z* 1590.80) was identified in fraction 3. The mass difference corresponds 289.22 Da or the addition of two labels at the N-terminus and the ε-amino groups of lysine side chain. For peptides only containing one label at the N-terminus the basic shift was, as previously described by Ross and co-workers, in general more important (Ross *et al.*, 2004). For instance NYTNAFQALYR (*m/z* 1504.76), exhibiting only one potential iTRAQ modification site, the labelled form of this peptide was found in fraction 12 while its native counterpart at *m/z* 1359.65 was focused in fraction 10. Most of the peptides in group A followed the same trend with a shift of 1 to 2 fractions to the basic end of the strip (Table 2.1, group A). Some others (7 peptides) pursued the observed basic shift tendency but are focussed irreproducible using the OGE fractionator (Chapter 2, additional file S2.1, group D).

Table 2.1: Observed basic pI shifts in OGE fractionation after iTRAQ labelling.
This table presents 70 peptides shifted to more basic OGE fraction after iTRAQ labelling. The non-labelled (NL) and iTRAQ labelled (L) peptide masses are shown in this table together with the mass difference induced by the labelling. The OGE fractions (F) of iTRAQ labelled peptides and their native counterparts are as well presented.

	Sequence	Mass NL	Mass L	Difference	F NL	F L
1	ECADLWPR	1045.46	1190.57	145.11	1	3,4
2	AYLEDFYR	1075.50	1220.61	145.11	1	3,4
3	EQMGYTFDALK	1301.58	1590.81	289.23	1	3,4
4	TMADEGVVALWR	1346.65	1491.77	145.12	1,2	3,4
5	ECSGVEPQLWAR	1430.66	1575.77	145.11	1	3,4
6	NQIDEIVLVGGSTR	1499.78	1644.90	145.13	1	3,4
7	LAEMPADSGYPAYLAAR	1794.84	1939.97	145.13	1	3,4
8	ELEFYMK	958.46	1247.66	289.20	1	3
9	IPSAVGYQPTLSTDLGGLQER	2201.13	2346.24	145.11	1	3,4
10	AQIWDTAGQER	1273.59	1418.71	145.12	1	3,4
11	AGGECLTFDQLALR	1549.77	1694.87	145.10	1	3,4
12	VDFAYSFFEK	1251.61	1540.79	289.18	1	3
13	IFDKPEDFIAER	1478.74	1767.95	289.22	1	3,4
14	GLFTSDQILFTDTR	1612.79	1757.92	145.13	1	3,4
15	TTPSYVAFTDSER	1472.66	1617.79	145.13	1	3,4
16	LDTGNFSWGSEAVTR	1638.76	1783.87	145.11	1	3,4
17	LWQVPETLPAEVVGK	1664.93	1954.13	289.19	2	3,4
18	QLDAHIEEQFGGGR	1555.73	1700.85	145.11	2	3,4
19	GFGFVTFAEEK	1230.61	1519.80	289.19	2	3,4
20	AFLVEEQK	962.51	1251.72	289.21	2	3,4
21	IFEGEALLR	1046.59	1191.69	145.10	2	3,4
22	ISGLIYEETR	1179.61	1324.72	145.11	2	3,4
23	TTAEEGVVALWR	1330.71	1475.80	145.09	2	3,4
24	LLIQNQDEMIK	1343.72	1632.92	289.21	2	3,4
25	IQDKEGIPPDQQR	1522.77	1811.99	289.22	2	3,4
26	TMVYPEAGFELQR	1539.74	1684.85	145.10	2	3,4
27	EQDVSLGANKFPER	1588.77	1878.00	289.22	2	3,4
28	GQGGIQQLLAAEQEAQR	1795.93	1941.03	145.10	2	3,4
29	QYAVFDEK[$]	981.46	1287.68	306.22	2	3,4
30	QLDSHIEEQFGGGR[$]	1554.71	1716.84	162.13	2	3,4
31	FDVGVKEIEGWTAR	1605.84	1895.03	289.19	2	3,4
32	HFEVDLSAFR	1219.61	1364.71	145.10	3	4
33	CALVYGQMNEPPGAR	1661.78	1806.87	145.10	4	6
34	NAVVTVPAYFNDSQR	1679.84	1824.94	145.10	4	5,6
35	QPTELELAQAFHQGK	1695.85	1985.07	289.22	4	5
36	TALTYVDNNDGSWHR	1747.80	1892.90	145.10	4	5

37	QQFPLALYQVDK	1448.78	1737.98	289.20	4	5,6
38	ADGFAGVFPEHK	1273.60	1562.82	289.22	4	5
39	SLEGLQANVQR	1213.63	1358.75	145.13	4	6
40	TFDNVYYK	1048.47	1337.70	289.23	4	5
41	MLSPLILGDEHYQTAR	1842.96	1988.04	145.08	4	5
42	SSFDAFQQILK	1282.67	1571.87	289.20	4	5
43	SSDFLMYGIK	1159.57	1448.77	289.20	4	5
44	SSMDAFQQILK	1282.67	1571.83	289.17	5	5
45	FTQANSEVSALLGR	1491.77	1636.88	145.11	5	6
46	STLVWEVR	988.56	1133.64	145.08	5	6
47	IFLENVIR	1002.62	1147.70	145.07	5	6
48	FFCEFCGK	1093.48	1382.65	289.17	5	6
49	EVAGFAPYEKR	1265.65	1554.85	289.20	5,6	6
50	SFGPAVIFNNEK	1321.70	1610.88	289.18	5	6
51	VALINYGPEYGR	1350.75	1495.80	145.06	5	6
52	YIAPEQVPVK	1142.63	1431.85	289.21	5	5,6
53	VEPLVNMGQITR	1355.72	1500.83	145.12	5	6
54	AYEPILLLGR	1143.67	1288.77	145.10	5	6
55	LVGEYGLR	905.51	1050.61	145.10	5	6
56	EALGGLPLYQR	1215.66	1360.77	145.11	5	6
57	ADAFLLVGTQPR	1286.70	1431.81	145.10	5	6,7
58	HGWEYVVK	1016.51	1305.72	289.21	6	8
59	FVIGGPHGDAGLTGR	1452.75	1597.86	145.10	7	8
60	LVNVFTIGK	989.60	1278.80	289.20	7	9,10
61	THAVVEPFVIATNR	1552.86	1697.95	145.09	7	8,9
62	SVHEPMQTGLK	1225.62	1514.82	289.21	7	8
63	SVVYALSPFQQK	1365.74	1654.94	289.20	7	10
64	YGGGANFVHDGYNK	1497.61	1786.88	289.27	7	8
65	TALTYIDGNGNWHR	1616.76	1761.88	145.12	8	9
66	AHLQDYIQTHYTAPR	1812.89	1958.00	145.11	8	9
67	NYTNAFQALYR	1359.66	1504.77	145.11	10	12
68	TLHPNWSPAAIK	1333.72	1622.93	289.21	10	11
69	FHQYQVVGR	1132.56	1277.69	145.13	11	12
70	FQSLGVAFYR	1186.64	1331.72	145.08	11	12

As shown in Table 2.2, 34 peptides were categorized in group B where peptides in both label-free and iTRAQ labelled experiments are focussed in the same OGE fraction. Among them, 10 peptides were recovered in fraction 12 the most basic fraction. Hence, even if iTRAQ labelling rendered them more basic, fraction 12 stands for the last and most basic region of the 12 cm strip (pH 3-10) a peptide could

reach. Furthermore, 10 of the 34 peptides were discerned (marked with an asterisk * in Table 2.2) to register the expected basic shift in at least one experiment but this shift could not be observed in all replicates. The fourteen remaining peptides were focused in the same OGE fraction before and after iTRAQ labelling. The most reliable explanation to this observation was that the iTRAQ tag did induce an increase in the peptide pI, but this shift was not pronounced enough and therefore did not provoke a shift in fraction since every fraction corresponds to 0.6 pH-unit. To look into this further, peptide amino acid structures were manually drawn in MarvinSketch calculator and peptide isoelectric points were calculated for the native and iTRAQ modified peptides. For example, the non-modified peptide GFGFVTFANEK of *m/z* 1215.62 was found in the same OGE fraction (fraction 6) of its doubly labelled peptide of *m/z* 1504.80. The calculated pI of the unlabelled peptide is 5.94 while a pI of 5.97 is assigned to the iTRAQ labelled form. Thus, the pI was slightly modified after iTRAQ labelling and remained below the edge of 0.6 pH-units.

Table 2.2: Co-migration of iTRAQ- and unlabelled peptides in the same OGE fraction. Thirty-four peptides focused in the same OGE fraction in both label-free and iTRAQ labelled experiments are shown in this table. Peptides shifted to more basic fractions in at least one experiment are indicated with an asterisk (*).

	Sequence	Mass NL	Mass L	Difference	F NL	F L
1	MFDAGLYEHCR*	1397.58	1542.69	145.12	4	4
2	EAFPGDVFYLHSR*	1536.75	1681.85	145.09	4	5
3	TLHGLQPPESSGIFNEK*	1852.93	2142.14	289.22	4	4
4	ATFDCLMK*	984.49	1273.65	289.16	5	5
5	GIPYLNTYDGR*	1267.67	1412.73	145.06	5,6	5,6
6	GFGFVTFANEK	1215.62	1504.80	289.18	2,6	6
7	GKDFAELIASGR	1262.67	1551.87	289.21	6	6
8	AALNDFDRFK	1195.60	1484.81	289.21	6	6
9	EAQWAHAQR*	1095.52	1240.63	145.11	8	8
10	SRFFHSTGQR*	1221.54	1366.71	145.17	8	8
11	AGDFFHSAQSR*	1221.56	1366.66	145.11	8	8
12	ASALIQHDWSR*	1282.63	1427.75	145.12	8	8
13	AHGGFSVFAGVGER	1389.69	1534.79	145.10	8	8
14	VGPFHNPSETYR	1402.65	1547.77	145.12	8	8
15	GVDKEHVMLLAAR	1437.77	1726.99	289.22	8	8
16	EVHFLPFNPVDKR	1596.85	1886.05	289.20	8	8
17	EIHFLPFNPVDKR	1610.87	1900.07	289.20	8	8

18	ALYHDLNAYR	1234.61	1379.72	145.11	8	8
19	AGVKPHELVF	1095.61	1384.82	289.21	8	8
20	LAWHSAGTFDSK*	1318.61	1607.84	289.23	8	8
21	YDTVHGQWK	1132.52	1421.74	289.22	8	8
22	NGGANFVAPGYTK	1294.54	1583.84	289.31	10	10
23	AASFNIIPSSTGAAK	1433.76	1722.96	289.21	10	10
24	FVTAVVGFGK	1023.57	1312.79	289.21	10	10
25	AGQYNFLIR	1080.58	1225.68	145.10	12	12
26	AYGGVLSGGAVR	1105.59	1250.70	145.10	12	12
27	GFQTSYYNR	1134.50	1279.62	145.12	11,12	12
28	VLNTGSPISVPVGR	1394.76	1539.90	145.13	12	12
29	SSSVFIPHGPGAVR	1409.73	1554.85	145.12	12	12
30	LVSAHSSQQIYTR	1488.75	1633.88	145.13	12	12
31	GGGHTSQIYAIR	1258.65	1403.75	145.11	12	12
32	HGSLGFLPR	982.53	1127.64	145.12	12	12
33	GGQLIYGGPLGR	1186.63	1331.76	145.12	12	12
34	AGGAYTLNTASAVTVR	1550.79	1695.91	145.12	12	12

Table 2.3 shows the eleven peptides of group C that were focused in more acidic fractions when they were iTRAQ labelled. Initially, the native form of these peptides was found in fractions 11 and 12, gathering the most basic peptides. The observed acidic shift is furthermore in agreement with Chenau *et al.* (2008). These authors found that the peptide pI average in fraction 24 (most basic fraction in their experiment, strip pH 3-10, 24 cm) decreased from 9.22 to 8.74 in non-labelled and iTRAQ labelled samples, respectively (Chenau *et al.*, 2008). To further investigate the acidic shift induced by iTRAQ labels, MarvinSketch Calculator was again implemented for pI calculations. The calculated pI of SKFDNLYGCR is 8.32 and it decreases to 7.72 after labelling, which corresponds to a shift of one OGE fraction. Indeed, the non-modified peptide was focused in fraction 11 while its iTRAQ labelled form was retrieved in fraction 10. Moreover, ASALIQHEWRPK, focused in fraction 12 when non-modified, was found in a more acidic fraction (fraction 10) after iTRAQ labelling. Interestingly, the calculated pI of the native peptide is 9.12 while this is 7.04 for its doubly labelled form, which corresponds accurately to the experimentally observed pI shifts.

Table 2.3: Acidic pI shifts in OGE as a result of iTRAQ labelling.
Eleven peptides shifted to more acidic OGE fraction after iTRAQ labelling are presented in this table
$^{\$}$Gln- > pyro-Glu@N-term

	Sequence	Mass NL	Mass L	Difference	F NL	F L
1	SKFDNLYGCR	1258.56	1547.79	289.22	11	10
2	QFNGLVDVYKK$^{\$}$	1292.69	1743.02	450.33	11	9,10
3	KGPLIVYGTEGAK	1331.73	1765.06	433.33	11	9
4	YLQPQESGWKPK	1459.80	1893.06	433.26	11	9,10
5	GVQQVLQNYK	1175.61	1464.84	289.23	12	10
6	KQFVIDVLHPGR	1407.81	1697.01	289.20	12	10
7	ASALIQHEWRPK	1434.76	1723.98	289.22	12	10
8	LSEPYKGIGDCFKR	1668.82	2102.14	433.33	12	9,10
9	GVLPQNQPFVVK	1324.74	1613.96	289.22	12	10,11
10	INWLTNPVHK	1220.65	1509.88	289.22	12	10
11	IAGFSTHLMK	1103.57	1392.79	289.22	12	10

Acidic and basic amino acid distribution per peptide

Some molecular considerations have been introduced to explain the behaviour of the 111 peptides in groups A, B and D presenting the expected basic shift and the 11 peptides in group C showing an acidic shift after iTRAQ labelling. Peptide amino acid composition has been investigated with a special attention to the acidic (E and D) and basic (K and R) amino acids. Thus, the average number of each amino acid by peptide per fraction was calculated (Figure 2.5). In peptides that shifted to basic regions (groups A, B and D), the number of acidic amino acids D and E by peptide globally decreased from acidic to more basic fractions to be absent in fraction 10 and above, a finding in agreement with Chenau *et al.* (2008) (Chenau *et al.*, 2008). Contrary to this, 7 of the 11 peptides that shifted to a more acidic fraction after labelling (Table 2.3, group C) contain at least one acidic residue and were nonetheless found in the fractions 11 and 12 when not labelled. Furthermore, the number of basic amino acids is higher in peptides that have an acidic shift compared to peptides that have a basic shift (Figure 2.5). Exclusively in the group showing acidic shifts, 4 peptides (KGPLIVYGTEGAK, QFNGLVDVYKK, YLQPQESGWKPK and LSEPYKGIGDCFKR) of the 11 had 3 iTRAQ tags due to the presence of two lysines

in their sequences while no similar case has been observed in peptides shifting to more basic fractions. The experimental finding that iTRAQ labelling shifts the pI of lysine-containing peptides to more acidic values was corroborated by pI calculations in MarvinSketch Calculator on the different forms of lysine. The calculated pI of native, free lysine (9.82) decreases to 7.60 for the double-tagged amino acid.

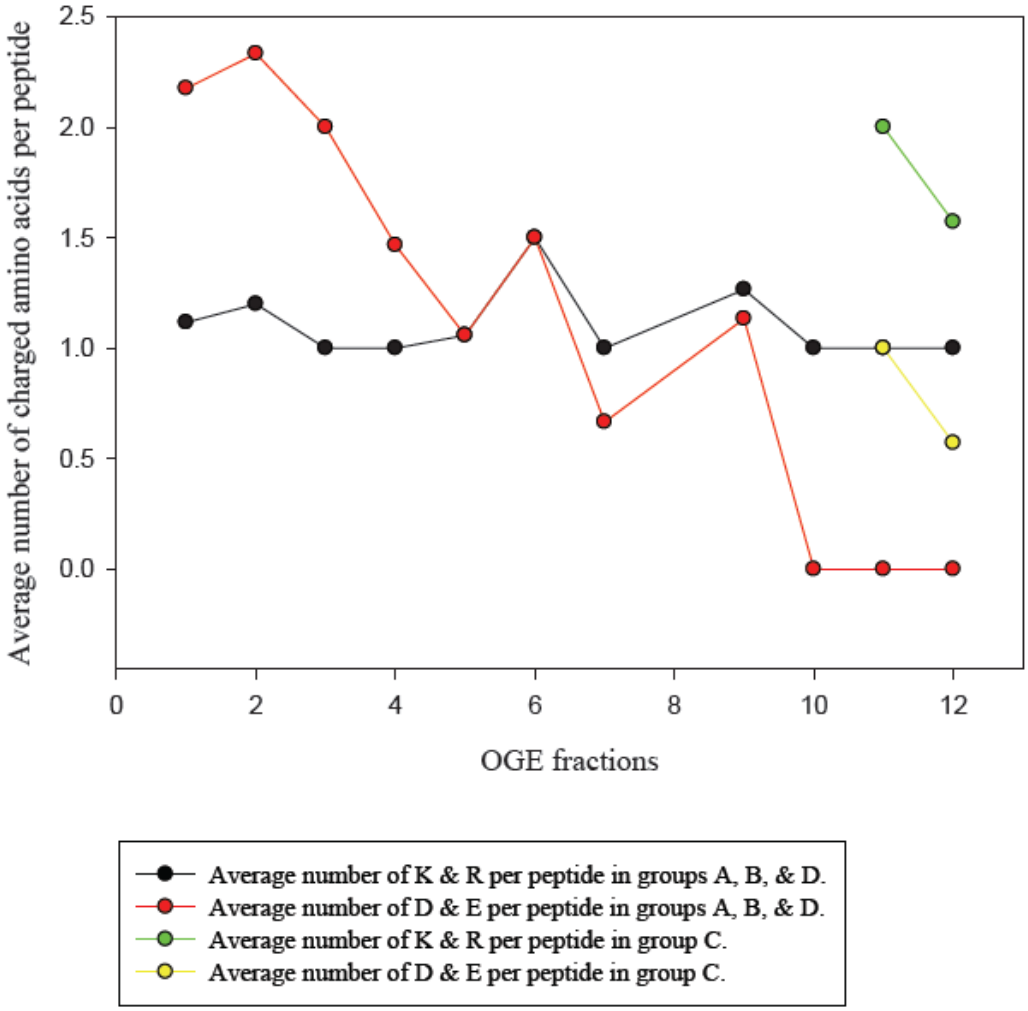

Figure 2.5: Average distribution of basic and acidic amino acids per peptide in each OGE fraction.
Average number of acidic (red plot) and basic (black plot) amino acids per peptide in groups A, B and D. Yellow and Green plots correspond to the average number of acidic and basic amino acids per peptide in OGE fractions 11 and 12 in group C, respectively.

iTRAQ impact on peptide elution time

The degree of retention time variation in LC separation after iTRAQ labelling was examined in groups A, B and D. Resulting retention time values were plotted per fraction for the unlabelled and iTRAQ labelled samples as shown in Figure 2.6. Clearly, iTRAQ labelling increased the retention time of 17 peptides initially focused in OGE fraction 1 and shifted to more basic fractions after the iTRAQ modification by approximately 6 minutes (Chapter 2, additional file S2.2). This variation decreased to less than 1 minute in other OGE fractions, to be entirely gone in fractions 3, 4, 8 and 12 where iTRAQ labelled peptides and their native counterparts eluted at approximately the same time. For group C, label-free and iTRAQ labelled peptides recorded almost the same elution time in LC separation (results not shown). Thus, iTRAQ labelling drastically affected peptide retention time in OGE fraction 1 and lost its effect for the more basic fractions.

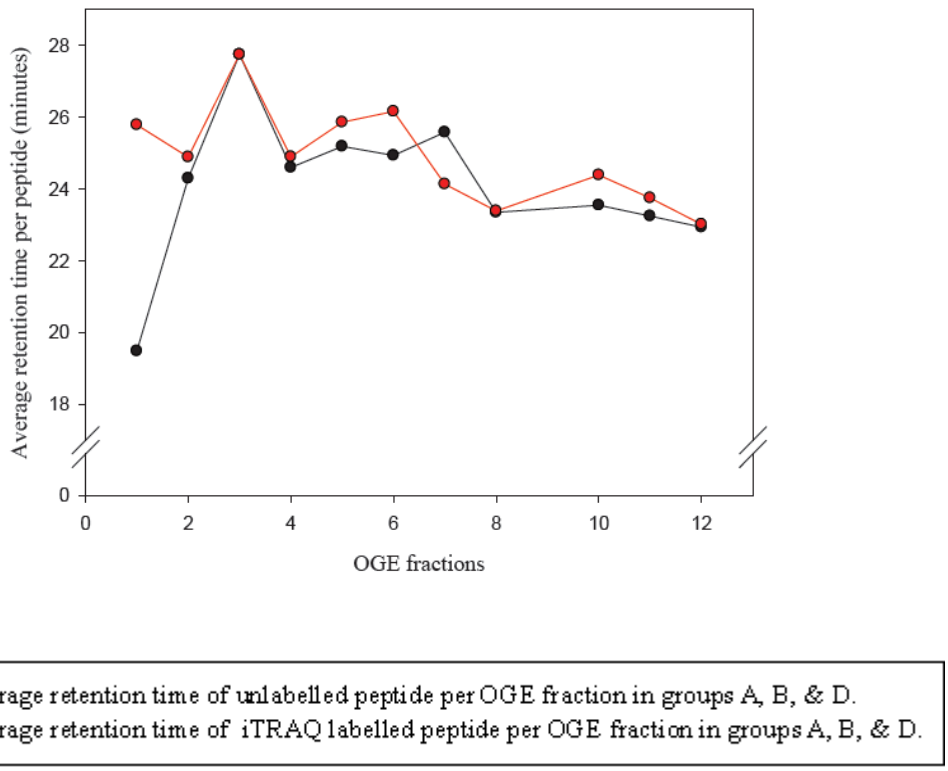

Figure 2.6: Peptide elution time in LC separation.
Average retention time (in minutes) of iTRAQ labelled peptides (red plot) and their native counterparts (black plot) in each OGE fraction in groups A, B and D.

Conclusions

In plants, MS-based proteomics has been largely used for protein identification while quantitative proteomics is still fully developing. In the present work microsomal proteins of *Medicago truncatula* roots were, for the first time, scrutinised by the state-of-the-art gel-free proteomic approach iTRAQ-OGE-LC-MS/MS. Herein, we described a straightforward, robust, and iTRAQ compatible method for in-solution protein digestion. Besides, the practical applicability of this tailored workflow allows users to successfully employ it with different kind of matrices. Another positive aspect of the current work includes the power of peptide fractionation according to their pI in OGE with respect to the focusing quality observed in free and iTRAQ labelled peptide electrophoresis.

Although Ross and co-workers described minimal iTRAQ reactivity with tyrosyl residue side-chain (<3%) (Ross *et al.*, 2004), a recent study has reported an evidence of O-acylation of hydroxylated side-chains of amino acid residues with iTRAQ especially in positions near histidyl residue (Wiktorowicz *et al.*, 2012). Herein, the examination of the peptide electrofocusing behaviour before and after iTRAQ labelling revealed a non-negligible basic pI shift in OGE fractionation on a wide pH range 3-10 and an important increase in retention time in LC separation of labelled peptides focused in OGE fraction 1. It was furthermore found that this basic shift is not global, specific peptides, with specific sequence-determined properties, may even have a shift to a more acidic pI. In this study, a first effort was done to describe these properties. It is noteworthy to point out that to date, most pI calculator algorithms use only native peptide sequences without taking into account the iTRAQ tags. Consequently, further experiments in combination with trustworthier, advanced pI calculator software are crucial to enhance our understanding on the observed basic shift and routinely describe the pI of iTRAQ labelled peptides. Thus, the experimental isoelectric points can be used as an efficient additional filtering tool for the validation of peptide identifications and increase the reliability of the identification procedure.

Methods

Biological material and growth conditions

Medicago truncatula cv Jemalong 5 seeds were surface sterilised and germinated at 27°C in the dark on 0.7% sterile agar (Bestel-Corre *et al.*, 2002). Two-day old seedlings were then transplanted into 400 mL plastic pots containing a mix of sterile soil of Epoisses and sand (1:2 v/v). Mycorrhizal inoculation was realized by adding Epoisses soil-based inoculum (spores, roots and hyphae) of the AM fungus *Rhizophagus irregularis* DAOM 181602 (formerly known as *Glomus intraradices*) (Kruger *et al.*, 2012). Seedlings (3 per pot) were grown for 4 weeks under controlled conditions (16 h photoperiod, 23°C/18°C day/night, 60% relative humidity, 220 µEinstein $m^{-2}.s^{-1}$ photon flux density). Control and *R. irregularis*-inoculated plants were watered each day with demineralised water and twice a week with a nitrogen-enriched nutrient solution. At harvest, roots were removed from their substrate, gently rinsed with deionised water, deep frozen, and stored at -80°C for later protein extraction.

Microsomal protein extraction

Microsome extraction of *M. truncatula* roots was performed at 4°C and obtained by differential centrifugation as previously described by Stanislas and co-authors (Stanislas *et al.*, 2009). Briefly, roots were homogenized using a Waring Blendor in grinding buffer (50 mM Tris-MES, pH 8.0, 500 mM sucrose, 20 mM EDTA, 10 mM DTT and 1 mM PMSF). The homogenate was centrifuged at 16,000x*g* for 20 minutes (rotor JA 14 Beckman, CA, USA). After centrifugation, supernatants were collected, filtered through two successive meshes (63 and 38 µm), and centrifuged at 96,000x*g* for 1 h (rotor 45 Ti, Beckman). Pellets, representing the microsomal fraction, were resuspended in 10 mM Tris-MES, pH 7.3 250 mM sucrose, 1 mM EDTA, 1 mM DTT, 1 mM PMSF, 10 µg/ml aprotinin and 10 µg/ml leupeptin. Protein amount was measured using the 2-D Quant Kit (GE Healthcare, Little Chalfont, UK).

In-solution protein digestion

Amicon Ultra-4 10 K centrifugal devices (Millipore, Bedford, MA, USA) were used for in-filter protein digestion. In the filtration devices, proteins (50 µg) from each control and mycorrhized plants were mixed with 10 mM DTT in solution A (8 M urea in 0.1 M Tris–HCl, pH 8.5) for 20 minutes to reduce protein disulphide bonds, and the

excess reducing solution eliminated by centrifugation at 5,000x*g* for 40 minutes (Sanyo MSE Harrier 18/80, Japan). The protein sample was further cleaned by rinsing with 200 µl of solution A and repetition of the centrifugation step at 5,000x*g* for 40 minutes. One hundred microliters of 50 mM iodoacetamide in solution A were added on the filter and the filter was incubated in the dark at room temperature (RT) for 30 minutes followed by a centrifugation at 5,000x*g* for 30 minutes. Afterwards, 100 µl of solution B (8 M urea in 0.1 M Tris–HCl, pH 8.0) was added on the filter to adjust the pH, and centrifuged again. After repeating the latter step twice, trypsin (Trypsin Gold, mass spectrometry grade, Promega, Madison, WI, USA) was added in 30 µl of triethylammonium bicarbonate (TEAB) to an enzyme/protein ratio of 1:100. Protein digestion was carried out overnight at RT. Finally the peptides were collected by centrifugation of the filter units at 5,000x*g* for 40 minutes.

iTRAQ peptides labelling

Each tryptic digest was either labelled with iTRAQ reagent 114 or 117 following the manufacturer's instructions (AB SCIEX, Foster City, CA, USA). Control and mycorrhized samples were labelled by alternating 114 and 117 tags to avoid labelling bias. Some experiments were labelled with single use of one iTRAQ tag (114, 115, 116 and 117) targeting an overview of the iTRAQ 4-plex effect on peptide pI. iTRAQ reagents were dissolved in 70 µl of ethanol and added to the protein digest. After 1 h of incubation at RT, equal amounts of the different samples were pooled and concentrated by evaporation using a SpeedVac (Heto, Saskatoon, SK, Canada). The excess of iTRAQ reagents was removed by desalting the labelled peptides using C18 columns Supelco (Discovery^{TM} DSC-18, 1 ml, 100 mg, Supelco Bellefonte, PA, USA). Peptides were eluted in 50% ACN (v/v), 0.1% TFA (v/v) and subsequently dried in SpeedVac (Heto) prior to peptides OGE fractionation.

Peptide OGE

3100 OFFGEL Fractionator and OFFGEL Kit pH 3–10 (Agilent Technologies, CA, USA) with 12 wells setup were used. Peptides were diluted in 1.8 ml of the focusing buffer containing only 5% (v/v) of glycerol in deviation from the supplier's protocol. IPG strips were rehydrated by adding 40 µl of peptide IPG strip rehydration solution per well for 15 minutes. Then, 150 µl of sample were loaded in each well. Peptide focusing was performed until it reached 20 kVh with a maximum voltage of 8,000 V

and maximum current of 50 µA. After focusing, the 12 peptide fractions were withdrawn and wells rinsed with 150 µl of H_2O/MeOH/TFA (49/50/1 v/v) for 15 minutes. Rinsing solutions were pooled with their corresponding peptide fractions and concentrated in SpeedVac (Heto) prior to LC-MS/MS analysis.

LC-MS/MS analysis

The dried peptides were re-dissolved in 25 µl 0.1% TFA (v/v). Peptide separation was performed using an Ultimate 3000 nano LC system (Dionex, Sunnyvale, USA) equipped with a C18 column (PepMap 100, 3 µm, 100 Å, 75 µm id x 15 cm, Dionex) and connected to a Probot microfraction collector (Dionex). The mobile phase consisted of a gradient of solvents A 2% ACN (v/v), 0.2% TFA (v/v) in water and B 80% ACN (v/v), 0.08% TFA (v/v) in water. Peptides were separated at a flow rate of 0.3 µL/minute using a linear gradient of 60 minutes of solvent B from 0 to 5% in 5 minutes, followed by an increase to 30% in 5 minutes and to 65% in 30 minutes. The column was washed with 95% of solvent B for 5 minutes followed by regeneration with solvent A. Column effluent was mixed with MALDI matrix α-cyano-4-hydroxycinnamic acid (CHCA) and collected at a frequency of one spot every 30 seconds on an Opti-TOF LC/MALDI insert blank plate (AB SCIEX). MALDI plates were analyzed with a MALDI-TOF/TOF 4800 Proteomics Analyzer (AB SCIEX). The instrument was calibrated using the 4700 mass standard calibration kit (AB SCIEX). MS spectra between *m/z* 900 and 4,000 were acquired for every spot using 1,500 laser shots. The 8 most intense ion signals per spot having a S/N > 30 were selected as precursors for MS/MS acquisition.

Peptide and protein identifications were performed with the ProteinPilot™ Software 4.0.8085 revision 148085 (AB SCIEX) using the Paragon algorithm. Combined data and spectra from each OGE fraction were searched against the NCBI viridiplantae database (released on the 5th of May 2011) and a EST database of *M. truncatula* (www.medicago.org, released on the 18th of July 2011). The following search parameters were selected: iTRAQ 4-plex peptide label, cysteine alkylation, trypsin specificity, ID focus on biological modifications, and processing including quantitation and thorough ID. We only report protein identifications with a total ProtScore >1.3, which represents >95% statistical confidence in ProteinPilot. Proteins having at least one peptide above 95% of confidence were recorded.

MarvinSketch Calculator Plugin (http://www.chemaxon.com/marvin/sketch) (Csizmadia, 2000), was implemented in this study to overcome the main bottleneck of the current available pI calculator such as the pI/MW tool of the ExPASy Proteomic Server (www.expasy.org) not giving the opportunity to calculate the pI of chemically modified peptides and consequently the pI of iTRAQ labelled peptides. This tool has been used to calculate pI of unlabelled and iTRAQ labelled peptides to explain some experimentally observed pI shifts

Abbreviations

ACN, Acetonitrile; AM, Arbuscular mycorrhiza; CHCA, α-cyano-4-hydroxycinnamic acid; DTT, Dithiothreitol; EDTA, Ethylenediaminetetraacetic acid; IAA, 2-iodoacetamide; IEF, Isoelectric focusing; IPG, Immobilized pH gradient; ITRAQ, Isobaric tags for relative and absolute quantitation; LC, Liquid chromatography; MALDI-TOF, Matrix assisted laser desorption ionisation time of flight; MeOH, Methanol; MES, 2-(N-morpholino)ethanesulfonic acid; MS, Mass spectrometry; MW, Molecular weight; NMWL, Nominal molecular weight limit; OGE, OFFGEL electrophoresis; pI, Isoelectric point; PMSF, Phenylmethylsulfonyl fluoride; SCX, Strong-cation exchange; TEAB, Triethylammonium bicarbonate; TFA, Trifluoroacetic acid; Tris, Tris(hydroxymethyl)aminomethane; 2-DE, Two-dimensional gel electrophoresis.

Competing interests

The authors declare that they have no competing interests.

Authors' contributions

CA: has performed the experiment in the frame of her PhD thesis, from plant cultivation until the in-depth analysis of the data; KS: provided help for MS analysis, discussed the results and critically commented and worked on the manuscript; CG: helped for the plant material, and the microsome isolation; EDG: supervised the PhD work and critically commented the manuscript; CL: technical help and support, especially in liquid chromatography steps; JR: supervised the PhD work, discussed the results and critically commented and worked on the manuscript. All authors read and approved the final manuscript

Acknowledgements

This work was supported by grants from the "Fonds National de la Recherche du Luxembourg" AFR TR-PHD BFR 08-078. The authors appreciate helpful discussions with Ghislaine Recorbet (INRA, Dijon, France) and her proofreading. The authors also thank Sébastien Planchon for his technical help and his support for bioinformatic issues.

Additional files

Chapter 2, additional file S2.1: Impact of iTRAQ labelling on peptide pI and OGE fractionwise.
This table shows the reproducibility of observed peptide pI shifts in at least 3 independent experiments of labelled samples in groups A, B, C and D. It presents peptide sequences, Paragon confidence score, observed (Obs mass) and theoretical masses (Theo mass), the mass modification induced by iTRAQ labelling and OGE fractions (OGF) before and after the labelling. Moreover the retention time (Rt) of non-modified and labelled peptides together with the difference (Diff) in retention time due to the iTRAQ tags are as well shown in this table.

Chapter 2, additional file S2.2: Impact of iTRAQ labelling on peptide retention time in LC separation.
This table presents the 17 peptides that showed an increase in retention time after the labelling. These peptides were focused in OGE fraction 1 when non-labelled (NL) and shifted to more basic fractions after iTRAQ labelling (L) and. The table shows their retention time (Rt) in minutes in LC separation before and after the labelling.

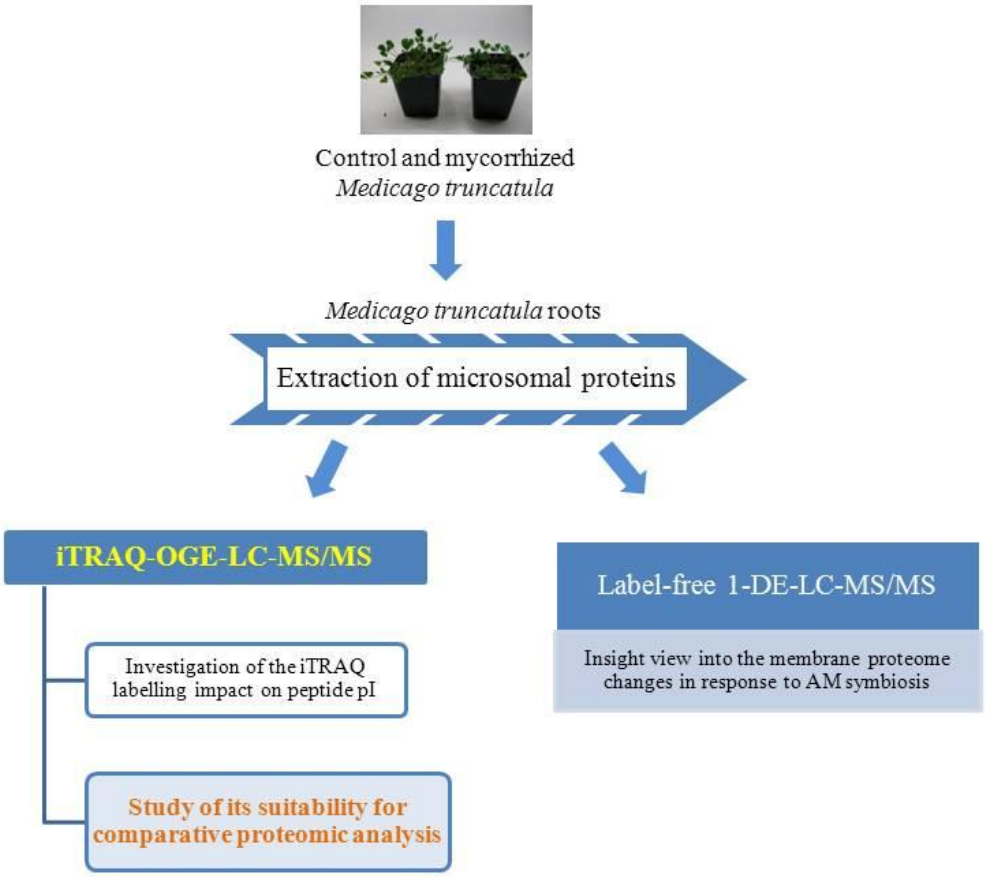

Abdallah *et al.*, 2012 Performance of isobaric labelling in quantitative proteomics of arbuscular mycorrhized *Medicago truncatula* roots. *Comparative Biochemistry and Physiology - Part D: Genomics and Proteomics*.

Chapter 3

Performance of isobaric labelling in quantitative proteomics of arbuscular mycorrhized *Medicago truncatula* roots

Cosette Abdallah[1,2], Kjell Sergeant[1], Céline C. Leclercq[1], Eliane Dumas-Gaudot[2] and Jenny Renaut[1]

[1]*Département Environnement et Agro-Biotechnologies, Centre de Recherche Public- Gabriel Lippmann, 41, rue du Brill, L-4422, Belvaux, Luxembourg.*

[2]*UMR Agroécologie INRA 1347/Agrosup/Université de Bourgogne, Pôle Interactions Plantes Microorganismes ERL 6300 CNRS, BP 86510, 21065 Dijon Cedex, France.*

Abdallah *et al.*, 2012 Performance of isobaric labelling in quantitative proteomics of arbuscular mycorrhized *Medicago truncatula* roots. *Comparative Biochemistry and Physiology - Part D: Genomics and Proteomics.*

Proteomics established itself as an indispensable technology to investigate and describe several biological processes. The plant proteomic field still relies on 2-DE gels and faces significant challenges in membrane proteomics. After the successful establishment of the iTRAQ-OGE-LC-MS/MS framework on *Medicago truncatula* microsomal proteins (chapter 2, (Abdallah *et al.*, 2012), this proteomic approach was afterwards implemented for in-depth study of *M. truncatula* membrane proteomics in response to the arbuscular mycorrhizal fungi invasion. The iTRAQ labelling quickly gained popularity in proteomics, however the protein quantification, that relies on reporter ions generated in MS/MS spectra, is not feasible through the standard collision induced dissociation (CID) in ion traps. The aforementioned drawback is overwhelmed in this study since iTRAQ labelled samples were analysed in the high performance Orbitrap Elite Velos mass spectrometer, in which the combination of hybrid fragmentation methods is possible. The CID-HCD couple provides a promising tool for iTRAQ labelled protein identification and their relative quantitation, giving that HCD fills the gap of the CID low mass cut-off limitation. This method combines the sensitivity of ion trap instruments with the very high resolution and mass accuracy capabilities. Its suitability in achieving accurate results and studying membrane proteomics in response to mycorrhiza is discussed in the following paper.

Abdallah *et al.*, 2012 Performance of isobaric labelling in quantitative proteomics of arbuscular mycorrhized *Medicago truncatula* roots. *Comparative Biochemistry and Physiology - Part D: Genomics and Proteomics*.

Abstract

Arbuscular mycorrhizal (AM) symbiosis, an intimate and mutualistic association between plant roots and fungi, is characterized by bilateral nutrient exchange between the two symbionts. Deep changes in the shape and number of organelles, together with profound modifications in various membrane compartments, are induced within AM symbiosis. Thus, important root microsomal protein modifications are assumed to be required to sustain the functioning of the interaction. However, proteomic analysis of symbiosis-related membrane proteins remains a major challenge due to their hydrophobicity, low abundance and precipitation at their isoelectric point, which precludes the use of two-dimensional electrophoresis (2-DE) for their large scale resolution and identification. In this context, to investigate the membrane-associated proteins that are regulated in the model interaction *Medicago truncatula* - *Rhizophagus irregularis*, a not yet implemented approach iTRAQ-OGE-LC-MS/MS to study plant-AM fungi symbiosis is employed as an alternative to 2-DE. The iTRAQ labelling has proven its compatibility with OFFGEL fractionation and has been widely used to study complex proteomes. An appropriate fractionation protocol is herein described allowing the recovery of membrane protein fractions. The suitability of the applied proteomic approach to track membrane proteome changes of *Medicago truncatula* roots in response to mycorrhiza is discussed.

Abdallah *et al.*, 2012 Performance of isobaric labelling in quantitative proteomics of arbuscular mycorrhized *Medicago truncatula* roots. *Comparative Biochemistry and Physiology - Part D: Genomics and Proteomics*.

Introduction

More than 80% of plants including all taxa except for Brassicaceae, and thus the model plant *Arabidopsis*, develop in their roots intimate association with arbuscular mycorrhizal (AM) fungi. While AM fungi are host dependant, plants can survive without the symbiotic partnership. By delivering phosphate, micronutrients and water, the fungi enhance the nutritional state of their hosts and in exchange benefit from an access to carbohydrates (Parniske, 2008; Bonfante & Genre, 2010). Besides improving the nutritional status, the symbiosis enables plants to perform better under harmful conditions and cope with adverse biotic and abiotic stresses (Parniske, 2008). AM symbiosis establishment elicits profound changes in the host plant and is characterized by the formation of "arbuscules", which are thought to be the major site of nutrient exchange between the two symbionts (Harrison, 1999). The invaded plant cell responds by the fragmentation of the vacuole, migration of the nucleus to a central position within the cell and an increase of the number of organelles (Carling & Brown, 1982; Balestrini *et al.*, 1992; Bonfante & Perotto, 1995). Moreover the plasma membrane extends around fourfold to form the periarbuscular membrane that envelops the arbuscule, therefore concomitant increases in membrane biosynthesis must be occurring (Harrison, 1999). Consequently, studies devoted to track membrane proteome changes in response to AM symbiosis could provide new insight into the understanding of how plants deal with the AM invasion. The *Medicago truncatula* root proteome is on the forefront of proteomic research and its dynamic alteration during interactions with fungi has been widely investigated as reviewed by Mathesius (2009) with a special focus in case of the symbiotic interaction with arbuscular mycorrhizal fungi (Bestel-Corre *et al.*, 2002; Valot *et al.*, 2005; Amiour *et al.*, 2006; Valot *et al.*, 2006; Recorbet *et al.*, 2010). *M. truncatula* became a model plant to study root legume-fungi symbiosis due to its diploid genome structure, relatively small genome size of about ~550 million base pair (Mbp) (Bell *et al.*, 2001) and short regeneration time. It is furthermore self-fertile, relatively easy to transform and its genome sequencing program is nearly completed, which offers further advantages through the increased number of available genomic tools (Colditz & Braun, 2010).

Lately, proteomics has emerged as an indispensable tool in the post-genomics era to study protein expression and changes in complex samples. One of the main differences between genomics and proteomics is that the former one is the study of a static entity whereas the protein content of organisms is highly dynamic. Unlike genomics, analogous to the polymerase chain reaction (PCR) does not exist in proteomics which hinders the study of low abundant proteins since they are often masked by high-abundant proteins. Two-dimensional gel electrophoresis (2-DE) remains the most commonly used technique in plant proteomics. More recently, substantial improvements in mass spectrometry (MS) and advances related to protein fractionation methods gave birth to a toolbox of novel and powerful gel-free proteomic approaches. MS-based proteomics is a young discipline and its development in plant biology is proceeding at a slow pace since studies using gel-free proteomics are still scant.

Membrane proteins are hydrophobic in nature and generally escape to 2-DE, thus gel-free quantitative approaches, such as isobaric tag for relative and absolute quantification (iTRAQ) coupled to LC-MS, seems to be well suited to study this class of proteins and has proven its ability to perform quantitative proteomic studies in plant membrane proteins (Kota & Goshe, 2011). The iTRAQ reagent labels peptide N-termini and ε-amino groups of lysine side chains and allows multiplexing of up to 8 samples in the same experiment. Protein quantification relies on reporter ion intensities yielded at low molecular mass (114-121) in MS/MS fragmentation (Ross *et al.*, 2004). To gain insight into the molecular mechanism of root hair cell biology, iTRAQ quantitative proteomics has recently been applied to characterize the phosphoproteome of the *Glycine max L.* root hairs during rhizobial colonization (Nguyen *et al.*, 2012). A broad range of MS instruments is capable of analysing iTRAQ labelled samples; however it is not feasible through the standard collision induced dissociation (CID fragmentation) in ion traps. This is due to CID low mass cut-off limitations, causing the mass spectra to be void below 25-30% of the precursor mass and thus iTRAQ reporter ions are missed (Kocher *et al.*, 2009). It has been demonstrated that the combination of two fragmentation methods -CID and higher energy collisional dissociation (HCD)- greatly enhances the analytical capacities of identifying and quantifying iTRAQ labelled peptides. While CID is performed in the

linear ion trap, HCD is done in an octopole collision cell (Savitski *et al.*, 2005; Falth *et al.*, 2007; Swaney *et al.*, 2008). Hence the same selected parent ion is fragmented twice, CID and HCD spectra are subsequently used for protein identification and quantification, respectively. Accordingly, the MS limitation is circumvented and iTRAQ reporter ions are detected (Kocher *et al.*, 2009).

The OFFGEL electrophoresis (OGE) apparatus, which permits isoelectric point peptide separation in solution, has proven its high resolution power, utility in reducing sample complexity and exclusivity in providing peptide isoelectric points. In recent years it has therefore proven to be a valuable tool for validating and filtering false positive identifications (Horth *et al.*, 2006; Hubner *et al.*, 2008). In addition, it has been shown that OGE is compatible with iTRAQ labelling for quantitative studies (Chenau *et al.*, 2008; Ernoult *et al.*, 2008).

In the current study, iTRAQ-OGE-LC-MS/MS proteomic approach is applied on the model legume *Medicago truncatula* roots inoculated with the AM fungus *Rhizophagus irregularis* to target protein pattern modifications and symbiosis-related microsomal proteins eligible for involvement in sustaining the interaction between the two symbionts.

Materials and methods

Plant material preparation, membrane protein extraction, protein digestion, iTRAQ labelling and OGE fractionation were performed as described in chapter 2 (Abdallah *et al.*, 2012).

LC-MS/MS analysis

The dried peptides were re-dissolved in 25 µl 0.1% TFA (v/v). Peptide separation was performed using an Ultimate 3000 nano LC system (Dionex, Sunnyvale, USA) equipped with a C18 column (PepMap 100, 3 µm, 100Å, 75 µm id x 15 cm, Dionex). The mobile phase consisted of a gradient of solvents A [2% ACN (v/v), 0.2% TFA (v/v) in water] and B [80% ACN (v/v), 0.08% TFA (v/v) in water]. Peptides were separated at a flow rate of 0.3 µL/minute using a gradient of 60 minutes of solvent B from 0 to 5% in 5 minutes, followed by an increase to 30 % in 5 minutes and to 65% in 30 minutes. The column was washed with 95% of solvent B for 5 minutes followed by regeneration with solvent A. The LC was online coupled to Orbitrap Elite Velos

(Thermo scientific, Bremen, Germany) in which *m/z* spectra (300-2,000 *m/z*) were acquired in a positive mode at a resolution of 60,000.

Data-dependent automatic survey MS scan and tandem mass spectra (MS/MS) acquisition were applied. For internal mass calibration the 371.101240 ion was used as a lock mass. Dynamic exclusion was enabled with exclusion size list of 500 and exclusion duration of 30 s. The 10 most intense precursors were selected for subsequent fragmentation, each selected parent ion was first fragmented by CID and then by HCD, the mono-charged precursor ions were excluded. The normalized collision energy was set to 35% and 65% in CID and HCD, respectively. For MS/MS *via* CID, the fragmentation was acquired in the ion trap with an isolation window of 2.0 *m/z*, a target value of 5,000, an activation Q of 0.25 and an activation time of 10 ms. For MS/MS *via* HCD a resolution of 15,000 was set in the Orbitrap with an isolation window of 2.0 *m/z*, a low mass cut-off at *m/z* 100, a target value of 30,000 ions and an activation time of 0.1 ms. Combined CID and HCD spectra were processed in Mascot using Proteome Discoverer (beta version 1.2.0.92) by searching against the NCBI viridiplantae database (released on the 5th of May 2011) and EST database of *Medicago truncatula* (www.medicago.org, released on the 18th of July 2011). The searches were performed with the following parameters: enzyme trypsin, 2 missed cleavage, mass accuracy precursor 10 ppm, mass accuracy fragments: 0.5 Da(CID)/0.02 Da (HCD), fixed modifications carbamidomethyl (C), iTRAQ 4-plex N-terminal and lysine (K) side chain, variable modifications methionine oxidation. Proteome Discoverer calculates reporter ion intensities through the HCD spectra with a target FDR of 5%.

Close homologues of the identified proteins in *M. truncatula* were searched against The *Arabidopsis* Information Resource (TAIR) database (http://www.arabidopsis.org/). Transmembrane domains (TMD) were predicted using the Tmpred server (http://www.ch.embnet.org/software/TMPRED_form.html) with a minimum score of 1000. The online tool PREDTMBB (http://biophysics.biol.uoa.gr/PRED-TMBB/input.jsp) was used to discriminate beta-barrel outer membrane proteins. Psort (http://psort.hgc.jp/form.html) was implemented to predict protein localisation.

Results and discussion

Proteomic analysis design for in-depth differential quantitative study.

Proteomic studies in response to AM symbiosis was to date performed scarcely by 2-DE, which represents the trademark method for plant proteomics. Microsomal proteins are out of the scope of this technique and highly underrepresented. Thus, many candidates involved in the establishment and functioning of the symbiosis remain to be discovered. An alternative approach iTRAQ-OGE-LC-MS/MS is herein discussed with the respect to the specific requirements for membrane proteomics. A protocol allowing the recovery of an enriched membrane protein fraction isolated from non-infected and mycorrhized *Medicago trun*catula roots has been used. Extracted proteins were digested in solution using trypsin, subsequently each digest was either labelled with iTRAQ reagents 114 or 117 and prefractionated in 12 wells using a 12 cm strip covering the pH range of 3-10 in OGE. The iTRAQ labelled and pre-fractionated samples were then separated on a C18 column online coupled to an orbitrap Elite Velos. Acquired MS/MS spectra were then provided to Proteome Discoverer for protein identification and quantification.

Comparison of peptide and protein identification results

Four independent experimental replicates of 100 µg of control and mycorrhized microsomal proteins were analysed by iTRAQ-OGE-LC-MS/MS. Table 3.1 represents a summary of the number of MS scans, peptides and proteins reported in the 12 OGE fractions per experiment. A similar number of proteins (77, 83, 94 and 112) were identified in each of the four replicates with an average of 158 peptides and 91 proteins in all experiments. Although the number of scans is relatively high, the number of identifications remains relatively low.

Table 3.1: Summary of the number of MS scans, identified peptides and proteins per experiment.

Experiments	Full scan	MS^2 scans	Number of peptides	Number of proteins
1	12461	83004	121	77
2	10572	100268	182	94
3	10834	97498	192	112
4	11472	96642	137	83

In order to explore the optimal HCD fragmentation conditions, iTRAQ labelled sample acquisition was performed under different HCD collision energy settings (35, 45, 55 and 65%). We found that 65% was the most appropriate collision energy for our samples yielding to the highest number of quantified peptides. Taking into account that HCD is limited by the low duty cycle of the Orbitrap which might decrease the number of quantified proteins, the number of the most intense precursor ions dedicated for MS/MS fragmentation, initially fixed at 10, was decreased to 5 and 3. Neither top 5 nor 3 parent ion selections were able to improve the overall number of identifications obtained in all experiments (data not shown). A straightforward interpretation of the generated datasets was possible with Proteome Discoverer software capable of searching and interpreting combined CID and HCD spectra. Thus HCD, containing the reporter ion information, was matched to the CID spectra of the corresponding precursor peptide prior to the searches in databases. To prove that the applied strategy is well suited to the quantitative proteomics of iTRAQ labelled samples, a trial search in the databases was done by omitting the CID spectra and keeping only HCD ones. Unsurprisingly the search results were missing a high number of proteins successfully identified when both spectra were combined (data not shown). HCD provides insufficient sequence-specific fragments for confident sequence assignment leading to low Mascot ion score and their minor contribution in increasing the number of identifications has been previously reported (Shen *et al.*, 2011).

The low number of identified proteins in the present study could be related to the offline pre-fractionation method (OGE prior to LC) which could lead to sample loss due to the number of desalting steps prior to MS analysis. Furthermore it has been previously reported that iTRAQ labelling significantly reduces the number of peptide identifications in an LC-MS workflow using CID and HCD peptide fragmentation (Thingholm *et al.*, 2010). This major drawback in isobaric tagging was related to the increased ion charge state of iTRAQ labelled peptides (Nogueira *et al.*, 2012). The setting of a perpendicular flow of ammonia vapour between the needle and MS orifice appeared to reduce the average charge state of labelled peptides, however it is

important to note that maintaining a constant flow of ammonia vapour is difficult (Thingholm *et al.*, 2010).

Degree of soluble contaminant proteins in the microsomal protein fractions.

For quantitative comparative proteomics, all experiments were loaded in Proteome Discoverer and a comparison view was obtained for the 151 proteins identified in all experiments. The first challenge faced in membrane proteomics is the elimination of abundant soluble proteins that contaminate the microsomal protein fractions, which makes an enrichment step crucial for a good membrane proteomic study. Such enrichment step is generally based on differential centrifugation (Santoni *et al.*, 2000). In the current study a previously described method on *Nicotiana tabacum* cells based on differential centrifugation has been employed (Stanislas *et al.*, 2009). After purification of the membrane protein fractions, the amount of contamination by non-targeted structures, soluble proteins, can be estimated after protein identifications by the use of tools available online and algorithms for protein localisation, transmembrane domain and beta barrel predictions. Close homologues displaying at least 70% pair-wise identity and/or a cut-off expectation value of e^{-40} (Nair & Rost, 2002) of the 151 proteins were found by searching against The *Arabidopsis* Information Resource (TAIR) database. A protein was considered as membrane-associated when it was experimentally demonstrated to have a membrane localisation on the basis of direct assay (Richly & Leister, 2004). When this criterion was not satisfied, a protein was considered as contaminant unless it displayed at least one transmembrane domain or formed a beta barrel embedded in the membrane lipid bilayer. Applying the aforementioned filters, only 18 out of the 151 proteins were recorded as soluble proteins and thus potential contaminants of the microsomal protein fractions which represent a percentage of 12%. Keeping in mind that membrane protein extraction methods are, by no mean, perfect and that the use of prediction algorithms must be done critically, we consider that the applied protocol gave access to membrane protein-enriched fractions.

Abdallah *et al.*, 2012 Performance of isobaric labelling in quantitative proteomics of arbuscular mycorrhized *Medicago truncatula* roots. *Comparative Biochemistry and Physiology - Part D: Genomics and Proteomics*.

Protein abundance changes and iTRAQ labelling accuracy.

The 151 proteins identified in all replicates can be sub-divided into 4 groups (Chapter 3; Additional file S3.1). The first one contained 12 identified proteins without quantitative data, which could be explained by a fragmentation performed better in CID leading to peptide and thus protein identification. The lack of quantitative data could not be fulfilled by HCD spectra as ions at *m/z* 114 and 117 could not be observed. The second group encompassed 45 proteins quantified in a single experiment while no quantification could be assigned to these proteins in other replicates. The third group included 36 proteins that were quantified in at least 2 experiments and presented the same trend in protein abundance changes even if the reproducibility was relatively low and the reporter ion ratio discrepancy was quite high from one experiment to another. As an example, the VDAC1.1 protein (TA20806_3880) was identified in two experiments and recorded reporter ion ratios (114/117) of 0.66 and 0.511 in both replicates. Although the quantification data showed a down-regulation of the protein expression in mycorrhized *M. truncatula* roots in both experiments, the low reproducibility of the measurements decrease the confidence in the calculated iTRAQ reporter ion ratios. Fifty eight proteins were classified in the fourth group. As described in material and methods, control and mycorrhized samples were labelled by alternating 114 and 117 tags to avoid labelling bias. In this group of proteins, the intensity of the iTRAQ reporter ion in MS/MS spectra at *m/z* 117 was in general higher than 114 leading to inconsistent quantitative data between experiments. Consequently the calculated ratio of the same protein showed either up- or down-regulation of the protein expression when mycorrhized proteins were labelled with iTRAQ tag 117 (calculated ratio 117/114) and 114 (calculated ratio 114/117), respectively. For instance, an iTRAQ reporter ion ratio (117/114) of 2.116 was assigned to histone H4 (gi22217761) in the fourth replicate while a ratio (114/117) of 0.58 was recorded in the first and second experiments. Aiming at in-depth understanding of the observed results, the same set of samples were analysed on MALDI-TOF/TOF and the same observation was noticed: the intensity of the iTRAQ reporter ion at *m/z* 117 was mainly higher than the one at 114 independently on the labelled sample (data not shown). Unlike the low accuracy in

protein quantification, some already known mycorrhiza-related proteins by Valot and colleagues (Valot *et al.*, 2005; Valot *et al.*, 2006) were successfully identified in this study such as lipoxygenase, cytochrome b5, elongation factor 1-alpha, vacuolar proton-inorganic pyrophosphatase and blue copper protein with 70% of query coverage with the one identified by Valot *et al.* (2006) when both sequences were aligned. The protein expression of putative phosphate transporter (gi97974044) was found to be down-regulated in response to AM symbiosis. Its sequence was aligned with MtPT1 (Javot *et al.*, 2007) and MtPT4 (Harrison *et al.*, 2002), it showed a query percentage of 36% and 35%, respectively. Despite the popularity of iTRAQ labelling for quantitative proteomic studies and its increased application, this technique is not without its shortcoming. Some concerns such as underestimation of ratios and limited accuracy were reported (Wang, H *et al.*, 2012). The expected influence of iTRAQ labelling on peptide fragmentation, by adding a high basic group on peptide N-termini, was recently proved on singly charged peptides analysed in MALDI (Gandhi *et al.*, 2012). This study has shown that iTRAQ labelling leads to a more pronounced set of b-ion peaks and distinct changes in the abundance of specific peptide types. Gandhi and co-workers highlighted that ion abundance depends on various factor such as instrumental set-up, chemical modifications and the used enzyme of cleavage. These parameters should be taken into account by search programs and it has shown that the relative abundance of ions can be correctly predicted (Gandhi *et al.*, 2012). In our case, the hypothesis that would more likely explain the high variability in reporter ion intensities and the non-homogeneity in reporter ion areas is what has been reported on iTRAQ labelling lack in both precision and accuracy in complex samples (Ow *et al.*, 2009). This imprecision was in part related to reporter ion signal intensity and the signal to noise ratio. The poor accuracy was also attributed to contaminants co-selected in the same precursor ion window leading to MS/MS spectra containing reporter ion derived from mixed sources and thus causing errors in reporter ion measurements (Christoforou & Lilley, 2012). The net effect of this co-selection is the unpredictable and distortion of reporter ion intensities (Christoforou & Lilley, 2012). Christoforou and Lilley reported that 90% of unlabelled sample spectra (supposed to be unable to produce reporter ions) contain at least two of eight "phantom" reporter

ions with almost 70% being fully quantifiable, which makes the co-selection of contaminants ubiquitous.

Conclusion and future prospects

This work aimed at further understanding membrane proteome modifications in *Medicago truncatula* roots infected by *Rhizophagus irregulare*. The main challenge in plant membrane proteomics was by-passed by using an appropriate fractionation protocol allowing the recovery of membrane protein-enriched fractions. An approach not yet implemented in the study of plant-AM fungi symbiosis, iTRAQ-OGE-LC-MS/MS, was herein applied to circumvent 2-DE-related shortcomings to study membrane proteins. Although the isobaric tagging method has many attractive attributes, it appeared less suited in the present large-scale study. The major constraints related to the applied labelling method, in the current study, were the low number of identified peptides/proteins and low accuracy in protein quantification. To deal with iTRAQ ratio distortions, many endeavours for robust solutions were suggested, such as preferences for peptide two dimensional separations to reduce sample complexity and application of novel MS fragmentation (introducing of hybrid method CID and HCD fragmentations). In our study both recommendations were respected, however it would be interesting to try narrowing the precursor ion isolation window in order to reduce the co-selection of contaminants and thus improve the reporter ion ratios (Wenger *et al.*, 2011). As previously shown to be compatible for iTRAQ labelled sample analyses, it would be also worthy to try analysing these samples in electron transfer dissociation followed by resonant excitation ETD/CAD, a new MS fragmentation method that could be more suited and lead to better results (Phanstiel *et al.*, 2009). With the increased discussions in the literature about iTRAQ poor quantification accuracy, a new method called iQuARI was recently described to reduce the distortion of the iTRAQ reporter ion ratios (Vaudel *et al.*, 2012). This method, based on the use of decoy sample, estimates the interference level in the sample and computes false discovery rates for reporter ion based quantification. Thus by revealing the substantial interference between the target and decoy samples iQuARI allows the correction of reporter ion ratio measurements (Vaudel *et al.*, 2012). Moreover, pilot experiments are mandatory and should be designed to

Abdallah *et al.*, 2012 Performance of isobaric labelling in quantitative proteomics of arbuscular mycorrhized *Medicago truncatula* roots. *Comparative Biochemistry and Physiology - Part D: Genomics and Proteomics*.

optimize the quantitative platform by adding spiked standard proteins in at known concentrations and test the performance of the system in terms of precision and accuracy. Large-scale multiplexed quantitative proteomics experiments using isobaric methods are suboptimal, therefore many described guidelines should be taken into account to select the best suited quantitative proteomic approach to a given experimental design.

Additional files

Chapter 3, additional file S3.1: Table of identified proteins by iTRAQ-OGE-LC-MS/MS.
For each experimental replicate, this table shows the 4 groups of identified proteins, their accession number and description, number of peptides and the iTRAQ reporter ion ratio of every protein.

Abdallah *et al.*, 2012 Performance of isobaric labelling in quantitative proteomics of arbuscular mycorrhized *Medicago truncatula* roots. *Comparative Biochemistry and Physiology - Part D: Genomics and Proteomics*.

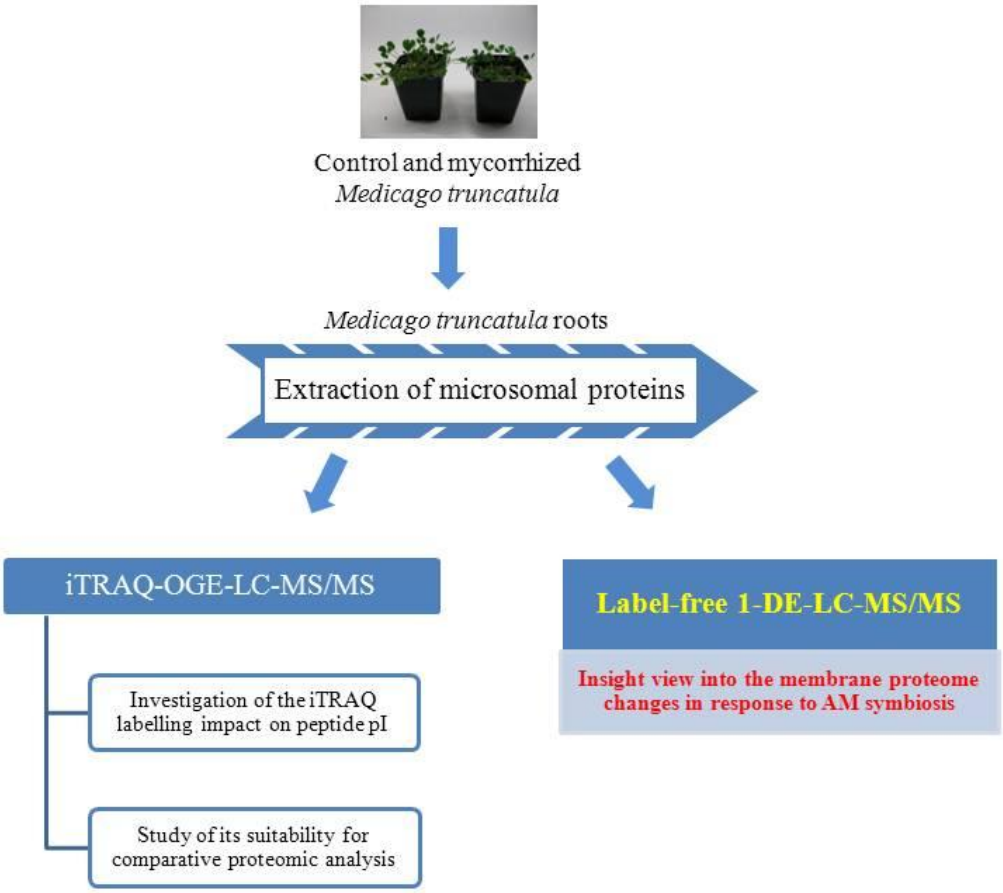

Abdallah *et al.*, 2012 A label-free 1-DE-LC-MS/MS workflow for inventorying the root microsomal proteome and its modifications upon arbuscular mycorrhizal symbiosis in the plant-microbe interacting model legume *Medicago truncatula*. *Journal of Proteomics* (submitted)

Chapter 4

A label-free 1-DE-LC-MS/MS workflow for inventorying the root microsomal proteome and its modifications upon arbuscular mycorrhizal symbiosis in the plant-microbe interacting model legume *Medicago truncatula*

Cosette Abdallah[1,2*], Ghislaine Recorbet[2*], Benoit Valot[3], Christelle Guillier[2], Michel Zivy[3], Diederik Van Tuinen[2], Daniel Wipf[2], Jenny Renaut[1] and Eliane Dumas-Gaudot[2]

[1]*Département Environnement et Agro-Biotechnologies, Centre de Recherche Public- Gabriel Lippmann, 41, rue du Brill, L-4422, Belvaux, Luxembourg.*

[2]*UMR Agroécologie INRA 1347/Agrosup/Université de Bourgogne, Pôle Interactions Plantes Microorganismes ERL 6300 CNRS, BP 86510, 21065 Dijon Cedex, France.*

[3]*UMR de Génétique Végétale, PAPPSO, Ferme du Moulon, 91190 Gif sur Yvette, Fance.*

*These authors contributed equally to this work
[§]Corresponding author
Email addresses:
BV: valot@moulon.inra.fr
CA: abdallah@lipmann.lu
CG: cguillier@dijon.inra.fr
DvT: tuinen@dijon.inra.fr
EDG: dumas@dijon.inra.fr
DW: Daniel.wipf@dijon.inra.fr
JR: renaut@lippmann.lu
MZ: zivy@moulon.inra.fr
GR: recorbet@dijon.inra.fr

Abdallah *et al.*, 2012 A label-free 1-DE-LC-MS/MS workflow for inventorying the root microsomal proteome and its modifications upon arbuscular mycorrhizal symbiosis in the plant-microbe interacting model legume *Medicago truncatula*. *Journal of Proteomics* (submitted)

The iTRAQ-OGE-LC-MS/MS approach appeared to be limited and less suited for large-scale analysis of *Medicago truncatula* microsomal proteins in response to an arbuscular mycorrhizal fungus colonisation, primarily due to the meagre reproducibility of iTRAQ reporter ion ratios. As an alternative, the promising label-free 1-DE-LC-MS/MS workflow was used for differential quantitative study of symbiosis-related membrane proteins. For in-depth and accurate relative quantification, label-free is more suited than isobaric tagging approaches (Vaudel *et al.*, 2012). This methodology takes advantage of both gel-based protein and gel-free peptide separation properties, which ensures protein solubility in SDS-PAGE and reduces sample complexity prior to LC, leading to higher chances in identifying low abundant proteins. The advent label-free methods are becoming increasingly popular as they do not require expensive protein labelling reagents and can accommodate any type of organism and most frameworks. In the current study, improved membrane protein extraction protocols and advanced techniques for their fractionation, identification and quantification are employed to detect low abundant and membrane proteins. This study can greatly expand the depth and breadth of membrane proteome changes and its fundamental role in the complex network of the AM interaction.

Graphical abstract

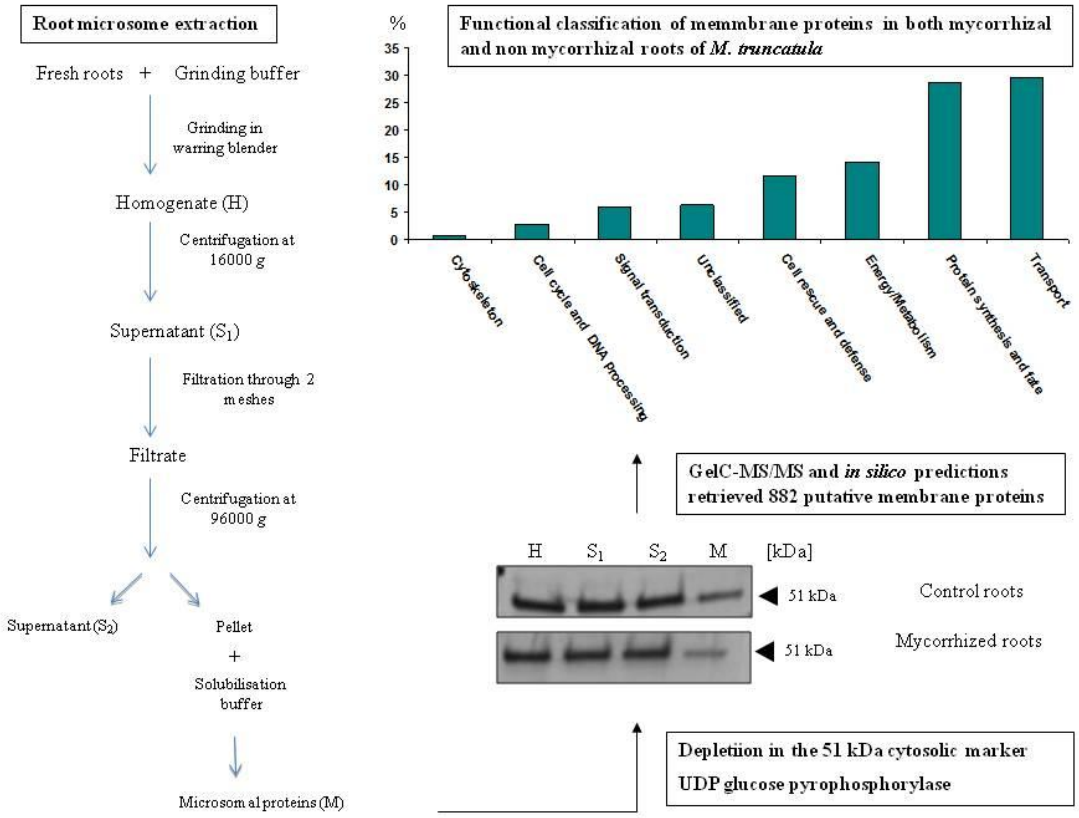

Abdallah *et al.*, 2012 A label-free 1-DE-LC-MS/MS workflow for inventorying the root microsomal proteome and its modifications upon arbuscular mycorrhizal symbiosis in the plant-microbe interacting model legume *Medicago truncatula*. *Journal of Proteomics* (submitted)

Abstract

Arbuscular mycorrhizal (AM) symbiosis, which associates most of plants roots with soil-borne fungi of the phylum *Glomeromycota*, is characterized by reciprocal nutritional benefits whereby plants supply associated fungi with carbohydrates while in turn, fungi provide mainly phosphorus and nitrogen to the host. Fungal colonization of plant roots induces massive changes in root cortical cells where the fungus differentiates into a tree-shaped haustorium, the arbuscule, which drives proliferation of the plasma membrane (PM), and the *de novo* synthesis of the periarbuscular membrane, an extension of the PM that surrounds the arbuscule, but displays novel biological features. Despite the recognized importance of membrane proteins in sustaining AM symbiosis, the root microsomal proteome elicited upon mycorrhiza, still remains to be explored. In this study, we used a device allowing the isolation of *Medicago truncatula* root microsomes with sufficient protein recovery and purity for their subsequent in depth analysis by GeLC-MS/MS. The results obtained highlighted the identification of 882 root membrane protein candidates whose cellular and functional classifications predispose plastids and transport as prevalent organelle and function, respectively. Consistently, besides alpha-helical *trans*-membrane spans, *in silico* predictions pointed out to the dominance of β-barrels domains coupled palmitate-modified proteins in the currently identified root microsomal proteome of *M. truncatula*, supporting the view of a highly fluent and dynamic membranous environment. Finally, the label-free peak integration strategy we used to quantify root membrane protein abundance changes upon AM symbiosis, indicated the prevalence of quantitative modifications, among which new candidates supporting the importance of membrane signalling/trafficking events in mycorrhiza establishment/functioning were identified.

Abdallah *et al.*, 2012 A label-free 1-DE-LC-MS/MS workflow for inventorying the root microsomal proteome and its modifications upon arbuscular mycorrhizal symbiosis in the plant-microbe interacting model legume *Medicago truncatula*. *Journal of Proteomics* (submitted)

Introduction

Arbuscular mycorrhizal (AM) symbiosis is the most widespread plant-microbe association on the planet, influencing plant nutrition, diversity and productivity. Plants hosting soil-borne AM fungi in their roots display an overall enhanced growth and a higher tolerance to biotic and abiotic stresses in adverse environments, making mycorrhiza of special interest in sustainable plant production systems (Smith, 1997; Gianinazzi *et al.*, 2010). AM symbiosis dates back to approximately 400 million years (Remy *et al.*, 1994), and is characterized by reciprocal nutritional benefits whereby plants supply associated fungi with carbohydrates while in turn, fungi provide mainly phosphorus and nitrogen to the host (Smith & Read, 2008). Fungal colonization of plant roots induces massive changes in root cortical cells into which the fungus branches dichotomously and differentiates into a tree-shaped haustorium, the arbuscule, which is thought to be the main site of signal and nutrient exchange between the two partners (Harrison, 2005; Parniske, 2008). Arbuscule development involves an extensive architectural reorganization of the colonized cell, including invagination of the plasma membrane (PM) and the tonoplast (Pumplin & Harrison, 2009), a dramatic PM proliferation (Harrison, 1999), and the *de novo* synthesis of the periarbuscular membrane (PAM), an extension of the PM that surrounds the arbuscule, but displays novel biological features such as the presence of MtPT4, an AM-specific phosphate transporter (Javot *et al.*, 2007), GmAMT4.1, an AM-inducible ammonium transporter (Kobae *et al.*, 2010), and the blue copper binding-like protein MtBcp1 of unknown function (Hohnjec *et al.*, 2005; Valot *et al.*, 2006; Pumplin & Harrison, 2009). Concomitantly, the cytoskeleton is rearranged to guide membrane deposition and the accumulation of Golgi, endoplasmic reticulum (ER), mitochondria, peroxisomes and plastids around the arbuscule (Genre *et al.*, 2005; Lohse *et al.*, 2005; Pumplin & Harrison, 2009). Noteworthy, remodelling of the cellular membrane system in AM roots is especially illustrated by strong alterations in the expression of genes related to lipid metabolism as indicated by up-regulation of transcripts encoding proteins involved in lipid breakdown and glycolipid synthesis, which sustain cell membrane composition and signalling processes (Gaude *et al.*, 2012). Likewise, mycorrhizal roots display a complex reprogramming of transporter gene expression among which belong those required for nutrient exchange and energetic requirements (Benedito *et al.*, 2010). As a result, the reorganization of the aforementioned

membranous compartments closely evokes the importance of getting knowledge on root microsomal protein modifications potentially sustaining AM symbiosis establishment and functioning, but also for creating a root membrane proteome database for comparative purposes with more recently evolved plant-microbe interactions that share root morphological commonalties with mycorrhiza (Paszkowski, 2006).

According to analyses of multiple complete genome sequences, it has been estimated that approximately 20 to 30% of the cellular proteome consists of *trans*-membrane (TM) proteins, also known as integral polytopic proteins, which correspond to proteins that are permanently attached to the lipid membrane and span at least once across the membrane. The *trans*-membrane regions of these proteins are either alpha-helical or beta-barrels, the former domains being present in all types of biological membranes including outer membranes, whereas beta-barrels being only found in outer membranes of Gram-negative bacteria, lipid-rich cell walls of a few Gram-positive bacteria, and outer membranes of mitochondria and chloroplasts (Wallin & von Heijne, 1998; Schwacke *et al.*, 2004). In parallel, many of other membrane-associated proteins, referred to as extrinsic, are anchored to the membrane *via* mechanisms that are distinct from those employed by *trans*-membrane proteins. Actually, lipid modifications facilitate the attachment of soluble proteins to biological membranes, but also enable protein–protein interactions and, in some cases, the shuttling of proteins between the plasma membrane and the cytosol or other membrane compartments. These modifications, which are found in all eukaryotic cells, fall into four major classes and are characterized by the type of lipid and the site of modification in the protein, including *N*-myristylation, palmitoylation and prenylation (Yalovsky *et al.*, 1999). The fourth and best-characterized lipid modification that occurs in the lumen of the secretory pathway is the attachment of glycosylphosphatidylinositol (GPI) anchors. This lipid modification is composed of a phosphatidylinositol connected through a carbohydrate linker to the protein. Following addition of the GPI moiety in the endoplasmic reticulum (ER), the protein traffics through the secretory pathway to the cell surface, where the GPI anchor tethers the protein to the extracellular face of the plasma membrane (Nadolski & Linder, 2007; Helbig *et al.*, 2010).

With regard to root proteomic analyses aiming at recording membrane protein changes elicited upon AM symbiosis, the use of two-dimensional gel electrophoresis (2-DE) performed on a microsome-enriched fraction from *Medicago truncatula* roots either inoculated or not with the mycorrhizal fungus *Glomus intraradices*, allowed retrieving 36 differentially-accumulated protein spots following mycorrhizal formation (Valot *et al.*, 2005). Nonetheless, this approach turned out to be limited by a rather low coverage (22%) of TM proteins, pointing to the necessity of increasing the proteomic repertoire of root membrane proteins to further assess their overall response to AM symbionts. Actually, 2-DE suffers from many limitations with respect to certain classes of proteins such as integral membrane proteins, proteins with high/low molecular weights or extreme isoelectric points. Moreover, gel spots can be populated with more than one protein making it often impossible to assign the correct quantitative values to the relevant protein identification (Ong & Pandey, 2001). Such limitations of 2-DE for analytical protein profiling have thus led to the more recent development of shotgun proteomic approaches designed to optimize proteome coverage, including one-dimensional (1-DE)-nanoscale capillary liquid chromatography-MS/MS, namely GeLC-MS/MS, which combines a size-based protein separation to an in-gel digestion of the resulting fractions, and proved valuable in expanding the depth and breadth of membrane protein detection in AM symbiosis (Valot *et al.*, 2006; Recorbet *et al.*, 2009). In parallel, the development of label-free technologies has allowed quantitating peptides in a relative manner using spectral characteristics such as peak area (peak integration) or frequency of peptide fragment spectra (spectral counting) during LC-MS/MS analysis, an advance that has been aided by progress in MS instrumentation (Bindschedler *et al.*, 2011). Spectral counting benefits from faster scan rates, higher sensitivity and faster MS to MS/MS conversions, while peak integration, based on the assumption that the chromatographic peak area of a peptide corresponds to its concentration (Filiou *et al.*, 2012), benefits from stable and precise LC systems and high accuracy mass analyzers (Thelen & Peck, 2007). These advent methods are becoming increasingly popular as they do not require expensive protein labelling and can accommodate any type of organism and most workflows, including plant systems such as beans (*Phaseolus vulgaris*), rice (*Oryza sativa)*, *Arabidopsis thaliana* (Bindschedler & Cramer, 2011) and *M. truncatula* in symbiosis with *Sinorhizobium meliloti* (Larrainzar *et al.*, 2007),

but however they have not yet been applied for tracking changes in root membrane protein abundance in response to mycorrhiza.

The elucidation of the root membrane proteome elicited upon mycorrhiza corresponding to a key milestone in understanding AM symbiosis development/functioning, the current study is thus intended to investigate, using a 2-DE- and label-free approach, the microsomal protein changes in response to the AM fungus *Rhizophagus irregularis* (formely *G. intraradices*) in the model leguminous host *M. truncatula*. For that purpose, a protocol aiming at isolating root microsomal proteins with sufficient recovery and purity for their subsequent in-depth analysis by GeLC-MS/MS was set up, and a new framework is herein described for the first application of quantitative label-free 1-DE-LC-MS/MS on arbuscular mycorrhized roots. Besides depicting the first large-scale depository of membrane proteins of *M. truncatula* roots, this article highlights new protein candidates potentially involved in sustaining the plant symbiotic program on the basis of a peak integration strategy.

Material and methods

Biological material and growth conditions

Medicago truncatula cv Jemalong 5 seeds were surface sterilised and germinated at 27°C in the dark on 0.7% sterile agar (Bestel-Corre *et al.*, 2002). Two-day old seedlings were then transplanted into 400 mL plastic pots containing a mix of sterile soil of Epoisses and sand (1:2 v/v). Mycorrhizal inoculation was realized by adding Epoisses soil-based inoculum (spores, roots and hyphae) of the AM fungus *Rhizophagus irregularis* DAOM 181602 (previously known as *Glomus intraradices*) (Kruger *et al.*, 2012). Seedlings (3 per pot) were grown for 4 weeks under controlled conditions (16 h photoperiod, 23°C/18°C day/night, 60% relative humidity, 220 µEinstein $m^{-2}.s^{-1}$ photon flux density). Control and *R. irregularis*-inoculated plants were watered each day with demineralised water and twice a week with a phosphate-starved but nitrogen-enriched nutrient solution, thus allowing mycorrhiza formation but impeding rhizobia development, respectively (Dumas-Gaudot *et al.*, 1994). Two independent biological experiments were conducted, each encompassing three replicates of mycorrhized and nonmycorrhized roots.

At harvest, roots were removed from their substrate, gently rinsed with running tap water and then with deionised water. Mycorrhizal parts were randomly collected from six replicated root systems per biological experiments and stained with trypan blue

after clearing with potassium hydroxide (Phillips & Hayman, 1970). Mycorrhizal colonisation parameters were estimated under light microscopy as described in (Trouvelot *et al.*, 1986). Calculations of frequency of mycorrhization (F%), percentage of root cortex colonisation (M%) and percentage of arbuscules (A%) were carried out with the MycoCalc program (http://www.dijon.inra.fr/mychintec/Mycocalc-prg/download.html). The remaining root parts were deep-frozen and stored at -80°C for later protein extraction. For mycorrhizal parameters, data were subjected to arcsin square root transformation before comparison of means using Student's *t*-test with a value of $P<0.01$ considered to be statistically significant (Recorbet *et al.*, 2010).

Root microsomal protein extraction

Extraction of microsomal proteins from *M. truncatula* roots was performed at 4°C using a differential centrifugation procedure described by Stanislas and co-authors for tobacco cell cultures (Stanislas *et al.*, 2009). As illustrated in Figure 4.2A, roots were homogenized using a Waring Blendor in grinding buffer (50 mM Tris-MES, pH 8.0, 500 mM sucrose, 20 mM EDTA, 10 mM DTT and 1 mM PMSF). The homogenate was centrifuged at 16,000x*g* for 20 minutes (rotor JA 14 Beckman, CA, USA). After centrifugation, supernatants were collected, filtered through two successive meshes (63 and 38 µm), and centrifuged at 96,000x*g* for 1h (rotor 45 Ti, Beckman). Pellets, representing the microsomal fraction, were resuspended in 10 mM Tris-MES, pH 7.3 250 mM sucrose, 1 mM EDTA, 1 mM DTT, 1 mM PMSF, 10 µg/ml aprotinin and 10 µg/ml leupeptin. Protein amount was measured using the Bradford's dye binding assay using BSA as a standard (Bradford, 1976).

To assess the efficiency of the afore-mentioned protocol in enriching membrane proteins from crude root extracts, depletion in the cytosolic marker UDP glucose pyrophosphorylase was compared between the various fractions resulting from the differential centrifugation procedure the in the two biological replicates using Western blot analysis. For that purpose, proteins (15 µg) separated on 12% SDS-PAGE for 45 min at 10°C and 20 mA (Hoefer Mightly Small II, Amersham Biosciences, Uppsala, Sweden) were further electrotransferred onto nitrocellulose membranes (Protan BA85, Shleider & Schuell, 0.45 μm pore size) using Trans-Blot SD semi-dry Electrophoretic Transfer Cell (BioRad). Membranes were incubated with barley UDP glucose pyrophosphorylase antibodies (Agrisera AB, http://www.agrisera.com/)

diluted 1:1000 as described in (Daher *et al.*, 2010). Antibody-bound proteins were detected using the ECL system according to the manufacturer's instructions (PerkinElmer, Western Lightning Plus ECL) after incubation with anti-rabbit secondary antibody conjugated to horseradish peroxidase.

Sample pre-fractionation using 1-DE

Twenty micrograms of the six control and six mycorrhized microsomal-enriched protein fractions were pre-fractionated by 0.7cm migration on 1D SDS-PAGE on linear 12%, pH 8.8 (Hoefer Mightly Small II, Amersham Biosciences, Uppsala, Sweden). Gels were stained with Coomassie Brilliant Blue (CBB) (Mathesius *et al.*, 2001). After CBB staining, the 0.7cm migration gel parts of each lane were sliced into 7 bands of equal size (1 mm). In-gel digestions were performed with trypsin in the Progest system (Genomic Solution, East Lyme, CT, USA) according to a standard protocol. Gel pieces were washed twice by successive baths of 10% (v/v) acetic acid, 40% (v/v) ethanol and ACN. They were then washed twice with successive baths of 25 mM NH_4CO_3 and ACN. Digestion was subsequently performed for 6 h at 37ºC with 125 ng of modified trypsin (Promega) dissolved in 20% (v/v) methanol and 20mM NH_4CO_3. Peptides were extracted successively with 2% (v/v) TFA and 50% (v/v) ACN and then with pure ACN. Peptide extracts were dried and suspended in 20 µL of 0.05% (v/v) TFA, 0.05% (v/v) HCOOH, and 2% (v/v) ACN.

LC-MS/MS analysis

Peptide separation was performed using an Eksigent 2D-ultra-nanoLC (Eksigent Technologies, Livermore, CA, USA) equipped with a C18 column (5 µm, 15cm x 75µm, PepMap, LC packing). The mobile phase consisted of a gradient of solvents A 0.1% HCOOH (v/v) in water and B 99.9% ACN (v/v), 0.1% HCOOH (v/v) in water. Peptides were separated at a flow rate of 0.3 µL/minute using a linear gradient of solvent B from 5 to 30% in 60 minutes, followed by an increase to 95 % in 10 minutes. Eluted peptides were online analysed with a LTQ XL ion trap (Thermo Electron) using a nanoelectrospray interface. Ionization (1.5 kV ionization potential) was performed with a liquid junction and a non-coated capillary probe (10 µm i.d.; New Objective). Peptide ions were analyzed using Xcalibur 2.0.7, with the following data-dependent acquisition steps (1) full MS scan (mass to charge ratio (*m/z*) 300-2000, centroid mode), (2) MS/MS (qz = 0.25, activation time = 30 ms, and collision

energy = 35%; centroid mode). Step 2 was repeated for the three major ions detected in step 1. Dynamic exclusion was set to 45 s.

Protein identification and quantification

Database search was performed with the X!Tandem software (version 2010.01.01.4) (http://www.thegpm.org/TANDEM/). Enzymatic cleavage was declared as a trypsin digestion with one possible missed cleavage. Cysteine carboxyamidomethylation and methionine oxidation were set to respectively static and possible modifications. Precursor mass precision was set to 2.0 Da with a fragment mass tolerance of 0.5. To minimize the generation of false-positive identifications and measurement time, spectra search was restricted against the *M. truncatula* EST database (http://medicago.toulouse.inra.fr/Mt/EST/). Identified proteins were filtered and grouped using X!Tandem parser (http:// pappso.inra.fr/bioinformatique.html) according to (i) the tolerated presence of only one peptide by reason of homologous search in *M. truncatula* database, with an E value smaller than 0.05 and (ii) a protein E value (calculated as the product of unique peptide E values) smaller than 10^{-4}. These criteria led to a False Discovery Rate (FDR) of 0.3% for peptide and protein identification. To take redundancy into account (i.e. the fact that the same peptide sequence can be found in several proteins), proteins with at least one peptide in common were grouped. When necessary, the protein sequences retrieved in the *M. truncatula* EST depository, which displayed either no annotation and/or an annotation to be updated according to the latest releases from the International *Medicago* Genome Annotated Group (IMGAG) V3.5 V3, were Blasted against Uniprot (http://www.uniprot.org/) /or NCBI (http://blast.ncbi.nlm.nih.gov/) non-redundant database.

Label-free quantification was performed using the open source software MassChroQ, which has previously demonstrated its efficiency to align and quantify LC-MS data on the basis of a peak integration strategy (Valot *et al.*, 2011). In order to take into account possible global quantitative variations between LC-MS runs, for each of them, the ratio of all peptide values to their value in the chosen reference LC-MS run was computed and normalization was performed by dividing peptide values by the median value of peptide ratios. To statistically assess significant protein abundance modifications upon AM symbiosis, an ANOVA was performed on $\log_{10}$ normalized data, thus allowing simultaneous comparison between treatments (mycorrhized and

nonmycorrhized plants) and biological replicates (independent experiments 1 and 2) by using the model Y= protein + treatment + experiment + interaction protein-experiment + interaction protein-treatment + residual variance. After discarding the effects due to the experiment and the interaction protein-experiment, mean protein abundance between mycorrhizal and nonmycorrhizal microsomal root fractions were compared using *t*-test with a value of $P<0.01$ considered to be statistically significant.

Protein sequence feature prediction

As a way to homogenize annotations, the identified proteins in *Medicago truncatula* EST (http://medicago.toulouse.inra.fr/Mt/EST/) were assigned to a Medtr accession number using (http://www.legoo.org/). Likewise, for comparative purposes with previous studies aiming at analyzing root protein accumulation in *M. truncatula*, either inoculated or not with AM symbionts (Valot *et al.*, 2005; Valot *et al.*, 2006; Aloui *et al.*, 2009; Recorbet *et al.*, 2009; Daher *et al.*, 2010; Recorbet *et al.*, 2010; Aloui *et al.*, 2011), the use of similar *in silico* protein predictors were favoured as far as possible in the current study. Accordingly, proteins were functionally classified using the FunCat scheme ((Ruepp *et al.*, 2004) as previously described (Recorbet *et al.*, 2009). Likewise, alpha-helical TM spans were predicted according to the Tmpred server (http://www.ch.embnet.org/software/TMPRED_form.html), with a minimum score of 1000 (Valot *et al.*, 2006) and/or (http://www.cbs.dtu.dk/services/TMHMM/), whereas the online tool (http://biophysics.biol.uoa.gr/PRED-TMBB/input.jsp) was employed to discriminate beta-barrel outer membrane proteins. Localisation prediction was performed by WoLF PSORT (http://wolfpsort.seq.cbrc.jp) as previously described in Daher *at al.* (2010). The targeting of membrane proteins to chloroplasts, mitochondria or the secretory pathway often accomplished by N-terminal signal sequences was assessed according to the SignalP 4.0 server (http://www.cbs.dtu.dk/services/SignalP). *N*-myristoylation, and S-palmitoylation predictions were inferred from the ExPASy tools (http://web.expasy.org/myristoylator/) and (http://csspalm.biocuckoo.org/online3.php), respectively. For prenylation prediction, the PrePS online tool (http://mendel.imp.ac.at/sat/PrePS/index.html) was used, while GPI anchor prediction was performed using the GPI Modification Site Prediction in Plants (http://mendel.imp.ac.at/gpi/plant_server.html). Close homologues of the

identified proteins in *Medicago* were searched against The *Arabidopsis* Information Resource (TAIR) (http://www.arabidopsis.org/) database.

Results and discussion

Biological parameters, protein identification and curation

As previously underlined by Zybailow and co-workers (Zybailov *et al.*, 2008), one weakness in quantitative shotgun membrane proteomics is the general lack of biological replicates that generates the inability to carry out standard statistical analyses of replicate datasets for biological interpretation. To satisfy this prerequisite, two independent biological experiments, each encompassing three replicates of each treatment (mycorrhized and nonmycorrhized roots) were performed in the current study. With regard to root colonization by the AM fungus, four weeks after inoculation, *R. irregularis* had developed symbiotic endomycorrhiza with *M. truncatula*, and on the basis of six root systems measured per experiment, the degree of root colonization, as estimated by trypan blue staining, was not found to differ between biological replicates, in that, for each of the three parameters (F, M, and A%), no significant differences at $P < 0.01$ were recorded (Figure 4.1). This result highlights the biological reproducibility of the two experiments conducted, especially with regard to the intensity of root cortex colonization (M%) and mean arbuscule abundance (A%), which likely represent the main root-intrinsic fungal structures factors generating membrane reorganization in established mycorrhiza, although such a phenomenon also occurs upon contact of symbionts (Genre *et al.*, 2005).

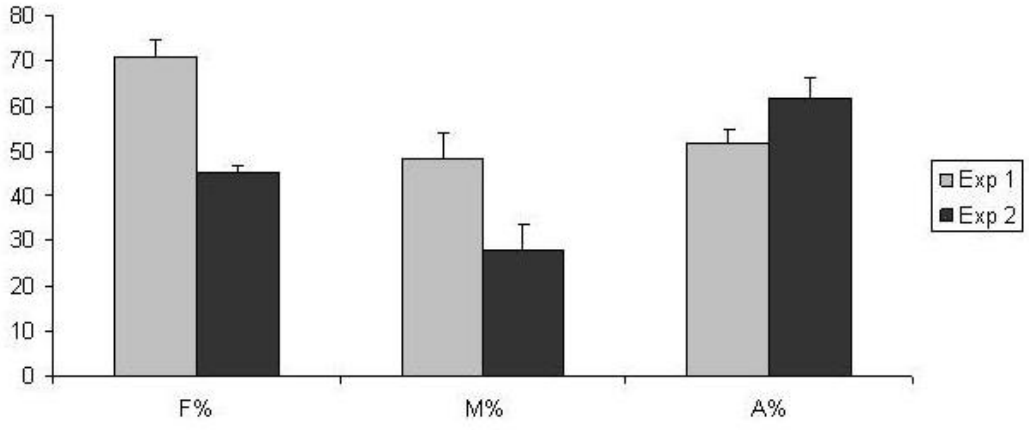

Figure 4.1: Development of *R. irregularis* within roots of four week-old *M. truncatula* plants.
Evaluated parameters, expressed as percentages, were frequency of mycorrhization (F%), intensity of root cortex colonization (M%) and arbuscule abundance (A%). For two independent biological experiments (Exp), histograms represent means for six plant replicates and vertical bars indicate SE. For each parameter, no significant differences at $P < 0.01$ were recorded between experiments after arcsin square root transformation.

In parallel, another main challenge in membrane proteomics is to minimize the presence of abundant soluble contaminants that might otherwise hinder the detection of less represented membrane-associated proteins, thus making crucial the initial enrichment step (Santoni *et al.*, 2000). In the current study, we used a differential centrifugation-based strategy originally developed for *Nicotiana tabacum* cultured cells (Stanislas *et al.*, 2009), which to our knowledge has never been performed to investigate membrane enrichment/modifications in roots originating from soil-grown plants. As a way to assess the adequacy of this protocol to the root system we investigated, a preliminary test was performed to check for cytosolic protein depletion upon the centrifugation procedure by using an antibody directed against the 51 kDa UDP-Glucose pyrophosphatase (Daher *et al.*, 2010). Figure 4.2B shows that in both AM fungus- free and -inoculated *M. truncatula* roots, the cytosolic marker was visually detected in a similar extent in all the supernatant fractions of the protocol that were tested, but that the immuno-detection signal fell down to a relative lesser intensity in the final membrane-enriched fractions from mycorrhized and nonmycorrhized roots. This result also holds true in the two biological repeats that

were performed (data not shown), thus suggesting a minimum contamination of the membrane-enriched fractions by soluble proteins.

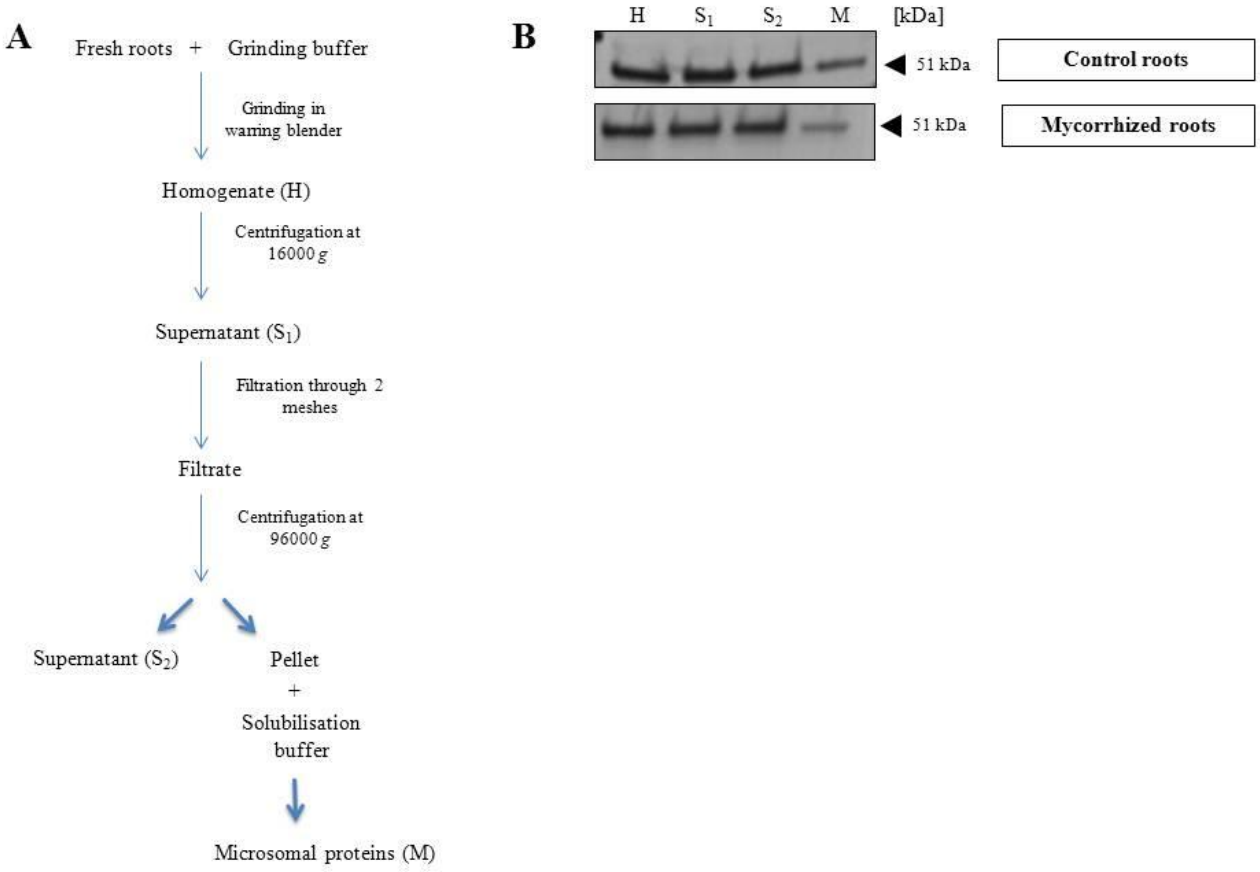

Figure 4.2: Enrichment in root microsomes from four week-old *M. truncatula* plants. (**A**) Schematic depiction of the microsome extraction workflow according to Stanislas *et al.*, 2009. (**B**) Western-blot analyses of the different purification steps (fractions H, S1, S2 and M) in control and mycorrhized *M. truncatula* roots using antibody directed against the 51 kDa-cytosolic UDP-glucose pyrophosphorylase (UGPase).

Subsequently, GeLC-MS/MS was chosen to resolve microsomal proteins of mycorrhizal and nonmycorrhized *M. truncatula* roots, in that this procedure gathers the advantages of both gel-based and gel-free separation approaches. Actually, the use of SDS ensures successful membrane protein solubilization, and its effectiveness arises from the ability of the nonpolar tail to infiltrate the lipid membrane, binding to protein in a high mass ratio (Jones, 1999). In-gel trapped protein tryptic digestion also allows removing detergents prior to MS analysis, which can otherwise dominate mass

spectra and preclude protein analysis. Additionally, the resolution of 1-DE prior to LC separation is enhanced since it occurs at both protein and peptide level, allowing the identification of less abundant proteins (Vertommen *et al.*, 2011). Using an E value smaller than 10^{-4} as a criterion to assign correct protein identification, a total of 1128 proteins was obtained from the twelve microsomal fractions analysed in the current study (Chapter 4, additional file S4.1). This initial repertoire was curated according to the principles of parsimony described in Nesvizhskii & Aebersold (2005) to provide a minimal list of proteins sufficient to explain all observed peptides, resulting in a final record of 1047 nonredundant proteins. Noticeably, the overlap in the proteins co-identified in the two independent experiments reached a common value of 96% in the mycorrhized and the nonmycorrhized plant roots, which points to the reproducibility of the protocol currently used for protein extraction and identification (Chapter 4, additional file S4.2).

Despite the depletion in the cytosolic marker that was investigated, we anticipated the detection of a pool of potential contaminants within the 1047 proteins initially identified, and the necessity of a curation procedure by reason of the ever-increasing sensitivity of LTQ mass spectrometers coupled to the likely presence of soluble proteins trapped within membrane vesicles. As a point of reference for *M. truncatula*, we used the rationale described by Daher and co-workers (2010) that favours similarity search on the basis of which homologous proteins share the same location in many organisms, a strategy recognized more confident than the use of *in silico* algorithmic predictors for protein localization (Nair & Rost, 2002). Consequently, the total 1047 pinpointed proteins were first BLASTed against the TAIR database and were considered as genuine microsomal *M. truncatula* proteins when homologous sequences displaying at least 70% pair-wise identity and a cut-off expectation value of e^{-40} were experimentally demonstrated to have a membrane localisation, including core integral or subunits of membrane complexes, on the basis of direct assays or "traceable author statement" (Daher *et al.*, 2010). When it was not the case, identified proteins were retained as contaminants unless predicted to display at least one TM domain, to form a beta barrel embedded in the membrane lipid bilayer, to be anchored to the membrane owing to hydrophobic tails, and/or to be targeted to plastids, mitochondria or the secretory pathway by signal sequences, as described in Marmagne *et al.* (2004); Schwacke *et al.* (2004).

Using these criteria, 164 (15.6%) proteins out of the 1047 nonredundant identifications were discarded as potential contaminants of the microsomal fractions isolated from nonmycorrhizal and mycorrhizal roots, although it is almost certain that authentic membrane proteins could have been included in this list, as exemplified for NADPH oxidase (59% identity, $7e^{-73}$) and protein kinase (69% identity $2e^{-63}$) described as membrane-associated in TAIR, but that escape the cut-of-points we choose, likely by reason of sequence divergence between *Arabidopsis* and *Medicago* spp. (Chapter 4, additional file S4.3). Regarding the functions of the retrieved contaminants, known or putative membrane-free ribosomal and histone proteins turned out to be the major sources of contaminations by representing 33 and 19% of the 164 identifications, respectively (Chapter 4, additional file S4.3). This dominant distribution appears consistent with the ability of histones to directly translocate biological membranes into phospholipid liposomes and/or to absorb the membrane surface owing to their positive charge (Hariton-Gazal *et al.*, 2003), together with the previously documented contamination of membrane-bound with free polyribosomes (Andrews & Tata, 1971). Consistent with the previously observed UDP glucose pyrophosphorylase depletion in the microsome-enriched fractions, the protocol used in the current study succeeded in retrieving 883 root membrane candidates (84.3%) out of the 1047 proteins identified (Chapter 4, additional file S4.4), a feature that largely over performs previous attempts in characterizing microsomal proteomes in *M. truncatula* and maize roots using OFFGEL fractionation of peptides (Abdallah *et al.*, 2012), or 2-DE coupled to either IPG-strips or OFFGEL fractionation (Valot *et al.*, 2005; Meisrimler & Luthje, 2012).

The microsomal proteome of *R. irregularis*-inoculated roots qualitatively resembles that of nonmycorrhized plants, thereby defining a core-set of membrane proteins in *M. truncatula*

As a result of the better resolution of microsomal proteins obtained through GeLC-MS/MS relative to 2-DE or OFFGEL fractionation, modifications of the root membrane proteome of *M. truncatula* upon symbiosis with *R. irregularis* could be more representatively assessed. Following the label-free MassChroQ-based analysis coupled to the ANOVA performed on the duplicated biological independent replicates that were conducted, a total of 52 proteins out of the 1047 initially identified in the microsome-enriched root fractions displayed a reproducible

significant (P<0.01) differential abundance in mycorrhizal plants relative to controls, which encompassed 29 and 23 up- and down-accumulated gene products, respectively, among which one protein was induced and another repressed (Tables 4.1 and 4.2). Irrespective of their known or predicted membrane location, the latter result strikingly points out to the existence of a rather conserved microsome-enriched fraction between mycorrhizal and nonmycorrhizal roots, as inferred from the only two proteins that turned out to display a differential qualitative accumulation between the two treatments. This observation also persists upon data curation in that only the protein Mtha1 regarded as a plasma membrane-associated happened to be AM-specific in the microsomes extracted in our experimental conditions (Table 4.1). Overall, comparison of the microsomal proteomes of *M. truncatula* between mycorrhized and nonmycorrhized roots allowed defining a core set of membrane proteins that is conserved irrespective of AM symbiosis, which consists of 882 curated accessions upon the exclusion of Mtha1.

When analyzing this core microsomal root proteome for subcellular location according to Wolf PSORT predictions, the three dominant cellular components that were retrieved encompassed the chloroplast, the nucleus and the plasma membrane after discarding the cytosolic-predicted proteins that were previously retained as genuine membrane-located according to the aforementioned criteria (Figure 4.3A). With regard to the first category, chloroplast-located proteins in roots refer to those belonging to non-photosynthetic plastids that have to import sugar phosphates and ATP from the cytosol in order to sustain their anabolic metabolism, thus contrasting with photosynthetic chloroplasts that synthesize sugar phosphates that are catabolized by oxidative processes to produce NADPH and ATP. In *M. truncatula*, the proteomic analysis of the relative contribution of soluble and membrane root plastid proteins to different biological processes had shown that root plastid proteins unique to the membrane-enriched fraction essentially contributed to withstand energy, signalling and transport mechanisms.

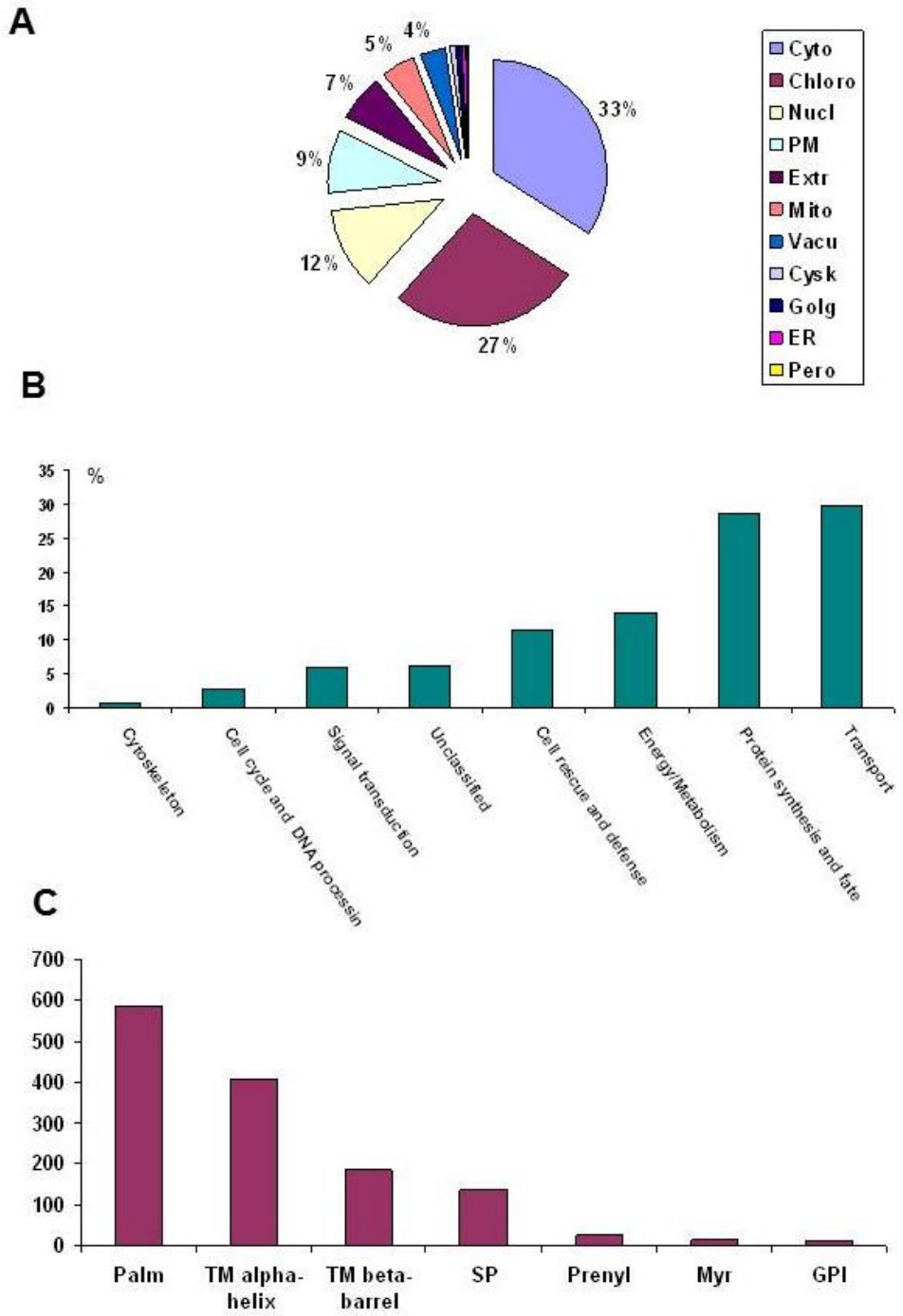

Figure 4.3: In silico characterization of the 882 putative membrane proteins conserved between control and mycorrhizal roots over the 883 root microsomal proteins that were recorded.

(**A**) Subcellular protein location according to Wolf PSORT predictions (Chloro, Cyto, Cysk, ER, Extr, Golg, Mito, Nucl, Pero, PM and Vacu, referring to as Chloroplast, Cytosol, Cytoskeleton, Endoplamic reticulum, Extracellular, Golgi apparatus, Mitochondria, Nucleus, Peroxisome, Plasma membrane, and Vacuolar membrane cellular components, respectively). (**B**) Functionally classification of root membrane proteins using the FunCat scheme (Ruepp *et al.*, 2004). (**C**) Distribution of the putative mechanisms by which the recorded proteins associate to root membranes of *M. truncatula*, as predicted according to the Tmpred server (http://www.ch.embnet.org/software/TMPRED_form.html), with a minimum score of 1000

(Valot *et al.*, 2006) and/or (http://www.cbs.dtu.dk/services/TMHMM/ for alpha-helical TM spans (**TM alpha-helix**), the online tool (http://biophysics.biol.uoa.gr/PRED-TMBB/input.jsp) to discriminate beta-barrel outer membrane proteins (**TM beta-barrel**), the SignalP 4.0 server (http://www.cbs.dtu.dk/services/SignalP) for membrane proteins targeted to chloroplasts, mitochondria or the secretory pathway (**SP**), the ExPASy tools (http://web.expasy.org/myristoylator/) and (http://csspalm.biocuckoo.org/online3.php) for assessing *N*-myristoylation (**Myr**), and S-palmitoylation (**Palm**) sites, respectively, the PrePS online tool (http://mendel.imp.ac.at/sat/PrePS/index.html for inferring prenylation modifications (**Prenyl)**, and the the GPI Modification Site Prediction in Plants (http://mendel.imp.ac.at/gpi/plant_server.html) for putative GPI anchorage to root membrane (**GPI**).

Consistently, as shown in chapter 4 additional file S4.4, most of the proteins known or predicted as plastid-located currently identified in the conserved root microsomal fraction turned-out to be involved in transport (ABC transporters, plant lipid transfer proteins, Ras small GTPases, ferritin, translocon, importin,…), energy/metabolism (malate dehydrogenases, aconitate hydratases, pyruvate dehydrogenases, fructose biphosphate aldolases, fumarate reductase, …) and signalling (small GTP-binding proteins, protein kinases, patatin…)-related processes. Proteins known or predicted to be nuclear occupied the second most abundant class (12%, Figure 4.3A) of the root microsomal proteome identified in *M. truncatula* and essentially consisted of ribosomal proteins that are known to attach the outermost membrane of the nuclear envelope. Actually, the nuclear envelope is a two-membrane system that includes the outer membrane that is continuous with the ER and lined with ribosomes, and the inner membrane that hosts integral proteins interacting with chromatin and the nuclear matrix (Kota & Goshe, 2011), as exemplified by the *trans*-membrane histones we identified in this study (Chapter 4, additional file S4.4). The eukaryotic nucleus is also important not only for DNA replication and transcription, as represented by the identification of several nuclear translation-initiation factors (Chapter 4, additional file S4.4), but also for cellular homeostasis and genomic responses to stress tolerance (Choudhary *et al.*, 2009). In this respect, numerous thioredoxins, glycoside hydrolases, lipoxigenases, high-mobility- and heat shock-like proteins, associated with cell rescue and defence mechanisms, were retrieved from the predicted membrane nuclear fraction (Chapter 4, additional file S4.4). Finally, 83 accessions, representing 9% of the 882 identifications regarded as genuine root membrane proteins conserved whatever the treatment (Chapter 4, additional file S4.4), were inferred as PM-associated according to Wolf PSORT predictions (Figure 4.3A).

Consistent with the role of the plasma membrane to establish a controlled exchange from the inside to the outside side of the cell, and reciprocally, a large majority of these known or putative root plasma membrane proteins was assigned to transporters, including ABC transporters which refer to ATP-binding cassette transporters that utilize the energy of ATP hydrolysis to carry out translocation of various substrates across extra- and intracellular membranes, including metabolic products, lipids and drugs and non-transport-related processes such as translation of RNA and DNA repair (Jones & George, 2004). Noticeably, additional to the presence of plasma-membrane proton-efflux P-type ATPases, we recorded within the list of the proteins annotated as PM transporters, the presence of aquaporins (PIP11, PIP2-7, Nodulin-26 like Intrinsic Protein-like NIP1-2), phosphate (MtPT1, 2, and 3), peptide, sugar, nitrate, nickel/cobalt, sulphate transporters and nonaspanin proteins (TM9SF9 superfamily), the latter group functioning as a channel or small molecule transporter. Likewise, the natural resistance-associated macrophage protein (Nramp) homologs form a family of proton-coupled transporters that facilitate the cellular absorption of divalent metal ions (Me^{2+}, including Mn^{2+}, Fe^{2+}, Co^{2+}, and Cd^{2+}) (Courville *et al.*, 2006) (Chapter 4, additional file S4.4). Although recent studies have initiated in the model legume *M. truncatula* the generation of systematic database dedicated to the characterization of all of the putative genome-encoded transporters, predicted to encompass from 3598 to 3830 proteins, data relative to their putative location to the root plasmalemma are missing, thereby making hardly possible assessing the representativeness of our data relative to the PM transporters currently identified (Benedito *et al.*, 2010; Miao *et al.*, 2012). Apart from transporters *sensu stricto*, putative PM proteins having role in membrane trafficking and signalling were also retrieved in the root microsome of *M. truncatula*, as demonstrated for example by the presence of secretory carrier membrane proteins (SCAMPs), tretraspanin, or phosphatidylinositol phosphate phosphatase (Chapter 4, additional file S4.4). Actually, SCAMPs are ubiquitously expressed integral membrane proteins with four TM spans. The prevalence and broad distribution of SCAMPs in membranes of endocytic recycling compartments, secretory vesicles, the *trans*-Golgi network, and the plasma membrane has raised the prospects that they participate in a variety of membrane trafficking events, including sorting, the formation of vesicular carriers, exocytosis, and endocytosis (Hubbard *et al.*, 2000). Regarding tetraspanins, which can localize at different membranes, they

facilitate cell-to-cell communication or sense the stimulus from the environment at the plasma membrane, and might also act as receptors (Wang, F *et al.*, 2012). Likewise, in plants, Ca^{2+}, phosphatidylinositol phosphates and inositol phosphates are major components of intracellular signalling, with several kinds of proteins and enzymes, such as calmodulin, protein kinase, protein phosphatase, including phosphatidylinositol phosphate phosphatase, and the Ca^{2+} channel, mediating the signalling (Kato *et al.*, 2010).

To obtain an overview of the functional significance of the core microsome of *M. truncatula* roots, the corresponding 882 identified proteins were classified according the FunCat annotation scheme that assigned them to eight biological processes, in which transport, protein synthesis/fate and energy/metabolism were the most prominent retrieved categories, whereas proteins of unknown function only encompassed 6.3% of the microsomal repertoire (Figure 4.3B). This functional grouping appears consistent with plastids and nucleus as prevalent cellular components of the root micosome in *M. truncatula* as previously described in Figure 4.3A. Actually, plastids, like mitochondria, are double-membrane organelles, the outer membrane representing a barrier to the movement of proteins and the inner a barrier to small metabolites, which perform many metabolic and anabolic biosynthesis tasks, such as N-assimilation (Esposito *et al.*, 2003), starch biosynthesis (Geigenberger *et al.*, 2004), and lipid biosynthesis (Rawsthorne, 2002). Depending on the function they need to play in the plant cell, plastids may differentiate into several forms, including chromoplasts for pigment synthesis, amyloplasts for starch storage, statoliths for detecting gravity or elaioplasts for storing fat (reviewed in Neuhaus & Emes, 2000), thereby implying energy and metabolism as essential functional processes. Although plastids have retained genes for a small number of polypeptides, the majority of plastid proteins are encoded in the nucleus, translated in the cytosol, imported into the organelle and targeted to one of its suborganellar compartments (Lopez-Juez, 2007), supporting a drastic role for transport- and protein synthesis/fate-related mechanisms. According to their denomination, plastids also have the ability to differentiate, or re-differentiate between these and other forms, a process resulting from specific differentiation programs that are controlled by the nucleus (reviewed in Vothknecht & Westhoff, 2001), thus linking plastidial and nuclear functioning as illustrated by our data (Figure 4.3A, B). Overall, both cellular and functional

classifications predispose plastids as prominent organelles sustaining membrane protein distribution in the root microsomal proteome currently identified in *M. truncatula*.

Finally, when analysing the root microsomal proteins of *M. truncatula* for the mechanisms by which they may associate to cell membranes, Figure 4.3 C showed that S-palmitoylation, alpha-helical and beta-barrel *trans*-membrane regions, were the prevalent processes, as predicted for 586, 409, and 187, accessions, respectively. On the whole, integral TM candidate proteins (596) embedded in the membrane bilayer dominate the microsomal proteome, when summing predictions for alpha-helices and beta-barrels. In the field of proteomics, the detection of integral membrane proteins has essentially considered alpha-helical domains that are present in all types of biological membranes, despite the development of beta-barrel prediction algorithms (Schwacke *et al.*, 2004; Imai *et al.*, 2011; Schleiff *et al.*, 2011). However, in plants, the outer membranes of mitochondria and chloroplasts all contain transmembrane β-barrel proteins that serve essential functions in cargo transport and signalling and are also vital for membrane biogenesis (Fairman *et al.*, 2011). Supporting this view, most of the β-barrel-containing proteins predicted in the current study were putatively located to plastids, encompassing transport-related proteins (chloroplastic outer envelope pores, importins, phosphate/phosphoenolpyruvate translocator, plant lipid transfer proteins, ABC transporters, phosphate/phosphoenolpyruvate translocator), and signalling/cargo associated components (putative receptor kinase, von Willebrand factor, and Rab-related proteins). Likewise, a putative mitochondrial flotillin referred to as a scaffolding protein was also recorded within those displaying a β-barrel domain (Chapter 4, additional file S4.4). Besides alpha-helices and beta-barrels domains that define integral membrane, S-palmitoylation was predicted as the most important lipid modification associating proteins to the membrane compartments in the root microsome of *M. truncatula* (Figure 4.3C). S-palmitoylation, a post-translational modification mediating the reversible addition of palmitate and other long-chain fatty acids to proteins at cysteine residues, has diverse functional consequences, among which it provides an important mechanism for regulating protein subcellular localization, stability, trafficking, translocation to lipid rafts, aggregation, and interaction with effectors (Nadolski & Linder, 2007). Noticeably, whereas N-myristoylation and prenylation are considered as irreversible attachments,

S-palmitoylation is a reversible process that allows proteins to rapidly shuttle between intracellular membrane compartments, which has been best illustrated for palmitoylated forms of the small GTPase Ras family (Aicart-Ramos *et al.*, 2011). Consequently, the important number of palmitate-modified microsomal proteins actually identified in the root proteome of *M. truncatula*, supports the view of a highly fluent and dynamic membranous environment (Figure 4.3C), a hypothesis that can be corroborated the identification of plastids and transport as prevalent organelles and functions in the root microsomal fractions, respectively (Figure 4.3A, B).

AM symbiosis quantitatively modifies the root membrane proteome of *M. truncatula*.

According to the peak integration label-free strategy we used to quantify protein abundance (MassChroQ), coupled to the ANOVA performed on the duplicated biological independent replicates that were conducted to compare protein accumulation between the curated microsomes of mycorrhizal and noncorrhizal roots, only the plasma-membrane proton-efflux P-type Mtha1ATPase turned-out to be induced upon AM symbiosis, whereas 22 and 19 proteins previously retained as genuine membrane proteins were revealed as up-and down- accumulated in mycorrhizal roots relative to controls, respectively (Tables 4.1 and 4.2). Whereas it cannot be ruled-out that mycorrhiza-specific membrane proteins could have escaped the protocols currently designed for microsome enrichment and protein curation, our data nonetheless corroborate the literature available on mycorrhiza-related membrane proteins, although very few of them so far have been described. Actually, the first reports on membrane proteins displaying an arbuscule-inducible accumulation in mycorrhizal roots were inferred a decade ago to Mtha1, a plasma membrane H^+ATPase considered to be involved in active uptake of nutrients from the symbiotic interface (Krajinski *et al.*, 2002), and MtPt4, a mycorrhiza-specific phosphate transporter (Harrison *et al.*, 2002). By the use of either reporter gene expression or membrane proteomic analyses, it was also demonstrated that one member of the AM-induced gene family encoding blue copper binding proteins (MtBcp1) was both specifically and strongly up-regulated in arbuscule-containing regions of mycorrhizal roots, suggesting its putative location within the periarbuscular membrane (Hohnjec *et al.*, 2005; Valot *et al.*, 2006). With regard to our results, not only Mtha1 was retrieved as induced in mycorrhizal roots, but MtBcp1 also displayed a near 10 fold over

accumulation relative to controls, thus corroborating previous data and the relevance of our protocol (Table 4.1).

Table 4.1. List of the proteins displaying an over-accumulation in mycorrhizal roots relative to controls.
Yellow-shaded lines refer to identifications escaping our criteria for assigning a protein as membrane associated.

Proteins up-accumulated in mycorrhizal roots relative to controls

MENS Toulouse 01/2003	Fold change	p value
MtC30183_1_AA Blast: XP_003611447 GMFP4 tetraspanin [Medicago truncatula].CD9/CD37/CD63 antigen	2,51	0,002
MtD01250_1_Blast: XP_003591547 ABC transporter C family protein [Medicago truncatula].	6,76	0,0004
MtC60823_1_AA Blast: OEP16_PEA Outer envelope pore protein 16, chloroplastic; AltName: Full=Chloroplastic outer envelope pore protein of 16 kDa.	1,62	0,002
MtC00088_1_AA Blast: XP_002881077 cyclophilin [Arabidopsis lyrata subsp. lyrata].Peptidyl-prolyl cis-trans isomerase, cyclophilin type	5, 01	0,004
MtC00605_1_AA Blast: XP_003592453 Blue copper protein [Medicago truncatula].Blue (type 1) copper domain	9,33	3.39279335048737e−06
MtC45467_1_AA Blast: XP_003614713 Transmembrane emp24 domain-containing protein [Medicagotruncatula].emp24/gp25L/p24 IPR001356:Homeobox	2,24	0,0030
MtC10070_1_AA Blast:XP_003627196 Lipoxygenase [Medicago truncatula].	8,13	1.54098955817972e−13
MtC00085.1_1_AA Histone core IPR009072:Histone-fold	2,14	1.81465612403287e−05
MtC60580_1_AA Peptidyl-prolyl cis-trans isomerase, cyclophilin type (blast ok)	2,14	0,0002
MtC20331_1_AA Histone H2A (blast ok)	6,92	5.7386174658891 1e−05
MtC92000_1_AA Histone core IPR009072:Histone-fold	2,95	4.30015229735403e−06
MtC00621_1_AA Histone H2A (blast ok)	3,55	0,0002
MtC00668_1_AA Ribosomal protein L1 (blast ok)	3,31	0,002
MtC00209_1_AA Ribosomal L28e protein	3,09	0,002
MtC00725_1_AA Ribosomal protein L29	2,45	2.73583877490324e−05
MtC00435_1_AA Ribosomal protein S13 (blast ok)	3,02	0,004
MtC00466_1_AA Blast: XP_003609172 H/ACA ribonucleoprotein complex subunit 2-like protein [Medicago truncatula].Ribosomal_L7Ae	1,7	0,009
MtC00190_1_AA Eukaryotic initiation factor 5A hypusine (eIF-5A)	2,82	0,001
MtD20646_1_AA Blast: XP_003628253 Prohibitin [Medicago truncatula].Band 7 protein	1,95	0,006
MtC10100.1_1_AA Blast: XP_003626103 Cathepsin B [Medicago truncatula].	1,51	0,0051
MtC60431_1_AA Blast: XP_003518654 PREDICTED: ras-related protein RABE1c-like [Glycine max]	1,91	0,0019
MtC00046_1_AA S-adenosylmethionine synthetase (ok blast)	2,69	0,006
MtC20060_1_AA Blast: A GAMMA carbonic anhydrase, partial [Silene latifolia].	2,04	0,0039
MtC10470_1_AA Actin/actin-like (blast ok) cd00012: NBD_sugar-kinase_HSP70_actin	2,6900	0,0089
MtC10339_1_AA Actin/actin-like (blast ok) cd00012: NBD_sugar-kinase_HSP70_actin	4,37	0,0011
MtD02792_1_AA Reticulon Blast: XP_003525365 PREDICTED: reticulon-like protein B2-like isoform 1 [Glycine max].	1,82	0,001
MtC00185_1_AA unknown Blast: XP_003616043.1 hypothetical protein MTR_5g075520 [Medicago truncatula]	3,16	0,0013

Protein induced in mycorrhizal roots relative to controls

MENS Toulouse 01/2003	Fold change	
MtC10290_1_AA Mtha1 PLASMA MEMBRANE ATPASE (plasma-membrane proton-efflux P-type ATPase)	43651,58	0,004

Nonetheless, imaging approaches also have recently revealed that the periarbuscular membrane is at least composed of two distinct specific protein-containing compartments, corresponding to an arbuscule-trunk domain that contains the blue copper-binding protein MtBcp1 (of unknown function) which also localizes to the host PM, as opposed to an arbuscule-branch domain that specifically harbours the AM symbiosis-specific phosphate transporters MtPt4 and OsPT11 (Harrison *et al.*, 2002; Kobae & Hata, 2010), the AM-inducible ammonium transporter GmAMT4.1 (Kobae *et al.*, 2010), STR half-ABC transporters (Zhang *et al.*, 2010; Gutjahr *et al.*, 2012) and vesicle-associated membrane proteins VAMP721d/e (Ivanov *et al.*, 2012). In view of these results that have suggested the occurrence of a *de novo* membrane biogenesis process associated with the dichotomous branching of the hyphae within plant cortical cells, together with the absence of proteins specific for the arbuscule-branch domain from our repertoire, with contrasts with the presence of MtBbp1 (Table 4.1 and Valot *et al.*, 2006), we propose that, unlike the trunk domain, the specific features displayed by the arbuscule-branch domain of the periarbuscular membrane likely make this compartment recalcitrant to the current methods used for PM enrichment. In this regard, the device of new proteomic protocols aiming at isolating the arbuscule-branch domain, probably on the basis of immunoassays targeting the enrichment in MtPt4 and/or GmAMT4.1, appears indispensable to increase our knowledge relative to the protein composition of the periarbuscular membrane. Nonetheless, when compared to previous proteomic studies targeting root microsomal proteins up-accumulated upon mycorrhiza (Valot *et al.*, 2005; Valot *et al.*, 2006), new candidates putatively supporting the AM symbiotic program in host plant roots happened to emerge from the current study as mainly exemplified by proteins having role in signalling/membrane trafficking (Table 4.1). Actually, tetraspanins, as previously mentioned, can localize at different membranes where they facilitate cell-to-cell communication or sense the stimulus from the environment at the plasma membrane, and might also act as receptors (Wang, F *et al.*, 2012). Likewise, the increase in membrane surface during arbuscule development may cause a significant portion of trans-Golgi vesicles to fuse with the periarbuscular membrane, and then to redirect proteins entering the secretory pathway to the periarbuscular space (Pumplin &

Harrison, 2009; Takeda *et al.*, 2009). In this regard, transmembrane emp24 domain-containing protein, prohibitin, ras-related protein RABE1c-like and reticulon-like protein, all having role in secretion or in membrane trafficking were recorded as up-accumulated membrane proteins upon symbiosis (Table 4.1), thus supporting the view of a transient reorientation of secretion favouring vesicle fusion during arbuscular development (Pumplin & Harrison, 2009). In the same line of reasoning, a predicted extracellular cathepsin, having role in both intracellular degradation and turnover of proteins, was currently identified as up-accumulated in symbiotic roots (Table 4.1), a record likely sustaining the previous identification of two AM-specific proteolytic subtilases located in the apoplastic symbiotic interface, for which a function in cleaving structural proteins to sustain hyphal elongation and plant penetration upon secretion to the periarbuscular space has been inferred (Takeda *et al.*, 2009). As illustrated by the aforementioned proteins sustaining membrane trafficking, the development of arbuscules also supposes a modification of architectural features to support newly synthesized membrane proteins (Genre *et al.*, 2005; Pumplin & Harrison, 2009; Gutjahr *et al.*, 2011). In the current study, this could be exemplified by the up-accumulation of cytoskeletal components that might direct secretion such as actin-like proteins, together with proteins playing role in protein synthesis and fate, including histones, ribosomal proteins, and cyclophilins (Table 4.1). Finally, compared to the 44 transporters predicted to be up-regulated in mycorrhizal roots on the basis of transcriptional analysis (Benedito *et al.*, 2010), only Mtha1, an ABC cassette, a pore protein, and a TM transporter, were actually identified as up-accumulated upon AM symbiosis (Table 4.1), thus pointing once again to the complementarities of transcriptional and proteomic approaches to resolve the AM symbiotic program.

When regarding the 19 identifications retained as genuine microsomal proteins that displayed a down-accumulation upon *R. irregularis* inoculation (Table 4.2), three prevalent classes were retrieved, which encompassed plasma membrane H^+ATPases (3 accessions), phosphate-related proteins (4 accessions), and signal transduction-associated proteins (5 accessions). In plants, H^+ATPases are primarily responsible for energizing the plasma membrane and generating the proton motive force for secondary membrane transport of cations, anions, sugars, and amino acids, and are of particular interest in AM plants, as a functional symbiosis is characterized by bi-

directional nutrient transport across a plant–fungal interface. Actually, Pi transporters are thought to operate in conjunction with H^+ATPases for inward transport of P (Schachtman *et al.*, 1998). Contrasting with previous reports showing the expression of H^+ATPases-encoding genes in arbuscule-containing cells, including the induction of the specific H^+ATPase isoform Mtha1 in *M. truncatula*, (Gianinazzi-Pearson *et al.*, 2000; Krajinski *et al.*, 2002), the three plasma membrane H^+ATPase isoforms we identified showed a reduced abundance upon AM symbiosis (Table 4.2).

Table 4.2. List of the proteins displaying a down-accumulation in mycorrhizal roots relative to controls.
Yellow-shaded lines refer to identifications escaping our criteria for assigning a protein as membrane-associated.

MENS Toulouse 01/2003	Fold change	P value
MtC60362_1_AA Blast: G7JCD0 Plasma membrane H+ ATPase , cation transport ATPase (P-type) family, proton efflux [Medicago truncatula].	0,56	0,005
MtC10646_1_AA Blast: G7JUD3 Plasma membrane H+-ATPase, cation transport ATPase (P-type) family, plasma-membrane proton-efflux P-type ATPase [Medicago truncatula].	0,48	0,000
MtC93235_1_AA Blast: XP_003594954 Plasma membrane ATPase, plasma-membrane proton-efflux P-type ATPase [Medicago truncatula].	0,41	0,001
MtC20134.1_1_AA MtPT2 PHOSPHATE TRANSPORTER Major facilitator superfamily (Liu *et al.*, 1998)	0,48	0,000
MtC20134.2_1_AA MtPT1 PHOSPHATE TRANSPORTER Major facilitator superfamily (Liu *et al.*, 1998)	0,5	0,003
MtC62284_1_AA Blast: A5H2U5 Phosphate transporter 3, phosphate:H+ symporter [Medicago truncatula] (Liu *et al.*, 2008)	0,26	5.3173146108420 6e−08
MtD06942_1_AA Blast: XP_003609464 Vacuolar proton-inorganic pyrophosphatase [Medicago truncatula]. IPR004131 Pyrophosphate-energised proton pump	0,49	0,001
MtD24902_1_AA Blast XP_003625400 Pleiotropic drug resistance protein [Medicago truncatula].	0,5	0,002
MtD19528_1_AA unknown Blast:XP_003627035.1 ABC transporter family pleiotropic drug resistance protein [Medicago truncatula]	0,5	0,007
MtC10149_1_AA Blast: ACJ83883 unknown [Medicago truncatula].Plastocyanin-like domain	0,47	0,001
MtD01112_1_AA Blast: XP_003517628.1 PREDICTED: probable LRR receptor-like serine/threonine-protein kinase At4g29180-like [Glycine max]	0,56	0,002
MtD11061_1_AA Blast: XP_003531816: probable LRR receptor-like serine/threonine-proteinkinase At1g56130-like [Glycine max]	0,62	0,008
MtD04430_1_AA Blast XP_003616753 Cysteine-rich receptor-like protein kinase [Medicago truncatula].	0,66	0,002
MtC10353_1_AA Blast: XP_003618047.1 Fasciclin-like arabinogalactan protein [Medicago truncatula]	0,59	0,004
MtC00322_1_AA Blast: XP_003597322 60S ribosomal protein L23a [Medicago truncatula].	0,32	0,000
MtD00010.1_1_AA Blast: XP_003618775 Elongation factor 1-alpha [Medicago truncatula].	0,28	0,0004
MtC20279_1_AA Blast: XP_003523765 PREDICTED: 26S protease regulatory subunit S10B homolog B-like isoform 1 [Glycine max].	0,6	0,002
MtC00419_1_AA Blast: BAA19156 HMG-1 [Canavalia gladiata].HMG1/2 (high mobility group) box	0,56	0,008
MtC10218_1_AA Blast: XP_003616180 UTP-glucose 1 phosphate uridylyltransferase [Medicago truncatula].	0,48	0,009
MtC30342_1_AA Blast: XP_003531547 PREDICTED: probable protein phosphatase 2C 10-like [Glycine max].	0,36	0,005
MtC40209_1_AA unknown Blast: ADV35716.2 root determined nodulation 1 [Medicago truncatula]	0,39	0,009

Protein displaying a suppressed accumulation in mycorrhizal roots relative to controls

MENS Toulouse 01/2003	Fold change	
MtC93047_1_AA Unkown Blast: XP_003635272.1 PREDICTED: clathrin light chain 1-like [Vitis vinifera]	01,58489E-05	0,0004

This repressed pattern is reminiscent of that reported in tomato plants, which displayed the selective down-expression of the ATPase encoding genes *LHA1* and *LHA4* in epidermal cells located in regions of the root that contain arbuscules, and could be involved in the generation of the proton gradient necessary for phosphate uptake at the epidermis (Ferrol *et al.*, 2002; Rosewarne *et al.*, 2007). According to the model described by Rosewarne *et al.* (1999), it has been proposed that a mycorrhizal plant in low-phosphate soils attains much of its P through a route provided by the fungus, thus expressing transport-related proteins at the arbuscular interface and alleviating the need to express plant transporters at sites directly in contact with the soil. As underlined by Ferrol and co-workers (2002), this hypothesis is consistent with the observation that, in some cases, phosphate uptake from the soil by the epidermal root cells becomes almost inactive during the mycorrhizal symbiosis (Pearson & Jakobsen, 1993). In this respect, three PM-located phosphate transporters, namely MtPT1, MtPT2 and MtPT3, were recorded as down-accumulated in response to *R. irregularis* relative to control roots (Table 4.2). These transporters of *M. truncatula* are members of the PHT1 Pi transporter family that mediate transfer of Pi into cells, whereas members of the PHT2, PHT3, PHT4, and pPT families are involved in Pi transfer across internal cellular membranes and organelle membranes. According to their recent characterization by Liu and co-workers (2008), MtPT1, MtPT2 and MtPT3 share a high level of sequence identity and low affinities for Pi, but display tissue-specific patterns in that *MtPT2* is expressed in epidermis, cortex, and vascular tissue, whereas *MtPT1* shows the same expression pattern but lacks expression in the vascular tissue, and *MtPT3* shows expression only in the vascular tissue. Noteworthy and consistent with our proteomic data, the expression of *MtPT1*/*MtPT2* and *MtPT3* was reported down-regulated in mycorrhizal roots, a process that was referred to as a consequence of an increase in the Pi level, which occurs as Pi is delivered to the roots by the AM fungal symbiont. As previously mentioned, during mycorrhiza plants are believed to activate symbiosis-associated Pi transporters to obtain Pi delivered by the AM fungal symbiont, and gradually down-regulate expression of their root Pi transporter genes (Liu *et al.*, 1998; Chiou *et al.*, 2001). Nonetheless, whereas this pattern of regulation holds true for root epidermal/cortical cell transporters having low affinity for Pi, including MtPT1, MtPT2 and MtPT3i, this model does not apply to a high affinity Pi transporter whose expression is maintained at the root-soil interface

during the AM symbiosis in *M. truncatula* (Liu *et al.*, 2008). Also in relation to Pi, a vacuolar proton-inorganic pyrophosphatase showed a reduced abundance in mycorrhizal roots relative to control (Table 4.2). Since large amount of inorganic pyrophosphate (PPi) are produced as a by product of macromolecule synthesis, reactions that utilize PPi in place of ATP are considered to confer a bioenergetic advantage to plant cells that have become ATP depleted owning to environmental stresses such as Pi starvation. Actually, the vacuolar H^+PPiase represents an enzyme that endows plants with the capability of utilizing PPi to circumvent an ATP-consuming cytosolic reaction together with facilitating Pi recycling during Pi stress, since two and one Pi molecules are produced per PPi and ATP hydrolyzed, respectively (Plaxton, 1999). In this respect, the up-regulation of H^+PPiase during Pi starvation in *Brassica napus* has been demonstrated, together with the utilization of this enzyme for maintaining vacuole acidification and employing PPi as an energy donor to conserve limited cellular pools of ATP while recycling valuable Pi (Palma *et al.*, 2000). Consequently, the decreased accumulation of the vacuolar proton-inorganic pyrophosphatase we recorded in mycorrhizal roots appears consistent when considering Pi supply as one of the main benefices conferred by AM symbiosis to their hosts. In the same line of reasoning, an UTP-glucose 1 phosphate uridylyltransferase also known as UDP–glucose pyrophosphorylase (UGPase) also displayed a reduced abundance upon mycorhization (Table 4.2). UGPase not only represents an important activity in carbohydrate metabolism, catalysing a reversible production of UDPG and PPi from Glc-1-P and UTP, but also constitutes an important mechanism increasing Pi availability during P stress. Noteworthy, in *Arabidopsis*, *UGP* expression and UGPase activity/protein content were strongly up-regulated by conditions resulting in phosphorus deficiency (Kleczkowski *et al.*, 2004). In pea (*Pisum sativum*) roots, UGPase protein increased after cadmium-excess stress, possibly reflecting Cd-induced Pi deficiency effects at the *UGP* expression level (Repetto, 2003). The UGPase step may thus constitute an important mechanism increasing Pi availability during P stress, in that the PPi released in the synthesis of UDPG by UGPase is hydrolyzed to Pi by pyrophosphatase(s), thereby increasing the availability of Pi for P-deprived plants (Kleczkowski *et al.*, 2004). Consequently, the decreased abundance we recorded in both vacuolar H^+PPiase and UGPase proteins in mycorrhizal roles, both having role in alleviating phosphorus deficiency, may

correlate the increased availability of Pi upon AM symbiosis in *M. truncatula* roots. Concomitantly, it has also been demonstrated that genes encoding protein proteases, PDR (pleiotropic drug resistant)-like ABC transporter, and protein phosphatase 2C, the latter acting as a general negative regulator of stress signalling through the regulation of the stress-activated mitogen-activated protein kinase pathway, were also are up-regulated under Pi limited conditions in pea plants (Tian *et al.*, 2007), thereby suggesting that the currently observed down accumulation of these proteins in mycorrhizal plants (Table 4.2), may actually also reflect an improved Pi uptake in *M. truncatula* roots upon AM symbiosis.

With regard to signalling processes, besides the three plant genes (*dmi1*, *dmi2*, and *dmi3*) relevant for the common early stages of signal transduction during nodulation and AM formation (Cullimore & Denarie, 2003), genes encoding putative AM-related receptors such as a Ser/Thr receptor kinase (TC86597) and a Leu-rich repeat (LRR) receptor-like protein kinase (TC80104) characterized by extracellular LRR domains mediating protein-protein interactions were reported by Hohnjec and co-workers (2005) as up-regulated upon mycorhization. By contract, two probable LRR receptor-like serine/threonine-protein kinases and a cysteine-rich receptor-like protein kinase were recorded in the current study as displaying a reduced abundance in response to *R. irregularis* inoculation (Table 4.2). Receptor-like kinases (RLKs) are animal receptor kinase orthologs in plants, so classified because of conserved structures that include an extracellular receptor, a transmembrane domain, and an intracellular kinase domain (Shiu & Li, 2004). RLK activation occurs upon binding of an extracellular ligand to the plasma membrane and subsequently, the RLK complex undergoes autotransphosphorylation that activate diverse signal transduction pathways, including those that control hormone and morphogenetic responses, cell differentiation, and defence signalling (Holland & Holland, 2002). Whether the down-accumulation of the three RLKs we observed could mediate reduced plant defence mechanisms in order to accommodate AM fungi is unknown, although previously described for genes encoding PR proteins and enzymes of phytoalexin biosynthesis that showed transcript level declines during the functional stage of the symbiosis (Liu *et al.*, 2003), but regulation of signalling activity at the cell surface (receptor down-regulation) has been documented. Actually, RLK internalization *via* encocytosis, which leads to degradation and recycling of receptor kinases, has been demonstrated (Shah *et al.*,

2002), thereby linking signal transduction pathways and membrane trafficking (Drakakaki *et al.*, 2009), as discussed above. In this regard, we also recorded the down-accumulation of a fasciclin-like arabinogalactan protein upon AM symbiosis (Table 4.2). Putative plant adhesion molecule include arabinogalactan-proteins (AGPs) having fasciclin-like domains (FLAs), among which 70% are predicted to be glycosylphosphatidylinositol-anchored to the plasma membrane in wheat and rice (Faik *et al.*, 2006). The functions of AGPs in undifferentiated protoplasts and cultured cells of several species have been investigated by using molecules that bind to and inactivate AGPs such as $(\beta\text{-d-Glc})_3$ or $(\beta\text{-d-Gal})_3$. Inhibition of cell expansion was evident in *Arabidopsis* seedlings, in which $(\beta\text{-d-Glc})_3$ causes a bulging of root epidermal cells (Willats & Knox, 1996). Current models suggest that an integrated control system regulates both the cell cycle and programmed cell death, and the results observed upon perturbation of AGPs in plant cell cultures indicate that AGPs may play a role in this integrated control system (Gao & Showalter, 1999) in that $(\beta\text{-d-Gal})_3$ disrupts plasmalemma-cell wall connections and thereby activates a signal transduction pathway that directs the cell away from cell cycle progression and toward programmed cell death. The connection of AM symbiosis with reduced amounts in plant AGPs, although quite unclear, may thus nonetheless reflect the reduced root elongation in mycorrhizal roots concomitant to the extension of the fungal extra-radical mycelium that provides extensive pathways for nutrient fluxes through the soil (Purin & Rillig, 2008). Finally, as very comprehensively reviewed in (Hause & Schaarschmidt, 2009), host plants indeed are able to control the degree of their associations with rhizobia and AM fungi in order to minimize the carbon resources they invest in symbiosis. Once first steps of interactions are initiated, further establishment of symbionts above a critical threshold level is restricted, leading to autoregulation (AUT) of mutualism. Recently, a screen for supernodulating *M. truncatula* mutants defective in this regulatory behaviour yielded loss-of-function alleles of a gene designated *ROOT DETERMINED NODULATION1* (*RDN1*), and a mutation in a putative *RDN1* ortholog was also identified in the supernodulating *nod3* mutant of pea (Schnabel *et al.*, 2011). Whereas previous key actors mediating loss-of-AUT mutants that display a supernodulating and supermycorrhizal phenotype (increased abundance of nodules and arbuscules, respectively), were identified as receptor-like kinases acting in the shoot, the *RDN1* promoter drove expression in the

vascular cylinder, suggesting that RDN1 may be involved in initiating, responding to, or transporting vascular signals. In the current study, we retrieved the protein RDN1 as down-accumulated in mycorrhizal roots *versus* controls (Table 4.2), thereby not only pointing out to another regulatory process shared between nitrogen-fixing rhizobial and mycorrhizal symbioses, but also to a mechanism favouring AM colonization in our experimental conditions.

Conclusions

For the first time, a protocol was designed that proved valuable in increasing the coverage of root membrane proteins in the model legume *M. truncatula*, relative to previous studies, as inferred from the 882 putative root microsomal proteins identified in the current study. On the basis of *in silico* predictions, the present work argued for plasticity as the main characteristic of the root microsomal proteins that were retrieved, as inferred from plastids and transport as prevalent organelle and function, respectively, together with the important representation of β-barrels domains coupled palmitate-modified proteins, two processes known to drive membrane signaling and trafficking events. Additionally, the label-free peak integration strategy we employed to record changes in membrane protein abundance in response to AM symbiosis, also gave arguments in favor of a conserved qualitative microsomal proteome upon the inoculation of *R. irregularis*, in that only the protein Mtha1was recorded as induced in mycorrhizal roots. Altogether, the current results sustain the view according to which the accommodation of AM fungi within root cortical cells implies a dynamic reorganisation of root membrane proteins, rather than the synthesis of AM-specific proteins. However, the present data also suggested that branch-related periarbuscular membrane proteins, by displaying specific features, could have escaped the procedure we employed for extracting root microsomal proteins, thus pointed out to the necessity of developing methods suitable for isolating/enriching periarbuscular membrane proteins. Nonetheless, besides getting knowledge on root microsomal protein modifications potentially sustaining AM symbiosis establishment and functioning, the protocol we described, by giving access to the largest coverage of root membrane proteins so far recorded in *M. truncatula*, may be helpful for creating a root membrane proteome database for comparative purposes with more recently evolved plant-microbe interactions that share root morphological commonalties with mycorrhiza.

Acknowledgments

CA, CG, EDG, DvT, DW, JR and GR acknowledge financial support by the Burgundy Regional Council (PARI Agrale 8) and "Fonds National de la Recherche du Luxembourg" AFR TR-PHD BFR 08-078.

Additional files

Chapter 4, additional file S4.1: List of the 1128 proteins.
Proteins are obtained from the twelve microsomal fractions analysed in the current study by using an E value smaller than 10^{-4} as a criterion to assign correct protein identification. Accessions and annotations refer to the *Medicago truncatula* EST database (http://medicago.toulouse.inra.fr/Mt/EST/).

Chapter 4, additional file S4.2: Overlap of the co-identified proteins in two biological experiments.
Overlap in the proteins co-identified in the two independent experiments (referred to as Exp 1 and Exp 2) after root microsome extractions that reached a common value of 96% both in the mycorrhized (M) and the nonmycorrhized (C) plant roots. Letters a, b, and c refer to each of the three replicates performed per experiment.

Chapter 4, additional file S4.3: List of the 164 (15.6%) proteins (yellow-shaded) out of the 1047 nonredundant identifications that were discarded as potential contaminants of the microsomal fractions isolated from nonmycorrhizal and mycorrhizal roots.
Red characters refer to Blast searches conducted on the NCBI nonredundant database. Purple lines refer to accessions displaying a membrane location according to TAIR but that escape our criteria for genuine microsomal *M. truncatula* proteins corresponding to homologous sequences displaying at least 70% pair-wise identity and a cut-off expectation value of e^{-40} were experimentally demonstrated to have a membrane localisation, including core integral or subunits of membrane complexes, on the basis of direct assays or "traceable author statement". The identified proteins in *Medicago truncatula* EST (http://medicago.toulouse.inra.fr/Mt/EST/) were assigned to a Medtr accession number using (http://www.legoo.org/). Proteins were functionally classified according to Ruepp *et al.* (2004). TM domains were predicted using the Tmpred server (http://www.ch.embnet.org/software/TMPRED_form.html), with a minimum score of 1000 (Valot *et al.*, 2006) and (http://www.cbs.dtu.dk/services/TMHMM/). WoLF PSORT (http://wolfpsort.seq.cbrc.jp) was used to predict protein localisation. The prediction of palmitoylation and N-terminal myristoylation sites was done using the ExPASy tools (http://csspalm.biocuckoo.org/online3.php) and (http://web.expasy.org/myristoylator/), respectively. For prenylation prediction, the PrePS online tool (http://mendel.imp.ac.at/sat/PrePS/index.html) was used, while GPI anchor prediction was performed using the GPI Modification Site Prediction in Plants (http://mendel.imp.ac.at/gpi/plant_server.html). SignalP 4.0 server (http://www.cbs.dtu.dk/services/SignalP/) was employed to predict the presence of signal peptide cleavage sites in protein sequences. The online tool (http://biophysics.biol.uoa.gr/PRED-TMBB/input.jsp) was used to discriminate beta-barrel outer membrane proteins.

Chapter 4, additional file S4.4: List of the 883 (84.3%) proteins out of the 1047 nonredundant identifications that were retained as genuine microsomal candidates from the fractions isolated from nonmycorrhizal and mycorrhizal roots.

Red characters refer to Blast searches conducted on the NCBI or Uniprot nonredundant database. Purple lines refer to accessions displaying a membrane location according to TAIR but that escape our criteria for genuine microsomal *M. truncatula* proteins corresponding to homologous sequences displaying at least 70% pair-wise identity and a cut-off expectation value of e^{-40} were experimentally demonstrated to have a membrane localisation, including core integral or subunits of membrane complexes, on the basis of direct assays or "traceable author statement". Green lines correspond to proteins satisfying the aforementioned criteria. Nonshaded lines correspond to proteins nonreferred as membrane-located according to TAIR annotations. The identified proteins in *Medicago truncatula* EST (http://medicago.toulouse.inra.fr/Mt/EST/) were assigned to a Medtr accession number using (http://www.legoo.org/). Proteins were functionally classified according to Ruepp *et al.* (2004). TM domains were predicted using the Tmpred server (http://www.ch.embnet.org/software/TMPRED_form.html), with a minimum score of 1000 (Valot *et al.*, 2006) and (http://www.cbs.dtu.dk/services/TMHMM/). WoLF PSORT (http://wolfpsort.seq.cbrc.jp) was used to predict protein localisation. The prediction of palmitoylation and N-terminal myristoylation sites was done using the ExPASy tools (http://csspalm.biocuckoo.org/online3.php) and (http://web.expasy.org/myristoylator/), respectively. For prenylation prediction, the PrePS online tool (http://mendel.imp.ac.at/sat/PrePS/index.html) was used, while GPI anchor prediction was performed using the GPI Modification Site Prediction in Plants (http://mendel.imp.ac.at/gpi/plant_server.html). SignalP 4.0 server (http://www.cbs.dtu.dk/services/SignalP/) was employed to predict the presence of signal peptide cleavage sites in protein sequences. The online tool (http://biophysics.biol.uoa.gr/PRED-TMBB/input.jsp) was used to discriminate beta-barrel outer membrane proteins.

Chapter 5

General discussion, conclusion and perspectives

Most plants live in close association with arbuscular mycorrhizal (AM) fungi, which colonize the plant roots and form typical intracellular structures, i.e. the arbuscules, thought to be the main sites of nutritional exchanges. Such AM fungi form an extensive hyphal network that reaches far beyond the root depletion zone, and are thus capable to acquire nutrients from the soil much more efficiently than the plant root system alone (Smith & Read, 2008). Together with genetics and thorough exploitation of plant mutants defective to the AM symbiosis at various stages, the development of large-scale untargeted approaches such as transcriptomics and proteomics has recently allowed decrypting some of the programmes that govern this particular plant root/AM fungal interaction. However, because the development of AM symbiosis is an asynchronous process, with mycorrhizal roots typically containing several symbiotic structures and various cell types, and in absence of any amplification strategy as for nucleic acids, proteomics of AM symbiosis is still a challenging task which will obviously benefit from subcellular enrichments of particular cell compartments.

Indeed, dynamic proteome alteration analyses in response to AM fungi have mainly used 2-DE gels with a special focus on soluble proteins regarding their ease of purification and high abundance. Because the AM association is mainly characterized by deep membrane changes in the host plant roots, our purpose was therefore to focus on membrane proteins. To achieve this, we choose to study *Medicago truncatula*, one of the key model systems for studying plant root interactions, inoculated with the representative AM fungus *Rhizophagus irregularis*. Moreover, using the substantial improvements in mass spectrometry (MS) and advances related to protein/peptides fractionation methods, we may expect increasing the coverage of the categories of proteins that escape canonical 2-DE separation, expanding the catalogue of membrane proteins. In the meantime, by developing accurate means to quantify the proteins, we look forward to unravelling proteins potentially involved in the functioning of the AM symbiosis.

Based on previous researches of the group “Mycorrhize” at the pole IPM of

the UMR Agroecology, a 4 weeks-AM infection system was deliberately chosen in order to get sufficient amounts of well-colonized young roots with reasonable arbuscule development to allow enrichment in membranes. Although membrane proteins are relatively few in number when compared to cytosolic proteins, almost all major processes and signalling pathways require membrane-associated proteins for proper function and regulation. However, membrane proteomics is still challenging due to 2-DE related limitations, therefore up to now only a few membrane proteins involved in the sustaining of the AM symbiosis were identified (Valot *et al.*, 2005) subsequently extend to some plasma membrane proteins after a first trial of plasma membrane enrichment followed by LC-MS/MS analysis (Valot *et al.*, 2006). However, at this time no convenient label free strategy for quantification was routinely available.

Therefore, first we tentatively improve the process for preparing microsomal proteins by applying to our root extracts a robust protocol for enrichment (Stanislas *et al.*, 2009). Such protocol has been proved to be efficient based on depletion in soluble proteins evaluated by western blots and by scrutinizing the membrane proteins of microsomal *M. truncatula* root fractions using available electronic tools after pilot LC-MS/MS analyses (data not shown).

Currently a large panel of shotgun MS-based proteomic approaches are available but their applications in plants are still scarce. To overcome 2-DE related concerns, microsomal proteins of *Medicago truncatula* roots were, for the first time, scrutinised by state-of-the-art MS-based proteomic approaches iTRAQ-OGE-LC-MS/MS and label-free 1-DE-LC-MS/MS. The applied workflows combine two novel proteomic procedures, label-based and -free, targeting an insight view on the membrane proteome changes in AM symbiosis. While the first approach is based on peptide chemical labelling by iTRAQ, the second one is label-free based on spectral peak intensity.

The first aim of the current work was methodological by analysing the impact of iTRAQ labelling on peptide pI and behaviour in OGE fractionation. In this objective, a straightforward and robust in-filter protein digestion, with easy recovery of a peptide fraction compatible with iTRAQ labelling, was successfully set up. Besides the practical applicability, this tailored workflow allows users to successfully employ it with different kind of matrices. Afterwards, the examination of peptide

electrofocusing behaviour before and after iTRAQ labelling revealed a non-negligible basic pI shift in OGE fractionation on a wide pH range (3-10). To further investigate and explain the experimental findings, MarvinSketch calculator was implemented, in which peptide amino acid structures can be manually drawn and peptide pI calculated for native and iTRAQ labelled peptides. To date most pI calculator algorithms use only native peptide sequences without taking into account the iTRAQ tags. In the current study, an effort was done to answer the question whether an iTRAQ labelled peptide will exhibit the same pI-value as its native counterpart. However, further experiments in combination with trustworthier, advanced pI calculator software are crucial to enhance our understanding on the observed basic shift and routinely describe the pI of iTRAQ labelled peptides.

Once iTRAQ-OGE-LC-MS/MS method was set up on *M. truncatula* microsomal proteins, it was subsequently used to track quantitative protein expression changes in response to AM symbiosis. The enrichment of membrane protein fractions, assessed by the subcellular localisation of the identified proteins and by some immunoblottings, highlighted the efficiency of the employed fractionation method to give access to membrane protein-enriched fractions. Isobaric tagging protocols involve multiple desalting steps and many procedures that may lead to sample loss and thus drastically decrease the number of identified proteins (151 proteins). Moreover, the results showed the difficulty in achieving reproducible and reliable quantitative data. Besides the use of a last generation mass spectrometer and application of the hybrid, recommended for iTRAQ labelled samples, fragmentation method (CID-HCD) the gained information was limited in terms of quantification accuracy. This method was suboptimal and appeared to be less suited to the current study. Although isobaric tagging methods have many attractive attributes, there are issues concerning their use in large-scale experiments. Therefore many described guidelines must be, for future application, taken into account such as the addition of spiked standard proteins in at known concentrations in order to test the performance of the system in terms of precision and accuracy.

Giving that iTRAQ approach appeared unable to yield accurate differential protein accumulations in mycorrhized plants, label-free 1-DE-LC-MS/MS technology becomes a surrogate tool to study the membrane proteins. This method benefits from both gel-based protein and gel-free peptide separation properties. Moreover, the in-gel

protein digestion allows detergent removal from peptide fractions prior to their further LC-MS analysis. This experimental strategy led to the identification of more than one thousand proteins with only 15.6% of potential soluble contaminant proteins in our experiments. This finding, coupled to the western blot results showing a depletion of the cytosolic marker "anti-UGPase" in microsomal protein fractions, strongly confirms the effectiveness of the employed protocol for root membrane enrichment with sufficient recovery and purity for their subsequent in-depth analysis. Our findings showed the existence of a conserved microsome-enriched fraction between mycorrhized and nonmycorrhized roots. The identified microsomal proteins were mainly chloroplast, nucleus and plasma membrane residents, while their functional classification revealed that transport, protein synthesis and metabolism are the prominent biological process categories of the core microsome. The expression of 22 and 19 membrane proteins displayed up-and down- accumulation in AM roots, respectively. Among the up-regulated proteins, a blue copper binding protein (MtBcp1) displayed a near 10 fold over accumulation in response to the AM symbiosis. It was previously shown that the arbuscule-trunk-located MtBcp1 is strongly up-regulated in arbuscule-containing regions of mycorrhizal roots. Furthermore, the presented study revealed new candidates putatively playing a role in signalling/membrane trafficking. For instance, transmembrane emp24 domain-containing protein, prohibitin, ras-related protein RABE1c-like and reticulon-like protein, all having roles in secretion or in membrane trafficking were recorded as up-accumulated membrane proteins upon symbiosis. It was previously demonstrated that the development of arbuscules induces architectural feature modification to support newly synthesized membrane proteins. This could be exemplified by the up-accumulation of cytoskeletal components such as actin-like proteins, together with proteins playing role in protein synthesis and fate, including histones, ribosomal proteins, and cyclophilins. The 19 proteins that showed a down-regulation of their expression in AM roots encompassed three prevalent classes: plasma membrane H^+ATPases (3 accessions), phosphate-related proteins (4 accessions), and signal transduction-associated proteins (5 accessions). The down-regulation of the plasma membrane H^+ATPase isoforms could be involved in the generation of the proton gradient necessary for phosphate uptake at the epidermis. Moreover, it has been proposed that a mycorrhizal plant reaches its phosphate needs through the fungus,

thus alleviating the expression of plant transporters. In this respect, three plasma membrane-located phosphate transporters, namely MtPT1, MtPT2 and MtPT3, were recorded as down-accumulated in response to *R. irregularis* inoculation. The protein abundance of vacuolar H^+PPiase, UDP–glucose pyrophosphorylase, protein proteases, PDR (pleiotropic drug resistant)-like ABC transporter, and protein phosphatase 2C was down-regulated in response to mycorrhiza. This observation may correlate with the increased availability of phosphate in AM *M. truncatula* roots. Our results shed the light on new membrane proteins that strongly support the importance of membrane signalling/trafficking events in mycorrhiza establishment and functioning.

Proteomics has become an important complementary tool to genomics providing novel information and greater insight into plant biology. The development of novel methods for protein quantification in parallel with the use of MS and bioinformatics techniques, as we have develop in our research, undoubtedly help in widening the application of these technologies for achieving a better understanding the key aspects of membrane proteins in AM plants. However, the presented study suggested that branch-related periarbuscular membrane proteins could have escaped the employed protocol for extracting root microsomal proteins. Thus, new proteomic protocols aiming at isolating the arbuscule-branch domain, probably on the basis of immunoassays appears indispensable to increase our knowledge relative to the protein composition of the periarbuscular membrane. Among the proteins differentially accumulated in response to *M. truncatula* root colonization, to our point of view RDN1, unknown protein (MtC00185, 3 times over-accumulated in AM roots) and unknown protein (MtC10149, plastocyanin-like domain, down-regulated in response to AM symbiosis) constitute good candidates for exploring their precise location and role in AM symbiosis. This could be achieved through different strategies i.e. use of already available *M. truncatula* mutants as done by Paradi *et al.* (2010) for a mycorrhizal specific blue copper-binding protein, production of RNA interference (RNAi) mutants, or targeted Rt-PCR of the corresponding genes after laser micro dissection of the appropriate cell compartments.

References

Abdallah C, Sergeant K, Guillier C, Dumas-Gaudot E, Leclercq C, Renaut J. 2012. Optimization of iTRAQ labelling coupled to OFFGEL fractionation as a proteomic workflow to the analysis of microsomal proteins of *Medicago truncatula* roots. *Proteome Sci* **10**(1): 37.

Aebersold R, Mann M. 2003. Mass spectrometry-based proteomics. *Nature* **422**(6928): 198-207.

Aggarwal K, Choe LH, Lee KH. 2006. Shotgun proteomics using the iTRAQ isobaric tags. *Brief Funct Genomic Proteomic* **5**(2): 112-120.

Aicart-Ramos C, Valero RA, Rodriguez-Crespo I. 2011. Protein palmitoylation and subcellular trafficking. *Biochim Biophys Acta* **1808**(12): 2981-2994.

Akiyama K. 2007. Chemical identification and functional analysis of apocarotenoids involved in the development of arbuscular mycorrhizal symbiosis. *Biosci Biotechnol Biochem* **71**(6): 1405-1414.

Akiyama K, Matsuzaki K, Hayashi H. 2005. Plant sesquiterpenes induce hyphal branching in arbuscular mycorrhizal fungi. *Nature* **435**(7043): 824-827.

Alban A, David SO, Bjorkesten L, Andersson C, Sloge E, Lewis S, Currie I. 2003. A novel experimental design for comparative two-dimensional gel analysis: two-dimensional difference gel electrophoresis incorporating a pooled internal standard. *Proteomics* **3**(1): 36-44.

Aloui A, Recorbet G, Gollotte A, Robert F, Valot B, Gianinazzi-Pearson V, Aschi-Smiti S, Dumas-Gaudot E. 2009. On the mechanisms of cadmium stress alleviation in *Medicago truncatula* by arbuscular mycorrhizal symbiosis: a root proteomic study. *Proteomics* **9**(2): 420-433.

Aloui A, Recorbet G, Robert F, Schoefs B, Bertrand M, Henry C, Gianinazzi-Pearson V, Dumas-Gaudot E, Aschi-Smiti S. 2011. Arbuscular mycorrhizal symbiosis elicits shoot proteome changes that are modified during cadmium stress alleviation in *Medicago truncatula*. *BMC Plant Biol* **11**: 75.

Alvarez S, Berla BM, Sheffield J, Cahoon RE, Jez JM, Hicks LM. 2009. Comprehensive analysis of the *Brassica juncea* root proteome in response to cadmium exposure by complementary proteomic approaches. *Proteomics* **9**(9): 2419-2431.

America AH, Cordewener JH. 2008. Comparative LC-MS: a landscape of peaks and valleys. *Proteomics* **8**(4): 731-749.

Amiour N, Recorbet G, Robert F, Gianinazzi S, Dumas-Gaudot E. 2006. Mutations in DMI3 and SUNN modify the appressorium-responsive root proteome in arbuscular mycorrhiza. *Mol Plant Microbe Interact* **19**(9): 988-997.

Anderson JP, Gleason CA, Foley RC, Thrall PH, Burdon JB, Singh KB. 2010. Plants versus pathogens: an evolutionary arms race. *Funct Plant Biol* **37**(6): 499-512.

Andrews TM, Tata JR. 1971. Protein synthesis by membrane-bound and free ribosomes of the developing rat cerebral cortex. *Biochem J* **124**(5): 883-889.

Ane JM, Zhu H, Frugoli J. 2008. Recent Advances in *Medicago truncatula* Genomics. *Int J Plant Genomics* **2008**: 256597.

AP VDW, Howlett BJ. 2011. Fungal pathogenicity genes in the age of 'omics'. *Mol Plant Pathol* **12**(5): 507-514.

Arnaud IL, Josserand J, Jensen H, Lion N, Roussel C, Girault HH. 2005. Salt removal during Off-Gel electrophoresis of protein samples. *Electrophoresis* **26**(9): 1650-1658.

Baerenfaller K, Grossmann J, Grobei MA, Hull R, Hirsch-Hoffmann M, Yalovsky S, Zimmermann P, Grossniklaus U, Gruissem W, Baginsky S. 2008. Genome-scale proteomics reveals *Arabidopsis thaliana* gene models and proteome dynamics. *Science* **320**(5878): 938-941.

Baier MC, Barsch A, Kuster H, Hohnjec N. 2007. Antisense repression of the *Medicago truncatula* nodule-enhanced sucrose synthase leads to a handicapped nitrogen fixation mirrored by specific alterations in the symbiotic transcriptome and metabolome. *Plant Physiol* **145**(4): 1600-1618.

Baier MC, Keck M, Godde V, Niehaus K, Kuster H, Hohnjec N. 2010. Knockdown of the symbiotic sucrose synthase MtSucS1 affects arbuscule maturation and maintenance in mycorrhizal roots of *Medicago truncatula*. *Plant Physiol* **152**(2): 1000-1014.

Balestrini R, Berta G, Bonfante P. 1992. The plant nucleus in mycorrhizal roots: positional and structural modifications. *Biol. Cell* **75**: 235–243.

Balestrini R, Cosgrove DJ, Bonfante P. 2005. Differential location of alpha-expansin proteins during the accommodation of root cells to an arbuscular mycorrhizal fungus. *Planta* **220**(6): 889-899.

Bell CJ, Dixon RA, Farmer AD, Flores R, Inman J, Gonzales RA, Harrison MJ, Paiva NL, Scott AD, Weller JW, May GD. 2001. The *Medicago* Genome Initiative: a model legume database. *Nucleic Acids Res* **29**(1): 114-117.

Benedito VA, Li H, Dai X, Wandrey M, He J, Kaundal R, Torres-Jerez I, Gomez SK, Harrison MJ, Tang Y, Zhao PX, Udvardi MK. 2010. Genomic inventory and transcriptional analysis of *Medicago truncatula* transporters. *Plant Physiol* **152**(3): 1716-1730.

Benschop JJ, Mohammed S, O'Flaherty M, Heck AJ, Slijper M, Menke FL. 2007. Quantitative phosphoproteomics of early elicitor signaling in *Arabidopsis*. *Mol Cell Proteomics* **6**(7): 1198-1214.

Besserer A, Becard G, Jauneau A, Roux C, Sejalon-Delmas N. 2008. GR24, a synthetic analog of strigolactones, stimulates the mitosis and growth of the arbuscular mycorrhizal fungus *Gigaspora rosea* by boosting its energy metabolism. *Plant Physiol* **148**(1): 402-413.

Besserer A, Becard G, Roux C, Sejalon-Delmas N. 2009. Role of mitochondria in the response of arbuscular mycorrhizal fungi to strigolactones. *Plant Signal Behav* **4**(1): 75-77.

Besserer A, Puech-Pages V, Kiefer P, Gomez-Roldan V, Jauneau A, Roy S, Portais JC, Roux C, Becard G, Sejalon-Delmas N. 2006. Strigolactones stimulate arbuscular mycorrhizal fungi by activating mitochondria. *PLoS Biol* **4**(7): e226.

Besson D, Pavageau AH, Valo I, Bourreau A, Belanger A, Eymerit-Morin C, Mouliere A, Chassevent A, Boisdron-Celle M, Morel A, Solassol J, Campone M, Gamelin E, Barre B, Coqueret O, Guette C. 2011. A quantitative proteomic approach of the different stages of colorectal cancer establishes OLFM4 as a new nonmetastatic tumor marker. *Mol Cell Proteomics* **10**(12): M111 009712.

Bestel-Corre G, Dumas-Gaudot E, Poinsot V, Dieu M, Dierick JF, van TD, Remacle J, Gianinazzi-Pearson V, Gianinazzi S. 2002. Proteome analysis and identification of symbiosis-related proteins from *Medicago truncatula Gaertn*. by two-dimensional electrophoresis and mass spectrometry. *Electrophoresis* **23**(1): 122-137.

Bhadauria V, Banniza S, Wei Y, Peng YL. 2009. Reverse genetics for functional genomics of phytopathogenic fungi and oomycetes. *Comp Funct Genomics*: 380719.

Bindschedler LV, Cramer R. 2011. Quantitative plant proteomics. *Proteomics* **11**(4): 756-775.

Bindschedler LV, Palmblad M, Cramer R. 2008. Hydroponic isotope labelling of entire plants (HILEP) for quantitative plant proteomics; an oxidative stress case study. *Phytochemistry* **69**(10): 1962-1972.

Blackburn K, Cheng FY, Williamson JD, Goshe MB. 2010a. Data-independent liquid chromatography/mass spectrometry (LC/MS$^{(E)}$) detection and quantification of the secreted *Apium graveolens* pathogen defense protein mannitol dehydrogenase. *Rapid Commun Mass Spectrom* **24**(7): 1009-1016.

Blackburn K, Mbeunkui F, Mitra SK, Mentzel T, Goshe MB. 2010b. Improving protein and proteome coverage through data-independent multiplexed peptide fragmentation. *J Proteome Res* **9**(7): 3621-3637.

Bohler S, Sergeant K, Hoffmann L, Dizengremel P, Hausman JF, Renaut J, Jolivet Y. 2011. A difference gel electrophoresis study on thylakoids isolated from poplar leaves reveals a negative impact of ozone exposure on membrane proteins. *J Proteome Res* **10**(7): 3003-3011.

Boldt K, Pors Y, Haupt B, Bitterlich M, Kuhn C, Grimm B, Franken P. 2011. Photochemical processes, carbon assimilation and RNA accumulation of sucrose transporter genes in tomato arbuscular mycorrhiza. *J Plant Physiol* **168**(11): 1256-1263.

Bondarenko PV, Chelius D, Shaler TA. 2002. Identification and relative quantitation of protein mixtures by enzymatic digestion followed by capillary reversed-phase liquid chromatography-tandem mass spectrometry. *Anal Chem* **74**(18): 4741-4749.

Bonfante P, Genre A. 2008. Plants and arbuscular mycorrhizal fungi: an evolutionary-developmental perspective. *Trends Plant Sci* **13**(9): 492-498.

Bonfante P, Genre A. 2010. Mechanisms underlying beneficial plant-fungus interactions in mycorrhizal symbiosis. *Nat Commun* **1**: 48.

Bonfante P, Perotto S. 1995. Strategies of arbuscular mycorrhizal fungi when infecting host plants. *New Phytol* **130**(1): 3-21.

Bonfante P, Requena N. 2011. Dating in the dark: how roots respond to fungal signals to establish arbuscular mycorrhizal symbiosis. *Curr Opin Plant Biol* **14**(4): 451-457.

Bradford MM. 1976. A rapid and sensitive method for the quantitation of microgram quantities of protein utilizing the principle of protein-dye binding. *Anal Biochem* **72**: 248-254.

Breuillin F, Schramm J, Hajirezaei M, Ahkami A, Favre P, Druege U, Hause B, Bucher M, Kretzschmar T, Bossolini E, Kuhlemeier C, Martinoia E, Franken P, Scholz U, Reinhardt D. 2010. Phosphate systemically inhibits development of arbuscular mycorrhiza in *Petunia hybrida* and represses genes involved in mycorrhizal functioning. *Plant J* **64**(6): 1002-1017.

Brunner A, Keidel EM, Dosch D, Kellermann J, Lottspeich F. 2010. ICPLQuant - A software for non-isobaric isotopic labeling proteomics. *Proteomics* **10**(2): 315-326.

Bucking H, Shachar-Hill Y. 2005. Phosphate uptake, transport and transfer by the arbuscular mycorrhizal fungus *Glomus intraradices* is stimulated by increased carbohydrate availability. *New Phytol* **165**(3): 899-911.

Buee M, Rossignol M, Jauneau A, Ranjeva R, Becard G. 2000. The pre-symbiotic growth of arbuscular mycorrhizal fungi is induced by a branching factor partially purified from plant root exudates. *Mol Plant Microbe Interact* **13**(6): 693-698.

Cairns DA. 2011. Statistical issues in quality control of proteomic analyses: good experimental design and planning. *Proteomics* **11**(6): 1037-1048.

Campos-Soriano L, Gomez-Ariza J, Bonfante P, San Segundo B. 2011. A rice calcium-dependent protein kinase is expressed in cortical root cells during the presymbiotic phase of the arbuscular mycorrhizal symbiosis. *BMC Plant Biol* **11**: 90.

Cappellazzo G, Lanfranco L, Fitz M, Wipf D, Bonfante P. 2008. Characterization of an amino acid permease from the endomycorrhizal fungus *Glomus mosseae*. *Plant Physiol* **147**(1): 429-437.

Cargile BJ, Sevinsky JR, Essader AS, Stephenson JL, Jr., Bundy JL. 2005. Immobilized pH gradient isoelectric focusing as a first-dimension separation in shotgun proteomics. *J Biomol Tech* **16**(3): 181-189.

Carling DE, Brown MF. 1982. Anatomy and physiology of vesicular-arbuscular and nonmycorrhizal roots. *Phytopathology* **72**: 1108–1114.

Carvalho PC, Han X, Xu T, Cociorva D, Carvalho Mda G, Barbosa VC, Yates JR, 3rd. 2010. XDIA: improving on the label-free data-independent analysis. *Bioinformatics* **26**(6): 847-848.

Catalano CM, Lane WS, Sherrier DJ. 2004. Biochemical characterization of symbiosome membrane proteins from *Medicago truncatula* root nodules. *Electrophoresis* **25**(3): 519-531.

Chelius D, Bondarenko PV. 2002. Quantitative profiling of proteins in complex mixtures using liquid chromatography and mass spectrometry. *J Proteome Res* **1**(4): 317-323.

Chen A, Gu M, Sun S, Zhu L, Hong S, Xu G. 2011. Identification of two conserved cis-acting elements, MYCS and P1BS, involved in the regulation of mycorrhiza-activated phosphate transporters in eudicot species. *New Phytol* **189**(4): 1157-1169.

Chen C, Gao M, Liu J, Zhu H. 2007. Fungal symbiosis in rice requires an ortholog of a legume common symbiosis gene encoding a Ca^{2+}/calmodulin-dependent protein kinase. *Plant Physiol* **145**(4): 1619-1628.

Chenau J, Michelland S, Sidibe J, Seve M. 2008. Peptides OFFGEL electrophoresis: a suitable pre-analytical step for complex eukaryotic samples fractionation compatible with quantitative iTRAQ labeling. *Proteome Sci* **6**: 9.

Cheng FY, Blackburn K, Lin YM, Goshe MB, Williamson JD. 2009. Absolute protein quantification by $LC/MS^{(E)}$ for global analysis of salicylic acid-induced plant protein secretion responses. *J Proteome Res* **8**(1): 82-93.

Chick JM, Haynes PA, Molloy MP, Bjellqvist B, Baker MS, Len AC. 2008. Characterization of the rat liver membrane proteome using peptide immobilized pH gradient isoelectric focusing. *J Proteome Res* **7**(3): 1036-1045.

Chiou TJ, Liu H, Harrison MJ. 2001. The spatial expression patterns of a phosphate transporter (MtPT1) from *Medicago truncatula* indicate a role in phosphate transport at the root/soil interface. *Plant J* **25**(3): 281-293.

Choudhary MK, Basu D, Datta A, Chakraborty N, Chakraborty S. 2009. Dehydration-responsive nuclear proteome of rice (*Oryza sativa L.*) illustrates protein network, novel regulators of cellular adaptation, and evolutionary perspective. *Mol Cell Proteomics* **8**(7): 1579-1598.

Christoforou AL, Lilley KS. 2012. Isobaric tagging approaches in quantitative proteomics: the ups and downs. *Anal Bioanal Chem.*

Colditz F, Braun HP. 2010. *Medicago truncatula* proteomics. *J Proteomics* **73**(10): 1974-1985.

Cook CE, Whichard LP, Turner B, Wall ME, Egley GH. 1966. Germination of Witchweed (*Striga lutea Lour.*): Isolation and Properties of a Potent Stimulant. *Science* **154**(3753): 1189-1190.

Cooper B, Feng J, Garrett WM. 2010. Relative, label-free protein quantitation: spectral counting error statistics from nine replicate MudPIT samples. *J Am Soc Mass Spectrom* **21**(9): 1534-1546.

Courville P, Chaloupka R, Cellier MF. 2006. Recent progress in structure-function analyses of Nramp proton-dependent metal-ion transporters. *Biochem Cell Biol* **84**(6): 960-978.

Csizmadia F. 2000. JChem: Java applets and modules supporting chemical database handling from web browsers. *J Chem Inf Comput Sci* **40**(2): 323-324.

Cullimore J, Denarie J. 2003. Plant sciences. How legumes select their sweet talking symbionts. *Science* **302**(5645): 575-578.

Czaja LF, Hogekamp C, Lamm P, Maillet F, Martinez EA, Samain E, Denarie J, Kuster H, Hohnjec N. 2012. Transcriptional Responses toward Diffusible Signals from Symbiotic Microbes Reveal MtNFP- and MtDMI3-Dependent Reprogramming of Host Gene Expression by Arbuscular Mycorrhizal Fungal Lipochitooligosaccharides. *Plant Physiol* **159**(4): 1671-1685.

Daher Z, Recorbet G, Valot B, Robert F, Balliau T, Potin S, Schoefs B, Dumas-Gaudot E. 2010. Proteomic analysis of *Medicago truncatula* root plastids. *Proteomics* **10**(11): 2123-2137.

De Jonge R, Bolton MD, Thomma BP. 2011. How filamentous pathogens co-opt plants: the ins and outs of fungal effectors. *Curr Opin Plant Biol* **14**(4): 400-406.

De Wit PJ, Mehrabi R, Van den Burg HA, Stergiopoulos I. 2009. Fungal effector proteins: past, present and future. *Mol Plant Pathol* **10**(6): 735-747.

Doidy J, Grace E, Kuhn C, Simon-Plas F, Casieri L, Wipf D. 2012. Sugar transporters in plants and in their interactions with fungi. *Trends Plant Sci* **17**(7): 413-422.

Drakakaki G, Robert S, Raikhel NV, Hicks GR. 2009. Chemical dissection of endosomal pathways. *Plant Signal Behav* **4**(1): 57-62.

Drissner D, Kunze G, Callewaert N, Gehrig P, Tamasloukht M, Boller T, Felix G, Amrhein N, Bucher M. 2007. Lyso-phosphatidylcholine is a signal in the arbuscular mycorrhizal symbiosis. *Science* **318**(5848): 265-268.

Dumas-Gaudot E, Asselin A, Gianinazzi-Pearson V, Gollotte A, Gianinazzi S. 1994. Chitinase isoforms in roots of various pea genotypes infected with arbuscular mycorrhizal fungi. *Plant Science* **99**: 27-37.

Dunkley TP, Watson R, Griffin JL, Dupree P, Lilley KS. 2004. Localization of organelle proteins by isotope tagging (LOPIT). *Mol Cell Proteomics* **3**(11): 1128-1134.

Durand TC, Sergeant K, Planchon S, Carpin S, Label P, Morabito D, Hausman JF, Renaut J. 2010. Acute metal stress in *Populus tremula x P. alba* (717-1B4 genotype): leaf and cambial proteome changes induced by cadmium $^{2+}$. *Proteomics* **10**(3): 349-368.

Elfstrand M, Feddermann N, Ineichen K, Nagaraj VJ, Wiemken A, Boller T, Salzer P. 2005. Ectopic expression of the mycorrhiza-specific chitinase gene Mtchit 3-3 in *Medicago truncatula* root-organ cultures stimulates spore germination of glomalean fungi. *New Phytol* **167**(2): 557-570.

Elschenbroich S, Ignatchenko V, Sharma P, Schmitt-Ulms G, Gramolini AO, Kislinger T. 2009. Peptide separations by on-line MudPIT compared to isoelectric focusing in an off-gel format: application to a membrane-enriched fraction from C2C12 mouse skeletal muscle cells. *J Proteome Res* **8**(10): 4860-4869.

Engelsberger WR, Erban A, Kopka J, Schulze WX. 2006. Metabolic labeling of plant cell cultures with $K^{(15)}NO_3$ as a tool for quantitative analysis of proteins and metabolites. *Plant Methods* **2**: 14.

Ephritikhine G, Ferro M, Rolland N. 2004. Plant membrane proteomics. *Plant Physiol Biochem* **42**(12): 943-962.

Ercolin F, Reinhardt D. 2011. Successful joint ventures of plants: arbuscular mycorrhiza and beyond. *Trends Plant Sci* **16**(7): 356-362.

Eriksson H, Lengqvist J, Hedlund J, Uhlen K, Orre LM, Bjellqvist B, Persson B, Lehtio J, Jakobsson PJ. 2008. Quantitative membrane proteomics applying narrow range peptide isoelectric focusing for studies of small cell lung cancer resistance mechanisms. *Proteomics* **8**(15): 3008-3018.

Ernoult E, Gamelin E, Guette C. 2008. Improved proteome coverage by using iTRAQ labelling and peptide OFFGEL fractionation. *Proteome Sci* **6**: 27.

Esposito S, Massaro G, Vona V, Di Martino Rigano V, Carfagna S. 2003. Glutamate synthesis in barley roots: the role of the plastidic glucose-6-phosphate dehydrogenase. *Planta* **216**(4): 639-647.

Essader AS, Cargile BJ, Bundy JL, Stephenson JL, Jr. 2005. A comparison of immobilized pH gradient isoelectric focusing and strong-cation-exchange chromatography as a first dimension in shotgun proteomics. *Proteomics* **5**(1): 24-34.

Eubel H, Braun HP, Millar AH. 2005. Blue-native PAGE in plants: a tool in analysis of protein-protein interactions. *Plant Methods* **1**(1): 11.

Faik A, Abouzouhair J, Sarhan F. 2006. Putative fasciclin-like arabinogalactan-proteins (FLA) in wheat (*Triticum aestivum*) and rice (*Oryza sativa*): identification and bioinformatic analyses. *Mol Genet Genomics* **276**(5): 478-494.

Fairman JW, Noinaj N, Buchanan SK. 2011. The structural biology of beta-barrel membrane proteins: a summary of recent reports. *Curr Opin Struct Biol* **21**(4): 523-531.

Falth M, Savitski MM, Nielsen ML, Kjeldsen F, Andren PE, Zubarev RA. 2007. SwedCAD, a database of annotated high-mass accuracy MS/MS spectra of tryptic peptides. *J Proteome Res* **6**(10): 4063-4067.

Fan J, Chen C, Yu Q, Brlansky RH, Li ZG, Gmitter FG, Jr. 2011. Comparative iTRAQ proteome and transcriptome analyses of sweet orange infected by "*Candidatus Liberibacter asiaticus*". *Physiol Plant* **143**(3): 235-245.

Fang Y, Robinson DP, Foster LJ. 2010. Quantitative analysis of proteome coverage and recovery rates for upstream fractionation methods in proteomics. *J Proteome Res* **9**(4): 1902-1912.

Fares A, Rossignol M, Peltier JB. 2011. Proteomics investigation of endogenous S-nitrosylation in *Arabidopsis*. *Biochem Biophys Res Commun* **416**(3-4): 331-336.

Feddermann N, Muni RR, Zeier T, Stuurman J, Ercolin F, Schorderet M, Reinhardt D. 2010. The PAM1 gene of petunia, required for intracellular accommodation and morphogenesis of arbuscular mycorrhizal fungi, encodes a homologue of VAPYRIN. *Plant J* **64**(3): 470-481.

Fernandez-Aparicio M, Flores F, Rubiales D. 2009. Recognition of root exudates by seeds of broomrape (*Orobanche and Phelipanche*) species. *Ann Bot* **103**(3): 423-431.

Ferrol N, Barea JM, Azcon-Aguilar C. 2002. Mechanisms of nutrient transport across interfaces in arbuscular mycorrhizas. *Plant Soil* **244**: 231-237.

Fester T, Hause B, Schmidt D, Halfmann K, Schmidt J, Wray V, Hause G, Strack D. 2002. Occurrence and localization of apocarotenoids in arbuscular mycorrhizal plant roots. *Plant Cell Physiol* **43**(3): 256-265.

Fields S. 2001. Proteomics. Proteomics in genomeland. *Science* **291**(5507): 1221-1224.

Filiou MD, Martins-de-Souza D, Guest PC, Bahn S, Turck CW. 2012. To label or not to label: Applications of quantitative proteomics in neuroscience research. *Proteomics* **12**(4-5): 736-747.

Fleron M, Greffe Y, Musmeci D, Massart AC, Hennequiere V, Mazzucchelli G, Waltregny D, De Pauw-Gillet MC, Castronovo V, De Pauw E, Turtoi A. 2010. Novel post-digest isotope coded protein labeling method for phospho- and glycoproteome analysis. *J Proteomics* **73**(10): 1986-2005.

Floss DS, Schliemann W, Schmidt J, Strack D, Walter MH. 2008. RNA interference-mediated repression of MtCCD1 in mycorrhizal roots of *Medicago truncatula* causes accumulation of C27 apocarotenoids, shedding light on the functional role of CCD1. *Plant Physiol* **148**(3): 1267-1282.

Fournier ML, Gilmore JM, Martin-Brown SA, Washburn MP. 2007. Multidimensional separations-based shotgun proteomics. *Chem Rev* **107**(8): 3654-3686.

Fraterman S, Zeiger U, Khurana TS, Rubinstein NA, Wilm M. 2007. Combination of peptide OFFGEL fractionation and label-free quantitation facilitated proteomics profiling of extraocular muscle. *Proteomics* **7**(18): 3404-3416.

Frenzel A, Manthey K, Perlick AM, Meyer F, Puhler A, Kuster H, Krajinski F. 2005. Combined transcriptome profiling reveals a novel family of arbuscular mycorrhizal-specific *Medicago truncatula* lectin genes. *Mol Plant Microbe Interact* **18**(8): 771-782.

Frenzel A, Tiller N, Hause B, Krajinski F. 2006. The conserved arbuscular mycorrhiza-specific transcription of the secretory lectin MtLec5 is mediated by a short upstream sequence containing specific protein binding sites. *Planta* **224**(4): 792-800.

Friedman DB, Hill S, Keller JW, Merchant NB, Levy SE, Coffey RJ, Caprioli RM. 2004. Proteome analysis of human colon cancer by two-dimensional difference gel electrophoresis and mass spectrometry. *Proteomics* **4**(3): 793-811.

Froehlich JE, Wilkerson CG, Ray WK, McAndrew RS, Osteryoung KW, Gage DA, Phinney BS. 2003. Proteomic study of the *Arabidopsis thaliana* chloroplastic envelope membrane utilizing alternatives to traditional two-dimensional electrophoresis. *J Proteome Res* **2**(4): 413-425.

Gabriel-Neumann E, Neumann G, Leggewie G, George E. 2011. Constitutive overexpression of the sucrose transporter SoSUT1 in potato plants increases arbuscular mycorrhiza fungal root colonization under high, but not under low, soil phosphorus availability. *J Plant Physiol* **168**(9): 911-919.

Gammulla CG, Pascovici D, Atwell BJ, Haynes PA. 2010. Differential metabolic response of cultured rice (*Oryza sativa*) cells exposed to high- and low-temperature stress. *Proteomics* **10**(16): 3001-3019.

Gammulla CG, Pascovici D, Atwell BJ, Haynes PA. 2011. Differential proteomic response of rice (*Oryza sativa*) leaves exposed to high- and low-temperature stress. *Proteomics* **11**(14): 2839-2850.

Gandhi T, Puri P, Fusetti F, Breitling R, Poolman B, Permentier HP. 2012. Effect of iTRAQ Labeling on the Relative Abundance of Peptide Fragment Ions Produced by MALDI-MS/MS. *J Proteome Res* **11**(8): 4044-4051.

Gao M, Showalter AM. 1999. Yariv reagent treatment induces programmed cell death in *Arabidopsis* cell cultures and implicates arabinogalactan protein involvement. *Plant J* **19**(3): 321-331.

Garcia-Garrido JM, Ocampo JA. 2002. Regulation of the plant defence response in arbuscular mycorrhizal symbiosis. *J Exp Bot* **53**(373): 1377-1386.

Gaude N, Schulze WX, Franken P, Krajinski F. 2012. Cell type-specific protein and transcription profiles implicate periarbuscular membrane synthesis as an important carbon sink in the mycorrhizal symbiosis. *Plant Signal Behav* **7**(4).

Ge L, Sun S, Chen A, Kapulnik Y, Xu G. 2008. Tomato sugar transporter genes associated with mycorrhiza and phosphate. *Plant Growth Regulation* **55**: 115-123.

Geigenberger P, Stitt M, Fernie AR. 2004. Metabolic control analysis and regulation of the conversion of sucrose to starch in growing potato tubers. *Plant, Cell & Environment* **27**(6): 655-673.

Genre A, Chabaud M, Timmers T, Bonfante P, Barker DG. 2005. Arbuscular mycorrhizal fungi elicit a novel intracellular apparatus in *Medicago truncatula* root epidermal cells before infection. *Plant Cell* **17**(12): 3489-3499.

Genre A, Ortu G, Bertoldo C, Martino E, Bonfante P. 2009. Biotic and abiotic stimulation of root epidermal cells reveals common and specific responses to arbuscular mycorrhizal fungi. *Plant Physiol* **149**(3): 1424-1434.

Geromanos SJ, Vissers JP, Silva JC, Dorschel CA, Li GZ, Gorenstein MV, Bateman RH, Langridge JI. 2009. The detection, correlation, and comparison of peptide precursor and product ions from data independent LC-MS with data dependant LC-MS/MS. *Proteomics* **9**(6): 1683-1695.

Gevaert K, Van Damme P, Ghesquiere B, Impens F, Martens L, Helsens K, Vandekerckhove J. 2007. A la carte proteomics with an emphasis on gel-free techniques. *Proteomics* **7**(16): 2698-2718.

Gianinazzi-Pearson V, Arnould C, Oufattole M, Arango M, Gianinazzi S. 2000. Differential activation of H^+-ATPase genes by an arbuscular mycorrhizal fungus in root cells of transgenic tobacco. *Planta* **211**(5): 609-613.

Gianinazzi S, Gollotte A, Binet MN, van Tuinen D, Redecker D, Wipf D. 2010. Agroecology: the key role of arbuscular mycorrhizas in ecosystem services. *Mycorrhiza* **20**(8): 519-530.

Giovannetti M, Sbrana C, Avio L, Citernesi AS, Logi C. 1993. Differential hyphal morphogenesis in arbuscular mycorrhizal fungi during pre-infection stages. *New Phytologist* **125**: 587-594.

Gomez-Roldan V, Fermas S, Brewer PB, Puech-Pages V, Dun EA, Pillot JP, Letisse F, Matusova R, Danoun S, Portais JC, Bouwmeester H, Becard G, Beveridge CA, Rameau C, Rochange SF. 2008. Strigolactone inhibition of shoot branching. *Nature* **455**(7210): 189-194.

Gordon JA, Jencks WP. 1963. The relationship of structure to the effectiveness of denaturing agents for proteins. *Biochemistry* **2**: 47-57.

Groth M, Takeda N, Perry J, Uchida H, Draxl S, Brachmann A, Sato S, Tabata S, Kawaguchi M, Wang TL, Parniske M. 2010. NENA, a *Lotus japonicus* homolog of Sec13, is required for rhizodermal infection by arbuscular mycorrhiza fungi and rhizobia but dispensable for cortical endosymbiotic development. *Plant Cell* **22**(7): 2509-2526.

Gruhler A, Schulze WX, Matthiesen R, Mann M, Jensen ON. 2005. Stable isotope labeling of *Arabidopsis thaliana* cells and quantitative proteomics by mass spectrometry. *Mol Cell Proteomics* **4**(11): 1697-1709.

Grunwald U, Nyamsuren O, Tamasloukht M, Lapopin L, Becker A, Mann P, Gianinazzi-Pearson V, Krajinski F, Franken P. 2004. Identification of mycorrhiza-regulated genes with arbuscule development-related expression profile. *Plant Mol Biol* **55**(4): 553-566.

Guether M, Neuhauser B, Balestrini R, Dynowski M, Ludewig U, Bonfante P. 2009. A mycorrhizal-specific ammonium transporter from *Lotus japonicus* acquires nitrogen released by arbuscular mycorrhizal fungi. *Plant Physiol* **150**(1): 73-83.

Guimil S, Chang HS, Zhu T, Sesma A, Osbourn A, Roux C, Ioannidis V, Oakeley EJ, Docquier M, Descombes P, Briggs SP, Paszkowski U. 2005. Comparative transcriptomics of rice reveals an ancient pattern of response to microbial colonization. *Proc Natl Acad Sci U S A* **102**(22): 8066-8070.

Gutjahr C, Banba M, Croset V, An K, Miyao A, An G, Hirochika H, Imaizumi-Anraku H, Paszkowski U. 2008. Arbuscular mycorrhiza-specific signaling in rice transcends the common symbiosis signaling pathway. *Plant Cell* **20**(11): 2989-3005.

Gutjahr C, Novero M, Welham T, Wang T, Bonfante P. 2011. Root starch accumulation in response to arbuscular mycorrhizal colonization differs among *Lotus japonicus* starch mutants. *Planta* **234**(3): 639-646.

Gutjahr C, Radovanovic D, Geoffroy J, Zhang Q, Siegler H, Chiapello M, Casieri L, An K, An G, Guiderdoni E, Kumar CS, Sundaresan V, Harrison MJ, Paszkowski U. 2012. The half-size ABC transporters STR1 and STR2 are indispensable for mycorrhizal arbuscule formation in rice. *Plant J* **69**(5): 906-920.

Gygi SP, Corthals GL, Zhang Y, Rochon Y, Aebersold R. 2000. Evaluation of two-dimensional gel electrophoresis-based proteome analysis technology. *Proc Natl Acad Sci U S A* **97**(17): 9390-9395.

Gygi SP, Rist B, Gerber SA, Turecek F, Gelb MH, Aebersold R. 1999. Quantitative analysis of complex protein mixtures using isotope-coded affinity tags. *Nat Biotechnol* **17**(10): 994-999.

Hagglund P, Bunkenborg J, Maeda K, Svensson B. 2008. Identification of thioredoxin disulfide targets using a quantitative proteomics approach based on isotope-coded affinity tags. *J Proteome Res* **7**(12): 5270-5276.

Hagglund P, Bunkenborg J, Yang F, Harder LM, Finnie C, Svensson B. 2010. Identification of thioredoxin target disulfides in proteins released from barley aleurone layers. *J Proteomics* **73**(6): 1133-1136.

Hahne H, Wolff S, Hecker M, Becher D. 2008. From complementarity to comprehensiveness--targeting the membrane proteome of growing *Bacillus subtilis* by divergent approaches. *Proteomics* **8**(19): 4123-4136.

Hariton-Gazal E, Rosenbluh J, Graessmann A, Gilon C, Loyter A. 2003. Direct translocation of histone molecules across cell membranes. *J Cell Sci* **116**(Pt 22): 4577-4586.

Harrison MJ. 1999. Molecular and Cellular Aspects of the Arbuscular Mycorrhizal Symbiosis. *Annu Rev Plant Physiol Plant Mol Biol* **50**: 361-389.

Harrison MJ. 2005. Signaling in the arbuscular mycorrhizal symbiosis. *Annu Rev Microbiol* **59**: 19-42.

Harrison MJ, Dewbre GR, Liu J. 2002. A phosphate transporter from *Medicago truncatula* involved in the acquisition of phosphate released by arbuscular mycorrhizal fungi. *Plant Cell* **14**(10): 2413-2429.

Harrison MJ, van Buuren ML. 1995. A phosphate transporter from the mycorrhizal fungus *Glomus versiforme*. *Nature* **378**(6557): 626-629.

Hartman NT, Sicilia F, Lilley KS, Dupree P. 2007. Proteomic complex detection using sedimentation. *Anal Chem* **79**(5): 2078-2083.

Hause B, Schaarschmidt S. 2009. The role of jasmonates in mutualistic symbioses between plants and soil-born microorganisms. *Phytochemistry* **70**(13-14): 1589-1599.

Hayashi T, Banba M, Shimoda Y, Kouchi H, Hayashi M, Imaizumi-Anraku H. 2010. A dominant function of CCaMK in intracellular accommodation of bacterial and fungal endosymbionts. *Plant J* **63**(1): 141-154.

Haynes PA, Roberts TH. 2007. Subcellular shotgun proteomics in plants: looking beyond the usual suspects. *Proteomics* **7**(16): 2963-2975.

Helber N, Wippel K, Sauer N, Schaarschmidt S, Hause B, Requena N. 2011. A versatile monosaccharide transporter that operates in the arbuscular mycorrhizal fungus *Glomus sp* is crucial for the symbiotic relationship with plants. *Plant Cell* **23**(10): 3812-3823.

Helbig AO, Heck AJ, Slijper M. 2010. Exploring the membrane proteome--challenges and analytical strategies. *J Proteomics* **73**(5): 868-878.

Henckel K, Runte KJ, Bekel T, Dondrup M, Jakobi T, Kuster H, Goesmann A. 2009. TRUNCATULIX--a data warehouse for the legume community. *BMC Plant Biol* **9**: 19.

Heupel S, Roser B, Kuhn H, Lebrun MH, Villalba F, Requena N. 2010. Erl1, a novel era-like GTPase from *Magnaporthe oryzae*, is required for full root virulence and is conserved in the mutualistic symbiont *Glomus intraradices*. *Mol Plant Microbe Interact* **23**(1): 67-81.

Hirochika H, Guiderdoni E, An G, Hsing YI, Eun MY, Han CD, Upadhyaya N, Ramachandran S, Zhang Q, Pereira A, Sundaresan V, Leung H. 2004. Rice mutant resources for gene discovery. *Plant Mol Biol* **54**(3): 325-334.

Hodge A, Campbell CD, Fitter AH. 2001. An arbuscular mycorrhizal fungus accelerates decomposition and acquires nitrogen directly from organic material. *Nature* **413**(6853): 297-299.

Hogenhout SA, Van der Hoorn RA, Terauchi R, Kamoun S. 2009. Emerging concepts in effector biology of plant-associated organisms. *Mol Plant Microbe Interact* **22**(2): 115-122.

Hohnjec N, Vieweg MF, Puhler A, Becker A, Kuster H. 2005. Overlaps in the transcriptional profiles of *Medicago truncatula* roots inoculated with two different *Glomus* fungi provide insights into the genetic program activated during arbuscular mycorrhiza. *Plant Physiol* **137**(4): 1283-1301.

Holland KA, Holland IB. 2002. Transmembrane signalling. In Nature Encyclopedia of Life Sciences. London: Nature Publishing Group.

Horth P, Miller CA, Preckel T, Wenz C. 2006. Efficient fractionation and improved protein identification by peptide OFFGEL electrophoresis. *Mol Cell Proteomics* **5**(10): 1968-1974.

Hubbard C, Singleton D, Rauch M, Jayasinghe S, Cafiso D, Castle D. 2000. The secretory carrier membrane protein family: structure and membrane topology. *Mol Biol Cell* **11**(9): 2933-2947.

Hubner NC, Ren S, Mann M. 2008. Peptide separation with immobilized pI strips is an attractive alternative to in-gel protein digestion for proteome analysis. *Proteomics* **8**(23-24): 4862-4872.

Huttlin EL, Hegeman AD, Harms AC, Sussman MR. 2007. Comparison of full versus partial metabolic labeling for quantitative proteomics analysis in *Arabidopsis thaliana*. *Mol Cell Proteomics* **6**(5): 860-881.

Imai K, Fujita N, Gromiha MM, Horton P. 2011. Eukaryote-wide sequence analysis of mitochondrial beta-barrel outer membrane proteins. *BMC Genomics* **12**: 79.

Ippel JH, Pouvreau L, Kroef T, Gruppen H, Versteeg G, van den Putten P, Struik PC, van Mierlo CP. 2004. In vivo uniform $^{(15)}$N-isotope labelling of plants: using the greenhouse for structural proteomics. *Proteomics* **4**(1): 226-234.

Isayenkov S, Mrosk C, Stenzel I, Strack D, Hause B. 2005. Suppression of allene oxide cyclase in hairy roots of *Medicago truncatula* reduces jasmonate levels and the degree of mycorrhization with *Glomus intraradices*. *Plant Physiol* **139**(3): 1401-1410.

Ishihama Y, Oda Y, Tabata T, Sato T, Nagasu T, Rappsilber J, Mann M. 2005. Exponentially modified protein abundance index (emPAI) for estimation of absolute protein amount in proteomics by the number of sequenced peptides per protein. *Mol Cell Proteomics* **4**(9): 1265-1272.

Islam N, Tsujimoto H, Hirano H. 2003. Wheat proteomics: relationship between fine chromosome deletion and protein expression. *Proteomics* **3**(3): 307-316.

Ivanov S, Fedorova EE, Limpens E, De Mita S, Genre A, Bonfante P, Bisseling T. 2012. Rhizobium-legume symbiosis shares an exocytotic pathway required for arbuscule formation. *Proc Natl Acad Sci U S A* **109**(21): 8316-8321.

Javot H, Penmetsa RV, Breuillin F, Bhattarai KK, Noar RD, Gomez SK, Zhang Q, Cook DR, Harrison MJ. 2011. *Medicago truncatula* mtpt4 mutants reveal a role for nitrogen in the regulation of arbuscule degeneration in arbuscular mycorrhizal symbiosis. *Plant J* **68**(6): 954-965.

Javot H, Penmetsa RV, Terzaghi N, Cook DR, Harrison MJ. 2007. A *Medicago truncatula* phosphate transporter indispensable for the arbuscular mycorrhizal symbiosis. *Proc Natl Acad Sci U S A* **104**(5): 1720-1725.

Jones AM, Bennett MH, Mansfield JW, Grant M. 2006. Analysis of the defence phosphoproteome of *Arabidopsis thaliana* using differential mass tagging. *Proteomics* **6**(14): 4155-4165.

Jones MN. 1999. Surfactants in membrane solubilisation. *Int J Pharm* **177**(2): 137-159.

Jones PM, George AM. 2004. The ABC transporter structure and mechanism: perspectives on recent research. *Cell Mol Life Sci* **61**(6): 682-699.

Jorrin JV, Maldonado AM, Castillejo MA. 2007. Plant proteome analysis: a 2006 update. *Proteomics* **7**(16): 2947-2962.

Kaffarnik FA, Jones AM, Rathjen JP, Peck SC. 2009. Effector proteins of the bacterial pathogen *Pseudomonas syringae* alter the extracellular proteome of the host plant, *Arabidopsis thaliana*. *Mol Cell Proteomics* **8**(1): 145-156.

Karp NA, Lilley KS. 2009. Investigating sample pooling strategies for DIGE experiments to address biological variability. *Proteomics* **9**(2): 388-397.

Kaspar S, Matros A, Mock HP. 2010. Proteome and flavonoid analysis reveals distinct responses of epidermal tissue and whole leaves upon UV-B radiation of barley (*Hordeum vulgare L.*) seedlings. *J Proteome Res* **9**(5): 2402-2411.

Kato M, Nagasaki-Takeuchi N, Ide Y, Tomioka R, Maeshima M. 2010. PCaPs, possible regulators of PtdInsP signals on plasma membrane. *Plant Signal Behav* **5**(7): 848-850.

Kieffer P, Dommes J, Hoffmann L, Hausman JF, Renaut J. 2008. Quantitative changes in protein expression of cadmium-exposed poplar plants. *Proteomics* **8**(12): 2514-2530.

Kiirika LM, Bergmann HF, Schikowsky C, Wimmer D, Korte J, Schmitz U, Niehaus K, Colditz F. 2012. Silencing of the Rac1 GTPase MtROP9 in *Medicago truncatula* stimulates early mycorrhizal and oomycete root colonizations but negatively affects rhizobial infection. *Plant Physiol* **159**(1): 501-516.

Kistner C, Winzer T, Pitzschke A, Mulder L, Sato S, Kaneko T, Tabata S, Sandal N, Stougaard J, Webb KJ, Szczyglowski K, Parniske M. 2005. Seven *Lotus japonicus* genes required for transcriptional reprogramming of the root during fungal and bacterial symbiosis. *Plant Cell* **17**(8): 2217-2229.

Kleczkowski LA, Geisler M, Ciereszko I, Johansson H. 2004. UDP-glucose pyrophosphorylase. An old protein with new tricks. *Plant Physiol* **134**(3): 912-918.

Kleparnik K, Bocek P. 2010. Electrophoresis today and tomorrow: Helping biologists' dreams come true. *Bioessays* **32**(3): 218-226.

Kloppholz S, Kuhn H, Requena N. 2011. A secreted fungal effector of *Glomus intraradices* promotes symbiotic biotrophy. *Curr Biol* **21**(14): 1204-1209.

Kobae Y, Hata S. 2010. Dynamics of periarbuscular membranes visualized with a fluorescent phosphate transporter in arbuscular mycorrhizal roots of rice. *Plant Cell Physiol* **51**(3): 341-353.

Kobae Y, Tamura Y, Takai S, Banba M, Hata S. 2010. Localized expression of arbuscular mycorrhiza-inducible ammonium transporters in soybean. *Plant Cell Physiol* **51**(9): 1411-1415.

Kocher T, Pichler P, Schutzbier M, Stingl C, Kaul A, Teucher N, Hasenfuss G, Penninger JM, Mechtler K. 2009. High precision quantitative proteomics using iTRAQ on an LTQ Orbitrap: a new mass spectrometric method combining the benefits of all. *J Proteome Res* **8**(10): 4743-4752.

Kohlen W, Charnikhova T, Liu Q, Bours R, Domagalska MA, Beguerie S, Verstappen F, Leyser O, Bouwmeester H, Ruyter-Spira C. 2011. Strigolactones are transported through the xylem and play a key role in shoot architectural response to phosphate deficiency in nonarbuscular mycorrhizal host *Arabidopsis*. *Plant Physiol* **155**(2): 974-987.

Koltai H, LekKala SP, Bhattacharya C, Mayzlish-Gati E, Resnick N, Wininger S, Dor E, Yoneyama K, Hershenhorn J, Joel DM, Kapulnik Y. 2010. A tomato strigolactone-impaired mutant displays aberrant shoot morphology and plant interactions. *J Exp Bot* **61**(6): 1739-1749.

Komatsu S, Wada T, Abalea Y, Nouri MZ, Nanjo Y, Nakayama N, Shimamura S, Yamamoto R, Nakamura T, Furukawa K. 2009. Analysis of plasma membrane proteome in soybean and application to flooding stress response. *J Proteome Res* **8**(10): 4487-4499.

Kosuta S, Hazledine S, Sun J, Miwa H, Morris RJ, Downie JA, Oldroyd GE. 2008. Differential and chaotic calcium signatures in the symbiosis signaling pathway of legumes. *Proc Natl Acad Sci U S A* **105**(28): 9823-9828.

Kota U, Goshe MB. 2011. Advances in qualitative and quantitative plant membrane proteomics. *Phytochemistry* **72**(10): 1040-1060.

Kouchi H, Imaizumi-Anraku H, Hayashi M, Hakoyama T, Nakagawa T, Umehara Y, Suganuma N, Kawaguchi M. 2010. How many peas in a pod? Legume genes responsible for mutualistic symbioses underground. *Plant Cell Physiol* **51**(9): 1381-1397.

Krajinski F, Frenzel A. 2007. Towards the elucidation of AM-specific transcription in *Medicago truncatula*. *Phytochemistry* **68**(1): 75-81.

Krajinski F, Hause B, Gianinazzi-Pearson V, Franken P. 2002. Mtha1, a plasma membrane H^+-ATPase gene from *Medicago truncatula*, shows arbuscule-specific induced expression in mycorrhizal tissue. *Plant Biol* **4**: 754-761.

Kretzschmar T, Kohlen W, Sasse J, Borghi L, Schlegel M, Bachelier JB, Reinhardt D, Bours R, Bouwmeester HJ, Martinoia E. 2012. A petunia ABC protein controls strigolactone-dependent symbiotic signalling and branching. *Nature* **483**(7389): 341-344.

Kruger M, Kruger C, Walker C, Stockinger H, Schussler A. 2012. Phylogenetic reference data for systematics and phylotaxonomy of arbuscular mycorrhizal fungi from phylum to species level. *New Phytol* **193**(4): 970-984.

Kubo M, Ueda H, Park P, Kawaguchi M, Sugimoto Y. 2009. Reactions of *Lotus japonicus* ecotypes and mutants to root parasitic plants. *J Plant Physiol* **166**(4): 353-362.

Kuhn H, Kuster H, Requena N. 2010. Membrane steroid-binding protein 1 induced by a diffusible fungal signal is critical for mycorrhization in *Medicago truncatula*. *New Phytol* **185**(3): 716-733.

Kuromori T, Takahashi S, Kondou Y, Shinozaki K, Matsui M. 2009. Phenome analysis in plant species using loss-of-function and gain-of-function mutants. *Plant Cell Physiol* **50**(7): 1215-1231.

Kuster H, Vieweg MF, Manthey K, Baier MC, Hohnjec N, Perlick AM. 2007. Identification and expression regulation of symbiotically activated legume genes. *Phytochemistry* **68**(1): 8-18.

Kwon C, Neu C, Pajonk S, Yun HS, Lipka U, Humphry M, Bau S, Straus M, Kwaaitaal M, Rampelt H, El Kasmi F, Jurgens G, Parker J, Panstruga R, Lipka V, Schulze-Lefert P. 2008. Co-option of a default secretory pathway for plant immune responses. *Nature* **451**(7180): 835-840.

Lanquar V, Kuhn L, Lelievre F, Khafif M, Espagne C, Bruley C, Barbier-Brygoo H, Garin J, Thomine S. 2007. ^{15}N-metabolic labeling for comparative plasma membrane proteomics in *Arabidopsis* cells. *Proteomics* **7**(5): 750-754.

Larrainzar E, Wienkoop S, Weckwerth W, Ladrera R, Arrese-Igor C, Gonzalez EM. 2007. *Medicago truncatula* root nodule proteome analysis reveals differential plant and bacteroid responses to drought stress. *Plant Physiol* **144**(3): 1495-1507.

Lasserre JP, Menard A. 2012. Two-dimensional blue native/SDS gel electrophoresis of multiprotein complexes. *Methods Mol Biol* **869**: 317-337.

Lee J, Feng J, Campbell KB, Scheffler BE, Garrett WM, Thibivilliers S, Stacey G, Naiman DQ, Tucker ML, Pastor-Corrales MA, Cooper B. 2009. Quantitative proteomic analysis of bean plants infected by a virulent and avirulent obligate rust fungus. *Mol Cell Proteomics* **8**(1): 19-31.

Leggewie G, Kolbe A, Lemoine R, Roessner U, Lytovchenko A, Zuther E, Kehr J, Frommer WB, Riesmeier JW, Willmitzer L, Fernie AR. 2003. Overexpression of the sucrose transporter SoSUT1 in potato results in alterations in leaf carbon partitioning and in tuber metabolism but has little impact on tuber morphology. *Planta* **217**(1): 158-167.

Lengqvist J, Uhlen K, Lehtio J. 2007. iTRAQ compatibility of peptide immobilized pH gradient isoelectric focusing. *Proteomics* **7**(11): 1746-1752.

Leroy B, Rosier C, Erculisse V, Leys N, Mergeay M, Wattiez R. 2010. Differential proteomic analysis using isotope-coded protein-labeling strategies: comparison, improvements and application to simulated microgravity effect on *Cupriavidus metallidurans* CH34. *Proteomics* **10**(12): 2281-2291.

Levy J, Bres C, Geurts R, Chalhoub B, Kulikova O, Duc G, Journet EP, Ane JM, Lauber E, Bisseling T, Denarie J, Rosenberg C, Debelle F. 2004. A putative Ca^{2+} and calmodulin-dependent protein kinase required for bacterial and fungal symbioses. *Science* **303**(5662): 1361-1364.

Li T, Xu SL, Oses-Prieto JA, Putil S, Xu P, Wang RJ, Li KH, Maltby DA, An LH, Burlingame AL, Deng ZP, Wang ZY. 2011. Proteomics analysis reveals post-translational mechanisms for cold-induced metabolic changes in *Arabidopsis*. *Mol Plant* **4**(2): 361-374.

Liao J, Singh S, Hossain MS, Andersen SU, Ross L, Bonetta D, Zhou Y, Sato S, Tabata S, Stougaard J, Szczyglowski K, Parniske M. 2012. Negative regulation of CCaMK is essential for symbiotic infection. *Plant J*.

Lilley KS, Razzaq A, Dupree P. 2002. Two-dimensional gel electrophoresis: recent advances in sample preparation, detection and quantitation. *Curr Opin Chem Biol* **6**(1): 46-50.

Liu H, Sadygov RG, Yates JR, 3rd. 2004. A model for random sampling and estimation of relative protein abundance in shotgun proteomics. *Anal Chem* **76**(14): 4193-4201.

Liu H, Trieu AT, Blaylock LA, Harrison MJ. 1998. Cloning and characterisation of two phosphate transporters from *Medicago trunculata* roots: regulation in response to phosphate and response to colonization by arbuscular mycorrhizal (AM) fungi *Mol Plant Microbe Interact* **11**: 14-22.

Liu J, Blaylock LA, Endre G, Cho J, Town CD, VandenBosch KA, Harrison MJ. 2003. Transcript profiling coupled with spatial expression analyses reveals genes involved in distinct developmental stages of an arbuscular mycorrhizal symbiosis. *Plant Cell* **15**(9): 2106-2123.

Liu J, Maldonado-Mendoza I, Lopez-Meyer M, Cheung F, Town CD, Harrison MJ. 2007. Arbuscular mycorrhizal symbiosis is accompanied by local and systemic alterations in gene expression and an increase in disease resistance in the shoots. *Plant J* **50**(3): 529-544.

Liu J, Versaw WK, Pumplin N, Gomez SK, Blaylock LA, Harrison MJ. 2008. Closely related members of the *Medicago truncatula* PHT1 phosphate transporter gene family encode phosphate transporters with distinct biochemical activities. *J Biol Chem* **283**(36): 24673-24681.

Liu W, Kohlen W, Lillo A, Op den Camp R, Ivanov S, Hartog M, Limpens E, Jamil M, Smaczniak C, Kaufmann K, Yang WC, Hooiveld GJ, Charnikhova T, Bouwmeester HJ, Bisseling T, Geurts R. 2011. Strigolactone biosynthesis in *Medicago truncatula* and rice requires the symbiotic GRAS-type transcription factors NSP1 and NSP2. *Plant Cell* **23**(10): 3853-3865.

Lohse S, Schliemann W, Ammer C, Kopka J, Strack D, Fester T. 2005. Organization and metabolism of plastids and mitochondria in arbuscular mycorrhizal roots of *Medicago truncatula*. *Plant Physiol* **139**(1): 329-340.

Lopez-Juez E. 2007. Plastid biogenesis, between light and shadows. *J Exp Bot* **58**(1): 11-26.

Lopez-Pedrosa A, Gonzalez-Guerrero M, Valderas A, Azcon-Aguilar C, Ferrol N. 2006. GintAMT1 encodes a functional high-affinity ammonium transporter that is expressed in the extraradical mycelium of *Glomus intraradices*. *Fungal Genet Biol* **43**(2): 102-110.

Lu P, Vogel C, Wang R, Yao X, Marcotte EM. 2007. Absolute protein expression profiling estimates the relative contributions of transcriptional and translational regulation. *Nat Biotechnol* **25**(1): 117-124.

Lundgren DH, Hwang SI, Wu L, Han DK. 2010. Role of spectral counting in quantitative proteomics. *Expert Rev Proteomics* **7**(1): 39-53.

Maeda D, Ashida K, Iguchi K, Chechetka SA, Hijikata A, Okusako Y, Deguchi Y, Izui K, Hata S. 2006. Knockdown of an arbuscular mycorrhiza-inducible phosphate transporter gene of *Lotus japonicus* suppresses mutualistic symbiosis. *Plant Cell Physiol* **47**(7): 807-817.

Maillet F, Poinsot V, Andre O, Puech-Pages V, Haouy A, Gueunier M, Cromer L, Giraudet D, Formey D, Niebel A, Martinez EA, Driguez H, Becard G, Denarie J. 2011. Fungal lipochitooligosaccharide symbiotic signals in arbuscular mycorrhiza. *Nature* **469**(7328): 58-63.

Majeran W, Cai Y, Sun Q, van Wijk KJ. 2005. Functional differentiation of bundle sheath and mesophyll maize chloroplasts determined by comparative proteomics. *Plant Cell* **17**(11): 3111-3140.

Majeran W, Zybailov B, Ytterberg AJ, Dunsmore J, Sun Q, van Wijk KJ. 2008. Consequences of C4 differentiation for chloroplast membrane proteomes in maize mesophyll and bundle sheath cells. *Mol Cell Proteomics* **7**(9): 1609-1638.

Manadas B, English JA, Wynne KJ, Cotter DR, Dunn MJ. 2009. Comparative analysis of OFFGel, strong cation exchange with pH gradient, and RP at high pH for first-dimensional separation of peptides from a membrane-enriched protein fraction. *Proteomics* **9**(22): 5194-5198.

Manadas B, Mendes VM, English J, Dunn MJ. 2010. Peptide fractionation in proteomics approaches. *Expert Rev Proteomics* **7**(5): 655-663.

Mann M. 2006. Functional and quantitative proteomics using SILAC. *Nat Rev Mol Cell Biol* **7**(12): 952-958.

Manthey K, Krajinski F, Hohnjec N, Firnhaber C, Puhler A, Perlick AM, Kuster H. 2004. Transcriptome profiling in root nodules and arbuscular mycorrhiza identifies a collection of novel genes induced during *Medicago truncatula* root endosymbioses. *Mol Plant Microbe Interact* **17**(10): 1063-1077.

Manza LL, Stamer SL, Ham AJ, Codreanu SG, Liebler DC. 2005. Sample preparation and digestion for proteomic analyses using spin filters. *Proteomics* **5**(7): 1742-1745.

Marmagne A, Rouet MA, Ferro M, Rolland N, Alcon C, Joyard J, Garin J, Barbier-Brygoo H, Ephritikhine G. 2004. Identification of new intrinsic proteins in *Arabidopsis* plasma membrane proteome. *Mol Cell Proteomics* **3**(7): 675-691.

Marsh E, Alvarez S, Hicks LM, Barbazuk WB, Qiu W, Kovacs L, Schachtman D. 2010. Changes in protein abundance during powdery mildew infection of leaf tissues of Cabernet Sauvignon grapevine (*Vitis vinifera L.*). *Proteomics* **10**(10): 2057-2064.

Marsh JF, Schultze M. 2001. Analysis of arbuscular mycorrhizas using symbiosis-defective plant mutants. *New Phytologist* **150**: 525–532.

Martin F, Gianinazzi-Pearson V, Hijri M, Lammers P, Requena N, Sanders IR, Shachar-Hill Y, Shapiro H, Tuskan GA, Young JP. 2008. The long hard road to a completed *Glomus intraradices* genome. *New Phytol* **180**(4): 747-750.

Martin SF, Munagapati VS, Salvo-Chirnside E, Kerr LE, Le Bihan T. 2012. Proteome turnover in the green alga *Ostreococcus tauri* by time course ^{15}N metabolic labeling mass spectrometry. *J Proteome Res* **11**(1): 476-486.

Mastrobuoni G, Irgang S, Pietzke M, Wenzel M, Assmus HE, Schulze WX, Kempa S. 2012. Proteome dynamics and early salt stress response of the photosynthetic organism *Chlamydomonas reinhardtii*. *BMC Genomics* **13**(1): 215.

Mathesius U. 2009. Comparative proteomic studies of root-microbe interactions. *J Proteomics* **72**(3): 353-366.

Mathesius U, Keijzers G, Natera SH, Weinman JJ, Djordjevic MA, Rolfe BG. 2001. Establishment of a root proteome reference map for the model legume *Medicago truncatula* using the expressed sequence tag database for peptide mass fingerprinting. *Proteomics* **1**(11): 1424-1440.

Mathy G, Sluse FE. 2008. Mitochondrial comparative proteomics: strengths and pitfalls. *Biochim Biophys Acta* **1777**(7-8): 1072-1077.

Meisrimler CN, Luthje S. 2012. IPG-strips versus off-gel fractionation: advantages and limits of two-dimensional PAGE in separation of microsomal fractions of frequently used plant species and tissues. *J Proteomics* **75**(9): 2550-2562.

Melo-Braga MN, Verano-Braga T, Leon IR, Antonacci D, Nogueira FC, Thelen JJ, Larsen MR, Palmisano G. 2012. Modulation of protein phosphorylation, glycosylation and acetylation in grape (*Vitis vinifera*) mesocarp and exocarp due to *Lobesia botrana* infection. *Mol Cell Proteomics*.

Meng Q, Rao L, Xiang X, Zhou C, Zhang X, Pan Y. 2011. A systematic strategy for proteomic analysis of chloroplast protein complexes in wheat. *Biosci Biotechnol Biochem* **75**(11): 2194-2199.

Messinese E, Mun JH, Yeun LH, Jayaraman D, Rouge P, Barre A, Lougnon G, Schornack S, Bono JJ, Cook DR, Ane JM. 2007. A novel nuclear protein interacts with the symbiotic DMI3 calcium- and calmodulin-dependent protein kinase of *Medicago truncatula*. *Mol Plant Microbe Interact* **20**(8): 912-921.

Miao Z, Li D, Zhang Z, Dong J, Su Z, Wang T. 2012. *Medicago truncatula* transporter database: a comprehensive database resource for *M. truncatula* transporters. *BMC Genomics* **13**: 60.

Miles GP, Samuel MA, Ranish JA, Donohoe SM, Sperrazzo GM, Ellis BE. 2009. Quantitative proteomics identifies oxidant-induced, AtMPK6-dependent changes in *Arabidopsis* thaliana protein profiles. *Plant Signal Behav* **4**(6): 497-505.

Mohammadi M, Anoop V, Gleddie S, Harris LJ. 2011. Proteomic profiling of two maize inbreds during early gibberella ear rot infection. *Proteomics* **11**(18): 3675-3684.

Morandi D, le Signor C, Gianinazzi-Pearson V, Duc G. 2009. A *Medicago truncatula* mutant hyper-responsive to mycorrhiza and defective for nodulation. *Mycorrhiza* **19**(6): 435-441.

Morandi D, Prado E, Sagan M, Duc G. 2005. Characterisation of new symbiotic *Medicago truncatula* (*Gaertn*.) mutants, and phenotypic or genotypic complementary information on previously described mutants. *Mycorrhiza* **15**(4): 283-289.

Murray JD, Muni RR, Torres-Jerez I, Tang Y, Allen S, Andriankaja M, Li G, Laxmi A, Cheng X, Wen J, Vaughan D, Schultze M, Sun J, Charpentier M, Oldroyd G, Tadege M, Ratet P, Mysore KS, Chen R, Udvardi MK. 2011. Vapyrin, a gene essential for intracellular progression of arbuscular mycorrhizal symbiosis, is also essential for infection by rhizobia in the nodule symbiosis of *Medicago truncatula*. *Plant J* **65**(2): 244-252.

Nadolski MJ, Linder ME. 2007. Protein lipidation. *FEBS J* **274**(20): 5202-5210.

Nagaraj N, Lu A, Mann M, Wisniewski JR. 2008. Detergent-based but gel-free method allows identification of several hundred membrane proteins in single LC-MS runs. *J Proteome Res* **7**(11): 5028-5032.

Nair R, Rost B. 2002. Sequence conserved for subcellular localization. *Protein Sci* **11**(12): 2836-2847.

Naumann B, Busch A, Allmer J, Ostendorf E, Zeller M, Kirchhoff H, Hippler M. 2007. Comparative quantitative proteomics to investigate the remodeling of bioenergetic pathways under iron deficiency in *Chlamydomonas reinhardtii*. *Proteomics* **7**(21): 3964-3979.

Neilson KA, Ali NA, Muralidharan S, Mirzaei M, Mariani M, Assadourian G, Lee A, van Sluyter SC, Haynes PA. 2011a. Less label, more free: approaches in label-free quantitative mass spectrometry. *Proteomics* **11**(4): 535-553.

Neilson KA, Mariani M, Haynes PA. 2011b. Quantitative proteomic analysis of cold-responsive proteins in rice. *Proteomics* **11**(9): 1696-1706.

Nelson CJ, Hegeman AD, Harms AC, Sussman MR. 2006. A quantitative analysis of *Arabidopsis* plasma membrane using trypsin-catalyzed $^{(18)}$O labeling. *Mol Cell Proteomics* **5**(8): 1382-1395.

Nesvizhskii AI, Aebersold R. 2005. Interpretation of shotgun proteomic data: the protein inference problem. *Mol Cell Proteomics* **4**(10): 1419-1440.

Neuhaus HE, Emes MJ. 2000. Nonphotosynthetic Metabolism in Plastids. *Annu Rev Plant Physiol Plant Mol Biol* **51**: 111-140.

Nguyen TH, Brechenmacher L, Aldrich J, Clauss T, Gritsenko M, Hixson K, Libault M, Tanaka K, Yang F, Yao Q, Pasa-Tolic L, Xu D, Nguyen HT, Stacey G. 2012. Quantitative Phosphoproteomic Analysis of Soybean Root Hairs Inoculated with *Bradyrhizobium japonicum*. *Mol Cell Proteomics*.

Niittyla T, Fuglsang AT, Palmgren MG, Frommer WB, Schulze WX. 2007. Temporal analysis of sucrose-induced phosphorylation changes in plasma membrane proteins of *Arabidopsis*. *Mol Cell Proteomics* **6**(10): 1711-1726.

Nogueira FC, Palmisano G, Schwammle V, Campos FA, Larsen MR, Domont GB, Roepstorff P. 2012. Performance of isobaric and isotopic labeling in quantitative plant proteomics. *J Proteome Res* **11**(5): 3046-3052.

Nouri MZ, Komatsu S. 2010. Comparative analysis of soybean plasma membrane proteins under osmotic stress using gel-based and LC MS/MS-based proteomics approaches. *Proteomics* **10**(10): 1930-1945.

Nuhse TS, Bottrill AR, Jones AM, Peck SC. 2007. Quantitative phosphoproteomic analysis of plasma membrane proteins reveals regulatory mechanisms of plant innate immune responses. *Plant J* **51**(5): 931-940.

Nunes CC, Dean RA. 2012. Host-induced gene silencing: a tool for understanding fungal host interaction and for developing novel disease control strategies. *Mol Plant Pathol* **13**(5): 519-529.

O'Connell RJ, Panstruga R. 2006. Tete a tete inside a plant cell: establishing compatibility between plants and biotrophic fungi and oomycetes. *New Phytol* **171**(4): 699-718.

O'Farrell PH. 1975. High resolution two-dimensional electrophoresis of proteins. *J Biol Chem* **250**(10): 4007-4021.

Old WM, Meyer-Arendt K, Aveline-Wolf L, Pierce KG, Mendoza A, Sevinsky JR, Resing KA, Ahn NG. 2005. Comparison of label-free methods for quantifying human proteins by shotgun proteomics. *Mol Cell Proteomics* **4**(10): 1487-1502.

Ong SE, Mann M. 2005. Mass spectrometry-based proteomics turns quantitative. *Nat Chem Biol* **1**(5): 252-262.

Ong SE, Pandey A. 2001. An evaluation of the use of two-dimensional gel electrophoresis in proteomics. *Biomol Eng* **18**(5): 195-205.

Op den Camp R, Streng A, De Mita S, Cao Q, Polone E, Liu W, Ammiraju JS, Kudrna D, Wing R, Untergasser A, Bisseling T, Geurts R. 2011. LysM-type mycorrhizal receptor recruited for rhizobium symbiosis in nonlegume *Parasponia*. *Science* **331**(6019): 909-912.

Ow SY, Salim M, Noirel J, Evans C, Rehman I, Wright PC. 2009. iTRAQ underestimation in simple and complex mixtures: "the good, the bad and the ugly". *J Proteome Res* **8**(11): 5347-5355.

Palma DA, Blumwald E, Plaxton WC. 2000. Upregulation of vacuolar $H^{(+)}$-translocating pyrophosphatase by phosphate starvation of *Brassica napus* (rapeseed) suspension cell cultures. *FEBS Lett* **486**(2): 155-158.

Palmblad M, Bindschedler LV, Cramer R. 2007a. Quantitative proteomics using uniform $^{(15)}$N-labeling, MASCOT, and the trans-proteomic pipeline. *Proteomics* **7**(19): 3462-3469.

Palmblad M, Mills DJ, Bindschedler LV, Cramer R. 2007b. Chromatographic alignment of LC-MS and LC-MS/MS datasets by genetic algorithm feature extraction. *J Am Soc Mass Spectrom* **18**(10): 1835-1843.

Panstruga R. 2003. Establishing compatibility between plants and obligate biotrophic pathogens. *Curr Opin Plant Biol* **6**(4): 320-326.

Paradi I, van Tuinen D, Morandi D, Ochatt S, Robert F, Jacas L, Dumas-Gaudot E. 2010. Transcription of two blue copper-binding protein isogenes is highly correlated with arbuscular mycorrhizal development in *Medicago truncatula*. *Mol Plant Microbe Interact* **23**(9): 1175-1183.

Park OK. 2004. Proteomic studies in plants. *J Biochem Mol Biol* **37**(1): 133-138.

Parker J, Zhu N, Zhu M, Chen S. 2012. Profiling thiol redox proteome using isotope tagging mass spectrometry. *J Vis Exp*(61).

Parniske M. 2000. Intracellular accommodation of microbes by plants: a common developmental program for symbiosis and disease? *Curr Opin Plant Biol* **3**(4): 320-328.

Parniske M. 2008. Arbuscular mycorrhiza: the mother of plant root endosymbioses. *Nat Rev Microbiol* **6**(10): 763-775.

Paszkowski U. 2006. A journey through signaling in arbuscular mycorrhizal symbioses 2006. *New Phytol* **172**(1): 35-46.

Patterson J, Ford K, Cassin A, Natera S, Bacic A. 2007. Increased abundance of proteins involved in phytosiderophore production in boron-tolerant barley. *Plant Physiol* **144**(3): 1612-1631.

Pearson JN, Jakobsen I. 1993. The relative contribution of hyphae and roots to phosphorus uptake by arbuscular mycorrhizal plants measured by dual labelling with ^{32}P and ^{33}P. *New Phytol* **124**: 489-494.

Perfect SE, Green JR. 2001. Infection structures of biotrophic and hemibiotrophic fungal plant pathogens. *Mol Plant Pathol* **2**(2): 101-108.

Perkel JM. 2009. iTRAQ gets put to the test. *J Proteome Res* **8**(11): 4885.

Petricka JJ, Schauer MA, Megraw M, Breakfield NW, Thompson JW, Georgiev S, Soderblom EJ, Ohler U, Moseley MA, Grossniklaus U, Benfey PN. 2012. The protein expression landscape of the *Arabidopsis* root. *Proc Natl Acad Sci U S A* **109**(18): 6811-6818.

Phanstiel D, Unwin R, McAlister GC, Coon JJ. 2009. Peptide quantification using 8-plex isobaric tags and electron transfer dissociation tandem mass spectrometry. *Anal Chem* **81**(4): 1693-1698.

Phillips JM, Hayman DS. 1970. Improved procedures for clearing roots and staining parasitic and vesicular-arbuscular mycorrhizal fungi for rapid assessment of infection. *Transactions of the British Mycological Society* **55**: 157-160.

Pichler P, Kocher T, Holzmann J, Mazanek M, Taus T, Ammerer G, Mechtler K. 2010. Peptide labeling with isobaric tags yields higher identification rates using iTRAQ 4-plex compared to TMT 6-plex and iTRAQ 8-plex on LTQ Orbitrap. *Anal Chem* **82**(15): 6549-6558.

Piersma SR, Fiedler U, Span S, Lingnau A, Pham TV, Hoffmann S, Kubbutat MH, Jimenez CR. 2010. Workflow comparison for label-free, quantitative secretome proteomics for cancer biomarker discovery: method evaluation, differential analysis, and verification in serum. *J Proteome Res* **9**(4): 1913-1922.

Plaxton WC. 1999. Metabolic aspects of the phosphate starvation in plants. In: Phosphorus in plant biology: regulatory roles in molecular, cellular, organismic, and ecosystem processes. Rockville, Maryland: American Society of Plant Physiologists.

Porceddu A, Panara F, Calderini O, Molinari L, Taviani P, Lanfaloni L, Scotti C, Carelli M, Scaramelli L, Bruschi G, Cosson V, Ratet P, de Larembergue H, Duc G, Piano E, Arcioni S. 2008. An Italian functional genomic resource for *Medicago truncatula*. *BMC Res Notes* **1**: 129.

Pozo MJ, Azcon-Aguilar C. 2007. Unraveling mycorrhiza-induced resistance. *Curr Opin Plant Biol* **10**(4): 393-398.

Pumplin N, Harrison MJ. 2009. Live-cell imaging reveals periarbuscular membrane domains and organelle location in *Medicago truncatula* roots during arbuscular mycorrhizal symbiosis. *Plant Physiol* **151**(2): 809-819.

Pumplin N, Mondo SJ, Topp S, Starker CG, Gantt JS, Harrison MJ. 2010. *Medicago truncatula* Vapyrin is a novel protein required for arbuscular mycorrhizal symbiosis. *Plant J* **61**(3): 482-494.

Pumplin N, Zhang X, Noar RD, Harrison MJ. 2012. Polar localization of a symbiosis-specific phosphate transporter is mediated by a transient reorientation of secretion. *Proc Natl Acad Sci U S A* **109**(11): E665-672.

Purin S, Rillig MC. 2008. Parasitism of arbuscular mycorrhizal fungi: reviewing the evidence. *FEMS Microbiol Lett* **279**(1): 8-14.

Rappsilber J, Ryder U, Lamond AI, Mann M. 2002. Large-scale proteomic analysis of the human spliceosome. *Genome Res* **12**(8): 1231-1245.

Rawsthorne S. 2002. Carbon flux and fatty acid synthesis in plants. *Prog Lipid Res* **41**(2): 182-196.

Recorbet G, Rogniaux H, Gianinazzi-Pearson V, Dumasgaudot E. 2009. Fungal proteins in the extra-radical phase of arbuscular mycorrhiza: a shotgun proteomic picture. *New Phytol* **181**(2): 248-260.

Recorbet G, Valot B, Robert F, Gianinazzi-Pearson V, Dumas-Gaudot E. 2010. Identification of in planta-expressed arbuscular mycorrhizal fungal proteins upon comparison of the root

proteomes of *Medicago truncatula* colonised with two *Glomus* species. *Fungal Genet Biol* **47**(7): 608-618.

Reddy DMRS, Schorderet M, Feller U, Reinhardt D. 2007. A petunia mutant affected in intracellular accommodation and morphogenesis of arbuscular mycorrhizal fungi. *Plant J* **51**(5): 739-750.

Reinhardt D. 2007. Programming good relations--development of the arbuscular mycorrhizal symbiosis. *Curr Opin Plant Biol* **10**(1): 98-105.

Remy W, Taylor TN, Hass H, Kerp H. 1994. Four hundred-million-year-old vesicular arbuscular mycorrhizae. *Proc Natl Acad Sci U S A* **91**(25): 11841-11843.

Repetto O, Bestel-Corre, G., Dumas-Gaudot, E., Berta, G., Gianinazzi-Pearson, V., Gianinazzi, S. 2003. Targeted proteomics to identify cadmium-induced protein modifications in *Glomus mosseae*-inoculated pea roots. *New Phytol* **157**: 555–567.

Revalska M, Vassileva V, Goormachtig S, Van Hautegem T, Ratet P, Iantcheva A. 2011. Recent Progress in Development of Tnt1 Functional Genomics Platform for *Medicago truncatula* and *Lotus japonicus* in Bulgaria. *Curr Genomics* **12**(2): 147-152.

Richly E, Leister D. 2004. An improved prediction of chloroplast proteins reveals diversities and commonalities in the chloroplast proteomes of *Arabidopsis* and rice. *Gene* **329**: 11-16.

Rosewarne GM, Barker SJ, Smith SE, Smith FA, Schachtman DP. 1999. A *Lycopersicon esculentum* phosphate transporter (LePT1) involved in phosphorus uptake from a vesicular-arbuscular mycorrhizal fungus. *New Phytol* **144**: 507-516.

Rosewarne GM, Smith FA, Schachtman DP, Smith SE. 2007. Localization of proton-ATPase genes expressed in arbuscular mycorrhizal tomato plants. *Mycorrhiza* **17**(3): 249-258.

Ross PL, Huang YN, Marchese JN, Williamson B, Parker K, Hattan S, Khainovski N, Pillai S, Dey S, Daniels S, Purkayastha S, Juhasz P, Martin S, Bartlet-Jones M, He F, Jacobson A, Pappin DJ. 2004. Multiplexed protein quantitation in *Saccharomyces cerevisiae* using amine-reactive isobaric tagging reagents. *Mol Cell Proteomics* **3**(12): 1154-1169.

Rudella A, Friso G, Alonso JM, Ecker JR, van Wijk KJ. 2006. Downregulation of ClpR2 leads to reduced accumulation of the ClpPRS protease complex and defects in chloroplast biogenesis in *Arabidopsis*. *Plant Cell* **18**(7): 1704-1721.

Ruepp A, Zollner A, Maier D, Albermann K, Hani J, Mokrejs M, Tetko I, Guldener U, Mannhaupt G, Munsterkotter M, Mewes HW. 2004. The FunCat, a functional annotation scheme for systematic classification of proteins from whole genomes. *Nucleic Acids Res* **32**(18): 5539-5545.

Sanders IR, Croll D. 2010. Arbuscular mycorrhiza: the challenge to understand the genetics of the fungal partner. *Annu Rev Genet* **44**: 271-292.

Santoni V, Molloy M, Rabilloud T. 2000. Membrane proteins and proteomics: un amour impossible? *Electrophoresis* **21**(6): 1054-1070.

Savitski MM, Nielsen ML, Kjeldsen F, Zubarev RA. 2005. Proteomics-grade de novo sequencing approach. *J Proteome Res* **4**(6): 2348-2354.

Sbrana C, Giovannetti M. 2005. Chemotropism in the arbuscular mycorrhizal fungus *Glomus mosseae*. *Mycorrhiza* **15**(7): 539-545.

Schaarschmidt S, Gonzalez MC, Roitsch T, Strack D, Sonnewald U, Hause B. 2007. Regulation of arbuscular mycorrhization by carbon. The symbiotic interaction cannot be improved by increased carbon availability accomplished by root-specifically enhanced invertase activity. *Plant Physiol* **143**(4): 1827-1840.

Schachtman DP, Reid RJ, Ayling SM. 1998. Phosphorus Uptake by Plants: From Soil to Cell. *Plant Physiol* **116**(2): 447-453.

Schaff JE, Mbeunkui F, Blackburn K, Bird DM, Goshe MB. 2008. SILIP: a novel stable isotope labeling method for in planta quantitative proteomic analysis. *Plant J* **56**(5): 840-854.

Schagger H, von Jagow G. 1991. Blue native electrophoresis for isolation of membrane protein complexes in enzymatically active form. *Anal Biochem* **199**(2): 223-231.

Schenkluhn L, Hohnjec N, Niehaus K, Schmitz U, Colditz F. 2010. Differential gel electrophoresis (DIGE) to quantitatively monitor early symbiosis- and pathogenesis-induced changes of the *Medicago truncatula* root proteome. *J Proteomics* **73**(4): 753-768.

Scherl A, Francois P, Charbonnier Y, Deshusses JM, Koessler T, Huyghe A, Bento M, Stahl-Zeng J, Fischer A, Masselot A, Vaezzadeh A, Galle F, Renzoni A, Vaudaux P, Lew D, Zimmermann-Ivol CG, Binz PA, Sanchez JC, Hochstrasser DF, Schrenzel J. 2006. Exploring glycopeptide-resistance in *Staphylococcus aureus*: a combined proteomics and transcriptomics approach for the identification of resistance-related markers. *BMC Genomics* **7**: 296.

Schleiff E, Maier UG, Becker T. 2011. Omp85 in eukaryotic systems: one protein family with distinct functions. *Biol Chem* **392**(1-2): 21-27.

Schliemann W, Schmidt J, Nimtz M, Wray V, Fester T, Strack D. 2006. Accumulation of apocarotenoids in mycorrhizal roots of *Ornithogalum umbellatum*. *Phytochemistry* **67**(12): 1196-1205.

Schmidt A, Kellermann J, Lottspeich F. 2005. A novel strategy for quantitative proteomics using isotope-coded protein labels. *Proteomics* **5**(1): 4-15.

Schmidt SM, Panstruga R. 2011. Pathogenomics of fungal plant parasites: what have we learnt about pathogenesis? *Curr Opin Plant Biol* **14**(4): 392-399.

Schnabel EL, Kassaw TK, Smith LS, Marsh JF, Oldroyd GE, Long SR, Frugoli JA. 2011. The ROOT DETERMINED NODULATION1 gene regulates nodule number in roots of *Medicago truncatula* and defines a highly conserved, uncharacterized plant gene family. *Plant Physiol* **157**(1): 328-340.

Schneider LV, Hall MP. 2005. Stable isotope methods for high-precision proteomics. *Drug Discov Today* **10**(5): 353-363.

Schneider T, Schellenberg M, Meyer S, Keller F, Gehrig P, Riedel K, Lee Y, Eberl L, Martinoia E. 2009. Quantitative detection of changes in the leaf-mesophyll tonoplast proteome in dependency of a cadmium exposure of barley (*Hordeum vulgare L.*) plants. *Proteomics* **9**(10): 2668-2677.

Schulze-Lefert P, Panstruga R. 2003. Establishment of biotrophy by parasitic fungi and reprogramming of host cells for disease resistance. *Annu Rev Phytopathol* **41**: 641-667.

Schulze WX, Usadel B. 2010. Quantitation in mass-spectrometry-based proteomics. *Annu Rev Plant Biol* **61**: 491-516.

Schussler A, Martin H, Cohen D, Fitz M, Wipf D. 2006. Characterization of a carbohydrate transporter from symbiotic *glomeromycotan* fungi. *Nature* **444**(7121): 933-936.

Schussler A, Martin H, Cohen D, Fitz M, Wipf D. 2007. Arbuscular Mycorrhiza: Studies on the *Geosiphon* Symbiosis Lead to the Characterization of the First *Glomeromycotan* Sugar Transporter. *Plant Signal Behav* **2**(5): 431-434.

Schwacke R, Flugge UI, Kunze R. 2004. Plant membrane proteome databases. *Plant Physiol Biochem* **42**(12): 1023-1034.

Sergeant K, Spiess N, Renaut J, Wilhelm E, Hausman JF. 2011. One dry summer: a leaf proteome study on the response of oak to drought exposure. *J Proteomics* **74**(8): 1385-1395.

Shah K, Russinova E, Gadella TW, Jr., Willemse J, De Vries SC. 2002. The *Arabidopsis* kinase-associated protein phosphatase controls internalization of the somatic embryogenesis receptor kinase 1. *Genes Dev* **16**(13): 1707-1720.

Sharda JN, Koide RT. 2008. Can hypodermal passage cell distribution limit root penetration by mycorrhizal fungi? *New Phytol* **180**(3): 696-701.

Shen Y, Tolic N, Xie F, Zhao R, Purvine SO, Schepmoes AA, Moore RJ, Anderson GA, Smith RD. 2011. Effectiveness of CID, HCD, and ETD with FT MS/MS for degradomic-peptidomic analysis: comparison of peptide identification methods. *J Proteome Res* **10**(9): 3929-3943.

Shen Z, Li P, Ni RJ, Ritchie M, Yang CP, Liu GF, Ma W, Liu GJ, Ma L, Li SJ, Wei ZG, Wang HX, Wang BC. 2009. Label-free quantitative proteomics analysis of etiolated maize seedling leaves during greening. *Mol Cell Proteomics* **8**(11): 2443-2460.

Shiu SH, Li WH. 2004. Origins, lineage-specific expansions, and multiple losses of tyrosine kinases in eukaryotes. *Mol Biol Evol* **21**(5): 828-840.

Siciliano V, Genre A, Balestrini R, Cappellazzo G, deWit PJ, Bonfante P. 2007a. Transcriptome analysis of arbuscular mycorrhizal roots during development of the prepenetration apparatus. *Plant Physiol* **144**(3): 1455-1466.

Siciliano V, Genre A, Balestrini R, Dewit PJ, Bonfante P. 2007b. Pre-Penetration Apparatus Formation During AM Infection is Associated With a Specific Transcriptome Response in Epidermal Cells. *Plant Signal Behav* **2**(6): 533-535.

Sieberer BJ, Chabaud M, Fournier J, Timmers AC, Barker DG. 2012. A switch in Ca^{2+} spiking signature is concomitant with endosymbiotic microbe entry into cortical root cells of *Medicago truncatula*. *Plant J* **69**(5): 822-830.

Silva JC, Denny R, Dorschel CA, Gorenstein M, Kass IJ, Li GZ, McKenna T, Nold MJ, Richardson K, Young P, Geromanos S. 2005. Quantitative proteomic analysis by accurate mass retention time pairs. *Anal Chem* **77**(7): 2187-2200.

Simon L, Levesque RC, Lalonde M. 1993. Identification of endomycorrhizal fungi colonizing roots by fluorescent single-strand conformation polymorphism-polymerase chain reaction. *Appl Environ Microbiol* **59**(12): 4211-4215.

Singh S, Parniske M. 2012. Activation of calcium- and calmodulin-dependent protein kinase (CCaMK), the central regulator of plant root endosymbiosis. *Curr Opin Plant Biol* **15**(4): 444-453.

Smith SE, Gianinazzi-Pearson V. 1988. Physiological interactions between symbionts in vesicular-arbuscular mycorrhizal plants. *Annu Rev Plant Physiol Plant Mol Biol* **39**: 221–224.

Smith SE, Read DJ. 2008. *Mycorrhizal Symbiosis*. London, New York: Academic Press.

Smith SE, Read, D. J. 1997. Mycorrhizal Symbiosis. Academic Press, London: 81–104.

Smith SE, Smith FA. 1990. Structure and function of the interfaces in biotrophic symbioses as they relate to nutrient transport. *New Phytologist* **114**: 1-38.

Staehelin C, Xie ZP, Illana A, Vierheilig H. 2011. Long-distance transport of signals during symbiosis: are nodule formation and mycorrhization autoregulated in a similar way? *Plant Signal Behav* **6**(3): 372-377.

Staes A, Demol H, Van Damme J, Martens L, Vandekerckhove J, Gevaert K. 2004. Global differential non-gel proteomics by quantitative and stable labeling of tryptic peptides with oxygen-18. *J Proteome Res* **3**(4): 786-791.

Stanislas T, Bouyssie D, Rossignol M, Vesa S, Fromentin J, Morel J, Pichereaux C, Monsarrat B, Simon-Plas F. 2009. Quantitative proteomics reveals a dynamic association of proteins to detergent-resistant membranes upon elicitor signaling in tobacco. *Mol Cell Proteomics* **8**(9): 2186-2198.

Stevenson SE, Chu Y, Ozias-Akins P, Thelen JJ. 2009. Validation of gel-free, label-free quantitative proteomics approaches: applications for seed allergen profiling. *J Proteomics* **72**(3): 555-566.

Stewart, II, Thomson T, Figeys D. 2001. ^{18}O labeling: a tool for proteomics. *Rapid Commun Mass Spectrom* **15**(24): 2456-2465.

Stroher E, Dietz KJ. 2006. Concepts and approaches towards understanding the cellular redox proteome. *Plant Biol (Stuttg)* **8**(4): 407-418.

Stulemeijer IJ, Joosten MH, Jensen ON. 2009. Quantitative phosphoproteomics of tomato mounting a hypersensitive response reveals a swift suppression of photosynthetic activity and a differential role for hsp90 isoforms. *J Proteome Res* **8**(3): 1168-1182.

Sun Q, Hu C, Hu J, Li S, Zhu Y. 2009. Quantitative proteomic analysis of CMS-related changes in Honglian CMS rice anther. *Protein J* **28**(7-8): 341-348.

Swaney DL, McAlister GC, Coon JJ. 2008. Decision tree-driven tandem mass spectrometry for shotgun proteomics. *Nat Methods* **5**(11): 959-964.

Takeda N, Sato S, Asamizu E, Tabata S, Parniske M. 2009. Apoplastic plant subtilases support arbuscular mycorrhiza development in *Lotus japonicus*. *Plant J* **58**(5): 766-777.

Tan Z, Hu Y, Lin Z. 2012. PhPT4 Is a Mycorrhizal-Phosphate Transporter Suppressed by Lysophosphatidylcholine in Petunia Roots. *Plant Molecular Biology Reporter*.

Tejeda-Sartorius M, Martinez de la Vega O, Delano-Frier JP. 2008. Jasmonic acid influences mycorrhizal colonization in tomato plants by modifying the expression of genes involved in carbohydrate partitioning. *Physiol Plant* **133**(2): 339-353.

Thelen JJ, Peck SC. 2007. Quantitative proteomics in plants: choices in abundance. *Plant Cell* **19**(11): 3339-3346.

Thingholm TE, Palmisano G, Kjeldsen F, Larsen MR. 2010. Undesirable charge-enhancement of isobaric tagged phosphopeptides leads to reduced identification efficiency. *J Proteome Res* **9**(8): 4045-4052.

Thompson A, Schafer J, Kuhn K, Kienle S, Schwarz J, Schmidt G, Neumann T, Johnstone R, Mohammed AK, Hamon C. 2003. Tandem mass tags: a novel quantification strategy for comparative analysis of complex protein mixtures by MS/MS. *Anal Chem* **75**(8): 1895-1904.

Tian J, Venkatachalam P, Liao H, Yan X, Raghothama K. 2007. Molecular cloning and characterization of phosphorus starvation responsive genes in common bean (*Phaseolus vulgaris L.*). *Planta* **227**(1): 151-165.

Tisserant E, Kohler A, Dozolme-Seddas P, Balestrini R, Benabdellah K, Colard A, Croll D, Da Silva C, Gomez SK, Koul R, Ferrol N, Fiorilli V, Formey D, Franken P, Helber N, Hijri M, Lanfranco L, Lindquist E, Liu Y, Malbreil M, Morin E, Poulain J, Shapiro H, van Tuinen D, Waschke A, Azcon-Aguilar C, Becard G, Bonfante P, Harrison MJ, Kuster H, Lammers P, Paszkowski U, Requena N, Rensing SA, Roux C, Sanders IR, Shachar-Hill Y, Tuskan G, Young JP, Gianinazzi-Pearson V, Martin F. 2012. The transcriptome of the arbuscular mycorrhizal fungus *Glomus intraradices* (DAOM 197198) reveals functional tradeoffs in an obligate symbiont. *New Phytol* **193**(3): 755-769.

Tollot M, Wong Sak Hoi J, van Tuinen D, Arnould C, Chatagnier O, Dumas B, Gianinazzi-Pearson V, Seddas PM. 2009. An STE12 gene identified in the mycorrhizal fungus *Glomus*

intraradices restores infectivity of a hemibiotrophic plant pathogen. *New Phytol* **181**(3): 693-707.

Tonge R, Shaw J, Middleton B, Rowlinson R, Rayner S, Young J, Pognan F, Hawkins E, Currie I, Davison M. 2001. Validation and development of fluorescence two-dimensional differential gel electrophoresis proteomics technology. *Proteomics* **1**(3): 377-396.

Trouvelot A, Kough JL, Gianinazzi-Pearson V. 1986. Mesure du taux de mycorhization VA d'un système radiculaire. Recherche de méthodes d'estimation ayant une signification fonctionnelle. In Physiological and Genetical Aspects of Mycorrhizae. France: INRA.

Umehara M, Hanada A, Yoshida S, Akiyama K, Arite T, Takeda-Kamiya N, Magome H, Kamiya Y, Shirasu K, Yoneyama K, Kyozuka J, Yamaguchi S. 2008. Inhibition of shoot branching by new terpenoid plant hormones. *Nature* **455**(7210): 195-200.

Unlu M, Morgan ME, Minden JS. 1997. Difference gel electrophoresis: a single gel method for detecting changes in protein extracts. *Electrophoresis* **18**(11): 2071-2077.

Valot B, Dieu M, Recorbet G, Raes M, Gianinazzi S, Dumas-Gaudot E. 2005. Identification of membrane-associated proteins regulated by the arbuscular mycorrhizal symbiosis. *Plant Mol Biol* **59**(4): 565-580.

Valot B, Langella O, Nano E, Zivy M. 2011. MassChroQ: a versatile tool for mass spectrometry quantification. *Proteomics* **11**(17): 3572-3577.

Valot B, Negroni L, Zivy M, Gianinazzi S, Dumas-Gaudot E. 2006. A mass spectrometric approach to identify arbuscular mycorrhiza-related proteins in root plasma membrane fractions. *Proteomics* **6 Suppl 1**: S145-155.

van Noorden GE, Kerim T, Goffard N, Wiblin R, Pellerone FI, Rolfe BG, Mathesius U. 2007. Overlap of proteome changes in *Medicago truncatula* in response to auxin and *Sinorhizobium meliloti*. *Plant Physiol* **144**(2): 1115-1131.

Vaudel M, Burkhart JM, Radau S, Zahedi RP, Martens L, Sickmann A. 2012. Integral Quantification Accuracy Estimation for Reporter Ion-based Quantitative Proteomics (iQuARI). *J Proteome Res*.

Venable JD, Dong MQ, Wohlschlegel J, Dillin A, Yates JR. 2004. Automated approach for quantitative analysis of complex peptide mixtures from tandem mass spectra. *Nat Methods* **1**(1): 39-45.

Vertommen A, Panis B, Swennen R, Carpentier SC. 2011. Challenges and solutions for the identification of membrane proteins in non-model plants. *J Proteomics* **74**(8): 1165-1181.

Vincent D SP. 2011. Development of an in-house protocol for the OFFGEL fractionation of plant proteins. *J Integrated omics* **DOI: 10.5584/jiomics.v2011i2011.59**.

Vogel JT, Walter MH, Giavalisco P, Lytovchenko A, Kohlen W, Charnikhova T, Simkin AJ, Goulet C, Strack D, Bouwmeester HJ, Fernie AR, Klee HJ. 2010. SlCCD7 controls strigolactone biosynthesis, shoot branching and mycorrhiza-induced apocarotenoid formation in tomato. *Plant J* **61**(2): 300-311.

Vothknecht UC, Westhoff P. 2001. Biogenesis and origin of thylakoid membranes. *Biochim Biophys Acta* **1541**(1-2): 91-101.

Wallin E, von Heijne G. 1998. Genome-wide analysis of integral membrane proteins from eubacterial, archaean, and eukaryotic organisms. *Protein Sci* **7**(4): 1029-1038.

Walter MH, Floss DS, Hans J, Fester T, Strack D. 2007. Apocarotenoid biosynthesis in arbuscular mycorrhizal roots: contributions from methylerythritol phosphate pathway isogenes and tools for its manipulation. *Phytochemistry* **68**(1): 130-138.

Walter MH, Floss DS, Strack D. 2010. Apocarotenoids: hormones, mycorrhizal metabolites and aroma volatiles. *Planta* **232**(1): 1-17.

Wang F, Vandepoele K, Van Lijsebettens M. 2012. Tetraspanin genes in plants. *Plant Sci* **190**: 9-15.

Wang H, Alvarez S, Hicks LM. 2012. Comprehensive comparison of iTRAQ and label-free LC-based quantitative proteomics approaches using two *Chlamydomonas reinhardtii* strains of interest for biofuels engineering. *J Proteome Res* **11**(1): 487-501.

Warren CM, Geenen DL, Helseth DL, Jr., Xu H, Solaro RJ. 2010. Sub-proteomic fractionation, iTRAQ, and OFFGEL-LC-MS/MS approaches to cardiac proteomics. *J Proteomics* **73**(8): 1551-1561.

Washburn MP, Wolters D, Yates JR, 3rd. 2001. Large-scale analysis of the yeast proteome by multidimensional protein identification technology. *Nat Biotechnol* **19**(3): 242-247.

Weidmann S, Sanchez L, Descombin J, Chatagnier O, Gianinazzi S, Gianinazzi-Pearson V. 2004. Fungal elicitation of signal transduction-related plant genes precedes mycorrhiza establishment and requires the dmi3 gene in *Medicago truncatula*. *Mol Plant Microbe Interact* **17**(12): 1385-1393.

Wenger CD, Lee MV, Hebert AS, McAlister GC, Phanstiel DH, Westphall MS, Coon JJ. 2011. Gas-phase purification enables accurate, multiplexed proteome quantification with isobaric tagging. *Nat Methods* **8**(11): 933-935.

Wienkoop S, Larrainzar E, Niemann M, Gonzalez EM, Lehmann U, Weckwerth W. 2006. Stable isotope-free quantitative shotgun proteomics combined with sample pattern recognition for rapid diagnostics. *J Sep Sci* **29**(18): 2793-2801.

Wiktorowicz JE, English RD, Wu Z, Kurosky A. 2012. Model Studies on iTRAQ Modification of Peptides: Sequence-dependent Reaction Specificity. *J Proteome Res* **11**(3): 1512-1520.

Wilkins MR, Sanchez JC, Gooley AA, Appel RD, Humphery-Smith I, Hochstrasser DF, Williams KL. 1996. Progress with proteome projects: why all proteins expressed by a genome should be identified and how to do it. *Biotechnol Genet Eng Rev* **13**: 19-50.

Willats WG, Knox JP. 1996. A role for arabinogalactan-proteins in plant cell expansion: evidence from studies on the interaction of beta-glucosyl Yariv reagent with seedlings of *Arabidopsis thaliana*. *Plant J* **9**(6): 919-925.

Wisniewski JR, Zougman A, Nagaraj N, Mann M. 2009. Universal sample preparation method for proteome analysis. *Nat Methods* **6**(5): 359-362.

Wright DP, Read DJ, Scholes JD. 1998. Mycorrhizal sink strength influences whole plant carbon balance of *Trifolium repens L. Plant Cell Environ* **21**: 881-891.

Wulf A, Manthey K, Doll J, Perlick AM, Linke B, Bekel T, Meyer F, Franken P, Kuster H, Krajinski F. 2003. Transcriptional changes in response to arbuscular mycorrhiza development in the model plant *Medicago truncatula*. *Mol Plant Microbe Interact* **16**(4): 306-314.

Xie X, Yoneyama K. 2010. The strigolactone story. *Annu Rev Phytopathol* **48**: 93-117.

Yalovsky S, Rodr Guez-Concepcion M, Gruissem W. 1999. Lipid modifications of proteins - slipping in and out of membranes. *Trends Plant Sci* **4**(11): 439-445.

Yang Y, Qiang X, Owsiany K, Zhang S, Thannhauser TW, Li L. 2011. Evaluation of different multidimensional LC-MS/MS pipelines for isobaric tags for relative and absolute quantitation (iTRAQ)-based proteomic analysis of potato tubers in response to cold storage. *J Proteome Res* **10**(10): 4647-4660.

Yano K, Yoshida S, Muller J, Singh S, Banba M, Vickers K, Markmann K, White C, Schuller B, Sato S, Asamizu E, Tabata S, Murooka Y, Perry J, Wang TL, Kawaguchi M, Imaizumi-Anraku H, Hayashi M, Parniske M. 2008. CYCLOPS, a mediator of symbiotic intracellular accommodation. *Proc Natl Acad Sci U S A* **105**(51): 20540-20545.

Yao X, Freas A, Ramirez J, Demirev PA, Fenselau C. 2001. Proteolytic ^{18}O labeling for comparative proteomics: model studies with two serotypes of adenovirus. *Anal Chem* **73**(13): 2836-2842.

Zamioudis C, Pieterse CM. 2012. Modulation of host immunity by beneficial microbes. *Mol Plant Microbe Interact* **25**(2): 139-150.

Zhang Q, Blaylock LA, Harrison MJ. 2010. Two *Medicago truncatula* half-ABC transporters are essential for arbuscule development in arbuscular mycorrhizal symbiosis. *Plant Cell* **22**(5): 1483-1497.

Zieske LR. 2006. A perspective on the use of iTRAQ reagent technology for protein complex and profiling studies. *J Exp Bot* **57**(7): 1501-1508.

Zybailov B, Rutschow H, Friso G, Rudella A, Emanuelsson O, Sun Q, van Wijk KJ. 2008. Sorting signals, N-terminal modifications and abundance of the chloroplast proteome. *PLoS One* **3**(4): e1994.

Additional files

Chapter 2, additional file S2.1.

Group A: Peptides shifted to more basic OGE fraction.

		Sequence	Score	Obs mass	Theo mass	Modification	OGF	Rt (min)	Rt	Diff
1	Unlabelled	ECADLWPR	99	1045.46	1045.46		frac 1	17.25		
	iTRAQ 1	ECADLWPR	99	1190.62	1190.57	145.11	frac 3	24	23.63	6.38
	iTRAQ 3	ECADLWPR	99	1190.62	1190.57	145.11	frac 3	23.5		
	iTRAQ 5	ECADLWPR	99	1190.61	1190.57	145.11	frac 4	23.5		
	iTRAQ 6	ECADLWPR	99	1190.48	1190.57	145.11	frac 4	23.5		
2	Unlabelled	AYLEDFYR	99	1075.50	1075.50		frac 1	18.75		
	iTRAQ 1	AYLEDFYR	99	1220.66	1220.61	145.11	frac 3	27	26.41	7.66
	iTRAQ 2	AYLEDFYR	95	1220.62	1220.61	145.11	frac 3	26		
	iTRAQ 3	AYLEDFYR	99	1220.67	1220.61	145.11	frac 3	26.5		
	iTRAQ 4	AYLEDFYR	99	1220.69	1220.61	145.11	frac 4	27		
	iTRAQ 6	AYLEDFYR	99	1220.67	1220.61	145.11	frac 4	26		
	iTRAQ 7	AYLEDFYR	99	1220.60	1220.61	145.11	frac 2,3	26.25		
	iTRAQ 8	AYLEDFYR	99	1220.60	1220.61	145.11	frac 3	26.25		
	iTRAQ 9	AYLEDFYR	99	1220.54	1220.61	145.11	frac 3	26.25		
3	Unlabelled	EQMGYTFDALK	99	1301.57	1301.58		frac 1	18.75		
	iTRAQ 1	EQMGYTFDALK	99	1590.88	1590.81	289.23	frac 3	25.5	24.95	6.2
	iTRAQ 3	EQMGYTFDALK	99	1590.88	1590.81	289.23	frac 3	25		
	iTRAQ 4	EQMGYTFDALK	99	1590.89	1590.81	289.23	frac 3	25		
	iTRAQ 6	EQMGYTFDALK	99	1590.87	1590.81	289.23	frac 4	24.5		
	iTRAQ 8	EQMGYTFDALK	99	1590.80	1590.81	289.23	frac 3	24.75		
4	Unlabelled	TMADEGVVALWR	99	1346.66	1346.65		frac 1	23.25		
	iTRAQ 1	TMADEGVVALWR	99	1491.86	1491.77	145.12	frac 3	30.5	29.29	6.04

	iTRAQ 2	TMADEGVVALWR	99	1491.80	1491.77	145.12	frac 3	29		
	iTRAQ 3	TMADEGVVALWR	99	1491.85	1491.77	145.12	frac 3	30		
	iTRAQ 6	TMADEGVVALWR	99	1491.88	1491.77	145.12	frac 3,4	30		
	iTRAQ 7	TMADEGVVALWR	99	1491.70	1491.77	145.12	frac 1,2,3,4	28.5		
	iTRAQ 8	TMADEGVVALWR	99	1491.75	1491.77	145.12	frac 1,2,3	28.5		
	iTRAQ 9	TMADEGVVALWR	99	1491.70	1491.77	145.12	frac 3,4	28.5		
5	Unlabelled	ECSGVEPQLWAR	99	1430.66	1430.66		frac 1	17.25		
	iTRAQ 1	ECSGVEPQLWAR	99	1575.84	1575.77	145.11	frac 3	24.5	24.13	6.88
	iTRAQ 3	ECSGVEPQLWAR	99	1575.83	1575.77	145.11	frac 3	24		
	iTRAQ 4	ECSGVEPQLWAR	99	1575.87	1575.77	145.11	frac 4	24		
	iTRAQ 6	ECSGVEPQLWAR	99	1575.83	1575.77	145.11	frac 3	24		
6	Unlabelled	NQIDEIVLVGGSTR	99	1499.77	1499.78		frac 1	18.75		
	iTRAQ 1	NQIDEIVLVGGSTR	99	1644.98	1644.90	145.13	frac 3	26.5	25.64	6.89
	iTRAQ 2	NQIDEIVLVGGSTR	99	1644.91	1644.90	145.13	frac 3	25		
	iTRAQ 3	NQIDEIVLVGGSTR	99	1644.98	1644.90	145.13	frac 3,4	26		
	iTRAQ 4	NQIDEIVLVGGSTR	99	1644.99	1644.90	145.13	frac 3,4	26		
	iTRAQ 6	NQIDEIVLVGGSTR	99	1644.98	1644.90	145.13	frac 4	25		
	iTRAQ 8	NQIDEIVLVGGSTR	99	1644.89	1644.90	145.13	frac 2,3	25.5		
	iTRAQ 9	NQIDEIVLVGGSTR	99	1644.82	1644.90	145.13	frac 3	25.5		
7	Unlabelled	LAEMPADSGYPAYLAAR	99	1794.81	1794.84		frac 1	18.75		
	iTRAQ 1	LAEMPADSGYPAYLAAR	99	1940.06	1939.97	145.13	frac 3	26.5	26.13	7.38
	iTRAQ 3	LAEMPADSGYPAYLAAR	99	1940.07	1939.97	145.13	frac 3	26		
	iTRAQ 4	LAEMPADSGYPAYLAAR	99	1940.09	1939.97	145.13	frac 4	26.5		
	iTRAQ 8	LAEMPADSGYPAYLAAR	99	1939.95	1939.97	145.13	frac 3	25.5		
8	Unlabelled	ELEFYMK	99	958.45	958.46		frac 1	18.75		
	iTRAQ 1	ELEFYMK	99	1247.72	1247.66	289.20	frac 3	26.5	25.83	7.08

	iTRAQ 8	ELEFYMK	99	1247.65	1247.66	289.20	frac 3	25.5		
	iTRAQ 9	ELEFYMK	99	1247.60	1247.66	289.20	frac 3	25.5		
9	Unlabelled	IPSAVGYQPTLSTDLGGLQER	99	2201.03	2201.13		frac 1	18.25	26.58	8.33
	iTRAQ 4	IPSAVGYQPTLSTDLGGLQER	99	2346.39	2346.24	145.11	frac 4	27.5		
	iTRAQ 6	IPSAVGYQPTLSTDLGGLQER	99	2346.25	2346.24	145.11	frac 4	26		
	iTRAQ 8	IPSAVGYQPTLSTDLGGLQER	99	2346.21	2346.24	145.11	frac 3	26.25		
10	Unlabelled	AQIWDTAGQER	99	1273.55	1273.59		frac 1	19		
	iTRAQ 1	AQIWDTAGQER	99	1418.76	1418.71	145.12	frac 3	21.5	21.3	2.3
	iTRAQ 2	AQIWDTAGQER	99	1418.70	1418.71	145.12	frac 3	21		
	iTRAQ 3	AQIWDTAGQER	99	1418.77	1418.71	145.12	frac 3	21.5		
	iTRAQ 4	AQIWDTAGQER	99	1418.82	1418.71	145.12	frac 4	21.5		
	iTRAQ 6	AQIWDTAGQER	99	1418.76	1418.71	145.12	frac 4	21		
11	Unlabelled	AGGECLTFDQLALR	99	1549.70	1549.77		frac 1	18.75	27.3	8.55
	iTRAQ 1	AGGECLTFDQLALR	99	1694.94	1694.87	145.10	frac 3	28		
	iTRAQ 4	AGGECLTFDQLALR	99	1694.97	1694.87	145.10	frac 4	28		
	iTRAQ 6	AGGECLTFDQLALR	99	1694.74	1694.87	145.10	frac 4	26.5		
	iTRAQ 8	AGGECLTFDQLALR	99	1694.84	1694.87	145.10	frac 3	27		
	iTRAQ 9	AGGECLTFDQLALR	99	1694.77	1694.87	145.10	frac 4	27		
12	Unlabelled	VDFAYSFFEK	99	1251.57	1251.61	289.18	frac 1	23	30	7
	iTRAQ 6	VDFAYSFFEK	99	1540.77	1540.79	289.18	frac 3	30		
	iTRAQ 8	VDFAYSFFEK	99	1540.77	1540.79	289.18	frac 3	30		
	iTRAQ 9	VDFAYSFFEK	99	1540.70	1540.79	289.18	frac 3	30		
13	Unlabelled	IFDKPEDFIAER	99	1478.68	1478.74	289.22	frac 1	20		
	iTRAQ 6	IFDKPEDFIAER	99	1767.91	1767.95	289.22	frac 4	26	26.17	6.17
	iTRAQ 7	IFDKPEDFIAER	99	1767.93	1767.95	289.22	frac 3	26.25		
	iTRAQ 8	IFDKPEDFIAER	99	1767.93	1767.95	289.22	frac 3	26.25		

14	Unlabelled	GLFTSDQILFTDTR	99	1612.80	1612.79		frac 1	24		
	iTRAQ 6	GLFTSDQILFTDTR	99	1757.89	1757.92	145.13	frac 4	30	30	6
	iTRAQ 8	GLFTSDQILFTDTR	99	1757.89	1757.92	145.13	frac 3	30		
	iTRAQ 9	GLFTSDQILFTDTR	99	1757.83	1757.92	145.13	frac 3	30		
15	Unlabelled	TTPSYVAFTDSER	99	1472.60	1472.66	145.13	frac 1	19	22.33	3.33
	iTRAQ 3	TTPSYVAFTDSER	99	1617.86	1617.79	145.13	frac 3	22.5		
	iTRAQ 6	TTPSYVAFTDSER	99	1617.78	1617.79	145.13	frac 4	22		
	iTRAQ 9	TTPSYVAFTDSER	99	1617.72	1617.79	145.13	frac 3	22.5		
16	Unlabelled	LDTGNFSWGSEAVTR	99	1638.69	1638.76		frac 1	22	25.42	3.42
	iTRAQ 6	LDTGNFSWGSEAVTR	99	1783.74	1783.87	145.11	frac 4	25		
	iTRAQ 8	LDTGNFSWGSEAVTR	99	1783.85	1783.87	145.11	frac 2,3	25.5		
	iTRAQ 9	LDTGNFSWGSEAVTR	99	1783.81	1783.87	145.11	frac 3	25.75		
17	Unlabelled	LWQVPETLPAEVVGK	99	1664.87	1664.93		frac 2	28.5	29.67	1.17
	iTRAQ 4	LWQVPETLPAEVVGK	99	1954.26	1954.13	289.19	frac 4	30.5		
	iTRAQ 6	LWQVPETLPAEVVGK	99	1954.09	1954.13	289.19	frac 3	29.25		
	iTRAQ 8	LWQVPETLPAEVVGK	99	1954.09	1954.13	289.19	frac 3	29.25		
18	Unlabelled	QLDAHIEEQFGGGR	99	1555.68	1555.73		frac 2	21.75	22.6	0.85
	iTRAQ 1	QLDAHIEEQFGGGR	99	1700.90	1700.85	145.11	frac 3	23		
	iTRAQ 3	QLDAHIEEQFGGGR	99	1700.91	1700.85	145.11	frac 3	22.5		
	iTRAQ 4	QLDAHIEEQFGGGR	99	1700.95	1700.85	145.11	frac 4	23		
	iTRAQ 6	QLDAHIEEQFGGGR	99	1700.73	1700.85	145.11	frac 4	22		
	iTRAQ 9	QLDAHIEEQFGGGR	99	1700.79	1700.85	145.11	frac 3	22.5		
19	Unlabelled	GFGFVTFAEEK	99	1230.60	1230.61		frac 2	28.5	28.9	0.4
	iTRAQ 1	GFGFVTFAEEK	99	1519.88	1519.80	289.19	frac 3	29.5		
	iTRAQ 3	GFGFVTFAEEK	99	1519.88	1519.80	289.19	frac 3	29		

	iTRAQ 4	GFGFVTFAEEK	99	1519.90	1519.80	289.19	frac 3,4	29.5		
	iTRAQ 6	GFGFVTFAEEK	99	1519.68	1519.80	289.19	frac 4	28		
	iTRAQ 8	GFGFVTFAEEK	99	1519.78	1519.80	289.19	frac 3	28.5		
20	Unlabelled	AFLVEEQK	99	962.50	962.51		frac 2	21.75		
	iTRAQ 1	AFLVEEQK	99	1251.75	1251.72	289.21	frac 3	21.5	21.91	0.16
	iTRAQ 2	AFLVEEQK	99	1251.70	1251.72	289.21	frac 3	21.5		
	iTRAQ 3	AFLVEEQK	99	1251.76	1251.72	289.21	frac 3	22		
	iTRAQ 4	AFLVEEQK	99	1251.80	1251.72	289.21	frac 4	22		
	iTRAQ 6	AFLVEEQK	99	1251.76	1251.72	289.21	frac 4	21.5		
	iTRAQ 7	AFLVEEQK	99	1251.70	1251.72	289.21	frac 3	22.5		
	iTRAQ 8	AFLVEEQK	99	1251.72	1251.72	289.21	frac 3	22.5		
	iTRAQ 9	AFLVEEQK	99	1251.64	1251.72	289.21	frac 3, 4	21.75		
21	Unlabelled	IFEGEALLR	99	1046.60	1046.59		frac 2	25.5		
	iTRAQ 1	IFEGEALLR	99	1191.74	1191.69	145.10	frac 3	28.5	27.86	2.36
	iTRAQ 3	IFEGEALLR	99	1191.74	1191.69	145.10	frac 3	28		
	iTRAQ 4	IFEGEALLR	99	1191.77	1191.69	145.10	frac 4	28.5		
	iTRAQ 5	IFEGEALLR	99	1191.72	1191.69	145.10	frac 4	27.5		
	iTRAQ 6	IFEGEALLR	99	1191.61	1191.69	145.10	frac 4	27		
	iTRAQ 8	IFEGEALLR	99	1191.67	1191.69	145.10	frac 3	27.75		
	iTRAQ 9	IFEGEALLR	99	1191.64	1191.69	145.10	frac 3,4	27.75		
22	Unlabelled	ISGLIYEETR	99	1179.61	1179.61		frac 2	22.5		
	iTRAQ 1	ISGLIYEETR	99	1324.77	1324.72	145.11	frac 1,2,3	26	25.21	2.71
	iTRAQ 2	ISGLIYEETR	99	1324.73	1324.72	145.11	frac 3	25		
	iTRAQ 3	ISGLIYEETR	99	1324.78	1324.72	145.11	frac 3,4	25.5		
	iTRAQ 4	ISGLIYEETR	99	1324.79	1324.72	145.11	frac 3,4	25.5		
	iTRAQ 6	ISGLIYEETR	99	1324.64	1324.72	145.11	frac 3,4	25		
	iTRAQ 8	ISGLIYEETR	99	1324.72	1324.72	145.11	frac 1,2,3	24.75		
	iTRAQ 9	ISGLIYEETR	99	1324.67	1324.72	145.11	frac 3	24.75		

23	Unlabelled	TTAEEGVVALWR	99	1330.73	1330.71		frac 2	27.75		
	iTRAQ 1	TTAEEGVVALWR	99	1475.87	1475.80	145.09	frac 3	29	28.43	0.68
	iTRAQ 2	TTAEEGVVALWR	99	1475.82	1475.80	145.09	frac 3	28		
	iTRAQ 3	TTAEEGVVALWR	99	1475.87	1475.80	145.09	frac 3	28.5		
	iTRAQ 4	TTAEEGVVALWR	99	1475.90	1475.80	145.09	frac 4	29		
	iTRAQ 6	TTAEEGVVALWR	99	1475.79	1475.80	145.09	frac 4	29		
	iTRAQ 8	TTAEEGVVALWR	99	1475.78	1475.80	145.09	frac 3	27.75		
	iTRAQ 9	TTAEEGVVALWR	99	1475.74	1475.80	145.09	frac 3	27.75		
24	Unlabelled	LLIQNQDEMIK	99	1343.72	1343.72		frac 2	23.25		
	iTRAQ 1	LLIQNQDEMIK	99	1632.98	1632.92	289.21	frac 3	25	24.42	1.17
	iTRAQ 2	LLIQNQDEMIK	99	1632.91	1632.92	289.21	frac 3	24		
	iTRAQ 3	LLIQNQDEMIK	99	1632.99	1632.92	289.21	frac 3	24.5		
	iTRAQ 4	LLIQNQDEMIK	99	1633.01	1632.92	289.21	frac 3,4	25		
	iTRAQ 6	LLIQNQDEMIK	99	1632.98	1632.92	289.21	frac 3,4	24		
	iTRAQ 9	LLIQNQDEMIK	99	1632.84	1632.92	289.21	frac 3,4	24		
25	Unlabelled	IQDKEGIPPDQQR	99	1522.75	1522.77		frac 2	20.25		
	iTRAQ 1	IQDKEGIPPDQQR	99	1812.04	1811.99	289.22	frac 3	20	19.79	-0.46
	iTRAQ 2	IQDKEGIPPDQQR	99	1811.98	1811.99	289.22	frac 3	19.5		
	iTRAQ 3	IQDKEGIPPDQQR	99	1812.06	1811.99	289.22	frac 3	18.5		
	iTRAQ 4	IQDKEGIPPDQQR	99	1812.11	1811.99	289.22	frac 3	20		
	iTRAQ 6	IQDKEGIPPDQQR	99	1811.99	1811.99	289.22	frac 4	20		
	iTRAQ 8	IQDKEGIPPDQQR	99	1812.00	1811.99	289.22	frac 3	20.25		
	iTRAQ 9	IQDKEGIPPDQQR	99	1811.91	1811.99	289.22	frac 3	20.25		
26	Unlabelled	TMVYPEAGFELQR	99	1539.75	1539.74		frac 2	24.75		
	iTRAQ 1	TMVYPEAGFELQR	99	1684.92	1684.85	145.10	frac 3	26.5	25.75	1
	iTRAQ 3	TMVYPEAGFELQR	99	1684.93	1684.85	145.10	frac 3	26		
	iTRAQ 4	TMVYPEAGFELQR	99	1684.95	1684.85	145.10	frac 3,4	26		

	iTRAQ 6	TMVYPEAGFELQR	99	1684.87	1684.85	145.10	frac 4	25		
	iTRAQ 8	TMVYPEAGFELQR	99	1684.83	1684.85	145.10	frac 3	25.5		
	iTRAQ 9	TMVYPEAGFELQR	99	1684.78	1684.85	145.10	frac 3,4	25.5		
27	Unlabelled	EQDVSLGANKFPER	99	1588.76	1588.77		frac 2	21		
	iTRAQ 1	EQDVSLGANKFPER	99	1878.05	1878.00	289.22	frac 3	21	20.86	-0.14
	iTRAQ 2	EQDVSLGANKFPER	99	1877.97	1878.00	289.22	frac 3	20.5		
	iTRAQ 3	EQDVSLGANKFPER	99	1878.07	1878.00	289.22	frac 3	20.5		
	iTRAQ 4	EQDVSLGANKFPER	99	1878.13	1878.00	289.22	frac 3,4	21		
	iTRAQ 6	EQDVSLGANKFPER	99	1877.86	1878.00	289.22	frac 3,4	21		
	iTRAQ 8	EQDVSLGANKFPER	99	1877.99	1878.00	289.22	frac 3	21		
	iTRAQ 9	EQDVSLGANKFPER	99	1877.91	1878.00	289.22	frac 3,4	21		
28	Unlabelled	GQGGIQQLLAAEQEAQR	99	1795.94	1795.93		frac 2	25.5		
	iTRAQ 1	GQGGIQQLLAAEQEAQR	99	1941.09	1941.03	145.10	frac 3	27	26.45	0.95
	iTRAQ 3	GQGGIQQLLAAEQEAQR	99	1941.12	1941.03	145.10	frac 3	26.5		
	iTRAQ 4	GQGGIQQLLAAEQEAQR	99	1941.13	1941.03	145.10	frac 4	27		
	iTRAQ 6	GQGGIQQLLAAEQEAQR	99	1941.10	1941.03	145.10	frac 4	25.5		
	iTRAQ 8	GQGGIQQLLAAEQEAQR	99	1940.99	1941.03	145.10	frac 3	26.25		
29	Unlabelled	QYAVFDEK	99	981.44	981.46		frac 2	23.25		
	iTRAQ 1	QYAVFDEK	99	1287.72	1287.68	306.22	frac 3	22	21.7	-1.55
	iTRAQ 3	QYAVFDEK	99	1287.73	1287.68	306.22	frac 3	21.5		
	iTRAQ 6	QYAVFDEK	99	1287.63	1287.68	306.22	frac 4	21.5		
	iTRAQ 8	QYAVFDEK	99	1287.68	1287.68	306.22	frac 3	21.75		
	iTRAQ 9	QYAVFDEK	99	1287.61	1287.68	306.22	frac 3	21.75		
30	Unlabelled	QLDSHIEEQFGGGR	99	1554.70	1554.71		frac 2	23.25		
	iTRAQ 1	QLDSHIEEQFGGGR	99	1716.89	1716.84	162.13	frac 3	22.5	22.13	-1.13
	iTRAQ 3	QLDSHIEEQFGGGR	99	1716.91	1716.84	162.13	frac 3	22		
	iTRAQ 4	QLDSHIEEQFGGGR	99	1716.95	1716.84	162.13	frac 4	22.5		

	iTRAQ 6	QLDSHIEEQFGGGR	99	1716.88	1716.84	162.13	frac 4	21.5		
	iTRAQ 7	QLDSHIEEQFGGGR	99	1716.81	1716.84	162.13	frac 3	22.5		
	iTRAQ 9	QLDSHIEEQFGGGR	99	1716.83	1716.84	162.13	frac 3	21.75		
31	Unlabelled	FDVGVKEIEGWTAR	99	1605.76	1605.84		frac 2	27	28.67	1.67
	iTRAQ 4	FDVGVKEIEGWTAR	99	1895.15	1895.03	289.19	frac 4	29.5		
	iTRAQ 6	FDVGVKEIEGWTAR	99	1894.88	1895.03	289.19	frac 4	28		
	iTRAQ 8	FDVGVKEIEGWTAR	99	1895.00	1895.03	289.19	frac 3	28.5		
32	Unlabelled	HFEVDLSAFR	99	1220.61	1219.61		frac 3	27.75	27.75	0
	iTRAQ 7	HFEVDLSAFR	99	1364.70	1364.71	145.10	frac 4	27.75		
	iTRAQ 8	HFEVDLSAFR	99	1364.69	1364.71	145.10	frac 4	27.75		
	iTRAQ 9	HFEVDLSAFR	99	1364.65	1364.71	145.10	frac 4	27.75		
33	Unlabelled	CALVYGQMNEPPGAR	99	1661.75	1661.78		frac 4	21.75		
	iTRAQ 1	CALVYGQMNEPPGAR	99	1806.93	1806.87	145.10	frac 6	22	21.79	0.04
	iTRAQ 2	CALVYGQMNEPPGAR	99	1806.89	1806.87	145.10	frac 6	21.5		
	iTRAQ 3	CALVYGQMNEPPGAR	99	1806.94	1806.87	145.10	frac 6	21.5		
	iTRAQ 4	CALVYGQMNEPPGAR	99	1806.98	1806.87	145.10	frac 5,6,7,8	22		
	iTRAQ 6	CALVYGQMNEPPGAR	99	1806.76	1806.87	145.10	frac 6,7	22		
	iTRAQ 8	CALVYGQMNEPPGAR	99	1806.82	1806.87	145.10	frac 6	21.75		
	iTRAQ 9	CALVYGQMNEPPGAR	99	1806.81	1806.87	145.10	frac 6	21.75		
34	Unlabelled	NAVVTVPAYFNDSQR	99	1679.81	1679.84		frac 4	24		
	iTRAQ 1	NAVVTVPAYFNDSQR	99	1825.00	1824.94	145.10	frac 5,6	25	24.36	0.36
	iTRAQ 2	NAVVTVPAYFNDSQR	99	1824.93	1824.94	145.10	frac 5,6	24		
	iTRAQ 3	NAVVTVPAYFNDSQR	99	1825.02	1824.94	145.10	frac 5,6	24.5		
	iTRAQ 4	NAVVTVPAYFNDSQR	99	1825.02	1824.94	145.10	frac 6	24.5		
	iTRAQ 6	NAVVTVPAYFNDSQR	99	1824.82	1824.94	145.10	frac 5,6	24.5		
	iTRAQ 8	NAVVTVPAYFNDSQR	99	1824.89	1824.94	145.10	frac 5, 6,7	24		

	iTRAQ 9	NAVVTVPAYFNDSQR	99	1824.87	1824.94	145.10	frac 5,6	24		
35	Unlabelled	QPTELELAQAFHQGK	99	1695.85	1695.85		frac 4	24.75		
	iTRAQ 1	QPTELELAQAFHQGK	99	1985.13	1985.07	289.22	frac 4	25.5	25.08	0.33
	iTRAQ 3	QPTELELAQAFHQGK	99	1985.17	1985.07	289.22	frac 5	25		
	iTRAQ 4	QPTELELAQAFHQGK	99	1985.18	1985.07	289.22	frac 5	26		
	iTRAQ 6	QPTELELAQAFHQGK	99	1984.92	1985.07	289.22	frac 5	24.5		
	iTRAQ 8	QPTELELAQAFHQGK	99	1985.01	1985.07	289.22	frac 5	24.75		
	iTRAQ 9	QPTELELAQAFHQGK	99	1984.98	1985.07	289.22	frac 5	24.75		
36	Unlabelled	TALTYVDNNDGSWHR	99	1747.81	1747.80		frac 4	22.5		
	iTRAQ 1	TALTYVDNNDGSWHR	99	1892.96	1892.90	145.10	frac 5	22.5	22.6	0.1
	iTRAQ 3	TALTYVDNNDGSWHR	99	1892.99	1892.90	145.10	frac 5	22.5		
	iTRAQ 4	TALTYVDNNDGSWHR	99	1893.01	1892.90	145.10	frac 5	23		
	iTRAQ 6	TALTYVDNNDGSWHR	99	1892.76	1892.90	145.10	frac 5	22.5		
	iTRAQ 9	TALTYVDNNDGSWHR	99	1892.84	1892.90	145.10	frac 5	22.5		
37	Unlabelled	QQFPLALYQVDK	99	1448.75	1448.78		frac 4	27		
	iTRAQ 4	QQFPLALYQVDK	99	1738.06	1737.98	289.20	frac 6	27.5	26.92	-0.08
	iTRAQ 8	QQFPLALYQVDK	99	1737.92	1737.98	289.20	frac 4,5, 6	27		
	iTRAQ 9	QQFPLALYQVDK	99	1737.89	1737.98	289.20	frac 5	26.25		
38	Unlabelled	ADGFAGVFPEHK	99	1273.58	1273.60		frac 4	23.25		
	iTRAQ 5	ADGFAGVFPEHK	99	1562.87	1562.82	289.22	frac 5	23	24	0.75
	iTRAQ 8	ADGFAGVFPEHK	99	1562.84	1562.82	289.22	frac 5	25		
	iTRAQ 9	ADGFAGVFPEHK	99	1562.76	1562.82	289.22	frac 5	24		
39	Unlabelled	SLEGLQANVQR	99	1213.61	1213.63		frac 4	20.25		
	iTRAQ 1	SLEGLQANVQR	99	1358.82	1358.75	145.13	frac 6	21	21	0.75
	iTRAQ 7	SLEGLQANVQR	99	1358.72	1358.75	145.13	frac 6	21		
	iTRAQ 8	SLEGLQANVQR	99	1358.72	1358.75	145.13	frac 6	21		

	iTRAQ 9	SLEGLQANVQR	99	1358.70	1358.75	145.13	frac 6	21		
40	Unlabelled	TFDNVYYK	99	1048.46	1048.47		frac 4	21		
	iTRAQ 1	TFDNVYYK	99	1337.74	1337.70	289.23	frac 5	22	21.9	0.9
	iTRAQ 5	TFDNVYYK	99	1337.74	1337.70	289.23	frac 5	21		
	iTRAQ 6	TFDNVYYK	99	1337.59	1337.70	289.23	frac 5	21.5		
	iTRAQ 8	TFDNVYYK	99	1337.68	1337.70	289.23	frac 5	21.75		
	iTRAQ 9	TFDNVYYK	99	1337.76	1337.70	289.23	frac 5	23.25		
41	Unlabelled	MLSPLILGDEHYQTAR	99	1842.91	1842.96		frac 4	27.75		
	iTRAQ 3	MLSPLILGDEHYQTAR	99	1988.16	1988.04	145.08	frac 5	29	28.5	0.75
	iTRAQ 6	MLSPLILGDEHYQTAR	99	1988.04	1988.04	145.08	frac 5	28		
	iTRAQ 8	MLSPLILGDEHYQTAR	99	1987.96	1988.04	145.08	frac 5	28.5		
42	Unlabelled	SSFDAFQQILK	99	1282.65	1282.67		frac 4	28.5		
	iTRAQ 3	SSFDAFQQILK	99	1571.95	1571.87	289.20	frac 5	29	28.42	-0.08
	iTRAQ 8	SSFDAFQQILK	99	1571.81	1571.87	289.20	frac 4.5	28.5		
	iTRAQ 9	SSFDAFQQILK	99	1571.79	1571.87	289.20	frac 5	27.75		
43	Unlabelled	SSDFLMYGIK	99	1159.55	1159.57		frac 4	27		
	iTRAQ 2	SSDFLMYGIK	99	1448.83	1448.77	289.20	frac 5	28	27.33	0.33
	iTRAQ 8	SSDFLMYGIK	99	1448.73	1448.77	289.20	frac 5	27		
	iTRAQ 9	SSDFLMYGIK	99	1448.71	1448.77	289.20	frac 5	27		
44	Unlabelled	SSMDAFQQILK	99	1282.65	1282.67		frac 4	28.5		
	iTRAQ 7	SSMDAFQQILK	99	1571.75	1571.83	289.17	frac 5	28.5	28.25	-0.25
	iTRAQ 8	SSMDAFQQILK	99	1571.81	1571.83	289.17	frac 4,5	28.5		
	iTRAQ 9	SSMDAFQQILK	99	1571.79	1571.83	289.17	frac 5	27.75		
45	Unlabelled	FTQANSEVSALLGR	99	1491.75	1491.77		frac 5	25.5		
	iTRAQ 4	FTQANSEVSALLGR	99	1636.97	1636.88	145.11	frac 6	28	27.08	1.58

	iTRAQ 6	FTQANSEVSALLGR	99	1636.87	1636.88	145.11	frac 6	27		
	iTRAQ 8	FTQANSEVSALLGR	99	1636.75	1636.88	145.11	frac 6	26.25		
46	Unlabelled	STLVWEVR	99	988.59	988.56		frac 5	25.5		
	iTRAQ 1	STLVWEVR	99	1133.70	1133.64	145.08	frac 6	26.5	25.69	0.19
	iTRAQ 2	STLVWEVR	99	1133.67	1133.64	145.08	frac 6	25.5		
	iTRAQ 3	STLVWEVR	99	1133.69	1133.64	145.08	frac 6	25.5		
	iTRAQ 4	STLVWEVR	99	1133.71	1133.64	145.08	frac 6	26		
	iTRAQ 6	STLVWEVR	99	1133.57	1133.64	145.08	frac 6	25.5		
	iTRAQ 7	STLVWEVR	99	1133.67	1133.64	145.08	frac 6	25.5		
	iTRAQ 8	STLVWEVR	99	1133.60	1133.64	145.08	frac 6	25.5		
	iTRAQ 9	STLVWEVR	99	1133.60	1133.64	145.08	frac 6	25.5		
47	Unlabelled	IFLENVIR	99	1002.65	1002.62		frac 5	27.75		
	iTRAQ 1	IFLENVIR	99	1147.77	1147.70	145.07	frac 6	30.5	29.59	1.84
	iTRAQ 2	IFLENVIR	99	1147.74	1147.70	145.07	frac 6	29.5		
	iTRAQ 3	IFLENVIR	99	1147.75	1147.70	145.07	frac 6	30		
	iTRAQ 4	IFLENVIR	99	1147.77	1147.70	145.07	frac 6	30		
	iTRAQ 6	IFLENVIR	99	1147.65	1147.70	145.07	frac 6	29		
	iTRAQ 7	IFLENVIR	99	1147.65	1147.70	145.07	frac 6	29.25		
	iTRAQ 8	IFLENVIR	99	1147.64	1147.70	145.07	frac 6	29.25		
	iTRAQ 9	IFLENVIR	99	1147.66	1147.70	145.07	frac 6,7	29.25		
48	Unlabelled	FFCEFCGK	99	1093.53	1093.48		frac 5	24		
	iTRAQ 1	FFCEFCGK	99	1382.72	1382.65	289.17	frac 6	27	26.21	2.21
	iTRAQ 3	FFCEFCGK	99	1382.71	1382.65	289.17	frac 6	26		
	iTRAQ 4	FFCEFCGK	99	1382.71	1382.65	289.17	frac 6	26.5		
	iTRAQ 6	FFCEFCGK	99	1382.55	1382.65	289.17	frac 6	26		
	iTRAQ 8	FFCEFCGK	99	1382.60	1382.65	289.17	frac 6	25.5		
	iTRAQ 9	FFCEFCGK	99	1382.60	1382.65	289.17	frac 6	26.25		

49	Unlabelled	EVAGFAPYEKR	99	1265.66	1265.65		frac 5,6	21.75		
	iTRAQ 1	EVAGFAPYEKR	99	1554.90	1554.85	289.20	frac 6	22	21.75	0
	iTRAQ 3	EVAGFAPYEKR	99	1554.91	1554.85	289.20	frac 6	21.5		
	iTRAQ 4	EVAGFAPYEKR	99	1554.95	1554.85	289.20	frac 6	21.5		
	iTRAQ 6	EVAGFAPYEKR	99	1554.74	1554.85	289.20	frac 6	22		
	iTRAQ 8	EVAGFAPYEKR	99	1554.80	1554.85	289.20	frac 6	21.75		
	iTRAQ 9	EVAGFAPYEKR	99	1554.81	1554.85	289.20	frac 6	21.75		
50	Unlabelled	SFGPAVIFNNEK	99	1321.74	1321.70		frac 5	26.25		
	iTRAQ 1	SFGPAVIFNNEK	99	1610.96	1610.88	289.18	frac 2,6	27	26.36	0.11
	iTRAQ 2	SFGPAVIFNNEK	99	1610.89	1610.88	289.18	frac 6	26		
	iTRAQ 3	SFGPAVIFNNEK	99	1610.95	1610.88	289.18	frac 6	26.5		
	iTRAQ 4	SFGPAVIFNNEK	99	1610.95	1610.88	289.18	frac 6	26.5		
	iTRAQ 6	SFGPAVIFNNEK	99	1610.77	1610.88	289.18	frac 6	26		
	iTRAQ 8	SFGPAVIFNNEK	99	1610.82	1610.88	289.18	frac 6	26.25		
	iTRAQ 9	SFGPAVIFNNEK	99	1610.81	1610.88	289.18	frac 6	26.25		
51	Unlabelled	VALINYGPEYGR	99	1350.80	1350.75		frac 5	24		
	iTRAQ 1	VALINYGPEYGR	99	1495.87	1495.80	145.06	frac 6	25	24.17	0.17
	iTRAQ 2	VALINYGPEYGR	99	1495.82	1495.80	145.06	frac 6	24		
	iTRAQ 3	VALINYGPEYGR	99	1495.86	1495.80	145.06	frac 6	24		
	iTRAQ 6	VALINYGPEYGR	99	1495.69	1495.80	145.06	frac 6	24		
	iTRAQ 8	VALINYGPEYGR	99	1495.76	1495.80	145.06	frac 6,7	24		
	iTRAQ 9	VALINYGPEYGR	99	1495.75	1495.80	145.06	frac 6	24		
52	Unlabelled	YIAPEQVPVK	99	1142.63	1142.63		frac 5	21		
	iTRAQ 1	YIAPEQVPVK	99	1431.88	1431.85	289.21	frac 5,6	21.5	21.5	0.5
	iTRAQ 7	YIAPEQVPVK	99	1431.82	1431.85	289.21	frac 5,6	21.75		
	iTRAQ 8	YIAPEQVPVK	99	1431.82	1431.85	289.21	frac 5,6	21.75		
	iTRAQ 9	YIAPEQVPVK	99	1431.77	1431.85	289.21	frac 5	21		

53	Unlabelled	VEPLVNMGQITR	99	1355.71	1355.72		frac 5	24		
	iTRAQ 1	VEPLVNMGQITR	99	1500.90	1500.83	145.12	frac 6	26	25.41	1.41
	iTRAQ 2	VEPLVNMGQITR	99	1500.84	1500.83	145.12	frac 6	25		
	iTRAQ 3	VEPLVNMGQITR	99	1500.90	1500.83	145.12	frac 6	25.5		
	iTRAQ 4	VEPLVNMGQITR	99	1500.90	1500.83	145.12	frac 6	25.5		
	iTRAQ 5	VEPLVNMGQITR	99	1500.89	1500.83	145.12	frac 6	25.5		
	iTRAQ 6	VEPLVNMGQITR	99	1500.73	1500.83	145.12	frac 6, 7	25.5		
	iTRAQ 8	VEPLVNMGQITR	99	1500.78	1500.83	145.12	frac 6	24.75		
	iTRAQ 9	VEPLVNMGQITR	99	1500.77	1500.83	145.12	frac 6	25.5		
54	Unlabelled	AYEPILLLGR	99	1143.67	1143.67		frac 5	30		
	iTRAQ 6	AYEPILLLGR	99	1288.66	1288.77	145.10	frac 6	30	30.25	0.25
	iTRAQ 8	AYEPILLLGR	99	1288.72	1288.77	145.10	frac 6	30		
	iTRAQ 9	AYEPILLLGR	99	1288.74	1288.77	145.10	frac 6	30.75		
55	Unlabelled	LVGEYGLR	99	905.49	905.51		frac 5	22.5		
	iTRAQ 6	LVGEYGLR	99	1050.54	1050.61	145.10	frac 6	23.5	23.31	0.81
	iTRAQ 7	LVGEYGLR	99	1050.60	1050.61	145.10	frac 6	23.25		
	iTRAQ 8	LVGEYGLR	99	1050.58	1050.61	145.10	frac 6	23.25		
	iTRAQ 9	LVGEYGLR	99	1050.57	1050.61	145.10	frac 6	23.25		
56	Unlabelled	EALGGLPLYQR	99		1215.66		frac 5	24.75		
	iTRAQ 1	EALGGLPLYQR	99	1360.83	1360.77	145.11	frac 6	26	25.15	0.4
	iTRAQ 2	EALGGLPLYQR	99	1360.78	1360.77	145.11	frac 6	25		
	iTRAQ 3	EALGGLPLYQR	99	1360.83	1360.77	145.11	frac 6	25		
	iTRAQ 6	EALGGLPLYQR	99	1360.68	1360.77	145.11	frac 6,7	25		
	iTRAQ 9	EALGGLPLYQR	99	1360.72	1360.77	145.11	frac 5	24.75		
57	Unlabelled	ADAFLLVGTQPR	99		1286.70		frac 5	26.25		
	iTRAQ 3	ADAFLLVGTQPR	99	1431.88	1431.81	145.10	frac 6	26	26.83	0.58
	iTRAQ 4	ADAFLLVGTQPR	99	1431.86	1431.81	145.10	frac 7	27.5		

	iTRAQ 6	ADAFLLVGTQPR	99	1431.72	1431.81	145.10	frac 6	27		
58	Unlabelled	HGWEYVVK	99	1016.50	1016.51		frac 6	22.5		
	iTRAQ 1	HGWEYVVK	99	1305.79	1305.72	289.21	frac 8	23.5	23.22	0.72
	iTRAQ 2	HGWEYVVK	99	1305.71	1305.72	289.21	frac 8	23		
	iTRAQ 3	HGWEYVVK	99	1305.76	1305.72	289.21	frac 8	23.5		
	iTRAQ 4	HGWEYVVK	99	1305.75	1305.72	289.21	frac 8	23.5		
	iTRAQ 5	HGWEYVVK	99	1305.77	1305.72	289.21	frac 8	23		
	iTRAQ 6	HGWEYVVK	99	1305.66	1305.72	289.21	frac 8	23		
	iTRAQ 8	HGWEYVVK	99	1305.67	1305.72	289.21	frac 8	23		
	iTRAQ 9	HGWEYVVK	99	1305.73	1305.72	289.21	frac 8	23.25		
59	Unlabelled	FVIGGPHGDAGLTGR	99	1452.76	1452.75		frac 7	23.25		
	iTRAQ 1	FVIGGPHGDAGLTGR	99	1597.94	1597.86	145.10	frac 8	24	23.5	0.25
	iTRAQ 2	FVIGGPHGDAGLTGR	98	1597.85	1597.86	145.10	frac 8	23.5		
	iTRAQ 3	FVIGGPHGDAGLTGR	99	1597.91	1597.86	145.10	frac 8	23.5		
	iTRAQ 4	FVIGGPHGDAGLTGR	98	1597.92	1597.86	145.10	frac 9	23.5		
	iTRAQ 6	FVIGGPHGDAGLTGR	99	1597.77	1597.86	145.10	frac 8	23.5		
	iTRAQ 8	FVIGGPHGDAGLTGR	99	1597.80	1597.86	145.10	frac 8	23.25		
	iTRAQ 9	FVIGGPHGDAGLTGR	99	1597.83	1597.86	145.10	frac 8	23.25		
60	Unlabelled	THAVVEPFVIATNR	99	1552.88	1552.86		frac 7	25.5		
	iTRAQ 2	THAVVEPFVIATNR	99	1697.94	1697.95	145.09	frac 8	25.5	25.6	0.1
	iTRAQ 3	THAVVEPFVIATNR	99	1698.01	1697.95	145.09	frac 8	26		
	iTRAQ 5	THAVVEPFVIATNR	99	1698.02	1697.95	145.09	frac 8	25.5		
	iTRAQ 8	THAVVEPFVIATNR	99	1697.89	1697.95	145.09	frac 8, 9	25.5		
	iTRAQ 9	THAVVEPFVIATNR	99	1697.90	1697.95	145.09	frac 8, 9	25.5		
61	Unlabelled	SVHEPMQTGLK	99	1225.63	1225.62		frac 7	21		
	iTRAQ 1	SVHEPMQTGLK	99	1514.90	1514.82	289.21	frac 8	20	19.92	-1.08
	iTRAQ 6	SVHEPMQTGLK	99	1514.90	1514.82	289.21	frac 8	19.5		

	iTRAQ 8	SVHEPMQTGLK	99	1514.78	1514.82	289.21	frac 8	20.25		
62	Unlabelled	SVVYALSPFQQK	99	1362.72	1365.74		frac 7	25.5		
	iTRAQ 2	SVVYALSPFQQK	99	1654.98	1654.94	289.20	frac 10	27	26.46	0.96
	iTRAQ 3	SVVYALSPFQQK	99	1654.98	1654.94	289.20	frac 10	27		
	iTRAQ 6	SVVYALSPFQQK	99	1654.81	1654.94	289.20	frac 10	26		
	iTRAQ 7	SVVYALSPFQQK	99	1654.92	1654.94	289.20	frac 10	26.25		
	iTRAQ 8	SVVYALSPFQQK	99	1654.85	1654.94	289.20	frac 10	26.25		
	iTRAQ 9	SVVYALSPFQQK	99	1654.84	1654.94	289.20	frac 10	26.25		
63	Unlabelled	YGGGANFVHDGYNK	99	1497.62	1497.61	289.27	frac 7	20.25		
	iTRAQ 1	YGGGANFVHDGYNK	99	1786.97	1786.88	289.27	frac 8	21	21	0.75
	iTRAQ 8	YGGGANFVHDGYNK	99	1786.83	1786.88	289.27	frac 8	21		
	iTRAQ 9	YGGGANFVHDGYNK	99	1786.83	1786.88	289.27	frac 8	21		
64	Unlabelled	LVNVFTIGK	99	989.49	989.60		frac 7	26		
	iTRAQ 3	LVNVFTIGK	99	1278.84	1278.80	289.20	frac 10	29	28.35	2.35
	iTRAQ 5	LVNVFTIGK	99	1278.86	1278.80	289.20	frac 10	28		
	iTRAQ 7	LVNVFTIGK	99	1278.81	1278.80	289.20	frac 10	28.5		
	iTRAQ 8	LVNVFTIGK	99	1278.76	1278.80	289.20	frac 10	27.75		
	iTRAQ 9	LVNVFTIGK	99	1278.84	1278.80	289.20	frac 9	28.5		
65	Unlabelled	TALTYIDGNGNWHR	99	1616.74	1616.76		frac 8	23.25		
	iTRAQ 1	TALTYIDGNGNWHR	99	1761.97	1761.88	145.12	frac 9	24.5	24.17	0.92
	iTRAQ 2	TALTYIDGNGNWHR	99	1761.90	1761.88	145.12	frac 9	24.5		
	iTRAQ 3	TALTYIDGNGNWHR	99	1761.92	1761.88	145.12	frac 9	24.5		
	iTRAQ 4	TALTYIDGNGNWHR	99	1761.94	1761.88	145.12	frac 9	24		
	iTRAQ 6	TALTYIDGNGNWHR	99	1761.87	1761.88	145.12	frac 9	23.5		
	iTRAQ 8	TALTYIDGNGNWHR	99	1761.81	1761.88	145.12	frac 9	24		
66	Unlabelled	AHLQDYIQTHYTAPR	99	1812.89	1812.89		frac 8	22.5		

	iTRAQ 3	AHLQDYIQTHYTAPR	99	1958.05	1958.00	145.11	frac 9	23.5	23	0.5
	iTRAQ 4	AHLQDYIQTHYTAPR	99	1958.08	1958.00	145.11	frac 9	23		
	iTRAQ 5	AHLQDYIQTHYTAPR	99	1958.09	1958.00	145.11	frac 9	22.5		
	iTRAQ 8	AHLQDYIQTHYTAPR	99	1958.06	1958.00	145.11	frac 9	23		
67	Unlabelled	NYTNAFQALYR	99	1359.66	1359.66		frac 10	27.75		
	iTRAQ 1	NYTNAFQALYR	99	1504.85	1504.77	145.11	frac 12	27.5	27.19	-0.56
	iTRAQ 2	NYTNAFQALYR	99	1504.82	1504.77	145.11	frac 12	27.5		
	iTRAQ 3	NYTNAFQALYR	99	1504.83	1504.77	145.11	frac 12	27.5		
	iTRAQ 4	NYTNAFQALYR	99	1504.83	1504.77	145.11	frac 12	27.5		
	iTRAQ 6	NYTNAFQALYR	99	1504.67	1504.77	145.11	frac 12	26.5		
	iTRAQ 7	NYTNAFQALYR	99	1504.74	1504.77	145.11	frac 12	27		
	iTRAQ 8	NYTNAFQALYR	99	1504.70	1504.77	145.11	frac 12	27		
	iTRAQ 9	NYTNAFQALYR	99	1504.70	1504.77	145.11	frac 12	27		
68	Unlabelled	TLHPNWSPAAIK	99	1333.66	1333.72		frac 10	22.5		
	iTRAQ 1	TLHPNWSPAAIK	99	1623.02	1622.93	289.21	frac 11	24	23.53	1.03
	iTRAQ 2	TLHPNWSPAAIK	99	1622.94	1622.93	289.21	frac 11	23.5		
	iTRAQ 3	TLHPNWSPAAIK	99	1622.96	1622.93	289.21	frac 11	23.5		
	iTRAQ 4	TLHPNWSPAAIK	99	1622.98	1622.93	289.21	frac 11	24		
	iTRAQ 5	TLHPNWSPAAIK	99	1622.97	1622.93	289.21	frac 11	23		
	iTRAQ 6	TLHPNWSPAAIK	99	1622.82	1622.93	289.21	frac 11	24		
	iTRAQ 7	TLHPNWSPAAIK	99	1622.90	1622.93	289.21	frac 11	23.25		
	iTRAQ 8	TLHPNWSPAAIK	99	1622.85	1622.93	289.21	frac 11	23.25		
	iTRAQ 9	TLHPNWSPAAIK	99	1623.91	1622.93	289.21	frac 11	23.25		
69	Unlabelled	FHQYQVVGR	99	1132.54	1132.56		frac 11	21		
	iTRAQ 3	FHQYQVVGR	99	1277.73	1277.69	145.13	frac 12	20.5	20.8	-0.2
	iTRAQ 4	FHQYQVVGR	99	1277.77	1277.69	145.13	frac 12	21		
	iTRAQ 5	FHQYQVVGR	99	1277.72	1277.69	145.13	frac 12	20.5		
	iTRAQ 8	FHQYQVVGR	99	1277.66	1277.69	145.13	frac 12	21		

	iTRAQ 9	FHQYQVVGR	99	1277.64	1277.69	145.13	frac 12	21		
70	Unlabelled	FQSLGVAFYR	99	1186.62	1186.64		frac 11	27		
	iTRAQ 6	FQSLGVAFYR	99	1331.65	1331.72	145.08	frac 12	27.5	26.75	-0.25
	iTRAQ 8	FQSLGVAFYR	99	1331.70	1331.72	145.08	frac 12	25		
	iTRAQ 9	FQSLGVAFYR	99	1331.65	1331.72	145.08	frac 12	27.75		

Group B: Peptides focused in the same OGE fraction.

		Sequence	Score	Obs mass	Theo mass	Modification	OGF	Rt (min)	Rt	Diff
1	Unlabelled	MFDAGLYEHCR*	99	1397.57	1397.58		frac 4	23.25		
	iTRAQ 1	MFDAGLYEHCR	99	1542.75	1542.69	145.12	frac 4	24.5	24.42	1.17
	iTRAQ 3	MFDAGLYEHCR	99	1542.77	1542.69	145.12	frac 4	24.5		
	iTRAQ 4	MFDAGLYEHCR	99	1542.78	1542.69	145.12	frac 5	25		
	iTRAQ 6	MFDAGLYEHCR	99	1542.59	1542.69	145.12	frac 5	24.5		
	iTRAQ 8	MFDAGLYEHCR	99	1542.70	1542.69	145.12	frac 4	24		
	iTRAQ 9	MFDAGLYEHCR	99	1542.63	1542.69	145.12	frac 4	24		
2	Unlabelled	EAFPGDVFYLHSR*	99	1536.77	1536.75		frac 4	27.75		
	iTRAQ 1	EAFPGDVFYLHSR	99	1681.93	1681.85	145.09	frac 4	28	28.08	0.33
	iTRAQ 3	EAFPGDVFYLHSR	99	1681.94	1681.85	145.09	frac 4	28.5		
	iTRAQ 4	EAFPGDVFYLHSR	95	1681.96	1681.85	145.09	frac 5	29		
	iTRAQ 6	EAFPGDVFYLHSR	99	1681.87	1681.85	145.09	frac 5	27.5		
	iTRAQ 8	EAFPGDVFYLHSR	99	1681.82	1681.85	145.09	frac 4	27.75		
	iTRAQ 9	EAFPGDVFYLHSR	99	1681.76	1681.85	145.09	frac 4	27.75		
3	Unlabelled	TLHGLQPPESSGIFNEK*	99	1852.92	1852.93		frac 4	24		
	iTRAQ 1	TLHGLQPPESSGIFNEK	99	2142.21	2142.14	289.22	frac 4	24	24.38	0.38
	iTRAQ 2	TLHGLQPPESSGIFNEK	99	2142.25	2142.14	289.22	frac 4	24.5		

	iTRAQ 4	TLHGLQPPESSGIFNEK	99	2142.25	2142.14	289.22	frac 5	25		
	iTRAQ 8	TLHGLQPPESSGIFNEK	99	2142.13	2142.14	289.22	frac 4	24		
4	Unlabelled	ATFDCLMK*	99	984.53	984.49		frac 5	23.25		
	iTRAQ 1	ATFDCLMK	99	1273.70	1273.65	289.16	frac 5	24	23.63	0.38
	iTRAQ 2	ATFDCLMK	99	1273.66	1273.65	289.16	frac 5	23.5		
	iTRAQ 3	ATFDCLMK	99	1273.72	1273.65	289.16	frac 5	23.5		
	iTRAQ 4	ATFDCLMK	99	1273.73	1273.65	289.16	frac 5,6	24		
	iTRAQ 6	ATFDCLMK	99	1273.56	1273.65	289.16	frac 6	23.5		
	iTRAQ 9	ATFDCLMK	99	1273.61	1273.65	289.16	frac 5	23.25		
5	Unlabelled	GIPYLNTYDGR*	99	1267.72	1267.67		frac 5,6	24		
	iTRAQ 1	GIPYLNTYDGR	99	1412.79	1412.73	145.06	frac 5,6	25	24.56	0.56
	iTRAQ 2	GIPYLNTYDGR	99	1412.74	1412.73	145.06	frac 5,6	24.5		
	iTRAQ 3	GIPYLNTYDGR	99	1412.79	1412.73	145.06	frac 5,6	24.5		
	iTRAQ 4	GIPYLNTYDGR	99	1412.80	1412.73	145.06	frac 5,6	24.5		
	iTRAQ 6	GIPYLNTYDGR	99	1412.63	1412.73	145.06	frac 5,6	24.5		
	iTRAQ 7	GIPYLNTYDGR	99	1412.71	1412.73	145.06	frac 5,6	24.75		
	iTRAQ 8	GIPYLNTYDGR	99	1412.69	1412.73	145.06	frac 5,6,7	24.75		
	iTRAQ 9	GIPYLNTYDGR	99	1412.69	1412.73	145.06	frac 5,6	24		
6	Unlabelled	GFGFVTFANEK	99	1215.66	1215.62		frac 2,6	28.5		
	iTRAQ 1	GFGFVTFANEK	99	1504.89	1504.80	289.18	frac 6	29	28	-0.5
	iTRAQ 2	GFGFVTFANEK	99	1504.85	1504.80	289.18	frac 6	28		
	iTRAQ 3	GFGFVTFANEK	99	1504.87	1504.80	289.18	frac 6	28		
	iTRAQ 4	GFGFVTFANEK	99	1504.88	1504.80	289.18	frac 6	28		
	iTRAQ 6	GFGFVTFANEK	99	1504.71	1504.80	289.18	frac 6	27.5		
	iTRAQ 8	GFGFVTFANEK	99	1504.74	1504.80	289.18	frac 6	27.75		
	iTRAQ 9	GFGFVTFANEK	99	1504.74	1504.80	289.18	frac 6	27.75		
7	Unlabelled	GKDFAELIASGR	99	1263.65	1262.67		frac 6	25.5		

	iTRAQ 1	GKDFAELIASGR	99	1551.96	1551.87	289.21	frac 6	27	25.83	0.33
	iTRAQ 3	GKDFAELIASGR	99	1551.94	1551.87	289.21	frac 6	26		
	iTRAQ 6	GKDFAELIASGR	99	1551.86	1551.87	289.21	frac 6	25.5		
	iTRAQ 7	GKDFAELIASGR	99	1551.74	1551.87	289.21	frac 6	25.5		
	iTRAQ 8	GKDFAELIASGR	99	1551.81	1551.87	289.21	frac 6	25.5		
	iTRAQ 9	GKDFAELIASGR	99	1551.81	1551.87	289.21	frac 6	25.5		
8	Unlabelled	AALNDFDRFK	99	1195.58	1195.60	289.21	frac 6	23.25		
	iTRAQ 3	AALNDFDRFK	99	1484.87	1484.81	289.21	frac 6	24	24	0.75
	iTRAQ 6	AALNDFDRFK	99	1484.71	1484.81	289.21	frac 6	24		
	iTRAQ 8	AALNDFDRFK	99	1484.77	1484.81	289.21	frac 6	24		
	iTRAQ 9	AALNDFDRFK	99	1484.76	1484.81	289.21	frac 6	24		
9	Unlabelled	EAQWAHAQR*	99	1095.52	1095.52		frac 8	21.75		
	iTRAQ 1	EAQWAHAQR	99	1240.70	1240.63	145.11	frac 8	19	19.07	-2.68
	iTRAQ 3	EAQWAHAQR	99	1240.67	1240.63	145.11	frac 8	19		
	iTRAQ 4	EAQWAHAQR	99	1240.70	1240.63	145.11	frac 9	19		
	iTRAQ 5	EAQWAHAQR	95	1240.68	1240.63	145.11	frac 9	19		
	iTRAQ 6	EAQWAHAQR	99	1240.56	1240.63	145.11	frac 8	18.5		
	iTRAQ 7	EAQWAHAQR	99	1240.65	1240.63	145.11	frac 8	19.5		
	iTRAQ 8	EAQWAHAQR	99	1240.59	1240.63	145.11	frac 8	19.5		
10	Unlabelled	SRFFHSTGQR*	99	1221.48	1221.54		frac 8	21.75		
	iTRAQ 1	SRFFHSTGQR	99	1366.73	1366.71	145.17	frac 8	21.5	21.4	-0.35
	iTRAQ 2	SRFFHSTGQR	99	1366.66	1366.71	145.17	frac 8	21.5		
	iTRAQ 3	SRFFHSTGQR	99	1366.70	1366.71	145.17	frac 9	21.5		
	iTRAQ 4	SRFFHSTGQR	99	1366.72	1366.71	145.17	frac 9	21.5		
	iTRAQ 6	SRFFHSTGQR	99	1366.72	1366.71	145.17	frac 8	21		
11	Unlabelled	AGDFFHSAQSR*	99	1221.56	1221.56		frac 8	21.75		
	iTRAQ 1	AGDFFHSAQSR	99	1366.73	1366.66	145.11	frac 8	21.5	21.5	-0.25

	iTRAQ 2	AGDFFHSAQSR	99	1366.66	1366.66	145.11	frac 8	21.5		
	iTRAQ 3	AGDFFHSAQSR	99	1366.70	1366.66	145.11	frac 9	21.5		
	iTRAQ 4	AGDFFHSAQSR	99	1366.72	1366.66	145.11	frac 9	21.5		
	iTRAQ 5	AGDFFHSAQSR	99	1366.72	1366.66	145.11	frac 9	21		
	iTRAQ 6	AGDFFHSAQSR	99	1366.59	1366.66	145.11	frac 8	21.5		
	iTRAQ 7	AGDFFHSAQSR	99	1366.64	1366.66	145.11	frac 8	21.75		
	iTRAQ 8	AGDFFHSAQSR	99	1366.62	1366.66	145.11	frac 8	21.75		
12	Unlabelled	ASALIQHDWSR*	99	1282.62	1282.63		frac 8	22.5		
	iTRAQ 1	ASALIQHDWSR	99	1427.83	1427.75	145.12	frac 8	23.5	22.83	0.33
	iTRAQ 2	ASALIQHDWSR	99	1427.75	1427.75	145.12	frac 8	22.5		
	iTRAQ 3	ASALIQHDWSR	99	1427.80	1427.75	145.12	frac 8	23		
	iTRAQ 4	ASALIQHDWSR	99	1427.81	1427.75	145.12	frac 8,9	22.5		
	iTRAQ 6	ASALIQHDWSR	99	1427.66	1427.75	145.12	frac 8	23		
	iTRAQ 8	ASALIQHDWSR	99	1427.71	1427.75	145.12	frac 8	22.5		
13	Unlabelled	AHGGFSVFAGVGER	99	1389.69	1389.69		frac 8	26.25		
	iTRAQ 2	AHGGFSVFAGVGER	99	1534.81	1534.79	145.10	frac 8	26	25.92	-0.33
	iTRAQ 3	AHGGFSVFAGVGER	99	1534.85	1534.79	145.10	frac 8	26.5		
	iTRAQ 5	AHGGFSVFAGVGER	99	1534.86	1534.79	145.10	frac 8	26		
	iTRAQ 6	AHGGFSVFAGVGER	99	1534.83	1534.79	145.10	frac 8	26		
	iTRAQ 8	AHGGFSVFAGVGER	99	1534.73	1534.79	145.10	frac 8	25.5		
	iTRAQ 9	AHGGFSVFAGVGER	99	1534.73	1534.79	145.10	frac 8	25.5		
14	Unlabelled	VGPFHNPSETYR	99	1402.63	1402.65		frac 8	21.75		
	iTRAQ 1	VGPFHNPSETYR	97	1547.85	1547.77	145.12	frac 8	21.5	21.43	-0.32
	iTRAQ 2	VGPFHNPSETYR	99	1547.77	1547.77	145.12	frac 8	21		
	iTRAQ 3	VGPFHNPSETYR	99	1547.82	1547.77	145.12	frac 8	21.5		
	iTRAQ 5	VGPFHNPSETYR	99	1547.83	1547.77	145.12	frac 8	21		
	iTRAQ 6	VGPFHNPSETYR	99	1547.69	1547.77	145.12	frac 8	21.5		
	iTRAQ 8	VGPFHNPSETYR	99	1547.73	1547.77	145.12	frac 8	21.75		

	iTRAQ 9	VGPFHNPSETYR	99	1547.73	1547.77	145.12	frac 8	21.75		
15	Unlabelled	GVDKEHVMLLAAR	99	1437.76	1437.77		frac 8	23.25		
	iTRAQ 1	GVDKEHVMLLAAR	99	1727.08	1726.99	289.22	frac 8	24	23.83	0.58
	iTRAQ 2	GVDKEHVMLLAAR	99	1726.97	1726.99	289.22	frac 8	23.5		
	iTRAQ 3	GVDKEHVMLLAAR	99	1727.04	1726.99	289.22	frac 8	24		
	iTRAQ 4	GVDKEHVMLLAAR	99	1727.05	1726.99	289.22	frac 8	24		
	iTRAQ 6	GVDKEHVMLLAAR	99	1726.89	1726.99	289.22	frac 8	24		
	iTRAQ 8	GVDKEHVMLLAAR	99	1726.93	1726.99	289.22	frac 8	23.5		
16	Unlabelled	EVHFLPFNPVDKR	99	1596.86	1596.85		frac 8	27		
	iTRAQ 3	EVHFLPFNPVDKR	99	1886.12	1886.05	289.20	frac 8	27.5	27.05	0.05
	iTRAQ 4	EVHFLPFNPVDKR	99	1886.13	1886.05	289.20	frac 8	27.5		
	iTRAQ 5	EVHFLPFNPVDKR	99	1886.14	1886.05	289.20	frac 8	27		
	iTRAQ 7	EVHFLPFNPVDKR	99	1886.13	1886.05	289.20	frac 8	27		
	iTRAQ 8	EVHFLPFNPVDKR	99	1885.98	1886.05	289.20	frac 8	26.25		
17	Unlabelled	EIHFLPFNPVDKR	99	1610.87	1610.87		frac 8	28.5		
	iTRAQ 3	EIHFLPFNPVDKR	99	1900.14	1900.07	289.20	frac 8	28.5	28	-0.5
	iTRAQ 4	EIHFLPFNPVDKR	99	1900.16	1900.07	289.20	frac 8	28.5		
	iTRAQ 5	EIHFLPFNPVDKR	99	1900.17	1900.07	289.20	frac 8	28		
	iTRAQ 6	EIHFLPFNPVDKR	99	1900.06	1900.07	289.20	frac 8	27.5		
	iTRAQ 8	EIHFLPFNPVDKR	99	1900.00	1900.07	289.20	frac 8	27.5		
18	Unlabelled	ALYHDLNAYR	99	1234.63	1234.61		frac 8	22.5		
	iTRAQ 6	ALYHDLNAYR	99	1379.64	1379.72	145.11	frac 8	23	23.19	0.69
	iTRAQ 7	ALYHDLNAYR	99	1379.71	1379.72	145.11	frac 8	23.25		
	iTRAQ 8	ALYHDLNAYR	99	1379.67	1379.72	145.11	frac 8	23.25		
	iTRAQ 9	ALYHDLNAYR	99	1379.70	1379.72	145.11	frac 8	23.25		
19	Unlabelled	AGVKPHELVF	99	1095.58	1095.61		frac 8	25.5		

	iTRAQ 1	AGVKPHELVF	99	1384.90	1384.82	289.21	frac 8	26	25.34	-0.16
	iTRAQ 2	AGVKPHELVF	99	1384.82	1384.82	289.21	frac 8	25.5		
	iTRAQ 3	AGVKPHELVF	99	1384.87	1384.82	289.21	frac 8	25.5		
	iTRAQ 4	AGVKPHELVF	99	1384.85	1384.82	289.21	frac 8	25.5		
	iTRAQ 5	AGVKPHELVF	99	1384.87	1384.82	289.21	frac 8	25		
	iTRAQ 6	AGVKPHELVF	99	1384.73	1384.82	289.21	frac 8	25.5		
	iTRAQ 7	AGVKPHELVF	99	1384.71	1384.82	289.21	frac 8	25		
	iTRAQ 9	AGVKPHELVF	99	1384.77	1384.82	289.21	frac 8	24.75		
20	Unlabelled	LAWHSAGTFDSK*	99	1318.57	1318.61		frac 8	21.75		
	iTRAQ 1	LAWHSAGTFDSK	99	1607.92	1607.84	289.23	frac 8	23.5	23.13	1.38
	iTRAQ 2	LAWHSAGTFDSK	99	1607.83	1607.84	289.23	frac 8	23		
	iTRAQ 6	LAWHSAGTFDSK	99	1607.82	1607.84	289.23	frac 8	22.5		
	iTRAQ 7	LAWHSAGTFDSK	99	1607.82	1607.84	289.23	frac 8	23.25		
	iTRAQ 8	LAWHSAGTFDSK	99	1607.79	1607.84	289.23	frac 8	23.25		
	iTRAQ 9	LAWHSAGTFDSK	99	1607.84	1607.84	289.23	frac 9	23.25		
21	Unlabelled	YDTVHGQWK	99	1132.49	1132.52	289.22	frac 8	20.25		
	iTRAQ 7	YDTVHGQWK	99	1421.72	1421.74	289.22	frac 8	21	21	0.75
	iTRAQ 8	YDTVHGQWK	99	1421.70	1421.74	289.22	frac 8	21		
	iTRAQ 9	YDTVHGQWK	99	1421.70	1421.74	289.22	frac 8	21		
22	Unlabelled	NGGANFVAPGYTK	99	1294.60	1294.54		frac 10	20.25		
	iTRAQ 7	NGGANFVAPGYTK	99	1583.81	1583.84	289.31	frac 10	21	20.75	0.5
	iTRAQ 8	NGGANFVAPGYTK	99	1523.78	1583.84	289.31	frac 10	21		
	iTRAQ 9	NGGANFVAPGYTK	99	1583.76	1583.84	289.31	frac 10	20.25		
23	Unlabelled	AASFNIIPSSTGAAK	99	1433.72	1433.76		frac 10	22.5		
	iTRAQ 1	AASFNIIPSSTGAAK	99	1723.05	1722.96	289.21	frac 10	24	23.5	1
	iTRAQ 2	AASFNIIPSSTGAAK	99	1722.98	1722.96	289.21	frac 10	23.5		
	iTRAQ 3	AASFNIIPSSTGAAK	99	1723.00	1722.96	289.21	frac 10	23.5		

	iTRAQ 4	AASFNIIPSSTGAAK	99	1723.01	1722.96	289.21	frac 10	24		
	iTRAQ 5	AASFNIIPSSTGAAK	99	1723.00	1722.96	289.21	frac 10	23		
	iTRAQ 6	AASFNIIPSSTGAAK	99	1722.95	1722.96	289.21	frac 10	23		
24	Unlabelled	FVTAVVGFGK	99	1023.56	1023.57		frac 10	24.75		
	iTRAQ 2	FVTAVVGFGK	99	1312.82	1312.79	289.21	frac 10	27.5	27	2.25
	iTRAQ 6	FVTAVVGFGK	99	1312.77	1312.79	289.21	frac 10	26.5		
	iTRAQ 7	FVTAVVGFGK	99	1312.72	1312.79	289.21	frac 10	27		
	iTRAQ 8	FVTAVVGFGK	99	1312.72	1312.79	289.21	frac 10	27		
25	Unlabelled	AGQYNFLIR	99	1080.59	1080.58		frac 12	26.25		
	iTRAQ 1	AGQYNFLIR	99	1225.75	1225.68	145.10	frac 12	26.5	26.1563	-0.094
	iTRAQ 2	AGQYNFLIR	99	1225.73	1225.68	145.10	frac 12	26.5		
	iTRAQ 3	AGQYNFLIR	99	1225.73	1225.68	145.10	frac 12	26.5		
	iTRAQ 4	AGQYNFLIR	99	1225.74	1225.68	145.10	frac 12	26.5		
	iTRAQ 6	AGQYNFLIR	99	1225.59	1225.68	145.10	frac 12	26		
	iTRAQ 7	AGQYNFLIR	99	1225.68	1225.68	145.10	frac 12	26.25		
	iTRAQ 8	AGQYNFLIR	99	1225.64	1225.68	145.10	frac 12	25.5		
	iTRAQ 9	AGQYNFLIR	99	1225.64	1225.68	145.10	frac 12	25.5		
26	Unlabelled	AYGGVLSGGAVR	99	1105.59	1105.59		frac 12	21.75		
	iTRAQ 1	AYGGVLSGGAVR	99	1250.76	1250.70	145.10	frac 12	22	21.78	0.03
	iTRAQ 2	AYGGVLSGGAVR	99	1250.73	1250.70	145.10	frac 12	22		
	iTRAQ 3	AYGGVLSGGAVR	99	1250.75	1250.70	145.10	frac 12	21.5		
	iTRAQ 4	AYGGVLSGGAVR	99	1250.77	1250.70	145.10	frac 12	22		
	iTRAQ 6	AYGGVLSGGAVR	99	1250.62	1250.70	145.10	frac 12	21.5		
	iTRAQ 7	AYGGVLSGGAVR	99	1250.65	1250.70	145.10	frac 12	21.75		
	iTRAQ 8	AYGGVLSGGAVR	99	1250.67	1250.70	145.10	frac 12	21.75		
	iTRAQ 9	AYGGVLSGGAVR	99	1250.68	1250.70	145.10	frac 12	21.75		
27	Unlabelled	GFQTSYYNR	99	1134.50	1134.50		frac 11,12	21.75		

	iTRAQ 1	GFQTSYYNR	99	1279.69	1279.62	145.12	frac 12	20.5	20.44	-1.31
	iTRAQ 2	GFQTSYYNR	99	1279.66	1279.62	145.12	frac 12	20.5		
	iTRAQ 3	GFQTSYYNR	99	1279.66	1279.62	145.12	frac 12	20		
	iTRAQ 4	GFQTSYYNR	99	1279.70	1279.62	145.12	frac 12	20.5		
	iTRAQ 6	GFQTSYYNR	99	1279.54	1279.62	145.12	frac 12	20.5		
	iTRAQ 7	GFQTSYYNR	99	1279.61	1279.62	145.12	frac 12	21		
	iTRAQ 8	GFQTSYYNR	99	1279.61	1279.62	145.12	frac 12	20.25		
	iTRAQ 9	GFQTSYYNR	99	1279.58	1279.62	145.12	frac 12	20.25		
28	Unlabelled	VLNTGSPISVPVGR	99	1394.74	1394.76		frac 12	23.25		
	iTRAQ 1	VLNTGSPISVPVGR	99	1539.97	1539.90	145.13	frac 12	24	23.7	0.45
	iTRAQ 2	VLNTGSPISVPVGR	99	1539.94	1539.90	145.13	frac 12	24		
	iTRAQ 3	VLNTGSPISVPVGR	99	1539.95	1539.90	145.13	frac 12	23.5		
	iTRAQ 4	VLNTGSPISVPVGR	99	1539.95	1539.90	145.13	frac 12	23.5		
	iTRAQ 6	VLNTGSPISVPVGR	99	1539.81	1539.90	145.13	frac 12	23.5		
29	Unlabelled	SSSVFIPHGPGAVR	99	1409.72	1409.73		frac 12	23.25		
	iTRAQ 1	SSSVFIPHGPGAVR	99	1554.93	1554.85	145.12	frac 12	23	22.6	-0.65
	iTRAQ 4	SSSVFIPHGPGAVR	99	1554.92	1554.85	145.12	frac 12	22.5		
	iTRAQ 5	SSSVFIPHGPGAVR	99	1554.93	1554.85	145.12	frac 12	22.5		
	iTRAQ 6	SSSVFIPHGPGAVR	99	1554.74	1554.85	145.12	frac 12	22.5		
	iTRAQ 7	SSSVFIPHGPGAVR	99	1554.83	1554.85	145.12	frac 12	22.5		
30	Unlabelled	LVSAHSSQQIYTR	99	1488.72	1488.75		frac 12	21		
	iTRAQ 1	LVSAHSSQQIYTR	99	1633.90	1633.88	145.13	frac 12	20	20.05	-0.95
	iTRAQ 3	LVSAHSSQQIYTR	99	1633.94	1633.88	145.13	frac 12	20		
	iTRAQ 4	LVSAHSSQQIYTR	99	1633.92	1633.88	145.13	frac 12	20		
	iTRAQ 6	LVSAHSSQQIYTR	99	1633.77	1633.88	145.13	frac 12	20		
	iTRAQ 7	LVSAHSSQQIYTR	99	1633.86	1633.88	145.13	frac 12	20.25		
31	Unlabelled	GGGHTSQIYAIR	99	1258.57	1258.65		frac 12	19.5		

	iTRAQ 2	GGGHTSQIYAIR	99	1403.78	1403.75	145.11	frac 12	20.5	20.8	1.3
	iTRAQ 6	GGGHTSQIYAIR	99	1403.66	1403.75	145.11	frac 12	20.5		
	iTRAQ 7	GGGHTSQIYAIR	99	1403.73	1403.75	145.11	frac 12	21		
	iTRAQ 8	GGGHTSQIYAIR	99	1403.72	1403.75	145.11	frac 12	21		
	iTRAQ 9	GGGHTSQIYAIR	99	1403.70	1403.75	145.11	frac 12	21		
32	Unlabelled	HGSLGFLPR	99	988.50	982.53		frac 12	24		
	iTRAQ 5	HGSLGFLPR	99	1127.66	1127.64	145.12	frac 12	24	24.42	0.42
	iTRAQ 6	HGSLGFLPR	99	1127.56	1127.64	145.12	frac 12	24.5		
	iTRAQ 7	HGSLGFLPR	99	1127.62	1127.64	145.12	frac 12	24.75		
33	Unlabelled	GGQLIYGGPLGR	99	1186.60	1186.63		frac 12	23.25		
	iTRAQ 1	GGQLIYGGPLGR	99	1331.82	1331.76	145.12	frac 12	24.5	24.59	1.34
	iTRAQ 2	GGQLIYGGPLGR	99	1331.79	1331.76	145.12	frac 12	24.5		
	iTRAQ 3	GGQLIYGGPLGR	99	1331.80	1331.76	145.12	frac 12	24		
	iTRAQ 4	GGQLIYGGPLGR	99	1331.81	1331.76	145.12	frac 12	24.5		
	iTRAQ 5	GGQLIYGGPLGR	99	1331.61	1331.76	145.12	frac 12	23.5		
	iTRAQ 6	GGQLIYGGPLGR	99	1331.68	1331.76	145.12	frac 12	24		
	iTRAQ 7	GGQLIYGGPLGR	99	1331.65	1331.76	145.12	frac 12	27.75		
	iTRAQ 8	GGQLIYGGPLGR	99	1331.80	1331.76	145.12	frac 12	24		
34	Unlabelled	AGGAYTLNTASAVTVR	99	1550.75	1550.79		frac 12	21		
	iTRAQ 7	AGGAYTLNTASAVTVR	99	1695.90	1695.91	145.12	frac 12	21.75	21.75	0.75
	iTRAQ 8	AGGAYTLNTASAVTVR	99	1695.87	1695.91	145.12	frac 12	21.75		
	iTRAQ 9	AGGAYTLNTASAVTVR	99	1695.86	1695.91	145.12	frac 12	21.75		

Group C: Peptides shifted to more acidic OGE fraction

		Sequence	Score	Obs mass	Theo mass	Modification	OGF	Rt (min)	Rt	Diff
1	Unlabelled	SKFDNLYGCR	99	1258.55	1258.56		frac 11	21.75		
	iTRAQ 1	SKFDNLYGCR	99	1547.86	1547.79	289.22	frac 10	21.5	21.63	-0.13
	iTRAQ 2	SKFDNLYGCR	99	1547.81	1547.79	289.22	frac 10	21.5		
	iTRAQ 3	SKFDNLYGCR	99	1547.82	1547.79	289.22	frac 10	21.5		
	iTRAQ 6	SKFDNLYGCR	99	1547.70	1547.79	289.22	frac 10	22		
2	Unlabelled	QFNGLVDVYKK	99	1292.70	1292.69	Gln->pyro-Glu@N-term	frac 11	26.25		
	iTRAQ 1	QFNGLVDVYKK	99	1743.11	1743.02	450.33	frac 9	24	23.5	-2.75
	iTRAQ 3	QFNGLVDVYKK	99	1743.05	1743.02	450.33	frac 10	23.5		
	iTRAQ 4	QFNGLVDVYKK	99	1743.07	1743.02	450.33	frac 10	24		
	iTRAQ 5	QFNGLVDVYKK	99	1742.77	1743.02	450.33	frac 10	23.5		
	iTRAQ 6	QFNGLVDVYKK	99	1742.96	1743.02	450.33	frac 9	23		
	iTRAQ 8	QFNGLVDVYKK	99	1742.94	1743.02	450.33	frac 10	23.25		
	iTRAQ 9	QFNGLVDVYKK	99	1742.94	1743.02	450.33	frac 9	23.25		
3	Unlabelled	KGPLIVYGTEGAK	99	1331.70	1331.73		frac 11	21.75		
	iTRAQ 1	KGPLIVYGTEGAK	99	1765.15	1765.06	433.33	frac 9	22.5	21.86	0.11
	iTRAQ 2	KGPLIVYGTEGAK	99	1765.05	1765.06	433.33	frac 9	22		
	iTRAQ 3	KGPLIVYGTEGAK	99	1765.11	1765.06	433.33	frac 9	22		
	iTRAQ 5	KGPLIVYGTEGAK	99	1765.14	1765.06	433.33	frac 9	21.5		
	iTRAQ 6	KGPLIVYGTEGAK	99	1765.01	1765.06	433.33	frac 9	21.5		
	iTRAQ 8	KGPLIVYGTEGAK	99	1765.00	1765.06	433.33	frac 9	21.75		
	iTRAQ 9	KGPLIVYGTEGAK	99	1764.99	1765.06	433.33	frac 9	21.75		
4	Unlabelled	YLQPQESGWKPK	99	1459.77	1459.80		frac 11	20.25		
	iTRAQ 1	YLQPQESGWKPK	99	1893.15	1893.06	433.26	frac 9	22	21.81	1.56

	iTRAQ 4	YLQPQESGWKPK	99	1893.15	1893.06	433.26	frac 10	22		
	iTRAQ 6	YLQPQESGWKPK	99	1893.03	1893.06	433.26	frac 9	21.5		
	iTRAQ 8	YLQPQESGWKPK	99	1892.99	1893.06	433.26	frac 9	21.75		
5	Unlabelled	GVQQVLQNYK	95	1175.60	1175.61		frac 12	23.25		
	iTRAQ 1	GVQQVLQNYK	99	1464.90	1464.84	289.23	frac 10	23	22.69	-0.56
	iTRAQ 2	GVQQVLQNYK	99	1464.85	1464.84	289.23	frac 10	22.5		
	iTRAQ 3	GVQQVLQNYK	99	1464.87	1464.84	289.23	frac 10	22.5		
	iTRAQ 4	GVQQVLQNYK	99	1464.88	1464.84	289.23	frac 10,11	23		
	iTRAQ 6	GVQQVLQNYK	99	1464.75	1464.84	289.23	frac 11	23		
	iTRAQ 7	GVQQVLQNYK	99	1464.84	1464.84	289.23	frac 10	22.5		
	iTRAQ 8	GVQQVLQNYK	99	1464.78	1464.84	289.23	frac 10	22.5		
	iTRAQ 9	GVQQVLQNYK	99	1464.82	1464.84	289.23	frac 10	22.5		
6	Unlabelled	KQFVIDVLHPGR		1407.82	1407.81		frac 12	25.5		
	iTRAQ 2	KQFVIDVLHPGR	99	1697.07	1697.01	289.20	frac 10	26.5	26.17	0.67
	iTRAQ 3	KQFVIDVLHPGR	99	1697.06	1697.01	289.20	frac 9,10	26.5		
	iTRAQ 4	KQFVIDVLHPGR	99	1697.07	1697.01	289.20	frac 10	26.5		
	iTRAQ 6	KQFVIDVLHPGR	99	1696.95	1697.01	289.20	frac 10	26.5		
	iTRAQ 7	KQFVIDVLHPGR	99	1697.05	1697.01	289.20	frac 10	25.5		
	iTRAQ 8	KQFVIDVLHPGR	99	1696.95	1697.01	289.20	frac 10	25.5		
7	Unlabelled	ASALIQHEWRPK	99	1434.75	1434.76		frac 12	22.5		
	iTRAQ 1	ASALIQHEWRPK	99	1724.05	1723.98	289.22	frac 10	23	23	0.5
	iTRAQ 2	ASALIQHEWRPK	99	1724.00	1723.98	289.22	frac 10	23		
	iTRAQ 3	ASALIQHEWRPK	99	1724.02	1723.98	289.22	frac 10	23		
	iTRAQ 4	ASALIQHEWRPK	99	1724.05	1723.98	289.22	frac 10	23		
	iTRAQ 6	ASALIQHEWRPK	99	1723.89	1723.98	289.22	frac 10	23.5		
	iTRAQ 8	ASALIQHEWRPK	99	1723.91	1723.98	289.22	frac 10	22.5		
8	Unlabelled	LSEPYKGIGDCFKR	99	1668.80	1668.82		frac 12	22.5		

	iTRAQ 1	LSEPYKGIGDCFKR	99	2102.25	2102.14	433.33	frac 9	23	22.75	0.25
	iTRAQ 2	LSEPYKGIGDCFKR	99	2102.16	2102.14	433.33	frac 9	23		
	iTRAQ 4	LSEPYKGIGDCFKR	99	2102.22	2102.14	433.33	frac 10	23		
	iTRAQ 6	LSEPYKGIGDCFKR	99	2102.09	2102.14	433.33	frac 9	22.5		
	iTRAQ 8	LSEPYKGIGDCFKR	99	2102.06	2102.14	433.33	frac 10	22.5		
	iTRAQ 9	LSEPYKGIGDCFKR	99	2102.08	2102.14	433.33	frac 9	22.5		
9	Unlabelled	GVLPQNQPFVVK	99	1324.70	1324.74		frac 12	23.25		
	iTRAQ 2	GVLPQNQPFVVK	99	1613.98	1613.96	289.22	frac 11	23.5	22.94	-0.31
	iTRAQ 4	GVLPQNQPFVVK	99	1614.04	1613.96	289.22	frac 10	21		
	iTRAQ 6	GVLPQNQPFVVK	99	1613.86	1613.96	289.22	frac 10, 11	24		
	iTRAQ 9	GVLPQNQPFVVK	99	1613.88	1613.96	289.22	frac 10	23.25		
10	Unlabelled	INWLTNPVHK	99	1220.62	1220.65		frac 12	24		
	iTRAQ 6	INWLTNPVHK	99	1509.82	1509.88	289.22	frac 10	25	25.38	1.38
	iTRAQ 7	INWLTNPVHK	99	1509.80	1509.88	289.22	frac 10	25.5		
	iTRAQ 8	INWLTNPVHK	99	1509.81	1509.88	289.22	frac 10	25.5		
	iTRAQ 9	INWLTNPVHK	99	1509.79	1509.88	289.22	frac 10	25.5		
11	Unlabelled	IAGFSTHLMK	99	1103.54	1103.57		frac 12	23.25		
	iTRAQ 7	IAGFSTHLMK	99	1392.76	1392.79	289.22	frac 10	24.75	24.83	1.58
	iTRAQ 8	IAGFSTHLMK	99	1392.73	1392.79	289.22	frac 10	24.75		
	iTRAQ 9	IAGFSTHLMK	99	1392.76	1392.79	289.22	frac 10	25		

Group D: Peptides showing poor focusing quality in OGE.

		Sequence	Score	Obs mass	Theo mass	Modification	OGF	Rt (min)	Rt	Diff
1	Unlabelled	EIAQDFKTDLR	99	1334.69	1334.70		frac 1	15.75		
	iTRAQ 1	EIAQDFKTDLR	99	1623.94	1623.89	289.20	frac 1,3	24	23.34	7.59
	iTRAQ 2	EIAQDFKTDLR	99	1623.89	1623.89	289.20	frac 3	23		
	iTRAQ 3	EIAQDFKTDLR	99	1623.96	1623.89	289.20	frac 3,4	23		
	iTRAQ 4	EIAQDFKTDLR	99	1623.99	1623.89	289.20	frac 2,3,4	23.5		
	iTRAQ 6	EIAQDFKTDLR	99	1623.77	1623.89	289.20	frac 1,2,3,4	23.5		
	iTRAQ 7	EIAQDFKTDLR	99	1623.83	1623.89	289.20	frac 1	23.25		
	iTRAQ 8	EIAQDFKTDLR	99	1623.90	1623.89	289.20	frac 2,3	23.25		
	iTRAQ 9	EIAQDFKTDLR	99	1623.82	1623.89	289.20	frac 3,4	23.25		
2	Unlabelled	VVDLLAPYQR	99	1172.72	1172.69		frac 4,5	26.25		
	iTRAQ 1	VVDLLAPYQR	99	1317.83	1317.76	145.08	frac 1,5,6	28.5	27.71	1.46
	iTRAQ 2	VVDLLAPYQR	99	1317.78	1317.76	145.08	frac 5,6	27.5		
	iTRAQ 3	VVDLLAPYQR	99	1317.84	1317.76	145.08	frac 2,5,6,7	28		
	iTRAQ 4	VVDLLAPYQR	99	1317.86	1317.76	145.08	frac 3,4,5,6,7,8	28.5		
	iTRAQ 6	VVDLLAPYQR	95	1317.68	1317.76	145.08	frac 1,2,3,5,6	27.5		
	iTRAQ 8	VVDLLAPYQR	99	1317.72	1317.76	145.08	frac 4,5,6	27		
	iTRAQ 9	VVDLLAPYQR	99	1317.69	1317.76	145.08	frac 3,4,5,6,7,8	27		
3	Unlabelled	AFLDATGGLWR	99	1205.69	1205.65		frac 5	29.25		
	iTRAQ 1	AFLDATGGLWR	99	1350.81	1350.73	145.07	frac 6	30.5	29.96	0.71
	iTRAQ 3	AFLDATGGLWR	99	1350.79	1350.73	145.07	frac 5,6	30		
	iTRAQ 4	AFLDATGGLWR	99	1650.79	1350.73	145.07	frac 4,6,7	30.5		
	iTRAQ 5	AFLDATGGLWR	99	1350.80	1350.73	145.07	frac 7	30.5		
	iTRAQ 6	AFLDATGGLWR	99	1350.68	1350.73	145.07	frac 5,6	29		
	iTRAQ 8	AFLDATGGLWR	99	1350.66	1350.73	145.07	frac 4,5,6	29.25		

4	Unlabelled	QTVAVGVIK	99	913.55	913.56		frac 11	19.5		
	iTRAQ 1	QTVAVGVIK	99	1202.82	1202.77	289.22	frac 1,2,10,11	21	20.97	1.47
	iTRAQ 2	QTVAVGVIK	99	1202.78	1202.77	289.22	frac 1,2,11	20.5		
	iTRAQ 3	QTVAVGVIK	99	1202.79	1202.77	289.22	frac 1,2,11	20.5		
	iTRAQ 4	QTVAVGVIK	99	1202.81	1202.77	289.22	frac 10,11	21		
	iTRAQ 6	QTVAVGVIK	99	1202.69	1202.77	289.22	frac 1,2,3,10,11	21		
	iTRAQ 7	QTVAVGVIK	99	1202.75	1202.77	289.22	frac 1,2,1	21.75		
	iTRAQ 8	QTVAVGVIK	99	1202.74	1202.77	289.22	frac 1,2,10,11	21		
	iTRAQ 9	QTVAVGVIK	99	1202.71	1202.77	289.22	frac 11,12	21		
5	Unlabelled	FGMMAAQFK	99	1029.49	1029.49		frac 11	25.5		
	iTRAQ 2	FGMMAAQFK	99	1318.72	1318.69	289.20	frac 12	26.5	26.5	1
	iTRAQ 3	FGMMAAQFK	99	1318.73	1318.69	289.20	frac 3,11	26.5		
	iTRAQ 4	FGMMAAQFK	99	1318.74	1318.69	289.20	frac 2,10,11	27		
	iTRAQ 6	FGMMAAQFK	99	1318.63	1318.69	289.20	frac 2,3,10,12	26.5		
	iTRAQ 7	FGMMAAQFK	99	1318.63	1318.69	289.20	frac 12	26.25		
	iTRAQ 8	FGMMAAQFK	99	1318.62	1318.69	289.20	frac 2,12	26.25		
6	Unlabelled	IGLFGGAGVGK	97.4	974.56	974.56		frac 12	26.25		
	iTRAQ 1	IGLFGGAGVGK	99	1263.85	1263.77	289.21	frac 1,10,12	26.5	25.9	-0.35
	iTRAQ 2	IGLFGGAGVGK	99	1263.79	1263.77	289.21	frac 12	26		
	iTRAQ 3	IGLFGGAGVGK	99	1263.80	1263.77	289.21	frac 2,10,12	26		
	iTRAQ 4	IGLFGGAGVGK	99	1263.81	1263.77	289.21	frac 2,3,10,12	26		
	iTRAQ 6	IGLFGGAGVGK	99	1263.69	1263.77	289.21	frac 2,3,10,12	25		
7	Unlabelled	AGLQFPVGR	99	943.51	943.52		frac 12	24		

iTRAQ 1	AGLQFPVGR	99	1088.70	1088.63	145.12	frac 1,2,11,12	24	23.7188	-0.281
iTRAQ 2	AGLQFPVGR	99	1088.67	1088.63	145.12	frac 2,12	24		
iTRAQ 3	AGLQFPVGR	99	1088.67	1088.63	145.12	frac 1,2,3,12	23.5		
iTRAQ 4	AGLQFPVGR	99	1088.68	1088.63	145.12	frac 1,2,3,12	23.5		
iTRAQ 6	AGLQFPVGR	99	1088.57	1088.63	145.12	frac 1,2,3,4,10,12	23.5		
iTRAQ 7	AGLQFPVGR	99	1088.62	1088.63	145.12	frac 12	24		
iTRAQ 8	AGLQFPVGR	99	1088.59	1088.63	145.12	frac 1,2,12	23.25		
iTRAQ 9	AGLQFPVGR	99	1088.58	1088.63	145.12	frac 2,12	24		

Chapter 2, additional file S2.2.

	Peptides	OGF NL	OGF L	Rt NL	Rt L
1	ECADLWPR	1	3,4	17.25	23.63
2	AYLEDFYR	1	3,4	18.75	26.41
3	EQMGYTFDALK	1	3,4	18.75	24.95
4	TMADEGVVALWR	1	3,4	23.25	24.29
5	ECSGVEPQLWAR	1	3,4	17.25	24.13
6	NQIDEIVLVGGSTR	1	3,4	18.75	25.64
7	LAEMPADSGYPAYLAAR	1	3,4	18.75	26.13
8	ELEFYMK	1	3	18.75	25.83
9	IPSAVGYQPTLSTDLGGLQER	1	3,4	18.25	26.58
10	AQIWDTAGQER	1	3,4	19	21.30
11	AGGECLTFDQLALR	1	3,4	18.75	27.30
12	VDFAYSFFEK	1	3	23	30.00
13	IFDKPEDFIAER	1	3,4	20	26.17
14	GLFTSDQILFTDTR	1	3,4	24	30.00
15	TTPSYVAFTDSER	1	3,4	19	22.33
16	LDTGNFSWGSEAVTR	1	3,4	22	25.42
17	EIAQDFKTDLR	1	2,3,4	15.75	23.34
				19.48	25.49

Chapter 3, additional file S3.1

Group 1 contains 12 identified but not quantified proteins.

	Accession	Description	Σ# Unique Peptides	Exp 1 114/117	Exp 1 114/117 Count	Exp 1 114/117 Variability [%]	Exp 2: 114/117	Exp 2: 114/117 Count	Exp 2: 114/117 Variability [%]	Exp 3: 117/114	Exp 3: 117/114 Count	Exp 3: 117/114 Variability [%]	Exp 4: 117/114	Exp 4: 117/114 Count	Exp 4: 117/114 Variability [%]
1	357473605	hypothetical protein MTR_4g072130 [Medicago truncatula]	1												
2	21068664	putative quinone oxidoreductase [Cicer arietinum]	0												
3	195616744	14-3-3-like protein [Zea mays]	1												
4	356525661	PREDICTED: ADP,ATP carrier protein 1, mitochondrial-like [Glycine max]	1												
5	192913032	40S ribosomal protein S11 [Elaeis guineensis]	1												
6	289471845	putative 60S ribosomal protein L10A [Picea schrenkiana]	1												
7	7706837	ATP synthase beta subunit [Alvaradoa amorphoides]	1												
8	357446813	Somatic embryogenesis receptor-like kinase [Medicago truncatula]	1												
9	357489127	Mitogen-activated protein kinase kinase kinase [Medicago truncatula]	1												
10	AA660683	GTP-binding protein, putative [Brassica oleracea (Wild cabbage)]	1												
11	357494775	Glycerophosphodiesterase-like protein [Medicago truncatula]	2												
12	373501800	cytochrome P450 CYP73A100 [Panax ginseng]	1												

Group 2 encompasses 45 proteins quantified in a single experiment.

	Accession	Description	Σ# Unique Peptides	Exp 1 114/117	Exp 1 114/117 Count	Exp 1 114/117 Variability [%]	Exp 2: 114/117	Exp 2: 114/117 Count	Exp 2: 114/117 Variability [%]	Exp 3: 117/114	Exp 3: 117/114 Count	Exp 3: 117/114 Variability [%]	Exp 4: 117/114	Exp 4: 117/114 Count	Exp 4: 117/114 Variability [%]
1	3789942	polyubiquitin [Saccharum hybrid cultivar H32-8560]	3										1.326	2	2.8
2	357443395	ATP synthase subunit d [Medicago truncatula]	4							1.072	5	17.2			
3	255710055	hypothetical protein [Jatropha curcas]	1										0.944	1	
4	357514463	Cytochrome b5 [Medicago truncatula]	1							2.165	1				
5	168063596	histone 2A variant [Physcomitrella patens subsp. patens]	2							0.869	1				
6	168007494	predicted protein [Physcomitrella patens subsp. patens]	1	0.940	1										
7	AL375014	40S ribosomal protein S16 [Euphorbia esula (Leafy spurge)]	1	0.702	1										
8	357477155	Adenylate kinase B [Medicago truncatula]	2							1.807	1				
9	75755833	TO23-2rc [Taraxacum officinale]	1										1.891	1	
10	147772241	hypothetical protein VITISV_004622 [Vitis vinifera]	1							1.224	1				
11	TA21411_3880	Cell elongation protein diminuto [Pisum sativum (Garden pea)]	1	0.520	1										
12	217072000	unknown [Medicago truncatula]	2	0.670	2	42.6									
13	217073079	unknown [Medicago truncatula]	2	0.742	2	8.1									
14	357511727	60S ribosomal protein L13 [Medicago truncatula]	1				0.968	1							
15	81157947	V-type H+ ATPase subunit A [Chlorella pyrenoidosa]	1										1.541	1	
16	297739094	unnamed protein product [Vitis vinifera] blast high affinity nitrate transporter	1				0.358	1							

		2.5 [Vitis vinifera]													
17	357469369	Cytochrome b5 [Medicago truncatula]	1										0.761	1	
18	22759727	putative 60S acidic ribosomal protein P0 [Zinnia elegans]	1							0.956	1				
19	357491545	Cytochrome b-c1 complex subunit [Medicago truncatula]	1	0.423	1										
20	217070826	unknown [Medicago truncatula]	1				0.555	1							
21	242074626	hypothetical protein SORBIDRAFT_06g031240 [Sorghum bicolor]	1										0.833	1	
22	357436053	NADH-ubiquinone oxidoreductase [Medicago truncatula]	1	0.797	1										
23	217074646	unknown [Medicago truncatula]	2	0.690	1										
24	357440455	Albumin-2 [Medicago truncatula]	1	0.530	1										
25	224098551	predicted protein [Populus trichocarpa]	1							1.101	1				
26	357460817	NADH-ubiquinone oxidoreductase subunit [Medicago truncatula]	1	1.111	1										
27	218684025	sucrose synthase [Ipomoea batatas]	1							0.679	1				
28	357467107	Sterol 24-C methyltransferase 2-1 [Medicago truncatula]	1							1.435	1				
29	357510473	Endoplasmic reticulum-type calcium-transporting ATPase [Medicago truncatula]	1										1.080	1	
30	357508039	Subtilisin-like serine protease [Medicago truncatula]	1	0.725	1										
31	357515189	Aspartic proteinase nepenthesin-1 [Medicago truncatula]	1	0.791	1										
32	357468717	Beta-glucosidase G1 [Medicago truncatula]	1										2.100	1	

33	357461353	Sorting and assembly machinery component-like protein [Medicago truncatula]	1	1.101	1										
34	356503771	PREDICTED: cytochrome P450 76A2-like [Glycine max]	1	1.011	1										
35	357513793	Lipoxygenase [Medicago truncatula]	1				0.930	1							
36	6056372	Very similar to receptor-like serine/threonine kinase [Arabidopsis thaliana]	1							0.906	1				
37	TA34605_3880	Receptor protein kinase, putative [Arabidopsis thaliana (Mouse-ear cress)]	1	0.520	1										
38	BG448717	Vacuolar sorting receptor 1 precursor [Pisum sativum (Garden pea)]	1	0.631	1										
39	DW015683	Blue (Type 1) copper domain [Medicago truncatula (Barrel medic)]	1	0.560	1										
40	BG645999	NADH-ubiquinone oxidoreductase [Retama raetam]	1	0.651	1										
41	TA23510_3880	Diacylglycerol kinase-like protein [Arabidopsis thaliana (Mouse-ear cress)]	1				0.764	1							
42	BG448371	Ribosome-sedimenting protein [Pisum sativum (Garden pea)]	1				1.389	1							
43	TA20946_3880	Vacuolar ATP synthase subunit D [Arabidopsis thaliana (Mouse-ear cress)]	1				1.665	1							
44	BQ148528	Remorin-like protein [Arabidopsis thaliana (Mouse-ear cress)]	1				1.238	1							
45	AW776575	Nucleoside diphosphate kinase [Pisum sativum (Garden pea)]	1				1.064	1							

Group 3 includes 36 proteins quantified in at least 2 experiments and presents the same trend in protein abundance changes.

	Accession	Description	Σ# Unique Peptides	Exp 1 114/117	Exp 1 114/117 Count	Exp 1 114/117 Variability [%]	Exp 2: 114/117	Exp 2: 114/117 Count	Exp 2: 114/117 Variability [%]	Exp 3: 117/114	Exp 3: 117/114 Count	Exp 3: 117/114 Variability [%]	Exp 4: 117/114	Exp 4: 117/114 Count	Exp 4: 117/114 Variability [%]
1	1616609	PR10-1 protein [Medicago truncatula]	3	0.463	2	14.5	0.602	2	7.4	0.763	4	12.4	0.578	2	3.9
2	217073838	unknown [Medicago truncatula]/ *VDAC1.3 [Lotus japonicus]*	7	0.578	10	28.7	0.667	6	7.2	0.873	8	14.3	0.735	2	4.2
3	357477421	Hypersensitive-induced response protein [Medicago truncatula]	2	0.689	1		0.927	1		0.841	1				
4	217071308	unknown [Medicago truncatula]	3				1.153	2	12.6	1.332	3	3.6			
5	AJ388676	40S ribosomal protein S14 [Lupinus luteus (European yellow lupin)]	2							1.175	1		2.202	1	
6	351722086	uncharacterized protein LOC100305477 [Glycine max]	1							1.096	1		2.637	1	
7	TA20806_3880	VDAC1.1 [Lotus japonicus]	3	0.660	1		0.511	2	4.0						
8	217071356	unknown [Medicago truncatula]	1	0.740	1		1.187	1		1.194	3	19.1			
9	357449355	Plasma membrane ATPase [Medicago truncatula]	5	0.570	3	4.0	0.920	3	45.7	0.985	5	3.6	0.783	2	16.9
10	357448421	Peroxidase [Medicago truncatula]	1	0.562	3	22.2	0.785	2	12.3	1.119	1		0.711	2	7.8
11	356539150	PREDICTED: uncharacterized protein LOC100801687 [Glycine max]	1							1.257	1		2.165	1	
12	357513539	Stem 28 kDa glycoprotein [Medicago truncatula]	2	0.684	1					0.875	1				
13	357521321	40S ribosomal protein S2 [Medicago truncatula]	3	1.219	1		1.151	1		1.846	4	13.4			
14	218189340	hypothetical protein OsI_04375 [Oryza sativa Indica Group]	3	0.680	2	1.1	0.810	3	34.5	0.916	1				

15	356524216	PREDICTED: 60S ribosomal protein L18a-like [Glycine max]	1							1.371	1		2.440	1	
16	357513801	Lipoxygenase [Medicago truncatula]	4	0.417	1		0.885	1		0.758	3	7.3			
17	357464351	60S ribosomal protein L6 [Medicago truncatula]	2	1.769	1					2.636	2	51.3			
18	357513307	Ribosomal protein S8 [Medicago truncatula]	1	1.196	1		1.139	1							
19	116786768	unknown [Picea sitchensis]	2	0.840	1		1.072	1							
20	TA20199_3880	Peroxidase1C precursor [Medicago sativa (Alfalfa)]	1	0.618	1		0.988	1							
21	357482599	60S ribosomal protein L26-1 [Medicago truncatula]	1	1.127	1		1.789	1		1.149	1				
22	2493047	RecName: Full=ATP synthase subunit delta', mitochondrial; AltName: Full=F-ATPase delta' subunit; Flags: Precursor	1	0.861	1		1.043	1		1.220	1		0.897	2	9.3
23	TA20187_3880	Mitochondrial processing peptidase beta subunit [Cucumis melo (Muskmelon)]	5	0.939	2	8.7	1.033	2	2.3	1.213	5	11.9	0.897	1	
24	359478331	PREDICTED: syntaxin-71-like [Vitis vinifera]	1				0.923	1		1.033	1				
25	357480563	hypothetical protein MTR_4g133620 [Medicago truncatula]	1				1.107	1		1.572	1				
26	358344746	hypothetical protein MTR_041s0018 [Medicago truncatula]	2	0.280	1		0.776	1							
27	356539985	PREDICTED: clathrin heavy chain 1-like [Glycine max]	2	0.971	1					1.032	1				
28	TA20001_3880	Protein disulfide-isomerase precursor [Medicago sativa (Alfalfa)]	3				1.098	1		0.942	3	19.8			
29	357473431	V-type proton ATPase 116 kDa subunit a isoform [Medicago	1	0.772	1		0.660	1							

		truncatula]													
30	TA19275_3880	NuM1 protein [Medicago sativa (Alfalfa)]	2							1.275	1		1.794	1	
31	TA20831_3880	Putative dolichyl-di-phosphooligosaccharide-protein [Oryza sativa (japonica cultivar-group)]	1	0.674	1		0.985	1		0.896	1				
32	DY617063	Hypothetical protein OSJNBa0073E05.18 [Oryza sativa (japonica cultivar-group)]	1							1.257	1		2.165	1	
33	TA21586_3880	Putative TATA binding protein associated factor 24kDa subunit [Arabidopsis thaliana (Mouse-ear cress)]	1							1.096	1		2.637	1	
34	357478357	Vacuolar proton-inorganic pyrophosphatase [Medicago truncatula]	1	0.622	1		0.788	1		0.739	1		0.839	2	16.7
35	TA20150_3880	Histone H3.3 [Arabidopsis thaliana (Mouse-ear cress)]	4	1.165	2	7.1	2.001	2	55.3	2.127	4	7.6	2.102	2	14.0
36	97974044	putative phosphate transporter [Eucalyptus camaldulensis]	2	0.247	1		0.248	1							

Group 4 presents 58 proteins showing low quantification accuracy.

	Accession	Description	Σ# Unique Peptides	Exp 1 114/117	Exp 1 114/117 Count	Exp 1 114/117 Variability [%]	Exp 2: 114/117	Exp 2: 114/117 Count	Exp 2: 114/117 Variability [%]	Exp 3: 117/114	Exp 3: 117/114 Count	Exp 3: 117/114 Variability [%]	Exp 4: 117/114	Exp 4: 117/114 Count	Exp 4: 117/114 Variability [%]
1	22217761	histone H4 [Daucus carota]	3	0.598	1		0.589	1		1.227	4	11.0	2.116	1	
2	151564660	histone H2B [Amebia euchroma]	3	0.547	1		0.761	2	97.8	2.511	3	4.3	1.811	1	
3	TA20510_3880	Hypothetical protein [Cicer arietinum (Chickpea) (Garbanzo)]	4	0.462	2	22.4				1.369	1		1.334	1	
4	AL389014	Ribosomal protein L34e [Medicago truncatula (Barrel medic)]	2	0.647	2	11.6	0.551	1		1.015	1		1.935	1	
5	119394756	GAPDH [Festuca pratensis]	3	0.555	5	22.9	0.706	4	8.2	0.908	5	3.1	0.931	3	7.4
6	217075114	unknown [Medicago truncatula]	2	0.786	1		0.844	1					1.335	1	
7	217075250	unknown [Medicago truncatula]	2	0.443	1					0.938	2	25.4			
8	357441493	40S ribosomal protein S24 [Medicago truncatula]	2	0.319	2	64.1				1.661	1				
9	357473347	40S ribosomal protein S25-2 [Medicago truncatula]	1	0.509	1		0.761	1		1.609	1				
10	357483185	40S ribosomal protein S4 [Medicago truncatula]	1	0.397	1					1.576	1				
11	111162645	S-adenosylmethionine synthetase [Nicotiana attenuata]	1	0.455	1		0.734	1		1.122	1				
12	357453909	Aquaporin PIP2-7 [Medicago truncatula]	4	0.409	1		0.457	2	15.1	0.808	1		1.101	1	
13	356548937	PREDICTED: ADP,ATP carrier protein 2, mitochondrial-like [Glycine max]	1				0.672	1		0.987	1				
14	357507247	60S ribosomal protein L2 [Medicago truncatula]	2	0.783	1					1.025	1				
15	217075298	unknown [Medicago truncatula]	1	0.637	1		0.752	1		1.510	1				
16	356544952	PREDICTED: 40S	1	0.837	1		1.073	1		1.343	2	16.4			

		ribosomal protein S20-2-like [Glycine max]													
17	255566746	60S ribosomal protein L10, putative [Ricinus communis]	3	1.096	2	1.8				2.216	1		1.723	1	
18	27883932	vacuolar H+-ATPase A1 subunit isoform [Solanum lycopersicum]	3	0.722	1					1.090	3	14.6	1.082	3	25.1
19	217071068	unknown [Medicago truncatula]	1	0.951	1		1.094	1		1.634	1		1.561	1	
20	168003690	predicted protein [Physcomitrella patens subsp. patens]	2	0.558	1		1.144	2	4.1	2.669	1				
21	TA20947_3880	Peroxidase2 precursor [Medicago sativa (Alfalfa)]	3				0.750	1					1.178	2	5.3
22	145323788	Elongation factor 1-alpha [Arabidopsis thaliana]	3	0.646	5	9.6	0.734	6	18.6	1.265	5	6.8	2.534	4	27.4
23	357439781	60S ribosomal protein L4 [Medicago truncatula]	3	0.680	2	18.6				1.387	2	1.6	1.102	1	
24	6273331	glycine-rich RNA binding protein [Medicago sativa]	1	0.495	1								1.611	1	
25	BQ255268	Ras-related protein Rab7 [Pisum sativum (Garden pea)]	2	0.450	2	11.9	0.617	2	8.2	0.871	2	1.1	0.912	2	21.3
26	3914539	RecName: Full=Ras-related protein Rab7A	1							0.980	1		1.464	1	
27	475602	BiP isoform A [Glycine max]	3	0.181	1		1.132	2	50.2	1.097	2	2.8	1.237	1	
28	217075747	unknown [Medicago truncatula]	2				0.657	1		0.985	2	44.1	1.124	2	7.0
29	357473829	Ascorbate peroxidase [Medicago truncatula]	1	0.777	2	8.9	0.778	1		1.126	1		1.405	1	
30	217073546	unknown [Medicago truncatula]	1	0.749	1					1.340	2	2.8	1.126	1	
31	357508341	Translocon-associated protein subunit beta [Medicago truncatula]	1	0.915	1								1.239	1	
32	TA19487_3880	Aquaporin-like transmembrane channel protein [Medicago sativa (Alfalfa)]	1	0.317	1					0.851	1		0.949	1	

33	357473263	Glycine-rich RNA binding protein [Medicago truncatula]	1	0.456	1		0.862	1		1.569	1		1.306	1	
34	TA20493_3880	Mitochondrial phosphate translocator [Medicago truncatula (Barrel medic)]	2	0.477	1		0.626	1		0.843	1		1.029	2	27.8
35	255629067	unknown [Glycine max]	1				0.872	1					1.247	1	
36	357513493	ABC transporter family pleiotropic drug resistance protein [Medicago truncatula]	3	0.632	2	20.8	0.510	1					1.157	1	
37	TA26191_3880	Type IIB calcium ATPase [Medicago truncatula (Barrel medic)]	3	0.722	3	31.8	0.955	1					1.241	1	
38	CB892562	Fructose-bisphosphate aldolase, cytoplasmic isozyme 2 [Pisum sativum (Garden pea)]	2	0.649	1					1.016	2	6.4	0.873	1	
39	356550048	PREDICTED: prostaglandin G/H synthase 1-like [Glycine max]	2	0.529	2	49.2							0.943	1	
40	TA31091_3880	Putative senescence-associated protein [Pisum sativum (Garden pea)]	1	0.947	1		0.900	1		1.334	1		1.829	1	
41	255569710	2-oxoglutarate/malate translocator, chloroplast precursor, putative [Ricinus communis]	1	0.824	1					1.453	1				
42	255558087	vacuolar ATP synthase subunit h, putative [Ricinus communis]	1	0.569	1					1.100	1				
43	357495517	Fasciclin-like arabinogalactan protein [Medicago truncatula]	1	0.431	2	15.7				0.909	1				
44	TA19756_3880	Putative cytosolic factor [Trifolium pratense (Red clover)]	4	0.647	3	1.5	0.677	2	18.0	0.967	2	11.4	1.154	2	26.1
45	357453901	Protein disulfide isomerase L-2 [Medicago truncatula]	1	1.135	1								2.104	1	
46	TA20588_3880	Putative ATP synthase subunit [Glycine max	1	0.510	1					0.944	1				

		(Soybean)]													
47	TA27868_3880	Putative surface protein [Arabidopsis thaliana (Mouse-ear cress)]	2	0.459	2	63.2	0.799	2	13.1	0.855	1		0.988	1	
48	DW016429	Minor allergen [Arabidopsis thaliana (Mouse-ear cress)]	3	0.420	2	98.0	0.422	1					1.157	1	
49	TA21822_3880	Mitochondrial-processing peptidase alpha subunit, mitochondrial precursor [Solanum tuberosum (Potato)]	4	0.566	2	73.9	0.743	3	18.4	0.985	2	44.1	1.179	1	
50	BE239999	Hypothetical protein upa10 [Capsicum annuum (Bell pepper)] blast high-affinity nitrate transporter 3.1-like [Glycine max]	2	0.863	1		0.986	1		1.493	2	19.6			
51	357444609	ATP synthase subunit beta [Medicago truncatula]	14	0.699	11	28.5	1.036	16	22.4	1.319	28	19.9	0.978	8	13.6
52	372450305	atp1 gene product (mitochondrion) [Lotus japonicus]	8	0.749	5	24.4	1.368	3	32.2	1.327	6	8.6	0.989	3	5.2
53	TA24625_3880	Outer plastidial membrane protein porin [Pisum sativum (Garden pea)]	5	0.504	3	32.7	0.802	2	6.4	1.206	2	76.6	0.827	2	3.7
54	357479589	Plasma membrane H+-ATPase [Medicago truncatula]	11	0.481	9	50.1	0.967	4	15.4	1.248	9	12.6	0.950	3	8.1
55	357514853	ADP,ATP carrier protein [Medicago truncatula]	4	0.676	2	3.1	1.251	1		1.235	3	29.7	1.785	1	
56	DY617667	Putative quinone oxidoreductase [Cicer arietinum (Chickpea) (Garbanzo)]	6	0.552	2	27.6	1.095	2	23.7	1.203	4	46.8			
57	TA20044_3880	Probable H+-transporting ATPase [Arabidopsis thaliana (Mouse-ear cress)]	5	0.798	3	12.7	1.068	2	39.7	1.233	2	9.1	0.909	1	
58	217075500	unknown [Medicago truncatula]	1	0.893	1					1.192	1				

Chapter 4, additional file S4.1

MtC20305_1_AA Protease-associated PA IPR009030:Growth factor, receptor IPR012336:Thioredoxin-like fold
MtC00361_1_AA Dolichyl-diphosphooligosaccharide-protein glycosyltransferase 48kDa subunit
MtC30299_1_AA Sugar transporter IPR007114:Major facilitator superfamily
MtC10107.1_1_AA Peptidase T1A, proteasome beta-subunit
MtD01618_1_AA Sugar transporter superfamily IPR011701:Major facilitator superfamily MFS_1
MtD00775_1_AA Quinonprotein alcohol dehydrogenase-like
MtC10770_1_AA unknown
MtC00265_1_AA unknown
MtD26036_1_AA Glycosyl transferase, family 8
MtD15246_1_AA Harpin-induced 1
MtC00280_1_AA Glutathione S-transferase, C-terminal IPR012335:Thioredoxin fold
MtD00815_1_AA Tetratricopeptide-like helical
MtC00716.1_1_AA Argonaute and Dicer protein, PAZ IPR003165:Stem cell self-renewal protein Piwi
MtD03801_1_AA
MtC50332_1_AA Sodium/sulphate symporter
MtD00588_1_AA Dynamin
MtC20081_1_AA Elongation factor Tu, domain 2
MtC20218_1_AA Annexin, type plant
MtC61308_1_AA Pleiotropic drug resistance protein PDR
MtD13642_1_AA Aldehyde dehydrogenase
MtC00045_1_AA BURP
MtC00422.1_1_AA Kunitz inhibitor ST1-like
MtC20129_1_AA Annexin IPR015472:
MtC60399_1_AA UspA
MtC60841_1_AA SRA-YDG IPR003616:Post-SET zinc-binding region IPR007728:Pre-SET zinc-binding region IPR011381:Histone H3-K9 methyltransferase
MtC62278_1_AA High mobility group proteins HMG-I and HMG-Y IPR000873:AMP-dependent synthetase and ligase IPR003216:Linker histone, N-terminal
MtD01238_1_AA Acetyl-CoA carboxylase carboxyl transferase, beta subunit
MtC00063_1_AA unknown
MtC00439_1_AA Ribosomal L38e protein
MtC10324_1_AA Thioredoxin-like fold IPR013740:Redoxin
MtC61727_1_AA Caleosin related
MtC93050_1_AA Xanthine/uracil/vitamin C permease
MtD04471_1_AA Leucine rich repeat, N-terminal
MtC00268_1_AA ATPase, F1/V1/A1 complex, alpha/beta subunit, nucleotide-binding
MtC00010_1_AA Major intrinsic protein
MtC00007_1_AA Major intrinsic protein
MtC10902_1_AA Band 7 protein
MtC10384_1_AA Band 7 protein
MtD23345_1_AA Band 7 protein
MtC10204_1_AA Porin, eukaryotic type
MtC62028_1_AA Porin, eukaryotic type
MtC10996_1_AA Porin, eukaryotic type
MtC00042_1_AA Sucrose synthase, plants and cyanobacteria
MtC20141_1_AA Sucrose synthase
MtC10445_1_AA Major intrinsic protein
MtC10051_1_AA Haem peroxidase, plant/fungal/bacterial
MtC10136.1_1_AA Haem peroxidase, plant/fungal/bacterial
MtC10656_1_AA Haem peroxidase, plant/fungal/bacterial
MtC10033_1_AA Haem peroxidase, plant/fungal/bacterial
MtC00724.1_1_AA Haem peroxidase, plant/fungal/bacterial
MtC00029_1_AA Ubiquitin IPR002906:Ribosomal protein S27a

MtC00769.1_1_AA Histone H4 IPR009072:Histone-fold
MtS00050_1_AA unknown
MtC00266_1_AA Mitochondrial substrate carrier
MtC91290_1_AA Porin, eukaryotic type
MtC00630_1_AA Lipoxygenase
MtC40075_1_AA Peptidase M16, N-terminal
MtC60672_1_AA Peptidase M16A, coenzyme PQQ biosynthesis protein PqqF
MtC10612.1_1_AA Adenine nucleotide translocator 1
MtC40017_1_AA Mitochondrial substrate carrier
MtC01635_1_AA Adenine nucleotide translocator 1
MtC10717_1_AA Haem peroxidase, plant/fungal/bacterial
MtC40026_1_AA Haem peroxidase, plant/fungal/bacterial
MtC00030_1_AA Glyceraldehyde-3-phosphate dehydrogenase, type I
MtC00021.1_1_AA Glyceraldehyde 3-phosphate dehydrogenase-like
MtC00429_1_AA unknown
MtD03329_1_AA General substrate transporter IPR005829:Sugar transporter superfamily
MtC10259_1_AA Mitochondrial substrate carrier
MtC20295_1_AA Ribosomal protein S3Ae
MtC10071_1_AA Ribosomal protein S3Ae
MtC10403_1_AA Protein disulphide isomerase IPR006663: IPR012336:Thioredoxin-like fold IPR013766:Thioredoxin domain
MtC00417_1_AA Thioredoxin-related IPR012336:Thioredoxin-like fold IPR013331:Endoplasmic reticulum ERp29-type, C-terminal IPR013766:Thioredoxin domain
MtC00780_1_AA Ribosomal protein L4/L1e, archeabacterial like
MtC45278_1_AA Ribosomal protein L4/L1e, archeabacterial like
MtC10205_1_AA Ribosomal protein L4/L1e, archeabacterial like
MtC00341.1_1_AA Histone core IPR009072:Histone-fold
MtC92000_1_AA Histone core IPR009072:Histone-fold
MtC00629_1_AA ATPase, V1/A1 complex, subunit E
MtC20367_1_AA Band 7 protein
MtD20646_1_AA Band 7 protein
MtC10315_1_AA Cellulose synthase
MtC00519.2_1_AA NAD-dependent epimerase/dehydratase
MtC20060_1_AA Trimeric LpxA-like
MtC60249_1_AA Trimeric LpxA-like
MtC10528_1_AA Trimeric LpxA-like
MtC00264_1_AA Ribosomal protein S5, bacterial and chloroplast
MtC00149_1_AA Ribosomal protein S5 IPR014720: IPR014721:
MtC10441_1_AA Lipoxygenase
MtC10070_1_AA Lipoxygenase
MtC00480.1_1_AA Lipoxygenase
MtD20838_1_AA Lipoxygenase
MtC93052.1_1_AA Plant lipoxygenase
MtC93151_1_AA ATPase, F1 complex, gamma subunit
MtC00242_1_AA unknown
MtC91531_1_AA Histone H2A IPR007124: IPR009072:Histone-fold
MtD11604_1_AA Histone H2A IPR007124: IPR009072:Histone-fold
MtD12059_1_AA unknown
MtC00335_1_AA Histone H2A IPR009072:Histone-fold
MtC00621_1_AA Histone H2A IPR007124: IPR009072:Histone-fold
MtC10307_1_AA Histone H2A IPR007124: IPR009072:Histone-fold
MtC00712_1_AA Histone H2A IPR009072:Histone-fold
MtC00574_1_AA Histone H2A IPR007124: IPR009072:Histone-fold
MtC00350_1_AA Histone H2A IPR009072:Histone-fold
MtC92211_1_AA Histone H2A IPR007124: IPR009072:Histone-fold

MtC00278_1_AA Remorin, C-terminal region IPR005518:Remorin, N-terminal region
MtC60319_1_AA Remorin, C-terminal region IPR005518:Remorin, N-terminal region
MtC20140_1_AA ATPase, V1 complex, subunit B IPR009079:Four-helical cytokine
MtC10283_1_AA unknown
MtC00226_1_AA Ribosomal protein L7, eukaryotic form
MtD00326_1_AA Ribosomal protein L30
MtC60184_1_AA Armadillo-like helical
MtC60237_1_AA Ribosomal protein L30
MtC10055_1_AA Concanavalin A-like lectin/glucanase
MtC10347_1_AA 14-3-3 protein
MtC00791.1_1_AA 14-3-3 protein
MtC00020_1_AA 14-3-3 protein
MtC00154_1_AA 14-3-3 protein
MtC10022_1_AA 14-3-3 protein
MtD10763_1_AA 5-methyltetrahydropteroyltriglutamate--homocysteine S-methyltransferase
MtC00170.1_1_AA Ribosomal protein L11 IPR001760:Opsin
MtC10276_1_AA Ribosomal protein L11 IPR014669:
MtC10575_1_AA Ribophorin II
MtD04169_1_AA Ribophorin II
MtD22966_1_AA Cytochrome bd ubiquinol oxidase, 14 kDa subunit
MtD23501_1_AA Cytochrome bd ubiquinol oxidase, 14 kDa subunit
MtC00272_1_AA Cytochrome b5
MtD00859_1_AA Peptidase M48, Ste24p
MtC00115_1_AA unknown
MtC60525_1_AA ATPase, F1 complex, delta/epsilon subunit
MtC00135_1_AA Ribosomal protein S8E
MtC00199_1_AA Ribosomal protein S8E
MtC00015_1_AA Peptidyl-prolyl cis-trans isomerase, cyclophilin type
MtC10908_1_AA Cytochrome b5
MtC10080_1_AA Cytochrome b5
MtC93078_1_AA Sigma-54 factor, interaction region IPR013753:Ras
MtC20086_1_AA Sigma-54 factor, interaction region IPR003579:Ras small GTPase, Rab type
MtC60316_1_AA Sigma-54 factor, interaction region IPR013753:Ras IPR015595:
MtC00594_1_AA Sigma-54 factor, interaction region IPR013753:Ras IPR015595:
MtD01385_1_AA Small GTP-binding protein domain IPR015595:
MtC62304_1_AA Ras small GTPase, Rab type
MtC00162_1_AA Kunitz inhibitor ST1-like
MtC61398_1_AA Sigma-54 factor, interaction region IPR013753:Ras
MtC30233_1_AA Sigma-54 factor, interaction region IPR003579:Ras small GTPase, Rab type
MtC00207_1_AA Sigma-54 factor, interaction region IPR013753:Ras
MtC90027_1_AA Sigma-54 factor, interaction region IPR013753:Ras
MtC60221_1_AA Sigma-54 factor, interaction region IPR003579:Ras small GTPase, Rab type
MtC00385_1_AA Ras small GTPase, Rab type
MtC00581_1_AA Ras small GTPase, Rab type
MtC10068_1_AA Enolase
MtC10113_1_AA Phosphoglucose isomerase (PGI)
MtC00100_1_AA Fructose-bisphosphate aldolase, class-I
MtC60154_1_AA Fructose-bisphosphate aldolase, class-I
MtC60189_1_AA ATPase, V1 complex, subunit C
MtC00032.1_1_AA Ribosomal protein S13
MtC00435_1_AA Ribosomal protein S13
MtC10375_1_AA Glycerophosphoryl diester phosphodiesterase
MtC00037_1_AA Ribosomal protein S4E
MtC00189_1_AA ATP-binding region, ATPase-like IPR009079:Four-helical cytokine

MtC10218_1_AA UTP--glucose-1-phosphate uridylyltransferase
MtC00040_1_AA Ribosomal protein S11
MtC00327_1_AA Ribosomal protein S11
MtC30197_1_AA IQ calmodulin-binding region
MtC00750_1_AA Complex 1 LYR protein
MtD00010.1_1_AA Translation elongation factor EF-1, alpha subunit
MtC00009_1_AA Bet v I allergen
MtC00227_1_AA Bet v I allergen
MtC00219_1_AA Bet v I allergen
MtC20134.2_1_AA Phosphate permease
MtC00168_1_AA Bet v I allergen
MtC00552_1_AA DOMON related IPR006593:Cytochrome b561 / ferric reductase transmembrane
MtC01542_1_AA Translation factor
MtC62284_1_AA Major facilitator superfamily
MtC50199_1_AA Ubiquinol cytochrome reductase transmembrane region IPR005805:Rieske iron-sulfur protein IPR014349:
MtC30089_1_AA unknown
MtD00014_1_AA ATP-binding region, ATPase-like IPR009079:Four-helical cytokine
MtD00238_1_AA ATP-binding region, ATPase-like IPR015566:
MtC20003_1_AA Respiratory-chain NADH dehydrogenase domain, 51 kDa subunit
MtC00460_1_AA Beta-Ig-H3/fasciclin
MtC20134.1_1_AA Major facilitator superfamily
MtC00742_1_AA Band 7 protein
MtC10854_1_AA unknown
MtS10732_1_AA Elongation factor Tu, C-terminal
MtC00544_1_AA ETC complex I subunit
MtC00081_1_AA ARF/SAR superfamily
MtC20040_1_AA Cytochrome b5 IPR011987:ATPase, V1 complex, subunit H, C-terminal
MtC00001_1_AA Major intrinsic protein
MtD00930_1_AA AAA ATPase IPR013525:ABC-2 type transporter IPR013581:Plant PDR ABC transporter associated
MtC11005_1_AA Glycoside hydrolase, family 18, catalytic domain
MtS10750_1_AA unknown
MtC90574_1_AA Pleiotropic drug resistance protein PDR
MtD03898_1_AA Pleiotropic drug resistance protein PDR
MtD08577_1_AA ABC-2 type transporter
MtC10110_1_AA Phosphoglycerate kinase
MtC20119_1_AA Actin/actin-like
MtC10470_1_AA Actin/actin-like
MtC30134_1_AA ATPase, F1 complex, gamma subunit IPR002020:Citrate synthase
MtC50329_1_AA Actin/actin-like
MtC10339_1_AA Actin/actin-like
MtC00550.2_1_AA Peptidase S7, flavivirus helicase (NS3) IPR013126:Heat shock protein 70
MtC00550.3_1_AA Heat shock protein 70
MtC00642_1_AA Protein of unknown function DUF588
MtC10184_1_AA Flavoprotein pyridine nucleotide cytochrome reductase
MtC10626_1_AA Flavoprotein pyridine nucleotide cytochrome reductase
MtD24950_1_AA Heat shock protein 70
MtC93197_1_AA Beta-Ig-H3/fasciclin
MtC60719_1_AA Tetratricopeptide-like helical
MtC10116.1_1_AA Sigma-54 factor, interaction region IPR003579:Ras small GTPase, Rab type
MtC60431_1_AA Sigma-54 factor, interaction region IPR013753:Ras
MtC10611_1_AA Sigma-54 factor, interaction region IPR003579:Ras small GTPase, Rab type
MtC10076.1_1_AA Sigma-54 factor, interaction region IPR003579:Ras small GTPase, Rab type
MtC93295_1_AA Sigma-54 factor, interaction region IPR003579:Ras small GTPase, Rab type

MtC30186_1_AA Sigma-54 factor, interaction region IPR013753:Ras
MtC00146_1_AA Sigma-54 factor, interaction region IPR003579:Ras small GTPase, Rab type
MtC61535_1_AA Sigma-54 factor, interaction region IPR013753:Ras IPR015598:
MtD02358_1_AA Heat shock protein 70
MtC00477_1_AA Patatin IPR008271:Serine/threonine protein kinase, active site
MtC10323_1_AA Complex 1 LYR protein
MtC00239_1_AA Heat shock protein 70
MtC60886_1_AA Ribosomal protein L15
MtC00413_1_AA Ribosomal protein L15
MtC00664.1_1_AA Haem peroxidase, plant/fungal/bacterial
MtC60441_1_AA Cytochrome b5
MtC00113_1_AA Ribosomal protein L13e
MtC00176_1_AA Ribosomal protein L13e
MtC00424_1_AA Vacuolar (H+)-ATPase G subunit
MtC00230_1_AA Plectin/S10, N-terminal
MtD01002_1_AA Tetratricopeptide TPR_1
MtC00121_1_AA S-adenosyl-L-homocysteine hydrolase
MtC30011_1_AA S-adenosyl-L-homocysteine hydrolase
MtC61065_1_AA Reticulon
MtC10115_1_AA unknown
MtC60575_1_AA TolB, C-terminal
MtC00108_1_AA Ribosomal protein L24/L26
MtC00414_1_AA Ribosomal protein L24/L26 IPR014723:
MtC45548_1_AA Ribosomal protein L24/L26 IPR014723:
MtD06379_1_AA unknown
MtC10213_1_AA ATPase, V0/A0 complex, subunit C/D
MtC30094_1_AA Protein kinase
MtC11009_1_AA Tyrosine protein kinase, active site
MtC00166.1_1_AA Translation factor IPR009022:Elongation factor G, III and V
MtC20024_1_AA Translation factor IPR009022:Elongation factor G, III and V
MtC00148_1_AA Ribosomal protein S7E
MtC00103_1_AA Ribosomal protein L2 IPR008994:Nucleic acid-binding, OB-fold IPR014726:
MtC00192_1_AA Ribosomal protein L6E IPR005568:Ribosomal protein L6, N-terminal
MtC00155.1_1_AA Ribosomal protein L6E IPR005568:Ribosomal protein L6, N-terminal
MtC00008_1_AA Haem peroxidase, plant/fungal/bacterial
MtC30022_1_AA Malic oxidoreductase
MtC00747.1_1_AA Cytochrome P450
MtC60677_1_AA Haem peroxidase, plant/fungal/bacterial
MtD11469_1_AA Inorganic H+ pyrophosphatase
MtC00101_1_AA Ribosomal protein S19/S15
MtC00089_1_AA Ribosomal protein L10 IPR001813:Ribosomal protein 60S
MtC00072.1_1_AA Major intrinsic protein
MtC00471_1_AA Tubulin IPR013838:Beta tubulin, autoregulation binding site
MtC00356.2_1_AA Tubulin
MtC00047_1_AA Ribosomal protein S24e
MtC10379_1_AA unknown
MtD00921_1_AA Alpha/beta hydrolase fold-1
MtC00077_1_AA S25 ribosomal protein
MtC00734_1_AA E-class P450, group I
MtC10905_1_AA Squalene/phytoene synthase
MtC00177_1_AA GRIM-19
MtC00566_1_AA Cytochrome oxidase c, subunit VIb
MtC00128_1_AA Ribosomal protein S7
MtC00661_1_AA ATPase, V1/A1 complex, subunit D

MtC00017.2_1_AA RNA-binding S4
MtC00184.1_1_AA Ribosomal L18ae protein
MtC93190_1_AA Syntaxin, N-terminal
MtC10028_1_AA unknown
MtC00572_1_AA unknown
MtC00011_1_AA Ribosomal protein L6, signature 2
MtD01494_1_AA unknown
MtC00091_1_AA S15/NS1, RNA-binding IPR012606:Ribosomal S13S15 N-terminal
MtC00306_1_AA Thioredoxin fold
MtC00104_1_AA Granulin IPR000169:Peptidase, cysteine peptidase active site
MtC10353_1_AA unknown
MtD12058_1_AA Nucleotide-binding, alpha-beta plait
MtD07266_1_AA Protein kinase
MtC30457.2_1_AA Protein kinase IPR011990:Tetratricopeptide-like helical
MtD23458_1_AA ATPase, F1/V1/A1 complex, alpha/beta subunit, nucleotide-binding
MtC00075_1_AA Ribosomal protein L18e
MtC60397_1_AA Ribosomal protein L18e
MtC00676_1_AA Superoxide dismutase, copper/zinc binding
MtC00299_1_AA Ribosomal protein L18e
MtC10414_1_AA unknown
MtC10444_1_AA NADH-ubiquinone oxidoreductase B18 subunit
MtC10182_1_AA Peptidase S8 and S53, subtilisin, kexin, sedolisin
MtC00400_1_AA Ribosomal protein L32e
MtC00744_1_AA unknown
MtC20114_1_AA Glutamine synthetase type I IPR014746:
MtC61283_1_AA Protein of unknown function UPF0172
MtC30184_1_AA Methyltransferase type 11 IPR013705:Sterol methyltransferase C-terminal
MtC20240_1_AA Multicopper oxidase, type 1
MtD01450_1_AA Porin, eukaryotic type
MtC10090.1_1_AA Protein of unknown function DUF250
MtC00039_1_AA Ribosomal protein L14
MtC00602_1_AA Ribosomal protein L14
MtC00124_2_AA unknown
MtC10536_1_AA Ribosomal protein S9
MtC00111_1_AA Ribosomal protein S19e
MtC20311_1_AA Ribosomal protein S19e
MtC10170_1_AA Alpha-helical ferredoxin
MtC20110_1_AA Pre-mRNA processing ribonucleoprotein, binding region IPR012974:NOP5, N-terminal IPR012976:NOSIC
MtC00083.1_1_AA Nascent polypeptide-associated complex NAC IPR009060:UBA-like
MtC10650_1_AA Ras small GTPase, Rab type IPR013567:EF hand associated, type-2
MtC20007_1_AA FAD linked oxidase, N-terminal
MtD15931_1_AA unknown
MtD07408_1_AA Cytochrome P450
MtC40021_1_AA Cytochrome P450
MtC90770_1_AA Calcium-binding EF-hand IPR013027:FAD-dependent pyridine nucleotide-disulphide oxidoreductase
MtC00093_1_AA Microsomal signal peptidase 25 kDa subunit
MtC00105_1_AA B12D
MtD18545_1_AA Sodium/calcium exchanger membrane region IPR011992:EF-Hand type
MtC10857.1_1_AA unknown
MtC00698_1_AA Malate dehydrogenase, active site
MtC00218.1_1_AA Malate dehydrogenase, active site
MtC60257_1_AA Phosphoenolpyruvate carboxylase IPR015813:
MtD08369_1_AA Elongation factor 1, gamma chain IPR004046:Glutathione S-transferase, C-terminal

IPR012335:Thioredoxin fold
MtC40173_1_AA Elongation factor 1, gamma chain IPR004046:Glutathione S-transferase, C-terminal IPR012335:Thioredoxin fold
MtD00118_1_AA GroEL-like chaperone, ATPase
MtC20083.1_1_AA GroEL-like chaperone, ATPase
MtC00173_1_AA Adenylate kinase
MtC30077.1_1_AA Aminoacyl-tRNA synthetase, class I IPR006861:Hyaluronan/mRNA binding protein
MtC60898_1_AA Phosphatidylinositol-specific phospholipase C, X region
MtD02232_1_AA Phosphoenolpyruvate carboxylase
MtC20035_1_AA Dynamin central region IPR001401:Dynamin IPR003130:Dynamin GTPase effector
MtC40192_1_AA Dynamin central region IPR001401:Dynamin IPR003130:Dynamin GTPase effector
MtD10710_1_AA AAA ATPase
MtC93032_1_AA Dynamin central region IPR001401:Dynamin IPR003130:Dynamin GTPase effector
MtD00070_1_AA Dihydrolipoamide acetyltransferase, long form
MtC60502_1_AA Mitochondrial import inner membrane translocase, subunit Tim17/22
MtD05591_1_AA Cytochrome P450
MtC10066_1_AA TRASH
MtC61265_1_AA Plant disease resistance response protein
MtC00035_1_AA Ribosomal protein L13, archea and eukaryotic form
MtC00251_1_AA Ribosomal protein L13, archea and eukaryotic form
MtC20341_1_AA Ribosomal protein L13, archea and eukaryotic form
MtC00748_1_AA ATPase, V0 complex, proteolipid subunit C,
MtC63141_1_AA Peroxysomal long chain fatty acyl transporter
MtC20165_1_AA Peroxysomal long chain fatty acyl transporter
MtC30266_1_AA Small GTP-binding protein domain
MtC30399_1_AA ATPase, V1/A1 complex, subunit F
MtC00096_1_AA Ribosomal protein S6e IPR014401:
MtC00469_1_AA Ribosomal protein S6e IPR014401:
MtC00568_1_AA Translocon-associated beta
MtC00087.1_1_AA Ras
MtC00606_1_AA IPR008089:Nucleotide sugar epimerase
MtC10807_1_AA NAD-dependent epimerase/dehydratase
MtD03747_1_AA NAD-dependent epimerase/dehydratase
MtC00049_1_AA Ribosomal protein L10E
MtC20133_1_AA Nonaspanin (TM9SF)
MtC30154.1_1_AA unknown
MtC30235_1_AA Glycoside hydrolase, catalytic core
MtC92247_1_AA E-class P450, group I
MtC40093_1_AA Nonaspanin (TM9SF)
MtD04425_1_AA von Willebrand factor, type A IPR006692:Coatomer WD associated region IPR010714:Coatomer alpha subunit, C-terminal
MtC00059_1_AA Triosephosphate isomerase
MtD00173_1_AA Blue (type 1) copper domain
MtC00328_1_AA Mitochondrial ribosomal protein L5
MtC20131_1_AA Rubrerythrin IPR009040:Ferritin-like IPR014034:
MtC00085.1_1_AA Histone core IPR009072:Histone-fold
MtC00508_1_AA Sec61beta
MtC91970_1_AA Histone H3 IPR007124: IPR009072:Histone-fold
MtC00491_1_AA Histone H3 IPR007124: IPR009072:Histone-fold
MtC10405_1_AA Peptidase A1, pepsin
MtC10752_1_AA Peptidase A1, pepsin
MtC10430_1_AA Major intrinsic protein
MtC10909_1_AA Reticulon
MtC10407_1_AA ATPase, F1/V1/A1 complex, alpha/beta subunit, nucleotide-binding
MtC63279_1_AA Scramblase

MtD16182_1_AA Protein of unknown function DUF588
MtC00233_1_AA MIR
MtC00535_1_AA Sigma-54 factor, interaction region IPR003579:Ras small GTPase, Rab type
MtD03445_1_AA Sigma-54 factor, interaction region IPR003579:Ras small GTPase, Rab type
MtC20143_1_AA Haem peroxidase, plant/fungal/bacterial
MtC00322_1_AA Ribosomal protein L23, N-terminal IPR013025:Ribosomal protein L25/L23
MtC00095_1_AA Ribosomal protein L23, N-terminal IPR013025:Ribosomal protein L25/L23
MtC10251_1_AA Prenylated rab acceptor PRA1
MtC20228.1_1_AA Thioredoxin-related IPR012336:Thioredoxin-like fold IPR013766:Thioredoxin domain
MtC40096_1_AA Protein disulphide isomerase IPR012336:Thioredoxin-like fold IPR013766:Thioredoxin domain
MtC45398_1_AA Glycoside transferase, six-hairpin, subgroup
MtD05256_1_AA Seryl-tRNA synthetase, class IIa IPR015866:
MtC10984_1_AA AMP-dependent synthetase and ligase
MtD02891_1_AA unknown
MtC91392_1_AA unknown
MtD05399_1_AA unknown
MtC00580.1_1_AA Eukaryotic ribosomal protein L5
MtD06307_1_AA unknown
MtC00137_1_AA Ribosomal protein L1
MtC00668_1_AA Ribosomal protein L1
MtC00506_1_AA Ribosomal protein L1
MtD00252_1_AA Prefoldin IPR010989:t-snare
MtD22970_2_AA unknown
MtC10185.1_1_AA E-class P450, group I
MtD27821_1_AA Dynamin central region
MtC00623_1_AA Cell division protein FtsZ
MtC20031_1_AA Cell division protein FtsZ
MtC00684_1_AA unknown
MtC10241_1_AA Ribosomal protein S10, eukaryotic and archaeal form
MtC10627_1_AA Ribosomal protein S10, eukaryotic and archaeal form
MtC00521_1_AA Ribosomal protein S10, eukaryotic and archaeal form
MtC00138_1_AA Ribosomal protein S17e
MtC00407_1_AA Peroxisomal biogenesis factor 11
MtD25003_1_AA unknown
MtC00194_1_AA unknown
MtC10351_1_AA unknown
MtC60783_1_AA Protein kinase IPR002048:Calcium-binding EF-hand
MtC00304_1_AA unknown
MtC60699_1_AA Protein of unknown function DUF248, methyltransferase putative
MtC30445_1_AA Protein kinase
MtC61176_1_AA Protein kinase
MtD02090_1_AA Protein kinase
MtC00144_1_AA Ribosomal protein L22/L17, eukaryotic and archaeal form
MtC00315_1_AA Ribosomal protein L22/L17, eukaryotic and archaeal form
MtD01335_1_AA Eukaryotic/archaeal ribosomal protein S3
MtC00318_1_AA Eukaryotic/archaeal ribosomal protein S3
MtD01818_1_AA ATP-grasp fold
MtC60808_1_AA ATPase, P-type cation-transporter, C-terminal
MtC00338_1_AA Transaldolase subfamily
MtC30387_1_AA unknown
MtC10629_1_AA Synaptobrevin IPR011012:Longin-like
MtC10402_1_AA Malate dehydrogenase, active site
MtD02749_1_AA unknown

MtC60899_1_AA Cytochrome b5
MtD12105_1_AA Major intrinsic protein
MtC00209_1_AA Ribosomal L28e protein
MtC00134_1_AA Ribosomal L28e protein
MtD13928_1_AA Cold-shock protein, DNA-binding
MtC45457_1_AA unknown
MtC10092_1_AA unknown
MtC10679_1_AA NADH:ubiquinone oxidoreductase 17.2 kD subunit
MtC00556_1_AA unknown
MtC10643_1_AA Calcium-binding EF-hand IPR015757:
MtC10646_1_AA ATPase, P-type, K/Mg/Cd/Cu/Zn/Na/Ca/Na/H-transporter
MtC93235_1_AA ATPase, P-type, K/Mg/Cd/Cu/Zn/Na/Ca/Na/H-transporter
MtC10159_1_AA Carbohydrate kinase, PfkB
MtC60476_1_AA Carbohydrate kinase, PfkB
MtC60362_1_AA Haloacid dehalogenase-like hydrolase
MtD10584_1_AA ATPase, P-type, K/Mg/Cd/Cu/Zn/Na/Ca/Na/H-transporter
MtD13438_1_AA E1-E2 ATPase-associated region
MtC00402_1_AA Nascent polypeptide-associated complex NAC
MtC00683_1_AA Nascent polypeptide-associated complex NAC
MtC60845_1_AA Protein of unknown function DUF1077
MtC00031_1_AA Major intrinsic protein
MtC00086_1_AA Ribosomal protein L19e
MtC00051_1_AA Ribosomal protein L19e
MtC30080_1_AA Deoxyxylulose-5-phosphate synthase
MtC00454_1_AA unknown
MtD01246_1_AA Protein kinase
MtD05462_1_AA Staphylococcus nuclease subtype
MtC20271_1_AA Ubiquinol-cytochrome C reductase, UQCRXQCR9 like
MtC30211_1_AA K+ potassium transporter
MtC50890_1_AA AAA-protein subdomain IPR005938:AAA ATPase, CDC48
MtD08475_1_AA AAA ATPase, central region
MtC90568_1_AA Major sperm protein
MtD00721_1_AA Protein of unknown function DUF250
MtC50602_1_AA Major sperm protein
MtC00735_1_AA Ribosomal protein 60S
MtD08074_1_AA Major intrinsic protein
MtC00078_1_AA Ribosomal protein 60S
MtC62382_1_AA Ribosomal protein 60S
MtC00127_1_AA Ferritin-like
MtC00046_1_AA S-adenosylmethionine synthetase
MtC00034_1_AA S-adenosylmethionine synthetase
MtC30195_1_AA Haem peroxidase, plant/fungal/bacterial IPR002133:S-adenosylmethionine synthetase
MtC45479_1_AA Major facilitator superfamily MFS_1
MtC00421_1_AA Haem peroxidase, plant/fungal/bacterial
MtC30297_1_AA Major sperm protein
MtC30183_1_AA CD9/CD37/CD63 antigen
MtD06241_1_AA CD9/CD37/CD63 antigen
MtC10659_1_AA C2 calcium-dependent membrane targeting
MtC45339_1_AA Sulphate transporter
MtC00438_1_AA ATPase, F1 complex, epsilon subunit, mitochondrial
MtC00016_1_AA Nucleoside diphosphate kinase
MtC30456.1_1_AA Ribophorin I
MtC10855_1_AA unknown

MtD13578_1_AA unknown
MtC00169_1_AA Elongation factor 1, beta/beta/delta chain IPR010987:Glutathione S-transferase, C-terminal-like IPR014038: IPR014717:
MtC10130_1_AA Metallophosphoesterase
MtD00400_1_AA Nonaspanin (TM9SF) IPR005479:Carbamoyl-phosphate synthase L chain, ATP-binding
MtC10600.1_1_AA Nonaspanin (TM9SF)
MtD00397_1_AA unknown
MtC00145_1_AA Ribosomal L22e protein
MtC20223_1_AA GroEL-like chaperone, ATPase
MtC10630_1_AA Ribosomal L22e protein
MtC00653_1_AA Flavoprotein pyridine nucleotide cytochrome reductase IPR008254:Flavodoxin/nitric oxide synthase IPR015702:
MtD00539_1_AA unknown
MtC10663_1_AA Flavoprotein pyridine nucleotide cytochrome reductase IPR008254:Flavodoxin/nitric oxide synthase
MtC10312_1_AA Glycoside hydrolase, family 19, catalytic IPR001002:Chitin-binding, type 1
MtC10145_1_AA Proteasome alpha-subunit
MtC20137_1_AA GroEL-like chaperone, ATPase
MtC10461_1_AA emp24/gp25L/p24
MtC30349_1_AA ER lumen protein retaining receptor
MtD00845_1_AA Protein of unknown function DUF221
MtC30054_1_AA DEAD-like helicases, N-terminal IPR014014:DEAD-box RNA helicase Q motif
MtC10085.1_1_AA Glycoside hydrolase, catalytic core
MtC60333_1_AA Cytochrome c oxidase, subunit Vb
MtD17495_1_AA t-snare
MtD02792_1_AA Reticulon
MtC00069_1_AA Ribosomal protein L14b/L23e
MtC01440_1_AA Peptidase T1A, proteasome beta-subunit
MtC00181.1_1_AA Mitochondrial import inner membrane translocase, subunit Tim17/22
MtC62673_1_AA Peroxysomal long chain fatty acyl transporter
MtD00950_1_AA Porin, eukaryotic type
MtC00161_1_AA Cytochrome b561 / ferric reductase transmembrane
MtC10149_1_AA Blue (type 1) copper domain
MtD04199_1_AA Blue (type 1) copper domain
MtC40087_1_AA Ribosomal protein L7AE
MtD16310_1_AA Ribosomal protein L7A IPR004342:EXS, C-terminal
MtC00722_1_AA Proteasome alpha-subunit
MtC20045_1_AA DnaJ central region
MtC60155_1_AA Heat shock protein DnaJ
MtC10231_1_AA Heat shock protein DnaJ
MtC10221_1_AA Proteasome alpha-subunit
MtC00254_1_AA HMG1/2 (high mobility group) box
MtD04793_1_AA Bacterial surface antigen (D15)
MtD06341_1_AA Leucine rich repeat, N-terminal
MtD03001_1_AA ABC-2 type transporter IPR013581:Plant PDR ABC transporter associated
MtC10121.1_1_AA E-class P450, group I
MtD02601_1_AA Cytochrome P450
MtC50269.2_1_AA Tudor IPR006022:Staphylococcus nuclease subtype
MtC50311_1_AA LMBR1-like conserved region
MtC20142_1_AA Tetratricopeptide region
MtD01112_1_AA unknown
MtC93099_1_AA Growth factor, receptor
MtC30069_1_AA Proteasome alpha-subunit
MtC20048_1_AA unknown

MtC93375_1_AA unknown
MtC93047_1_AA Clathrin light chain
MtD11061_1_AA Leucine-rich repeat
MtC20051.2_1_AA Transketolase, central region
MtS00138_1_AA unknown
MtD14618_1_AA Mitochondrial carrier protein
MtD02555_1_AA unknown
MtD07002_1_AA Mitochondrial substrate carrier
MtC00167_1_AA Ribosomal protein S17
MtC00024_1_AA Ribosomal protein S17
MtC40004.1_1_AA E-class P450, group I
MtC00518_1_AA Major intrinsic protein IPR002208:SecY protein IPR003439:ABC transporter related
MtD00748_1_AA Peptidase S8 and S53, subtilisin, kexin, sedolisin IPR015500:
MtD03426_1_AA unknown
MtC30292_1_AA ATPase, P-type cation-transporter, C-terminal
MtC10961_1_AA unknown
MtC00416_1_AA Universal stress protein (Usp) IPR014729:
MtC40095_1_AA Aspartyl-tRNA synthetase, class IIb IPR004365:nucleic acid binding, OB-fold, tRNA/helicase-type
MtC60711_1_AA NADH dehydrogenase (ubiquinone), 20 kDa subunit
MtD24909_1_AA Cytochrome c oxidase, subunit Vb
MtC30120_1_AA Annexin, type plant IPR015472:
MtD00644_1_AA Diacylglycerol kinase, catalytic region
MtD09396_1_AA Oligosaccharyl transferase, STT3 subunit
MtC10530_1_AA CHCH
MtC00092.1_1_AA Peptidase, cysteine peptidase active site
MtC62969_1_AA Tetratricopeptide-like helical
MtC30030_1_AA Peptidase M16, N-terminal
MtC00591_1_AA E-class P450, group I
MtC61192_1_AA Ribosomal protein S8
MtC20071_1_AA 2OG-Fe(II) oxygenase
MtD06942_1_AA Inorganic H+ pyrophosphatase
MtC30210_1_AA Nonaspanin (TM9SF)
MtD02094_1_AA Eukaryotic translation initiation factor 3, subunit 7
MtC91364_1_AA Strictosidine synthase IPR011042:TolB, C-terminal
MtC91949_1_AA Protein phosphatase 2C-like
MtC00129_1_AA unknown
MtC30575.1_1_AA TonB box, N-terminal
MtD07674_1_AA Surface antigen variable number
MtC93228_1_AA Haem peroxidase, plant/fungal/bacterial
MtC20102_1_AA Cupredoxin
MtC45631_1_AA Protein of unknown function DUF850, transmembrane eukaryotic
MtC60334_1_AA ETC complex I subunit conserved region
MtC00312.1_1_AA 20S proteasome, A and B subunits
MtC10355_1_AA unknown
MtC30087_1_AA E-class P450, group I
MtD15950_1_AA SOUL heme-binding protein
MtC00122.1_1_AA Ribosomal protein L34e
MtC00307_1_AA Major intrinsic protein
MtC10229_1_AA unknown
MtC00359_1_AA Haem peroxidase, plant/fungal/bacterial
MtC00680.1_1_AA Glycoside hydrolase, family 18, catalytic domain
MtC61024_1_AA Peptidase S24, S26A and S26B IPR015927:
MtC93300_1_AA unknown

MtC20379_1_AA General substrate transporter
MtC93387_1_AA Diacylglycerol kinase accessory region
MtD26107_1_AA Protein of unknown function DUF248, methyltransferase putative
MtC45338.1_1_AA
MtC40200_1_AA
MtC93412_1_AA Cytochrome P450
MtC00110_1_AA Ribosomal protein S26E IPR008957:Fibronectin, type III-like fold
MtD18706_1_AA unknown
MtC00231_1_AA Calcium-binding EF-hand
MtC90917_1_AA unknown
MtC00064_1_AA Ribosomal protein L36E
MtC00005_1_AA Plant lipid transfer protein/seed storage/trypsin-alpha amylase inhibitor
MtC00590_1_AA unknown
MtC20389_1_AA Dihydrolipoamide acetyltransferase, long form
MtC40005_1_AA Glycosyl transferase, family 2
MtC00066_1_AA Ribosomal protein L21e
MtC00539_1_AA Ribosomal protein L21e
MtC10096_1_AA Manganese and iron superoxide dismutase
MtC00772_1_AA Glycine hydroxymethyltransferase
MtC00153_1_AA Peptidase S24, S26A and S26B IPR015927:
MtC10610_1_AA Tetratricopeptide-like helical
MtC45345_1_AA Concanavalin A-like lectin/glucanase
MtC10052_1_AA ArgE/dapE/ACY1/CPG2/yscS IPR002715:Nascent polypeptide-associated complex NAC IPR009060:UBA-like
MtC00689_1_AA Peptidylprolyl isomerase, FKBP-type
MtC00326_1_AA 6-phosphogluconate dehydrogenase, C-terminal extension
MtC20220_1_AA Mov34-1
MtD03607_1_AA 6-phosphogluconate-binding site
MtC00571_1_AA 6-phosphogluconate dehydrogenase, C-terminal extension
MtC60231_1_AA Carotenoid oxygenase
MtC60716_1_AA Nicastrin
MtC10442_1_AA Annexin
MtD17397_1_AA ATPase, P-type, K/Mg/Cd/Cu/Zn/Na/Ca/Na/H-transporter
MtD20233_1_AA Succinate dehydrogenase/fumarate reductase iron-sulfur protein IPR012285:Fumarate reductase, C-terminal
MtC00288_1_AA Cytochrome c oxidase subunit Vc
MtC93129_1_AA Protein of unknown function UPF0136, Transmembrane
MtD00177_1_AA Mitochondrial import inner membrane translocase, subunit Tim17/22
MtC10064_1_AA Adenosine kinase
MtC10533_1_AA unknown
MtD07270_1_AA Optic atrophy 3
MtD13384_1_AA C2 calcium-dependent membrane targeting
MtC10104_1_AA Peptidase T1A, proteasome beta-subunit
MtD07825_1_AA Protein kinase IPR001150:Formate C-acetyltransferase glycine radical
MtC00102_1_AA Eukaryotic initiation factor 5A hypusine (eIF-5A) IPR012340:Nucleic acid-binding, OB-fold, subgroup IPR014722:
MtC00190_1_AA Eukaryotic initiation factor 5A hypusine (eIF-5A)
MtC10874_1_AA Disulphide isomerase IPR006663: IPR012336:Thioredoxin-like fold IPR013766:Thioredoxin domain
MtC00143_1_AA Ribosomal protein S27E
MtC20393_1_AA Phosphoinositide-specific phospholipase C, C-terminal (PLC) IPR011992:EF-Hand type IPR015359:
MtC00404_1_AA Ribosomal protein L27e IPR005824:KOW
MtC00106_1_AA HMG1/2 (high mobility group) box
MtD00941_1_AA Band 7 protein

MtC00094_1_AA Chalcone-flavanone isomerase
MtD01733_1_AA Linker histone, N-terminal
MtC20234_1_AA IPR013216:Methyltransferase type 11 IPR013705:Sterol methyltransferase C-terminal
MtC30033_1_AA Thiolase
MtC00067_1_AA Flavodoxin/nitric oxide synthase
MtC10046_1_AA Flavodoxin/nitric oxide synthase
MtC10675_1_AA Small GTP-binding protein domain
MtD03039_1_AA Flavodoxin/nitric oxide synthase
MtC01434.1_1_AA Heat shock protein 70
MtD00691_1_AA Heat shock protein 70
MtC40216_1_AA E-class P450, group I
MtD01243_1_AA Concanavalin A-like lectin/glucanase
MtC62070_1_AA Diacylglycerol kinase, catalytic region
MtC10783_1_AA ATP-citrate lyase/succinyl-CoA ligase
MtC50144_1_AA Nuclear transport factor 2 IPR012677:Nucleotide-binding, alpha-beta plait
MtC61028_1_AA Alba, DNA/RNA-binding protein
MtD00232_1_AA Cleft lip and palate transmembrane 1
MtC61888_1_AA Kunitz inhibitor ST1-like
MtC10298_1_AA Flavodoxin/nitric oxide synthase
MtC61089_1_AA Mitochondrial ribosome
MtC20250.1_1_AA Peroxysomal long chain fatty acyl transporter
MtC00348_1_AA Alkaline phosphatase IPR005995:Phosphoglycerate mutase, 2,3-bisphosphoglycerate-independent
MtC62895_1_AA Band 7 protein
MtD24902_1_AA ABC transporter related
MtD00351_1_AA unknown
MtD07414_1_AA Leucine-rich repeat
MtC00324_1_AA Ribosomal protein L29
MtC00725_1_AA Ribosomal protein L29
MtC10007_1_AA Bet v I allergen
MtC00597_1_AA SCAMP
MtC93030_1_AA Succinyl-CoA ligase, alpha subunit
MtC93061_1_AA SCAMP
MtC00463_1_AA Pyruvate kinase IPR015793: IPR015794: IPR015795: IPR015813:
MtC00531_1_AA Pyrophosphate-dependent phosphofructokinase PfpB IPR015913:
MtD17620_1_AA Protein of unknown function DUF588
MtC90955_1_AA Short-chain dehydrogenase/reductase SDR
MtC10982_1_AA unknown
MtC10331_1_AA WD40-like
MtD11268_1_AA tRNA-binding arm
MtC30086.2_1_AA Protein of unknown function DUF248, methyltransferase putative
MtC40018_1_AA
MtC30114_1_AA unknown
MtC30248_1_AA Reticulon
MtD01059_1_AA Reticulon
MtD11510_1_AA OST3/OST6
MtD17080_1_AA unknown
MtC00200_1_AA Ribosomal protein L30e
MtC91735_1_AA unknown
MtC30185_1_AA Peptidase aspartic, active site
MtC62988_1_AA unknown
MtC30342_1_AA Protein phosphatase 2C-like
MtC20331_1_AA Histone H2A IPR007124: IPR009072:Histone-fold
MtC45435_1_AA Proteasome alpha-subunit

MtD01191_1_AA unknown
MtC00234.1_1_AA NmrA-like
MtC10502_1_AA NmrA-like
MtD12603_1_AA 7-Fold repeat in clathrin and VPS proteins
MtC45570_1_AA Mitochondrial import inner membrane translocase, subunit Tim17/22
MtD11146_1_AA unknown
MtC10417_1_AA SAC3/GANP/Nin1/mts3/eIF-3 p25
MtD00123_1_AA Protein of unknown function DUF248, methyltransferase putative
MtD00856_1_AA Nitrate reductase NADH dependant
MtD11751_1_AA unknown
MtC20025_1_AA Mitochondrial substrate carrier
MtD00535_1_AA Fumarate reductase/succinate dehydrogenase, FAD-binding site IPR013027:FAD-dependent pyridine nucleotide-disulphide oxidoreductase
MtC00028_1_AA Kunitz inhibitor ST1-like
MtC10385_1_AA unknown
MtD12678_1_AA Cupin 1 IPR007113:
MtD15605_1_AA Cytochrome P450
MtC10267.1_1_AA Proteasome alpha-subunit
MtC93113_1_AA Proteasome component region PCI IPR011990:Tetratricopeptide-like helical IPR013143:PCI/PINT associated module
MtC00140_1_AA Ribosomal protein 60S
MtC10267.2_1_AA Proteasome alpha-subunit
MtD00114_1_AA Hydroxymethylglutaryl-coenzyme A synthase
MtC00493_1_AA IPR012336:Thioredoxin-like fold IPR013766:Thioredoxin domain
MtS10012_1_AA E-class P450, group I
MtC00249_1_AA Ribosomal protein L37e
MtC00793_1_AA Nucleotide-binding, alpha-beta plait
MtC62546_1_AA ATPase, F0 complex, subunit G, mitochondrial
MtD00571_1_AA Protein of unknown function DUF1682
MtC00159_1_AA emp24/gp25L/p24 IPR001071:Cellular retinaldehyde binding/alpha-tocopherol transport IPR008273:Cellular retinaldehyde-binding/triple function, N-terminal
MtD03626_1_AA Stomatin
MtD14276_1_AA Chaperonin TCP-1
MtD04957_1_AA Soluble quinoprotein glucose dehydrogenase
MtC00082_1_AA Universal stress protein (Usp)
MtC00466_1_AA High mobility group-like nuclear protein
MtC00258_1_AA Ribosomal protein S2, eukaryotic and archaeal form
MtD04430_1_AA
MtC00700_1_AA unknown
MtC30417_1_AA emp24/gp25L/p24 IPR008273:Cellular retinaldehyde-binding/triple function, N-terminal
MtC00088_1_AA Peptidyl-prolyl cis-trans isomerase, cyclophilin type IPR015891:
MtC00732_1_AA unknown
MtC10835_1_AA Nickel/cobalt transporter, high-affinity
MtC20008_1_AA Metal-dependent hydrolase, composite
MtC11011_1_AA Thioredoxin-like fold
MtC61893_1_AA unknown
MtC00366_1_AA Small GTP-binding protein domain
MtC00221_1_AA Ras GTPase
MtC10242_1_AA Nucleoside diphosphate kinase
MtC90388_1_AA unknown
MtC93035_1_AA Peptidase A1, pepsin
MtD01562_1_AA B-cell receptor-associated 31-like IPR009053:Prefoldin
MtD01568_1_AA Putative rRNA pseudouridine synthase
MtC00688_1_AA Bet v I allergen

MtC60945_1_AA Natural resistance-associated macrophage protein
MtC00343.1_1_AA Bet v I allergen
MtC00074_1_AA Bet v I allergen
MtC20248_1_AA General substrate transporter
MtD00484_1_AA DOMON related IPR006593:Cytochrome b561 / ferric reductase transmembrane
MtC90816_1_AA Fibrillarin
MtC30296_1_AA Carbohydrate-binding-like fold
MtC00245_1_AA Bet v I allergen
MtC00252.1_1_AA Protein of unknown function DUF1138
MtC10095_1_AA Chalcone-flavanone isomerase
MtC00054_1_AA Actin-binding, cofilin/tropomyosin type
MtC30123.1_1_AA unknown
MtC10018_1_AA Glutathione S-transferase, C-terminal IPR012335:Thioredoxin fold
MtC60596_1_AA Kunitz inhibitor ST1-like
MtD00112_1_AA Rh-like protein/ammonium transporter
MtC10194_1_AA unknown
MtD00116.1_1_AA DOMON related
MtC45586_1_AA ATPase, P-type cation-transporter, C-terminal
MtC30065_1_AA E-class P450, group I
MtC00320_1_AA O-methyltransferase, family 2 IPR001601: IPR012967:Dimerisation
MtC20377_1_AA Synaptobrevin IPR011012:Longin-like
MtC00216_1_AA Synaptobrevin IPR011012:Longin-like
MtD01574_1_AA E-class P450, group I
MtC10069_1_AA Tetratricopeptide TPR_1
MtC00331_1_AA Plant acid phosphatase
MtC00656_1_AA Protein secE/sec61-gamma protein
MtC00118.1_1_AA Nucleic acid-binding, OB-fold, subgroup
MtC30281.1_1_AA Prenyltransferase/squalene oxidase
MtC60823_1_AA Mitochondrial import inner membrane translocase, subunit Tim17/22
MtC10091_1_AA DREPP plasma membrane polypeptide
MtC61096_1_AA emp24/gp25L/p24
MtD12384_1_AA Protein kinase IPR007090:
MtC00708_1_AA Protein kinase
MtC45467_1_AA emp24/gp25L/p24 IPR001356:Homeobox
MtC30193_1_AA N-acyl-L-amino-acid amidohydrolase
MtC20115_1_AA Pyridine nucleotide-disulphide oxidoreductase, class I
MtC30561_1_AA Plant disease resistance response protein
MtC61652_1_AA Bacterial surface antigen (D15)
MtC93137_1_AA emp24/gp25L/p24
MtC10373_1_AA Peptidase T1A, proteasome beta-subunit
MtC63034_1_AA Calcium-binding EF-hand
MtC10547_1_AA ATPase, F0 complex, subunit G, mitochondrial
MtD00237_1_AA Protease-associated PA
MtD26753_1_AA Bacterial surface antigen (D15)
MtC20277_1_AA unknown
MtC61099_1_AA Helix-turn-helix type 3 IPR013729:Multiprotein bridging factor 1, N-terminal
MtC00261_1_AA Thioredoxin-like fold IPR013740:Redoxin
MtS00040_1_AA unknown
MtD01344_1_AA Cytochrome P450
MtD08046_1_AA C2 calcium/lipid-binding region, CaLB
MtD04304_1_AA AAA ATPase
MtD03384_1_AA Peroxysomal long chain fatty acyl transporter
MtD01250_1_AA AAA ATPase
MtC30059_1_AA Alpha-1,4-glucan-protein synthase, UDP-forming

MtC10969_1_AA Alpha-1,4-glucan-protein synthase, UDP-forming
MtD02820_1_AA Protein kinase IPR002048:Calcium-binding EF-hand
MtC90224_1_AA Alpha-1,4-glucan-protein synthase, UDP-forming
MtC20347_1_AA Concanavalin A-like lectin/glucanase
MtC60191_1_AA E-class P450, group I
MtC10154_1_AA NAD-dependent epimerase/dehydratase
MtC10336_1_AA SAC3/GANP/Nin1/mts3/eIF-3 p25 IPR011991:Winged helix repressor DNA-binding
MtC00151_1_AA Ribosomal protein L31e
MtC00367_1_AA Dienelactone hydrolase
MtC00501_1_AA Ctr copper transporter
MtC10483_2_AA unknown
MtD06042_1_AA Protein kinase
MtC00297_1_AA Plant acid phosphatase IPR014403:
MtD01690_1_AA Annexin
MtC40038_1_AA Clathrin light chain
MtC60580_1_AA Peptidyl-prolyl cis-trans isomerase, cyclophilin type IPR015891:
MtD03040_1_AA SCAMP
MtC00534_1_AA C2 calcium-dependent membrane targeting
MtC00778_1_AA General substrate transporter
MtC10834_1_AA Plant disease resistance response protein
MtC62227_1_AA Zinc finger, Tim10/DDP-type
MtD19684_1_AA unknown
MtD19528_1_AA unknown
MtC40039_1_AA Lipase, class 3
MtC10600.2_1_AA Hexokinase
MtC93146_1_AA WD40-like
MtD00178_1_AA Protein of unknown function DUF248, methyltransferase putative
MtD07370_1_AA Protein of unknown function DUF248, methyltransferase putative
MtC00228_1_AA Leucine rich repeat, N-terminal
MtC60137_1_AA Peptidase aspartic, active site
MtD22772_1_AA Ubiquinol-cytochrome C reductase hinge protein
MtC10138_1_AA Ubiquinol-cytochrome C reductase hinge protein
MtC10596_1_AA Alternative oxidase
MtC91778_1_AA Peptidase M17, leucyl aminopeptidase
MtC00726_1_AA Protein of unknown function Cys-rich
MtC60359_1_AA Protein of unknown function Cys-rich
MtC10429_1_AA Heat shock chaperonin-binding IPR011595:Tetratricopeptide-related region
MtC90489_1_AA Protein of unknown function UPF0041
MtC00163_1_AA Ribosomal protein 60S
MtC00208_1_AA Ribosomal protein S28e IPR012340:Nucleic acid-binding, OB-fold, subgroup
MtC40031_1_AA Pectinesterase IPR006501:Pectinesterase inhibitor
MtC10168_1_AA unknown
MtC30101_1_AA Pectinesterase IPR006501:Pectinesterase inhibitor
MtC00423.1_1_AA Deoxyxylulose-5-phosphate synthase
MtC61146_1_AA Prenylated rab acceptor PRA1 IPR014475: IPR014690:
MtD01017_1_AA Purple acid phosphatase, N-terminal
MtD16665_1_AA unknown
MtC00415_1_AA Cytochrome c, monohaem
MtC20107_1_AA Peptidase M24, methionine aminopeptidase
MtC10736.1_1_AA Bet v I allergen
MtC93060_1_AA unknown
MtD09807_1_AA Prolyl-tRNA synthetase, class IIa
MtC10806.1_1_AA Phosphoesterase At2g46880
MtD13497_1_AA ABC transporter, transmembrane region, type 1

MtC00357_1_AA Thaumatin, pathogenesis-related
MtC50630_1_AA Lipase/lipooxygenase, PLAT/LH2
MtD06527_1_AA Beta-Ig-H3/fasciclin
MtC00212_1_AA Aldo/keto reductase
MtC00739.1_1_AA Succinate dehydrogenase or fumarate reductase, flavoprotein subunit, low-GC Gram-positive bacteria
MtC90369_1_AA unknown
MtC00160_1_AA Thioredoxin-related IPR012336:Thioredoxin-like fold IPR013766:Thioredoxin domain IPR015467:
MtC00375_1_AA Thioredoxin-related IPR006663: IPR012336:Thioredoxin-like fold IPR013766:Thioredoxin domain
MtD18613_1_AA Sodium/hydrogen exchanger
MtC00310_1_AA Thioredoxin-related IPR006663: IPR012336:Thioredoxin-like fold IPR013766:Thioredoxin domain
MtD00538_1_AA Short-chain dehydrogenase/reductase SDR
MtC10023_1_AA Haem peroxidase
MtC30380_1_AA unknown
MtD00231_1_AA Peptidase T1A, proteasome beta-subunit
MtD02943_1_AA Peptidase S8 and S53, subtilisin, kexin, sedolisin
MtC62065_1_AA
MtC00269_1_AA unknown
MtC93168_1_AA Like-Sm ribonucleoprotein-related, core
MtD15227_1_AA Aldehyde dehydrogenase IPR015590:
MtD00865_1_AA ENTH/VHS IPR013809:Epsin-like, N-terminal
MtD01946_1_AA AB-hydrolase YheT, putative
MtD02436_1_AA Phosphatidate cytidylyltransferase
MtC10112_1_AA Haem peroxidase, plant/fungal/bacterial
MtC30290.1_1_AA Eukaryotic translation initiation factor 2, alpha subunit IPR012340:Nucleic acid-binding, OB-fold, subgroup
MtD15465_1_AA Eukaryotic translation initiation factor 2, alpha subunit
MtC40189_1_AA Nucleosome assembly protein (NAP)
MtC20273.1_1_AA Nucleotide-binding, alpha-beta plait
MtC00185_1_AA unknown
MtC90316_1_AA E-class P450, group I
MtC93021.1_1_AA Importin alpha-like protein, beta-binding region
MtC20235_1_AA U2A/phosphoprotein 32 family A, C-terminal IPR007092:
MtC00080_1_AA EF-Hand type
MtD23826_1_AA EF-Hand type
MtC00492_1_AA E1 protein and Def2/Der2 allergen
MtC30238_1_AA t-snare
MtC60733_1_AA emp24/gp25L/p24
MtC93173_1_AA unknown
MtC45043.1_1_AA Acetyl-coenzyme A carboxyltransferase, C-terminal
MtC00349_1_AA Aconitate hydratase 1
MtC20002_1_AA Aconitate hydratase 1
MtD00498_1_AA Protein of unknown function DUF579, plant
MtD07435_1_AA Glycosyl transferase, family 48
MtD03985_1_AA Protein kinase IPR001452:Src homology-3
MtD08148_1_AA Glycosyl transferase, family 48
MtD23422_1_AA E-class P450, group I
MtS10792_1_AA Short-chain dehydrogenase/reductase SDR
MtC10150_1_AA Linker histone, N-terminal
MtC00323_1_AA Protein kinase
MtC60903_1_AA unknown
MtC00294_1_AA Aldo/keto reductase

MtC00308_1_AA Thioredoxin fold
MtD01122_1_AA Lipase/lipooxygenase, PLAT/LH2
MtC00419_1_AA HMG1/2 (high mobility group) box
MtC40030_1_AA Chloroplast protein import component Toc34
MtC93020_1_AA Dehydrogenase, E1 component
MtC30278_1_AA Dehydrogenase, E1 component
MtC00451_1_AA unknown
MtD18276_1_AA unknown
MtC10102_1_AA HMG1/2 (high mobility group) box
MtC00205.1_1_AA Cold acclimation WCOR413
MtC00502_1_AA Phenylalanine/histidine ammonia-lyase
MtC20149_1_AA unknown
MtC00512_1_AA E-class P450, group I
MtC20026_1_AA Thiolase
MtC00295.1_1_AA Ribosomal L37ae protein IPR011331: IPR011332:
MtC00527_1_AA Protein of unknown function DUF791
MtC30078_1_AA Cupin 1
MtD00492_1_AA Thymidine kinase IPR001739:Methyl-CpG binding IPR011124:Zinc finger, CW-type
MtC62650_1_AA unknown
MtD05586_1_AA unknown
MtD01393_1_AA unknown
MtD06161_1_AA C2 calcium-dependent membrane targeting
MtD07475_1_AA E-class P450, group I
MtC00012_1_AA Haem peroxidase, plant/fungal/bacterial
MtC00057_1_AA unknown
MtC20251_1_AA Adrenodoxin reductase IPR002937:Amine oxidase IPR014103:
MtC00300_1_AA unknown
MtC00743_1_AA unknown
MtC10198_1_AA E-class P450, group I
MtD00388_1_AA unknown
MtC00053_1_AA Ribosomal protein 60S
MtD07462_1_AA Cystinosin/ERS1p repeat
MtD15850_1_AA ABC transporter, transmembrane region, type 1
MtD27293_1_AA Heat shock protein DnaJ, N-terminal IPR004179:Sec63
MtC10419.1_1_AA Annexin, type plant
MtD01629_1_AA E-class P450, group I
MtD02821_1_AA unknown
MtC00058_1_AA Ribosomal L23 and L15e, core
MtC20018_1_AA Deoxyxylulose-5-phosphate synthase
MtC30291_1_AA Protein of unknown function DUF1620
MtC45672_1_AA Aminoacyl-transfer RNA synthetase, class II
MtC30415_1_AA Signal peptidase 22 kDa subunit IPR008978:HSP20-like chaperone
MtC90728_1_AA unknown
MtC00291_1_AA CBS
MtC61295_1_AA Rhodopsin-like GPCR superfamily IPR001078:Catalytic domain of components of various dehydrogenase complexes
MtC20039_1_AA Rhodopsin-like GPCR superfamily IPR006256:Dihydrolipoamide acetyltransferase
MtD01202_1_AA unknown
MtC61426_1_AA unknown
MtC91534.1_1_AA Syntaxin/epimorphin family
MtC10100.1_1_AA Peptidase C1A, papain C-terminal IPR001400:Somatotropin hormone
MtC10233_1_AA Aldehyde dehydrogenase
MtC10280_1_AA CD9/CD37/CD63 antigen
MtC10641_1_AA Cytochrome c, monohaem

MtC30199_1_AA Xylose isomerase, bacterial type
MtC20380_1_AA unknown
MtC00523_1_AA GroES-like
MtC60645_1_AA Metridin-like ShK toxin IPR005123:2OG-Fe(II) oxygenase
MtC30566.1_1_AA Proteasome component region PCI
MtC61244_1_AA Catalase
MtD00882_1_AA Surfeit locus 4-related
MtC20047_1_AA Late embryogenesis abundant protein 2
MtC60757_1_AA Peptidylprolyl isomerase, FKBP-type
MtS10582_1_AA Eukaryotic initiation factor 1A (eIF-1A)
MtC61549_1_AA unknown
MtC00292_1_AA Proteasome alpha-subunit
MtD07835_1_AA Chalcone-flavanone isomerase
MtC10613_1_AA Ubiquitin-conjugating enzyme, E2
MtC61084_1_AA unknown
MtC93171_1_AA unknown
MtC10472_1_AA unknown
MtC60692_1_AA unknown
MtC60813_1_AA
MtD02273_1_AA Adenine nucleotide translocator 1
MtC40045_1_AA Protein of unknown function DUF81
MtC00314_1_AA Calcium-binding EF-hand
MtC60275_1_AA Protein of unknown function UPF0016
MtC00753_1_AA Thiamine biosynthesis Thi4 protein
MtC30202_1_AA Synaptojanin, N-terminal
MtC10369_1_AA IPR013210:Leucine rich repeat, N-terminal
MtC30138_1_AA Aminotransferase, class I and II
MtC20350.1_1_AA Pyridine nucleotide-disulphide oxidoreductase, NAD-binding region
MtC93236_1_AA unknown
MtC10139_1_AA Hyaluronan/mRNA binding protein
MtC61464_1_AA Pyridine nucleotide-disulphide oxidoreductase, class I
MtC00201_1_AA Like-Sm ribonucleoprotein-related, core
MtC30111_1_AA AAA ATPase IPR005937:26S proteasome subunit P45
MtC30567_1_AA Eukaryotic rRNA processing
MtC60497_1_AA Major intrinsic protein
MtC90553_1_AA Expansin 45, endoglucanase-like
MtC61439_1_AA unknown
MtD01782_1_AA Zinc finger, C2H2-type IPR009060:UBA-like
MtC91170_1_AA Ribosomal protein L23, N-terminal IPR013025:Ribosomal protein L25/L23
MtC00696_1_AA unknown
MtD01985_1_AA Mitochondrial import inner membrane translocase, subunit Tim17/22
MtC61447_1_AA Plant lipid transfer protein/Par allergen
MtC93345_1_AA Ras small GTPase, Rab type IPR015600:
MtD01540_1_AA Peroxysomal long chain fatty acyl transporter
MtD15136_1_AA tRNA-binding arm
MtC00241_1_AA unknown
MtC00273_1_AA Ribosomal L38e protein
MtC00395_1_AA Cytochrome c oxidase, subunit VIa
MtD26762_1_AA unknown
MtD27326_1_AA unknown
MtC10243_1_AA Defender against death DAD protein
MtC10913_1_AA unknown
MtC20046_1_AA Glycoside transferase, six-hairpin, subgroup
MtC40209_1_AA unknown

MtC20037_1_AA E-class P450, group I
MtC60727_1_AA Alpha/beta hydrolase fold-1 IPR000379:
MtC61633_1_AA ATPase, P-type, K/Mg/Cd/Cu/Zn/Na/Ca/Na/H-transporter
MtC00443_1_AA Protein of unknown function UPF0041
MtC90041_1_AA Prefoldin
MtC00615_1_AA unknown
MtC10361_1_AA Protein of unknown function UPF0057
MtC60621.1_1_AA Protein of unknown function DUF124
MtC60870_1_AA Ubiquitin
MtC00779_1_AA Thioredoxin-related IPR012336:Thioredoxin-like fold IPR013766:Thioredoxin domain IPR015467:
MtC30132_1_AA unknown
MtD00766_1_AA Peptidase M18, aminopeptidase I
MtC10290_1_AA ATPase, P-type, K/Mg/Cd/Cu/Zn/Na/Ca/Na/H-transporter
MtC10773_1_AA Ribonucleoprotein complex SRP, Srp19 component
MtC10945_1_AA O-methyltransferase, family 3
MtC30106_1_AA Pre-mRNA processing ribonucleoprotein, binding region IPR012974:NOP5, N-terminal IPR012976:NOSIC
MtD02058_1_AA unknown
MtD00211_1_AA Protease-associated PA IPR007369:Peptidase A22B, minor histocompatibility antigen H13
MtD02197_1_AA unknown
MtC60857_1_AA unknown
MtD00583_1_AA Citrate synthase
MtD07098_1_AA Lipase/lipooxygenase, PLAT/LH2
MtD01586_1_AA unknown
MtD12421_1_AA unknown
MtC10898_1_AA Protein kinase
MtD17959_1_AA Mov34-1
MtC20011_1_AA Aminotransferase, class-II
MtC93344_1_AA Anticodon-binding IPR015263:
MtC00432_1_AA Harpin-induced 1
MtD00256_1_AA Peptidase A22B, minor histocompatibility antigen H13
MtC50546_1_AA Short-chain dehydrogenase/reductase SDR
MtC10273_1_AA Dynamin GTPase effector IPR011993:Pleckstrin homology-type
MtD17572_1_AA 7-Fold repeat in clathrin and VPS proteins
MtC20285_1_AA Cupredoxin
MtC62032_1_AA Protein of unknown function UPF0057
MtC92209_1_AA Nucleotide-binding, alpha-beta plait
MtD00926_1_AA Oligopeptide transporter OPT superfamily
MtC10653_1_AA unknown
MtC10412_1_AA unknown
MtC20303_1_AA Phosphatidylinositol-specific phospholipase C, X region
MtD02247_1_AA Prenylcysteine lyase
MtC61847_1_AA High mobility group-like nuclear protein
MtD17526_1_AA Cytochrome b5
MtD18850_1_AA Mitochondrial substrate carrier
MtC00525_1_AA Glyoxalase/bleomycin resistance protein/dioxygenase
MtC10099_1_AA Fructose-bisphosphate aldolase, class-I
MtC10394_1_AA unknown
MtC10579.1_1_AA Isocitrate dehydrogenase NADP-dependent, C-terminal, plant
MtD03619_1_AA Protein kinase
MtD07207_1_AA Protein kinase
MtD07440_1_AA Protein of unknown function DUF248, methyltransferase putative
MtD22800_1_AA Mpv17/PMP22

MtC10684_1_AA 26S proteasome subunit P45 IPR013093:ATPase AAA-2
MtC10897_1_AA AAA ATPase IPR005937:26S proteasome subunit P45
MtC20279_1_AA AAA ATPase IPR005937:26S proteasome subunit P45 IPR008994:Nucleic acid-binding, OB-fold
MtD25171_1_AA Clathrin propeller, N-terminal
MtC00545_1_AA GroEL-like chaperone, ATPase
MtC00731_1_AA AAA ATPase IPR005937:26S proteasome subunit P45
MtC91353_1_AA Flavodoxin/nitric oxide synthase
MtD00713_1_AA Helix-hairpin-helix motif
MtC30064_1_AA Aldo/keto reductase
MtC00638_1_AA Major facilitator superfamily
MtC10141_1_AA Proteasome component region PCI
MtC10504.1_1_AA ATP citrate synthase, small subunit IPR013816:ATP-grasp fold, subdomain 2
MtC20269_1_AA Paraneoplastic encephalomyelitis antigen
MtC30209_1_AA RNA-binding region RNP-1 (RNA recognition motif) IPR001865:Ribosomal protein S2
MtC10449_1_AA HR-like lesion-inducer
MtC00445_1_AA Heat shock protein DnaJ
MtC45629_1_AA von Willebrand factor, type A IPR010734:Copine
MtC62738_1_AA unknown
MtC00141_1_AA Ribosomal protein S14
MtC91888_1_AA Blue (type 1) copper domain
MtC10060_1_AA Glutathione S-transferase, C-terminal IPR012335:Thioredoxin fold
MtD01219_1_AA AAA ATPase
MtC60311_1_AA Protein kinase
MtC00330_1_AA 2OG-Fe(II) oxygenase
MtC00354_1_AA Ribosomal L38e protein
MtC00387_1_AA Protein of unknown function UPF0136, Transmembrane
MtC00538_1_AA Nitrite and sulphite reductase 4Fe-4S region IPR015825:
MtC10486_1_AA Mov34-1 IPR011002:Flagellar motor switch protein FliG-like
MtD17162_1_AA ATPase, F1/V1/A1 complex, alpha/beta subunit, N-terminal
MtC20198_1_AA unknown
MtC91716_1_AA Membrane-associated proteins in eicosanoid and glutathione metabolism (MAPEG)
MtD05273_1_AA unknown
MtS10375_1_AA General substrate transporter
MtC30180_1_AA Peptidoglycan-binding LysM
MtC40103_1_AA Protein kinase IPR013210:Leucine rich repeat, N-terminal
MtD02573_1_AA E-class P450, group II
MtC60219_1_AA UDP-glucose 4-epimerase
MtD00884_1_AA E-class P450, group IV
MtC00605_1_AA Blue (type 1) copper domain
MtD06497_1_AA FAD-dependent pyridine nucleotide-disulphide oxidoreductase
MtC10285_1_AA NAD-dependent epimerase/dehydratase
MtC30240_1_AA Protein of unknown function DUF284, transmembrane eukaryotic
MtD12444_1_AA unknown
MtD18142_1_AA unknown
MtC30386_1_AA WD40-like
MtC00504_1_AA Ferredoxin
MtC40046_1_AA ATPase, V0/A0 complex, 116-kDa subunit
MtC10131.1_1_AA ATPase, F1 complex, OSCP/delta subunit
MtC10318_1_AA unknown
MtC00558_1_AA unknown
MtC00650_1_AA GHMP kinase, C-terminal IPR014721:
MtC20111_1_AA Glu/Leu/Phe/Val dehydrogenase, dimerisation region
MtC61689_1_AA Protein of unknown function DUF1692

MtD04586_1_AA Cupin 1 IPR007113:
MtD11294_1_AA Mitochondrial glycoprotein
MtD13218_1_AA Importin alpha-like protein, beta-binding region
MtD01837_1_AA unknown
MtC30201_1_AA Proteasome component region PCI IPR013143:PCI/PINT associated module IPR013586:26S proteasome regulatory subunit, C-terminal
MtC61309_1_AA Thioredoxin fold
MtC93161_1_AA Der1-like
MtC50840.2_1_AA Nucleotide-binding, alpha-beta plait
MtD00747_1_AA Calcium-binding EF-hand IPR003100:Argonaute and Dicer protein, PAZ IPR014811:
MtD01060_1_AA AAA ATPase, central region IPR010339:TIP49, C-terminal
MtC30389_1_AA unknown
MtC30458_1_AA Cupin 1 IPR007113:
MtD06754_1_AA MscS Mechanosensitive ion channel, transmembrane
MtC93153_1_AA unknown
MtC60082_1_AA Aldehyde dehydrogenase
MtD03699_1_AA Protein kinase
MtC00633_1_AA unknown
MtC10209_1_AA ATPase, F0 complex, subunit C IPR006402:HAD-superfamily hydrolase, subfamily IA, variant 3
MtC20030_1_AA Nicotinate phosphoribosyltransferase related
MtC40118_1_AA Alanyl-tRNA synthetase, class IIc
MtD15872_1_AA Late embryogenesis abundant (LEA) group 1
MtD23115_1_AA Alpha/beta hydrolase fold-1 IPR000379:
MtC10930.1_1_AA Glycoside hydrolase, family 47
MtD17510_1_AA IPR013210:Leucine rich repeat, N-terminal

Chapter 4, additional file S4.2.

	Control roots	Total number of nonredundant proteins identified	Number of proteins co-identified in the two experiments
Exp 1	C1 (a+b+c)	1096	
Exp 2	C2 (a+b+c)	1076	1051

	Mycorrhizal roots	Total number of nonredundant proteins identified	Number of proteins co-identified in the two experiments
Exp 1	M1 (a+b+c)	1079	
Exp 2	M2 (a+b+c)	1082	1041

Chapter 4, additional file S4.3.

	Mt3,5 accession	MENS Toulouse 01/2003	Biological function	Localisation WolfPsort	TM	BB	GPI	SP	Palmitoylation	Prenylation	N-myrostylation	% Homologie TAIR	E value	Accession TAIR	Localisation according TAIR
3	Medtr2g035100	MtC00009_1_AA Bet v I allergen	Cell rescue and defense	cyto	0/0							31	1.00E-04	AT1G24020	membrane
40	Medtr4g097170	MtC00085.1_1_AA Histone core IPR009072:Histone-fold	Cell cycle and DNA processing	nucl	0//0							97	6.00E-72	AT5G65360	chloroplast, nucleosome
41	Medtr4g097170	MtC00085.2_1_AA Histone core IPR009072:Histone-fold	Cell cycle and DNA processing	nucl	0//0							97	2.00E-55	AT5G65360	chloroplast, nucleosome
43	Medtr3g107710	MtC00087.1_1_AA Ras Blast: GTP-binding protein [Cicer arietinum]	Signal transduction	cyto	0//0							96	e-128	AT5G55190	intracellular, plasmodesma
44	Medtr3g107710	MtC00087.3_1_AA Ras Blast: ABM73376.1Ran1 [Pisum sativum]	Transport	cyto	0//0							96	e-128	AT5G55190	intracellular, plasmodesma
46	Medtr4g024270	MtC00091_1_AA S15/NS1, RNA-binding IPR012606:Ribosomal S13S15 N-terminal	Protein synthesis and fate	cyto_nucl	0//0							91	8.00E-77	AT3G60770	cell wall, chloroplast, cytosol, cytosolic ribosome, cytosolic small ribosomal subunit, nucleolus
49	Medtr4g075450	MtC00101_1_AA Ribosomal protein S19/S15	Protein synthesis and fate	cyto	0//0							94	2.00E-74	AT5G09510	Cytosolic ribo, nucleolus, plasmodesma, ribosome
51	Medtr5g024180	MtC00106_1_AA HMG1/2 (high mobility group) box	Protein synthesis and fate	nucl	0//0							72	2.00E-27	AT1G20696	Chromatin
61	Medtr5g040570	MtC00122.1_1_AA Ribosomal protein L34e	Protein synthesis and fate	pero	0//0							93	2.00E-47	AT1G26880	Nucleolus / Chloro
65	Medtr2g037990	MtC00129_1_AA unknown Blast: XP_003595072.1 Fiber protein Fb15 [Medicago truncatula]	unclassified	cyto	0//0							63	2.00E-29	AT4G30010	Mitochondrion/ Plastid
70	AC146550_1006	MtC00138_1_AA Ribosomal protein S17e	Protein synthesis and fate	chlo	0//0							90	6.00E-57	AT5G04800	cytosolic small ribosomal subunit, ribosome
81	Medtr3g094570	MtC00155.1_1_AA Ribosomal protein L6E IPR005568:Ribosomal protein L6, N-terminal	Protein synthesis and fate	nucl	0//0							72	3.00E-81	AT1G74060	Cytos rib / ribos / Nucleolus
82	Medtr3g094570	MtC00155.2_1_AA Ribosomal protein L6E IPR005568:Ribosomal protein L6, N-terminal	Protein synthesis and fate	nucl	0//0							72	3.00E-81	AT1G74060	Cytos rib / ribos / Nucleolus
83	Medtr8g095360	MtC00159_1_AA emp24/gp25L/p24 IPR001071:Cellular retinaldehyde binding/alpha-tocopherol transport IPR008273:Cellular retinaldehyde-binding/triple function, N-terminal	Transport	cyto	0//0							65	e-120	AT1G72160	Chloroplast
84	Medtr8g059790	MtC00162_1_AA Kunitz inhibitor ST1-like	Cell rescue and defense	extr	0//0							31	2.00E-12	AT1G73260	Mitochondrion
92	Medtr4g130910	MtC00190_1_AA Eukaryotic initiation factor 5A hypusine (eIF-5A)	Protein synthesis and fate	chlo	0//0							91	2.00E-73	AT1G13950	undefined
96	Medtr7g021030	MtC00200_1_AA Ribosomal protein L30e	Protein synthesis and	chlo	0//0							86	2.00E-51	AT1G36240	cytosol, cytosolic large ribosomal

			fate												subunit
97	Medtr5g072530	**MtC00201_1_AA Like-Sm ribonucleoprotein-related, core**	Protein synthesis and fate	mito	0//0							89	5.00E-35	AT2G18740	cytosol
100	Medtr6g013210	**MtC00208_1_AA Ribosomal protein S28e IPR012340:Nucleic acid-binding, OB-fold, subgroup**	Protein synthesis and fate	cyto	0//0							88	2.00E-16	AT5G03850	cell wall, cytosol, cytosolic small ribosomal subunit, intracellular, plasma membrane, rRNA export from nucleus, ribosome,
101	Medtr2g100410	**MtC00209_1_AA Ribosomal L28e protein**	Protein synthesis and fate	chlo	0//0							66	6.00E-37	AT2G19730	cell wall, chloroplast, cytosolic large ribosomal subunit, cytosolic ribosome, plasma membrane, plasmodesma
102	Medtr3g083130	**MtC00212_1_AA Aldo/keto reductase**	Energy metabolism	chlo	0//0							51	6.00E-91	AT1G59960	Cyto
113	Medtr5g088740	**MtC00236_1_AA Ribosomal protein L30e**	Protein synthesis and fate	chlo	0//0							88	4.00E-55	AT1G36240	cytosol, cytosolic large ribosomal subunit
118	Medtr7g068280	**MtC00254_1_AA HMG 1/2 (high mobility group) box**	Protein synthesis and fate	nucl	0//0							45	2.00E-11	AT1G20693	chromatin, nucleus
126	Medtr4g068040	**MtC00273_1_AA Ribosomal L38e protein**	Protein synthesis and fate	cyto	0//0							91	2.00E-28	AT3G59540	cytosolic large ribosomal subunit
133	Medtr4g103340	**MtC00295.1_1_AA Ribosomal L37ae protein IPR011331: IPR011332:**	Protein synthesis and fate	chlo	0//0							93	6.00E-34	AT3G10950	cytosol, cytosolic large ribosomal subunit,
142	Medtr3g096050	MtC00320_1_AA O-methyltransferase, family 2 IPR001601: IPR012967:Dimerisation	Protein synthesis and fate	cyto	0//0							57	e-121	AT3G53140	undefined
145	Medtr4g062410	**MtC00324_1_AA Ribosomal protein L29**	Protein synthesis and fate	cyto	0//0							79	6.00E-30	AT5G02610	cytosolic large ribosomal subunit, cytosolic ribosome, plasma membrane, plasmodesma, ribosome, vacuolar membrane
148	Medtr4g096790	**MtC00327_1_AA Ribosomal protein S11**	Protein synthesis and fate	cyto	0//0							81	2.00E-54	AT3G11510	cytosolic ribosome, cytosolic small ribosomal subunit, nucleolus
149	Medtr4g080740	**MtC00328_1_AA Mitochondrial ribosomal protein L5**	Protein synthesis and fate	cyto	0//0							87	5.00E-79	AT5G45775	vacuole
152	Medtr4g063200	**MtC00341.1_1_AA Histone core IPR009072:Histone-fold**	Cell cycle and DNA processing	nucl	0//0							98	1.00E-41	AT1G07790	Chloro
153	Medtr3g099900	**MtC00341.2_1_AA Histone core IPR009072:Histone-fold**	Cell cycle and DNA processing	nucl	0//0							98	4.00E-40	AT1G07790	Chloro
171	Medtr4g071000	**MtC00402_1_AA Nascent polypeptide-associated complex NAC**	Protein synthesis and fate	mito	0//0							77	7.00E-48	AT1G73230	undefined

175	Medtr2g012450, Medtr2g012440, Medtr2g012110	MtC00414_1_AA Ribosomal protein L24/L26 IPR014723:	Protein synthesis and fate	cyto	0//0							64	3.00E-40	AT5G67510	cytosolic large ribosomal subunit, cytosolic ribosome
177	Medtr7g082820	MtC00419_1_AA HMG1/2 (high mobility group) box	Protein synthesis and fate	nucl	0//0							70	3.00E-18	AT1G20696	chromatin
186	Medtr4g068040	MtC00439_1_AA Ribosomal L38e protein	Protein synthesis and fate	nucl	0//0							53	2.00E-14	AT3G59540	cytosolic large ribosomal subunit
194	Medtr8g018550	MtC00480.1_1_AA Lipoxygenase	Cell rescue and defense	cyto	0//0							49	0	AT3G22400	Choro
195	Medtr7g013610	MtC00491_1_AA Histone H3 IPR007124: IPR009072:Histone-fold	Cell cycle and DNA processing	nucl	0//0							99	9.00E-74	AT5G65360	chloroplast, nucleosome
201	Medtr3g025230	MtC00512_1_AA E-class P450, group I	Energy metabolism	cyto	0//0							68	5.00E-70	AT4G22690	cell wall, mitochondrion, plasma membrane, vacuolar membrane
203	Medtr4g034030	MtC00521_1_AA Ribosomal protein S10, eukaryotic and archaeal form	Protein synthesis and fate	cyto	0//0							90	7.00E-49	AT5G62300	cell wall, cytosolic small ribosomal subunit
204	AC225518_12	MtC00523_1_AA GroES-like	Protein synthesis and fate	cyto	0//0							75	1.00E-36	AT1G23100	Mitochondrium
209	AC235488_9	MtC00539_1_AA Ribosomal protein L21e	Protein synthesis and fate	cyto	0//0							81	5.00E-73	AT1G09690	cytosolic large ribosomal subunit
210	Medtr7g013610	MtC00543_1_AA Histone H3 IPR009072:Histone-fold	Cell cycle and DNA processing	nucl	0//0							99	2.00E-57	AT5G65360	chloroplast, nucleosome
220	Medtr2g104440	MtC00587_1_AA Like-Sm ribonucleoprotein-related, core	Energy metabolism	mito	0//0							89	5.00E-42	AT4G30330	Cytos
238	Medtr2g036260, Medtr2g036290, AC229724_1028, Medtr2g036240	MtC00680.1_1_AA Glycoside hydrolase, family 18, catalytic domain	Energy metabolism	chlo	0//0							30	0.1	AT3G49142	undefined
239	Medtr3g020660	MtC00683_1_AA Nascent polypeptide-associated complex NAC	Protein synthesis and fate	cyto	0//0							80	4.00E-50	AT1G17880	undefined
240	Medtr8g045570	MtC00688_1_AA Bet v I allergen	Cell rescue and defense	cyto	0//0							35	5.00E-19	AT1G70890	chlo
245	Medtr4g062410	MtC00725_1_AA Ribosomal protein L29	Protein synthesis and fate	cyto_nucl	0//0							88	2.00E-53	AT5G02610	cytosolic large ribosomal subunit, cytosolic ribosome
247	Medtr7g010150	MtC00727_1_AA Ribosomal protein L34e	Protein synthesis and fate	cyto	0//0							93	3.00E-47	AT1G26880	Nucleolus / Chloro
253	Medtr8g040150	MtC00750_1_AA Complex 1 LYR protein	Energy metabolism	cyto	0//0							63	6.00E-44	AT3G12260	Mitochondrium / M
255	Medtr4g128150	MtC00769.1_1_AA Histone H4 IPR009072:Histone-fold	Cell cycle and DNA processing		0//0							100	4.00E-33	AT5G59970	V
256	Medtr4g128150	MtC00769.3_1_AA Histone H4 IPR009072:Histone-fold	Cell cycle and DNA processing	nucl	0//0							100	4.00E-33	AT5G59970	V
261	AC146550_1006	MtC00790_1_AA Ribosomal protein S17e	Protein synthesis and fate	chlo	0//0							90	1.00E-54	AT2G05220	cytosolic small ribosomal subunit

267	Medtr8g045570	MtC10007_1_AA Bet v I allergen	Cell rescue and defense	cysk	0//0							37	5.00E-25	AT1G70890	chloroplast
268	Medtr2g066630	MtC10018_1_AA Glutathione S-transferase, C-terminal IPR012335:Thioredoxin fold	Cell rescue and defense	cyto	0//0							63	6.00E-83	AT1G17180	cytoplasm
276	Medtr1g061670	MtC10066_1_AA TRASH Blast:XP_003590400.1 60S ribosomal protein L24 [Medicago truncatula]	Protein synthesis and fate	nucl	0//0							94	1.00E-62	AT3G53020	cytosolic large ribosomal subunit, nucleolus
281	Medtr4g015460	MtC10085.1_1_AA Glycoside hydrolase, catalytic core	Energy metabolism	chlo	0//0							45	e-120	AT2G44450	Plasmodesma / CW
283	unfound	MtC10092_1_AA unknown Blast: AAS20985.1 At1g67350-like protein [Hyacinthus orientalis]	Unclassified	nucl	0//0							74	1.00E-31	AT1G67350	Mitoch memb
284	Medtr1g115840	MtC10095_1_AA Chalcone-flavanone isomerase	Energy metabolism	cyto	0//0							50	1.00E-52	AT3G55120	endoplasmic reticulum, extrinsic to endoplasmic reticulum membrane, nucleus, plant-type vacuole membrane
285	unfound	MtC10096_1_AA Manganese and iron superoxide dismutase	Cell rescue and defense	mito	0//0							77	6.00E-96	AT3G10920	Mitochondriom
288	Medtr7g068280	MtC10102_1_AA HMG1/2 (high mobility group) box	Protein synthesis and fate	nucl	0//0							49	7.00E-18	AT3G51880	Chromatin / Nucleus
301	Medtr5g021730	MtC10150_1_AA Linker histone, N-terminal	Cell cycle and DNA processing	nucl	0//0							68	2.00E-13	AT1G06760	nucleosome, nucleus
310	Medtr7g013610	MtC10216_1_AA Histone H3 IPR007124: IPR009072:Histone-fold	Cell cycle and DNA processing	chlo	0//0							99	2.00E-58	AT5G65360	chloroplast, nucleosome
314	Medtr6g086300	MtC10233_1_AA Aldehyde dehydrogenase	Energy metabolism	cyto	0//0							56	e-161	AT3G48000	Mitochondrium / Chloro
317	Medtr7g010150	MtC10257.1_1_AA Ribosomal protein L34e	Protein synthesis and fate	cyto	0//0							93	4.00E-34	AT1G26880	chloroplast, nucleolus
329	Medtr6g087990	MtC10324_1_AA Thioredoxin-like fold IPR013740:Redoxin	Cell rescue and defense	mito	0//0							79	7.00E-75	AT3G06050	Mitochondriom
331	Medtr2g096100	MtC10341_1_AA Histone H4 IPR009072:Histone-fold	Cell cycle and DNA processing	nucl	0//0							100	3.00E-41	AT5G59970	V
339	Medtr5g081710	MtC10412_1_AA unknown Blast: ADR71255.1 60S ribosomal protein L35aA [Hevea brasiliensis]	Protein synthesis and fate	cyto	0//0							91	6.00E-57	AT1G74270	cytosol, cytosolic large ribosomal subunit
345	Medtr8g018430	MtC10441_1_AA Lipoxygenase	Cell rescue and defense	chlo	0//0							59	1.00E-52	AT3G22400	Chloro
346	unfound	MtC10444_1_AA NADH-ubiquinone oxidoreductase B18 subunit	Transport	mito	0//0							75	6.00E-39	AT2G02050	mitochondrial membrane, mitochondrion, respiratory chain complex I
351	Medtr5g020740	MtC10502_1_AA NmrA-like Blast: XP_003612049.1 Isoflavone reductase-like protein [Medicago truncatula]	Energy metabolism	cyto	0//0							68	e-122	AT1G75280	PM
354	Medtr5g069410	MtC10533_1_AA unknown Blast: NP_192621.1 calcium ion binding protein [Arabidopsis thaliana]	Unclassified	nucl	0//0							80	e-128	AT4G12700	undefined

374	unfound	MtC10679_1_AA NADH:ubiquinone oxidoreductase 17.2 kD subunit	Energy metabolism	cyto	0//0							78	8.00E-73	AT3G03100	Mitochondriom
379	Medtr8g038460	MtC10749_1_AA Histone H4 IPR007124: IPR009072:Histone-fold	Cell cycle and DNA processing	nucl	0//0							100	3.00E-41	AT5G59970	V
386	Medtr2g096660	MtC10807_1_AA NAD-dependent epimerase/dehydratase	Energy metabolism	chlo	0//0							89	e-179	AT3G46440	Cytos
399	Medtr2g036220, Medtr2g036190	MtC11005_1_AA Glycoside hydrolase, family 18, catalytic domain	Energy metabolism	Cyto	0//0							34	0.97	NS	undefined
405	Medtr4g024630	MtC20018_1_AA Deoxyxylulose-5-phosphate synthase	Energy metabolism	cyto	0							83	0	AT2G45290	chloroplast, chloroplast stroma
418	Medtr2g021300	MtC20081_1_AA Elongation factor Tu, domain 2	Protein synthesis and fate	chlo	0							82	0	AT4G02930	cell wall, mitochondrion
421	Medtr4g070910	MtC20110_1_AA Pre-mRNA processing ribonucleoprotein, binding region IPR012974:NOP5, N-terminal IPR012976:NOSIC	Cell cycle and DNA processing	cyto	0							78	0	AT5G27120	nucleolus, plasmodesma
435	Medtr8g038210	MtC20218_1_AA Annexin, type plant	Signal transduction	cyto	0							54	6.00E-92	AT5G12380	undefined
444	Medtr7g104570	MtC20271_1_AA Ubiquinol-cytochrome C reductase, UQCRXQCR9 like	Energy metabolism	cyto	0							80	2.00E-29	AT3G52730	membrane, mitochondrial respiratory chain complex III, mitochondrion
446	Medtr4g080090	MtC20277_1_AA unknown Blast: XP_003607599.1 Multiprotein bridging factor 1 [Medicago truncatula]	Protein synthesis and fate	nucl	0							73	3.00E-54	AT3G58680	Nucleolus
474	Medtr5g091930	MtC30134_1_AA ATPase, F1 complex, gamma subunit IPR002020:Citrate synthase	Energy metabolism	mito	0							69	0	AT2G44350	cell wall, chloroplast, mitochondrion
490	Medtr2g096030	MtC30235_1_AA Glycoside hydrolase, catalytic core	Energy metabolism	cysk	0							29	0	AT1G53780	membrane
504	Medtr8g095360	MtC30417_1_AA emp24/gp25L/p24 IPR008273:Cellular retinaldehyde-binding/triple function, N-terminal	Transport	nucl	0							62	e-111	AT4G09160	Chloro
509	Medtr5g028350	MtC30567_1_AA Eukaryotic rRNA processing	Protein synthesis and fate	nucl	0							56	2.00E-61	AT3G22660	undefined
513	Medtr7g088050	MtC40030_1_AA Chloroplast protein import component Toc34	Transport	cyto	0							64	e-115	AT5G05000	Choro/ choro Inner M
524	Medtr8g093880	MtC40200_1_AA Blast: XP_003630288.1 Ankyrin-like protein [Medicago truncatula]	Signal transduction	chlo	0							73	e-148	AT5G64030	Golgi
527	Medtr5g063620	MtC45254_1_AA unknown Blast: ACG30677.1 histone H4 [Zea mays]	Cell cycle and DNA processing	nucl	0							100	3.00E-41	AT5G59970	V
538	Medtr4g083150	MtC50144_1_AA Nuclear transport factor 2 IPR012677:Nucleotide-binding, alpha-beta plait	Transport	cyto	0							37	5.00E-62	AT3G25150	undefined
545	Medtr1g108290	MtC50840.2_1_AA Nucleotide-binding, alpha-beta plait	Cell cycle and DNA processing	cyto	0							59	2.00E-63	AT5G04600	Nucleolus
546	Medtr4g103340	MtC50879_1_AA Ribosomal L37ae protein	Protein synthesis and fate	chlo	0							95	4.00E-45	AT3G10950	Cyto / Cytos Rib
550	Medtr1g023630	MtC60141_1_AA Histone H3 IPR007124: IPR009072:Histone-fold	Cell cycle and DNA	chlo	0							97	1.00E-71	AT5G65360	chloroplast, nucleosome

			processing												
553	Medtr4g097170	MtC60204.1_1_AA Histone H3 IPR009072:Histone-fold	Cell cycle and DNA processing	nucl	0							100	8.00E-60	AT4G40030	undefined
554	Medtr4g097170	MtC60204.2_1_AA Histone H3 IPR009072:Histone-fold	Cell cycle and DNA processing	nucl	0							100	8.00E-60	AT4G40030	undefined
579	Medtr7g113020	MtC60727_1_AA Alpha/beta hydrolase fold-1 IPR000379:	energy metabolism	cysk	0							34	5.00E-50	AT4G02340	Perox
580	Medtr4g063430, Medtr4g063240	MtC60748_1_AA Histone core IPR009072:Histone-fold	Cell cycle and DNA processing	nucl	0							98	4.00E-49	AT1G07790	Chloro
582	Medtr4g071180	MtC60761_1_AA Histone core IPR009072:Histone-fold	Cell cycle and DNA processing	nucl	0							98	5.00E-49	AT1G07790	Chloro
584	Medtr4g071180	MtC60774_1_AA IPR007125:Histone core IPR009072:Histone-fold	Cell cycle and DNA processing	nucl	0							98	4.00E-49	AT1G07790	Chloro
587	Medtr7g088370	MtC60841_1_AA SRA-YDG IPR003616:Post-SET zinc-binding region IPR007728:Pre-SET zinc-binding region IPR011381:Histone H3-K9 methyltransferase	Cell cycle and DNA processing	nucl	0							59	e-165	AT5G04940	Nucleus
601	Medtr4g080090	MtC61099_1_AA Helix-turn-helix type 3 IPR013729:Multiprotein bridging factor 1, N-terminal	Protein synthesis and fate	mito	0							70	3.00E-52	AT3G58680	Nucleolus / Nucleus/ Cytos
603	Medtr8g092720	MtC61188_1_AA Histone H3 IPR007124: IPR009072:Histone-fold	Cell cycle and DNA processing	chlo	0							99	1.00E-73	AT5G65360	chloroplast, nucleosome
611	Medtr8g037810	MtC61426_1_AA unknown Blast: XP_003627750.1 Chaperone protein dnaJ [Medicago truncatula]	Protein synthesis and fate	cyto	0							70	e-128	AT2G22730	cytosol
614	unfound	MtC61464_1_AA Pyridine nucleotide-disulphide oxidoreductase, class I	Cell rescue and defense	cyto	0							70	e-169	AT5G03630	chloroplast stroma, cytosol
622	Medtr2g019020	MtC61893_1_AA unknown Blast: XP_003593890.1 ABC transporter C family member [Medicago truncatula]	Transport	extr	0							67	3.00E-35	AT1G30400	plant-type vacuole, plasmodesma, vacuolar membrane, vacuole
626	Medtr8g037810	MtC62065_1_AA Blast: XP_002278176.1 PREDICTED: chaperone protein dnaJ 10 [Vitis vinifera]	Protein synthesis and fate	nucl	0							64	2.00E-83	AT1G21080	undefined
629	Medtr3g065570	MtC62278_1_AA High mobility group proteins HMG-I and HMG-Y IPR000873:AMP-dependent synthetase and ligase IPR003216:Linker histone, N-terminal	Protein synthesis and fate	nucl	0							51	9.00E-19	AT1G14900	cytosol, nuclear chromatin, nucleus
638	Medtr4g063220, Medtr4g063450	MtC62627_1_AA Histone core IPR009072:Histone-fold	Cell cycle and DNA processing	nucl	0							98	2.00E-49	AT1G07790	Chloro
642	Medtr4g103340	MtC62792_1_AA Ribosomal L37ae protein	Protein synthesis and fate	chlo	0							93	3.00E-45	AT3G10950	Cyto / Cytos Rib
644	Medtr2g086610	MtC62861_1_AA S25 ribosomal protein	Protein synthesis and fate	nucl	0							93	1.00E-36	AT2G21580	cytosolic ribosome, cytosolic small ribosomal subunit, plasmodesma,

															vacuolar membrane
650	Medtr5g081710	MtC63127_1_AA Ribosomal protein L35Ae	Protein synthesis and fate	cyto	0							91	2.00E-46	AT1G74270	cytosolic large ribosomal subunit
656	Medtr7g013610	MtC63364_1_AA Histone H3 IPR007124: IPR009072:Histone-fold	Cell cycle and DNA processing	chlo	0							92	4.00E-50	AT5G65360	chloroplast, nucleosome
662	Medtr2g025480	MtC90489_1_AA Protein of unknown function UPF0041 Blast: XP_002518402.1 Brain protein, putative [Ricinus communis]	Unclassified	extr	0							87	1.00E-49	AT4G22310	mitochondrion
666	Medtr4g121900	MtC90728_1_AA unknown Blast: Q41050.1 Chloroplastic outer envelope pore protein of 16 kDa [Pisum sativum]	Transport	cyto	0							49	6.00E-37	AT2G28900	chloroplast, chloroplast envelope, plastid outer membrane, vacuole
670	Medtr4g128150	MtC91063_1_AA Histone H4 IPR007124: IPR009072:Histone-fold	Cell cycle and DNA processing	nucl	0							100	4.00E-33	AT5G59970	V
671	Medtr4g063060	MtC91170_1_AA Ribosomal protein L23, N-terminal IPR013025:Ribosomal protein L25/L23	Protein synthesis and fate	cyto	0							58	5.00E-23	AT3G55280	Cytosol,/cytosolic ribo/ M
679	Medtr8g059790	MtC91818_1_AA Kunitz inhibitor ST1-like	Cell rescue and defense	chlo	0							37	7.00E-04	AT1G17860	apoplast, cell wall
680	Medtr7g013610	MtC91970_1_AA Histone H3 IPR007124: IPR009072:Histone-fold	Cell cycle and DNA processing	nucl	0							83	3.00E-46	AT3G27360	chloroplast, nucleosome
681	Medtr4g071180	MtC92000_1_AA Histone core IPR009072:Histone-fold	Cell cycle and DNA processing	nucl	0							71	2.00E-33	AT5G22880	Nucleus / Nucleolus
683	Medtr2g082510	MtC92211_1_AA Histone H2A IPR007124: IPR009072:Histone-fold	Cell cycle and DNA processing	nucl	0							65	2.00E-28	AT1G08880	Nucleolus
713	Medtr4g129070	MtC93387_1_AA Diacylglycerol kinase accessory region	Signal transduction	cyto	0							76	2.00E-25	AT5G57690	undefined
717	Medtr5g093300, Medtr2g006820	MtD00072_1_AA Dihydrolipoamide acetyltransferase, long form	Energy metabolism	mito	0							68	e-138	AT4G26910	membrane, mitochondrion
728	Medtr6g084450	MtD00231_1_AA Peptidase T1A, proteasome beta-subunit	Protein synthesis and fate	cyto	0							83	e-116	AT1G56450	Cytosol /proteasome cxp
737	Medtr1g083290	MtD00387_1_AA NADPH oxidase Respiratory burst	Cell rescue and defense	nucl	0							59	7.00E-73	AT1G09090	integral to membrane, membrane
740	Medtr7g113130	MtD00415_1_AA NADPH oxidase Respiratory burst	Cell rescue and defense	nucl	0							59	7.00E-73	AT1G09090	integral to membrane, membrane
741	Medtr1g089750	MtD00492_1_AA Thymidine kinase IPR001739:Methyl-CpG binding IPR011124:Zinc finger, CW-type	Protein synthesis and fate	chlo	0							64	4.00E-52	AT3G63030	Nucleus
747	unfound	MtD00539_1_AA unknown Blast: AAM28290.1 putative ATP/GTP binding protein [Ananas comosus]	Signal transduction	chlo	0							54	e-101	AT5G10010	Nucleolus
755	Medtr3g088860	MtD00766_1_AA Peptidase M18, aminopeptidase I	Protein synthesis and fate	cyto	0							69	2.00E-89	AT5G60160	V / VM / cytosol
766	Medtr4g097790	MtD00934_1_AA unknown Blast: XP_003608579.1hypothetical protein	Unclassified	nucl	0							76	7.1	AT2G22795	undefined

		MTR_4g097790 [Medicago truncatula]													
795	Medtr5g083910	MtD02090_1_AA Protein kinase	Signal transduction	cyto	0							69	2.00E-63	AT1G53430	plasma membrane
807	Medtr4g083250	MtD02749_1_AA unknown Blast: AFK35211.1 unknown [Medicago truncatula]	Unclassified	nucl	0							58	7.00E-70	AT2G45060	Mitochondrion
816	Medtr4g096790	MtD03194_1_AA Ribosomal protein S11	Protein synthesis and fate	cyto	0							81	2.00E-61	AT3G11510	Cytos Ribos / Nucleous/ mitochondrion
823	Medtr3g086980	MtD03754_1_AA Small GTP-binding protein domain IPR015595:	Signal transduction	cyto	0							95	e-101	AT3G12160	Exocytic vesicule
846	Medtr7g073340	MtD06307_1_AA unknown Blast:AFK48380.1 unknown [Medicago truncatula]	Unclassified	chlo	0							34	7.00E-09	AT2G38550	chloroplast, chloroplast envelope, chloroplast inner membrane, mitochondrion, plastid
866	Medtr3g071450	MtD07674_1_AA Surface antigen variable number	Unclassified	cyto	0							49	5.00E-35	AT5G05520	Mitochondrion /Plastd
868	Medtr1g115890	MtD07835_1_AA Chalcone-flavanone isomerase	Energy metabolism	cysk	0							57	6.00E-65	AT5G05270	undefined
883	Medtr7g081660	MtD09722_1_AA Hyaluroman/mRNA binding protein	Protein synthesis and fate	nucl	0							36	1.00E-21	AT4G16830	Cytos / Nucleus
896	Medtr5g091710	MtD11268_1_AA XP_003617451 hypothetical protein MTR_5g091710 [Medicago truncatula].t	Unclassified	nucl	0							55	4.1	AT5G05870	undefined
919	Medtr8g056940	MtD12652_1_AA Glutathione S-transferase, C-terminal IPR012335:Thioredoxin fold	Cell rescue and defense	cyto	0							65	2.00E-80	AT1G78380	chloroplast, chloroplast stroma, cytoplasm, cytosol, plasma membrane, vacuolar membrane
923	Medtr1g105310	MtD12827_1_AA Histone H3 IPR009072:Histone-fold	Cell cycle and DNA processing	chlo	0							94	5.00E-70	AT5G65360	chloroplast, nucleosome
925	Medtr2g034900	MtD13218_1_AA Importin alpha-like protein, beta-binding region	Transport	chlo	0							84	6.00E-87	AT4G16143	Cytos / Nucleolus / plasmodesma
926	Medtr5g023050	MtD13384_1_AA C2 calcium-dependent membrane targeting	Signal transduction	cyto	0							64	2.00E-68	AT4G35790	membrane, plasma membrane, plasmodesma, vacuole
943	Medtr3g107710	MtD14892_1_AA Ras Blast: CAC10213.1 GTP-binding protein [Cicer arietinum]	Signal transduction	cyto	0							98	e-116	AT5G55190	plasmodesma
956	Medtr7g093170	MtD15872_1_AA Late embryogenesis abundant (LEA) group 1	Cell rescue and defense	mito	0							52	1.00E-19	AT5G06760	undefined
959	Medtr4g092290	MtD16132_1_AA Histone core IPR009072:Histone-fold	Cell cycle and DNA processing	nucl	0							98	1.00E-41	AT1G07790	Chloro
962	Medtr8g056940	MtD16413_1_AA Glutathione S-transferase, C-terminal IPR012335:Thioredoxin fold	Cell rescue and defense	cyto	0							65	6.00E-83	AT1G17180	chloroplast, chloroplast stroma, cytoplasm, cytosol, plasma membrane, vacuolar membrane
964	Medtr8g091480	MtD16665_1_AA unknown Blast: XP_003630077.1 hypothetical protein	Unclassified	nucl	0							25	1.9	AT2G33700	undefined

		MTR_8g091480 [Medicago truncatula]													
966	Medtr7g081810	MtD17080_1_AA unknown Blast: XP_003624308.1 Subtilisin-like serine protease [Medicago truncatula]	Protein synthesis and fate	cysk	0							57	3.00E-56	AT2G04160	cell wall, endomembrane system
975	Medtr7g076900	MtD17726_1_AA C2 calcium/lipid-binding region, CaLB	Signal transduction	cyto	0							53	3.00E-30	AT3G57880	Plasmodesma /CW /ER
976	Medtr4g096790	MtD17745_1_AA unknown Blast: XP_003623908.1 Extended synaptotagmin-2 [Medicago truncatula]	Transport	cyto	0							81	2.00E-54	AT3G11510	cytosolic ribosome, cytosolic small ribosomal subunit, nucleolus
989	Medtr8g014360	MtD19528_1_AA unknown Blast:XP_003627035.1 ABC transporter family pleiotropic drug resistance protein [Medicago truncatula]	Transport	chlo	0							61	5.00E-40	AT1G59870	chloroplast, membrane, plasma membrane
999	Medtr8g018550	MtD20838_1_AA Lipoxygenase	Cell rescue and defense	nucl	0							50	5.00E-56	AT3G22400	Chloro
1002	Medtr5g040570	MtD22210_1_AA Ribosomal protein L34e	Protein synthesis and fate	cyto	0							95	1.00E-28	AT1G26880	Chloro / Nucleolus
1004	Medtr7g013610	MtD22633_1_AA Histone H3 IPR009072:Histone-fold	Cell cycle and DNA processing	chlo	0							99	1.00E-73	AT5G65360	chloroplast, nucleosome
1005	Medtr7g013610	MtD22675_1_AA Histone H3 IPR007124: IPR009072:Histone-fold	Cell cycle and DNA processing	nucl	0							99	7.00E-74	AT5G65360	chloroplast, nucleosome
166	Medtr4g075160	**MtC00379_1_AA unknown Blast: XP_003540566.1 PREDICTED: NADH dehydrogenase [ubiquinone]**	Transport	cyto	0//0							83	3.00E-15	AT1G76200	mitochondrion respiratory chain complex I
1017	Medtr1g011880	MtD23501_1_AA Cytochrome bd ubiquinol oxidase, 14 kDa subunit	Energy metabolism	mito	0							63	7.00E-32	AT4G32470	membrane, mitochondrial respiratory chain complex III, mitochondrion, plastid, vacuolar membrane
25	Medtr4g016510	**MtC00057_1_AA SGNH hydrolase-type esterase superfamily protein**	Energy metabolism	chlo	0//0							56	7.00E-71	AT2G38180	undefined
35	Medtr4g070600	**MtC00077_1_AA S25 ribosomal protein**	Protein synthesis and fate	nucl	0//0							93	1.00E-36	AT2G21580	Cytos ribos / plasmodesma / Vm
128	Medtr7g065630	**MtC00280_1_AA Glutathione S-transferase, C-terminal IPR012335:Thioredoxin fold**	Cell rescue and defense	cyto	0//0							51	3.00E-53	AT3G09270	Cyto
439	unfound	MtC20235_1_AA U2A'/phosphoprotein 32 family A, C-terminal IPR007092:	Cell cycle and DNA processing	cyto_nucl	0							72	5.00E-92	AT1G09760	Cajal body, chloroplast, cytoplasm, cytosol, nucleolus, nucleoplasm, nucleus
810	unfound	MtD02821_1_AA unknown Blast: XP_003548304.1 PREDICTED: eukaryotic translation initiation factor 3 subunit J-like [Glycine max]	Protein synthesis and fate	nucl	0							50	2.00E-36	AT5G37475	cytosol, plasmodesma
836	Medtr5g093300, Medtr2g006820	MtD04868_1_AA Dihydrolipoamide acetyltransferase, long form	Energy metabolism	chlo	0							67	e-137	AT4G26910	M / mitochondrion
918	Medtr8g040150	MtD12624_1_AA ABC transporter	Transport	cysk	0							63	4.00E-44	AT3G12260	M / mitochondrion

		related IPR008011:Complex 1 LYR protein													
	Medtr2g013220	MtC93047_1_AA Unkown Blast: XP_003635272.1 PREDICTED: clathrin light chain 1-like [Vitis vinifera]	Transport	Nucl	0							59	2.00E-45	AT3G51890	clathrin coat of coated pit, clathrin coat of trans-Golgi network vesicle

Chapter 4, additional file S4.4.

Accession Mt3,5	Accession MENS Toulouse 01/2003_Identification	Functional classification	Localisation WolfPsort	TM	BB	GPI	SP	Palmitoylation	Prenylation	N-myrostylation	% Homologie TAIR	E value	Accession TAIR	Localisation TAIR
Medtr4g101280	MtC00005_1_AA Plant lipid transfer protein/seed storage/trypsin-alpha amylase inhibitor	Transport	chlo	1//1 TM			SP	P 6			66	2.00E-24	AT1G62510	endomembrane system
Medtr4te061140	MtC00008_1_AA Haem peroxidase, plant/fungal/bacterial	Cell rescue and defense	cyto	0//0							70	e-102	AT1G07890	CW / chloro /cytosol / PM / plasmodesma
Medtr3g070210	MtC00010_1_AA Major intrinsic protein, Blast: XP_003600863 Aquaporin protein PIP11	Transport	plas	5//5 TM	BB			**P 2**			86	e-102	AT1G01620	chloroplast, membrane, plasma membrane
Medtr3g093110	MtC00011_1_AA Ribosomal protein L6, signature 2	Protein synthesis and fate	cyto	0//0							87	4.00E-94	AT1G33140	chloroplast envelope, cytosolic large ribosomal subunit, large ribosomal subunit, membrane, plasmodesma, vacuole
Medtr4g132110	MtC00012_1_AA Haem peroxidase, plant/fungal/bacterial	Cell rescue and defense	cyto	0//1 TM			SP	**P 2**			81	e-152	AT4G21960	endomembrane system
Medtr4g075290	MtC00015_1_AA Peptidyl-prolyl cis-trans isomerase, cyclophilin type	Protein synthesis and fate	chlo	0//0				**P 1**			76	2.00E-76	AT2G16600	chloro / cytosol / PM / plasmodesma
Medtr4g104030	MtC00016_1_AA Nucleoside diphosphate kinase	Energy metabolism	cyto	0//0							76	1.00E-64	AT4G09320	Apoplast, chlorop, cytosol, perox, PM, plasmodesma, Vm, V
Medtr3g005430	MtC00017.3_1_AA 40S ribosomal protein S9	Protein synthesis and fate	cyto	0//0							92	1.00E-81	AT5G39850	cytosol, cytosolic small ribosomal subunit, membrane, plasmodesma
Medtr4g116410	MtC00024_1_AA Ribosomal protein S17	Protein synthesis and fate	cyto	0//0				**P 2**			82	1.00E-73	AT5G23740	cytosolic small ribosomal subunit, membrane
Medtr2g094270	MtC00027_1_AA Major intrinsic protein, Blast: XP_003597235 Aquaporin PIP2-7	Transport	plas	6//6 TM							78	e-128	AT3G53420	chloroplast, membrane, plasma membrane, plasmodesma, vacuole
Medtr8g088060	MtC00029_1_AA Blast: DF36485 ubiquitin extension protein, partial [Ageratina adenophora].	Protein synthesis and fate	cyto	0//0				**P 3**			82	4.00E-69	AT2G47110	Intra Cell / Cytos Rib
Medtr1g098220	MtC00032.2_1_AA Ribosomal protein S13	Protein synthesis and fate	cyto	0//0				**P 2**			84	1.00E-72	AT4G09800	Cytosol / V/ Plamodesma / CW / Nucleolus / cytos Rib
Medtr7g110310	MtC00034_1_AA S-adenosylmethionine synthetase	Energy metabolism	cyto	0//0				**P 3**			89	0	AT1G02500	cell wall, cytosol, membrane, plasma membrane
Medtr5g083790	MtC00035_1_AA Ribosomal protein L13, archea and eukaryotic form	Protein synthesis and fate	cyto	0//0				**P 2**			85	e-104	AT5G48760	Cytos rib /
Medtr5g018940	MtC00037_1_AA Ribosomal protein S4E	Protein synthesis and fate	chlo	0//0				**P 1**			91	e-135	AT5G07090	cytosolic ribosome, cytosolic small ribosomal subunit,VM
Medtr5g081710	MtC00038_1_AA Ribosomal protein L35Ae	Protein synthesis and fate	chlo	0//0				**P 1**			89	4.00E-55	AT1G41880	cytosolic large ribosomal subunit, membrane, ribosome
Medtr1g075720	MtC00039_1_AA Ribosomal protein L14	Protein synthesis and fate	cyto	0//0				**P 1**			85	1.00E-59	AT4G27090	chloroplast, cytosol, cytosolic large ribosomal subunit, cytosolic ribosome, endoplasmic reticulum, nucleolus,

														plasmodesma, ribosome, vacuolar membrane, vacuole
Medtr2g081610	MtC00045_1_AA BURP Blast:XP_003596540.1Embryonic abundant protein USP92 [Medicago truncatula] (BURP domain)	Cell rescue and defense	extr	1//1 TM			SP	**P 2**			33	5.00E-11	AT5G25610	endomembrane system
Medtr4g123810	MtC00046_1_AA S-adenosylmethionine synthetase	Energy metabolism	cyto	0//1 TM				**P 3**			91	0	AT3G17390	cell wall, membrane, nucleolus, plasma membrane, plasmodesma
AC140545_25	MtC00049_1_AA Ribosomal protein L10E	Protein synthesis and fate	chlo_mito	0//0				**P 4**	FT - CaaX Farnesyltransferase/ GGT1 - CaaX Geranylgeranyltransferase		88	e-114	AT1G26910	chloroplast envelope, membrane, ribosome
Medtr1g088070	MtC00051_1_AA Ribosomal protein L19e	Protein synthesis and fate	chlo	0//0				**P 4**			84	2.00E-61	AT4G02230	cytosol, cytosolic large ribosomal subunit, cytosolic ribosome, plasma membrane, ribosome
Medtr7g118060	MtC00053_1_AA Ribosomal protein 60S	Protein synthesis and fate	extr	0//0	BB			**P 2**			66	1.00E-16	AT5G24510	cytosolic ribosome, ribosome
Medtr2g028670	MtC00054_1_AA Blast: XP_003594440 Actin depolymerizing factor (cofilin) [Medicago truncatula	Cytoskeleton	cyto	0//0				**P 1**			82	2.00E-63	AT5G59880	Chloro / cytosol, mitochondrion, PM, plasmodesma
Medtr2g014220	MtC00058_1_AA Ribosomal L23 and L15e, core	Protein synthesis and fate	nucl	0//0							81	4.00E-94	AT4G16720	Cytosol,/cytosolic ribo/ PM / Vm
Medtr2g035930	MtC00061_1_AA Ribosomal protein L27e IPR005824:KOW	Protein synthesis and fate	nucl	0//0				**P 1**			74	1.00E-42	AT4G15000	Cytosol,/cytosolic ribo/ ribos
Medtr4g082860	MtC00063_1_AA unknown Blast: XP_003607781.1 Low-temperature inducible [Medicago truncatula]	Cell rescue and defense	mito	0//0	BB						55	2.00E-07	AT2G03440	undefined
Medtr1g100960	MtC00064_1_AA Ribosomal protein L36E	Protein synthesis and fate	chlo	0//0							80	5.00E-44	AT3G53740	Cytosol, cytosolic ribo, M, Vm
AC235488_9.1	MtC00066_1_AA Ribosomal protein L21e	Protein synthesis and fate	cyto	0//0			SP				81	2.00E-73	AT1G09690	Cytos rib / rib
Medtr7g098290	MtC00069_1_AA Ribosomal protein L14b/L23e	Protein synthesis and fate	cyto	0//0	BB			**P 1**			98	9.00E-67	AT3G04400	Cytos rib / ribos
Medtr8g046140	MtC00073_1_AA Ribosomal protein L5	Protein synthesis and fate	cyto	0//0				**P 1**			87	1.00E-88	AT2G42740	chloro / cytoso / cytos ribos / nucleolus / plasmodesma / V
Medtr8g045570	MtC00074_1_AA Bet v I allergen	Cell rescue and defense	cyto	0//0				**P 1**			36	7.00E-22	AT5G28010	ND
Medtr1g083460.	MtC00075_1_AA Ribosomal protein L18e	Protein synthesis and fate	nucl	0//0							84	3.00E-88	AT5G27850	Cytoso / cytos ribos / M / plasmodesma / V
unfound	MtC00078_1_AA Ribosomal protein 60S	Protein synthesis and fate	chlo	0//1	BB		SP				72	2.00E-16	AT2G27710	chloro / cytoso / cytos ribos / nucleolus / PM / plasmodesma / V
Medtr5g088320	MtC00080_1_AA Blast: CALM3_PETHY Calmodulin-related protein.	Signal transduction (calcium-mediated signal transduction)	nucl	0//0							99	3.00E-82	AT2G27030	vacuolar membrane
Medtr5g077130	MtC00082_1_AA Universal stress protein (Usp)	Cell rescue and defense	cyto	0//1 TM				**P 1**			76	9.00E-66	AT3G53990	Plasmodesma
Medtr7g088680	MtC00083.1_1_AA Nascent polypeptide-associated complex NAC IPR009060:UBA-like	Protein synthesis and fate	nucl	0//0	BB						68	9.00E-61	AT3G49470	cytosol, cytosolic ribosome, plasmodesma

Medtr1g088070	MtC00086_1_AA Ribosomal protein L19e	Protein synthesis and fate	nucl	0//0				**P 1**			85	4.00E-88	AT1G02780	cytosol, cytosolic large ribosomal subunit, cytosolic ribosome, membrane, nucleolus, plasma membrane, plasmodesma, ribosome
Medtr3g070500	MtC00088_1_AA Peptidyl-prolyl cis-trans isomerase, cyclophilin type IPR015891:	Protein synthesis and fate	extr	0//1 TM	BB		SP				90	1.00E-87	AT5G58710	Chloro / plasmodesma
Medtr4g063060	MtC00095_1_AA Ribosomal protein L23, N-terminal IPR013025:Ribosomal protein L25/L23	Protein synthesis and fate	cyto	0//0	BB						81	4.00E-49	AT3G55280	Cytosol,/cytosolic ribo/ M
Medtr2g014030	MtC00096_1_AA Ribosomal protein S6e IPR014401:	Protein synthesis and fate	nucl	0//0							79	3.00E-95	AT4G31700	chloro / cytoso / cytos ribos / nucleolus / PM / plasmodesma / V
Medtr3g078630	MtC00105_1_AA Blast: ACJ84101 unknown [Medicago truncatula].	Unclassified	chlo	1//1 TM				**P 1**			74	4.00E-34	AT3G48140	Peroxisome
Medtr5g015570	MtC00108_1_AA Ribosomal protein L24/L26	Protein synthesis and fate	cyto	1//0 TM						Predicted as myristoylated	98	e-104	AT1G10630	cytosol, membrane, plasma membrane, vacuolar membrane
Medtr7g109960	MtC00109.1_1_AA Blast: XP_003618207 ADP-ribosylation factor [Medicago truncatula]. ARF/SAR superfamily; Ras small GTPase, Rab type; ADP-ribosylation factor	Transport	chlo	0//1 TM		GPI				Predicted as myristoylated	98	e-103	AT1G10630	cytosol, membrane, plasma membrane, vacuolar membrane
Medtr5g034130	MtC00109.2_1_AA ARF/SAR superfamily.ARF/SAR superfamily; Ras small GTPase, Rab type; ADP-ribosylation factor	Transport	mito	0//0						Predicted as myristoylated	98	e-103	AT1G10630	cytosol, membrane, plasma membrane, vacuolar membrane
Medtr5g097200	MtC00110_1_AA Ribosomal protein S26E IPR008957:Fibronectin, type III-like fold	Protein synthesis and fate	cyto	0//0				**P 3**			62	6.00E-33	AT3G56340	cytosolic ribosome, cytosolic small ribosomal subunit, membrane
Medtr3g013640	MtC00111_1_AA Ribosomal protein S19e	Protein synthesis and fate	cysk	0//0				**P 1**			82	7.00E-70	AT5G61170	Cytosol,/cytosolic ribo/ ribos / V
Medtr7g111590	MtC00113_1_AA Ribosomal protein L13e	Protein synthesis and fate	chlo	0//0							87	6.00E-98	AT3G49010	Cell wall, cytosol, cytosolic ribo, M, PM / plasmodesma / Nucleolus /Vm
Medtr4g070080	MtC00115_1_AA unknown Blast: XP_003606910.1Glycine-rich RNA binding protein [Medicago truncatula]	Cell rescue and defense	chlo	0//0	BB						81	3.00E-36	AT2G21660	Chloro / cytoso / cytos ribos / Perosisome / Nucleolus / plasmodesma /
Medtr7g100720	MtC00118.1_1_AA 40S RIBOSOMAL PROTEIN S23	Protein synthesis and fate	cyto	0//0				**P 1**			96	8.00E-76	AT5G02960	cytosolic ribosome, cytosolic small ribosomal subunit, ribosome
Medtr8g083090	MtC00121_1_AA S-adenosyl-L-homocysteine hydrolase	Energy metabolism	chlo	0//0				**P 3**			85	e-159	AT4G13940	Cytosol / M / PM / Plasmodesma / Vm / V
Medtr8g106080	MtC00124_2_AA unknown Blast: XP_003535496.1 PREDICTED: conserved oligomeric Golgi complex subunit 1-like [Glycine max]	Transport	nucl	0//0				**P 1**			89	2.00E-71	AT2G09990	Plasmodesma / Chloro/ Cytos Rib / CW / M /
Medtr5g083170	MtC00127_1_AA Ferritin-like	Transport (iron ion transport)	chlo	0//0							72	4.00E-84	AT2G40300	chloroplast, chloroplast envelope, chloroplast stroma, mitochondrion

AC235488_13.1	MtC00128_1_AA Ribosomal protein S7	Protein synthesis and fate	cyto	0//0				**P 2**			92	e-101	AT2G37270	M / Ribos / CW / PM / cytos / Plasmodesma / Chloro
Medtr5g097200	MtC00132_1_AA Ribosomal protein S26E IPR008957:Fibronectin, type III-like fold	Protein synthesis and fate	cyto	0//0				**P 4**			62	2.00E-32	AT2G40590	Cytos rib
Medtr2g100410	MtC00134_1_AA Ribosomal L28e protein	Protein synthesis and fate	nucl	0//0							73	1.00E-56	AT4G29410	Cytos ribos / plasmodesma / PM
Medtr4g016670	MtC00135_1_AA Ribosomal protein S8E	Protein synthesis and fate	nucl	0//0				**P 1**			76	1.00E-85	AT5G59240	Cytosol,/cytosolic ribo/ Vm
Medtr3g070930	MtC00137_1_AA Ribosomal protein L1	Protein synthesis and fate	cyto	0//0				**P 1**			81	2.00E-99	AT1G08360	Cytosol, cytosolic ribo, PM, plasmodesma, ribosome
Medtr5g005130	MtC00141_1_AA Ribosomal protein S14	Protein synthesis and fate	nucl	0//0				**P 3**			92	3.00E-25	AT4G33865	cytosolic small ribosomal subunit
AC235488_13	MtC00142_1_AA Ribosomal protein S7	Protein synthesis and fate	cyto	0//0				**P 3**			89	e-100	AT3G11940	cell wall, chloroplast, cytosolic ribosome, plasma membrane, plasmodesma,vacuole
Medtr2g015680	MtC00143_1_AA Ribosomal protein S27E	Protein synthesis and fate	vacu	0//1 TM			SP	**P 2**			82	1.00E-36	AT3G61110	cell wall, cytosolic ribosome, cytosolic small ribosomal subunit, plasmodesma, ribosome
Medtr3g085490	MtC00144_1_AA Ribosomal protein L22/L17, eukaryotic and archaeal form	Protein synthesis and fate	nucl	0//0				**P 1**			87	1.00E-89	AT1G67430	Cytosolic ribo, M, nucleolus, V, plasmodesma, ribosome
Medtr1g088450	MtC00145_1_AA Ribosomal L22e protein	Protein synthesis and fate	nucl	0//0				**P 1**			77	4.00E-48	AT3G05560	Cytos Ribos / cytos/ Nucleolus / PM / Plsmodesma
Medtr7g076670	MtC00147_1_AA Ribosomal protein S14	Protein synthesis and fate	nucl	0//0				**P 3**			92	3.00E-25	AT4G33865	cytosolic small ribosomal subunit, ribosome
Medtr6g021670	MtC00148_1_AA Ribosomal protein S7E	Protein synthesis and fate	cyto	0//0							81	1.00E-90	AT1G48830	cell wall, chloroplast, cytosol, cytosolic ribosome, plasma membrane
Medtr8g105340	MtC00149_1_AA Ribosomal protein S5 IPR014720: IPR014721:	Protein synthesis and fate	plas	0//1 TM			SP	**P 1**			92	e-120	AT3G57490	Plasmodesmata /M
Medtr8g101980	MtC00151_1_AA Ribosomal protein L31e	Protein synthesis and fate	cyto	0//0				**P 1**			73	2.00E-43	AT5G56710	Cytos Ribos /Plasmodesmata / CW
Medtr2te077360	MtC00154_1_AA 14-3-3 protein	Signal transduction	nucl	0//0				**P 1**			75	e-115	AT2G42590	chloroplast stroma, cytoplasm, cytosol, nucleus, plasma membrane
Medtr8g076830	MtC00167_1_AA Ribosomal protein S17	Protein synthesis and fate	cyto	0//0				**P 2**			83	6.00E-73	AT3G48930	cell wall, cytosol, cytosolic ribosome, membrane, plasmodesma
Medtr2g035150.	MtC00168_1_AA Bet v I allergen	Cell rescue and defense	cyto	0//0	BB						34	0.009	AT5G45870	undefined
Medtr7g111590	MtC00176_1_AA Ribosomal protein L13e	Protein synthesis and fate	chlo	0//0							86	1.00E-81	AT3G49010	cell wall, cytosol, cytosolic large ribosomal subunit, cytosolic ribosome, membrane, nucleolus, plasma membrane, plasmodesma, vacuolar membrane

Medtr7g092890	MtC00181.1_1_AA Mitochondrial import inner membrane translocase, subunit Tim17/22	Transport	cyto	3//4 TM	BB						59	3.00E-43	AT2G42210	chloroplast, membrane,mitochondrion, plastid outer membrane
Medtr5g091130	MtC00184.1_1_AA Ribosomal L18ae protein	Protein synthesis and fate	cyto	0//0				**P 1**			90	2.00E-81	AT2G34480	cytosol, cytosolic large ribosomal subunit, cytosolic ribosome, plasma membrane, vacuolar membrane
Medtr2g098000	MtC00184.2_1_AA Ribosomal L18ae protein	Protein synthesis and fate	nucl	0//0				**P 1**			90	2.00E-81	AT2G34480	cytosol, cytosolic large ribosomal subunit, cytosolic ribosome, plasma membrane, vacuolar membrane
Medtr5g075520	MtC00185_1_AA unknown Blast: XP_003616043.1 hypothetical protein MTR_5g075520 [Medicago truncatula]	Unclassified	cyto	1//1 TM							24	1.00E-04	AT5G49350	endomembrane system
Medtr8g091910	MtC00192_1_AA Ribosomal protein L6E IPR005568:Ribosomal protein L6, N-terminal	Protein synthesis and fate	nucl	0//0							73	3.00E-82	AT1G74050	cytosol, cytosolic large ribosomal subunit, membrane, plasma membrane, plasmodesma
Medtr3g115930	MtC00194_1_AA unknown Blast: XP_003603853.1 hypothetical protein MTR_3g115930 [Medicago truncatula]	Unclassified	chlo	2//2 TM	BB		SP	**P 2**			77	1.00E-27	AT1G42960	chloroplast, chloroplast envelope, chloroplast inner membrane, chloroplast thylakoid membrane, membrane, mitochondrion, plastid
Medtr8g012330	MtC00199_1_AA Ribosomal protein S8E	Protein synthesis and fate	nucl	0//0							72	1.00E-72	AT5G59240	cytosolic ribosome, cytosolic small ribosomal subunit, membrane
Medtr5g005130	MtC00202_1_AA Ribosomal protein S14	Protein synthesis and fate	nucl	0//0				**P 3**			92	6.00E-21	AT4G33865	cytosolic small ribosomal subunit
Medtr4g068510	MtC00205.1_1_AA Cold acclimation WCOR413	Cell rescue and defense	vacu	5//6 TM							61	1.00E-51	AT2G15970	plasma membrane, vacuole
Medtr1g043040	MtC00218.2_1_AA Malate dehydrogenase, active site	Energy metabolism	chlo	0//1 TM	BB			**P 2**			73	e-137	AT1G04410	apoplast, chloroplast, chloroplast stroma, membrane, nucleus, plasma membrane, plasmodesma, vacuolar membrane, vacuole
Medtr2g034640	MtC00221_1_AA Ras GTPase	Signal transduction	cyto	0//1 TM							86	1.00E-95	AT4G02080	PM
Medtr7g098290	MtC00225_1_AA Ribosomal protein L14b/L23e	Protein synthesis and fate	cyto	0//0				**P 1**			98	5.00E-67	AT3G04400	cytosolic large ribosomal subunit
Medtr2g035320	MtC00227_1_AA Bet v I allergen	Cell rescue and defense	cyto	0//0	BB						28	AT5G45870	AT5G45870	undefined
Medtr7g023630	MtC00228_1_AA Polygalacturonase inhibitor precursor, Leucine rich repeat, N-terminal	Cell rescue and defense	extr	1//1 TM			SP	**P 2**			42	4.00E-30	AT5G06860	cell wall, plant-type cell wall, plasmodesma
Medtr5g010020	MtC00230_1_AA 40S RIBOSOMAL PROTEIN S10	Protein synthesis and fate	extr	1//0 TM				**P 1**			87	3.00E-47	AT5G52650	cell wall, cytosolic ribosome, membrane
Medtr3g106130	MtC00233_1_AA MIR Blast: XP_003603304.1 Stromal cell-derived factor 2-like protein [Medicago truncatula]	Protein synthesis and fate	extr	0//1 TM			SP				77	2.00E-93	AT2G25110	ER
Medtr5g020800	MtC00234.1_1_AA Blast: XP_003612051 Isoflavone reductase [Medicago truncatula].	Cell rescue and defense 'Phytoalexin biosynthesis; pterocarpan phytoalexin	cyto	0//0				**P 1**			53	4.00E-93	AT1G75280	PM

		biosynthesis.)												
Medtr5g020800	MtC00234.2_1_AA Isoflavone reductase [Medicago truncatula].	Cell rescue and defense 'Phytoalexin biosynthesis; pterocarpan phytoalexin biosynthesis.)	cyto	0//0				**P 1**			53	4.00E-93	AT1G75280	PM
Medtr5g020800	MtC00234.3_1_AA Isoflavone reductase [Medicago truncatula].	Cell rescue and defense 'Phytoalexin biosynthesis; pterocarpan phytoalexin biosynthesis.)	cyto	0//0				**P 1**			53	4.00E-93	AT1G75280	PM
Medtr2g101900	MtC00249_1_AA Ribosomal protein L37e	Protein synthesis and fate	chlo	0//0				**P 2**			88	2.00E-43	AT1G52300	cytosolic large ribosomal subunit
Medtr1g023590	MtC00251_1_AA Ribosomal protein L13, archea and eukaryotic form	Protein synthesis and fate	chlo	0//0				**P 1**			80	8.00E-95	AT5G48760	cytosolic large ribosomal subunit, cytosolic ribosome
unfound	MtC00252.1_1_AA Protein of unknown function DUF1138 Blast:BAM13305.1 ozone-responsive stress related protein [Oryza latifolia]	Cell rescue and defense	extr	0//1TM				**P 1**			68	3.00E-26	AT1G01170	M/ Mito
unfound	MtC00252.2_1_AA Protein of unknown function DUF1138 Blast: BAM13305.1 ozone-responsive stress related protein [Oryza latifolia]	Cell rescue and defense	extr	0//1 TM				**P 1**			68	3.00E-26	AT1G01170	M/ Mito
Medtr6g005820	MtC00257_1_AA Ras small GTPase, Rab type	Transport	mito	0//0						Predicted as myristoylated	98	e-104	AT1G10630	Cytosol/PM / PM / VM
Medtr6g087990	MtC00261_1_AA Blast: XP_003620633 Peroxiredoxin [Medicago truncatula].	Cell rescue and defense (Reduces hydrogen peroxide and alkyl hydroperoxides with reducing equivalents provided through the thioredoxin or glutaredoxin system. May be involved in mitochondrial redox homeostasis.)	cysk	0//0							73	5.00E-70	AT1G65980	PM/Chloro/PM
Medtr8g105340	MtC00264_1_AA Ribosomal protein S5, bacterial and chloroplast	Protein synthesis and fate	cyto	0//0				**P 1**			92	e-116	AT3G57490	cytosol, cytosolic ribosome, membrane, nucleolus, plasmodesma
Medtr4g101140	MtC00265_1_AA unknown Blast: XP_003549910.1 PREDICTED: NADH dehydrogenase [ubiquinone] 1 beta subcomplex subunit 8, mitochondrial-like [Glycine max]	Transport	mito	1//1 TM							81	9.00E-48	AT5G47570	undefined
Medtr7g083790	MtC00266_1_AA Mitochondrial substrate carrier	Transport	chlo	0//2 TM				**P 3**			85	e-144	AT5G14040	cell wall, chloroplast, membrane,mitochondrion, vacuolar membrane
Medtr5g075690	MtC00269_1_AA unknown Blast:XP_003616060.1Cytochrome b-c1 complex subunit [Medicago truncatula]	Transport	cyto	1//1 TM							79	7.00E-25	AT5G05370	Mitochondrium
Medtr3g092090	MtC00272_1_AA Cytochrome b5	Transport	mito	1//1 TM							79	2.00E-58	AT5G53560	Chloro thylakoid membrane / ER / Vm / PM
AC235674_1	MtC00278_1_AA Blast: XP_002511833 Remorin, putative [Ricinus communis]	Signal transduction	cyto	0//0	BB			**P 1**			62	1.00E-23	AT3G61260	V / PM / Plasmodesmata
AC140545_25	MtC00286_1_AA Ribosomal protein L10E	Protein synthesis and fate	chlo_mito	0//0				**P 3**			89	e-110	AT1G26910	M / Ribosome / Chloro envelope

Medtr1g087020	MtC00288_1_AA Cytochrome c oxidase subunit Vc	Transport	cyto	2//1 TM				**P 1**			81	3.00E-25	AT5G61310	endomembrane system, mitochondrial respiratory chain
Medtr4g012740	MtC00292_1_AA Proteasome alpha-subunit	Protein synthesis and fate	cyto	0//0				**P 2**			86	e-122	AT5G42790	cytosol, plasma membrane, proteasome complex, proteasome core complex
Medtr5g097910	MtC00294_1_AA Aldo/keto reductase	Energy metabolism	cyto	0//0				**P 2**			54	9.00E-83	AT1G59960	Cytos
Medtr1g045120	MtC00297_1_AA Plant acid phosphatase	Energy metabolism	extr	1//1 TM			SP	**P 2**			50	5.00E-73	AT1G04040	V / CW / Vm / Plasmodesmata
Medtr6g059410	MtC00300_1_AA unknown Blast: XP_003619561.1 Kunitz-type trypsin inhibitor-like 2 protein [Medicago truncatula]	Cell rescue and defense	extr	0//1 TM			SP				31	2.00E-10		mitochondrion
Medtr1g006490	MtC00307_1_AA Major intrinsic protein Blast XP_003588369 Aquaporin TIP4-1	Transport	vacu	7//7 TM	BB			**P 3**			79	9.00E-97	AT2G25810	central vacuole, membrane, plant-type vacuole membrane
Medtr8g105630	MtC00308_1_AA Thioredoxin fold	Cell rescue and defense	chlo	1//1 TM				**P 1**			74	2.00E-65	AT2G31570	cytosol
Medtr4g111950	MtC00310_1_AA Thioredoxin-related IPR006663: IPR012336:Thioredoxin-like fold IPR013766:Thioredoxin domain	Cell rescue and defense	chlo	0//0				**P 1**		Predicted as myristoylated	69	2.00E-54	AT3G08710	cytosol, nucleus, plasma membrane, plastid
Medtr5g012470	MtC00312.1_1_AA 20S proteasome, A and B subunits	Protein synthesis and fate	cyto	1//0 TM							87	e-105	AT3G22630	apoplast, cytosol, plasma membrane, proteasome core complex, vacuolar membrane, vacuole
Medtr3g085490	MtC00315_1_AA Ribosomal protein L22/L17, eukaryotic and archaeal form	Protein synthesis and fate	nucl	0//0				**P 1**			88	3.00E-76	AT1G27400	chloroplast, cytosol, cytosolic large ribosomal subunit, plasma membrane, plasmodesma, ribosome, vacuolar membrane, vacuole
Medtr6g052220	MtC00318_1_AA Eukaryotic/archaeal ribosomal protein S3	Protein synthesis and fate	chlo	0//0				**P 3**			92	e-109	AT3G53870	cytosolic ribosome, cytosolic small ribosomal subunit, membrane, plasmodesma
Medtr2g096340	MtC00322_1_AA Ribosomal protein L23, N-terminal IPR013025:Ribosomal protein L25/L23	Protein synthesis and fate	nucl	0//0							82	3.00E-41	AT3G55280	cytosolic large ribosomal subunit, cytosolic ribosome, ,membrane
Medtr6g088610	MtC00323_1_AA Blast: XP_003620684 Somatic embryogenesis receptor kinase [Medicago truncatula].	Signal transduction	nucl	0//0				**P 2**			74	e-127	AT3G24550	PM
Medtr2g014220	MtC00325_1_AA Ribosomal L23 and L15e, core	Protein synthesis and fate	nucl	0//0							81	9.00E-79	AT4G16720	cytosol, cytosolic large ribosomal subunit, cytosolic ribosome, plasma membrane, vacuolar membrane
AC146721_1013	MtC00326_1_AA 6-phosphogluconate dehydrogenase, C-terminal extension	Energy metabolism	chlo	0//0				**P 1**			87	0	AT3G02360	chloroplast stroma, cytosol, peroxisome
Medtr7g090520	MtC00330_1_AA Blast: XP_002284968 gibberellin 20 oxidase 3 [Vitis vinifera].	Energy metabolism	cyto	0//0				**P 1**			65	e-126	AT1G52820	undefined

Medtr7g017700	MtC00335_1_AA Histone H2A IPR009072:Histone-fold	Cell cycle and DNA processing	nucl	0//0	BB						75	3.00E-36	AT5G02560	nucleosome, nucleus
Medtr8g045570	MtC00343.1_1_AA Bet v I allergen	Cell rescue and defense	cyto	0//0				**P 1**			38	2.00E-17	AT5G28010	undefined
Medtr5g088320	MtC00346_1_AA Calcium-binding EF-hand	Signal transduction	chlo	0//0							98	1.00E-71	AT2G27030	Vm/PM
Medtr7g074570	MtC00348_1_AA Phosphoglycerate mutase, 2,3-bisphosphoglycerate-independent	Energy metabolism	cyto	0//0				**P 1**			82	0	AT1G09780	chloroplast, cytosol, mitochondrial envelope, plasma membrane, plasmodesma
Medtr2g088360	MtC00349_1_AA Aconitate hydratase 1	Energy metabolism	chlo	0//1 TM			SP	**P 2**			85	0	AT2G05710	cell wall, chloroplast, chloroplast stroma, cytosol, mitochondrion, vacuolar membrane
Medtr7g093910	MtC00350_1_AA Histone H2A IPR009072:Histone-fold	Cell cycle and DNA processing	chlo	0//0	BB			**P 1**			84	3.00E-56	AT1G54690	nucleolus, Nucleus
Medtr4g068040	MtC00354_1_AA Ribosomal L38e protein	Protein synthesis and fate	nucl	0//0				**P 1**			91	5.00E-26	AT3G59540	cytosolic large ribosomal subunit
Medtr5g010640	MtC00357_1_AA Thaumatin, pathogenesis-related	Cell rescue and defense	chlo	1//1 TM			SP	**P 1**			78	1.00E-89	AT4G11650	EndoM system
AC235488_1	MtC00359_1_AA Haem peroxidase, plant/fungal/bacterial	Cell rescue and defense	chlo	1//1 TM			SP	**P 4**			55	2.00E-95	AT1G05260	ER
Medtr2g034640	MtC00366_1_AA Small GTP-binding protein domain	Signal transduction	cyto	2//2 TM				**P 2**	FT - CaaX Farnesyltransferase/ GGT1 - CaaX Geranylgeranyltransferase		86	3.00E-96	AT4G02080	plasma membrane
Medtr3g005060	MtC00367_1_AA Endo-1,3;1,4-beta-D-glucanase, Dienelactone hydrolase	Energy metabolism	cyto	0//0				**P 2**			57	1.00E-80	AT3G23600	Nucleus / PM / Cytos / Apoplast
Medtr6g021670	MtC00369_1_AA Ribosomal protein S7E	Protein synthesis and fate	chlo	0//0				**P 1**			81	2.00E-81	AT1G48830	cell wall, chloroplast, cytosol, cytosolic ribosome, cytosolic small ribosomal subunit, plasma membrane
Medtr1g023140	MtC00375_1_AA Thioredoxin-relatedIPR006663: IPR012336:Thioredoxin-like fold IPR013766:Thioredoxin domain	Cell rescue and defense	cyto	0//0				**P 1**			69	7.00E-42	AT3G51030	Cytos
Medtr5g076590	MtC00385_1_AA Ras small GTPase, Rab type	Transport	chlo	1//1 TM				**P 2**	GGT2 - Rab Geranylgeranyltransferase		80	2.00E-85	AT5G45130	Vm
Medtr5g092160	MtC00387_1_AA Protein of unknown function UPF0136, Transmembrane	Unclassified	plas	4//4 TM	BB						52	AT1G50740	AT1G50740	undefined
Medtr4g097800	MtC00395_1_AA Cytochrome c oxidase, subunit VIa	Transport	mito	0//1 TM							72	7.00E-34	AT4G37830	Mitochondrium
Medtr8te085740	MtC00400_1_AA Ribosomal protein L32e	Protein synthesis and fate	cyto	0//0				**P 1**			81	9.00E-55	AT4G18100	cytosol, cytosolic large ribosomal subunit, cytosolic ribosome, nucleolus,
Medtr2g006610, Medtr2g006170	MtC00404_1_AA Ribosomal protein L27e IPR005824:KOW	Protein synthesis and fate	chlo	0//0				**P 2**			73	6.00E-38	AT4G15000	cytosolic large ribosomal subunit, cytosolic ribosome
Medtr7g076200	MtC00407_1_AA Unknown Blast: XP_003623838 Peroxisomal membrane protein 11-1 Peroxisomal biogenesis factor 11	Protein synthesis and fate	golg	0//2 TM	BB		SP	**P 1**			80	e-106	AT1G01820	Peroxisome/Intergral to M peroxsisoms/ Plasmodesmata

Medtr5g033090	MtC00413_1_AA Ribosomal protein L15	Protein synthesis and fate	nucl	0//0							77	3.00E-54	AT1G70600	cytosolic large ribosomal subunit / nucleus / M/ plasmodesma
Medtr7g080800	MtC00415_1_AA Cytochrome c, monohaem	Transport	mito	0//0				**P 1**			90	5.00E-52	AT4G10040	cytosol, mitochondrion, vacuolar membrane
AC150841_2, Medtr3g014870, Medtr3g014820	MtC00422.1_1_AA Kunitz inhibitor ST1-like	Cell rescue and defense	extr	1//1 TM			SP				32	6.00E-11	AT1G73260	mitochondrion
Medtr3g014870	MtC00422.2_1_AA Kunitz inhibitor ST1-like	Cell rescue and defense	extr	1//1 TM			SP				28	4.00E-11	AT1G17860	apoplast, cell wall
Medtr3g076630	MtC00423.1_1_AA Pyruvate dehydrogenase E1 component subunit beta-like	Energy metabolism	chlo	0//0			SP				73	e-173	AT2G34590	Choro/ Chloro envloppe
Medtr3g076630	MtC00423.2_1_AA Pyruvate dehydrogenase E1 component subunit beta-like	Energy metabolism	chlo	0//0				**P 2**			73	e-173	AT2G34590	Choro/ Chloro envloppe
Medtr2g065470	MtC00429_1_AA unknown Blast: XP_003596038.1 Glyceraldehyde-3-phosphate dehydrogenase [Medicago truncatula]	Energy metabolism	chlo	0//0	BB		SP	**P 3**			83	0	AT1G79530	Plastid/ M
Medtr4g051880	MtC00432_1_AA Harpin-induced 1	Cell rescue and defense	chlo	1//1 TM				**P 2**			64	7.00E-64	AT3G52470	plasmodesma
Medtr1g106900	MtC00435_1_AA Ribosomal protein S13	Protein synthesis and fate	nucl	0//0				**P 2**			82	5.00E-72	AT4G09800	Plasmodesmata/ Cell Wall / Cytosol Ribos/ Nucleaus / V
Medtr5g040610	MtC00438_1_AA ATPase, F1 complex, epsilon subunit, mitochondrial	Transport	chlo	0//0				**P 1**			78	3.00E-31	AT1G51650	Mitochondrium
Medtr2g025480	MtC00443_1_AA Protein of unknown function UPF0041 Blast:XP_003555865.1 PREDICTED: brain protein 44-like protein-like [Glycine max]	Unclassified	mito	1//1 TM				**P 2**			85	5.00E-46	AT5G20090	M / Vm / mitochondrion/ PM
Medtr7g109340	MtC00445_1_AA Heat shock protein DnaJ	Cell rescue and defense	cyto	0//0							75	e-108	AT3G62600	PM/ endoplasmic reticulum lumen
Medtr4g077840	MtC00451_1_AA unknown Blast: XP_003537717.1 PREDICTED: NADH dehydrogenase [ubiquinone] iron-sulfur protein 6, mitochondrial-like [Glycine max]	Transport	mito	0//0				**P 1**			86	1.00E-36	AT3G03070	Mitochondrium
Medtr1g061630	MtC00463_1_AA Pyruvate kinase	Energy metabolism	cyto	0//0				**P 3**			87	0	AT3G52990	cytosol, membrane
Medtr4g112780	MtC00466_1_AA Blast: XP_003609172 H/ACA ribonucleoprotein complex subunit 2-like protein [Medicago truncatula].Ribosomal_L7Ae	Protein synthesis and fate	chlo	0//0				**P 3**			61	1.00E-50	AT5G08180	Nucleus
Medtr3g113970	MtC00469_1_AA Ribosomal protein S6e IPR014401:	Protein synthesis and fate	nucl	0//0				**P 7**			91	0	AT1G75780	vacuole
Medtr5g017670	MtC00477_1_AA Patatin IPR008271:Serine/threonine protein kinase, active site	Signal transduction	chlo	0//0				**P 1**			53	e-119	AT4G37050	undefined
Medtr2g010750	MtC00493_1_AA IPR012336:Thioredoxin-like fold IPR013766:Thioredoxin domain	Cell rescue and defense	cyto	0//3 TM							67	9.00E-41	AT1G11530	Cytos

Medtr3g105330	MtC00501_1_AA Ctr copper transporter	Transport	vacu	3//3 TM	BB			**P 2**	FT - CaaX Farnesyltransferase/ GGT1 - CaaX Geranylgeranyltransferase		50	1.00E-36	AT5G20650	Late endosome / Vm / V / Plasmodesma
Medtr1g064090	MtC00502_1_AA Phenylalanine/histidine ammonia-lyase	Energy metabolism	chlo	0//1 TM				**P 7**			82	0	NS	cytoplasm
Medtr5g012930	MtC00506_1_AA Ribosomal protein L1	Protein synthesis and fate	chlo	0//0				**P 2**			81	e-100	AT1G08360	cytosolic large ribosomal subunit/ PM / Cytos / Plasmodesma
Medtr8g086330	MtC00508_1_AA Sec61beta family	Transport	chlo	1//1 TM							75	2.00E-22	AT3G60540	undefined
Medtr8g076770	MtC00518_1_AA Major intrinsic protein IPR002208:SecY protein IPR003439:ABC transporter related	Transport	plas	10//8 TM				**P 3**			93	0	AT4G35100	Membrane
Medtr4g132270	MtC00525_1_AA Glyoxalase/Bleomycin resistance protein/dioxygenase domain; Glyoxalase I XP_003534533 Blast: XP_003534533 putative lactoylglutathione lyase-like	Cell rescue and defense	cyto	0//0	BB						79	e-137	AT1G11840	chloroplast envelope, cytosol, peroxisome, plasma membrane, vacuole
Medtr3g092030	MtC00527_1_AA Protein of unknown function DUF791 Blast:XP_003602305.1Major facilitator superfamily domain-containing protein [Medicago truncatula]	Transport	vacu	11//10 TM				**P 4**			77	0	AT4G27720	plasma membrane
Medtr1g035230	MtC00531_1_AA Pyrophosphate-dependent phosphofructokinase PfpB IPR015913:	Energy metabolism	cyto	0//0				**P 2**			81	0	AT1G20950	cytosol
Medtr8g035590	MtC00534_1_AA Calcium-dependent lipid binding	Signal transduction	chlo	2//2 TM	BB						64	4.00E-74	AT3G61050	PM / Nuclear M
Medtr7g067470	MtC00545_1_AA GroEL-like chaperone, ATPase	Protein synthesis and fate	cyto	0//0	BB			**P 3**			90	e-153	AT5G20890	Cytos / CW / PM anchored
Medtr2g104110	MtC00556_1_AA unknown Blast: XP_003597927.1 NADH-ubiquinone oxidoreductase 24 kDa subunit [Medicago truncatula]	Transport	mito	0//0				**P 6**			85	e-128	AT4G02580	Mitochondrium
unfound	MtC00558_1_AA unknown Blast: XP_002523307.1 ormdl, putative [Ricinus communis]	Protein synthesis and fate	plas	3//2 TM							85	2.00E-48	AT5G42000	E.R.
Medtr7g083560	MtC00568_1_AA Translocon-associated beta	Transport	chlo	3//3 TM	BB			**P 2**			62	3.00E-58	AT5G14030	plasmodesma, vacuolar membrane
AC146721_1013	MtC00571_1_AA 6-phosphogluconate dehydrogenase, C-terminal extension	Energy metabolism	chlo	0//1 TM			SP	**P 5**			88	e-106	AT1G64190	chloroplast, chloroplast stroma, cytosol, membrane
Medtr2g082220	MtC00574_1_AA Histone H2A IPR007124: IPR009072:Histone-fold	Cell cycle and DNA processing	chlo	0//0	BB			**P 3**			80	5.00E-47	AT5G54640	Nucleolus
Medtr3g118030	MtC00580.1_1_AA Eukaryotic ribosomal protein L5	Protein synthesis and fate	chlo	0//1 TM	BB						79	e-123	AT5G39740	cytosol, cytosolic large ribosomal subunit, cytosolic ribosome, nucleolus, plasma membrane, vacuole

Medtr3g064390	MtC00581_1_AA Ras small GTPase, Rab type	Transport	mito	0//0	BB			**P 2**	GGT2 - Rab Geranylgeranyltransferase	Predicted as myristoylated	80	3.00E-87	AT5G45130	Vm
Medtr6g091630	MtC00586_1_AA Ribosomal protein L31e	Protein synthesis and fate	cyto	0//0				**P 1**			72	3.00E-34	AT5G56710	cell wall, cytosolic large ribosomal subunit, cytosolic ribosome, plasmodesma, ribosome
Medtr4g090120	MtC00590_1_AA unknown Blast: MLP3.2 protein [Medicago truncatula]	Unclassified	nucl	1//1 TM			SP	**P 1**			47	7.00E-15	AT3G07568	undefined
Medtr7g027960	MtC00591_1_AA cytochrome P450	Transport	cyto	0//1 TM				**P 1**			48	3.00E-46	AT3G32047	endomembrane system
Medtr2g005510	MtC00594_1_AA Ras GTPase superfamily; Ras small GTPase, Rab type	Transport	cyto	0//0				**P 2**	FT - CaaX Farnesyltransferase/ GGT1 - CaaX Geranylgeranyltransferase/ GGT2 - Rab Geranylgeranyltransferase		87	e-105	AT1G09630	cell plate, cytosol, endosome, plasma membrane
Medtr2g012560	MtC00597_1_AA SCAMP	Transport	plas	4//4 TM							63	e-101	AT1G61250	PM
Medtr4g120770	MtC00602_1_AA Ribosomal protein L14	Protein synthesis and fate	cyto	0//0							83	1.00E-57	AT2G20450	chloroplast, cytosol, cytosolic large ribosomal subunit, cytosolic ribosome, endoplasmic reticulum, nucleolus, plasmodesma, vacuolar membrane, vacuole
Medtr7g086190	MtC00605_1_AA Blue (type 1) copper domain; XP_003592453	Transport	chlo	2//2 TM			SP	**P 1**			40	5.00E-18	AT3G17675	undefined
Medtr1g088480	MtC00606_1_AA NAD-dependent epimerase/dehydratase; NAD binding site "NADB_Rossmann"	Transport	cyto	1//1 TM							78	0	AT3G53520	Golgi membrane, membrane, plasma membrane
Medtr7g009330	MtC00615_1_AA probable mitochondrial porin	Transport	nucl	0//0	BB						23	3.00E-08	AT5G15090	cell wall, chloroplast, chloroplast envelope, membrane, mitochondrion, nucleolus, plasma membrane, plastid, vacuolar membrane, vacuole
Medtr1g011850	MtC00621_1_AA Histone H2A IPR007124: IPR009072:Histone-fold	Cell cycle and DNA processing	nucl	0//0	BB			**P 1**			91	6.00E-54	AT1G52740	V
Medtr4g097830	MtC00623_1_AA Tubulin/FtsZ protein	Cytoskeleton	mito	0//1TM				**P 7**			93	0	AT1G50010	cell wall, cytosol, membrane
Medtr8g018730	MtC00630_1_AA Lipoxygenase	Cell rescue and defense	cyto	0//1 TM				**P 1**			53	0	AT3G22400	chloroplast
Medtr4g087310	MtC00633_1_AA unknown Blast: XP_003608067.1 15 kDa selenoprotein [Medicago truncatula]	Cell rescue and defense	cyto	1//1 TM			SP	**P 4**			76	6.00E-65	AT1G05720	endomembrane system
Medtr5g068140	MtC00638_1_AA Inorganic phosphate transporter (MIP)	Transport	plas	5//4 TM							50	4.00E-46	AT5G43350	M
unfound	MtC00650_1_AA GHMP kinase, Diphosphomevalonate decarboxylase	Energy metabolism	cyto	0//1 TM				**P 1**			78	0	AT3G54250	undefined

Medtr4g128020	MtC00653_1_AA NADPH-CYTOCHROME P450 REDUCTASE, Flavoprotein pyridine nucleotide cytochrome reductase	Transport	chlo	1//1 TM				**P 2**			64	0	AT3G02280	chloroplast, endoplasmic reticulum
Medtr5g084060	MtC00656_1_AA Protein secE/sec61-gamma protein	Transport	cyto	1//1 TM							70	4.00E-21	AT3G48570	PM
Medtr7g114240	MtC00676_1_AA Superoxide dismutase, copper/zinc binding	Cell rescue and defense	cyto	0//0	BB			**P 1**			83	1.00E-68	AT1G08830	cytoplasm, cytosol
unfound	MtC00700_1_AA unknown Blast: Unknown	Unclassified	chlo	0//0			SP				74	2.00E-31	AT4G20150	Mitochondrium / Vm
Medtr7g108320	MtC00712_1_AA Histone H2A IPR009072:Histone-fold	Cell cycle and DNA processing	nucl	0//0	BB						79	1.00E-45	AT1G54690	Nucleus / Nucleolus
Medtr4g113200	MtC00716.1_1_AA Argonaute and Dicer protein	Cell cycle and DNA processing	cyto	0//0				**P 4**			83	0	AT1G69440	cytoplasm, cytosol, nucleus
Medtr8g104870	MtC00726_1_AA Protein of unknown function Cys-rich Blast: XP_003630909.1 Fruit weight 2.2-like protein [Medicago truncatula]	Unclassified	chlo	1//1 TM				**P 14**			68	2.00E-44	AT1G14870	PM
Medtr1g083330, Medtr1g083340	MtC00731_1_AA 26S proteasome subunit P45	Protein synthesis and fate	cyto	0//0				**P 1**			91	0	AT3G05530	cytoplasm, cytosol, nucleus, proteasome regulatory particle, base subcomplex
Medtr2g014950	MtC00732_1_AA unknown Blast: XP_003593680.1 28 kDa heat- and acid-stable phosphoprotein [Medicago truncatula]	Signal transduction	chlo	0//0				**P 2**			55	1.00E-35	AT5G46020	Cytos
AC235671_19	MtC00734_1_AA E-class P450, group I	Transport	plas	1//1 TM				**P 3**			51	e-150	AT4G37370	PM / ER
unfound	MtC00735_1_AA Ribosomal protein 60S	Protein synthesis and fate	chlo	0//0	BB						67	9.00E-18	AT2G27710	chloroplast, cytosol, cytosolic ribosome, membrane, nucleolus, nucleus, plasma membrane, ribosome
Medtr5g075450	MtC00747.1_1_AA Cytochrome P450	Transport	cyto	1//2 TM				**P 1**			80	0	AT2G40890	endoplasmic reticulum, membrane, plant-type cell wall, plasma membrane, plasmodesma, vacuolar membrane
Medtr4g081130	MtC00753_1_AA Thiamine biosynthesis Thi4 protein	Energy metabolism	chlo	0//0	BB			**P 2**			81	e-146	AT5G54770	chloroplast, chloroplast envelope, chloroplast stroma, mitochondrion, thylakoid
Medtr8g083420	MtC00772_1_AA Glycine hydroxymethyltransferase	Energy metabolism	chlo	0//0				**P 3**			87	0	AT4G13930	cytosol, membrane, plasma membrane, plasmodesma
Medtr3g118530	MtC00778_1_AA Sugar transporter Blast: XP_003604104 Monosaccharide-sensing protein	Transport	plas	5//5 TM	BB			**P 4**	FT - CaaX Farnesyltransferase/ GGT1 - CaaX Geranylgeranyltransferase		69	e-122	AT4G35300	V / Vm
Medtr7g009070	MtC00779_1_AA Thioredoxin-related IPR012336:Thioredoxin-like fold IPR013766:Thioredoxin domain IPR015467:	Cell rescue and defense	nucl	0//0						Predicted as myristoylated	55	1.00E-38	AT5G39950	PM / Mitochiondrium / cytos
Medtr1g045410	MtC00780_1_AA Ribosomal protein L4/L1e, archeabacterial like	Protein synthesis and fate	cyto	0//1 TM							76	0	AT3G09630	M / Nucleolus / Cytos Ribo / CW / Plamodesmata / PM / V / Chloro

Medtr2g076960, Medtr2te077360	MtC00791.1_1_AA 14-3-3 protein	Signal transduction	nucl	0//0				**P 2**			76	e-105	AT1G22300	chloroplast stroma, cytoplasm, cytosol, mitochondrion, plasma membrane, plasmodesma
Medtr4g063550	MtC00793_1_AA RNA-binding region RNP-1	Protein synthesis and fate	nucl	0//0	BB						53	2.00E-48	AT5G59950	undefined
Medtr4g092920	MtC01434.1_1_AA Heat shock protein 70	Cell rescue and defense	mito	0//0	BB		SP	**P 2**			80	0	AT5G09590	cell wall, chloroplast, mitochondrial matrix, mitochondrion, vacuolar membrane
Medtr3g109210	MtC01440_1_AA Peptidase T1A, proteasome beta-subunit	Protein synthesis and fate	cyto	0//0	BB						85	e-113	AT4G31300	V / Cytos / Proteasome core cplx / Vm /
Medtr8g036880	MtC01635_1_AA Adenine nucleotide translocator 1	Transport	chlo	3//3 TM	BB						71	e-144	AT4G28390	M / Chloro m / mitochondrion
Medtr8g106800	MtC10023_1_AA Haem peroxidase	Cell rescue and defense	cyto	0//0							72	0	NS	endomembrane system
unfound	MtC10028_1_AA unknown Blast: XP_003549822.1 PREDICTED: high-affinity nitrate transporter 3.1-like [Glycine max]	Transport	plas	1//2 TM			SP	**P 3**			48	7.00E-41	AT5G50200	plasma membrane
Medtr2g029850	MtC10033_1_AA Haem peroxidase, plant/fungal/bacterial	Cell rescue and defense	extr	0//1 TM			SP	**P 3**			52	9.00E-87	AT3G49110	plant-type cell wall, vacuole
Medtr2g081810	MtC10046_1_AA 1,4-benzoquinone reductase-like; Trp repressor binding protein-like	Protein synthesis and fate	mito	0//0							84	3.00E-97	AT5G54500	M / PM / V / Vm
Medtr3g092970	MtC10052_1_AA ArgE/dapE/ACY1/CPG2/yscS IPR002715:Nascent polypeptide-associated complex NAC IPR009060:UBA-like	Protein synthesis and fate	cyto	0//0	BB						66	5.00E-46	AT3G49470	Cytos
Medtr2g066630	MtC10060_1_AA Glutathione S-transferase, C-terminal IPR012335:Thioredoxin fold	Cell rescue and defense	cyto	0//0							72	4.00E-89	AT1G19570	Chloro / Mitochondruim / Cytos / Perox / PM / apoplast / V
Medtr1g064060	MtC10064_1_AA Adenosine kinase	Energy metabolism	cyto	0//0				**P 3**			84	e-150	AT3G09820	apoplast, chloroplast, cytosol, membrane, plasma membrane, plasmodesma
Medtr6g060570	MtC10068_1_AA Enolase	Energy metabolism	cyto	0//0				**P 1**			89	0	AT2G36530	Mitochondrial envelope
Medtr3g072080	MtC10069_1_AA Vesicular-fusion protein SEC17	Transport	chlo	0//0				**P 3**			69	e-102	AT3G56190	PM / V / Vm / Plasmodesmata / M
Medtr5g006440	MtC10071_1_AA Ribosomal protein S3Ae	Protein synthesis and fate	cyto	0//0				**P 2**			84	e-122	AT3G04840	chloroplast, cytosol, cytosolic ribosome, cytosolic small ribosomal subunit, plasma membrane, plasmodesma
Medtr1g068730, Medtr1g068740	MtC10076.1_1_AA Sigma-54 factor, interaction region IPR003579:Ras small GTPase, Rab type	Transport	nucl	0//0				**P 2**	fT - CaaX Farnesyltransferase/ GGT1 - CaaX Geranylgeranyltransferase/GGT2 - Rab Geranylgeranyltransferase		83	2.00E-89	AT3G09900	cytosol, plasma membrane
Medtr3g049400	MtC10090.1_1_AA Protein of unknown function DUF250 Blast: XP_003599946.1 Glucose-6-phosphate/phosphate-translocator [Medicago truncatula]	Transport	plas	6//6 TM				**P 2**			73	e-144	AT1G61800	vacuolar membrane

Medtr4g071860	MtC10099_1_AA Fructose-bisphosphate aldolase, class-I	Energy metabolism	chlo	0//0	BB						83	0	AT2G01140	chloroplast, chloroplast stroma, chloroplast thylakoid, mitochondrion, plastoglobule
Medtr7g079230	MtC10100.1_1_AA Blast: XP_003626103 Cathepsin B [Medicago truncatula].	Protein synthesis and fate	extr	0//2 TM			SP	**P 2**			71	e-140	AT4G01610	cytosol, vacuole
Medtr7g088490	MtC10107.1_1_AA Peptidase T1A, proteasome beta-subunit	Protein synthesis and fate	chlo	0//0				**P 1**			93	e-112	AT1G21720	Proteasome cpx/ Vm / Cytos
Medtr2g066120	MtC10110_1_AA Phosphoglycerate kinase	Energy metabolism	cyto	0//0	BB						89	0	AT1G79550	apoplast, chloroplast stroma, cytosol, membrane, nucleus, plasma membrane, plasmodesma, vacuolar membrane
Medtr2g029910	MtC10112_1_AA Haem peroxidase, plant/fungal/bacterial	Cell rescue and defense	extr	1//1 TM			SP	**P 3**			59	3.00E-94	AT5G06730	Vm
Medtr5g065880	MtC10113_1_AA Phosphoglucose isomerase (PGI)	Energy metabolism	chlo	0//0	BB			**P 2**			79	0	AT4G24620	chloroplast, chloroplast envelope, chloroplast stroma, cytosol, plastid
Medtr5g007210	MtC10115_1_AA unknown Blast: XP_003610804 hypothetical protein MTR_5g007210	Unclassified	chlo	1//1 TM							52	5.00E-36	AT5G16660	Choro / Chloro m / M
Medtr5g095230	MtC10121.1_1_AA E-class P450, group I	Transport	cyto	1//1 TM				**P 1**			53	e-157	AT3G14630	endomembrane system
Medtr2g029800	MtC10136.1_1_AA Haem peroxidase, plant/fungal/bacterial	Cell rescue and defense	extr	1//1 TM		GPI	SP	**P 4**			55	e-102	AT2G38380	plant-type cell wall
Medtr2g008080	MtC10138_1_AA Ubiquinol-cytochrome C reductase hinge protein	Transport	mito	0//0				**P 1**			86	9.00E-29	AT1G15120	Mitochondrium
Medtr7g081660	MtC10139_1_AA Hyaluronan/mRNA binding protein	Protein synthesis and fate	nucl	0//0				**P 1**			47	8.00E-32	AT4G16830	Cytos / Nucleus
Medtr8g075320	MtC10145_1_AA Proteasome alpha-subunit	Protein synthesis and fate	cyto	0//0				**P 1**			91	e-108	AT5G66140	Proteasome cpx V / Cytos/ Chloro
Medtr3g099580	MtC10149_1_AA Blast: ACJ83883 unknown [Medicago truncatula].Plastocyanin-like domain	Transport	extr	0//2 TM	BB	GPI	SP				52	1.00E-24	AT3G60270	M anchored
Medtr1g108530	MtC10154_1_AA NAD-dependent epimerase/dehydratase	Transport	mito	1//1 TM							89	0	AT2G27860	cytoplasm, cytosol
Medtr8g052030	MtC10166.1_1_AA KOW Blast: XP_003611879.1 40S ribosomal protein S4 [Medicago truncatula]	Protein synthesis and fate	chlo	0//0				**P 1**			91	e-135	AT5G07090	cytosolic ribosome, vacuolar membrane
Medtr7g081810	MtC10182_1_AA Peptidase S8 and S53, subtilisin, kexin, sedolisin	Protein synthesis and fate	cyto	0//0				**P 2**			52	5.00E-71	AT5G59810	cell wall, endomembrane system
Medtr4g031820	MtC10185.1_1_AA E-class P450, group I	Transport	plas	1//1 TM							51	e-158	AT3G14680	endomembrane system
unfound	MtC10194_1_AA unknown Blast: NP_001147556 arabinogalactan protein [Zea mays].	Protein synthesis and fate	cyto	0//0				**P 1**			76	5.00E-85	AT5G11680	PM
Medtr5g072930, Medtr5g072980	MtC10198_1_AA E-class P450, group I	Transport	vacu	2//2 TM			SP	**P 2**			43	e-112	AT4G31500	M / RE /Mitochondrion / PM
Medtr5g025120	MtC10205_1_AA Ribosomal protein L4/L1e, archeabacterial like	Protein synthesis and fate	cyto	0//1 TM							76	e-173	AT3G09630	cell wall, chloroplast, cytosol, cytosolic large ribosomal subunit, cytosolic ribosome,

														membrane, nucleolus, plasma membrane, plasmodesma, vacuole
Medtr5g013910	MtC10209_1_AA ATPase, F0 complex, subunit C	Transport	cyto	0//0				**P 1**			70	3.00E-95	AT2G38740	Cytos / PM
Medtr5g077000	MtC10218_1_AA UTP--glucose-1-phosphate uridylyltransferase	Energy metabolism	mito	0//0				**P 1**			84	0	AT5G17310	cytosol, plasma membrane
Medtr6g013300	MtC10221_1_AA Proteasome alpha-subunit	Protein synthesis and fate	cyto	0//0	BB						97	e-128	AT3G14290	Cytos Ribos / Proteasome Core cpx / cytos
Medtr8g006430	MtC10231_1_AA Heat shock protein DnaJ	Cell rescue and defense	nucl	0//0				**P 3**	fT - CaaX Farnesyltransferase/ GGT1 - CaaX Geranylgeranyltransferase		69	e-117	AT3G44110	CW / PM / Cytos / Plasmodesma / Nucleolus
Medtr4g104030	MtC10242_1_AA Nucleoside diphosphate kinase	Energy metabolism	mito	0//1 TM				**P 1**			68	2.00E-93	AT4G11010	Mitoch memb / Mitochondrion / plastid
Medtr3g023120	MtC10243_1_AA Defender against death DAD protein	Cell rescue and defense	chlo	3//3 TM				**P 3**			89	4.00E-48	AT1G32210	ER / M
Medtr5g016590	MtC10267.1_1_AA Proteasome alpha-subunit	Protein synthesis and fate	chlo	0//0				**P 1**			85	e-119	AT3G22110	Cytos / Proteasome cpx / V / Cytos Ribos
Medtr7g070070	MtC10267.2_1_AA Proteasome alpha-subunit	Protein synthesis and fate	chlo	0//0				**P 1**			85	e-119	AT3G22110	Cytos / Proteasome cpx / V / Cytos Ribos
Medtr4g030140	MtC10273_1_AA Dynamin GTPase effector; Pleckstrin-like	Transport	nucl	0//0	BB			**P 1**			61	e-128	AT1G59610	clathrin-coated endocytic vesicle / PM / Cell Plate / Cytos / V
Medtr4g059400	MtC10276_1_AA Ribosomal protein L11 IPR014669:	Protein synthesis and fate	cyto	0//0	BB			**P 1**			90	7.00E-74	AT5G60670	cytosol, cytosolic large ribosomal subunit
Medtr5g014080	MtC10280_1_AA CD9/CD37/CD63 antigen Blast: NP_194606 Tetraspanin family protein [Arabidopsis thaliana].	Signal transduction	plas	4//4 TM				**P 8**			43	4.00E-38	AT4G28770	Vm / V / M
Medtr3g109330	MtC10283_1_AA unknown Blast:NP_567873 myosin heavy chain-related protein [Arabidopsis thaliana].	Cytoskeleton	vacu	1//2 TM				**P 2**			51	3.00E-96	AT4G31340	ER / Vm
Medtr1g009600	MtC10285_1_AA NAD-dependent epimerase/dehydratase	Transport	cyto	0//0							83	e-146	AT1G63000	PM / cytos / plasmodesma
Medtr4g127710	MtC10290_1_AA Mtha1 PLASMA MEMBRANE ATPASE (ATPase, P-type, K/Mg/Cd/Cu/Zn/Na/Ca/Na/H-transporter)	Transport	mito	1//1 TM							45	7.00E-27	AT5G62670	M / PM
Medtr2g011080	MtC10298_1_AA Blast: XP_003593404 Flavoprotein wrbA [Medicago truncatula].	Transport	chlo	0//0							78	1.00E-68	AT5G54500	M / PM / V / Vm
Medtr3g118390	MtC10312_1_AA Glycoside hydrolase, family 19, catalytic IPR001002:Chitin-binding, type 1	Cell rescue and defense	extr	1//1 TM			SP	**P 3**			64	e-109	AT3G12500	Vm/cytos
Medtr7g079110	MtC10315_1_AA Cellulose synthase	Energy metabolism	plas	4//4 TM				**P 2**			35	e-115	AT4G23990	Membrane
Medtr2g008050	MtC10339_1_AA Actin/actin-like	Cytoskeleton	cysk	0//0				**P 1**			94	e-173	AT5G09810	cell wall, chloroplast envelope, chloroplast stroma, cytoskeleton, cytosol, mitochondrion, nucleolus, plasma membrane, plasmodesma

Medtr5g024680	MtC10351_1_AA unknown Blast: XP_003612406.1 hypothetical protein MTR_5g024680 [Medicago truncatula]	Unclassified	nucl	1//1 TM	BB			**P 2**			63	4.00E-37	AT1G42960	chloroplast, chloroplast envelope, chloroplast inner membrane, chloroplast thylakoid membrane, membrane, mitochondrion, plastid
Medtr4g022610, Medtr4g022580	MtC10355_1_AA Glycosyltransferase	Energy metabolism	chlo	0//0				**P 1**			75	e-141	AT3G07020	M / PM
Medtr4g130670	MtC10361_1_AA Protein of unknown function UPF0057 Blast: XP_003610299.1 Stress-induced hydrophobic peptide [Medicago truncatula]	Cell rescue and defense	chlo	1//1 TM				**P 5**			80	2.00E-31	AT4G28088	endomembrane system, integral to membrane
Medtr7g092730	MtC10369_1_AA Polygalacturonase inhibitor	Cell rescue and defense	extr	1//1 TM			SP	**P 4**			50	9.00E-77	AT5G06860	cell wall, plant-type cell wall, plasmodesma
Medtr2g098010	MtC10373_1_AA Peptidase T1A, proteasome beta-subunit	Protein synthesis and fate	cyto	0//0				**P 1**			87	e-117	AT3G60820	chloroplast, cytosol, plasma membrane, proteasome core complex
Medtr4g072130	MtC10394_1_AA unknown Blast: XP_003607087.1 hypothetical protein MTR_4g072130 [Medicago truncatula]	Unclassified	chlo	1//1 TM	BB						80	9.00E-12	AT5G15320	undefined
Medtr5g014710	MtC10402_1_AA Malate dehydrogenase, active site	Energy metabolism	chlo	0//0	BB			**P 2**			80	e-160	AT3G15020	Mitochondrium / M / Apoplast
Medtr5g005100	MtC10414_1_AA Vacuolar-sorting receptor, EGF-like calcium-binding	Transport	cyto	1//1 TM				**P 2**			77	e-111	AT2G14740	Golgi transport complex, integral to plasma membrane, intracellular, membrane
Medtr5g063670	MtC10419.1_1_AA Annexin, type plant	Signal transduction	cyto	0//0				**P 2**			69	e-130	AT1G35720	apoplast, cell wall, chloroplast, chloroplast stroma, cytosol, membrane, mitochondrion, plasma membrane, plasmodesma, thylakoid, vacuolar membrane, vacuole
Medtr8g107460	MtC10429_1_AA Heat shock chaperonin-binding	Cell rescue and defense	nucl	0//0	BB						63	2.00E-83	AT4G22670	Cytos
Medtr8g087710	MtC10430_1_AA Aquaporin NIP1-2	Transport	plas	5//6 TM	BB						71	e-103	AT4G18910	PM

Medtr1g088070	MtC10440_1_AA Ribosomal protein L19e	Protein synthesis and fate	chlo	0//0				**P 4**			84	1.00E-88	AT1G02780	Cytos / Nucleolus /cytos Ribos/ M /Plasmodesma / PM
Medtr5te046150	MtC10449_1_AA HR-like lesion-inducer	Cell rescue and defense	plas	2//3 TM	BB						51	5.00E-34	AT4G14420	endoplasmic reticulum
Medtr4g127150	MtC10465_1_AA Protein secE/sec61-gamma protein	Transport	cyto	1//1 TM							75	2.00E-22	AT5G50460	intracellular
Medtr3g100940	MtC10472_1_AA unknown Blast: XP_003602965.1 Transmembrane protein [Medicago truncatula]	Unclassified	cyto	6//6 TM				**P 2**			87	e-116	AT1G47640	Mitochondriom
Medtr4g103810	MtC10483_2_AA unknown Blast:AFK46423.1 unknown [Medicago truncatula]	Unclassified	mito	0//2 TM							70	2.00E-27	AT1G22520	Mitochondriom
Medtr2g062920	MtC10504.1_1_AA ATP citrate synthase, small subunit IPR013816:ATP-grasp fold, subdomain 2	Energy metabolism	cyto	0//0				**P 2**			85	0	AT1G60810	citrate lyase complex
AC233070_1015, AC225458_90	MtC10530_1_AA BlastXP_003627680 NADH dehydrogenase [Medicago truncatula].	Transport	chlo	0//0				**P 1**	fT - CaaX Farnesyltransferase/ GGT1 - CaaX Geranylgeranyltransferase		85	3.00E-50	AT5G18800	mitochondrial respiratory chain complex I
Medtr4g085580	MtC10536_1_AA Ribosomal protein S9	Protein synthesis and fate	cyto	0//0				**P 2**	fT - CaaX Farnesyltransferase/ GGT1 - CaaX Geranylgeranyltransferase		89	8.00E-70	AT2G09990	cell wall, chloroplast, cytosol, cytosolic ribosome, membrane, plasmodesma
Medtr8g101890, Medtr8g101880	MtC10547_1_AA ATPase, F0 complex, subunit G, mitochondrial	Transport	mito	0//0				**P 1**			80	3.00E-54	AT4G26210	mitochondrial proton-transporting ATP synthase complex, coupling factor F(o)
Medtr5g077070	MtC10579.1_1_AA Isocitrate dehydrogenase NADP-dependent, C-terminal, plant	Energy metabolism	extr	0//0							88	0	AT1G65930	apoplast, chloroplast stroma, cytosol, plasma membrane, plasmodesma
Medtr5g070680, Medtr5g070880	MtC10596_1_AA Alternative oxidase	Transport	cyto	1//1 TM							65	5.00E-95	AT5G64210	mitochondrial envelope, mitochondrion
Medtr5g077170	MtC10600.1_1_AA Nonaspanin \(TM9SF\) Blast: ACQ90591 putative transmembrane transporter [Eutrema halophilum].	Transport		3//4 TM				**P 2**			78	e-152	AT1G14670	Golgi apparatus, integral to membrane, membrane
Medtr6g074910	MtC10600.3_1_AA Nonaspanin (TM9SF)	Transport	plas	9//10 TM			SP	**P 2**			82	0	AT1G08350	Golgi apparatus, plant-type cell wall, plasmodesma, vacuolar membrane
unfound	MtC10610_1_AA coatomer epsilon subunit [Medicago truncatula].	Transport	nucl	0//0			SP	**P 2**			76	e-127	AT2G34840	Cytos
Medtr7g100020	MtC10611_1_AA Sigma-54 factor, interaction region IPR003579:Ras small GTPase, Rab type	Transport	cyto	0//0	BB			**P 2**	fT - CaaX Farnesyltransferase/ GGT1 - CaaX Geranylgeranyltransferase/GGT2 - Rab Geranylgeranyltransferase		81	1.00E-91	AT5G59840	intracellular, plasma membrane, plasmodesma
Medtr5g075580	MtC10613_1_AA Ubiquitin-conjugating enzyme, E2	Protein synthesis and fate	mito	0//0	BB						100	2.00E-67	AT1G16890	cytosol, plasma membrane
Medtr3g079510, Medtr1g100550	MtC10626_1_AA Flavoprotein pyridine nucleotide cytochrome	Transport	cyto	0//0				**P 1**			76	8.00E-90	AT5G17770	PM /RE

	reductase													
Medtr7g092720	MtC10627_1_AA Ribosomal protein S10, eukaryotic and archaeal form	Protein synthesis and fate	cyto	0//0							89	6.00E-59	AT3G47370	cell wall, cytosol, cytosolic ribosome, cytosolic small ribosomal subunit, membrane, nucleolus, plasmodesma
Medtr5g089370	MtC10629_1_AA SYNAPTOBREVIN-LIKE / VESICLE-ASSOCIATED MEMBRANE PROTEIN	Transport	chlo	1//1 TM				**P 3**			81	e-104	AT5G22360.1	Golgi / V
Medtr1g083430	MtC10630_1_AA Ribosomal L22e protein	Protein synthesis and fate	cyto	0//0				**P 1**			72	1.00E-46	AT3G05560	cytosol, cytosolic large ribosomal subunit, cytosolic ribosome, nucleolus, plasma membrane, plasmodesma, ribosome
Medtr5g096420	MtC10643_1_AA Calcium-binding EF-hand IPR015757:	Signal transduction	extr	0//0				**P 3**			89	e-117	AT5G55990	cytosolic ribosome, membrane, plant-type vacuole membrane, vacuole
Medtr4g127710	MtC10646_1_AA Blast: G7JUD3 Plasma membrane H+-ATPase, cation transport ATPase (P-type) family, plasma-membrane proton-efflux P-type ATPase	Transport	plas	5//5 TM							82	e-154	AT2G18960	integral to membrane, membrane, nucleus, plasma membrane, plasmodesma, vacuole
Medtr1g082870	MtC10650_1_AA Ras small GTPase, Rab type IPR013567:EF hand associated, type-2	Transport	chlo	1//1 TM				**P 6**			64	0	AT5G27540	mitochondrion
Medtr2g029820	MtC10656_1_AA Haem peroxidase, plant/fungal/bacterial	Cell rescue and defense	vacu	1//1 TM		GPI	SP	**P 4**			54	6.00E-98	AT5G06730	Vm
Medtr3g100160	MtC10663_1_AA Flavoprotein pyridine nucleotide cytochrome reductase	Transport	chlo	1//1 TM				**P 2**			70	0	AT4G24520	cytosol, endoplasmic reticulum
Medtr8g075240	MtC10675_1_AA Small GTP-binding protein domain	Signal transduction	chlo	0//0				**P 3**	fT - CaaX Farnesyltransferase/ GGT1 - CaaX Geranylgeranyltransferase/GGT2 - Rab Geranylgeranyltransferase		88	e-100	AT2G17800	cytoplasm, nucleus, phragmoplast, spindle
Medtr7g100720	MtC10714_1_AA Ribosomal protein S23, eukaryotic and archaeal form	Protein synthesis and fate	cyto	0//0				**P 1**			95	1.00E-73	AT5G02960	cytosolic ribosome, cytosolic small ribosomal subunit
Medtr5g022600	MtC10715_1_AA Ras small GTPase, Rab type	Transport	chlo	0//0				**P 2**	fT - CaaX Farnesyltransferase/ GGT1 - CaaX Geranylgeranyltransferase/GGT2 - Rab Geranylgeranyltransferase		91	1.00E-94	AT1G75840	cytoplasm, nucleolus, nucleus, phragmoplast, plasma membrane
Medtr3g055130	MtC10736.1_1_AA Bet v I allergen	Cell rescue and defense	cyto	0//0	BB						27	0.003	AT1G24020	Membrane
Medtr7g111530	MtC10752_1_AA Peptidase A1, pepsin	Protein synthesis and fate	nucl	0//0				**P 3**			58	2.00E-78	AT1G11910	V /Cytos/ Plasmodesma
Medtr5g048060	MtC10770_1_AA unknown	Unclassified	golg	3//3 TM				**P 3**			63	2.00E-45	AT1G48440	intracellular
unfound	MtC10773_1_AA Ribonucleoprotein complex SRP, Srp19 component	Transport	cyto	0//0				**P 3**			70	1.00E-43	AT1G48160	intracellular, signal recognition particle, endoplasmic reticulum targeting

Medtr3g115880	MtC10782_1_AA unknown Blast: XP_003603847.1 Canopy-like protein [Medicago truncatula]	Unclassified	extr	0//1 TM			SP	**P 4**			59	4.00E-29	AT1G42480	undefined
unfound	MtC10783_1_AA ATP-citrate lyase/succinyl-CoA ligase	Energy metabolism	cyto	0//0	BB			**P 1**			92	1.00E-56	AT2G20420	Mitochondriom
Medtr2g038080	MtC10806.1_1_AA Metallo-phosphoesterase	Energy metabolism	cyto	1//1 TM			SP	**P 1**			63	e-145	AT5G63140	endomembrane system
Medtr7g093870	MtC10834_1_AA Plant disease resistance response protein	Cell rescue and defense	vacu	1//1 TM			SP	**P 1**			47	2.00E-37	AT1G65870	CW
Medtr4g073010	MtC10835_1_AA Nickel/cobalt transporter, high-affinity	Transport	plas	5//5 TM	BB			**P 1**			68	2.00E-81	AT4G35080	chloroplast, integral to membrane
Medtr1g094870	MtC10855_1_AA RIBOPHORIN I	Protein synthesis and fate	plas	2//2 TM			SP				68	e-178	AT2G01720	endoplasmic reticulum, plant-type cell wall, plasma membrane, vacuolar membrane
Medtr8g061940	MtC10868_1_AA Histone H3 IPR007124: IPR009072:Histone-fold	Cell cycle and DNA processing	chlo	0//0				**P 1**			100	5.00E-62	AT4G40030	undefined
Medtr5g084930	MtC10874_1_AA Disulphide isomerase	Protein synthesis and fate	chlo	1//1 TM				**P 3**			72	e-180	AT2G32920	ER/ V/ PM
Medtr7g099640	MtC10897_1_AA AAA ATPase IPR005937:26S proteasome subunit P45	Protein synthesis and fate	Cyto	0//0				**P 1**			89	0	AT5G19990	proteasome complex
Medtr4g107810, Medtr4g107760	MtC10902_1_AA Band 7 protein Blast: XP_003608997 Hypersensitive-induced response protein [Medicago truncatula].	Protein synthesis and fateMembrane protease subunits, stomatin/prohibitin homologs [Posttranslational modification, protein turnover, chaperones]; COG0330"Band 7 protein is an integral membrane protein which is thought to regulate cation conductance. A variety of proteins belong to this family. These include the prohibitins, cytoplasmic anti-proliferative proteins and stomatin,A subgroup of the band 7 domain of flotillin (reggie) like proteins. This subgroup contains proteins similar to stomatin, prohibitin, flotillin, HlfK/C and podicin. Many of these band 7 domain-containing proteins are lipid raft-associated. Individual...; cd03407" /db_xref="CDD:48219"	Cyto	0//0				**P 2**		Predicted as myristoylated	84	e-134	AT5G62740	M /V/ PM/ Vm / Plasmodesma
Medtr4g071520	MtC10905_1_AA Squalene/phytoene synthase	Energy metabolism	Cyto	2//2 TM				**P 2**			73	e-174	AT4G34650	integral to membrane

Medtr5g090340	MtC10909_1_AA Reticulon	Transport	plas	3//3 TM			SP	**P 2**			56	4.00E-75	AT3G10260	endoplasmic reticulum, mitochondrion
Medtr4g127310	MtC10930.1_1_AA Glycoside hydrolase, family 47	Cell rescue and defense	cyto	0//0				**P 2**			82	0	AT1G51590	Golgi
Medtr7g090890	MtC10982_1_AA unknown	Unclassified	plas	4//4 TM				**P 3**			54	3.00E-61	AT3G57280	chloroplast, chloroplast envelope, chloroplast inner membrane
Medtr3g082660, Medtr4g027260	MtC10984_1_AA AMP-dependent synthetase and ligase	Energy metabolism	Cyto	1//1 TM				**P 3**			70	0	AT2G04350	chloroplast envelope, endoplasmic reticulum
Medtr1g116520	MtC11009_1_AA Tyrosine protein kinase, active site	Signal transduction	chlo	1//1TM				**P 4**			81	e-170	AT3G59350	PM
Medtr2g038560	MtC11011_1_AA Thioredoxin-like fold	Cell rescue and defense	extr	TM 1			SP	**P 1**			66	5.00E-41	AT5G20500	undefined
Medtr5g022940	MtC20002_1_AA Aconitate hydratase 1	Energy metabolism	chlo	TM 1			SP	**P 2**			86	0	AT4G35830	apoplast, cytosol, mitochondrion, plasma membrane, plasmodesma, vacuole
Medtr5g089200	MtC20008_1_AA Metal-dependent hydrolase, composite	Energy metabolism	chlo	TM 1			SP	**P 1**			75	0	AT5G12200	endomembrane system
Medtr5g072020	MtC20011_1_AA Aminotransferase, class-II	Energy metabolism	extr	TM 2			SP	**P 2**			82	0	AT5G23670	endoplasmic reticulum, membrane, vacuole
Medtr2g069310	MtC20024_1_AA Translation factor IPR009022:Elongation factor G, III and V	Protein synthesis and fate	chlo	0				**P 6**			92	0	AT1G06220	chloroplast, cytosol, membrane, nucleolus, plasma membrane, plasmodesma, vacuolar membrane
Medtr5g009500	MtC20025_1_AA Mitochondrial substrate carrier	Transport	cyto	TM 2	BB			**P 2**			77	e-164	AT4G01100	membrane, mitochondrion, plastid, vacuolar membrane
Medtr4te022430	MtC20026_1_AA Thiolase	Energy metabolism	cyto	TM1	BB			**P 1**			72	0	AT2G33150	chloroplast, membrane, mitochondrion, nucleolus, peroxisome, vacuolar membrane
Medtr5g017050	MtC20030_1_AA Nicotinate phosphoribosyltransferase related	Energy metabolism	cyto	0				**P 2**			80	0	AT2G23420	undefined
Medtr2g019640	MtC20037_1_AA E-class P450, group I	Transport	chlo	TM 2				**P 1**			70	0	AT2G34500	undefined
Medtr8g018770	MtC20039_1_AA DIHYDROLIPOAMIDE S-ACETYLTRANSFERASE COMPONENT (E2) OF PYRUVATE DEHYDROGENASE COMPLEX	Energy metabolism	chlo	0	BB						71	e-169	AT3G25860	chloroplast, chloroplast envelope, chloroplast stroma, chloroplast thylakoid, cytosolic ribosome, membrane
Medtr2g087660	MtC20045_1_AA DnaJ central region	Cell rescue and defense	nucl	0					fT - CaaX Farnesyltransferase/ GGT1 - CaaX Geranylgeranyltransferase		75	e-135	AT3G44110	CW / PM / Cytos / Plasmodesma / Nucleolus
Medtr2g028480	MtC20046_1_AA Glycoside hydrolase	Cell rescue and defense	nucl	TM 1							77	0	AT5G49720	Golgi apparatus, cell plate, early endosome, plasma membrane
Medtr6g084520	MtC20048_1_AA NADH-UBIQUINONE OXIDOREDUCTASE	Transport	cyto	0				**P 2**			69	2.00E-38	AT3G18410	Mitochondrion
Medtr1g116120, Medtr5g059410	MtC20051.2_1_AA Transketolase, central region	Energy metabolism	chlo	0							84	0	AT3G60750	chloroplast, chloroplast envelope, chloroplast stroma

Medtr5g020850	MtC20060_1_AA Blast: A GAMMA carbonic anhydrase, partial [Silene latifolia].	Energy metabolism	Cyto	0							87	5.00E-91	AT1G19580	Mitochondrion M
Medtr5g022960	MtC20071_1_AA 2OG-Fe(II) oxygenase	Energy metabolism	mito	TM 1				**P 1**			75	e-113	AT2G17720	undefined
Medtr1g090130	MtC20083.1_1_AA GroEL-like chaperone, ATPase	Protein synthesis and fate	Mito	0	BB						83	0	AT5G56500	cytosol, cytosolic ribosome, mitochondrial matrix, mitochondrion, vacuolar membrane
Medtr7g069390	MtC20107_1_AA Peptidase M24, methionine aminopeptidase	Protein synthesis and fate	chlo	0							76	e-119	AT3G51800	PM / Nucleolus
Medtr6g029460	MtC20111_1_AA Glu/Leu/Phe/Val dehydrogenase, dimerisation region	Energy metabolism	cyto	0							78	e-141	AT5G07440	Mitochondrion / Vm
Medtr6g071070	MtC20114_1_AA Glutamine synthetase type I IPR014746:	Energy metabolism	cyto	0							86	e-172	AT1G66200	Apoplast / V / cytos / cytos Ribos / Chloro m
Medtr4g121880	MtC20115_1_AA DIHYDROLIPOAMIDE DEHYDROGENASE	Energy metabolism	cyto	0	BB						81	0	AT3G17240	chloroplast, mitochondrial matrix, mitochondrion
Medtr8g038220	MtC20129_1_AA Annexin IPR015472:	Signal transduction	cyto	0				**P 1**			54	e-100	AT5G12380	undefined
Medtr1g014080	MtC20133_1_AA Nonaspanin (TM9SF)	Transport	plas	TM 8			SP	**P 4**			78	0	AT5G10840	Golgi apparatus, plant-type cell wall, vacuolar membrane
Medtr1g043290	MtC20134.1_1_AA MtPT2 PHOSPHATE TRANSPORTER Major facilitator superfamily	Transport	plas	TM 11				**P 1**			71	0	AT5G43360	PM
Medtr1g090140	MtC20137_1_AA GroEL-like chaperone, ATPase	Protein synthesis and fate	chlo	0	BB			**P 4**			89	0	AT1G55490	apoplast, chloroplast, chloroplast envelope, chloroplast stroma, cytosolic ribosome, membrane, plasma membrane
Medtr4g124660	MtC20141_1_AA Sucrose synthase	Energy metabolism	cyto	0				**P 2**			80	0	AT3G43190	cytosol, membrane, plasma membrane, vacuole
Medtr7g114810	MtC20142_1_AA Tetratricopeptide region	Protein synthesis and fate	nucl	0				**P 3**			78	e-134	AT3G04830	undefined
Medtr5g074970	MtC20143_1_AA Haem peroxidase, plant/fungal/bacterial	Cell rescue and defense	extr	TM 1			SP	**P 1**			65	e-113	AT5G58400	EndoM system
Medtr8g088620	MtC20149_1_AA Rab GDP dissociation inhibitor	Signal transduction	cyto	0				**P 1**			85	0	AT2G44100	Cytosol
Medtr1g088680	MtC20165_1_AA Peroxysomal long chain fatty acyl transporter	Transport	plas	TM 4				**P 2**			75	0	AT2G47800	plant-type vacuole, plasma membrane, plasmodesma, vacuolar membrane, vacuole
Medtr8g005360	MtC20198_1_AA unknown Blast: XP_003552331.1 PREDICTED: NADH dehydrogenase [ubiquinone] 1 alpha subcomplex subunit 1-like [Glycine max]	Transport	cyto	TM 1				**P 2**			75	7.00E-25	AT3G08610	mitochondrial respiratory chain complex I
Medtr3g086330	MtC20223_1_AA GroEL-like chaperone, ATPase	Protein synthesis and fate	chlo	0				**P 3**			89	0	AT1G24510	cytosol, plasma membrane, plasmodesma
Medtr2g094180	MtC20228.1_1_AA Thioredoxin-related IPR012336:Thioredoxin-like fold IPR013766:Thioredoxin domain	Cell rescue and defense	pero	0							71	e-141	AT5G60640	Vm / Chloro / Mitoch / ER

Medtr3g032530	MtC20234_1_AA (S)-ADENOSYL-L-METHIONINE:DELTA 24-STEROL METHYLTRANSFERASE	Energy metabolism	vacu	TM 1				**P 3**			86	e-179	AT5G13710	V / Plamodesmata
Medtr4g124000	MtC20250.1_1_AA Peroxysomal long chain fatty acyl transporter	Transport	plas	TM 5	BB			**P 1**			71	e-138	AT5G39040	V / Vm
Medtr1g081290	MtC20251_1_AA Adrenodoxin reductase IPR002937:Amine oxidase IPR014103:	Energy metabolism	chlo	0				**P 1**			83	0	AT3G04870	chloroplast, chloroplast envelope
Medtr7g065210	MtC20261_1_AA Plant lipid transfer protein/seed storage/trypsin-alpha amylase inhibitor	Transport	extr	TM 1			SP	**P 2**			68	4.00E-39	AT2G37870	Plasmodesmata
Medtr4g085540	MtC20269_1_AA POLYADENYLATE-BINDING PROTEIN	Protein synthesis and fate	cyto	0	BB			**P 3**			76	0	AT1G49760	Cytosol
Medtr4g074800, Medtr4g074930	MtC20273.1_1_AA NUM1-LIKE PROTEIN	Cell cycle and DNA processing	chlo	0	BB						55	3.00E-61	AT3G18610	undefined
Medtr3g117230	MtC20279_1_AA Blast: XP_003523765 PREDICTED: 26S protease regulatory subunit S10B homolog B-like isoform 1 [Glycine max].	Protein synthesis and fate	chlo	0							71	e-154	AT1G45000	M / CW / Nucleolus / Plasmodesmata /PM / M
Medtr5g006440	MtC20295_1_AA Ribosomal protein S3Ae	Protein synthesis and fate	nucl	0				**P 3**			85	e-118	AT4G34670	cell wall, cytosol, cytosolic ribosome, membrane, nucleolus, plasma membrane, plasmodesma
Medtr1g106940	MtC20305_1_AA VACUOLAR SORTING RECEPTOR	Transport	vacu	TM 2			SP	**P 9**			82	0	AT2G14740	Golgi apparatus, membrane
Medtr3g013640	MtC20311_1_AA Ribosomal protein S19e	Protein synthesis and fate	cysk	0				**P 1**			81	2.00E-69	AT3G02080	cell wall, cytosol, cytosolic ribosome, plasmodesma, ribosome
Medtr7g108320	MtC20331_1_AA Histone H2A IPR007124: IPR009072:Histone-fold	Cell cycle and DNA processing	nucl	0	BB						77	7.00E-40	AT5G59870	plasmodesma/ Nucleolus
Medtr5g083790	MtC20341_1_AA Ribosomal protein L13, archea and eukaryotic form	Protein synthesis and fate	cyto	0				**P 2**			85	2.00E-96	AT4G13170	cytosolic large ribosomal subunit, membrane
Medtr7g080370	MtC20347_1_AA Calreticulin	Protein synthesis and fate	extr	TM 1			SP	**P 1**			78	e-159	AT1G08450	ERm / ER
Medtr5g071250	MtC20350.1_1_AA NADH-UBIQUINONE OXIDOREDUCTASE	Transport	cyto	0							82	e-138	AT2G29990	intrinsic to mitochondrial inner membrane
Medtr5g071250	MtC20350.2_1_AA NADH-UBIQUINONE OXIDOREDUCTASE	Transport	cyto	0							82	e-138	AT2G29990	intrinsic to mitochondrial inner membrane
Medtr4g083490	MtC20377_1_AA SYNAPTOBREVIN-LIKE / VESICLE-ASSOCIATED MEMBRANE PROTEIN	Transport	cyto	TM 1							80	1.00E-87	AT2G32670	chloroplast, endosome, plasma membrane
Medtr3g116060	MtC20379_1_AA General substrate transporter	Transport	plas	TM 12	BB			**P 4**			64	0	AT4G35300	V / Vm
unfound	MtC20380_1_AA unknown Blast: O49929.1 Chloroplastic outer envelope pore protein of 24 kDa [Pisum sativum]	Transport	cyto	0	BB			**P 1**			65	6.00E-76	AT5G42960	Mitochondrial M/ Chloro M / plastid

Medtr3g084340	MtC30011_1_AA S-adenosyl-L-homocysteine hydrolase	Energy metabolism	cyto	0				**P 3**			86	e-161	AT4G13940	M / Vm /Plasmodesma /PM / V / Cytos
Medtr5g098310	MtC30033_1_AA Thiolase	Energy metabolism	chlo	0	BB			**P 1**			77	e-179	AT5G48230	cytosol, peroxisome, plasma membrane
Medtr2g099620	MtC30054_1_AA EUKARYOTIC INITIATION FACTOR 4A	Protein synthesis and fate	chlo	0							92	0	AT1G54270	cytosol, plasma membrane, plasmodesma, vacuolar membrane
Medtr7g021820, Medtr7g021680	MtC30064_1_AA Aldo/keto reductase	Energy metabolism	chlo	0				**P 1**			77	e-154	AT1G60730	Cytosol
Medtr5g095230	MtC30065_1_AA E-class P450, group I	Transport	chlo	TM 1							50	e-150	AT3G14610	endoplasmic reticulum
Medtr2g060830	MtC30069_1_AA Proteasome alpha-subunit	Protein synthesis and fate	cyto	0	BB						94	e-128	AT1G16470	Cytosol /cyto Rib /
Medtr7g081660	MtC30077.1_1_AA Aminoacyl-tRNA synthetase, class I IPR006861:Hyaluronan/mRNA binding protein	Protein synthesis and fate	nucl	0	BB			**P 1**			43	5.00E-23	AT4G17520	cytoplasm, nucleus
Medtr8g088860	MtC30078_1_AA Cupin 1	Energy metabolism	cyto	0	BB						41	3.00E-80	AT1G07750	cytosol, plasmodesma
Medtr5g026930	MtC30086.2_1_AA methyltransferase putative	Energy metabolism	cyto	TM 1				**P 2**			73	0	AT1G31850	golgi apparatus
Medtr7g092620	MtC30087_1_AA E-class P450, group I	Transport	plas	TM 1				**P 5**			40	e-105	AT2G42250	endomembrane system
unfound	MtC30089_1_AA unknown Blast: XP_003524856.1 PREDICTED: uncharacterized protein LOC100777797 isoform 1 [Glycine max]	Unclassified	plas	TM 1				**P 2**			66	e-133	AT1G23170	M
Medtr4g103790	MtC30106_1_AA Pre-mRNA processing ribonucleoprotein, binding region	Protein synthesis and fate	nucl	0				**P 2**			79	0	AT1G56110	cell wall, nucleolus, plasmodesma
Medtr7g099640	MtC30111_1_AA AAA ATPase IPR005937:26S proteasome subunit P45	Protein synthesis and fate	cyto	0				**P 1**		Predicted as myristoylated	92	0	AT4G29040	membrane, nucleus, proteasome regulatory particle, base subcomplex
Medtr2g030560	MtC30114_1_AA unknown	Unclassified	plas	TM 2	BB		SP	**P 2**			45	4.00E-73	AT3G24160	ER /M / V
Medtr7g011990	MtC30132_1_AA Generic methyltransferase	Energy metabolism	cyto	TM 1				**P 2**			48	5.00E-90	AT5G54160	Nucleus /Cytosol / Plasmpdesma / PM
Medtr5g072020	MtC30138_1_AA Aminotransferase, class I and II	Energy metabolism	chlo	TM 1				**P 1**			24	1.00E-31	AT3G48780	undefined
Medtr3g013890, AC232874_1008, AC235748_1009	MtC30154.1_1_AA WOUND-INDUCED PROTEIN LIKE PROTEIN	Cell rescue and defense	cyto	TM 2				**P 2**			71	e-171	AT4G24220	Cytosol
AC235671_2	MtC30180_1_AA Peptidoglycan-binding LysM	Energy metabolism	plas	TM 2		GPI		**P 3**			44	2.00E-66	AT2G17120	anchored to membrane, anchored to plasma membrane, plasma membrane, plasmodesma
Medtr5g014080	MtC30183_1_AA Blast: XP_003611447 DEFINITION GMFP4 tetraspanin [Medicago truncatula].CD9/CD37/CD63 antigen	Signal transduction	vacu	TM 4				**P 9**	fT - CaaX Farnesyltransferase/ GGT1 - CaaX Geranylgeranyltransferase		56	7.00E-88	AT1G32400	membrane, plasmodesma, vacuole
Medtr1g039270	MtC30185_1_AA Peptidase aspartic, active site	Protein synthesis and fate	chlo	TM 3			SP	**P 1**			69	e-175	AT1G01300	M /CW

Medtr7g081700	MtC30186_1_AA RAB1, SMALL GTP-BINDING PROTEIN	Transport	chlo	TM 1	BB		SP	**P 2**	FT - CaaX Farnesyltransferase/ GGT1 - CaaX Geranylgeranyltransferase/ GGT2 - Rab Geranylgeranyltransferase		86	e-102	AT5G47200	Golgi / PM
Medtr1g038920	MtC30193_1_AA N-acyl-L-amino-acid amidohydrolase	Energy metabolism	chlo	TM 1			SP				68	e-171	AT4G38220	V
Medtr7g072480	MtC30195_1_AA Haem peroxidase, plant/fungal/bacterial IPR002133:S-adenosylmethionine synthetase	Cell rescue and defense	chlo	0			SP				58	6.00E-99	AT5G05340	Apoplast / CW / cytosol
AC233577_25	MtC30197_1_AA IQ calmodulin-binding region	Protein synthesis and fate	cyto	0							71	3.00E-67	AT5G62390	PM / plasmodesma / RE
Medtr4g128840	MtC30199_1_AA Xylose isomerase, bacterial type	Energy metabolism	cyto	TM 1			SP	**P 1**			75	e-113	AT5G57655	Vm / V / RE
Medtr3g114480	MtC30201_1_AA Proteasome component region PCI IPR013143:PCI/PINT associated module IPR013586:26S proteasome regulatory subunit, C-terminal	Protein synthesis and fate	cyto	0				**P 3**			75	0	AT1G20200	cytosol, plasma membrane, plasmodesma,
Medtr5g023960	MtC30202_1_AA PHOSPHATIDYLINOSITOL PHOSPHATE PHOSPHATASE	Signal transduction	plas	TM 3				**P 5**			46	0	AT3G51460	plasma membrane, plasma membrane of cell tip, plasmodesma
Medtr1g019150	MtC30209_1_AA RNA-binding region RNP-1 (RNA recognition motif) IPR001865:Ribosomal protein S2	Protein synthesis and fate	chlo	0	BB			**P 3**			67	e-171	AT2G23350	Cytosol
Medtr2g006300	MtC30210_1_AA Nonaspanin (TM9SF)	Transport	chlo	TM 10			SP	**P 2**			77	0	AT1G10950	Golgi
Medtr4g012940	MtC30233_1_AA Sigma-54 factor, interaction region IPR003579:Ras small GTPase, Rab type	Transport	chlo	0			SP	**P 2**	GGT2 - Rab Geranylgeranyltransferase		91	e-111	AT1G52280	Vm / V / PM /
Medtr3g055200	MtC30238_1_AA t-snare (SYNTAXIN-LIKE PROTEIN)	Transport	golg	TM 1				**P 3**			73	5.00E-86	AT1G79590	V / endosome M
Medtr5g025590	MtC30248_1_AA Reticulon	Transport	cyto	TM 1							70	0	AT1G19360	endoplasmic reticulum
Medtr5g036600	MtC30278_1_AA Dehydrogenase, E1 component	Energy metabolism	chlo	0				**P 1**			77	e-179	AT1G24180	cytosol, mitochondrion, nucleus
Medtr4g005190	MtC30281.1_1_AA Prenyltransferase/squalene oxidase	Energy metabolism	nucl	0				**P 1**			74	0	AT1G78950	undefined
Medtr3g071550	MtC30290.1_1_AA Eukaryotic translation initiation factor 2, alpha subunit IPR012340:Nucleic acid-binding, OB-fold, subgroup	Protein synthesis and fate	cyto	0				**P 1**			81	e-151	AT2G40290	Cytosol / Nucleus
AC225517_18	MtC30291_1_AA Protein of unknown function DUF1620	Unclassified	cyto	TM 1							73	e-152	AT5G11560	ER / PM / V /Vm
Medtr4g027050	MtC30297_1_AA Major sperm protein VESICLE-ASSOCIATED MEMBRANE PROTEIN (VAMP)	Transport	chlo	TM 1		GPI					74	1.00E-69	AT3G60600	PM / RE M/ Vm / nucleus / RE
Medtr2g008850	MtC30342_1_AA Protein phosphatase 2C-like	Signal transduction	nucl	0				**P 5**			67	e-108	AT1G34750	PM
Medtr3g109730	MtC30380_1_AA unknown Blast:ACJ84472.1 unknown [Medicago truncatula]	Unclassified	chlo	TM 1				**P 1**			72	4.00E-86	AT3G49720	M / Golgi / Vm/ Chloro M PM
unfound	MtC30386_1_AA WD40-like	Signal transduction	cyto	TM 1							64	e-143	AT3G52190	endoplasmic reticulum, intracellular, plasma membrane

Medtr5g089370	MtC30387_1_AA unknown Blast:XP_003617238.1 Vesicle-associated membrane protein 7C [Medicago truncatula]	Transport	cyto	TM 1				**P 2**			75	8.00E-98	AT4G32150	Intracellular / M / Vm
Medtr5g074740	MtC30389_1_AA unknown Blast:XP_003517003.1 PREDICTED: cationic peroxidase 1-like [Glycine max]	Cell rescue and defense	chlo	TM 1			SP	**P 1**			62	6.00E-97	AT5G05340	Apoplast / CW / cytosol
Medtr3g027890	MtC30415_1_AA Signal peptidase 22 kDa subunit IPR008978:HSP20-like chaperone	Protein synthesis and fate	vacu	TM 1				**P 1**			78	4.00E-73	AT5G27430	CW
Medtr3g115980	MtC30456.1_1_AA Ribophorin I	Protein synthesis and fate	plas	TM 2			SP	**P 2**			67	0	AT1G76400	endoplasmic reticulum, membrane
Medtr2g086640	MtC30458_1_AA Cupin 1 IPR007113:	Energy metabolism	chlo	TM 1	BB		SP				46	6.00E-26	AT1G09560	CW / Nucleus
Medtr4g122110, Medtr4g122330	MtC30561_1_AA Plant disease resistance response protein	Cell rescue and defense	extr	TM 1	BB						40	4.00E-23	AT1G22900	EndoM system
Medtr5g027960	MtC30566.1_1_AA Proteasome component region PCI	Protein synthesis and fate	cyto	0				**P 2**			67	e-171	AT5G15610	undefined
Medtr8g088430	MtC40004.1_1_AA E-class P450, group I	Transport	cyto	TM 1				**P 1**			62	e-163	AT5G36110	EndoM system
Medtr4g055520, AC225518_18	MtC40005_1_AA Glycosyl transferase, family 2	Cell rescue and defense	plas	TM 5				**P 1**			78	0	AT5G22740	undefined
Medtr8g055840	MtC40018_1_AA probable methyltransferase PMT14-like [Glycine max]	Energy metabolism	chlo	TM 1			SP				74	0	AT4G18030	Golgi apparatus, plant-type cell wall, vacuolar membrane
Medtr7g050870	MtC40031_1_AA Pectinesterase IPR006501:Pectinesterase inhibitor	Protein synthesis and fate	mito	TM 1							44	3.00E-47	AT1G11580	Vm / Cytosol / CW
Medtr3g079340	MtC40039_1_AA Lipase, class 3	Energy metabolism	cyto	TM 1				**P 1**			42	e-109	AT3G48090	undefined
AC225518_18	MtC40045_1_AA Protein of unknown function DUF81 Blast: NP_850068.1 Sulfite exporter TauE/SafE family protein [Arabidopsis thaliana]	Transport	plas	TM 10	BB		SP	**P 1**			68	e-163	AT2G25737	endomembrane system, integral to membrane
unfound	MtC40087_1_AA Ribosomal protein L7AE	Protein synthesis and fate	chlo	0				**P 2**			79	3.00E-99	AT2G47610	chloroplast, cytosol, cytosolic large ribosomal subunit, cytosolic ribosome, nucleolus, plasmodesma, vacuolar membrane
Medtr3g105950	MtC40093_1_AA Nonaspanin (TM9SF)	Transport	plas	TM 8			SP	**P 3**			79	e-110	AT5G10840	Golgi apparatus, plant-type cell wall, vacuolar membrane
Medtr2g036600	MtC40095_1_AA Aspartyl-tRNA synthetase, class IIb IPR004365:nucleic acid binding, OB-fold, tRNA/helicase-type	Protein synthesis and fate	chlo	0				**P 2**			74	0	AT3G11710	cytosol, plasmodesma
Medtr8g023560	MtC40103_1_AA Protein kinase IPR013210:Leucine rich repeat, N-terminal	Signal transduction	nucl	TM 3			SP	**P 1**			60	e-101	AT4G22130	PM
Medtr4g074640	MtC40118_1_AA Alanyl-tRNA synthetase, class IIc	Protein synthesis and fate	cyto	0				**P 2**			67	0	AT1G50200	chloroplast, cytosol, mitochondrion

Medtr2g039680	MtC40189_1_AA Nucleosome assembly protein (NAP)	Cell cycle and DNA processing	chlo	TM 1			SP	**P 2**	FT - CaaX Farnesyltransferase/ GGT1 - CaaX Geranylgeranyltransferase		62	e-106	AT5G56950	Nucleus / cytos
Medtr8g105580	MtC40192_1_AA Dynamin central region IPR001401:Dynamin IPR003130:Dynamin GTPase effector	Transport	cyto	0				**P 2**			84	0	AT1G14830	cell cortex, cell plate, cytoplasm, membrane, plasma membrane, plasmodesma
Medtr8g039290	MtC40209_1_AA unknown Blast: ADV35716.2 root determined nodulation 1 [Medicago truncatula]	Unclassified	chlo	TM 1			SP	**P 1**			71	e-152	AT5G13500	EndoM system
Medtr8g020940	MtC40216_1_AA E-class P450, group I	Transport	chlo	TM 2				**P 2**			79	0	AT2G40890	endoplasmic reticulum, microsome, mitochondrion, plasma membrane
Medtr1g045410	MtC45278_1_AA Ribosomal protein L4/L1e, archeabacterial like	Energy metabolism	cyto	TM 1							74	e-180	AT3G09630	cell wall, chloroplast, cytosol, cytosolic large ribosomal subunit, cytosolic ribosome, membrane, nucleolus, plasma membrane, plasmodesma, vacuole
Medtr3g113720	MtC45398_1_AA ENDO-BETA-1,4-D-GLUCANASE, Glycoside transferase, six-hairpin, subgroup	Cell rescue and defense	plas	TM 3		GPI		**P 6**			65	0	AT1G19940	undefined
Medtr5g016590	MtC45435_1_AA Proteasome alpha-subunit	Protein synthesis and fate	nucl	0				**P 1**			81	e-122	AT2G27020	Proteasome cpx
Medtr1g101030	MtC45457_1_AA unknown Blast: XP_003548182.1 PREDICTED: tripeptidyl-peptidase 2-like [Glycine max]	Protein synthesis and fate	chlo	0	BB						61	0	AT4G20850	chloroplast, cytoplasm, cytosolic ribosome, membrane, vacuolar membrane, vacuole
Medtr5g058140	MtC45467_1_AA Transmembrane emp24 domain-containing protein	Transport	plas	TM 2			SP	**P 4**			63	7.00E-67	AT1G09580	endomembrane system, integral to membrane, intracellular, membrane
Medtr2g012450	MtC45548_1_AA Ribosomal protein L24/L26 IPR014723:	Protein synthesis and fate	nucl	0				**P 1**			69	3.00E-56	AT3G49910	chloroplast, cytosol, cytosolic large ribosomal subunit, cytosolic ribosome, large ribosomal subunit, membrane, nucleolus, nucleus, plasma membrane, vacuolar membrane
Medtr5g094300	MtC45570_1_AA Mitochondrial import inner membrane translocase, subunit Tim17/22	Transport	chlo	TM 2				**P 1**			58	6.00E-42	AT5G55510	chloroplast envelope, mitochondrial inner membrane presequence translocase complex
Medtr7g114130	MtC45629_1_AA von Willebrand factor, type A IPR010734:Copine	Transport (memb traff)	cyto	TM 1	BB						80	e-136	AT5G61910	undefined
Medtr1g079890	MtC45631_1_AA transmembrane protein 111-like	Unclassified	plas	TM 2							78	e-106	AT4G12590	RE / mitochondrion
Medtr1g014140	MtC45672_1_AA Aminoacyl-transfer RNA synthetase, class II	Maternal tudor protein	mito	0			SP	**P 3**			67	0	AT4G31180	cytosol
Medtr3g098420	MtC50269.2_1_AA Maternal tudor protein	Maternal tudor protein	cyto	0				**P 1**			68	0	AT5G07350	cell, cell wall, chloroplast, cytosol, endoplasmic reticulum, nuclear envelope, plasma membrane
Medtr7g093260	MtC50329_1_AA Actin/actin-like	Cytoskeleton	extr	TM 1				**P 2**			71	e-162	AT2G42090	undefined

Medtr2g009220	MtC50332_1_AA Sodium/sulphate symporter	Transport	plas	TM 8				**P 4**			63	e-150	AT5G64290	M / Chloro m
Medtr3g086210	MtC50546_1_AA Short-chain dehydrogenase/reductase SDR	Energy metabolism	extr	TM 1	BB		SP	**P 4**			69	5.00E-94	AT3G03330	ER / PM
Medtr4g027050	MtC50602_1_AA Major sperm protein	Transport	chlo	TM 1		GPI					69	1.00E-97	AT3G03330	endoplasmic reticulum, plasma membrane
Medtr1g102420	MtC50630_1_AA Lipase/lipooxygenase, PLAT/LH2	Cell rescue and defense	extr	TM 2		GPI	SP	**P 2**			55	2.00E-43	AT5G62200	anchored to M /Vm
Medtr4g131180	MtC60082_1_AA Aldehyde dehydrogenase	Energy metabolism	extr	TM 1				**P 2**			87	0	AT2G24270	undefined
Medtr7g074570	MtC60086_1_AA Phosphoglycerate mutase, 2,3-bisphosphoglycerate-independent	Energy metabolism	cyto	0				**P 1**			82	0	AT1G09780	chloroplast, cytosol, mitochondrial envelope, plasma membrane, plasmodesma
Medtr5g091130, Medtr5g091120	MtC60113.2_1_AA Ribosomal L18ae protein	Protein synthesis and fate	nucl	0				**P 1**			90	1.00E-92	AT2G34480	cytosol, cytosolic large ribosomal subunit, cytosolic ribosome, plasma membrane, vacuolar membrane
Medtr4g050420	MtC60155_1_AA Heat shock protein DnaJ	Cell rescue and defense	nucl	0				**P 4**	FT - CaaX Farnesyltransferase/ GGT1 - CaaX Geranylgeranyltransferase		71	e-158	AT3G44110	CW / PM / Cytos / Plasmodesma / Nucleolus
Medtr8g020940	MtC60191_1_AA E-class P450, group I	Transport	cyto	TM 2							36	e-102	AT2G40890	Mitochondrium / PM / RE / M
Medtr8g089180	MtC60219_1_AA UDP-glucose 4-epimerase	Energy metabolism	plas	TM 2			SP	**P 2**			83	e-114	AT2G34850	ND
Medtr3g064390	MtC60221_1_AA Sigma-54 factor, interaction region IPR003579:Ras small GTPase, Rab type	Transport	chlo	0				**P 1**			86	1.00E-92	AT3G54840	Endosome /PM
Medtr5g025270	MtC60231_1_AA Carotenoid oxygenase	Energy metabolism	pero	0				**P 1**			80	0	AT3G63520	cytoplasm, plasma membrane, plasmodesma, vacuolar membrane, vacuole
Medtr2g038250	MtC60237_1_AA Ribosomal protein L30	Protein synthesis and fate	cyto	0							80	e-104	AT3G13580	chloroplast, cytosolic large ribosomal subunit, cytosolic ribosome, membrane
Medtr2g076670	MtC60257_1_AA Phosphoenolpyruvate carboxylase	Energy metabolism	cyto	0				**P 1**			81	0	AT1G53310	apoplast, cytosol
AC233660_17	MtC60275_1_AA Protein of unknown function	Unclassified	plas	TM 5	BB			**P 1**			71	5.00E-89	AT1G68650	M
Medtr2g103950	MtC60311_1_AA Protein kinase	Signal transduction	chlo	0				**P 4**			61	e-127	AT1G52540	PM /plasmodesma
Medtr2g083860	MtC60316_1_AA Sigma-54 factor, interaction region IPR013753:Ras IPR015595:	Transport	cyto	0	BB			**P 2**	FT - CaaX Farnesyltransferase/ GGT1 - CaaX Geranylgeranyltransferase/ GGT2 - Rab Geranylgeranyltransferase		80	e-100	AT1G06400	PM
Medtr5g017650	MtC60359_1_AA Protein of unknown function Cys-rich Blast: XP_003630909.1 Fruit weight 2.2-like protein [Medicago truncatula]	Unclassified	extr	TM 1				**P 13**			63	3.00E-48	AT1G14870	PM
Medtr1g083460	MtC60397_1_AA Ribosomal protein L18e	Protein synthesis and fate	chlo	0							77	2.00E-81	AT5G27850	chloroplast, cytosolic large ribosomal subunit,

														plasma membrane, vacuolar membrane, vacuole
Medtr3g116830	MtC60399_1_ AA Blast: XP_003603940 Universal stress protein A-like protein UspA	Cell rescue and defense	cyto	0				**P 3**			68	4.00E-70	AT2G21620	undefined
Medtr1g068740	MtC60431_1_AA Blast: XP_003518654 PREDICTED: ras-related protein RABE1c-like [Glycine max]	Transport	chlo	TM 1				**P 2**			80	1.00E-88	AT5G59840	Plasmodesma / PM
Medtr2g099550	MtC60502_1_AA Mitochondrial import inner membrane translocase, subunit Tim17/22	Transport	chlo	TM 2	BB						50	8.00E-45	AT1G72750	membrane, mitochondrial inner membrane,mitochondrion
AC233070_1029	MtC60580_1_AA Peptidyl-prolyl cis-trans isomerase, cyclophilin type IPR015891:	Protein synthesis and fate	chlo	TM 2				**P 1**			56	7.00E-66	AT3G66654	PM / Golgi
Medtr6g059650	MtC60596_1_AA Kunitz inhibitor ST1-like	Cell rescue and defense	extr	TM 1			SP				34	1.00E-16	AT1G17860	CW / Apolast
Medtr4g100740	MtC60621.1_1_AA Protein of unknown function DUF124 Blast: NP_199553.2 tryptophan RNA-binding attenuator-like protein [Arabidopsis thaliana]	Protein synthesis and fate	nucl	TM 2				**P 1**			74	e-118	AT5G47420	ER
Medtr4g118800	MtC60635.1_1_AA Protein of unknown function DUF588 Blast: NP_001238662.1 CASP-like protein 7 [Glycine max]	Unclassified	vacu	TM 2	BB						29	6.00E-07	NS	undefined
Medtr4g103340	MtC60636_1_AA Ribosomal L37ae protein IPR011331: IPR011332:	Protein synthesis and fate	chlo	0				**P 1**			93	1.00E-41	AT3G10950	Cyto / cytosolic large ribosomal subunit,
Medtr4g118560	MtC60645_1_AA Metridin-like ShK toxin IPR005123:2OG-Fe(II) oxygenase	Energy metabolism	nucl	0				**P 4**			76	e-127	AT5G18900	Nucleus / cytos
Medtr4g012910	MtC60657_1_AA Ribosomal protein L37e	Protein synthesis and fate	chlo	0			SP	**P 2**			89	5.00E-30	AT1G52300	cytosolic ribosome
Medtr4g083290, Medtr4g083250	MtC60692_1_AA unknown Blast:XP_003607819.1 hypothetical protein MTR_4g083250 [Medicago truncatula]	Unclassified	nucl_plas	0	BB			**P 1**			60	2.00E-58	AT4G26410	undefined
Medtr8g055840	MtC60699_1_AA Protein of unknown function DUF248, methyltransferase putative	Energy metabolism	cyto	0							80	6.00E-98	AT1G26850	Golgi apparatus, membrane
Medtr3g104310	MtC60711_1_AA NADH dehydrogenase (ubiquinone), 20 kDa subunit	Transport	chlo	TM 1				**P 1**			86	1.00E-78	AT5G11770	Mitochondrion
Medtr3g065110	MtC60716_1_AA Nicastrin	Protein synthesis and fate	plas	TM 1	BB		SP	**P 3**	FT - CaaX Farnesyltransferase/ GGT1 - CaaX Geranylgeranyltransferase/		56	e-164	AT3G52640	Vm / V
Medtr5g080300	MtC60757_1_AA Peptidylprolyl isomerase, FKBP-type	Protein synthesis and fate	chlo	0				**P 2**			78	5.00E-67	AT3G55520	chloroplast thylakoid lumen, membrane
Medtr2g005930	MtC60763_1_AA Protein of unknown function DUF1682 Blast: XP_003592937.1 hypothetical protein MTR_2g005930 [Medicago truncatula]	Unclassified	nucl	TM 1			SP	**P 1**			63	e-126	AT4G24330	ER
Medtr1g041150	MtC60783_1_AA Protein kinase IPR002048:Calcium-binding EF-hand	Signal transduction	chlo	TM 1				**P 3**			71	0	AT5G12480	PM

Medtr1g083620	MtC60813_1_AA Phospholipase D/Transphosphatidylase;Pleckstrin-like [Medicago truncatula]	Transport	chlo	TM 1							70	2.00E-63	AT3G16785	undefined
Medtr8g076150	MtC60854_1_AA ATPase, V0 complex, proteolipid subunit C,	Transport	chlo	TM 4	BB						73	4.00E-49	AT4G34720	V
Medtr6g034680	MtC60857_1_AA unknown Blast:AFK42380.1unknown [Medicago truncatula]	Unclassified	cyto	TM 1							64	5.00E-53	AT1G71780	ER
Medtr7g012560	MtC60870_1_AA Ubiquitin	Protein synthesis and fate	chlo	0				**P 3**	FT - CaaX Farnesyltransferase/ GGT1 - CaaX Geranylgeranyltransferase/		64	3.00E-33	AT5G15460	undefined
Medtr4g022350	MtC60899_1_AA Cytochrome b5	Transport	vacu	TM 1							75	2.00E-59	AT2G32720	undefined
Medtr2g010540	MtC60903_1_AA unknown Blast:XP_003593353.1 hypothetical protein MTR_2g010540 [Medicago truncatula]	Unclassified	chlo	TM 1				**P 1**			63	4.00E-94	AT5G65810	undefined
Medtr1g008700	MtC60941_1_AA Haem peroxidase, plant/fungal/bacterial	Cell rescue and defense	cyto	0							70	e-102	AT1G07890	cell wall, chloroplast, chloroplast stroma, cytosol, plasma membrane, plasmodesma
Medtr5g016270	MtC60945_1_AA Natural resistance-associated macrophage protein	Transport	plas	TM 10	BB			**P 1**			81	0	AT2G23150	plasmodesma, vacuolar membrane, vacuole
Medtr2g103570	MtC61024_1_AA Peptidase S24, S26A and S26B IPR015927:	Protein synthesis and fate	vacu	TM 1							71	7.00E-72	AT1G52600	endoplasmic reticulum, plasma membrane
Medtr2g103500	MtC61028_1_AA Alba, DNA/RNA-binding protein	Cell cycle and DNA processing	plas	0	BB						85	4.00E-51	AT1G29250	Cytos /PM / Nucleus
Medtr1g099500	MtC61065_1_AA Reticulon	Transport	plas	TM 3							71	5.00E-85	AT4G23630	endoplasmic reticulum membrane, endoplasmic reticulum tubular network, integral to cytosolic side of endoplasmic reticulum membrane, plasma membrane, vacuole
Medtr2g094180	MtC61084_1_AA unknown Blast: XP_003536390.1 PREDICTED: protein disulfide-isomerase 5-2-like [Glycine max]	Protein synthesis and fate	cyto	TM 1							49	9.00E-39	AT1G35620	Vm // CW / plasmodesma
Medtr2g034290	MtC61089_1_AA Mitochondrial ribosome	Protein synthesis and fate	mito	0				**P 3**			74	8.00E-41	AT5G47890	Mitochondrion
Medtr3g072600	MtC61096_1_AA emp24/gp25L/p24	Transport	plas	TM 2			SP	**P 2**			63	1.00E-76	AT1G09580	endomembrane system, integral to membrane, intracellular, membrane
Medtr4g014060, Medtr4g013710	MtC61146_1_AA Prenylated rab acceptor PRA1 IPR014475: IPR014690:	Transport	chlo	TM 2	BB			**P 1**			67	1.00E-65	AT2G38360	RE / Cytos
Medtr1g105370	MtC61192_1_AA Ribosomal protein S8	Protein synthesis and fate	cyto	0							98	9.00E-72	AT5G59850	Cytos ribos / M / CW
Medtr8g018770	MtC61295_1_AA Rhodopsin-like GPCR superfamily IPR001078:Catalytic domain of components of various dehydrogenase complexes, Dihydrolipoyllysine-residue acetyltransferase component of pyruvate dehydrogenase complex	Energy metabolism	chlo	0	BB			**P 1**			86	e-114	AT1G34430	PM/ Chloro / Chloro envel / Cytosol rib

Medtr1g072570	MtC61309_1_AA Thioredoxin fold	Cell rescue and defense	nucl	0						Predicted as myristoylated	70	1.00E-50	AT3G63080	ER /PM
Medtr2g038560	MtC61349_1_AA Thioredoxin-like fold	Cell rescue and defense	extr	TM 1			SP	P 1		Predicted as myristoylated	66	5.00E-41	AT5G20500	undefined
AC225474_12	MtC61398_1_AA Sigma-54 factor, interaction region IPR013753:Ras	Transport	chlo	0				3	GGT2 - Rab Geranylgeranyltransferase		82	e-101	AT4G09720	Vm
Medtr1g105370	MtC61411_1_AA Ribosomal protein S8	Protein synthesis and fate	cyto	0							98	9.00E-72	AT5G59850	cell wall, cytosolic small ribosomal subunit, membrane
Medtr1g072570	MtC61419_1_AA Thioredoxin fold	Cell rescue and defense	nucl	0						Predicted as myristoylated	70	5.00E-63	AT3G63080	endoplasmic reticulum, plasma membrane
Medtr5g030580	MtC61439_1_AA unknown Blast:XP_003612923.1 Spinster-like protein [Medicago truncatula]	Transport	plas	TM 5				P 1			65	2.00E-80	AT2G22730	membrane
Medtr7g065210	MtC61447_1_AA Plant lipid transfer protein/Par allergen	Transport	extr	TM 1			SP	P 2			69	2.00E-31	AT2G37870	Plasmodesmata
Medtr8g093740	MtC61535_1_AA Sigma-54 factor, interaction region IPR013753:Ras IPR015598:	Transport	nucl	0	BB			P3	GGT2 - Rab Geranylgeranyltransferase		83	9.00E-90	AT1G43890	peroxisome
Medtr7g091060	MtC61549_1_AA unknown Blast:AFK39184.1 unknown [Medicago truncatula]	Unclassified	chlo	TM 1	BB						66	4.00E-16	AT2G43780	Mitochondrion
Medtr4g127710	MtC61633_1_AA ATPase, P-type, K/Mg/Cd/Cu/Zn/Na/Ca/Na/H-transporter	Transport	vacu	TM 2							75	3.00E-80	AT3G47950	PM
Medtr3g071450	MtC61652_1_AA Bacterial surface antigen (D15), Blast: XP_003600958 Sorting and assembly machinery component-like protein [Medicago truncatula].	Transport	cyto	TM 1				P 1			55	7.00E-69	AT3G11070	M
Medtr4g080800	MtC61689_1_AA Protein of unknown function DUF1692 Blast: XP_003607653.1 Endoplasmic reticulum-Golgi intermediate compartment protein [Medicago truncatula]	Transport	cyto	TM 1							68	8.00E-79	AT4G27080	undefined
AC233676_19	MtC61727_1_AA Caleosin related	Cell rescue and defense	cyto	TM 1							66	8.00E-66	AT1G70670	undefined
Medtr4g114330	MtC61847_1_AA High mobility group-like nuclear protein	Protein synthesis and fate	cyto_nucl	0	BB			P 1			81	7.00E-56	AT4G22380	Nucleolus
Medtr4g130660	MtC62032_1_AA Protein of unknown function UPF0057 Blast:XP_003610299.1 Stress-induced hydrophobic peptide [Medicago truncatula]	Cell rescue and defense	plas	TM 1				P 3			57	1.00E-18	AT4G30660	endomembrane system, integral to membrane
Medtr8g098410	MtC62047_1_AA Thioredoxin-like IPR012335:Thioredoxin fold	Cell rescue and defense	chlo	0			SP				74	1.00E-79	AT4G11600	chloroplast, cytosol, mitochondrion, plasma membrane
Medtr7g099640	MtC62049_1_AA AAA ATPase IPR005937:26S proteasome subunit P45	Protein synthesis and fate	chlo	TM 1						Predicted as myristoylated	89	0	AT5G58290	proteasome complex
Medtr3g008260	MtC62070_1_AA Diacylglycerol kinase, catalytic region	Signal transduction	chlo	0				P 5			65	e-103	AT4G21540	plant-type vacuole membrane, vacuole
Medtr4g021710	MtC62227_1_AA Zinc finger, Tim10/DDP-type	Transport	nucl	0				P 4			78	3.00E-39	AT3G46560	mitochondrial intermembrane space, mitochondrion

Medtr1g043220, Medtr1g043290, Medtr1g043200	MtC62284_1_AA Blast: A5H2U5 Phosphate transporter 3, phosphate:H+ symporter [Medicago truncatula].Liu et al (2008)	Transport	plas	TM 11				**P 1**			71	0	AT5G43360	PM
Medtr1g043200	MtC62304_1_AA Ras small GTPase, Rab type	Transport	cyto	0				**P 6**			78	3.00E-60	AT4G09720	Vm
unfound	MtC62382_1_AA Ribosomal protein 60S	Protein synthesis and fate	chlo	0	BB		SP				72	4.00E-20	AT2G27710	chloroplast, cytosol, cytosolic ribosome, membrane, nucleolus, nucleus, plasma membrane, ribosome
Medtr2g082510	MtC62427_1_AA Histone H2A IPR009072:Histone-fold	Cell cycle and DNA processing	chlo	0	BB						80	9.00E-47	AT4G27230	Nucleus
Medtr4g101280	MtC62534_1_AA Plant lipid transfer protein/seed storage/trypsin-alpha amylase inhibitor	Transport	chlo	TM 1	BB		SP	**P 6**			66	2.00E-24	AT4G12510	endomembrane system
Medtr6g071330	MtC62537_1_AA unknown Blast: NP_564527.1 protein B-cell receptor-associated 31-like protein [Arabidopsis thaliana]	Transport	vacu	TM 3				**P 2**			64	9.00E-39	AT3G17780	endomembrane system, endoplasmic reticulum, integral to membrane
Medtr8g101880	MtC62546_1_AA ATPase, F0 complex, subunit G, mitochondrial	Transport	cyto_nucl	0				**P 3**			67	1.00E-43	AT4G29480	mitochondrion
Medtr2g069310	MtC62591_1_AA Translation factor IPR009022:Elongation factor G, III and V	Protein synthesis and fate	cyto	0				**P 5**			91	0	AT1G56070	chloroplast, cytosol, membrane, nucleolus, plasma membrane, plasmodesma, vacuolar membrane
AC225519_3	MtC62650_1_AA unknown Blast: AFK48658.1 unknown [Lotus japonicus]	Unclassified	nucl	TM 1							45	3.00E-26	AT1G55160	Mitochondrium / Plastid
Medtr4g062410	MtC62665_1_AA Ribosomal protein L29	Protein synthesis and fate	cyto	0							79	9.00E-48	AT5G02610	cytosolic large ribosomal subunit, cytosolic ribosome, plasma membrane, plasmodesma, vacuolar membrane
Medtr6g005540	MtC62738_1_AA unknown Blast: AFK41962.1 unknown [Medicago truncatula]	Unclassified	chlo	TM 3				**P 3**			52	1.00E-78	AT5G55610	Plastid / Chloro /mitochondrion /M
Medtr8g018430	MtC62828_1_AA unknown Blast:XP_003627187.1 Lipoxygenase [Medicago truncatula]	Cell rescue and defense	nucl	TM 1				**P 1**			59	2.00E-56	AT3G22400	Chloro
Medtr3g093220	MtC62895_1_AA Blast XP_003602426 Stomatin-like protein [Medicago truncatula]. Band-7	Protein synthesis and fate (voir raft et band 7)	nucl	0	BB						61	9.00E-23	AT5G54100	mitochondrion
Medtr5g088320	MtC62974_1_AA Calcium-binding EF-hand	Signal transduction	cyto	0			SP				98	4.00E-82	AT2G27030	PM /Vm
Medtr6g091630	MtC62977_1_AA Ribosomal protein L31e	Protein synthesis and fate	cyto	0				**P 1**			72	1.00E-42	AT5G56710	Cytos Ribos /Plasmodesmata / CW
Medtr2g075840	MtC62988_1_AA unknown Blast: XP_003596315.1 Ubiquitin domain-containing protein [Medicago truncatula]	Protein synthesis and fate	chlo	0				**P 2**		Predicted as myristoylated	71	1.00E-42	AT1G53400	undefined
Medtr2g104130	MtC63034_1_AA Calcium-binding EF-hand	Signal transduction	cyto	0				**P 1**		Predicted as myristoylated	78	3.00E-79	AT3G18430	V

Medtr2g035100	MtC63137_1_AA Bet v I allergen	Cell rescue and defense	cyto	0	BB						30	3.00E-04	AT1G24020	membrane
Medtr5g081710	MtC63140_1_AA Ribosomal protein L35Ae	Protein synthesis and fate	chlo	0				**P 1**			89	2.00E-49	AT3G55750	cytosolic large ribosomal subunit, cytosolic ribosome, membrane, ribosome
Medtr8g061970	MtC63141_1_AA Peroxysomal long chain fatty acyl transporter	Transport	plas	TM 5				**P 3**			67	0	AT2G47800	plant-type vacuole, plasma membrane, plasmodesma, vacuolar membrane, vacuole
AC140545_25	MtC63151_1_AA Ribosomal protein L10E	Protein synthesis and fate	chlo_mito	0				**P 4**	ft - CaaX Farnesyltransferase/ GGT1 - CaaX Geranylgeranyltransferase/		88	e-109	AT1G26910	chloroplast envelope, membrane
Medtr4g077510	MtC63279_1_AA Scramblase	Transport	cyto	0	BB						79	5.00E-44	AT2G04940	Mitochondrium / Plastid
Medtr5g072980	MtC63366_1_AA E-class P450, group I	Transport	vacu	TM 2			SP	**P 2**			43	e-112	AT4G31500	M / RE /Mitochondrion / PM
Medtr8g092020	MtC90027_1_AA Sigma-54 factor, interaction region IPR013753:Ras	Transport	cyto	0				**P 1**	GGT2 - Rab Geranylgeranyltransferase		73	6.00E-86	AT1G22740	V
Medtr3g009740	MtC90041_1_AA Prefoldin	Protein synthesis and fate	golg	TM 1				**P 3**			28	6.00E-21	AT4G26455	Nuclear env, Cell Plate
Medtr5g046030	MtC90224_1_AA Alpha-1,4-glucan-protein synthase, UDP-forming	Energy metabolism	extr	0				**P 1**			86	e-179	AT3G02230	Golgi apparatus, Golgi stack, Golgi trans cisterna, cell wall, cytosol, cytosolic ribosome, vacuolar membrane
Medtr1g116890	MtC90316_1_AA E-class P450, group I	Transport	cyto	TM 1				**P 1**	ft - CaaX Farnesyltransferase/ GGT1 - CaaX Geranylgeranyltransferase/		40	1.00E-26	AT3G52970	endomembrane system
Medtr1g026020	MtC90553_1_AA Expansin 45, endoglucanase-like	Energy metabolism	extr	0				**P 1**			77	e-105	AT1G20190	CW
Medtr4g101020	MtC90568_1_AA Major sperm protein	Transport	vacu	TM 1				**P 1**			75	8.00E-51	AT3G60600	cytosol, endoplasmic reticulum, endoplasmic reticulum membrane, integral to membrane, nucleus, plasma membrane, protein storage vacuole
Medtr2g102660	MtC90574_1_AA Pleiotropic drug resistance protein PDR	Transport	plas	TM 6				**P 1**			73	0	AT1G15520	PM
Medtr2g083180	MtC90770_1_AA Calcium-binding EF-hand	Signal transduction	chlo	TM 1			SP	**P 3**			73	0		extrinsic to mitochondrial inner membrane, mitochondrion
Medtr1g114000	MtC90816_1_AA Fibrillarin	Protein synthesis and fate	cyto	0	BB						90	e-132	AT4G25630	Nucleolus
Medtr4g101930	MtC90917_1_AA unknown Blast: XP_003608785.1 COX VIIa-like protein [Medicago truncatula]	Transport	cyto	TM 1							75	9.00E-26	AT4G21105	Vm / mitochondrion
Medtr5g019620	MtC91353_1_AA 1,4-BENZOQUINONE REDUCTASE / TRP REPRESSOR BINDING PROTEIN	Protein synthesis and fate	vacu	TM 1				**P 1**			63	2.00E-84	AT4G36750	PM
Medtr3g033620	MtC91392_1_AA unknown Blast: XP_003539855.1 PREDICTED: uncharacterized protein LOC100818590 [Glycine max]	Unclassified	chlo	TM 2	BB			**P 1**			73	e-123	AT5G12470	chloroplast, chloroplast envelope, chloroplast inner membrane, mitochondrion, plastid

Medtr4g071150	MtC91531_1_AA Histone H2A IPR007124: IPR009072:Histone-fold	Cell cycle and DNA processing	chlo	0	BB		SP	**P 1**			69	2.00E-38	AT5G02560	Nucleolus / Nucleus
Medtr8g066340	MtC91534.1_1_AA Syntaxin/epimorphin family	Transport	cyto	TM 1	BB			**P 1**			65	7.00E-72	AT4G17730	vacuolar membrane
Medtr5g076470	MtC91716_1_AA Syntaxin (MAPEG)	Transport	cyto	TM 3				**P 1**			65	4.00E-48	AT1G65820	V / ER / M
Medtr2g019240	MtC91735_1_AA unknown Blast: XP_003593909.1 hypothetical protein MTR_2g019240 [Medicago truncatula]	Unclassified	extr	TM 1				**P 2**			85	6.00E-07	AT2G34585	vacuolar membrane, vacuole
Medtr4g130860	MtC91778_1_AA Peptidase M17, leucyl aminopeptidase	Protein synthesis and fate	chlo	TM 1	BB			**P 1**			75	0	AT2G24200	chloroplast stroma, cytosol, vacuole
Medtr3g065490	MtC92209_1_AA Nucleotide-binding, alpha-beta plait	Protein synthesis and fate	nucl	0	BB						64	7.00E-50	AT5G37720	Nucleolus
Medtr7g092600	MtC92247_1_AA E-class P450, group I	Transport	cyto	TM 1				**P 2**			52	4.00E-69	AT2G42250	endomembrane system
Medtr8g062670	MtC93020_1_AA Dehydrogenase, E1 component	Energy metabolism	chlo	0				**P 2**			80	e-177	AT1G59900	cytosol, mitochondrion, nucleus
Medtr1g083810	MtC93021.1_1_AA Importin alpha-like protein, beta-binding region	Transport	chlo	0	BB			**P 2**			77	0	AT3G06720	cell wall, cytosol, nuclear envelope, nucleolus
Medtr8g008680	MtC93024_1_AA Initiation factor eIF-4 gamma, middle IPR003891:Initiation factor eIF-4 gamma, MA3	Protein synthesis and fate	nucl	0				**P 2**			56	0	AT3G60240	undefined
Medtr6g077820	MtC93030_1_AA Succinyl-CoA ligase, alpha subunit	Energy metabolism	chlo	0	BB			**P 1**			81	e-135	AT5G23250	Mitochondrion
Medtr8g009510	MtC93032_1_AA Dynamin central region IPR001401:Dynamin IPR003130:Dynamin GTPase effector	Transport	cyto	0				**P 3**			74	0	AT3G60190	mitochondrion, plasma membrane, plasmodesma, vacuolar membrane, vacuole
Medtr8g039540	MtC93035_1_AA Peptidase A1, pepsin	Protein synthesis and fate	extr	TM 1			SP	**P 7**			63	e-161	AT5G07030	CW, plant-type cell wall
Medtr4g106750	MtC93050_1_AA Xanthine/uracil/vitamin C permease	Transport	plas	TM 12				**P 3**			83	0	AT5G62890	cell wall, plasmodesma, vacuole
Medtr2g099570	MtC93052.1_1_AA Plant lipoxygenase	Cell rescue and defense	cyto	TM 1				**P 2**			60	0	AT3G22400	Chloro
Medtr3g106510	MtC93060_1_AA unknown Blast: AFK38721.1 unknown [Lotus japonicus]	Unclassified	vacu	TM 3			SP	**P 6**			52	2.00E-58	AT2G12400	Plasmodesma
Medtr2g012560	MtC93061_1_AA SCAMP	Transport	plas	TM 4							69	e-123	AT2G20840	PM
Medtr2g075950	MtC93078_1_AA Sigma-54 factor, interaction region IPR013753:Ras	Transport	cyto	0	BB			**P 2**	ft - CaaX Farnesyltransferase/ GGT1 - CaaX Geranylgeranyltransferase/GGT2 - Rab Geranylgeranyltransferase		88	e-111	AT1G16920	Golgi / PM / Vm
Medtr1g009010	MtC93113_1_AA Proteasome component region PCI IPR011990:Tetratricopeptide-like helical IPR013143:PCI/PINT associated module	Protein synthesis and fate	chlo	0	BB						76	0	AT1G29150	proteasome complex
unfound	MtC93129_1_AA Protein of unknown function UPF0136 Blast: XP_003609490.1 Transmembrane protein [Medicago truncatula]	Unclassified	E.R.	TM 3	BB						54	7.00E-29	AT3G43520	chloroplast, chloroplast envelope
Medtr5g098250	MtC93137_1_AA emp24/gp25L/p24	Transport	cyto	TM 1			SP	**P 1**			78	e-100	AT3G22845	V

Medtr3g116500	MtC93146_1_AA WD40-like	Signal transduction	nucl	0				**P 5**			76	e-149	AT4G34460	PM / / RE /
Medtr3g052270	MtC93151_1_AA ATPase, F1 complex, gamma subunit	Transport	chlo	0	BB			**P 2**			78	e-148	AT2G33040	Mitochondrion : CW/ Nucleus / Nucleolus / Chloro
Medtr4g059360	MtC93153_1_AA unknown Blast: XP_003539713.1 PREDICTED: uncharacterized protein LOC100787578 [Glycine max]	Unclassified	extr	0			SP				58	1.00E-20	AT2G28430	undefined
Medtr8g102300	MtC93161_1_AA Der1-like	Protein synthesis and fate	plas	TM 4							71	e-102	AT4G29330	undefined
Medtr8g105890	MtC93168_1_AA Like-Sm ribonucleoprotein-related, core	Protein synthesis and fate	cyto	0				**P 1**			93	1.00E-54	AT3G62840	undefined
unfound	MtC93171_1_AA unknown Blast:XP_003538104.1 PREDICTED: nicalin-1-like [Glycine max]	Protein synthesis and fate	cyto	TM 1			SP	**P 1**			55	2.00E-56	AT3G44330	endoplasmic reticulum, mitochondrion, plasma membrane, plasmodesma, vacuolar membrane, vacuole
Medtr2g088700	MtC93190_1_AA Syntaxin, N-terminal	Transport	extr	0			SP	**P 1**	ft - CaaX Farnesyltransferase/ GGT1 - CaaX Geranylgeranyltransferase		58	4.00E-38	AT5G08080	plasma membrane, plasmodesma
Medtr5g021060	MtC93228_1_AA Haem peroxidase, plant/fungal/bacterial	Cell rescue and defense	chlo	0				**P 4**			77	e-120	AT5G66390	EndoM system
Medtr2g036650	MtC93235_1_AA Blast: XP_003594954 Plasma membrane ATPase, plasma-membrane proton-efflux P-type ATPase[Medicago truncatula].	Transport	extr	TM 2			SP				81	3.00E-77	AT1G80660	PM / Vm
Medtr4g101930	MtC93300_1_AA unknown Blast: XP_003608785.1 COX VIIa-like protein [Medicago truncatula]	Transport	cyto	TM 1							73	5.00E-22	AT4G21105	Vm /mitochondrion
Medtr4g106750	MtC93315_1_AA Xanthine/uracil/vitamin C permease	Transport	plas	TM 10				**P 3**			83	0	AT1G49960	cell wall, plasmodesma, vacuole
Medtr7g110660	MtC93344_1_AA Anticodon-binding IPR015263:	Protein synthesis and fate	cyto	0				**P 2**			81	e-126	AT3G62120	Cytosol /M /Plasmodesma
Medtr5g013900	MtC93345_1_AA Ras small GTPase, Rab type IPR015600:	Transport	chlo	0				**P 2**	GGT2 - Rab Geranylgeranyltransferase		87	1.00E-65	AT2G44610	Golgi membrane, cell, cytosol, membrane fraction, plasma membrane, plasmodesma, vacuolar membrane
Medtr4g094240	MtC93375_1_AA unknown Blast:AAP42136.1 erg-1 [Solanum tuberosum]	Protein synthesis and fate	cyto	0	BB			**P 1**			83	5.00E-45	AT5G64260	Plasmodesma / cytosol / CW
AC233655_16	MtC93412_1_AA Cytochrome P450	Transport	cyto	0				**P 1**			62	e-102	AT5G25900	chloroplast outer membrane, endoplasmic reticulum, microsome
Medtr4g019170	MtD00010.1_1_AA Translation elongation factor EF-1, alpha subunit	Protein synthesis and fate	cyto	1 TM				**P5**			98	e-150	AT1G07930	mitochondrion, plasmodesma, vacuole
Medtr5g093300, Medtr2g006820	MtD00070_1_AA Dihydrolipoamide acetyltransferase, long form	Energy metabolism	mito	0							68	e-138	AT4G26910	membrane, mitochondrion
Medtr5g011040	MtD00114_1_AA Hydroxymethylglutaryl-coenzyme A synthase	Energy metabolism	extr	0				**P5**			79	e-156	AT4G11820	Cytosol /Plasmodesma
Medtr8g011900	MtD00116.2_1_AA DOMON related	Protein synthesis and fate	cyto	0	BB						44	2.00E-24	AT3G07390	anchored to membrane, anchored to plasma

														membrane, extracellular region, plasma membrane
Medtr1g090140	MtD00118_1_AA GroEL-like chaperone, ATPase	Protein synthesis and fate	cyto	0	BB						90	0	AT3G23990	cytosol, cytosolic ribosome, mitochondrial matrix, mitochondrion, vacuolar membrane
Medtr5g040360	MtD00123_1_AA Protein of unknown function DUF248, methyltransferase putative	Energy metabolism	chlo	TM 1				**P 3**			79	0	AT1G26850	Golgi /M
Medtr8g055840	MtD00145_1_AA Protein of unknown function DUF248, methyltransferase putative	Energy metabolism	chlo	TM 1				**P 3**			79	0	AT1G26850	Golgi /M
Medtr4g130570	MtD00162_1_AA unknown Blast: XP_003610290.1 Eukaryotic initiation factor iso-4F subunit p82-34 [Medicago truncatula]	Protein synthesis and fate	nucl	TM 1							50	3.00E-27	AT5G57870	Cytosol / Nucleus
Medtr4g114870	MtD00173_1_AA Blue (type 1) copper domain	Transport	extr	TM 1		100	SP	**P 1**			46	2.00E-19	AT5G20230	PM / V /
unfound	MtD00177_1_AA Mitochondrial import inner membrane translocase, subunit Tim17/22	Transport	cyto	TM 2				**P 1**			65	4.00E-52	AT2G37410	Mitochondrion / mitochondrion M
Medtr1g075900	MtD00178_1_AA Protein of unknown function DUF248, methyltransferase putative	Energy metabolism	chlo	TM 1				**P 2**			70	e-145	AT5G14430	Golgi / Vm / CW
Medtr1te116950	MtD00211_1_AA Protease-associated PA IPR007369:Peptidase A22B, minor histocompatibility antigen H13	Protein synthesis and fate	plas	TM 8			SP	**P 7**			53	e-128	AT1G05820	endomembrane system, integral to membrane
Medtr3g098210	MtD00232_1_AA Cleft lip and palate transmembrane 1	Cell cycle and DNA processing	cyto	TM 2	BB						66	e-132	AT5G08500	undefined
Medtr1g106940	MtD00237_1_AA Protease-associated PA	Protein synthesis and fate	chlo	TM 1			SP	**P 4**		Predicted as myristoylated	58	4.00E-88	AT4G20110	M/ golgi network
Medtr1g025430	MtD00238_1_AA ATP-binding region, ATPase-like IPR015566:	Energy metabolism	extr	TM 2		GPI	SP	**P 4**	ft - CaaX Farnesyltransferase/ GGT1 - CaaX Geranylgeranyltransferase		80	2.00E-85	AT4G24190	chloro / cytoso / cytos ribos / / PM / plasmodesma / V / Vm / ER / Nucleus
Medtr1g008280	MtD00256_1_AA Peptidase A22B, minor histocompatibility antigen H13	Protein synthesis and fate	plas	TM 8				**P 1**			78	e-147	AT2G03120	endoplasmic reticulum, endoplasmic reticulum membrane
AC146721_1013	MtD00321_1_AA 6-phosphogluconate dehydrogenase, C-terminal extension	Energy metabolism	chlo	0				**P 1**			87	0	AT3G02360	chloroplast stroma, cytosol, peroxisome
Medtr2g038250	MtD00326_1_AA Ribosomal protein L30	Protein synthesis and fate	cyto				SP				78	e-114	AT3G13580	cytosol Ribos / M / chloro /
Medtr1g008280	MtD00339_1_AA Peptidase A22B, minor histocompatibility antigen H13	Protein synthesis and fate	plas	TM 8				**P 2**			76	e-145	AT2G03120	endoplasmic reticulum, endoplasmic reticulum membrane
Medtr4g071550	MtD00351_1_AA unknown Blast: XP_003607043.1 Signal recognition particle receptor subunit beta [Medicago truncatula]	Transport	cyto	TM 1				**P 2**			69	e-104	AT5G05670	ER / PM
Medtr5g073020	MtD00388_1_AA unknown Blast: XP_003615846.1 Cytochrome P450 71B35 [Medicago truncatula]	Transport	plas	TM 2			SP	**P 3**			45	e-120	AT4G31500	M / RE /Mitochondrion / PM
Medtr6g074910	MtD00400_1_AA Nonaspanin (TM9SF) IPR005479:Carbamoyl-phosphate synthase L chain, ATP-	Transport	chlo	0			SP	**P 1**			76	4.00E-74	AT2G01970	Golgi apparatus, plant-type cell wall, plasmodesma, vacuolar

	binding													membrane
Medtr2g012560	MtD00493_1_AA SCAMP	Transport	plas	TM 4							65	e-109	AT1G61250	PM
Medtr3g085270	MtD00498_1_AA Protein of unknown function DUF579, plant Blast: AFK44106.1 unknown [Medicago truncatula]	Unclassified	cyto	TM 1				**P 3**			67	2.00E-90	AT1G27930	undefined
Medtr6g021800	MtD00512_1_AA Translation elongation factor EF-1, alpha subunit	Protein synthesis and fate	cyto	0				**P 4**			98	e-150	AT1G07930	mitochondrion, plasmodesma, vacuole
Medtr5g020050	MtD00535_1_AA Fumarate reductase/succinate dehydrogenase, FAD-binding site IPR013027:FAD-dependent pyridine nucleotide-disulphide oxidoreductase	Transport	mito	0				**P 3**			83	3.00E-86	AT2G18450	Mitochondrion
Medtr3g086210	MtD00538_1_AA Short-chain dehydrogenase/reductase SDR	Energy metabolism	chlo	TM 2				**P 4**			63	e-124	AT1G67730	ER / M
Medtr2g005930	MtD00571_1_AA Protein of unknown function DUF1682 Blast: XP_003592937.1 hypothetical protein MTR_2g005930 [Medicago truncatula]	Unclassified	cyto_nucl	TM 2							60	e-120	AT5G49945	ER
Medtr4g030140	MtD00588_1_AA Dynamin	Transport	cyto	0	BB						78	3.00E-93	AT1G59610	clathrin-coated endocytic vesicle / PM / Cell Plate / Cytos / V
Medtr4g129070	MtD00644_1_AA Diacylglycerol kinase, catalytic region	Signal transduction	cyto	0				**P 2**			61	e-114	AT2G18730	membrane, plasma membrane, plasmodesma
Medtr2g010020	MtD00691_1_AA Heat shock protein 70	Cell rescue and defense	chlo	TM 1	BB			**P 3**			82	0	AT5G09590	cell wall, chloroplast, mitochondrial matrix, mitochondrion, vacuolar membrane
Medtr5g074690	MtD00713_1_AA Helix-hairpin-helix motif	Cell cycle and DNA processing	cyto	0				**P 2**			71	0	AT1G06950	chloroplast, chloroplast envelope, membrane
Medtr3g077640	MtD00721_1_AA Protein of unknown function DUF250 Blast: XP_003601250.1 Phosphate/phosphoenolpyruvate translocator [Medicago truncatula]	Transport	chlo	TM 7	BB			**P 1**			79	e-144	AT5G33320	chloroplast, chloroplast envelope, mitochondrion, plastid, plastid inner membrane
Medtr1g106830	MtD00747_1_AA Calcium-binding EF-hand	Signal transduction	cyto	0				**P 1**			69	0	AT2G27040	Cajal body, nuclear euchromatin, nucleolus
AC225517_18	MtD00775_1_AA Unknown	Unclassified	cyto	TM 1							63	6.00E-81	AT5G11560	ER / PM / V /Vm
unfound	MtD00815_1_AA Tetratricopeptide-like helical	Protein synthesis and fate	cyto	0	BB			**P 2**			59	e-152	AT1G67680	undefined
Medtr2g018780	MtD00845_1_AA Protein of unknown function DUF221	Unclassified	plas	TM 8				**P 2**			64	0	AT1G30360	chloroplast, chloroplast envelope, membrane, plasma membrane, plasmodesma, vacuolar membrane, vacuole
Medtr4g114030	MtD00856_1_AA Blast: XP_003609284 NADH-cytochrome b5 reductase-like protein [Medicago truncatula].	Transport e	cyto	TM 1				**P 1**			67	e-106	AT5G20080	mitochondrial intermembrane space, mitochondrion, plant-type cell wall
Medtr7g078760	MtD00859_1_AA Peptidase M48, Ste24p	Protein synthesis and fate	E.R.	TM 4							80	0	AT4G01320	V / ER

Medtr7g006280	MtD00865_1_AA ENTH/VHS IPR013809:Epsin-like, N-terminal	Transport chlatrin endocytosis	nucl	0							77	5.00E-94	AT2G43160	PM / Vm / golgi
Medtr5te046150	MtD00882_1_AA Unknown	Unclassified	plas	TM 3	BB		SP				54	9.00E-36	AT4G14420	ER
Medtr1g019410	MtD00884_1_AA cytochrome P450 monooxygenase CYP51G1 [Medicago truncatula].	Transport €	vacu	TM 1			SP				82	0	AT1G11680	ER / PM
Medtr2g086290	MtD00921_1_AA Alpha/beta hydrolase fold-1	Energy metabolism	chlo	TM 2				**P 1**			61	e-132	AT2G36290	ER
Medtr7g028250	MtD00926_1_AA Oligopeptide transporter OPT superfamily	Transport	plas	TM 9				**P 2**			73	0	AT3G27020	Vm
Medtr3g100100	MtD01002_1_AA Tetratricopeptide TPR_1	Protein synthesis and fate	chlo	TM 1	BB						41	2.00E-29	AT5G65520	undefined
Medtr4g103520	MtD01017_1_AA Blast: ADM32503 purple acid phosphatase [Glycine max].Purple acid phosphatase, N-terminal (Calcineurin-like phosphoesterase; pfam00149), metallo-esterase-like	Energy metabolism	vacu	TM 1			SP				58	3.00E-59	AT4G24890	cell wall
Medtr8g072310	MtD01059_1_AA Reticulon	Transport	cyto	TM 1							72	0	Medtr8g072310	ER
Medtr3g061640	MtD01060_1_AA Blast: XP_003600480 RuvB DNA helicase-like protein [Medicago truncatula].	Cell rescue and defense	cyto	0	BB						80	2.00E-86	AT5G67630	Chloro Nucleolus
Medtr8g014820	MtD01112_1_AA unknown Blast: XP_003517628.1 PREDICTED: probable LRR receptor-like serine/threonine-protein kinase At4g29180-like [Glycine max]	Signal transduction	extr	TM 1	BB		SP	**P 1**			52	e-111	AT4G29180	EndoM system
Medtr4g073400	MtD01191_1_AA unknown Blast: XP_003607198.1 Synaptotagmin-7 [Medicago truncatula]	Transport okMay be involved in Ca2+-dependent exocytosis of secretory vesicles through Ca2+ and phospholipid binding to the C2 domain or may serve as Ca2+ sensors in the process of vesicular trafficking and exocytosis	extr	TM 1							78	1.00E-66	AT2G20990	endosome, internal side of plasma membrane, intracellular, membrane, plasma membrane, plasmodesma, vacuole
Medtr3g099990	MtD01219_1_AA Blast: XP_003602883 ABC transporter (lipid) the ABCA subfamily mediates the transport of a variety of lipid compounds.	Transport	cyto	0				**P 7**			72	e-171	AT5G61730	plasma membrane
Medtr4g050870	MtD01238_1_AA Acetyl-CoA carboxylase carboxyl transferase, beta subunit	Energy metabolism (Lipid bios)	nucl	0				**P 3**			72	6.00E-87	ATCG00500	chloroplast, chloroplast envelope, membrane
Medtr8g095680	MtD01243_1_AA Blast: XP_003630450 Calnexin-like protein [Medicago truncatula].	Protein synthesis and fate	vacu	TM 1			SP	**P 1**			78	8.00E-75	AT5G07340	chloroplast, endoplasmic reticulum, membrane, vacuolar membrane
Medtr1g088680	MtD01250_1_AA Blast: XP_003591547 ABC transporter C family protein [Medicago truncatula].	Transport	chlo	TM 3				**P 5**			68	e-176	AT2G47800	plant-type vacuole, plasma membrane, plasmodesma, vacuolar membrane, vacuole
Medtr5g072020	MtD01296_1_AA Blast: XP_003615764 Serine palmitoyltransferase [Medicago truncatula].	Energy metabolism (lipid meta)	chlo	TM 1				**P 1**			24	1.00E-31	AT3G48780	EndoM system

AC233655_16	MtD01344_1_AA Cytochrome P450	Transport	chlo	TM 2				**P 1**			61	1.00E-67	AT5G25900	chloroplast outer membrane, endoplasmic reticulum, microsome
Medtr7g051940	MtD01385_1_AA Small GTP-binding protein domain IPR015595:	Signal transduction	cyto	0				**P 2**	GGT2 - Rab Geranylgeranyltransferase		89	2.00E-84	AT2G31680	Cytosol
Medtr8g014700	MtD01393_1_AA Blast XP_003627062 Receptor-like protein kinase [Medicago truncatula].	Signal transduction	extr	TM 1			SP				51	4.00E-57	AT1G51790	EndoM system
Medtr7g074070	MtD01494_1_AA unknown Blast: XP_003623651 hypothetical protein MTR_7g074070 [Medicago truncatula].	Unclassified	chlo	TM 2	BB						64	5.00E-77	AT3G08640	chloro envelop / chloro
Medtr7g111590, Medtr5te026750	MtD01561_1_AA Ribosomal protein L13e	Protein synthesis and fate	chlo	0							86	9.00E-98	AT3G49010	cell wall, cytosol, cytosolic large ribosomal subunit, cytosolic ribosome, membrane, nucleolus, plasma membrane, plasmodesma, ribosome, vacuolar membrane
Medtr4g049540	MtD01562_1_AA Blast:NP_568607 B-cell receptor-associated 31-like protein [Arabidopsis thaliana].	Transport (protein)	plas	TM 3							70	3.00E-84	AT5G42570	ER / Plasmodesma / Vm
Medtr7g099920	MtD01568_1_AA Blast: XP_002540014 centromere/microtubule binding protein cbf5, putative, partial [Ricinus communis].	Cell cycle and DNA processing	cyto	0				**P 2**			89	e-108	AT3G57150	Nucleolus / Cytso Plamodesma
Medtr7g027960	MtD01574_1_AA E-class P450, group I	Transport	chlo	TM 1			SP				30	4.00E-37	AT5G06900	EndoM system
Medtr7g099920	MtD01586_1_AA unknown Blast:XP_003625506.1 Eukaryotic translation initiation factor 3 subunit A [Medicago truncatula]	Protein synthesis and fate	cyto	0				**P 1**			84	e-154	AT4G11420	PM
Medtr7g005910	MtD01618_1_AA Sugar transporter superfamily IPR011701:Major facilitator superfamily MFS_1	Transport	cyto	TM 6	BB						69	e-103	AT2G43330	Vm /V
Medtr8g107640	MtD01690_1_AA Annexin	signal transduction	cyto	0				**P 2**			51	1.00E-93	AT1G68090	undefined
Medtr8g106980	MtD01733_1_AA Linker histone, N-terminal	Cell cycle and DNA processing	nucl	0	BB						58	2.00E-14	AT1G48620	chloroplast, nucleolus
Medtr8g085380	MtD01782_1_AA Blast: XP_003629679 Peptide-N(4)-(N-acetyl-beta-glucosaminyl)asparagine amidase	Protein synthesis and fate	nucl	0				**P 1**			68	5.00E-70	AT1G04850	Cytosol
Medtr3g098990	MtD01837_1_AA unknown Blast: XP_003602786 Protein DEK [Medicago truncatula].	Cell cycle and DNA processing	nucl	0				**P 1**			68	1.00E-55	AT5G63550	undefined
Medtr1g096050	MtD01946_1_AA Blast: XP_003539999 embryogenesis-associated protein EMB8-like [Glycine max]	Energy metabolism	chlo	0				**P 1**			68	e-143	AT3G50790	undefined
Medtr4g078050	MtD01985_1_AA Mitochondrial import inner membrane translocase, subunit Tim17/22	Transport	E.R.	TM 2				**P 3**			52	2.00E-31	AT3G10110	chloroplast, mitochondrial inner membrane, mitochondrial inner membrane presequence

														translocase complex
Medtr3g116150	MtD02058_1_AA unknown Blast: XP_003602786.1 Protein DEK [Medicago truncatula]	Cell cycle and DNA processing	chlo	TM 1							70	2.00E-36	AT2G33585	undefined
Medtr2g013930	MtD02094_1_AA Eukaryotic translation initiation factor 3, subunit 7	Protein synthesis and fate	nucl	0				**P 2**			59	e-111	AT4G20980	Chloro
Medtr6g012880	MtD02197_1_AA unknown Blast: XP_003618550.1 Mitochondrial S1 ribosomal protein [Medicago truncatula]	Protein synthesis and fate	chlo	TM 1				**P 3**			28	1.8	NS	chloroplast
Medtr2g076670	MtD02232_1_AA Phosphoenolpyruvate carboxylase	Energy metabolism	chlo	0				**P 2**			87	e-170	AT3G14940	Cytosol
Medtr3g096670	MtD02247_1_AA Blat: XP_003526874 PREDICTED: farnesylcysteine lyase-like [Glycine max].	Protein synthesis and fate	chlo	TM 1	BB		SP	**P 1**			48	2.00E-55	AT5G63910	Vm / V
Medtr4g018750	MtD02273_1_AA Adenine nucleotide translocator 1	Transport	extr	TM 2				**P 2**			79	e-117	AT3G54110	mitochondrial inner M / mitochondrion / plamsodesma / chloro /
Medtr8g066340	MtD02291_1_AA Syntaxin/epimorphin family	Transport	cyto	TM 1	BB			**P 1**			65	4.00E-80	AT4G17730	VM
Medtr7g024390	MtD02358_1_AA Heat shock protein 70	Cell rescue and defense	mito	0				**P 2**			86	e-179	AT3G12580	apoplast, cell wall, chloroplast, cytosol, cytosolic ribosome, nuclear matrix, plasma membrane, plasmodesma, vacuolar membrane, vacuole
Medtr2g025550	MtD02436_1_AA Blast: XP_003594202 Phosphatidate cytidylyltransferase [Medicago truncatula].	lipid-dependent signal transduction cascade, phosphoinositide biosynthesis in the plasma membrane	chlo	TM 1				**P 1**			63	3.00E-35	AT4G22340	EndoM system / M
Medtr1g087320	MtD02555_1_AA unknown Blast: XP_003591427.1 Transmembrane protein [Medicago truncatula]	Unclassified	plas	TM 5							69	2.00E-83	AT3G62580	EndoM system
Medtr8g035760, AC233070_1002, AC225458_103	MtD02573_1_AA E-class P450, group II	Transport	chlo	TM 1							56	4.00E-53	AT2G45510	ER
Medtr5g095230	MtD02601_1_AA Cytochrome P450	Transport	cyto	TM 1							50	1.00E-51	AT3G14620	EndoM system
Medtr1g099500	MtD02792_1_AA Reticulon	Transport endoplasmic reticulum tubular network maintenance, May be involved in secretion or in membrane trafficking	E.R.	TM 2							62	2.00E-69	AT1G64090	endoplasmic reticulum membrane, endoplasmic reticulum tubular network, integral to cytosolic side of endoplasmic reticulum membrane, plasmodesma
Medtr1g041150	MtD02820_1_AA Protein kinase IPR002048:Calcium-binding EF-hand	Signal transduction	cyto	0						Predicted as myristoylated	79	e-105	AT3G57530	PM / Cytosol / plamodesma / nucleus
Medtr4g077000	MtD02891_1_AA unknown Blast:XP_003607364.1 hypothetical protein MTR_4g077000 [Medicago truncatula]	Unclassified	chlo	TM 2	BB			**P 1**			73	e-125	AT5G12470	chloroplast, chloroplast envelope, chloroplast inner membrane, mitochondrion, plastid
Medtr1g101030.	MtD02943_1_AA Peptidase S8 and S53, subtilisin, kexin, sedolisin	Protein synthesis and fate	nucl	TM 1				**P 1**			72	6.00E-33	AT4G20850	chloroplast, cytoplasm, cytosolic ribosome, membrane, vacuolar

														membrane, vacuole
Medtr2g101090, Medtr2g100990	MtD03001_1_AA ABC-2 type transporter IPR013581:Plant PDR ABC transporter associated	Transport	plas	TM 5				**P 1**			61	e-140	AT1G59870	chloroplast, chloroplast envelope, membrane, mitochondrion, plasma membrane, vacuolar membrane
Medtr2g081810	MtD03039_1_AA Flavodoxin/nitric oxide synthase	Transport €	cyto	0							87	3.00E-93	AT5G54500	M / PM / V / Vm
Medtr5g027790	MtD03040_1_AA SCAMP (Secretory carrier-associated membrane protein)	Transport prot, endo, exo	cyto	TM 1				**P 3**			63	3.00E-45	AT1G32050	Mitochondrion /PM
Medtr3g080240	MtD03329_1_AA Blast: XP_003541360 PREDICTED: plastidic glucose transporter 4-like [Glycine max].	Transport (hexose)	vacu	TM 7	BB						78	e-123	AT5G16150	chloroplast envelope,
Medtr1g088680	MtD03384_1_AA Blast: XP_003628563 Multidrug resistance protein ABC transporter family [Medicago	Transport	extr	TM 4				**P 3**			58	e-133	AT2G47800	plant-type vacuole, plasma membrane, plasmodesma, vacuolar membrane, vacuole
Medtr6g021790	MtD03445_1_AA Sigma-54 factor, interaction region IPR003579:Ras small GTPase, Rab type	Transport	cyto	0				**P 3**	GGT2 - Rab Geranylgeranyltransferase		81	e-100	AT4G35860	Chloro
AC146721_1013	MtD03607_1_AA Blast: ACM68927 6-phosphogluconate dehydrogenase [Cucumis sativus].	Energy metabolism (Pentose shunt)	chlo	0	BB						85	e-128	AT1G64190	chloroplast, chloroplast stroma, cytosol, membrane
Medtr2g028580	MtD03699_1_AA Protein kinase	Signal transduction	nucl	TM 1				**P 1**			46	e-118	AT5G49760	plasma membrane, vacuole
Medtr1g088480	MtD03747_1_AA NAD-dependent epimerase/dehydratase	Transport	chlo	0							85	3.00E-58	AT3G53520	M /Golgi /
Medtr4g132110	MtD03755.2_1_AA Haem peroxidase, plant/fungal/bacterial	Cell rescue and defense	cyto	TM 1			SP	**P 2**			81	e-152	AT4G21960	EndoM system
Medtr7g113420	MtD03801_1_AA Blast: XP_003626280 Protein AUXIN RESPONSE [Medicago truncatula] (auxin polar transport)	Transport	mito	TM 1							50	1.00E-74	AT1G54990	ER / Vm / Mitochondrodiun
Medtr7g098370, Medtr7g098760	MtD03898_1_AA Pleiotropic drug resistance protein PDR, ABC transporter associated	Transport	chlo	TM 2				**P 3**			71	e-168	AT1G15520	PM
Medtr7g113420	MtD03927_1_AA Protein AUXIN RESPONSE	Transport	mito	TM 1							50	1.00E-74	AT1G54990	ER / Vm / Mitochondrodiun
unfound	MtD04169_1_AA Ribophorin II	Protein synthesis and fate	chlo	TM 3	BB			**P 2**			49	4.00E-73	AT4G21150	endoplasmic reticulum, membrane, mitochondrion, plant-type cell wall, plasma membrane, plasmodesma, vacuolar membrane
Medtr2g088990	MtD04199_1_AA Blue (type 1) copper domain	Transport	extr	TM 2	BB	GPI	SP				54	8.00E-30	AT3G60270	Anchord to M
Medtr1g088680	MtD04304_1_AA Blast: XP_003628563 Multidrug resistance protein ABC transporter family [Medicagotruncatula].	Transport	chlo	0				**P 3**			61	e-137	AT2G47800	plant-type vacuole, plasma membrane, plasmodesma, vacuolar membrane, vacuole
Medtr4g071130	MtD04425_1_AA von Willebrand factor, type A IPR006692:Coatomer WD associated region	Transport	chlo	0	BB			**P 1**			69	0	AT1G62020	CUL4 RING ubiquitin ligase complex, cytosol, intracellular, membrane,

	IPR010714:Coatomer alpha subunit, C-terminal													plasma membrane
Medtr5g083910	MtD04430_1_AA Blast XP_003616753 Cysteine-rich receptor-like protein kinase [Medicago truncatula].	Signal transduction	extr	TM 1			SP				54	2.00E-43	AT3G14840	PM / plasmodsma /
Medtr2g014960	MtD04471_1_AA Blast: XP_003593681 Somatic embryogenesis receptor-like kinase [Medicago truncatula].Leucine rich repeat, N-terminal	Signal transduction	nucl	0	BB		SP	**P 1**			42	1.00E-35	AT1G79620	EndoM system
Medtr8g020610	MtD04586_1_AA Cupin 1 IPR007113:	Energy metabolism	chlo	TM 1	BB		SP	**P 1**			52	5.00E-56	AT1G72610	extracellular matrix
Medtr4g064780	MtD04793_1_AA Bacterial surface antigen (D15)	Transport	cyto	0							82	e-136	AT3G46740	chloroplast, chloroplast envelope, integral to chloroplast outer membrane, membrane, vacuolar membrane
Medtr3g107550	MtD05273_1_AA unknown Blast: XP_003603422.1 hypothetical protein MTR_3g107550 [Medicago truncatula]	Unclassified	chlo	TM 3	BB			**P 3**			72	5.00E-81	AT5G11280	undefined
Medtr3g098420	MtD05462_1_AA Blast: XP_003602730 nuclease domain-containing protein [Medicago truncatula].	Protein synthesis and fate	cyto	0	BB			**P 1**			70	2.00E-57	AT5G07350	cell, cell wall, chloroplast, cytosol, endoplasmic reticulum, nuclear envelope, plasma membrane
Medtr8g101880	MtD05491_1_AA ATPase, F0 complex, subunit G, mitochondrial	Transport	cyto_nucl	0				**P 1**			75	3.00E-20	AT4G29480	Mitochondrion
Medtr4g055520	MtD05516_1_AA unknown Blast: XP_003606274.1 Glucomannan 4-beta-mannosyltransferase [Medicago truncatula] Cellulose synthase-like protein	Energy metabolism (cw biogenesis, degradation)	plas	TM 3				**P 1**			84	0	AT5G22740	undefined
Medtr5g005100	MtD05586_1_AA unknown Blast: XP_003610620.1 Vacuolar-sorting receptor [Medicago truncatula]	Transport (vacuolar-sorting receptor (VSR) involved in clathrin-coated vesicles sorting from Golgi apparatus to vacuoles)	chlo	TM 1			SP				76	8.00E-69	AT2G14740	membrane
Medtr8g035810, AC225458_94, AC225458_98, Medtr8g035820, AC225458_99, AC233070_1006, AC233070_1007, AC233070_1011	MtD05591_1_AA Cytochrome P450	Transport	cyto	0				**P 1**			58	3.00E-85	AT2G45510	ER
Medtr3g116500	MtD05593_1_AA WD40-like	signal transduction	nucl	0				**P 5**			76	e-144	AT4G34460	PM / / RE /
Medtr4g130910	MtD05610_1_AA Translation protein SH3-like IPR012340:Nucleic acid-binding, OB-fold, subgroup IPR014722:	Protein synthesis and fate	chlo	0				**P 1**			91	1.00E-74	AT1G13950	undefined
Medtr1g025550	MtD06161_1_AA Blast: XP_003589515 Synaptotagmin-7 [Medicago truncatula].C2 calcium-dependent membrane targeting	Transport (May be involved in Ca2+-dependent exocytosis of secretory vesicles through Ca2+ and phospholipid binding to the C2 domain or may serve	extr	TM 1							68	e-122	AT1G20080	undefined

		as Ca2+ sensors in the process of vesicular trafficking and exocytosis)												
Medtr4g113100	MtD06341_1_AA Blast: AAK92807 putative receptor protein kinase [Arabidopsis thaliana].Leucine rich repeat, N-terminal	Signal transduction	chlo	TM 1	BB		SP	**P 1**			66	6.00E-73	AT2G26730	PM
Medtr5g026930	MtD06397_1_AA Blast: XP_003517079 PREDICTED: probable methyltransferase PMT20-like [Glycine max].	Energy metabolism (This is a family of putative S-adenosyl-L-methionine (SAM)-dependent methyltransferase)	cyto	TM 1				**P 2**			74	0	AT4G19120	undefined
Medtr2g035100	MtD06407_1_AA Bet v I allergen	Cell rescue and defense	cyto	0	BB						30	3.00E-04	NS	membrane
unfound	MtD06497_1_AA Blast XP_003524448 PREDICTED: PROTEIN: monodehydroascorbate reductase, chloroplastic-like [Glycine max].	Cell rescue and defense (cold, cad)	cyto	0	BB			**P 1**			79	6.00E-98	AT1G63940	Chloro / M / Mitochondrion
Medtr5g098420	MtD06527_1_AA Blast: XP_002316776 fasciclin-like arabinogalactan protein, partial [Populus trichocarpa].	Protein synthesis and fate (cell surface adhesion protein)	chlo	0				**P 1**			61	1.00E-95	AT5G55730	anchored to membrane, anchored to plasma membrane, cell wall, plasma membrane
Medtr7g038120	MtD06754_1_AA Blast: XP_003622471 Mechanosensitive ion channel domain-containing protein / MS ion channel domain-containing protein [Medicago truncatula].	Transport	golg	TM 4							63	1.00E-69	AT4G00290	chloroplast, chloroplast envelope
Medtr2g069310, Medtr2g069050	MtD06868_1_AA Elongation factor Tu	Protein synthesis and fate	chlo	0				**P 6**			92	0	AT1G56070	chloroplast, cytosol, membrane, nucleolus, plasma membrane, plasmodesma, vacuolar membrane
Medtr4g115970	MtD06942_1_AA Inorganic H+ pyrophosphatase Blast: XP_003609464 Vacuolar proton-inorganic pyrophosphatase [Medicago truncatula]. IPR004131 Pyrophosphate-energised proton pump	Transport (proton)	plas	TM 5	BB			**P 2**			95	2.00E-55	AT1G15690	chloroplast, chloroplast envelope, endosome membrane, membrane, mitochondrion, plant-type vacuole, plant-type vacuole membrane, plasma membrane, vacuolar membrane, vacuole
Medtr5g030530	MtD07002_1_AA Mitochondrial substrate carrier	Transport	cyto	TM 2	BB			**P 2**			74	3.00E-65	AT5G46800	chloroplast,mitochondrion, plastid
Medtr2g096160	MtD07207_1_AA Blast: NP_190214 receptor-like protein kinase HERK 1 [Arabidopsis thaliana]	Signal transduction	cyto	0							81	e-123	AT3G46290	PM / plasmodesma /
Medtr7g077150	MtD07266_1_AA Blast: XP_002511845 receptor protein kinase, putative [Ricinus communis].	Signal transduction	cyto	0				**P 4**			88	e-129	AT1G63500	PM / plasmodesma /
Medtr2g014860	MtD07270_1_AA Blast: XP_003593671 hypothetical protein MTR_2g014860 [Medicago truncatula].	Unclassified	chlo	TM 1							62	4.00E-40	AT1G28510	undefined

Medtr1g075900	MtD07370_1_AA Blast: XP_003541361 probable methyltransferase PMT8-like [Glycine max].	energy metabolism	mito	0				**P 1**			74	0	AT3G23300	Golgi / Nucleus / Vm
Medtr4g074930, Medtr4g074800	MtD07390_1_AA unknown Blast:CAA61298 Nuclear migration protein nuM1 [Medicago sativa] RNA-binding protein	Cell cycle and DNA processing	chlo	0	BB						55	4.00E-61	AT3G18610	undefined
Medtr5g083910	MtD07414_1_AA Blast: XP_003531816 probable LRR receptor-like serine/threonine-protein kinase At1g56130-like [Glycine max].Leucine-rich repeat	Signal transduction	extr	TM 1			SP	**P 3**			50	1.00E-56	AT1G56130	M / PM
AC235753_1023	MtD07435_1_AA Glycosyl transferase, family 48	Cell rescue and defense	cyto	TM 3				**P 1**			90	e-117	AT2G36850	PM / plasmodesma
Medtr7g076150	MtD07440_1_AA Blast: XP_003528881 probable methyltransferase PMT13-like [Glycine max].	energy metabolism (cell wall pectin metabolic process)	cyto	0				**P 1**			73	e-155	AT4G00740	Golgi /Integral to M
Medtr1g018800	MtD07462_1_AA Blast: ADN33725 mannose-P-dolichol utilization defect 1 protein [Cucumis melosubsp. melo].	Transport (Cystine Transporter) Part of the ABC transporter complex tcyJKLMN involved in L-cystine import. Is also involved in cystathionine, djenkolate, and S-methylcysteine transport	vacu	TM 3	BB			**P 2**			71	6.00E-93	AT4G07390	M
Medtr6g008530	MtD07475_1_AA E-class P450, group I	Transport	chlo	0				**P 1**			55	2.00E-68	AT4G31940	EndoM system
Medtr4g113100	MtD07825_1_AA Blast: AAK92807 putative receptor protein kinase [Arabidopsis thaliana].	Signal transduction	nucl	0				**P 2**			81	7.00E-87	AT2G26730	PM
Medtr2g094270	MtD08074_1_AA Blast: XP_003597235 Aquaporin PIP2-7 [Medicago truncatula].	Transport (Major intrinsic protein (MIP) superfamily. Members of the MIP superfamily function as membrane channels that selectively transport water, small neutral molecules, and ions out of and between cells.Aquaporins facilitate the transport of water and small neutral solutes across cell membranes	cyto	TM 6							77	e-131	AT5G60660	Plasmodesma
Medtr1g116470	MtD08148_1_AA Glycosyl transferase, family 48	Cell rescue and defense	nucl	TM 3							84	1.00E-71	AT3G07160	PM
Medtr2g005570	MtD08369_1_AA Blast: XP_002264400 PREDICTED: elongation factor 1-gamma-like [Vitis vinifera].Elongation factor 1, gamma chain	Protein synthesis and fate	cyto	0				**P 2**			67	e-170	AT1G57720	cell wall, cytosol, membrane, plasma membrane, plasmodesma, vacuole
AC235487_5	MtD08475_1_AA Blast: XP_003521403 PREDICTED: cell division cycle protein 48	Cell cycle and DNA processing	cysk	0				**P 4**			94	e-143	AT5G03340	CW / Cytosl

	homolog [Glycine max]													
Medtr3g095810	MtD08485_1_AA Ribosomal protein S2, eukaryotic and archaeal form	Protein synthesis and fate	cyto	0							82	e-107	AT1G72370	chloroplast, cytoplasm, cytosol, cytosolic ribosome, membrane, nucleus, plasma membrane, plasmodesma, small ribosomal subunit
Medtr2g101090, Medtr2g100990	MtD08577_1_AA ABC-2 type transporter	Transport	nucl	TM 1							73	2.00E-43	AT3G16340	PM
Medtr1g116120, Medtr5g059410	MtD08749_1_AA Transketolase, central region	Energy metabolism	chlo	0							85	0	AT3G60750	chloroplast, chloroplast envelope, chloroplast stroma
Medtr8g018690	MtD08844_1_AA Lipoxygenase	Cell rescue and defense	cyto	TM 1							56	0	AT3G22400	Chloro
Medtr1g098220	MtD08989_1_AA Ribosomal protein S13	Protein synthesis and fate	cyto	0				**P 2**			89	2.00E-60	AT4G09800	cell wall, cytosolic small ribosomal subunit, nucleolus, plasmodesma, small ribosomal subunit, vacuole
Medtr4g123810	MtD09341_1_AA S-adenosylmethionine synthetase	Energy metabolism	cyto	0				**P 3**			91	0	AT3G17390	CW / Plasmodesma / Nucleus / PM/ M/ G olgi
Medtr4g123810	MtD09358_1_AA S-adenosylmethionine synthetase	Energy metabolism	cyto	0				**P 3**			91	0	AT3G17390	CW / Plasmodesma / Nucleus / PM/ M/ G olgi
Medtr6g077750	MtD09396_1_AA Blast: XP_003620143 Dolichyl-diphosphooligosaccharide-protein glycosyltransferase subunit STT3A [Medicago truncatula].	Protein synthesis and fate	chlo	TM 2							83	e-162	AT1G34130	M / PM / ER
Medtr5g026930	MtD09432_1_AA Protein of unknown function DUF248, methyltransferase putative	Energy metabolism	cyto	TM 1				**P 2**			74	0	AT4G19120	undefined
Medtr5g022600	MtD09637_1_AA Ras small GTPase, Rab type	Transport	chlo	0				**P 4**	ft - CaaX Farnesyltransferase/ GGT1 - CaaX Geranylgeranyltransferase		88	1.00E-98	AT2G17800	cytoplasm, nucleus, phragmoplast, spindle
Medtr7g110660	MtD09807_1_AA Blast: XP_003626067 Bifunctional aminoacyl-tRNA synthetase [Medicago truncatula].	Protein synthesis and fate	nucl	0							89	1.00E-68	AT3G62120	Cytosol /M /Plasmodesma
Medtr7g110310	MtD09952_1_AA S-adenosylmethionine synthetase	Energy metabolism	cyto	0				**P 3**			91	0	AT3G17390	CW / Plasmodesma / Nucleus / PM/ M/ Golgi
Medtr2g015680	MtD10024_1_AA Ribosomal protein S27E	Protein synthesis and fate	chlo	0				**P 1**			82	6.00E-37	AT3G61110	cell wall, cytosolic ribosome, cytosolic small ribosomal subunit, plasmodesma, ribosome
Medtr4g024270	MtD10254_1_AA Ribosomal protein S15	Protein synthesis and fate	cyto_nucl	0							89	2.00E-64	AT4G00100	cytosolic small ribosomal subunit, membrane, nucleolus
Medtr1g018840	MtD10303_1_AA unknown Blast XP_003589133.1 Cysteine proteinase [Medicago truncatula]	Protein synthesis and fate	cyto	TM 1				**P 5**			66	0	AT1G47128	apoplast, chloroplast, plasmodesma, vacuole
Medtr5g026930	MtD10413_1_AA Protein of unknown function DUF248, methyltransferase putative	Energy metabolism	cyto	TM 1				**P 1**			74	0	AT4G19120	undefined
Medtr4g123810	MtD10563_1_AA S-adenosylmethionine synthetase	Energy metabolism	cyto	0				**P 3**			91	0	AT3G17390	CW / Plasmodesma / Nucleus / PM/ M/ G olgi

Medtr3g108800	MtD10584_1_AA ATPase, P-type, K/Mg/Cd/Cu/Zn/Na/Ca/Na/H-transporter	Transport	plas	TM 3							80	e-106	AT2G24520	PM
Medtr7g102070	MtD10710_1_AA Blast: XP_003625677 ABC transporter-like protein, partial [Medicago truncatula].	Transport	chlo	0	BB						77	e-112	AT2G36910	PM /plasmodesma
Medtr7g086300	MtD10763_1_AA 5-methyltetrahydropteroyltriglutamate--homocysteine S-methyltransferase	Energy metabolism	cyto	0				**P 1**			82	0	AT5G17920	Perox / cytos / Chloro / PM / apoplast / plasmodesma /Vm
Medtr2g069310	MtD10899.2_1_AA Translation factor IPR009022:Elongation factor G, III and V	Protein synthesis and fate	cyto	0				**P 5**			91	0	AT1G56070	Cytosol / M /chloro / Plasmodesma / Nucleus / V / PM
Medtr7g028160	MtD11172_1_AA TCP transcription factor IPR012340:Nucleic acid-binding, OB-fold, subgroup	Protein synthesis and fate	nucl	0				**P 1**			79	5.00E-55	AT5G23740	membrane
Medtr5g080880	MtD11294_1_AA Mitochondrial glycoprotein	Unclassified	mito	0				**P 1**			42	2.00E-20	AT2G39795	mitochondrial matrix, mitochondrion
Medtr3g065110	MtD11298_1_AA Nicastrin	Protein synthesis and fate	plas	TM 1			SP	**P 1**			57	e-131	AT3G52640	Vm / V
Medtr8g039290	MtD11446_1_AA unknown Blast: ADV35716.2 root determined nodulation 1 [Medicago truncatula]	Unclassified	chlo	TM 1			SP	**P 1**			71	e-152	AT5G13500	EndoM system
Medtr4g115970	MtD11469_1_AA Inorganic H+ pyrophosphatase Blast: XP_003609464 Vacuolar proton-inorganic pyrophosphatase [Medicago truncatula].	Transport	vacu	TM 6	BB			**P 1**			82	e-180	AT1G15690	PM /Vm /Cytos / Chloro / V / M / mitochondrion
Medtr8g086850	MtD11604_1_AA Histone H2A IPR007124: IPR009072:Histone-fold	Cell cycle and DNA processing	nucl	0	BB						73	7.00E-32	AT5G02560	Nucleolus / Nucleus
Medtr2g096660	MtD11611_1_AA NAD-dependent epimerase/dehydratase	Transport	chlo	0							87	e-175	AT2G28760	plasma membrane
Medtr5g098310	MtD11657_1_AA Thiolase	Energy metabolism	chlo	0	BB			**P 1**			77	e-165	AT5G48230	Cytosol/ perox / PM
Medtr7g118060	MtD11728_1_AA Ribosomal protein 60S	Protein synthesis and fate	chlo	TM 1	BB			**P 1**			66	6.00E-16	AT5G24510	cytosolic ribosome
Medtr3g077050	MtD11747_1_AA Ribosomal protein L15	Protein synthesis and fate	nucl	0							77	3.00E-54	AT1G70600	cytosol, cytosolic large ribosomal subunit, cytosolic ribosome, membrane, plasmodesma
Medtr7g076230	MtD11751_1_AA unknown Blast: BAA96978.1 protein transport protein SEC12p-like [Arabidopsis thaliana]	Transport	cyto	0				**P 2**			37	1.00E-15	AT5G50650	undefined
Medtr5g098250	MtD11890_1_AA emp24/gp25L/p24	Transport	cyto	0							75	5.00E-87	AT3G07680	M
Medtr4g070140	MtD12058_1_AA Nucleotide-binding, alpha-beta plait	Protein synthesis and fate	cyto	TM 1	BB		SP				77	9.00E-29	AT2G21660	chloroplast, cytoplasm, cytosol, nucleus, peroxisome, plasmodesma
Medtr1g099930	MtD12059_1_AA unknown Blast: XP_003533972.1 PREDICTED: putative substrate translocation pore, SPX domain-containing membrane protein At4g22990-like isoform 1 [Glycine max]	Transport	plas	TM 5	BB						70	e-102	AT4G22990	undefined

Medtr1g095070	MtD12105_1_AA Major intrinsic protein, Blast XP_003591905 Aquaporin PIP [Medicago truncatula].	Transport	plas	TM 5	BB			**P 2**			79	e-108	AT2G37170	chloroplast, membrane, plasma membrane, plasmodesma
Medtr2g104110	MtD12192_1_AA, Blast: XP_003597927 NADH-ubiquinone oxidoreductase 24 kDa subunit [Medicago truncatula].	Transport	cyto	0				**P 6**			78	e-116	AT4G02580	Mitochondrion
Medtr4g063090	MtD12237_1_AA Major intrinsic protein Blast: AF275315_1 water-selective transport intrinsic membrane protein 1 [Lotus japonicus].	Transport	cyto	TM 4	BB						76	3.00E-44	AT2G36830	central vacuole, chloroplast envelope, plant-type vacuole membrane, protein storage vacuole, vacuolar membrane, vacuole
Medtr8g014930	MtD12384_1_AA Protein kinase	Signal transduction	nucl	TM 1				**P 2**			44	e-107	AT2G19230	EndoM system
Medtr3g088150	MtD12421_1_AA unknown	Unclassified	nucl	0				**P 1**			59	3.00E-28	AT1G44170	endoplasmic reticulum, membrane, plasmodesma, plastid, vacuole
Medtr3g106480	MtD12444_1_AA Blast: FLOT1_MEDTR Full=Flotillin-like protein 1. ACCESSION D2XNQ8. Band_7_flotillin: a subgroup of the band 7 domain of flotillin (reggie) like proteins. This subgroup contains proteins similar to stomatin, prohibitin, flotillin, HlfK/C and podicin. These two proteins are lipid raft-associated.	Transport	mito	0	BB						52	4.00E-50	AT5G25260	vacuolar membrane
Medtr3g084340	MtD12580_1_AA S-adenosyl-L-homocysteine hydrolase IPR015878:	Energy metabolism	cyto	0				**P 3**			86	e-161	AT4G13940	cytosol, membrane, plasma membrane, plasmodesma, vacuolar membrane, vacuole
Medtr5g082900	MtD12603_1_AA 7-Fold repeat in clathrin and VPS proteins	Transport	cyto	0				**P 2**			81	e-101	AT3G08530	chloroplast, cytosol, membrane, plasma membrane, plasmodesma
Medtr1g085140	MtD12678_1_AA Blast: XP_003626121 Rhicadhesin receptor [Medicago truncatula]. Cupin 1 IPR007113:	Protein synthesis and fate (an attachment protein of rhizobiaceae.)	chlo	TM 1			SP				67	1.00E-48	AT1G09560	CW / Nucleus
Medtr4g132110	MtD12723.2_1_AA Haem peroxidase, plant/fungal/bacterial	Cell rescue and defense	cyto	TM 1			SP	**P 2**			81	e-152	AT4G21960	EndoM system
Medtr1g116520	MtD12821_1_AA Tyrosine protein kinase, active site	Signal transduction	cyto	0				**P 4**			81	e-170	AT3G59350	PM
Medtr7g086300	MtD13094.2_1_AA Blast: XP_003624677 Methionine synthase	Energy metabolism	cyto	0				**P 1**			82	0	AT5G17920	apoplast, chloroplast, chloroplast stroma, cytosol, membrane, peroxisome, plasma membrane, plasmodesma, vacuolar membrane
Medtr4g127710	MtD13438_1_AA Blast: PMA2_SOLLC Plasma membrane ATPase 2; AltName: Full=Proton pump	Transport (cation)	vacu	TM 1	BB						86	e-110	AT5G62670	M / PM

Medtr8g061970	MtD13497_1_AA ABC transporter, transmembrane region, type 1	Transport	cyto	TM 1				**P 1**			62	6.00E-74	AT3G62700	plant-type vacuole, vacuolar membrane, vacuole
Medtr6g013300	MtD13504_1_AA Proteasome alpha-subunit	Protein synthesis and fate	cyto	0	BB						97	e-137	AT3G14290	cytosol, cytosolic ribosome, proteasome core complex
Medtr5g088660	MtD13578_1_AA unknown Blast: XP_003617173.1 Elongation factor 1-beta [Medicago truncatula]	Protein synthesis and fate	nucl	0	BB						68	3.00E-26	AT5G19510	apoplast, cytosol, plasmodesma
Medtr3g088150	MtD13642_1_AA Aldehyde dehydrogenase	Energy metabolism	cyto	0				**P 1**			74	9.00E-68	AT1G44170	V / M / plamodesma / ER
Medtr5g098310	MtD13848_1_AA Thiolase	Energy metabolism	chlo	0	BB			**P 1**			77	e-179	AT5G48230	Cytosol/ perox / PM
Medtr8g075560	MtD13928_1_AA Cold-shock protein	Cell rescue and defense	cyto	0	BB						62	5.00E-24	AT2G21060	cytosol, nucleus
Medtr5g026930	MtD14084_1_AA Protein of unknown function DUF248, methyltransferase putative	Energy metabolism	cyto	TM 1				**P 2**			74	0	AT4G19120	undefined
Medtr5g087560	MtD14276_1_AA Chaperonin TCP-1	Protein synthesis and fate	chlo	0				**P 2**			95	e-106	AT3G11830	Cytosol
Medtr4g012910	MtD14407_1_AA Ribosomal protein L37e	Protein synthesis and fate	chlo	0				**P 2**			88	2.00E-43	AT3G16080	cytosolic large ribosomal subunit
Medtr8g077310	MtD14474_1_AA Sugar transporter IPR007114:Major facilitator superfamily	Transport	plas	TM 11	BB			**P 2**			76	e-178	AT1G19450	vacuolar membrane, vacuole
Medtr4g063090	MtD14539_1_AA unknown Blast:AAB41809.1 membrane channel protein [Medicago sativa]	Transport	chlo	TM 2							71	5.00E-25	AT2G36830	central vacuole, chloroplast envelope, plant-type vacuole membrane, protein storage vacuole, vacuolar membrane, vacuole
Medtr5g030530	MtD14618_1_AA Mitochondrial carrier protein	Transport	chlo	TM 2	BB			**P 3**			76	1.00E-79	AT5G46800	chloroplast, mitochondrion, plastid
Medtr1g018840	MtD14684_1_AA Blast: XP_003589133 Cysteine proteinase [Medicago truncatula].	Protein synthesis and fate	nucl	0				**P 5**			68	e-180	AT1G47128	apoplast, chloroplast, plasmodesma, vacuole
Medtr2g081610	MtD14864.1_1_AA BURP	Cell rescue and defense	extr	TM 1			SP	**P 2**			33	4.00E-11	AT1G49320	protein storage vacuole
Medtr2g081770	MtD14864.2_1_AA BURP	Cell rescue and defense	cyto	TM 1			SP	**P 1**			33	3.00E-11	AT1G49320	protein storage vacuole
Medtr2g039960	MtD14914_1_AA Blast: XP_003595233 Eukaryotic initiation factor 4A [Medicago truncatula].	Protein synthesis and fate	chlo	0							91	0	AT3G13920	cell wall, cytosol, membrane, nucleolus, plasmodesma
Medtr7g092730	MtD15021_1_AA Blast: XP_003625217 Polygalacturonase inhibitor [Medicago truncatula].Leucine rich repeat, N-terminal	Cell rescue and defense	chlo	0				**P 5**			50	2.00E-76	AT5G06860	cell wall, plant-type cell wall, plasmodesma
Medtr4g076030	MtD15136_1_AA Putative uncharacterized protein	Unclassified	nucl	0				**P 2**			49	3.00E-52	AT2G32240	PM
Medtr3g088150	MtD15227_1_AA Blast: XP_003544699 PREDICTED: aldehyde dehydrogenase family 3 member H1-like isoform 2 [Glycine max].	Energy metabolism	cyto	0	BB						74	3.00E-39	AT1G44170	endoplasmic reticulum, membrane, plasmodesma, plastid, vacuole

Medtr3g071560	MtD15465_1_AA Eukaryotic translation initiation factor 2, alpha subunit	Protein synthesis and fate	cyto	0				**P 1**			78	6.00E-71	AT2G40290	Cytosol / Nucleus
Medtr8g089190	MtD15605_1_AA Cytochrome P450	Transport	cyto	TM 1							36	2.00E-16	AT5G36110	endomembrane system
Medtr3g092090	MtD15630_1_AA Cytochrome b5	Transport	chlo	TM 1							79	4.00E-58	AT5G53560	chloroplast thylakoid membrane, endoplasmic reticulum, endoplasmic reticulum membrane, plasma membrane, vacuolar membrane, vacuole
Medtr7g110310	MtD15632_1_AA S-adenosylmethionine synthetase	Energy metabolism (aa)	cysk	0				**P 2**			85	0	AT4G01850	cell wall, cytosol, extracellular vesicular exosome, nucleolus, plasmodesma
unfound	MtD15666_1_AA ORMDL	Protein synthesis and fate	plas	TM 3							85	2.00E-48	AT1G01230	ER
Medtr4te061140	MtD15731_1_AA Haem peroxidase, plant/fungal/bacterial	Cell rescue and defense	cyto	0							70	2.00E-99	AT1G07890	cell wall, chloroplast, chloroplast stroma, cytosol, plasma membrane, plasmodesma
Medtr2g014030	MtD15801_1_AA Ribosomal protein S6e IPR014401:	Protein synthesis and fate	nucl	0							79	3.00E-95	AT4G31700	chloroplast, cytosol, cytosolic ribosome, cytosolic small ribosomal subunit, membrane, nucleolus, plasma membrane, plasmodesma
Medtr8g061970	MtD15850_1_AA Blast: XP_003628563 Multidrug resistance protein ABC transporter family [Medicagotruncatula].	Transport	cyto	TM 1							54	7.00E-35	AT3G62700	plant-type vacuole, vacuolar membrane, vacuole
Medtr1g083330, Medtr1g083340	MtD15929_1_AA Blast: XP_003591146 26S protease regulatory subunit 6A-like protein [Medicago truncatula].	Protein synthesis and fate	cyto	0				**P 1**			94	0	AT3G05530	cytoplasm, cytosol, nucleus, proteasome regulatory particle, base subcomplex
unfound	MtD15931_1_AA unknown Blast: AAK15493.1 brassinosteroid biosynthetic protein LKB [Pisum sativum]	Energy metabolism	cyto	TM 1				**P 1**			79	e-142	AT3G19820	integral to membrane, membrane, plasma membrane, vacuolar membrane, vacuole
Medtr6g073040	MtD16182_1_AA Protein of unknown function DUF588 Blast: XP_003619992.1 hypothetical protein MTR_6g073040 [Medicago truncatula]	Unclassified	vacu	TM 4	BB		SP	**P 1**			42	2.00E-06	AT2G39530	membrane
unfound	MtD16310_1_AA Ribosomal protein L7A IPR004342:EXS, C-terminal	Protein synthesis and fate	mito	0				**P 1**			61	1.00E-39	AT2G47610	chloroplast, cytosol, cytosolic large ribosomal subunit, cytosolic ribosome, nucleolus, plasmodesma, vacuolar membrane
Medtr4g071970	MtD16472_1_AA ATPase, V0 complex, proteolipid subunit C,	Transport	vacu	TM 4	BB			**P 1**			79	9.00E-54	AT4G34720	plasma membrane, vacuole
Medtr3g031610	MtD16981_1_AA Protein kinase Blast: XP_003529230 PREDICTED: G-type lectin S-receptor-like serine/threonine-protein kinase At1g34300-like	Signal transduction	nucl	TM 1							52	3.00E-27	AT4G32300	PM

	[Glycine max].													
Medtr1g005600, Medtr1g006010	MtD17162_1_AA ATPase, F1/V1/A1 complex, alpha/beta subunit, N-terminal	Transport	cyto	0	BB						88	4.00E-45	AT2G07698	chloroplast, chloroplast envelope, membrane, mitochondrion, nucleolus, vacuolar membrane, vacuole
Medtr5g094230	MtD17248_1_AA Glycerophosphoryl diester phosphodiesterase	Energy metabolism (glycerol et lipid)	chlo	TM 1	BB		SP	**P 4**			57	0	AT4G26690	anchored to membrane, anchored to plasma membrane, plant-type cell wall, plasma membrane
Medtr4g043690	MtD17397_1_AA ATPase, P-type, K/Mg/Cd/Cu/Zn/Na/Ca/Na/H-transporter	Transport	cyto	0				**P 1**			57	6.00E-29	AT3G57330	chloroplast, plant-type vacuole membrane, plasma membrane, vacuolar membrane, vacuole
Medtr2g028580	MtD17510_1_AA Blast: XP_003594434 Somatic embryogenesis receptor-like kinase [Medicago truncatula].IPR013210:Leucine rich repeat, N-terminal	Signal transduction	extr	TM 1	BB		SP				57	3.00E-38	AT5G49760	PM / V
Medtr5g045630	MtD17526_1_AA Cytochrome b5	Transport	cyto	0				**P 1**			67	6.00E-23	AT1G26340	chloroplast outer membrane, stromule
Medtr3g070940	MtD17572_1_AA Blast: XP_003600924 Clathrin heavy chain [Medicago truncatula].	Transport	cyto	0							88	1.00E-91	AT3G11130	PM / Plasmodesma / V / Vm
Medtr7g114130	MtD17614_1_AA Blast: XP_002511086 copine, putative [Ricinus communis].Copines are phospholipid-bindingC2 calcium/lipid-binding region, CaLB	Transport (M traffick)	chlo	0				**P 5**			55	1.00E-74	AT5G61910	undefined
Medtr2g035100	MtD17619_1_AA unknown Blast:XP_003594829.1 Pathogenesis-related protein PR10 [Medicago truncatula]	Cell rescue and defense	cyto	0	BB						30	3.00E-04	AT1G24020	membrane
Medtr1g081410	MtD17767_1_AA Ribosomal protein S24e	Protein synthesis and fate	chlo	0			SP	**P 2**			90	2.00E-42	AT3G04920	chloroplast, cytosol, cytosolic ribosome, cytosolic small ribosomal subunit, membrane, nucleolus, plasma membrane, vacuolar membrane
Medtr1g056390	MtD17917_1_AA unknown Blast: CAJ77501.1 expp1 protein precursor [Solanum tuberosum]	Unclassified	nucl	0				**P 2**			65	2.00E-79	AT3G44150	PM
Medtr1g106900	MtD17961_1_AA Ribosomal protein S13	Protein synthesis and fate	nucl	0				**P 2**			88	3.00E-51	AT4G09800	cell wall, cytosolic small ribosomal subunit, nucleolus, plasmodesma, small ribosomal subunit, vacuole
Medtr1g079890	MtD18059_1_AA Blast: XP_003590940 Transmembrane protein [Medicago truncatula].Protein of unknown function DUF850	Unclassified	cyto	TM 2				**P 2**			76	e-101	AT4G12590	RE / mitochondrion
Medtr1g083190, Medtr3g106420	MtD18142_1_AA unknown Blast: XP_003591134.1Flotillin-like	Transort	nucl	0	BB			**P 2**			46	2.00E-25	AT5G25260	vacuolar membrane

	protein [Medicago truncatula]													
Medtr3g118030	MtD18175_1_AA Eukaryotic ribosomal protein L5	Protein synthesis and fate	mito	TM 2				**P 1**			79	e-136	AT5G39740	cytosol, cytosolic large ribosomal subunit, cytosolic ribosome, nucleolus, plasma membrane, ribosome, vacuole
Medtr1g023210	MtD18210_1_AA Peptidase C1A, papain C-terminal	Protein synthesis and fate	chlo	0			SP	**P 3**			70	e-143	AT4G39090	V / Nucleus
Medtr7g114250	MtD18613_1_AA Blast: AAR19085 Na+/H+ antiporter [Medicago sativa].	Transport	chlo	TM 4							78	2.00E-75	AT3G05030	undefined
Medtr7g098200	MtD18706_1_AA unknown Blast:XP_003551296.1 PREDICTED: peptide transporter PTR1-like [Glycine max] (MFS)	Transport	plas	TM 5				**P 1**			68	e-106	AT3G54140	membrane, plasma membrane, plasmodesma
Medtr5g030530	MtD18850_1_AA Mitochondrial substrate carrier	Transport	chlo	TM 1							79	7.00E-33	AT5G46800	chloroplast,mitochondrion, plastid
Medtr4g128840	MtD19186_1_AA Xylose isomerase, bacterial type	Energy metabolism	mito	TM 1				**P 2**			75	e-114	AT5G57655	Vm / V / RE
Medtr1g018840	MtD19264_1_AA Peptidase C1A, papain C-terminal	Protein synthesis and fate	cyto	0				**P 3**			70	e-102	AT1G47128	apoplast, chloroplast, plasmodesma, vacuole
Medtr7te026930	MtD19684_1_AA unknown Blast: AAB97305.1 NADH ubiquinone oxidoreductase subunit 5 [Vicia faba]	Transport €	chlo	0				**P 1**			95	5.00E-56	ATMG00665	Mitochondrion
Medtr8g086070	MtD19776_1_AA Mitochondrial substrate carrier	Transport	cyto	TM 1							79	e-142	AT5G19760	cell wall, chloroplast, chloroplast envelope, mitochondrion, plasmodesma, vacuolar membrane
Medtr2g008070	MtD20057_1_AA Ubiquinol-cytochrome C reductase hinge protein	Transport	chlo	0			SP	**P 1**			86	2.00E-27	AT1G15120	Mitochondrium
Medtr4g051880	MtD20062_1_AA Harpin-induced 1	Cell rescue and defense	cyto	0				**P 1**			65	7.00E-49	AT3G11660	undefined
unfound	MtD20233_1_AA Succinate dehydrogenase/fumarate reductase iron-sulfur protein IPR012285:Fumarate reductase, C-terminal	Energy metabolism (TCA)	chlo	0				**P 4**			88	e-121	AT5G40650	Mitochondrion
Medtr4g075290	MtD20401_1_AA Peptidyl-prolyl cis-trans isomerase, cyclophilin type IPR015891:	Protein synthesis and fate	cyto	0				**P 1**			77	1.00E-72	AT2G16600	chloroplast, cytosol, plasma membrane, plasmodesma
Medtr1g108530	MtD20414_1_AA unknown Blast: ACJ11753.1 UDP-D-apiose/UPD-D-xylose synthetase [Gossypium hirsutum]	Energy metabolism(galactose)	plas	TM 2			SP	**P 1**			83	0	AT1G08200	apoplast, cytoplasm, cytosol
Medtr5g075240	MtD20427_1_AA Ribosomal protein S9	Protein synthesis and fate	cyto	0				**P 2**			89	3.00E-66	AT2G09990	cell wall, chloroplast, cytosol, cytosolic ribosome, cytosolic small ribosomal subunit, membrane, plasmodesma
Medtr3g008250	MtD20646_1_AA Blast: XP_003628253 Prohibitin [Medicago truncatula]. Band 7	Signal transductionBand_7_prohibitin. A subgroup of the band 7	cyto	0							76	6.00E-77	AT5G40770	membrane, mitochondrion, nucleolus, plasma membrane,

	protein	domain of flotillin (reggie) like proteins. This subgroup group includes proteins similar to prohibitin (a lipid raft-associated integral membrane protein). Individual proteins of this band 7 domain family may...; cd03401" /db_xref="CDD:48213"												vacuolar membrane, vacuole
Medtr6g074910	MtD20873.2_1_AA Nonaspanin (TM9SF)	Transport	plas	TM 10			SP	**P 2**			82	0	AT2G01970	Golgi apparatus, plant-type cell wall, plasmodesma, vacuolar membrane
Medtr4g101280	MtD22035_1_AA Plant lipid transfer protein/seed storage/trypsin-alpha amylase inhibitor	Transport	chlo	TM 1			SP	**P 6**			46	7.00E-20	AT4G12510	EndoM system
Medtr8g005360	MtD22323_1_AA unknown Blast: XP_003552331.1 PREDICTED: NADH dehydrogenase [ubiquinone] 1 alpha subcomplex subunit 1-like [Glycine max]	Transport	cyto	TM 1				**P 1**			77	4.00E-23	AT3G08610	Mitochondrion
Medtr7g114040	MtD22726_1_AA Histone H2A IPR007124: IPR009072:Histone-fold	Cell cycle and DNA processing	chlo	0	BB						78	3.00E-45	AT1G54690	nucleolus, nucleus
Medtr2g008070	MtD22772_1_AA Ubiquinol-cytochrome C reductase hinge protein	Transport	mito	0				**P 1**			78	9.00E-28	AT1G15120	Mitochondrium
Medtr1g075540	MtD22800_1_AA Blast: NP_192356 peroxisomal membrane protein PMP22 [Arabidopsis thaliana]Mpv17/PMP22	Cell rescue and defense	mito	TM 2							63	6.00E-66	AT4G04470	peroxisomal membrane
Medtr4g068040	MtD22835_1_AA Ribosomal L38e protein	Protein synthesis and fate		0				**P 1**			91	2.00E-31	AT3G59540	cytosolic large ribosomal subunit
Medtr1g026090	MtD22852_1_AA Ribosomal protein L14b/L23e	Protein synthesis and fate	cyto	0			SP				97	3.00E-75	AT3G04400	cytosolic large ribosomal subunit, ribosome
Medtr3g055120	MtD22970_2_AA unknown Blast: XP_003600177.1 Major pollen allergen Bet v 1-L [Medicago truncatula]	Cell rescue and defense	chlo	0	BB						31	0.82	AT1G25141	undefined
Medtr2g035130	MtD23030_1_AA Bet v I allergen	Cell rescue and defense	cyto	0	BB						29	0.002	AT5G45870	undefined
Medtr2g035130	MtD23062_1_AA Bet v I allergen	Cell rescue and defense	cyto	0	BB						29	0.002	AT5G45871	undefined
unfound	MtD23115_1_AA Alpha/beta hydrolase fold-1 IPR000379:	Energy metabolism	vacu	TM 2	BB						88	1.00E-95	AT5G20520	apoplast, cytoplasm, nucleus, vacuole
AC225458_44	MtD23422_1_AA E-class P450, group I	Transport	cyto	0				**P 1**			53	6.00E-69	AT3G48290	undefined
Medtr1g005600, Medtr1g006010	MtD23458_1_AA ATPase, F1/V1/A1 complex, alpha/beta subunit, nucleotide-binding	Transport	chlo	0	BB						98	8.00E-65	ATMG01190	cell wall, mitochondrion

Medtr3g115930	MtD23697_1_AA unknown Blast:XP_003603853.1 hypothetical protein MTR_3g115930 [Medicago truncatula]	Unclassified	vacu	TM 1				**P 1**			77	1.00E-29	AT1G42960	chloroplast, chloroplast envelope, chloroplast inner membrane, chloroplast thylakoid membrane, membrane, mitochondrion, plastid
Medtr5g088320	MtD23826_1_AA EF-Hand type	Protein synthesis and fate	chlo	0							100	1.00E-35	AT2G27030	Vm/PM
Medtr2g096570	MtD23832_1_AA Histone H2A IPR007124: IPR009072:Histone-fold	Cell cycle and DNA processing	nucl	0	BB						75	2.00E-41	AT5G02560	Nucleolus / Nucleus
Medtr1g108530	MtD23863_1_AA NAD-dependent epimerase/dehydratase	Transport	chlo	TM 1	BB			**P 1**			73	2.00E-61	AT1G08200	apoplast / cytosol
Medtr4g068040	MtD24497_1_AA Ribosomal L38e protein	Protein synthesis and fate	nucl	0				**P 1**			91	3.00E-31	AT3G59540	cytosolic large ribosomal subunit
Medtr7g068280	MtD24793_1_AA HMG1/2 (high mobility group) box	Protein synthesis and fate	nucl	0				**P 2**			56	4.00E-25	AT3G51880	Chromatin / Nucleus
Medtr7g098760	MtD24902_1_AA Blast XP_003625400 Pleiotropic drug resistance protein [Medicago truncatula].	Transport	cysk	0							71	7.00E-98	AT1G15520	PM
Medtr2g103150	MtD24909_1_AA Cytochrome c oxidase, subunit Vb	Transport	mito	0			SP				77	3.00E-43	AT1G80230	mitochondrial envelope, mitochondrion
Medtr7g024390	MtD24950_1_AA Heat shock protein 70	Cell rescue and defense	cyto	0				**P 2**			92	e-103	AT3G09440	apoplast, cell wall, chloroplast, cytosol, cytosolic ribosome, nuclear matrix, plasma membrane, plasmodesma, vacuolar membrane, vacuole
Medtr7g109730	MtD25003_1_AA unknown	Unclassified	cyto	0				**P 2**			60	4.00E-42	AT3G62360	endoplasmic reticulum, plant-type cell wall, vacuolar membrane
Medtr3g070940	MtD25171_1_AA Clathrin propeller, N-terminal	Transport	chlo	0				**P 1**			85	6.00E-59	AT3G08530	chloroplast, cytosol, membrane, plasma membrane, plasmodesma
Medtr5g081710	MtD25219_1_AA Ribosomal protein L35Ae	Protein synthesis and fate	cyto	0							85	9.00E-42	AT3G55750	cytosolic large ribosomal subunit, cytosolic ribosome, membrane
Medtr4g101140	MtD25998_1_AA unknown Blast: XP_003549910.1 PREDICTED: NADH dehydrogenase [ubiquinone] 1 beta subcomplex subunit 8, mitochondrial-like [Glycine max]	Transport	chlo	TM 1							80	4.00E-47	AT5G47570	mitochondriom
Medtr2g012560	MtD26020_1_AA SCAMP	Transport	E.R.	TM 2							68	6.00E-59	AT2G20840	PM
Medtr1g080460	MtD26036_1_AA Glycosyl transferase, family 8	Cell rescue and defense	chlo	0				**P 1**			79	2.00E-82	AT5G18480	M
Medtr4g064780	MtD26753_1_AA Bacterial surface antigen (D15)	Transport	cyto	0	BB						85	1.00E-53	AT3G46740	chloroplast, chloroplast envelope, integral to chloroplast outer membrane, membrane, vacuolar membrane
Medtr3g108190	MtD26762_1_AA unknown Blast:ABB59583.1 putative sulfate transporter, partial [Populus tremula x Populus alba]	Transport	plas					**P 1**			47	4.00E-38	AT2G25680	V / Mitochondrion

Medtr2g044580	MtD27293_1_AA Heat shock protein DnaJ, N-terminal IPR004179:Sec63	Cell rescue and defense	cyto	0							74	e-120	AT1G79940	endoplasmic reticulum, integral to endoplasmic reticulum membrane, mitochondrion, plasma membrane
Medtr5g099070	MtD27326_1_AA unknown Blast: XP_003618109.1 Niemann-Pick C1 protein [Medicago truncatula]	Transport	extr	TM 1				**P 1**			78	6.00E-96	AT4G38350	M / Vm /V/
Medtr4g030140	MtD27821_1_AA Blast: XP_003605375 Dynamin-2B [Medicago truncatula].	Transport (Clathrin-mediated endocutosis: An endocytosis process that begins when material is taken up into clathrin-coated pits, which then pinch off to form clathrin-coated endocytic vesicles.	cyto	0	BB			**P 1**			84	e-108	AT1G59610	cell plate, clathrin-coated endocytic vesicle, cytosol, plasma membrane, plasmodesma, vacuole
Medtr2g060830	MtC00722_1_AA Proteasome alpha-subunit	Protein synthesis and fate	cyto	0//0							88	e-116	AT2G05840	cytosolic ribosome, proteasome core complex
Medtr3g089040	MtC10104_1_AA Peptidase T1A, proteasome beta-subunit	Protein synthesis and fate	cyto	0//0							83	e-124	AT3G26340	proteasome complex
Medtr6g084450	MtD00231_1_AA Peptidase T1A, proteasome beta-subunit	Protein synthesis and fate	cyto	0							83	e-116	AT1G56450	Cytosol /proteasome cxp
Medtr3g062510	MtC10684_1_AA 26S proteasome subunit P45 IPR013093:ATPase AAA-2	Protein synthesis and fate	cyto	0//0							98	0	AT5G58290	proteasome complex
Medtr3g108800	MtC60362_1_AA Blast: G7JCD0 Plasma membrane H+ ATPase , cation transport ATPase (P-type) family	Transport	plas	TM 6				P 2			83	0	AT4G30190	integral to membrane, membrane, plasma membrane, plasmodesma, vacuolar membrane
Medtr1g043290	MtC20134.2_1_AAMtPT1 PHOSPHATE TRANSPORTER Major facilitator superfamily (Liu et al. 1998)	Transport	plas	TM 11				P 1			69	0	AT5G43360	membrane, plasma membrane
Medtr2g075250	MtD11061_1_AA Blast: XP_003531816 : probable LRR receptor-like serine/threonine-proteinkinase At1g56130-like [Glycine max].Leucine−rich repeat	Signal transduction	Chlo	TM 1							50	5.00E-57	AT1G56140	plasma membrane
Medtr5g098420	MtC10353_1_AA unknown Blast: XP_003618047.1 Fasciclin-like arabinogalactan protein [Medicago truncatula]	Protein synthesis and fate	Chlo	TM 2	BB		SP				66	e-123	AT4G12730	anchored to membrane, anchored to plasma membrane, membrane, plasma membrane, vacuolar membrane
Medtr2g034550	MtC60823_1_AA Blast: OEP16_PEA RecName: Full=Outer envelope pore protein 16, chloroplastic; AltName: Full=Chloroplastic outer envelope pore protein of 16 kDa.	Transport	Chlo	TM 1	BB						52	4.00E-40	AT2G28900	chloroplast, chloroplast envelope, plastid outer membrane, vacuole
Medtr8g018550	MtC10070_1_AA Lipoxygenase	Cell rescue and defense	cyto	TM 2							56	0.00E+00	AT3G22400	chloroplast
Medtr2g086500	MtC00668_1_AA Ribosomal protein L1	Protein synthesis and fate	cyto	0				P 1			81	e-100	AT1G08360	cytosol, cytosolic large ribosomal subunit, cytosolic ribosome, plasma membrane, plasmodesma, ribosome
Medtr7g026230	MtC10470_1_AA Actin/actin-like	Cytoskeleton	Chlo	TM 2				P 2			97	0	AT3G12110	chloroplast envelope, chloroplast stroma,

														cytoskeleton, mitochondrion, plasma membrane, plasmodesma